Institut de Duve
Ludwig Cancer Research, Brussels

Secondary site mutations restoring physiologic function for JAK2 V617F and identification of novel allosteric sites in oncoproteins: new therapeutic opportunities for blood malignancies

Emilie Leroy, MSc.

Promoteur: Prof. Stefan N. Constantinescu

-2016-

Thèse présentée en vue de l'obtention du grade de
Docteur en Sciences Biomédicales et Pharmaceutiques
Orientation: Signalisation et hématologie moléculaire

Ecole doctorale de génétique et d'immunologie (GIM)
Université Catholique de Louvain
Faculté de Pharmacie et Sciences Biomédicales
Institut de Duve
Ludwig Cancer Research, Brussels

Promoter:

Professor Stefan N. Constantinescu (UCL-SIGN, de Duve Institute, Cell signaling Unit and Ludwig Cancer Research, Brussels Branch)

Jury:

Internal members

- Professor Thomas Michiels (UCL de Duve Institute - MIPA, Microbial Pathogenesis Unit)
- Professor Jean-Christophe Renauld (UCL de Duve Institute - MEXP, Experimental Medecine Unit)
- Professor Miikka Vikkula (UCL de Duve Institute - GEHU, Human Molecular Genetic Unit)
- Professor Frédéric Lemaigre (UCL de Duve Institute – LPAD, Liver and Pancreas Differentiation)

External members

- Professor Radek Skoda (University Hospital Basel, Department of Biomedecine, Experimental Hematology)
- Dr. Andrew K. Shiau (Small Molecules Discovery Program, Ludwig Cancer Research, San Diego Branch)

This thesis was supported by PhD fellowship from FRIA (Fonds pour la formation à la recherche dans l'industrie et dans l'agriculture) and by Salus Sanguinis Foundation (Bourse Guillaume Franqui et Lucienne De Roover).

TABLE OF CONTENTS

TABLE OF CONTENTS **3**

TABLE OF FIGURES **5**

LIST OF TABLES **7**

LIST OF ANNEXES **9**

ABSTRACT **11**

ABBREVIATIONS **13**

INTRODUCTION **17**

1.Hematopoiesis **17**

2. Myeloproliferative neoplasms **17**

2.1 Activating mutations in JAK2 20

2.2 Activating mutations in the thrombopoietin receptor 22

2.3 What about CALR? 23

3. Cytokine receptors signaling **24**

3.1 General overview 24

3.2 Type-I cytokine receptors 26

3.3 Signaling pathways 32

4. Kinatown (protein kinases) **37**

4.1 General overview 37

4.2 Classification of kinases 38

4.3 Conserved structural features 38

4.4 Common activation mechanisms 46

4.5 Regulation mechanisms 49

4.5 Pseudokinases 50

4.6 Concluding remarks 52

5. Janus kinases **52**

5.1 Discovery and evolution 52

5.2 Structure of JAKs 53

5.3 Physiopathology of JAK2 58

6. JAK2 inhibitors: the current landscape **66**

6.1. JAK2, the Achilles' heel of MPNs. 66
6.2. Type-I inhibitors 68
6.3. Type-II inhibitors 72

OBJECTIVES 77

RESULTS 79
ARTICLE 1: Uncoupling JAK2 V617F activation from cytokine-induced signalling by modulation of the JH2 αC helix 79
ARTICLE 2. Inhibition of JAK2 V617F by Targeting the Aromatic Interactions Around F617 107

DISCUSSION 123
1. Physiological activation of JAK2 by cytokine receptor 123
1.1 Function of the pseudokinase domain during JAK2 activation: *cis* versus *trans* auto-inhibition 123
1.2 Function of the pseudokinase domain in the inter-molecular interface. 127
2. Pathological activation of JAK2 by the mutation V617F 130
3. Development of inhibitors specific for JAK2 V617F 137
3.1 Novel allosteric sites in the pseudokinase/kinase interface of JAK2. 137
3.2 *Ab initio* modeling of small molecules specific for JAK2 V617F 140

CONCLUSION 143

PERSPECTIVES 145
Rethinking JAK2 inhibition: towards novel strategies of more specific and versatile Janus kinase inhibition 145
1. Allosteric inhibitors 145
2. Covalent inhibitors 150
3. Tuning JAK2 signaling from the outside. 152
4. Targeting cytokine receptor-JAK2 interaction. 152
5. Conclusion 155

REFERENCES 157

Annex 183

TABLE OF FIGURES

Figure 1. Hematopoiesis 19
Figure 2. The cytokine receptor superfamily 25
Figure 3. Schematic representation of homodimeric type-I cytokine receptors 27
Figure 4. The cytokine receptor-JAK2 complex 28
Figure 5. Role of the TpoR transmembrane and juxtamembrane domains in receptor dimerization and activation 30
Figure 6. Major signaling pathways activated by cytokine receptors 33
Figure 7. The typical fold of a kinase and structural location of the important catalytic features 40
Figure 8. The ATP binding cleft 41
Figure 9. The activation segment 43
Figure 10. Residues participating in the phosphoryl transfer reaction 43
Figure 11. The αC- β4 loop participates in the motion of the αC helix 46
Figure 12. The two hydrophobic regulatory spines and the αF helix define the internal core of protein kinases 48
Figure 13. Anatomy of JAKs 53
Figure 14. Model of the interface between JH1 and JH2 in JAK2 derived from molecular dynamics simulations 62
Figure 15. V617F induces a conformational change in the JH2 αC helix 64
Figure 16. The FFV triad is conserved in JAKs 65
Figure 17. Comparison between type-I versus type-II inhibitors of JAK2 71
Figure 18. Definition of the different types of kinase inhibitors 76
Figure 19. Two models have been proposed for regulation of JAK kinase domain by the pseudokinase domain 124
Figure 20. Theoretical models of the inter-molecular interplay between two JAK2 molecules and the role of JH2 in the process 128
Figure 21. The domino model illustrates the sequential set of events propagating from the V617F site to the kinase active site 131
Figure 22. Modeling of the structural changes induced by V617F mutation from the JH2 αC helix to the N-lobe of JH1 132
Figure 23. Representation of the pockets and cavities in JAK2 JH2 V617F 138
Figure 24. Structural details of the JAK2 V617F inhibitory mutations 139

Figure 25. Location of a hydrophobic pocket underneath the JH2 αC and close to residue E596 140
Figure 26. Putative aromatic π-stacking disruptive chemicals 141
Figure 27. JAK2 structures and the possible allosteric sites 149
Figure 28. Possible strategy for the development of covalent allosteric inhibitor 151
Figure 29. The cytokine-receptor-JAK complex 154

LIST OF TABLES

Table 1. Comparison between JH1 and JH2 catalytic motifs 51
Table 2. Summary of published three-dimensional structures of JAKs 57
Table 3. Conservation of the residues involved in V617F-mediated activation across JAKs 137

LIST OF ANNEXES

Annex 1. Germ-line JAK2 mutations in the kinase domain are responsible for hereditary thrombocytosis and are resistant to JAK2 and HSP90 inhibitors. Marty, C., Saint-Martin, C., Pecquet, C., Grosjean, S., Saliba, J., Mouton, C., Leroy, E., Harutyunyan, A. S., Abgrall, J. F., Favier, R, Toussaint, A. Solary, E. Kralovics, R., Constantinescu, S. N., Najman, A., Vainchenker, W., Plo, I., Bellanne-Chantelot, C. *Blood* (2014), *123*, 1372-1383

Annex 2. Whole-exome sequencing identifies novel MPL and JAK2 mutations in triple-negative myeloproliferative neoplasms. Milosevic Feenstra, J. D., Nivarthi, H., Gisslinger, H., Leroy, E., Rumi, E., Chachoua, I., Bagienski, K., Kubesova, B., Pietra, D., Gisslinger, B, Milanesi, C., Jager, R., Chen, D., Berg, T., Schalling, M., Schuster, M., Bock, C., Constantinescu, S. N., Cazzola, M., Kralovics, R. *Blood* (2016*), 127*, 325-332.

Annex 3. His499 Regulates Dimerization and Prevents Oncogenic Activation by Asparagine Mutations of the Human Thrombopoietin Receptor. Leroy, E.*, Defour, J. P.*, Sato, T., Dass, S., Gryshkova, V., Shwe, M. M., Staerk, J., Constantinescu, S. N., and Smith, S. O**.** *J Biol Chem* (2016), *291*, 2974-2987

Annex 4. Orientation-specific signalling by thrombopoietin receptor dimers. Staerk, J.*, Defour, J. P.*, Pecquet, C., Leroy, E., Antoine-Poirel, H., Brett, I., Itaya, M., Smith, S. O., Vainchenker, W., and Constantinescu, S. N. *EMBO J* (2011), 30, 4398-4413

Annex 5. Activating Janus kinase pseudokinase domain mutations in myeloproliferative and other blood cancers. Constantinescu, S. N., Leroy, E., Gryshkova, V., Pecquet, C., and Dusa, A. Biochem Soc Trans (2013), *41*, 1048-1054.

Annex 6. Cooperation of germline JAK2 mutations E846D and R1063H in hereditary erythrocytosis with megakaryocytic atypia. Kapralova, K.*, Horvathova, M.*, Pecquet, C.*, Fialova Kucerova, J., Pospisilova, D., Leroy, E., Kralova, B., Milosevic Feenstra, J. D., Schischlik, F., Kralovics, R., Constantinescu, S. N., Divoky, V. *Blood* (2016). In Press.

*Co-authors

Annex 7. Table: Mutations in Janus kinases associated with hematological malignancies.

Annex 8. Table: List of the JAK2 inhibitors historically studied.

ABSTRACT

Cytokine receptors and their appended JAKs are necessary for the formation and function of hematopoietic and immune systems. JAKs are cytosolic tyrosine kinases with fundamental functions in biology, as well as key drug targets in JAK-STAT signaling pathway. A single point mutation resulting in the substitution of a valine for a phenylalanine at residue 617 in JAK2 has been recognized as the most common molecular event associated with myeloproliferative neoplasms (MPNs). V617F lies in the pseudokinase domain (JH2) and activates the adjacent catalytic JAK2 subunit, the kinase domain (JH1), by a process that is still unclear. Understanding the molecular mechanism by which V617F activates JAK2 is a key challenge for the field of MPNs. Indeed, understanding the mechanism of constitutive activation at the molecular level would allow not only a better comprehension of the structure and function of pseudokinase domains, but also guide future drug design towards more specific inhibitory strategies. Among all the pharmaceutical compounds that have been investigated over the past ten years only one has been accepted for clinical use. But there is still no curative treatment option for MPN patients to date.

Our major focus was on understanding the role of the JH2 and the JH1 domains in regulating both normal and V617F-mediated activation of JAK2. More precisely, we aimed to determine how V617F activation is transmitted from the JH2 to JH1. It was already known that the V617F-induced molecular effects involve the F594/F595 residues of the α helix C of JH2 where an aromatic stacking interaction between F617 and F594/F595 is required for constitutive signaling of JAK2 V617F, the first molecular step in triggering hyper-activation in JAK2.

In our first study, we emphasized the function of the JH2 αC in the oncoprotein JAK2 V617F and found additional key elements of V617F-mediated activation. We determined that V617F hyperactivity absolutely requires negative charge on the face of αC opposite to F595/F594. Reversing the charge of this helical face restores wild-type phenotype to

JAK2 and normal response to cytokine stimulation. The inhibitory mutations that remove negative charge or add positive charges, such as E596A/R, are suggested to not alter the JH2 domain structure, as shown by our X-ray crystal of JH2 V617F-E596A. In addition, we found by structure-guided modeling and mutageneses that V617F activates JAK2 through a community of residues across the JH2, SH2-JH2 linker and JH1 domains.

In a second study, we focused on how to directly destabilize the initial molecular step in V617F-mediated activation, namely the aromatic stacking between F617 and F594/F595. This interaction induced a change in conformation of the JH2 αC, which can be visualized in the X-ray crystal structure of JH2-V617F. We found that introducing another bulky aromatic residue, such as phenylalanine, in the vicinity of the aromatic stacking can inhibit JAK2 V617F hyperactivity without altering the normal function of the protein. These findings pave the way for further studies using small molecules able to disrupt the aromatic stacking interaction that only exist in the mutant form, presenting a valuable strategy in order to attain mutant-specific inhibition.

Altogether, we have identified several regulatory sites for novel allosteric modulation of the mutant protein JAK2 V617F. These new allosteric sites provide opportunities for the identification of a new class of pharmaceuticals that could potentially obtain improved specificity and potency toward the oncoprotein JAK2 V617F.

ABBREVIATIONS

ABL	Abelson
ADP	Adenosine Di Phosphate
AKT	AKT8 Virus Oncogene Cellular Homolog
ALL	Acute Lymphoid Leukemia
AML	Acute Myeloid Leukemia
ASXL1	Additional Sex Combs Like 1
ATP	Adenosine Tri Phosphate
ATPγS	Adenosine Tri Phosphate gamma S
B-ALL	B-cell Acute Lymphoblastic Leukemia
BCR	Breakpoint Cluster Region
BRAF	v-Raf Murine Sarcoma Viral Oncogene Homologue B1
BTK	Bruton Tyrosine Kinase
CALR	Calreticulin
CDK2	Cyclin-Dependent Kinase 2
CML	Chronic Myeloid Leukemia
CMP	Common Myeloid Progenitor
CRM	Cytokine Receptor Module
DNA	Deoxyribonucleic Acid
DNMT3A	DNA (cytokine-5)-Methyltransferase 3A
DQX	8-[3,5-difluoro-4-(morpholin-4-ylmethyl)phenyl]-2-(1-piperidin-4-yl-1H-pyrazol-4-yl)quinoxaline
ECL	Eosinophilic Leukemia
EDO	1,2-Ethanediol
EMA	European Medicines Agency
EGFR	Epithelial Growth Factor Receptor
Epo	Erythropoietin
ER	Endoplasmic Reticulum
ET	Essential Thrombocythemia
EZH2	Enhancer of Zeste Homolog 2
FAK	Focal Adhesion Kinase
FDA	Food and Drug Administration
FERM	Four-Point-One/Ezrin/Radixin/Moesin
FLT-3	Fms-like Tyrosine Kinase 3

FGFR-1	Fibroblast Growth Factor-1
FRET	Fluorescence Resonance Energy Transfer
GAS	Gamma-Activated Site
GCN2	General Control Non-Derepressible 2
G-CSFR	Granulocyte-Colony Stimulating Factor Receptor
GM-CSFR	Granulocyte-Macrophage Colony Stimulating Factor Receptor
GPCR	G Protein-Coupled Receptor
GOL	Glycerol
Gp130	Glycoprotein 130
GRH	Growth Hormone Receptor
HER2	Human Epithelial Growth Factor 2
HER3	Human Epithelial Growth Factor 3
Hop	Hopscotch
HSC	Hematopoietic Stem Cells
SHP90	Heat Shock Protein 90
IDH1/2	Isocitrate Dehydrogenase 1/2
IFN	Interferon
IK1	5-Phenyl-2-Ureidothiophene-3-Carboxamide
IL	Interleukin
IFNAR	Interferon Alpha Receptor
IRK	Insulin Receptor Kinase
ISRE	IFN-Stimulated Responsive Element
JAK	Janus Kinases
JH	JAK Homology
JSI	JAK Specific Insertion
Kd	Dissociation Constant
kDa	kiloDalton
KSR1	Kinase Suppressor of Ras 1
MAPK	Mitogen-Activated Protein Kinase
MD	Molecular Dynamics
Mg	Magnesium
Mn	Manganese
MLKL	Mixed Lineage Kinase domain-Like
MO25	MOuse Protein 25
MPL	Myeloproliferative Leukemia Virus Oncogene

MPN	Myeloproliferative Neoplasm
MDS	Myelodysplastic Syndrome
MF	Myelofibrosis
NMR	Nuclear Magnetic Resonance
NK	Natural Killer
NLS	Nuclear Signaling Sequence
NRTK	Non-receptor Tyrosine Kinase
PCR	Polymerase Chain Reaction
PDB	Protein Data Bank
PDGFR	Platelet-derived Growth Factor Receptor
PIAS	Protein Inhibitor of Activated STAT
PI3K	Phosphatydylinositol-3-kinase
PKA	Protein Kinase A
PMF	Primary Myelofibrosis
PO4	Phosphate Ion
PRLR	Prolactin Receptor
PTB	Phosphotyrosine Binding
PTK	Protein Tyrosine Kinase
PTP	Protein Tyrosine Phosphatase
PV	Polycythemia Vera
RA	Rheumatoid Arthritis
RAF	Rapidly Accelerated Fibrosarcoma
RET	REarranged During Transfection
RTK	Receptor Tyrosine Kinase
SAXS	Small Angle X-ray Scattering
SCID	Severe Combined Immunodeficiency
SgK223	Sugen Kinase 223
SCYL1	SCY1 Like Pseudokinase 1
SCYL3	SCY1 Like Pseudokinase 3
SH2	Src Homology Domain
SHP	SH2 Domain-containing Phosphatases
SOCS	Suppressor of Cytokine Signaling
Src	Rous sarcoma oncogene cellular homolog
SRSF2	Serine and Arginine Rich Splicing Factor 2
STAT	Signal Transducer and Activator of Transcription
STRADα	STe20-Related ADaptor α

TM	Transmembrane
TET	Ten-Eleven Translocation
TET2	Tet Methylcytosine Dioxygenase 2
Tpo	Thrombopoietin
TpoR	Thrombopoietin Receptor
TP53	Tumor Protein P53
TYK2	Tyrosine kinase 2
U2AF1	U2 Small Nuclear RNA Auxiliary Factor 1
WHO	World Health Organization
WNK	With No Lysine Kinases
WT	Wild Type
2TT	2-chloro-N-(2-((cyclopropylcarbonyl)amino)pyridin-4-yl) benzamide

Amino Acids

Hydrophobic	
A	Alanine
V	Valine
I	Isoleucine
L	Leucine
M	Methionine
F	Phenylalanine
Y	Tyrosine
W	Tryptophane

Polar	
S	Serine
T	Threonine
N	Asparagine
Q	Glutamine

Positively charged side chain	
R	Arginine
H	Histidine
K	Lysine

Negatively charge side chain	
D	Aspartate
E	Glutamate

Special cases	
C	Cysteine
G	Glycine
P	Proline

INTRODUCTION

1.Hematopoiesis

The rapid turnover of blood constituents requires a highly effective and tightly regulated process for regenerating new blood cells. This process, which is referred to as hematopoiesis, allows immature precursor cells to generate mature blood cells in the adult bone marrow. All blood cells arise from a unique type of pluripotent cell, namely the hematopoietic stem cell (HSC), which possesses the ability to self-replicate, to proliferate and to differentiate into increasingly specialized progenitors cells (**Figure 1**). In the steady state, hematopoiesis maintains basal levels of blood cells, but it can rapidly expand the numbers of progenitor cells to adapt to physiological stresses such as hemorrhage or infection (1). Hematopoiesis is controlled by inherited and environmental factors (2). Indeed, proliferation and differentiation are regulated by a paracrine stimulation of growth factors that modulate the transcription factor program governing progenitor cell fate. Blood cells comprise different cell types divided into two lineages: (i) the myeloid lineage composed of erythrocytes, thrombocytes, granulocytes and monocytes and (ii) the lymphoid lineage consisting of lymphocytes. This work focuses mainly focused on the former, which can give rise to clonal hematological disorders named myeloproliferative neoplasms (MPNs).

2. Myeloproliferative neoplasms

The unified concept of myeloproliferative disorders (MPDs) was initially proposed by William Dameshek in 1951 (3) and more recently re-named myeloproliferative neoplasms (MPNs) in 2008 (4). They are clonal hematological disorders initiated in hematopoietic stem cells and multipotent hematopoietic progenitors, resulting in the overproduction of mature myeloid cells (from the erythroid, megakaryocytic or granulocytic lineage). The term "MPNs" in this thesis refers to BCR-ABL-negative

myeloproliferative disorders and in practice groups polycythemia vera (PV), essential thrombocythemia (ET) and primary myelofibrosis (PMF), although the World Health Organization (WHO) classification also includes chronic myeloid leukemia (CML) and other entities such as eosinophilic leukemia (CEL) (5). MPNs have a chronic clinical progression with median survival under treatment of ~ 20 years for ET, 14 years for PV and 6 years for PMF (6). Unfortunately, current therapies in MPNs are not curative nor do they prevent disease progression. Inhibition of JAK2 has been shown to be beneficial in MPNs treatment, especially in myelofibrosis and PV resistant to antineoplastic agent such as hydroxyurea (7-9). The current JAK2 inhibitors used in MPNs treatment will be discussed in section 6. MPNs are characterized by bone marrow hypercellularity with or without fibrosis, elevated cell count of at least one blood lineage, frequent splenomegaly, increased risk of thrombosis and bleeding and a propensity to progress into secondary acute leukemia associated with a dismal prognosis (10, 11). Dysregulation of the JAK-STAT pathway underlies the molecular basis of MPN pathogenesis. MPNs are associated with mutually exclusive somatic mutations of Janus kinase 2 (JAK2), thrombopoietin receptor (TpoR) or most recently calreticulin (CALR) leading to hypersensitivity or independence of myeloid progenitors from cytokines and to subsequent malignant proliferation. The most recurrent mutation is JAK2 V617F, which is found in > 95% of PV patients and in 50-60% of ET and PMF patients. MPN patients that are negative for JAK2, CALR or TpoR mutations are commonly referred as "triple negative" (12, 13). While it is well accepted that these driver mutations are responsible for the phenotype of MPNs, removing cytokine control of survival, proliferation and differentiation, the precise contribution of inherited factors to the disease establishment, clonal dominance, development, progression and severity is less understood (14).

In addition to the common driver mutations, other somatic mutations have been associated with more rare cases of MPNs. Inactivating mutations in genes encoding negative regulators of the JAK/STAT pathway (such as LNK or SOCS) have been found in a minority of MPN patients (15-17) and associated with aberrant hematopoiesis (18-20). These mutations can either drive the disease or enhance the effect of another driver mutation such as JAK2 or MPL mutations. Finally, with the recent progress in whole-genome sequencing, an expanding catalog of somatic mutations in epigenetic

modifiers (TET2, ASXL1, IDH1/2, EZH2 or DNMT3A), in the splicing machinery (SRSF2, U2AF1) or in tumor suppression (TP53) has been associated with MPNs (12, 21). However, these mutations do not alone drive the disease. In fact, they are thought to be involved in the disease progression by occurring either before or after the mutation JAK2 V617F (22-24). Of importance, only mutated JAK2, TpoR and CALR and the loss of LNK are able to induce MPN in mouse models, giving the evidence that they are real driver mutations, as expected as they constitutively activate JAK2-STAT5/STAT3 pathways.

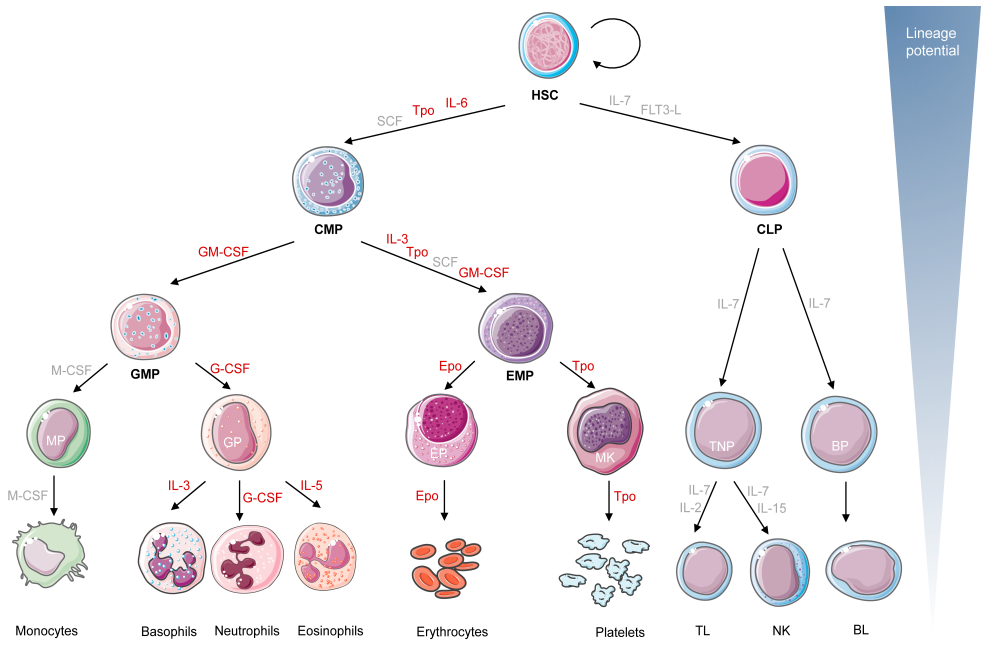

Figure 1. Hematopoiesis. Blood cells originate from a rare population of multipotent, self-renewing stem cells that undergo a progressive loss of differentiative potential to give rise to two lineage-restricted progenitors CMP and CLP. Cytokines utilizing JAK2 for signaling are denoted in red. JAK2 V617F occurs in HSCs and signal through EpoR, TpoR, and G-CSFR, which explains why V617F-induced proliferation affects the three myeloid lineages. HSC: hematopoietic stem cell, CMP: Common myeloid progenitors, CLP: common lymphoid progenitors, GMP: granulocyte and macrophage progenitors, EMP: erythroid and megakaryocyte progenitors, MP: macrophage progenitors, EP: erythroid progenitors, MK: megakaryocytes, TNP: T-cell and Natural Killer progenitors, BP: B-cell progenitors, TL: T-lymphocytes, NK: Natural Killers, BL: B-lymphocytes.

2.1 Activating mutations in JAK2

JAK2 V617F

In 2005, four independent studies published the identification of a novel acquired somatic point mutation in the gene encoding Janus kinase 2 (JAK2), namely JAK2 V617F (25-28). A guanine to a thymine transversion at nucleotide 1849 of the cDNA in exon 14 of the gene results in a substitution of the highly conserved valine to phenylalanine at codon 617. This residue is located in the N-terminal lobe of the pseudokinase domain. JAK2 V617F is a somatic mutation acquired at the level of HSC (**Figure 1**) and found in > 95% of PV patients and > 50% in ET and PMF (29).

How a unique mutation can give rise to three disease phenotypes has been extensively studied but is presently not completely understood. Several investigative routes have been taken to understand this particular pathogenesis: i) the mutation may occur in different subsets of HSCs already pre-committed to the erythroid or megakaryocytic lineage; ii) the phenotypic progression from the unique mutation depends on the patient genotypic background and the existence of predisposing genes (23, 30); iii) the "dosage hypothesis" has been one of the most reported theories; which implies that the number of copies of the JAK2 V617F allele (namely allele burden, translated into levels of active kinase) is correlated with a particular phenotype. In this scenario, a low allele burden favors ET, while a high allele burden leads to PV, and very high levels induce myelofibrosis (31, 32). In accordance with this notion, JAK2 V617F is found to be heterozygous in ET and homozygous in PV patients (33) iv) phenotype was suggested to be correlated with preferential binding of JAK2 V617F to certain cytokine receptors, but this model requires either genetic factors favoring such preferential binding and activation or occurrence of the mutation in specific stem and progenitor subsets.

JAK2 V617F requires a functional FERM domain (34) and binding to dimerized cytokine receptors to exert its constitutive activation (35). JAK2 V617F triggers constitutive signaling of STATs, MAPK and PI3K pathways (26). Of note, JAK2 V617F mediates transformation of cells only through hematopoietic homodimeric type-I cytokine receptors: TpoR, EpoR (erythropoietin receptor) and G-CSFR (granulocyte colony-stimulating factor receptor) (**see introduction, section 3**) (36).

It is interesting to note that even though GHR (growth hormone receptor) or PRLR (prolactin receptor) are typical homodimeric type-I receptors, they do not seem to constitutively signal via JAK2 V617F or any other activated forms of JAK2 as no acromegaly phenotype has ever been observed in any JAK2 V617F mouse model (37). Homologous substitution in JAK isoforms have been shown to be activating in JAK1 (JAK1 V658F) and in TYK2 (TYK2 V678F) (38), although only JAK1 V658F has been described in humans, in patients with T-cell lymphoblastic leukemia (39, 40).
The exact molecular mechanism by which the V617F mutation, located on the pseudokinase domain, actives the kinase domain of JAK2 remains unexplained and has been the main focus of the present work. Previous studies have given some insights into specific features of the V617F-mediated activation that will be discussed in the introduction, section 5.3.

Other Somatic mutations

Apart from V617F, a growing list of additional JAK2 somatic mutations has been associated with a small minority of MPN cases (41). Some of them have been shown to be activating while others have not been yet characterized. They principally cover regions from exon 12 to exon 15. They comprise three exon 14 PV-related mutations, C618R (42), D620E (43, 44) and C616Y (45), affecting residues in close proximity to valine 617. They also include a group of approximately 16 different mutations such as missense mutations, deletions and insertions around residues 538-543 that were grouped under the name of "exon 12 mutations", which are linked to a PV subset that is characterized by selective activation of proliferation in the erythroid lineage (46). These mutations are found in < 3% of PV negative for V617F and seem to preferentially induce erythrocytosis without changes in the megakaryocyte lineage (47). This was supported by the phenotype of transgenic mice expressing an exon 12 JAK2 mutant (48). All these "exon 12 mutations" are located in the linker between the pseudokinase domain and the SH2 domain (the SH2/JH2 linker) (**see introduction, section 5.2**). This region is critical for normal and pathological regulation of JAK2.

Germline mutations

In 2014, several groups reported germ-line JAK2 heterozygous mutations associated with hereditary thrombocytosis. The group of Hitchcock identified JAK2 R564Q(49), while the group of Vainchenker identified new heterozygous germline mutations in hereditary thrombocytosis. While one family harbors the JAK2 R867Q mutation (a kinase domain mutation), the other family carries two JAK2 mutations, S755R/R938Q (pseudokinase/ kinase domain mutations), on the same molecule. In a collaborative work with our group, they could identified that these mutations are indeed activating and that they confer to JAK2 a prolonged half-life that correlates with an increased binding to the heat shock protein 90 (HSP90) chaperone and with higher levels of TpoR at the cell surface (50) (**Annex 1**). Early in 2016, Kralovics and colleagues identified novel heterozygous germline mutations in "triple negative" cases of ET and PMF by applying whole-exome sequencing (WES). As part of this collaborative effort, we characterized these new germline mutations (G335D, G571S and V625F) and we could show that only V625F constitutively activates the JAK-STAT5 pathway (51) (**Annex 2**). The group of Sten-Eirik Jacobsen identified a family with hereditary thrombocytosis that harbors the heterozygous mutation JAK2 V617I (52) that our group described as a weakly activating mutation at V617 (53). Like the other JAK2 germline mutations associated with hereditary thrombocytosis, this mutation preferentially induced signaling in megakaryocytes and via TpoR (54). Our group could show that all these mutants, when expressed in heterozygous conditions, induce mainly activation of TpoR and STAT1 (50), which is known to promote megakaryocyte proliferation and differentiation (55, 56)

2.2 Activating mutations in the thrombopoietin receptor

The majority of TpoR mutations alter residue W515, which is located in the cytoplasmic juxtamembrane (JM) domain. This residue is part of an amphipathic and helical motif "RWQFP" that was shown to prevent spontaneous activation of the receptor in the absence of cytokine stimulation (57). In fact, W515 itself was shown to control dimerization and activation of the receptor (58). Mutations W515K/L/A/S/R/G are only found

in ET and PMF patients, with frequencies of 3% and 5-8% respectively (59-63). A recent study indicated that substitutions of W515 by 17 other amino acids (out of 20) induce constitutive activation of the receptor (64), suggesting that MPN patients should also be tested for these mutations. Mouse models of W515L/A mutants have shown to induce a rapid and fatal MPN with myelofibrosis and a large expansion of platelets, neutrophils and immature erythroid progenitors, which presents a much more severe phenotype than the one induced by JAK2 V617F (65).

Residue S505, located in the transmembrane domain of the receptor, is found mutated to asparagine (N) in familial and sporadic ET with low frequency (62, 66) and leads to constitutive activation of the receptor-JAK2 complex (67). S505N mutation results in a strong dimerization of the receptor in the absence of Tpo binding (68). Substitution of the serine (S) by a much more polar residue such as asparagine (N) is thought to lead to intermolecular hydrogen bounds formation, which is responsible for the cytokine-independent dimerization of the receptor, leading to activation of the downstream pathway. In extremely rare cases, TpoR mutations can be found together with JAK2 V617F in the same patient, but they are present in different cells, likely arising from different clones (51). All these mutations induce a MPN phenotype by mediating cytokine-independent cell proliferation. Autonomous dimerization of the mutated receptor in an active oncogenic conformation is thought to be the molecular mechanism by which the pathological signaling is triggered. The specific dimeric interfaces adopted by these receptors have been the subject of two studies (**Annexes 3, 4**).

2.3 What about CALR?

Late in 2013, the two groups of R. Kralovics and A. R. Green made the exciting discovery of mutations in the gene encoding calreticulin (CALR) in 25% cases of ET and PMF patients (12, 13). CALR is an endoplasmic reticulum (ER) lumen resident chaperone protein involved in the quality control system, certifying correct folding of proteins entering the secretory pathway (69). CALR possesses an ER retention signal made of the amino acids KDEL in its C-terminal sequence. Mutations found in MPN patients affect exon 9, which encode this region. The two most prevalent mutants

are the so-called "del52" or type-1 and "Ins5" or type-2 characterized by a 52 bp deletion and 5 bp insertions in the c-terminal region of CALR, respectively, leading to +1 frameshifting. (70). Studies have demonstrated that CALR mutants specifically activate TpoR, but not the other type-I and type-II cytokine receptors, through interaction with specific N-glycosylation sites of extracellular domain of the receptor (71).
CALR mutants induce pathological signaling mainly through JAK-STAT and MAPK pathways, which differ from JAK2 V617F-induced signaling that also induces significant activation of the PI3K pathway (71).

3. Cytokine receptors signaling

3.1 General overview

Cytokine receptors play a critical role in supporting hematopoiesis. Soluble cytokines circulating in the blood bind to their cognate receptors at the cell membrane and trigger various biological responses such as proliferation, differentiation and survival (72). The signaling pathways governing myeloid differentiation has been well characterized and mainly includes the JAK/**S**ignal **T**ransducers and **A**ctivators of **T**ranscription (STATs) pathway but also the Ras/**M**itogen-**A**ctivated **P**rotein **K**inase (MAPK) pathway and the **P**hosphatydyl**i**nositol-**3**'-**K**inase (PI3K)/AKT pathway which are both activated by cytokine receptors via Janus kinases (73).

The cytokine receptor superfamily consists of single membrane-spanning molecules lacking intrinsic kinase activity. Members of the Janus kinase (JAK) family are bound to their cytosolic tail to ensure signaling propagation. Of note, hematopoiesis also requires another class of receptors, which are receptor tyrosine kinase. In contrast with cytokine receptors, these receptors (e.g. FLT-3 or c-kit) possess an intrinsic kinase activity. Based on the conserved structural extracellular domain, the cytokine receptors superfamily is separated into type-I and type-II cytokine receptors (**Figure 2**) (74). These receptors have different JAK requirements (**Figure 2**). However, the lack of structural information on the intracellular tail of receptors clouds our understanding of the molecular details governing the specificity of this interaction. How individual JAKs distinctly interact with

their own receptors has always been an intriguing question and data, to date, have mainly come from mutagenesis studies (75-77). Until recently, structural studies on TYK2 (78) and JAK1 (79) provided the first visualization of the JAK-receptor interface (discussed later in the perspectives).

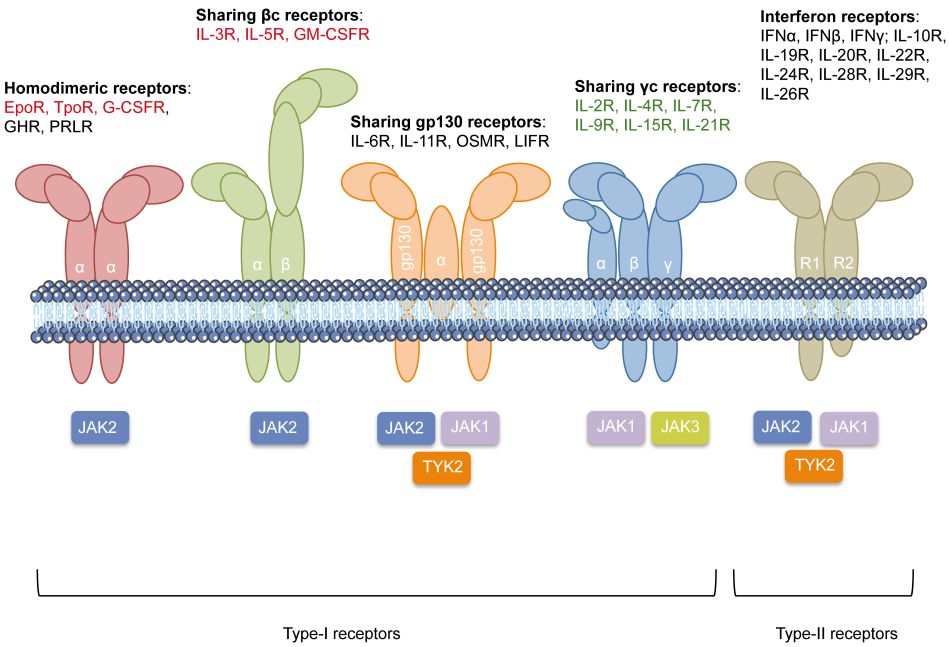

Figure 2. The cytokine receptor superfamily. Schematic representation of type-I and type-II subfamilies, based on homologies in the sequence of the extracellular domains. The JAKs (JAK1, JAK2, JAK3 and TYK2) utilized by each class of receptors are indicated. Type-I receptors can form homodimers (α/α), heterodimers (α/β) or oligomers (gp130/α/gp130);(α/β/γ). Within the type-I cytokine receptors, the α chain is mainly responsible for cytokine binding. Cytokine receptors composed of two or more different chains activate at least two different JAKs. Single chain receptors like homodimeric receptors only activate JAK2, although TpoR also uses TYK2 and G-CSFR, JAK1. The myelopoiesis-related cytokine receptors are denoted in red, while the lymphopoiesis-related cytokines receptors are denoted in green. JAK2 V617F requires any of the three hematopoietic homodimeric receptors to signal in the absence of cytokine.

3.2 Type-I cytokine receptors

Type-I cytokine receptors share a number of common extracellular structural features including a cytokine receptor module (CRM) containing two fibronectin type III-like domains, four spatially conserved extracellular cysteines and a membrane proximal WSXWS motif (**Figure 3**)(80). They also contain a single helical transmembrane domain of approximately 20-25 residues that are mainly hydrophobic. In their cytosolic tail, they possess the conserved box1 and box2 necessary for non-covalent binding of JAKs. Box1 is membrane proximal and is rich in proline and hydrophobic residues whereas box2 is less conserved and begins with a cluster of hydrophobic residues, followed by negatively charged residues and ends with one or two positive ones (81). Type-I receptors correspond to the hematopoietic receptors and can be themselves divided in subfamilies depending on the complex formed by the active receptor (**Figure 2**). Indeed, cytokine binding to the extracellular domain can induce the formation of homodimers, heterodimers or oligomers (**Figure 2**). The present study focuses on the homodimeric receptors subfamily that includes the erythropoietin receptor (EpoR) and the thrombopoietin receptor (TpoR).

Thrombopoietin receptor

The thrombopoietin receptor (TpoR) (also called c-Mpl, derived from the myeloproliferative leukemia virus) plays different roles at various stages of hematopoiesis. In fact, TpoR signaling regulates the proliferation of megakaryocyte progenitors, their differentiation into mature megakaryocytes, generation of platelets (82), as well as renewal and quiescence of HSCs (83, 84). *In vivo* studies have shown that TpoR deficient mice display significant reduction in megakaryocytes, platelets and HSCs (85). The CRM in TpoR is duplicated and is 466 residues long (**Figure 3**); its deletion results in a weakly constitutively activated form (86).

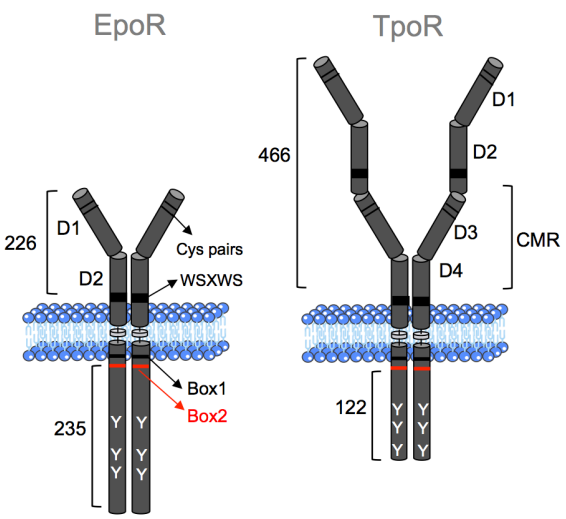

Figure 3.
Schematic representation of homodimeric type-I cytokine receptors.
The erythropoietin (EpoR) and thrombopoietin (TpoR) receptors exhibit extracellular and intracellular domain of different length. The WS-X-WS motif and the pairs of cysteines are both important for receptor folding and characterize the type I receptors. Box 1 and Box 2 are necessary for Janus kinase binding that phosphorylate tyrosine residues (Y) in the cytosolic tail.

Tpo binding to the receptor is though to stabilize a particular homodimeric interface, which in turn activates the pre-bound JAK2 kinases. In addition, TpoR can also activate TYK2 (87), but JAK2 remains the main kinase for its signaling, at least in myeloid progenitors (88). Moreover, both JAK2 and TYK2 promote cell surface localization of TpoR and an increase in the total level of the mature form of the receptor (89). Concomitant binding of JAK2 and TYK2 on the same TpoR receptor chain is not a conceivable model with respect to the sizes of the JAKs and the cytosolic tail of the receptor (**Figure 4**). Competition assays between JAK2 and TYK2 (using different DNA ratios while measuring STAT5 transcriptional activity) indicated that JAK2 might have a stronger affinity to TpoR than TYK2 (Defour J.P. & Chachoua I., Unpublished data). Finally, it has been shown that signaling via JAK2 and TYK2 can be induced via differentially oriented TpoR dimers (90). The exact role of TYK2 in TpoR signaling still remains to be deciphered, especially in order to determine whether TYK2 utilization by TpoR differs in different cell types and in physiological versus pathological signaling. TYK2 signaling might be relevant in cell types that express low JAK2 levels.

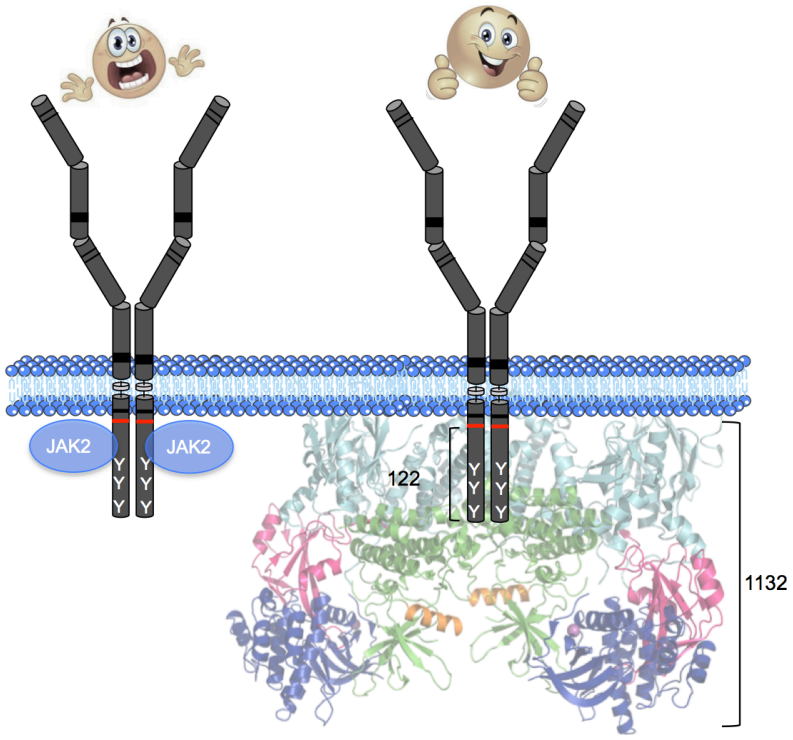

Figure 4. The cytokine receptor-JAK2 complex. This model provides a full view of a type-I cytokine receptor (here TpoR) in complex with JAK2. JAK2 is 1132 amino acids long (120 kDa), while the cytosolic tail of TpoR is 122 amino acids long (14 kDa). Given that JAK2 is almost 8 times bigger than the TpoR cytosolic tail, it strongly suggests that concomitant binding of both TYK2 and JAK2 on the same dimer is unlikely. This representation gives a better idea of what complexes should look like. JAK2 is a large enzyme appended to the cytosolic tail, whereas the extracellular domain is only the tip of the molecular iceberg.

TpoR contains a unique amphipathic motif, the so-called RWQFP motif, in the cytosolic JM domain that was shown to control receptor dimerization and is associated with MPN mutations. Deletion or mutation of this motif leads to ligand-independent activation of TpoR (57). The transmembrane domain (TM) of TpoR was demonstrated to be helical by nuclear magnetic resonance (NMR) (**Annex 3**). This domain is particularly important for receptor function. Indeed, when a cytokine binds to the receptor, the TM is responsible for transmitting the conformational changes from the extracellular portion to the downstream cytosolic tail and to the appended

JAKs. Since clinically relevant mutations have been found in the TpoR TM portion, the importance of this domain in controlling the activity of the receptor was highlighted. For instance, the TM S505N mutation, which is found in ET patients, leads to ligand-independent dimerization and the consequent constitutive activation of the receptor.

Introduction of a highly polar amino acid such as asparagine (N) in the TM domain is assumed to drive dimerization of the TM helices by forming hydrogen bonds, as long as the asparagines are found in close proximity. This concept has been used to study the different possible orientations adopted by the TpoR TM in the context of the wild-type full-length receptor. This work is described in a publication; **see Annex 3**. It was previously shown that TpoR signals through several conformations using an artificial TpoR model in which the extracellular domain was replaced by a dimerizing coiled-coil domain (Put-3). The Put-3 was fused to the TM domain in all seven possible orientations and imposed different conformations to the downstream TM and cytosolic domains. Using these constructs, one interface corresponding to the inactive dimeric state and one interface corresponding to the physiological dimeric state could be identified. Moreover, several other active dimeric orientations were identified and were shown to induce MPN-like phenotypes (**Annex 4**).

We conducted an asparagine-scanning mutagenesis of the TM domain in both human and murine TpoR (**Annex 3**). While the murine receptor exhibited several active conformations, as observed with the artificial Put-3 constructs, only one variant of the human receptor (the clinically relevant S505N mutation) was consistent with constitutive signaling. Our studies indicated that this discrepancy could be attributed to histidine 499, solely present in the human TpoR TM domain. In fact, second site mutational studies indicated that H499 was responsible for protecting the human receptor from activation by several asparagine mutations. By spectroscopy, using short TM peptides, we also showed that H499 accounts for a change in the conformation and secondary structure of the TM helix and shifts the monomer-dimer equilibrium toward monomer for the human receptor. We could conclude that H499 is critical for dimerization and orientation-dependent activation of the human TpoR.

Of note, H499 is the pharmacological target of a small molecule agonist, eltrombopag (Promacta/Reveled; GlaxoSmithKline, London, UK). H499 is only found in the TM domain of TpoR and G-CSFR within the type-I cytokine superfamily and only arose later in species evolution. This led us to consider its possible role in evolution in preventing oncogenic activation by multiple asparagines. Finally, we can conclude that TpoR possesses two "activation breaks", one at the extracellular proximal TM domain (H499) and one in the intracellular proximal TM domain (RWQFP/W515) (**Figure 5**).

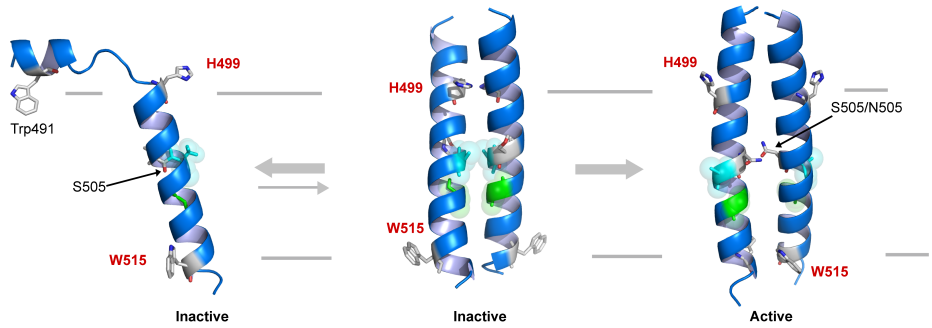

Figure 5. Role of the TpoR transmembrane and juxtamembrane domains in receptor dimerization and activation. Models of the monomeric and dimeric transmembrane domains of the human TpoR derived from nuclear magnetic resonance (NMR) data. The wild type and inactive receptor is primarily monomeric (left) with a break in helical secondary structure in the region N-terminal to H499 (toward the extracellular domain). In the mutant TpoR S505N, the transmembrane domain is oriented closer to the bilayer normal and a helix formation is induced in the region N-terminal to H499 (right). The model suggests that in the full-length receptor, the monomer and inactive dimer (middle) are in equilibrium and that either ligand or the S505N mutation shifts the equilibrium toward the active dimer with S505 or N505 being in the dimer interface.

Erythropoietin receptor

The erythropoietin receptor (EpoR) (with its ligand Epo) is responsible for survival, proliferation and differentiation of erythroid progenitors. EpoR localizes at the cell surface as a preformed dimer or higher oligomer that undergoes specific conformational changes upon ligand binding leading the receptor activation (91). Key residues within the TM domain are believed to maintain the unliganded dimer in an inactive state (92). In contrary to TpoR, the crystal structure of EpoR extracellular domain has been solved alone (93) and bound to Epo (94) and more recently in complex with diabodies (95). Much effort has been focused on the JM and TM domains that mediate the conformational change imposed by Epo binding to the extracellular domain of EpoR. Using a coiled-coil (Put3) fusion protein, Seubert and colleagues were able to identify which TM interfaces were involved in active and inactive orientations of the dimeric EpoR (96).
Receptor dimerization alone is not sufficient for EpoR activation; indeed, the orientation imposed to the EpoR dimers by ligand binding is critical. It was shown that the orientation of the extracellular domain is highly connected to the conformation of the downstream cytoplasmic domain and therefore signaling (97). This finding provided the first basis for the design of synthetic ligands able to finely tune EpoR signaling and cytokine receptors in general. This was later accomplished by K.C. Garcia's group that developed diabodies able to re-orient EpoR dimers (95). The use of these surrogate ligands is discussed in the **perspectives, section 3,** as a possible strategy for inhibiting JAK2.

Receptor dimerization and activation

Upon cytokine binding, cytokine receptors adopt an active dimeric/oligomeric conformation. This conformation is transmitted via the TM and JM domains to the cytoplasmic domain, which adopts a configuration that enables close proximity of the kinase domains of two pre-bound JAK molecules. Once adjacent and properly oriented, the JAKs will cross-phosphorylate each other and activate themselves to trigger downstream signaling. The usual model of receptor activation postulates

that a single ligand binds to two receptor monomers, which in turn, initiates dimerization and activation of the receptor.
However, the notion that pre-dimerized (mostly inactive) states exist in cytokine receptors is now generally accepted. Studies have shown that receptors such as EpoR (92, 93), GHR (98, 99), PRLR (100) or gp130 (101) can form homodimers in the absence of ligand. Thus, implying that dimerization is not sufficient to activate the receptor and that a forced rearrangement of the TM domain is also involved in the activation process. The chemical properties of the amino acids constituting the TM α-helices seem to play essential functions in receptor dimerization and activation. Cytokine binding to the inactive but pre-formed dimer induces critical conformational changes re-orienting the receptor in a productive configuration for signaling. Given that JAKs are pre-bound to the receptors, which can form homodimers, it is likely that JAK molecules possess a *trans* inhibitory mechanism (**see discussion, section 1.1**). Finally, taking into account that JAKs are ~ 5 fold larger than the average cytosolic domains (**Figure 4**), it is strongly suggested that receptors and JAKs form functional units (102) (discussed in **Annex 5**).

3.3 Signaling pathways

As previously mentioned, JAKs are activated by cross-phosphorylation (at tyrosines Y1007/1008) facilitated by dimerization of the receptor in an effective conformation. Once activated, JAKs phosphorylate tyrosine residues on the cytosolic tails of receptors, thereby providing a number of binding sites for SH2 (Src homology 2) and PTB (phosphotyrosine binding) domain containing proteins such as STATs, adaptor proteins (SHC) or negative regulators (SOCS or PTP). Tyrosine phosphorylation is the main mechanism by which transmembrane proteins transmit signals from the extracellular to the intracellular compartment. Protein tyrosine phosphorylation was serendipitously discovered in 1979 by Tony Hunter (103) and this process account for less than 1% of the intracellular phosphorylation events compared to serine phosphorylation (90%) and threonine phosphorylation (10%) (104). Hematopoietic cytokine receptors such as EpoR or TpoR typically trigger signaling cascades that include the

JAK-STAT pathway, as well as the PI3K and MAPK pathways, which also depend on JAK activation for initiation (**Figure 6**) (105).
Although activation of PI3K and MAPK will not be discussed here, it is important to note that they have been widely studied in cytokine signaling.

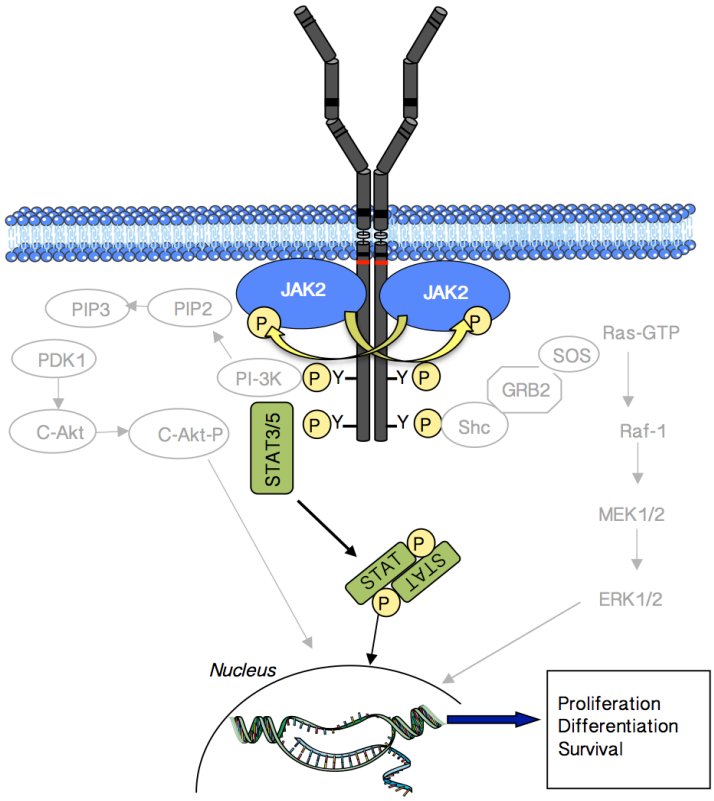

Figure 6. Major signaling pathways activated by cytokine receptors. In the absence of cytokines, cytokine receptors such as TpoR are preassembled with JAK in inactive complexes. Cytokine binding induces a conformational change that enables the appended JAKs to cross-phosphorylate and activate each other. As a result, JAKs phosphorylate tyrosine residues (Y) on the intracellular domain of receptors, which attract SH2 domain containing signaling molecules. Such molecules become phosphorylated and translocate into the nucleus (STATs) to modulate gene expression or initiate kinase signaling cascades (MAPK or PI3K pathways).

The JAK-STAT signaling pathway

What is striking about the JAK-STAT signaling pathway is that a relatively large number of cytokines receptors (approximately 40) use a limited number of JAKs (JAK1, JAK2, JAK3 and TYK2)(106). The receptor-JAKs association is a restrictive system as different classes of receptors preferentially use one JAK or a specific combination of JAKs (**Figure 2**). Also, this pathway is relatively simple in that it is composed of only two intracellular signaling components: the JAK tyrosine kinases and their main substrates, STATs, as well as cytosolic receptor tails, that then recruit other adaptors triggering PI3K and MAPK pathways. JAKs and STATs can form diverse combinations depending on the cytokine receptor, thus amplifying the variability of the signaling cascade. There are four JAK family members, JAK1-3 and TYK2, (a detailed description of JAKs is presented in the **introduction, section 5)**. As their name suggests, STATs are both signal transducer proteins and transcriptional activators. In mammals, seven different STATs have been described (STAT1, 2, 3, 4, 5a, 5b, 6). Specific phosphorylation of TpoR (Y112 and Y117 starting from the first residue of the cytosolic tail) (107) or EpoR (Y343 and Y401) (108, 109) results in the recruitment and phosphorylation of STAT5.

Once recruited to the receptors, STATs become phosphorylated by JAKs on single tyrosine residue (Y694 in STAT5a and Y699 in STAT5b). Phosphorylated STATs lose affinity for receptor phosphotyrosines in favor of other phosphorylated STATs and form dimers through their SH2 domains, which leads to the exposure of a nuclear localization sequence (NLS). STAT dimers then translocate to the nucleus where they bind to GAS (gamma-activated site) or GAS-like enhancer elements (110) to stimulate transcription of genes important in survival, proliferation and differentiation of myeloid cells. Notably, STATs are also activated in response to growth factors, such as platelet-derived growth factor (PDGF) or epidermal growth factors (EGF). Homodimeric receptors utilizing JAK2 commonly mobilize STAT5a/b. In addition, EpoR (111-113) and TpoR (87, 114) also activate STAT1 and STAT3.

Type-I interferons activate STAT1/STAT2/IRF9 (Interferon regulated factor 9) complexes (110) to induce via ISRE (IFN-stimulated response elements) expression of genes involved in inducing anti-proliferative, anti-viral and immunomodulatory effects.

Role of the JAK-STAT signaling pathway in cellular functions

Activation of the JAK-STAT signaling pathway stimulates cell proliferation, differentiation, survival and apoptosis. These cellular events are critical for different developmental and homeostatic processes, such as hematopoiesis, immune development, stem cell maintenance, organism growth or mammary gland development (115). Knock-out mice for each JAK and STAT have been engineered, which allowed scientists to gain insights into their physiological roles. Indeed, analysis of their respective phenotypes provided information on their non-redundant roles in cytokine signaling. Regarding JAKs, the phenotype of JAK1 and JAK2 deficient mice are both lethal due to failure in gp130/JAK1-dependent neurogenesis and in definitive erythropoiesis, respectively (116-118). Mice deficient in TYK2 only show increased susceptibility to pathogens due to impaired IFNα/β and IL2 signaling (119, 120). In contrast to the other JAKs that are ubiquitous, JAK3 is only expressed in the hematopoietic lineage. Lack of JAK3 causes SCID (Severe Combined Immune Deficiency) due to deficiency into γc-dependent signaling (121).

Dysregulation of the JAK-STAT pathway has several direct pathological consequences including hematological diseases, and can also be associated with solid cancers. An activated STAT3 signature is found in more than 50% of lung and breast cancers and in over 95% of head and neck tumors (122). Persistent activation of STAT5 has also been associated with prostate (123) and mammary cancer (124). An increased secretion of cytokines by cancer and stromal cells contribute to the pathogenesis of these malignancies along with a direct dysfunction of the JAK-STAT pathway in the tumor cells by genes amplification/mutations or inactivation of endogenous suppressors of the pathway (reviewed in (125)). Yet, a driver (initiator) effect for pathological activation of the JAK-STAT pathway has been established only for hematological malignancies.

Regulation of the JAK-STAT signaling pathway

In order to avoid hyperactivity, a series of intracellular processes conspire to temper the pathway. These regulatory mechanisms comprise protein tyrosine phosphatases (PTPs), suppressors of cytokine signaling (SOCS), protein inhibitors of activated STATs (PIAS), specific adaptor proteins (LNK), post-translational modifications of the signaling elements (e.g. ubiquitination or sumoylation) and receptor endocytosis and proteosomal degradation.

First, PTPs modulate the activities of kinases and other molecules by dephosphorylating tyrosine residues. Two SH2 domain-containing PTPs, namely SHP-1 and SHP-2, are key molecules in down-regulation of cytokine signaling in hematopoietic cells (126). Upon cytokine stimulation, SHPs bind to phosphotyrosines, undertake a conformational change, which unmasks the SHP catalytic site, thereby enabling dephosphorylation of JAKs, STATs and receptors. Secondly, the SOCS family members (SOCS1-7 and CIS) are involved in long-term regulation. In fact, transcriptions of genes encoding SOCS proteins are triggered by activation of STATs. Similarly to PTPs, SOCS bind through an SH2 domain to phosphotyrosines of activated JAKs and of receptors, and prevent binding of other signaling molecules. In addition SOCS proteins can recruit elements of the E3 ubiquitin ligase machinery, which leads to ubiquitination and proteosomal degradation of the targeted elements, such as receptors (127) or JAK2 (128). Of importance, crystallographic data have shown that SOCS3, a major regulator in the immune and hematopoietic systems, inhibits JAK2 by simultaneously recognizing specific sequences on JAK2 and the receptor (in this case, gp130) (129). This study provided evidence that SOCS target precise JAK-cytokine pairs. Third, PIAS proteins inhibit STAT transcriptional activity through several mechanisms. For instance, it has been proposed that PIAS-1 and PIAS-3 inhibit STAT1 and STAT3 respectively by recognizing activated STATs and by blocking their access to DNA(130, 131). Fourth, the SH2-containing adaptor protein LNK specifically inhibits Tpo (132) and Epo (133) signaling by targeting phosphotyrosines. Mice deficient for LNK have aberrant hematopoiesis (18, 19), while mutations in LNK have been associated with MPNs (15, 134) and certain leukemias (135).

Fifth, cell surface cytokine receptors can undergo endocytosis and subsequent intracellular degradation. It is worth noting that in some cases, down-regulation mechanisms can fail in inhibiting activated signaling, as it is the case with the MPNs-associated JAK2 V617F mutant that escapes from negative regulation by SOCS3, especially at high JAK2 V617F levels (136).

4. Kinatown (protein kinases)

4.1 General overview

Protein kinases are one of the largest families of eukaryotes proteins. Indeed, the human genome encodes 518 protein kinases, which represents about 2 % of the whole genome. Out of the 518 kinases, 10% have been classified as pseudokinases (137, 138). In 2002, Manning et al. presented an extensive catalogue of the human kinases and for the first time formulated the terms "kinome" and "pseudokinase", which constituted one of the milestones in molecular cell biology (138). Although this area has been intensively studied since then, the fundamental biology of many of these proteins remains to be fully determined. Kinases regulate the majority of the key cellular activities including proliferation, metabolism, gene expression and apoptosis, through phosphorylation. Hence, it is not surprising that following to the acquisition of mutations, uncontrolled kinases induce inappropriate cellular signaling and eventually disease. Approximately 180 kinases are associated with pathologies, especially cancer, and most of these have been the subject of pharmaceutical drug discovery development. Currently, more than 5% of the human kinome is targeted by clinically approved inhibitors. The function of protein kinases is to bind adenosine triphosphate (ATP) in their active site and then, transfer the third phosphate of ATP (γ-phosphate) to the hydroxyl group of a serine, a threonine or a tyrosine residue contained in substrates. This process, namely phosphorylation, constitutes the main post-translational modification involved in cell regulation. Addition of a phosphate can be reversed by the action of phosphatases (139).

4.2 Classification of kinases

Kinases are classified into two main groups based of their substrate recognition. The first group, the serine/threonine kinases, transfers phosphate on serine and threonine containing substrate. They include MAPK and protein kinase A (PKA). The second group, the tyrosine kinases (PTKs), catalyzes phosphorylation on tyrosines.
There are 91 known tyrosine kinases that can be further subdivided into receptors tyrosine kinases (RTKs) and non-receptor tyrosine kinases (NRTKs). There are 58 RTKs that are composed of an extracellular domain, a single TM helix and an intracellular domain with the PTK core responsible for phosphorylation. Examples of RTKs include the epidermal growth factor receptor (EGFR), the platelet-derived growth factor receptor (PDGFR) or the insulin receptor kinase (IRK). There are 32 NRTKs, which are cytosolic tyrosine kinases and include the Src subfamily, Abl, Fes, ZAP-70 and of course, JAKs. They lack transmembrane domains and therefore are predominantly found in the cytoplasm. They usually possess modular units such as SH2, SH3 or Pleckstrin Homology (PH) domains that facilitate their subcellular localization (140).

4.3 Conserved structural features

Structural biology has contributed significantly to our understanding of kinase function. The first crystal structure of a kinase to be solved was that of the cyclic AMP-dependent kinase (PKA) in 1991 (141). The overall structure of protein kinases is generally conserved. Kinases are roughly 300 amino acids long and typically display a bilobal structure with a smaller N-lobe and a larger C-lobe (**Figure 7**). While the N-lobe is composed of 5 β-strands positioned in an antiparallel fashion and a single α helix (α C), the C-lobe is mostly helical (**Figure 7**). The two lobes are connected by a single strand of residues, namely the hinge region, allowing a certain degree of flexibility necessary for the catalysis reaction (142). The deep region between the two lobes is commonly referred as the "cleft", the "active site" or the "ATP binding pocket" where ATP binds. The adenine ring of ATP forms hydrogen bonds with the hinge region (**Figure 8**). The kinase cleft is the region where catalysis occurs as follows: it binds and properly orients ATP (along with

divalent cation like Mg^{++} or Mn^{++}), then it binds and properly orientates the substrates residues hydroxyl group, and lastly transfers the γ-phosphate to the substrate. Many kinases structures have been solved in their active and inactive states (143) and comparison of these structures has brought insights into the mechanism of activation and ATP / substrate binding (144). Protein kinases maintain the balance between their inactive and active conformations through conformational plasticity.

While the structure of kinases in their active conformation is highly conserved, each kinase has developed its own molecular mechanisms to maintain their inactive conformation. Indeed, each kinase displays distinct features with respect to the different domains surrounding the kinase domain.

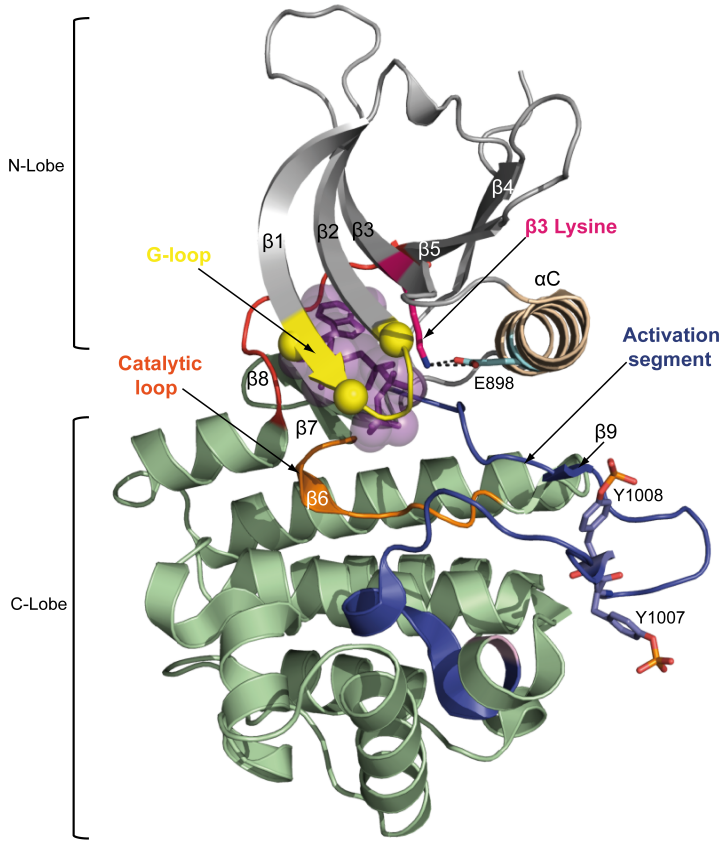

Figure 7. The typical fold of a kinase and structural location of the important catalytic features. The structure of JAK2 is displayed here (PDB: 3KRR). The smaller N-lobe is made of beta strands (β1-β5), while the C-lobe is larger and helical. The flexible hinge region between the two lobes is shown in red. The main structural elements are shown in different colors and the two tyrosines in the activation segment are shown in blue sticks. The critical salt bridge between the αC and the β3 strand lysine is shown as a dotted line. The αC is colored in wheat. The G-loop or glycine-rich loop is colored in yellow and the three glycines are shown as small spheres. The ATP location has been modeled and is displayed in purple.

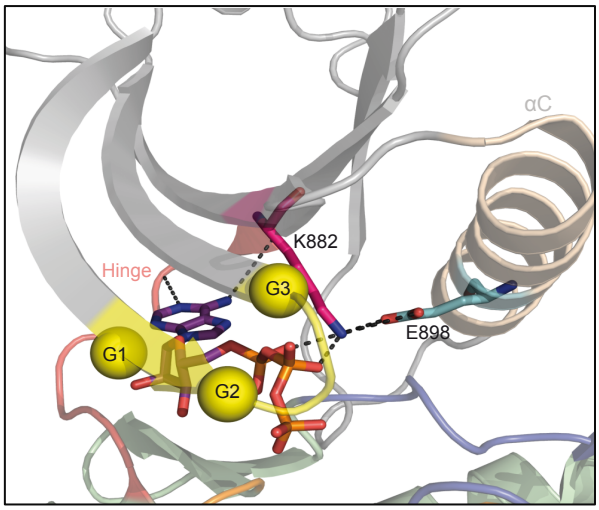

Figure 8. The ATP binding cleft. ATP binds to a region between the two lobes and its adenine ring is hydrogen bonded to hinge region residues. The salt bridge between β3 lysine (K882) is the αC glutamate (E898) is a hallmark of active kinase and helps to position the lysine correctly for coordinating the α and β phosphates of ATP (PDB: 3KRR).

Since kinases catalyze the same reaction, they all adopt a similar active conformation. Their conserved architecture is highlighted by specific structural elements where each residue has a defined role in the proper folding of the kinase core and in the catalysis reaction. The key structural elements that participate in the activation mechanism are conserved through the kinases and include:

The activation segment:

The activation segment runs from the triplet "DGF" (from the magnesium binding loop) to the triplet "APE" (from the P+1 loop). The middle portion consisting of β9 and the activation loop (AL) is highly flexible and largely varies in sequence and length (**Figure 9**). This segment is commonly referred as the "phosphorylation lip". Indeed, it contains tyrosine residues that are phosphorylated during the process of activation, which brings the kinase to its fully activated state. In the case of JAK2 it is Y1007 and Y1008. The length of the activation segment (~ 20-35 residues) can vary depending on the kinase (145). The DGF aspartate (D994 in JAK2 kinase domain) is strictly conserved and interacts with the divalent ion (Mg^{++} in JAKs) (**Figures 9-10**) to properly position the ATP phosphates for phosphotransfer (146).

The divalent ion can differ depending on the kinase and can influence the catalytic efficiency of the kinase (147). The motif APE is part of the so-called "P+1 loop" and plays critical important role in the substrate binding (**Figure 9**) (148). The activation loop has the capacity to undergo significant conformational changes depending on the activation states (149). *Phosphorylation* of the AL stabilizes the loop in an *open conformation*, which will have two consequences. First, it will allow access of ATP and the substrate to the active site and second, it will properly orient the DFG motif aspartate for the catalysis reaction (149). Phosphorylated tyrosines form a set of hydrogen bonds to key elements of the kinase core such as the αC and the HRD arginine to maintain the open conformation (**Figure 9**). *Dephosphorylation* of the AL leads to the formation of a totally disordered loop in a *closed conformation,* which means that the loop is inserted into the active site and hinders ATP and substrate access.

The catalytic loop:

The short catalytic loop is stretched between β6 and β7 at the base of the cleft (**Figure 7**) and contains the critical residues for catalysis. It includes the highly conserved HRD motif where the aspartate (D976 in JAK2) has been proposed to act as a catalytic base by deprotonating the substrate hydroxyl to catalyze the subsequent nucleophilic attack on the γ-phosphate of ATP during the phosphoryl transfer reaction (149). The arginine (R975 in JAK2) is thought to neutralize the negative charge of the γ-phosphate during transfer. An invariant asparagine (N981 in JAK2) located 5 residues downstream of the catalytic aspartate is hydrogen bonded to the aspartate and can contribute to the chelation of a second ion (**Figure 10**) (150).

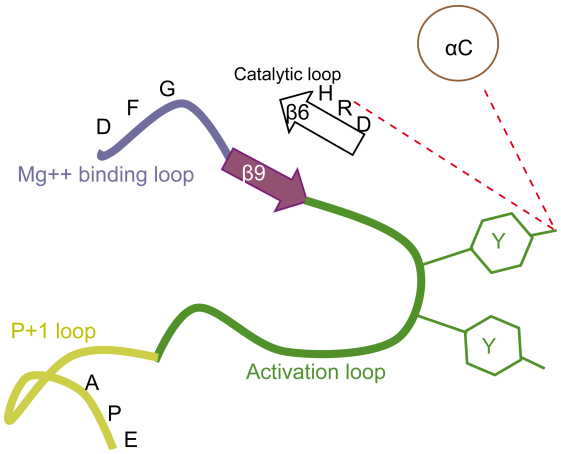

Figure 9. The activation segment. Nomenclature of the activation segment. It runs from DFG in the Mg^{++} binding loop to the conserved APE in the P+1 loop and includes β9 and the activation loop. (Adapted from (138)). In JAK2, the activation loop is maintained in an open conformation by formation of interactions with αC and catalytic loop residues.

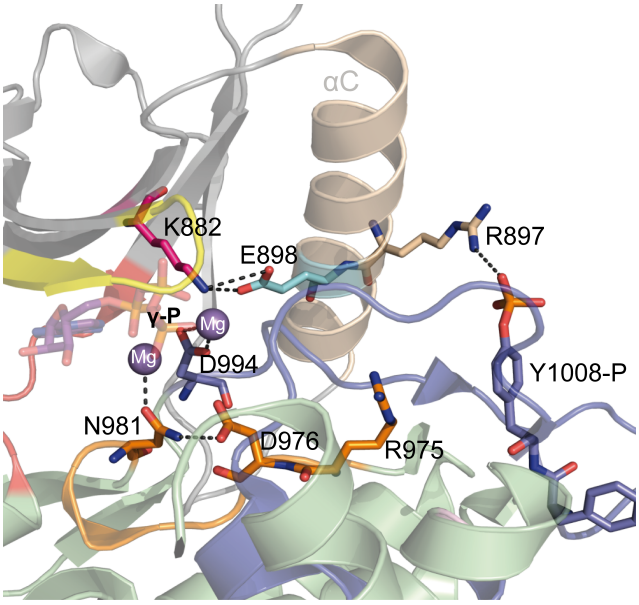

Figure 10. Residues participating in the phosphoryl transfer reaction. D994 (from DFG) binds the first Mg++, while N981 interacts with the second Mg++. The positively charged R975 (from HRD) neutralizes the γ-phosphate that becomes negatively charged when extracted from the ATP molecule (PDB: 3KRR).

The ATP binding loop:

The ATP binding loop, known as the "glycine-rich loop" or the "G-loop", is the most dynamic loop in the kinase core (151). Indeed, the glycines make it highly flexible in the absence of ATP. It lies between β1 and β2 strands at the edge of the active site cleft in the N-lobe. It contains three highly conserved glycines (**Figure 8**) that are part of the GxGxϕG motif (where ϕ is usually a phenylalanine or a tyrosine). The major function of this segment is to properly position the adenine ring and phosphates of ATP. The main chain nitrogens of the small glycines interact with the ATP phosphates, while the adenine ring is located in a hydrophobic pocket close to the hinge region. Of note, a charged residue usually located at the end of the motif reaches outwards to couple the G-loop to a distal segment and participate in closing of the G-loop (151). In JAK2, two charged residues are located in (K857) and after the G-loop (E864), but their role in maintaining the flexibility of the G-loop has to be determined. However, both have been associated with either constitutive activation of JAK2 (K857) (**Article 1**) or inhibitor resistant mutation (E864)(152), thus implying a potential role of these charged residues in maintaining the fold of the G-loop as this segment controls the positioning of both ATP and small molecules (153).

β3 strand:

This strand contains a universally conserved lysine (K882 in JAK2) which is part of the consensus motif "VAI(V)K" typical of all kinases (**Figure 8**). In the active state, this lysine coordinates the α and β phosphates of ATP when anchored to the αC via a key salt bridge with a conserved glutamate (E898 in JAK2). This ion pair is crucial to facilitate the appropriate positioning of the lysine and serves as a signature of active kinase. Its mutation to a similar arginine leads to complete inactivation of the kinase (a.k.a "kinase dead mutant") (154). The β3 strand terminates with a hydrophobic leucine (L884 in JAK2) whose role has only been recently appreciated with the discovery that it helps stabilize the αC (155). Interestingly, mutation of this leucine a phenylalanine leads to a constitutively active BRAF (L485F) associated with facial syndromes (156).

Recently, it was shown that mutation of this leucine to proline in JAK1 (L910P), JAK2 (L884P) and JAK3 (L857P) leads to constitutively activated kinases (157).

The α helix C:

The prominent αC from the N-lobe is inserted between β3 and β4 strands. It is positioned between the two lobes and its movement defines the whole dynamic behavior of the kinase. Indeed, movement of the αC can lead to disruption or the formation of the active conformation. The stability of the αC is therefore crucial and is promoted by multiple contacts all around the helix. The αC interacts with the kinase core via regularly conserved interactions. In the active kinase, the middle helix interacts with the β3 strand via the conserved glutamate (JAK2 E898), while the N-terminal portion usually interacts with the phosphorylated activation loop via a basic residue facilitating the inward conformation of the αC. In JAK2, R897 is hydrogen bonded to phosphotyrosine 1008 of the activation loop (**Figure 10**) (158). Other helical faces of the αC are engaged with segments lying outside the kinase core such as tails, linkers or other binding partners. These interactions greatly vary depending on the kinase (159). Altogether, these interactions participate in controlling the movement of the αC, thus regulating the activation of the kinase. It is noteworthy that the αC- β4 loop sustains key functions in the activation process of the kinase. It serves as a pivot point for the αC movement, enabling the helix to swing in and out during the activation process (**Figure 11**) (151). Moreover, basic residues that lie in this loop have been shown to be involved in the dimerization-dependent activation of EGFR (160) and RAF (161). Such residues are found in JAK2 JH1 αC- β4 loop (K912) (**Figure 11**) and in JAK2 JH2 αC- β4 loop (K607), but the role of these lysines in the dimerization-mediated activation of JAK2 still has to be investigated, whether it would be JH1 or JH2-mediated dimerization of two JAK2 molecules. Given that the JH2 homologous JAK2 K607N mutation has been found in acute myelogenous leukemia patients (162) and that K912 is conserved in all the JAKs, it implies a possible role of the αC- β4 loop of both JH1 and JH2 in JAK2 dimerization/cross-phosphorylation that still has to be explored.

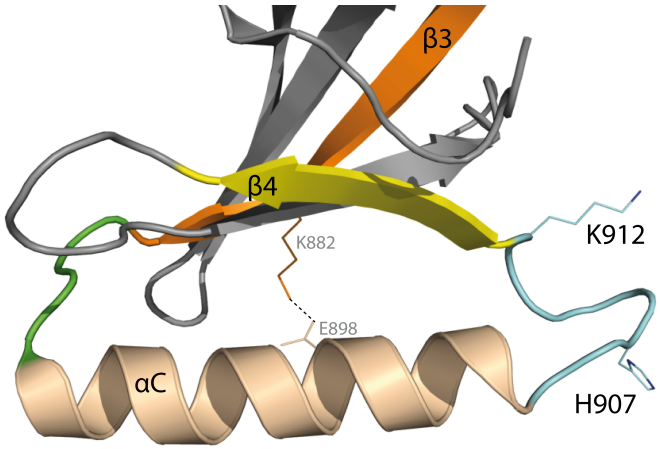

Figure 11. The αC- β4 loop participates in the motion of the αC helix. The αC is colored in wheat; the β4 strand is in yellow and β3 in orange. The αC- β4 loop, displayed in cyan, includes two basic residues: K912 and H907. (PDB: 3KRR).

4.4 Common activation mechanisms

A study of the conformation of surface-exposed residues between active and inactive structures of kinases suggested that the process of kinase activation involves the formation of two alignments of hydrophobic residues, namely the "hydrophobic spines" (144). The two spines, the regulatory spine (R-spine) and a catalytic spine (C-spine) (**Figure 12**), consist of a set of residues whose spatial positions are highly conserved throughout kinases (144). The dynamic assembly of these two spines during activation serves to create an internal hydrophobic core that stabilizes the active conformation of the kinase, bringing together all of the functional motifs that are essential for catalytic activity. The two spines traverse the kinase core from the C-lobe α helix F to the top of the N-lobe β strands. The α helix F seems to act as the central hub for the formation of the spines. Assembly of the R-spine is typically facilitated by phosphorylation of the activation segment and therefore defines *activation*. While, the assembly of the C-spine depends on the presence of ATP in the active site and therefore controls *catalysis* (163). JAK2 kinase domain will be used here to illustrate the concept of these spines (**Figure 12**).

R-spine:

This spine (*green*) consists of four residues (RS1-RS4), two from the C-lobe and two from the N-lobe and is anchored to the αF via a universally conserved aspartate (D1036). Each R-spine residue comes from a critical part of the kinase. RS1 is the catalytic loop HRD histidine (H974), RS2 is the activation loop DFG phenylalanine (F995), RS3 is a conserved aliphatic residue at the very C-terminus of αC (L902) and RS4 is an aliphatic residue at the base of β4 (Y913). Assembly of the R-spine drags the DFG phenylalanine into the spine while correctly positioning the HRD aspartate for catalysis. Moreover, the αC acquires a suitable configuration for catalysis and key salt bridge formation (**Figure 12**) (148).

C-spine:

This spine (*yellow*) is made up of a series of 8 hydrophobic residues and is completed by the adenine ring of ATP after nucleotide binding. They are 6 conserved residues from the C-lobe and 2 from the N-lobe. In the C-lobe, it starts at the C-terminus of αF with two aliphatic residues V1043 and L1047. The second level of the spine consists of a large aliphatic residue from αD (L937) capped by a triplet from β7 strand (I982, L983, V984).

L983 points toward the ATP binding pocket and serves as a base for the adenine ring of ATP. Then, on the opposite site of the adenine ring two aliphatic residues from the N-lobe β2 (V863) and β3 (A880) terminate the spine (**Figure 12**) (164).

Figure 12. The two hydrophobic regulatory spines and the αF helix define the internal core of protein kinases. a. The R-spine (green surface) and the C-spine (yellow surface) are anchored to the **α**F (pink), which lies in the middle of the rigid C-lobe. When the kinase is inactive (left), the spines are not complete. The DFG phenylalanine is translocated to a position not amenable for catalysis of phosphotransfer. In the active conformation (right), the C-spine is completed by the ATP molecule, whereas the R-spine is completed by the DFG phenylalanine. Phosphorylation of the activation segment causes a reorganization of the active site, such that the two spines are aligned and couple the two lobes. **b.** Detailed anatomy of the spines. Depiction of the precise residues that form the spines in JAK2 JH1. The R-spine is anchored to the **α**F via interaction with D1036. The C-spine is completed by the adenine ring of ATP locked-in between V863 and L983. (Active conformation, PDB: 3KRR, Inactive conformation: PDB: 3UGC).

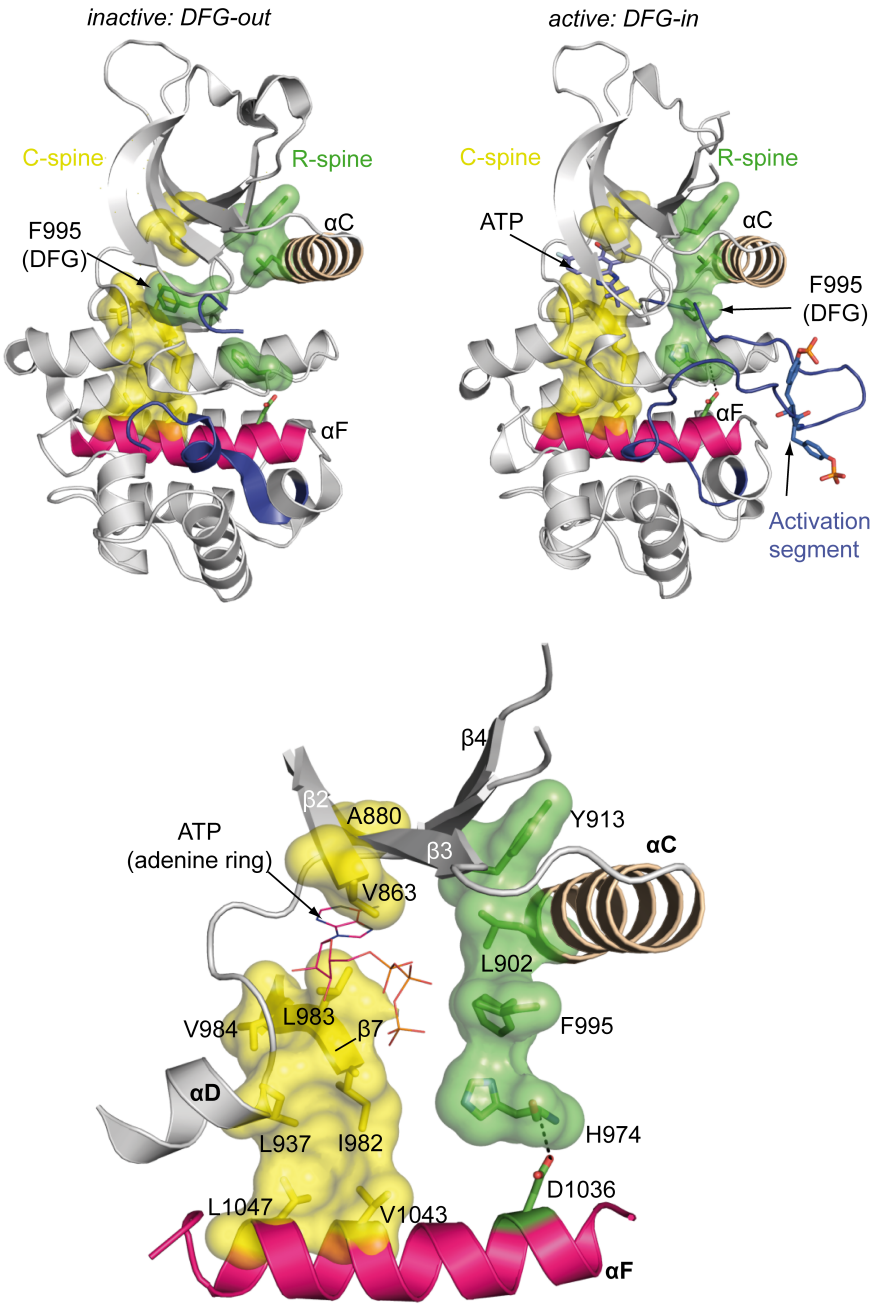
inactive: DFG-out
C-spine
R-spine
F995
(DFG)
αC
αF
active: DFG-in
C-spine
R-spine
ATP
αC
F995
(DFG)
αF
Activation
segment
β4
β2
A880
Y913
ATP
(adenine ring)
β3
αC
V863
L902
V984
L983
β7
F995
αD
H974
L937
I982
D1036
L1047
V1043
αF

Besides providing a model for kinase activation, the spines can also serve as a model to explain the mechanism of activation of mutations found in human cancer. A recent study identified a number of hydrophobic mutations in BRAF, ABL and EGFR whose mechanism could be described by their strategic localization around the spines (163). Notably, the importance of the hydrophobic environment that participates in the positioning of the αC was highlighted. Moreover, they reported an array of strategic hydrophobic mutations that can drive the assembly the active conformation of RAF that could potentially be extended to other kinases.

4.5 Regulation mechanisms

Most of the kinases are multi-domain proteins and thus, regulation arises at multiple levels to maintain the kinase in an inactive state. For this reason, every kinase has developed its own molecular mechanism to transit from the inactive to the active state. The kinase activity can be regulated at different levels including *trans* interaction with another molecule, cis interaction with another protein domain, phosphorylation / dephosphorylation of other residues within the protein, allosteric regulation by other binding partners and cellular localization. Within the kinase core, the position of the previously described motifs participates in the regulation of the kinase activity. Displacement of these segments is achieved through several mechanisms specific to every kinase. For instance, the *position of the αC* was revealed to the driving force for the activation of cyclin-dependent kinase 2 (CDK2). Binding of cyclin A to CDK2 reorients the αC in a position that allows the formation of the critical lysine-glutamate salt bridge (165, 166). The position of the αC can be also modified by the interactions with other protein domains, as it is the case for Src. The αC of Src kinase is held in an inactive conformation by indirect restraining interactions with its SH2 and SH3 domains (167, 168). Overall, we can say that a kinase is either blocked in an *inactive conformation* by steric constrains of inhibitory regulatory domains or binding partners; or adopts an *active conformation* by binding to other activating regulatory domains of binding partners. Whether JAKs are activated through one or the other mechanism, **see discussion, section 1**.

Every kinase possesses inherent regulatory mechanisms but the recent proposed model of kinase regulation based on the assembly of the hydrophobic spines has generally been accepted in the field. However, the driving forces for the assembly of the spines is specific to each kinase.

4.5 Pseudokinases

With GCN2, JAKs are the only proteins to have a pseudokinase domain adjacent to its kinase domain within the same molecule. The importance of the pseudokinase domain has been highlighted by the presence of the mutation JAK2 V617F that activates the contiguous kinase domain.

As previously mentioned, approximately 10% of the kinome actually lack one or several key residues that are necessary for catalysis and are presumed to be catalytically inactive kinases. These "inactive kinase" or pseudokinases are distributed throughout the diverse kinase subfamilies and seem to have evolved from active kinases that lost their activity during evolution (169). However, despite their lack of activity, many pseudokinases appeared to play important roles in signaling and seem to be essential functional regulators. A classification of pseudokinases has been proposed based of the missing key residues (HRD, DFG, VAIK) (170). The difference in the key motifs between the kinase (JH1) and the pseudokinase (JH2) domains of JAK2 is presented in **table 1**. Around 50 proteins were originally identified as pseudokinases, which may have been slightly overestimated. Some of these pseudokinases have since been shown to be catalytically active and hence, were reclassified as "atypical kinases" (171). More recently, an increasing number of pseudokinases such as KSR (kinase suppressor of Ras) (172), HER3 (human epidermal growth factor receptor 3) (173), CASK (calcium/calmodulin-dependent serine protein *kinase)* (174) or JAK2 JH2 (175) have been shown to retain some residual kinase activity despite exhibiting a non-canonical nucleotide binding mode. While the notion that some pseudokinases bind ATP is generally accepted, evidence supporting catalysis capacity is commonly subject to controversy. Whether this level of kinase activity is important for their function is however still debated.

	G-loop	β3 strand	Catalytic loop	Activation loop
JH1	GxGxΦG	VAIK	HRD	DFG
JH2	GxGxΦT	VLLK	HGN	DPG

Table1. Comparison between JH1 and JH2 catalytic motifs. The pseudokinase domain of JAK2 (JH2) lacks the conserved key motifs characteristic of canonical kinases.

To date, extensive structural and biochemical studies have revealed that despite their catalytically inactive nature, approximately 40% of the pseudokinome retain the ability to bind nucleotide (176), while only a small number are capable of catalysis leading to phosphoryl transfer at varying degrees (177). The persistence of so many pseudokinases in evolved organisms suggests that their non-catalytic roles might be important. Indeed, pseudokinases are frequently found in pair with kinase domain in a heterodimer complex (KSR1/BRAF; HER2/HER3; STRADα/MO25) where they have been suggested to function as allosteric activator of the adjacent kinase. Despite their lack of conserved residues necessary for ATP catalysis, the role of pseudokinases in signaling has emerged during the past few years. They display various signaling functions that are independent of phosphoryl transfer including protein scaffolding (KSR1, RAF, EGFR) or modulation of the activity of typical kinase (JAK2) (176). Studies have shown that ATP binding to pseudokinases typically leads to stabilization of the protein, which supports their role as important scaffolds in signaling complexes (176). A large number of in depth reviews on the advances of pseudokinase have been published during the past few years, but more interestingly on the potential roles of pseudokinases in cancer (178-180). As altered activity of pseudokinases can lead to impaired cellular function and malignancies, pseudokinases have even been suggested as potential therapeutic targets (180, 181). Several studies have confirmed that disease-associated pseudokinases are able to bind small molecules including HER3, JAKs, WNKs (with-no-lysine kinases), STRADα, MLKL (Mixed lineage kinase domain-like protein), KSR1/2 and Tribbles pseudokinases (reviewed in (180)).

4.6 Concluding remarks

Our understanding of kinase regulation has emerged from solved crystal structures and analysis of their active and inactive conformations. Furthermore, the finding of activating mutations within the kinase core often reveals additional mechanistic information. Yet, the exact role of all the structural features has not yet been fully determined. Many kinases such as JAKs display several domains of which the assembly is not known, as no crystal structure of the full-length protein exists. However, with the recent advances in molecular dynamics simulation and x-ray crystallography, a more detailed understanding of these multi-domain proteins has started to emerge. Since the initial cataloguing of the human kinome in 2002, the classification of kinases and pseudokinases has undergone some modification.

5. Janus kinases

5.1 Discovery and evolution

Janus kinases (JAKs) were first described in 1989 by using degenerate oligonucleotides probes corresponding to conserved PTKs proteins in a PCR with hematopoietic cells DNA and fairly named "just another kinase" (182). They were later renamed after the two-faced Roman god Janus, when it was discovered that JAKs are made up of both a kinase domain and a pseudokinase domain (183, 184). JAKs come in four flavors, JAK1-3 and TYK2. JAK1, JAK2 and TYK2 are ubiquitously expressed while JAK3 is restricted to the hematopoietic system (185). JAKs are found in all vertebrates but homologs have also been identified in zebrafish *Dario rerio* (186) and the fruit fly *drosophila melanogaster*- hopscotch (hop) (187, 188). Phylogenetic analysis revealed that the first gene duplication resulted in a common ancestor for JAK2/JAK3 and for TYK2/JAK1 while a second one gave rise to the four current members (189). JAKs appear to have evolved alongside the development of the innate and adaptive immune system, consistent with their multiple roles in immune cells (190). The four JAKs interact with more than 40 different cytokine receptors (191).

Generation of knockout animals has helped to determine the specificity of individual JAKs for particular receptors and define their biological functions.

5.2 Structure of JAKs

JAKs are relatively large proteins (JAK2 is 1132 amino acids) composed of seven defined regions called JAK homology (JH) domains based on their primary sequences. The carboxyl-terminal region contains the kinase (JH1) and pseudokinase (JH2) domains whereas the N-terminus region includes the SH2-like domain (JH3-JH4) and the FERM domain (JH5-JH6-JH7) (**Figure 13**). To date, no three-dimensional structure of any JAKs in their entirety is available, which occludes our understanding of the assembly of the different domains. While the entire JAK can be purified and concentrated to a appropriate level, it does not seem to be amendable to crystallization due to its high flexibility. However, we now possess structural information about all the domains of JAK1, JAK2 and TYK2, while only the JH1 structure is available for JAK3 (**Table 2**).

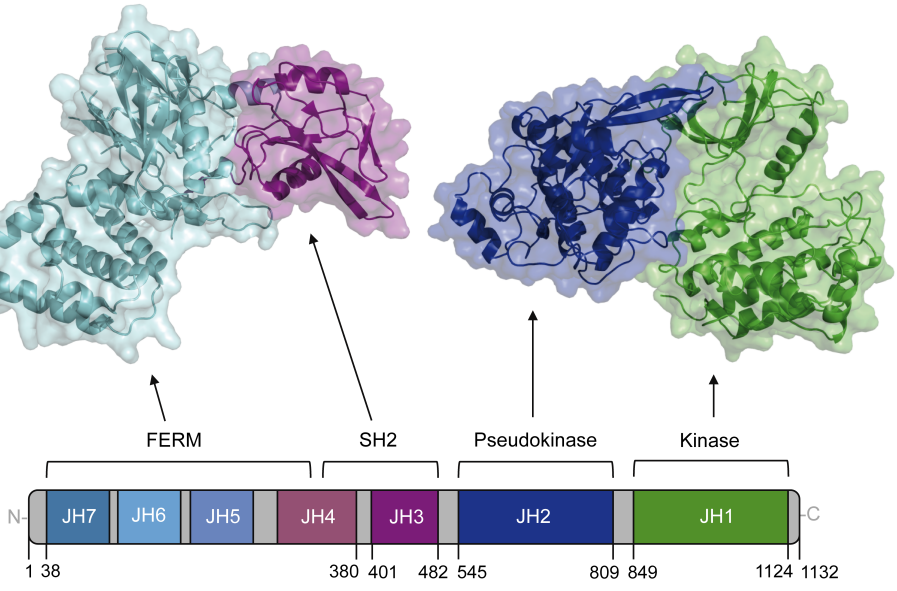

Figure 13. Anatomy of JAKs. The amino acid numbering and the three dimensional structures in the figure correspond to JAK2**.** (FERM SH2= PDB: 4Z32; JH1 JH2= model with JH1; PDB: 3KRR and JH2, PDB: 4FVQ).

FERM

The N-terminal regions of JAKs form the FERM (band 4.1, erzin, radixin, moeisin) domain, which is necessary for binding JAKs to their receptor. In addition, the FERM domain promotes cell surface localisation and stabilization of cytokine receptors including EpoR (192) and TpoR (89). This domain typically consists of a three-lobed structure, F1-F3, where F1 has an ubiquitin-like architecture, F2 has an acyl-coenzyme A binding protein-like fold and F3 shares similarities to a Pleckstrin domain (193). The first structure of a JAK FERM domain to be reported was that of TYK2 in May 2014, in complex with receptor chain (78), while the crystal structure of the FERM domain of JAK1 was recently published in April 2016, in complex with receptor peptide (79); followed by the FERM domain of JAK2, which was published in May 2016 (194). The JAK FERM domain also turns out to have a regulatory role in the activity of the kinase domain (195-197). A similar function has also been seen in another kinase containing a FERM domain, Focal Adhesion Kinase (FAK), where the FERM domain was shown to interact with the activation loop of its kinase domain, thereby preventing access to the active site. However, whether the same mechanism occurs in JAKs remains to be seen. A study also indicated that FERM controls the hyperactivity of JAK2 V617F. While the FERM domain seems to exert an inhibitory role in JAK2 WT kinase activity, it seems to play a positive regulatory role in JAK2 V617F activity (198).

SH2

The FERM domain is followed by JH3-JH4, which share similarities with Src homology 2 (SH2). However, this domain does not seem to fulfil a classical SH2 domain function namely binding to phosphorylated tyrosines (183, 184) and is often referred as a "SH2-like" domain. SH2 domains typically contain about 100 residues and consist of two αC and central antiparallel β-sheets. Commonly in SH2 domains, an invariant arginine on the βB-5 contacts the phosphate group of the phosphotyrosine. Mutation of the corresponding arginine in JAK1 and JAK2 had no effect on signaling (199, 200). Yet, the SH2 domain was shown to be necessary for receptor interaction and JAK activation (199). In addition, it was shown that JAK2 V617F requires an intact SH2 domain for constitutive activation and initiation of MPN phenotype in mice (201).The structures of the SH2-like domains have been solved along

with the FERM domain for TYK2 (78), JAK1 (79) and JAK2 (194). Interestingly, SH2 was shown to play a central role for TYK2 binding to the receptor. The structure shows that the SH2-like domain binds the box2 of IFNAR1's cytoplasmic domain in a manner similar to that of classical SH2 domain binding to a phosphotyrosine. In fact, TYK2 SH2 interacts with a glutamate residue from box2, which mimics the canonical phosphotyrosine.

JH2

The pseudokinase domain or JH2 precedes the kinase domain and its function in JAK2 had always been of particular interest. The first evidence that JH2 exerts an inhibitory function on JH1 came from hopscotch (Hop) mutations in drosophila, Hop Tum-l and Hop T42 in JH2, which result in constitutive kinase activity inducing a leukemia like phenotype in flies (202, 203). Biochemical studies of mammalian JAKs have shown that deletion of JH2 increases the phosphorylation of JAKs and the downstream STAT5 (204, 205). Despite showing typical features of functional kinases, JH2 lacks the critical residues required for proper catalytic activity and nucleotide binding (**Table 2**). The structures of the pseudokinase domain of JAK1, JAK2 and TYK2 have been solved over the last few years (**Table 2**) and show many similarities. They all display an accessible nucleotide binding site, a partially degraded G-loop and an unusually short activation loop. All these three JH2s were shown to bind ATP (**Table 2**). Thermal shift assays demonstrated that JH2 of JAK1 and JAK2 binds ATP and cation (176) and the crystal structure of JAK2 JH2 shows the domain bound to ATP and Mg^{++}(206). The ability of TYK2 JH2 to bind ATP was less clear until the recent crystal structure of an ATPγS-bound structure, which confirms that TYK2 JH2 is indeed capable of binding ATP (207). Fascinatingly, JH2 of TYK2 was shown to bind multiple small molecules inhibitors (**Table 2**), which opens perspectives for targeting JH2 with pharmacological agents in order to modulate the activity of JAKs. JAK2 JH2 has been found to possess weak kinase activity *in vitro* inducing phosphorylation of two regulatory residues (S523 and Y570) (175).

Once phosphorylated, these residues participate in inhibitory interactions between JH1 and JH2 (208, 209). Despite binding ATP, JAK1 and TYK2 JH2 do not possess catalytic activities (207, 210). The catalytic activity of JAK2

JH2 is still matter of debate and several lines of evidence either support or impugn the idea. On one side, structural comparison of the three JH2 shows that they all contain a small helix in their activation loop (αAL). This αAL is only stabilized by two salt bridges in the structures of JAK1 and TYK2, which probably blocks access to substrate (207, 210). Also, the JH2 substrate residues, S523 and Y570, are only present in JAK2. On the other side, ATP binds to JAK2 JH2 with relatively high binding affinity (Kd=1μM, which is 10% of the reported Kd for JH1) (175) and disruption of ATP binding to JH2 does not lead to constitutive activation of JAK2 (211). For this reason, ATP has been proposed to have a structural rather than a functional role in binding JH2 of JAKs. Binding of ATP to JH2 seems to stabilize an effective conformation that facilitates cytokine-induced activation of JAKs. The main structural effect of ATP binding on JAK2 JH2 is the rigidification of the αC (206).

JH1

JH1 is a typical kinase domain with all the conventional motifs (**Figure 7**). Mutation of the β3 strand lysine abrogating the kinase activity gave the first evidence of catalytic activity on JH1 (212). Phosphorylation of the two tyrosine of the activation loop stabilizes an active conformation of JAKs and constitutes the first event in the intracellular activation cascade. It was shown that the first out of the two tyrosines (Y1007 in JAK2) was the critical residue for the activity of JAKs (213-215). The first structure of JH1 in the JAK family was solved in 2005 for JAK3 (216), rapidly followed by the kinase domain of JAK2 in 2006 (158). To date, all the JH1 structures have been solved with multiple ligands (**Table 2**). When compared with other kinases, JH1 displays an unusual helix in the C-lobe (αH) named "JAK specific insertion" (JSI), deletion of which was shown to abrogate auto-phosphorylation in JAK2 (217). Whether the JSI plays a role in the intra or intermolecular regulation of JAKs remains unclear. One residue from the JSI in JAK2 was associated with germline mutation (R1063H) leading to hereditary erythrocytosis (**Annex 6**). In 2013, the first crystal structure of JAK2 JH1 in its inactive conformation was solved (218), which allows structural comparison between the inactive and the active state of the kinase domain. Activation of JH1 leads to the typical remodelling of the active site with the alignment of the two hydrophobic spines described earlier.

Protein	Domain	Ligand	Complex	PDB ID	Resolution	Ref.
JAK1	JH1	CP-690,550		3EYG	1.9 Å	(219)
	JH1	CMP6		3EYH	2.0 Å	(219)
	JH2			4L00	1.8 Å	(210)
	JH2 V658F			4L01	1.9 Å	(210)
	FERM-SH2		IFNLR1/IL10RA chimeric	5IXI	2.57 Å	(79)
	FERM-SH2		IFNRλ	5IXD	2.85 Å	(79)
JAK2	JH1	CMP6		2B7A	2.0 Å	(158)
	JH1	DQX		3KRR	1.8 Å	(220)
	JH1 *inactive*$	NVP-BBT594		3UGC	1.34 Å	(218)
	JH1	CMP6, PO4	SOCS3/GP130	4GL9	3.9 Å	(129)
	JH2*			4FVP	2.01 Å	(206)
	JH2 *	ATP, Mg^{++}		4FVQ	1.75 Å	(206)
	JH2 V617F*	ATP, Mg^{++}		4FVR	2.0 Å	(206)
	JH2 V617F/E596A*	ATP, Mg^{++}		5I4N	1.54 Å	(221)
	FERM-SH2			4Z32	3.0 Å	(194)
TYK2	JH1	ADP, Mg^{++}		4GVJ	2.03 Å	(222)
	JH2	IK1		3ZON	2.15 Å	SGC¥
		BMS-066		4WOV	1.8 Å	(223)
		ATPγS, Mg^{++}, GOL, EDO		5C03	1.9 Å	(207)
		Pyrazine compound		5C01	2.15 Å	(207)
	JH2-JH1	2TT		4OLI	2.8 Å	(208)
	FERM-SH2	GOL	IFNR1 peptide	4PO6	1.99 Å	(78)
JAK3	JH1	Staurosporine		1YVJ§	2.55 Å	(216)
	JH1	4LH(covalent inhibitor)		4Z16	2.9 Å	(224)

Table 2. Summary of published three-dimensional structures of JAKs.
(The list is not exhaustive and all the structural data are from X-Ray Diffraction)
* Contain surface mutations (W659A, W777A, F794H)
$ First JAK2 kinase domain that was solved in its inactive conformation bound to a type-II inhibitor.
¥ SGC= Structural genomics Consortium Gallery
§ First crystal structure of JAK determined.
GOL= glycerol; EDO=1,2-Ethanediol; PO4= Phosphate ion

5.3 Physiopathology of JAK2

JAK2 is crucial for mammalian development, as JAK2 deficient mice die at embryonic day 12.5 due to defective hematopoiesis (118). In fact, JAK2 is essential for signaling through EpoR, TpoR and cytokine receptors harboring the common beta chain (118). In addition it has been shown that JAK2 is also activated by GPCR (225, 226) and growth factor receptors.

Regulation of JAK2

JAK2 activity must be regulated at different levels. *In the absence of cytokine*, JAK2 activity must be maintained at a basal level while, *following activation*, JAK2 activity must be stopped by appropriate negative feedback. Collectively these two levels of regulation are completed through *cis* and *trans* mechanisms.

Regulation in cis

An initial level of auto-inhibition is thought to occur through JH2 inhibition of JH1 via an interface that will be discussed later. Secondly, JAK2 possesses several sites of phosphorylation besides Y1007 and Y1008 on the activation loop. Phospho amino acid analysis of JAK2 revealed that 20 tyrosine residues are phosphorylated upon stimulation (227). Phosphorylation of Y637, Y813, Y868, Y966 and Y972 was shown to increase JAK2 activity while phosphorylation of Y119, Y221, Y317, Y570 and Y913 negatively regulate JAK2 activity (227). In addition, in the absence of stimulation, JAK2 is constitutively phosphorylated on S523, which mediates negative regulation at the basal state (228, 229). The precise mechanisms by which these phosphorylation events regulate the activity of JAK2 have only been described for a few residues. Phosphorylation of Y119 within the FERM induces dissociation of JAK2 from the EpoR (195), while phosphorylation of Y813 (230) and Y966 (231) potentiates JAK2 activity through the recruitment of the adaptor proteins SH2-Bβ and p70, respectively. Phosphorylation of S523 and Y570 were shown to participate in the maintenance of inhibitory interactions between JH1 and JH2 by molecular dynamic simulation (209).

Regulation in Trans

Another level of regulation involves binding of a series of negative regulators after cytokine stimulation that has already been discussed in the introduction, section 3.3.

Role of the pseudokinase domain in the regulation of JAK2

Several biochemical data collected from three studies underlined the regulatory function of JH2 (204, 205, 232). JH2 was first shown to negatively regulate JH1 as its deletion led to constitutive activation of JAK2 (205). Then, it was also shown that JH2 is required for cytokine-induced activation of JAK2 (204, 205). It was proposed that JH2 is required to maintain JAK2 inactive in the absence of stimulation. In addition, it was demonstrated that the inhibitory function of JH2 on JH1 was not due to dephosphorylation (205) and independent of additional regulatory proteins (232). Therefore, the inhibitory function of JH2 is an intrinsic property of the domain. Following the discovery of JAK2 V617F, it was believed that the presence of the mutation on the pseudokinase domain abrogates the inhibitory effect of JH2 on JH1 thereby activating JAK2. Studies of the biochemical parameters of JH1 and JH2 have shown that JH2 actually decreases the activity of JH1 by diminishing its affinity for ATP (233).

Later, it was proposed that JH2 might also exert a positive regulatory role on JH1. Indeed, some mutations in JH2 of JAK3 (234) lead to loss of function causing severe combined immunodeficiency (SCID). Mutations in JH2 of TYK2 also lead to catalytically impaired enzyme (235). However, to date, no such mutations could be identified in JAK2. The dual function of JH2 was also supported by biochemical studies, which showed that when JH2 is deleted in JAK2, the basal activity couldn't be further stimulated by cytokine (204). The molecular mechanism underlying the stimulatory interaction mediated by JH2 on JH1 has been less investigated and only recently started to gain attention. JH2 plays a dual role in the regulation of JAK2. On one side, JH2 auto-inhibits JH1 in the absence of stimulation and on the other side is required to properly activate JH1 after stimulation.

One could assume that the auto-inhibitory function of JH2 occurs in *cis* while its activating function occurs in *trans*. Several theoretical models have been used to describe the effect of JH2 on JH1, based on the description of different JH2-JH1 interfaces (discussed in **Annex 5**).

The pseudokinase/kinase interface

The first hypothetical model showing the interface between JH1 and JH2 was based on the FGFR (fibroblast growth factor receptor) dimer. In this model, the C-lobe of one domain contacts the N-lobe of the other domain and the two αC are in contact with each other. This antiparallel asymmetric representation of the JH2-JH1 interface has served for years as a model for describing the effect of JH2 on JH1, but also to explain how V617F activates JH1. Moreover, this model has been used for years by many laboratories (including ours) to design JAK2 mutagenesis strategies that aim to understand the molecular interplay between the two domains. Subsequently, several other theoretical models have been proposed (**Annex 5**). In 2014, a collaboration between S. Hubbard (Skirball Institute, NYC) and D.E Shaw (D.E Shaw Research, NYC) led to a decisive work in which they uncovered the inhibitory interface between JH1 and JH2 of JAK2, which fundamentally differs from any models described before. They ran molecular-dynamics (MD) simulations in which they placed the atomic coordinates of JH2 and JH1 along with the JH2-JH1 linker and the SH2-JH2 linker (209). In their work, they describe an inhibitory interface that is facilitated by several inter-domain contacts, mainly salt bridges, which can be divided into four regions (**Figure 14**). Their model was supported by mutagenesis experiments based on reversing the salt bridges. Their model offers a molecular rationale for the mechanism of activation of JAK2 V617F and other activating mutations. Indeed, they could map MPN disease mutations in and around the inter-domain interface. Mutations located in the interface were proposed to destabilize this interface, thereby liberating the kinase domain from the inhibitory steric constraint of the pseudokinase domain. Remarkably, their results were supported by a crystallographic structure of the TYK2 tandem pseudokinase-kinase domains that was solved and published at approximately the same time (208).

The inhibitory interface is predominantly mediated by the N-lobes of each domain (**Figure 14**). JH2 interacts across the back of JH1 active site via an interface involving residues from the SH2-JH2 linker, the JH2 αC, the JH2 N-lobe as well as residues from the N-lobe and hinge region of JH1. Interestingly, a portion of the SH2-JH2 linker is clearly seen in the interface between JH1 and JH2. The C-terminal region of this linker was previously shown to have a negative regulatory role on JAK2 (236). Furthermore, it was later confirmed that the SH2-JH2 linker participates in negatively controlling the activity of JH1 by reducing its affinity for ATP (237).

Figure 14. Model of the interface between JH1 and JH2 in JAK2 derived molecular dynamics simulations. The interface between JH1 and JH2 is subdivided into four regions (I-IV), where interdomain contacts maintain the auto-inhibitory interplay between JH1 and JH2. Region I, II and IV essentially include salt bridges, whereas region III comprises hydrophobic contacts. The JH2 αC is largely part of this interface and comprises residues from region III (C-term) and region IV (N-term). In the small squares, residues that belong to JH1 are denoted in green, while JH2 residues are denoted in blue. S523 (from the SH2-JH2 linker) and Y570 are both phosphorylated. Mutations of residues from region II (R683S and D873N) and region III (P933R) have been associated with acute lymphoid leukemia (ALL)(Adapted from 2091.

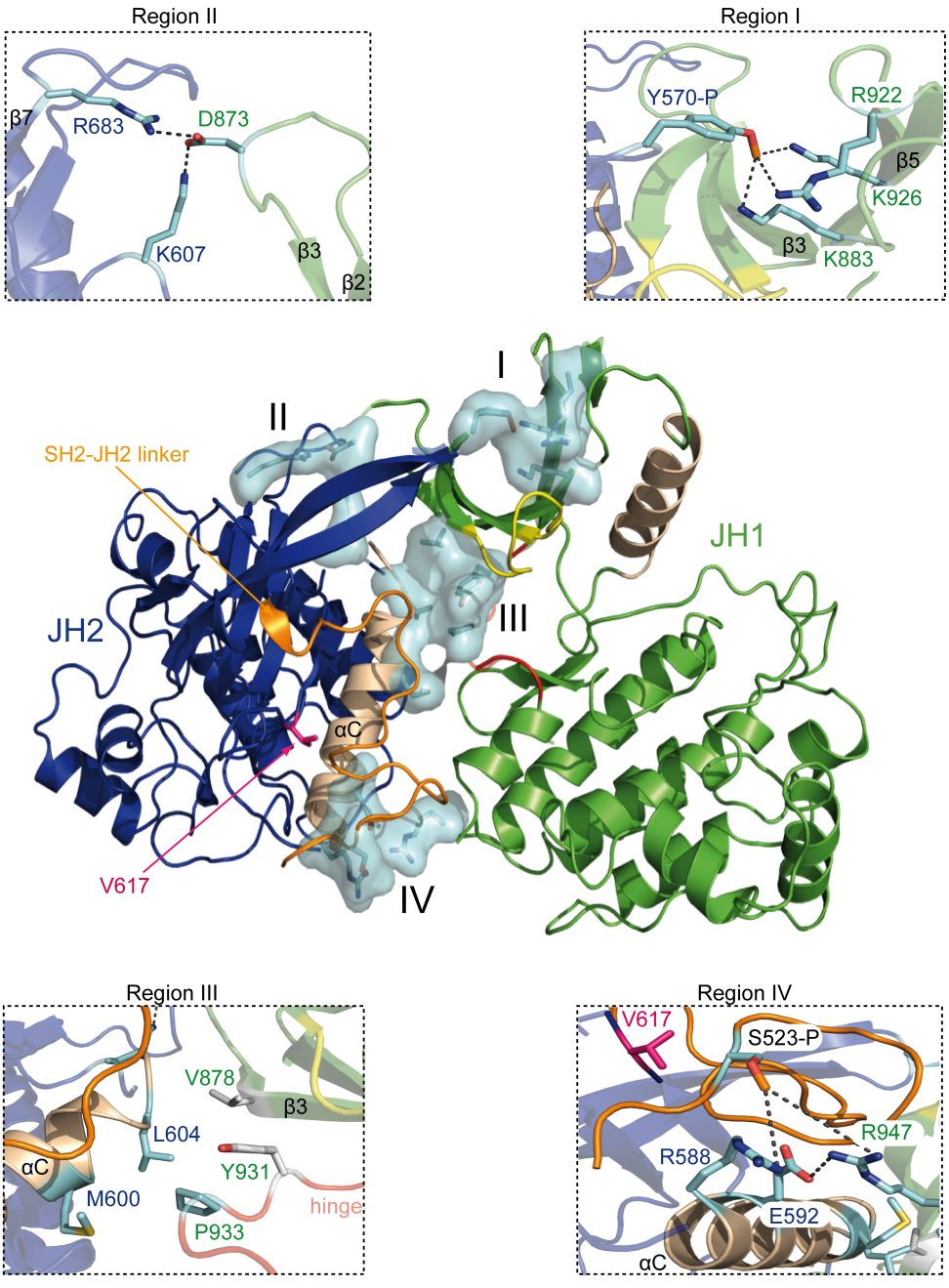
Region II
β7
R683
D873
K607
β3
β2
Region I
Y570-P
R922
β5
K926
β3
K883
I
II
SH2-JH2 linker
JH1
JH2
III
αC
V617
IV
Region III
V878
β3
L604
αC
Y931
M600
hinge
P933
Region IV
V617
S523-P
R947
R588
E592
αC

Once phosphorylated, S523 (from the SH2-JH2 linker) and Y570 (from JH2 N-lobe), participate in the formation of interdomain inhibitory salt bridges. Y570 is not conserved in the other JAKs, but is substituted by negatively charged residues located at homologous positions, which could also participate is similar salt bridge formation across the interface. This model supports the notion that JH2 inhibits JH1 through two mechanisms: i) *stabilization of an inactive state of JH1*. In fact, MD simulations suggested that the interaction with JH2 prevents the formation of the critical salt bridge necessary for catalytic activity of JH1 (K882-E898, section 4.3) (209). This was supported by the finding that JH2 restrains the activity of JH1 by reducing its affinity for ATP (237). ii) *sequestration of JH1*. The two JH1s must transphosphorylate each other, which constitutes the first activation event of the signaling cascade. But to do so, they need to be in close proximity and accessible to one another. The interdomain linker is around 30 amino acids long, which does not allow that much freedom to JH1. In the absence of stimulation, JH2 is thought to sterically limit the encounter between the two JH1 of each molecules associated with pre-dimerized receptor complex.

Mechanism of activation of JAK2 V617F

The mutation V617F is located in β4-β5 loop of JH2. The first molecular clue underlying the hyperactivity of this mutation came from a mutagenesis study. It was shown that an aromatic residue at position 617 was necessary to support hyperactivation. Substitution of V617 to tryptophan (W), leucine (L), isoleucine (I) or methionine (M) induced constitutive activation of JAK2 (53). Subsequently, it was demonstrated that F617 interacts with two phenylalanines located on the JH2 αC via an aromatic π-π stacking interaction (238). Substitution of F595 or F594 to alanine abrogates V617F-mediated activation while sustaining cytokine inducibility (238). A few years later, the crystal structure of JAK2 JH2 V617F was determined and confirmed the phenylalanine-to-phenylalanine interaction (206). Indeed, structural comparison of JH2 WT and JH2 V617F showed that in the presence of the mutation V617F, the JH2 αC changes its conformation probably due to the π-π stacking interaction between F594, F595 and F617

(**Figure 15**). The structure of JAK2 JH2 V617F displays an extended and more rigid αC with an additional turn on the N-terminal end, while the αC of JAK JH2 WT is more disordered and contains a kink in the middle (**Figure 15**).
This change of conformation provided the first insights into the molecular mechanism of JAK2 V617F activation and is thought to be the first molecular event driving hyperactivation of V617F.

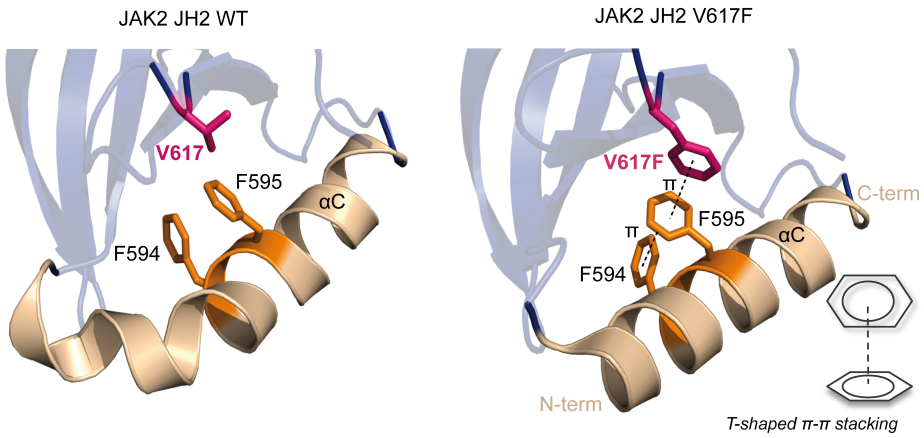

Figure 15. V617F induces a conformational change in the JH2 αC helix. The aromatic F617 interacts with F595 and F594 via a double π-π T-shaped stacking. This aromatic interaction seems to be responsible of the observed structural change in the αC in the mutant JAK2 JH2. While JAK2 JH2 WT displays a loose helix, the JAK2 JH2 V617F exhibits a rigid helix with an extra N-terminal turn.

In their MD simulation, Hubbard and colleagues showed that V617F does not directly interact with JH1 but rather makes contacts with the SH2-JH2 linker. In fact, MD simulation of JH2-JH1 V617F indicates that the mutation destabilizes the position of the SH2-JH2 linker normally positioned in the interface, thereby disrupting the JH2-JH1 inhibitory interface (209). Thus, the SH2-JH2 linker seems to be necessary to maintain auto-inhibition of JAK2 and seems to be part of the process by which V617F activates JH1.

A subsequent structural study of JAK1 V658F (JAK2 V617F homolog) brought additional lines of evidence into the mechanism of activation of JAK2 V617F. M. Eck and colleagues proposed a model in which V617F induces activation via a remodeling of JH2 and the SH2-JH2 linker again through aromatic interactions (210). This study revealed the presence of a F-F-V triad evolutionary conserved throughout JAKs consisting of F595 (of the αC), F537 (from the SH2-JH2 linker) and V617. Rearrangement of this triad is though to occur when V617 is substituted to phenylalanine, thus triggering activation. In the JAK1 JH2 V658F crystal structure (**Figure 16**), the phenyl ring of F658 (F617 in JAK2) occupies a pocket, which is normally occupied by the phenyl ring of F575 (F537 in JAK2) in the wild type structure (**Figure 16**). Therefore, F575 is pushed away (adopting a "out of the triad" conformation) and contacts the SH2-JH2 linker region (210). Interestingly, this "out of the triad" conformation can also be observed in the structure of JAK1 JH2 wild type suggesting that this region is highly prone to movement, likely to transmit activation to JH1. It is suggested that this "out of the triad" conformation of F575 (F537 in JAK2) is stabilized in the mutant conformation (210). While the exact molecular path by which V617F activates JH1 has still to be determined, the study presented in the first article attempted to provide some evidence on the mechanism.

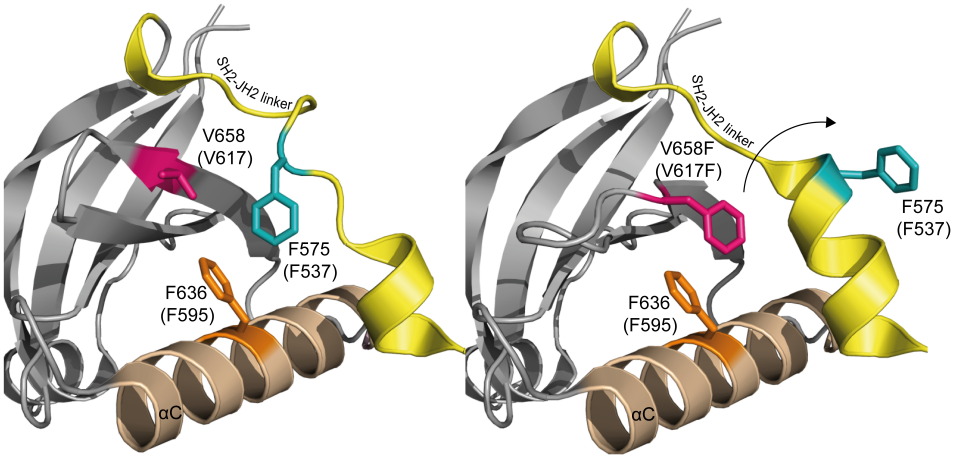

Figure 16. The FFV triad is conserved in JAKs. The crystal structures of JAK1 JH2 wild type (left, PDB: 4L00) and JAK1 JH2 V658F (right, PDB: 4L01) are shown. The JH2 αC is colored in wheat and the SH2-JH2 linker is colored in yellow. Residues forming the F-F-V triad in JAK1 are shown as sticks, with the corresponding JAK2 residues in parentheses. Substitution of V658 by phenylalanine pushes F575 away from its original location in the F-F-V triad.

Other activating mutations of JAK2

Other mutations were identified in PV patients (41, 46) and reported to induce constitutive activation of JAK2 (236) (**Annex 7**). Curiously, these mutations cluster in the exon 12, which encodes the SH2-JH2 linker region. The linker appears to act as a switch that transmits the cytokine-mediated activation of EpoR, relieving the JH2-mediated auto-inhibition, resulting in the kinase activation of JAK2 (236). Mutagenesis study indicated that the N-terminal region of the SH2-JH2 linker is important to mediate interaction with EpoR, whereas the C-terminal region is involved in auto-inhibition of JAK2. In fact, mutations of the C-terminal regions lead to constitutive activation of JAK2 (236). The clinically relevant mutations, such as K539L or N622I, lie on the C-terminal region of the linker. Similarly to what was proposed for JAK2 V617F, the exon 12 mutations were suggested to activate JAK2 through remodeling of the SH2-JH2 linker, which destabilizes the inhibitory JH2-JH1 interface (209). These exon 12 mutations highlight the critical regulatory role of the SH2-JH2 linker in JAK2. Further studies have to be undertaken to determine the exact role of this linker in the normal and pathogenic activation of JAK2.

6. JAK2 inhibitors: the current landscape

6.1. JAK2, the Achilles' heel of MPNs.

JAK2 became an intensive focus in the field of MPN after the discovery of an activating mutation in its pseudokinase domain, namely JAK2 V617F (25-28). The classical MPNs include the Philadelphia chromosome-negative (Ph^-) myeloproliferative diseases that are polycythemia Vera (PV), essential thrombocythemia (ET) and myelofibrosis (MF). The prevalence of MPNs in Europe is approximately 20 per 100,000 persons (239). Patients with MPNs develop splenomegaly, thrombosis, bleeding and can transform to acute myeloid leukemia (AML). Major efforts have been made in understanding the molecular pathogenesis of the disorders. Although several JAK2 activating mutations have been associated with MPNs, V617F remains the most predominant oncogene of these diseases as it is found in 95% of

patients with polycythemia vera (PV) and 60-65% of patients with essential thrombocythemia (ET) and primary myellfibrosis (MF). Other driver mutations have been associated with MPN. Activating mutations in the gene *c-MPL* encoding the thrombopoietin receptor (TpoR) such as TpoR W515K/L/S/A or TpoR S505N are found in 15% if JAK2 V617F-negative ET or MF (240). More recently frameshifting mutations in the last exon (exon 9) of the gene encoding the calreticulin gene (CALR), have been found in ET and MF patients negative for JAK2 V617F or TpoR mutations (12, 13). All things considered, JAK2 remains at the center of these disorders as both TpoR and CALR mutants depend on JAK2 for their signaling, which makes JAK2 the prime target for inhibition. Indeed, a genomic study carried out in 2014 indicates that activated JAK2 signaling is found in all patients with MPNs irrespective of the driver mutation or clinical diagnosis (241), which is in line with the observation that MPN patients may respond to JAK inhibitors regardless of their mutational status (242, 243).

Preceding the discovery of activating JAK2 mutations, safe long-term treatment for MPNs included cytoreductive drugs such as hydroxyurea, busulfan, anagrelide and IFNα (244). But since the description of the somatic mutation JAK2 V617F in 2005, major efforts have been devoted to the development of JAK2 inhibitors. **Annex 8** presents a table that lists all the JAK2 inhibitors that have been studied to date. At the moment, they have been around 20 compounds studied as JAK2 kinase domain inhibitors covering different chemical scaffolds ranging from pyrimidine based to pyridine derivatives.

Current JAK2 inhibitors cannot discriminate between mutant forms of JAK2 and JAK2 wild type (WT). As a consequence, inhibition of JAK2 WT in patients eventually causes anemia and thrombocytopenia as JAK2 specifically mediates cytokine signaling for red blood cell and platelet progenitors. Nevertheless, targeting JAK2 catalytic activity seems to be a reasonable approach in MPNs treatment. Development of potent JAK2 inhibitors for MPN treatment needs to satisfy several criteria. First, they must be specific to JAKs over all the other kinases to avoid any off-target toxicity. Kinases have always been highly attractive targets for anti-cancer drug design. Several years from today, it was difficult to believe that specific

targeting of the nucleotide binding site of specific kinases would be possible, as all the kinases share similar features and retain the same function. However, drug exploitation of different features of particular kinase ATP-binding pocket such as the gatekeeper residue side chains, non-covalent interactions, salt bridges and the DFG-loop position allows specificity to be achieved (245).. Secondly, the inhibitors have to display some specificity to JAK2 compared to other JAKs. Indeed, due to their promiscuous signaling, the four JAKs molecules (JAK1-3 and TYK2) might be affected by inhibitors showing low specificity. Third, and case specific, in order to treat patients harboring the most predominant mutation in MPN, JAK2 V617F, molecules should be specific to the mutant form of the protein and spare JAK2 WT.

Besides their role in blood disorders such as MPNs, hyperactivation of JAKs is also involved in immune-mediated disorders such as rheumatoid arthritis, psoriasis, Crohn's disease and lupus. That gives an impetus to develop novel JAK-specific inhibitors. This becomes possible because JAKs have been studied for many years with around hundred JAK structures being deposited in the protein data bank to date. The pharmaceutical industry has shown a flourishing interest into these kinases as therapeutic targets. Following ruxolitinib, several other JAK2 inhibitors as lestaurtinib, momelotinib, pacritinib, tocafitinib or baricitinib have been developed (**Annex 8**). Some of these compounds are still under investigation for the treatment of MPNs or rheumatological disorders, while others were stopped because of their toxicity or low efficiency. Our growing understanding of the JAK2 function and structure can definitely contribute to the development novel strategies to efficiently inhibit JAK2.

6.2. Type-I inhibitors

Protein kinases represent an important class of pharmaceutical drug targets, especially in the field of cancer. Type-1 inhibitors target the ATP-binding site of kinases in their active conformation. Naturally, targeting the catalytic activity of JAK2 has become a conceivable approach and small molecule inhibitor screenings were rapidly launched. The JAK1/JAK2 dual inhibitor ruxolitinib was the first molecule developed and the first targeted

therapy applied in MPN. FDA (Food and Drug Administration) and EMA (European Medicines Agency) first approved it for treatment of MF after the CONFORTI/ II trials (8, 9) and more recently for treatment of PV after the RESPONSE trial (246). Although ruxolitinib reduces myelofibrosis symptoms such as splenomegaly, it does not significantly decrease or eliminate the MPN clones. Furthermore, ruxolitinib has encountered side effects including thrombocytopenia and anemia, and to a lesser extent dose-dependent myelosuppression (247). This strongly encouraged the development of novel compounds showing more selectivity and thereby different safety profiles. Type-I JAK2 inhibitors have been tested in preclinical and clinical studies. Fedratinib (SAR302503), Lestaurtinib (CEP-701), Momelotinib (CYT-387), Pacritinib (SB1518), Gandotinib (LY2784544), BMS-911543, XL019 have been developed in MPNs treatment while Tofacitinib (CP-690,550) and Baricitinib (LY3009104) were developed for rheumatological disease for blocking JAK3/JAK1 and JAK2/JAK1, respectively. Finally, CEP-33779 was investigated in solid cancers (**Annex 8**). All these compounds are ATP-mimetics recognizing the ATP-binding pocket in the so-called active conformation of the kinase. In this active conformation, the DFG phenylalanine of the activation loop (F995) makes hydrophobic contacts with the N-lobe αC helix and the catalytic loop, thereby adopting a "DFG-in" conformation (**Figure 17a**). Some of these compounds show higher specificity to JAK2, such as BMS-911543 and Gandotinib (**Annex 8**).
Among inhibitors targeting active JH1, compounds NS-018 and gandotinib appear to be more effective to inhibit proliferation of JAK2 V617F cells versus cytokine-stimulated JAK2 WT cells (248, 249). An interaction between both these two molecules and G993 (preceding the DFG motif) was visualized by crystal structures (248, 249). However, G993 seems to be close to some of the other non-V617F-specific JAK inhibitors. Whether these molecules show preference to JAK2 V617F is due to targeting G993 in JH1, or addiction of transformed cells to JAK2 signaling remains to be determined.

By occupying the ATP binding pocket, type-I inhibitors abolish phosphoryl transfer from ATP to the substrate. Andraos *et al.* showed that this binding mode induces a paradoxical increased phosphorylation of the activation loop Y1007 of JAK2 despite inhibition of downstream signaling likely due to

transphosphorylation by other JAK partners or other kinases (218). This has been a complicating issue in many studies, as phosphorylation of Y1007 is a read-out of activation (213). Unwanted phosphorylation upon inhibitor addition was already reported for other kinases such as BRAF (250, 251) or AKT (252).

Similarly to other anti-kinases therapies, a prolonged use of inhibitors can confer resistance. Acquisition of mutations in the catalytic domain is a common mechanism used by kinases to resist to drug treatment. However, to date, no mutations were detected in patients treated with ruxolitinib, possibly underlying the limited efficacy of the current type-I inhibitors. Most of the studies investigating resistance to JAK2 inhibitors are either selection or mutagenesis and selection studies *in vitro* aimed at predicting future resistance-conferring mutations to type-I inhibitors before their appearance in the clinical setting (253-255). Yet, this knowledge can be used to inform decisions during drug design process but clearly as of now mutational-mediated conformational escape is not an issue in JAK2 inhibition therapy. Yet, certain patients that do not respond to one JAK2 inhibitor can respond to another JAK2 inhibitor due to unknown mechanisms. In 2012, the team of Dr. Ross Levine provided insights into the mechanism hindering MPN alleles reduction by type-I inhibitors, which they termed "persistence" (256). Indeed, they have shown that persistence of the mutated clones treated by ruxolitinib or fedratinib occurs by heterodimerization of JAK2 with JAK1 or TYK2 (256). They later extended their studies to other type-I inhibitors (momelotinib or BMS911543) and shown that persistence is induced through the same mechanism (257), underlying the insensitivity of the clones to structurally different type-I compounds. This phenomenon is promoted by an increase in JAK2 expression and can be reversible upon inhibitor withdrawal (256). Another mechanism of resistance appears to be acquisition of mutations that increase half-life of mutant JAK2. Germ-line JAK2 activating mutants were identified in hereditary thrombocytosis and induced not only activation, but also increased stability and resistance to type-I inhibitors (50). Curiously, inhibition of the HSP90 chaperon protein (heat shock protein 90), for which JAK2 is a client protein, restores sensitivity to JAK2 inhibitors, opening perspectives for alternate strategies of inhibition (152, 256).

Formation of heterodimeric complexes is possible because JAK2 is stabilized in an active (generally more accessible) conformation by type-I inhibitors. Therefore, type-II inhibitors that bind to the inactive conformation might have a better chance in eradicating persistent clones, as they would avoid the formation of such complexes.

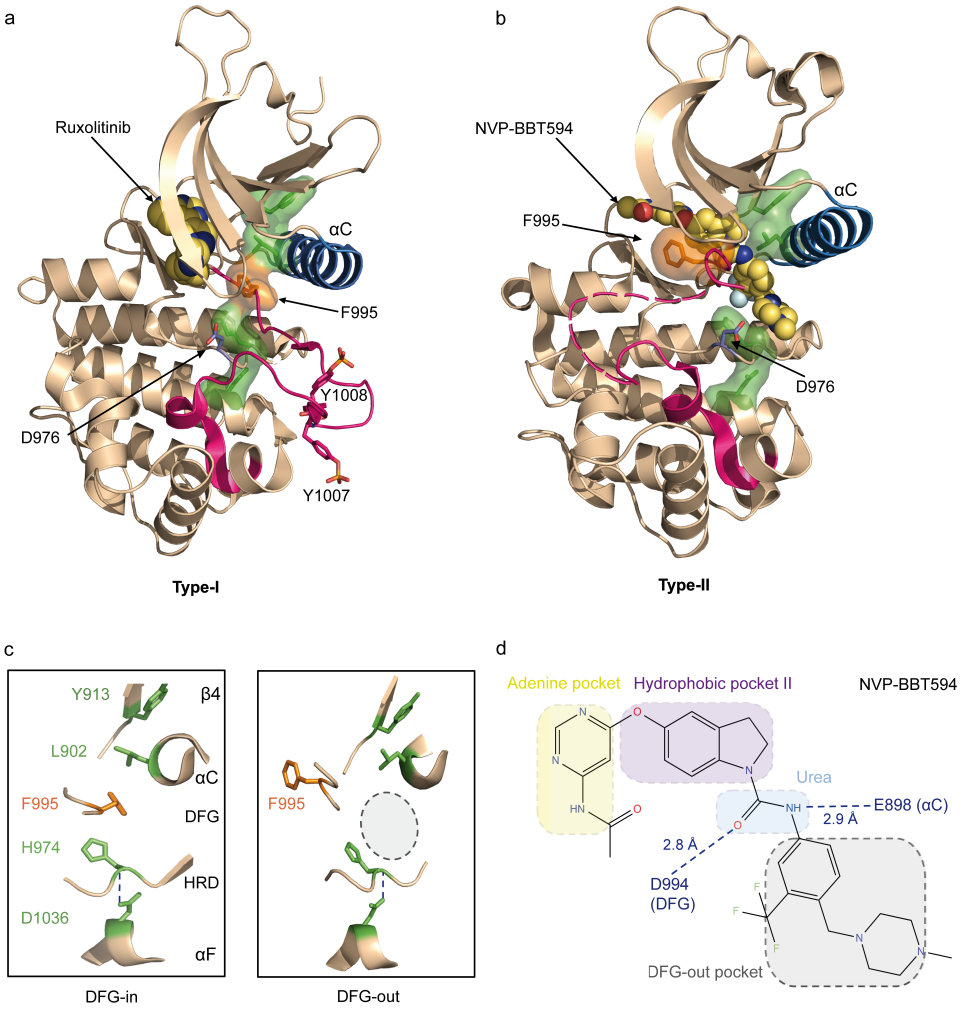

Figure 17. Comparison between a type-I versus type-II inhibitors of JAK2. a. Type-I binding mode. Ruxolitinib (shown is spheres) binding to the active conformation of JAK2 JH1 (PDB: 3KRR) has been modeled based on the co-crystal structure of ruxolitinib bound Src (PDB: 4U5J). The αC is colored in blue and the activation loop, colored in pink, adopts an open (active) conformation. D976 from the catalytic loop (HRD motif) colored in light blue is turned toward the active site. F995 from the DFG motif, located at the outset of the activation loop, is colored in orange and adopts an "in" position in the hydrophobic regulatory spine depicted in green. **b.** Type-II binding mode. Ribbon diagram of the co-crystal structure of NVP-BBT594 bound JAK2 JH1 (PDB: 3UGC). The inhibitor is shown in spheres and binds JH1 that exhibits an activation loop in a closed (inactive) conformation (pink dashed lines). D976 is turned outward of the active site, while F995 is translocated away from it original pocket and now resides "out" of the regulatory spine. **c.** A regulatory hydrophobic spine is composed of a series of 4 hydrophobic residues from β4, αC, DFG and HRD. These residues are only correctly aligned in the active conformation of kinases and that is stabilized by phosphorylation of the activation loop (left panel). This so-called regulatory spine is bound to the C-lobe α helix F (αF) via a conserved hydrogen bond between H974 and D1036 (dashed line). F995 from the DFG occupies its pocket and is aligned in the spine in the active stat (DFG-in). In the inactive conformation (right panel), the regulatory spine is "broken" since F995 is moved away from its original position in the spine leaving the pocket (grey oval) empty. This DFG-out pocket can now be occupied by type-II inhibitors. **d.** Schematic drawing of some important contacts specific of type-II inhibitor binding to kinase. Type-II inhibitors, such as NVP-BBT594, usually present an amide or an urea group in the molecule that makes hydrogen bonding with a conserved αC glutamate side chain and with the DFG aspartate backbone (blue dashed lines). The pyrimidine group of NVP-BBT594 occupies the adenine site of the ATP binding site (yellow) while the dihydroindole moiety occupies the adjacent hydrophobic pocket II (purple) in opposition to the hydrophobic pocket I occupied by type-I inhibitors (not shown). The Tri-fluoro-methyl-phenyl and the N-methylpiperazine occupy the DFG-out pocket (grey).

6.3. Type-II inhibitors

Type-II inhibitors recognize the inactive conformation of kinases and bind to the ATP binding pocket and to the extra "DFG-out" pocket only accessible in the conformation of inactive kinases (**Figure 17b**). The so-called "DFG-out" pocket is created by the DFG phenylalanine adopting an "out" conformation, which means that its side chain is out of the regulatory spine (**Figure 17b**). With the help of a plethora of crystallographic data and a better understanding of kinases regulation, the growing field of structure-based drug design could identify this second class of kinase inhibitors preferentially binding to the unphosphorylated inactive conformation of the

kinase. By exploiting supplementary binding sites contiguous to the ATP binding pocket (the DFG- pocket), type-II inhibitors gain in specificity and hence in selectivity (258). Importantly, the extra-pocket targeted by type-II inhibitors is less conserved within the kinome than the canonical ATP binding pocket, thus promising better selectivity of the compound and minimization of the off-target toxicity. This second generation of inhibitors prompted considerable interest for the treatment of Brc-Abl positive CML after the introduction of the earliest type-II inhibitor, imatinib (Gleevec®, STI-571). The solved structure of the Bcr-Abl co-crystallized with imatinib (PDB: 1IEP) (259) actually served as a model for further type-II drugs design.

To date, two compounds have been described to bind JAK2 in a type-II binding mode, namely NVP-CHZ868 and NVP-BBT594 (Novartis) (**Figure 17b**). Strikingly, both drugs were described to retain the capacity to inhibit persistence cells (256, 257, 260). Andraos and colleagues described that, in contrast to type-I inhibitors, the type-II inhibitor NVP-BBT594 stabilizes the inactive conformation of JAK2, which results in an unphosphorylated activation loop likely achieving a stronger inhibition (218). Moreover, this work reported the first structure of JAK2 kinase domain in its inactive state by co-crystallization of JH1 with NVP-BBT594, where the DFG phenylalanine is moved by approximately 10 Å from its position in the active state (PDB: 3UGC) (**Figure 17b**). NVP-BBT-594 recognizes structurally distinctive regions within the kinase cleft compared to type-I inhibitors such as ruxolitinib. This atomic structure will likely help the design of future type-II inhibitors. The dihydroindole NVP-BBT594 was originally developed as an inhibitor of the imatinib resistant Bcr-Abl T315I (261), and latter was found to inhibit JAK2. However, it retains some limitation in selectivity and its pharmacokinetic properties render it improper for *in vivo* use (260). For this reason, another type-II inhibitor was developed with improved physicochemical and pharmacokinetic properties, NVP-CHZ868, which shows strong efficacy against activated forms of JAK2 responsible for MPN development. Two accompanying publications reported the effect of NVP-CHZ868 in MPN (257) and in B-ALL (260) mouse models, showing that NVP-CHZ868 suppresses signaling of transformed cells resistant to type-I inhibitors and even displayed a significant reduction of the allele burden in PV and MF murine models.

NVP-CHZ868 exhibited selectivity for pathogenic JAK2 activation against JAK2 WT activation and remarkably, it did not only affect V617F-mediated but also the pathologic persistent MPL W515L-mediated activation of JAK2 WT (257).
One JAK2 kinase domain mutation conferring resistance, L884P, was isolated by a mutagenesis approach conducted on the B-ALL-associated JAK2 R683G mutant and was found to prevent inhibition by NVP-CHZ868 (260). Substitution of L884P, located in the N-lobe β3 strand of the kinase domain, by a proline is thought to disorganize the hydrophobic network regulating the shape of the ATP binding cleft and to prevent binding of the type-II inhibitor by changing the position of the αC helix. Interestingly, this mutation was also described as an activating mutation, in JAK2 and JAK3 (L857P) (157, 260) and reported in B-ALL cases (260). This mutation appears to intrinsically activate JH1, as it does not require receptor complex formation to signal (157). How this mutation enables JAKs to escape from receptor binding requirement still needs to be elucidated.

The mutation seems to maintain the kinase domain in a highly stabilized active conformation rather than just obstructing the type-II inhibitor-binding pocket. Such escape mechanism has to be taken into account when designing inhibitors. This also raises the question of whether each type of compound needs to expect the acquisition of respective escape mechanism. Nonetheless, the new type-II NVP-CHZ868 holds promising prospects for clinical use.

It still not evident how type-II compounds could be more potent on hyperactive mutants against JAK2 WT as they specifically target the inactive conformation which is assumed to be mainly adopted by normal JAK2 compared to activated forms of JAK2. Even though type-II inhibitors provide better kinase specificity, they cannot discriminate between wild-type and the mutant forms.

For this reason, a better understanding of the precise mechanism(s) governing the activation of JAK2 by mutations is required and determination of critical regions involved in mutation-mediation activation could possibly constitute new allosteric sites to target in order to achieve

mutants specific inhibition. Allosteric inhibitors that are defined as molecules binding to a region on the kinase that does not overlap with the ATP binding site are also referred as type-III inhibitors (262) (**Figure 18**). To date no such molecules have been clearly identified for JAK2. Two molecules, LS104 and ON044580 were described as allosteric inhibitors of JAK2 (263-265) and demonstrated inhibitory activity against native JAK2 and JAK2 V617F. However, their binding mode was never confirmed, neither by crystallographic data nor by mutagenesis and their development was not continued. At present, structural and mechanistic studies (210, 211, 221, 238) indicate that allosteric inhibition of JAK2 could be achieved by targeting other domains of JAK2, distinct from the kinase domain. This new class of compounds, sometimes referred as type-IV inhibitors (262) (**Figure 18**), could be possibly developed in order to achieve JAK2 V617F specific inhibition.

The different types of kinase inhibitors

The common *reversible* inhibitors are classified in four different groups from I to IV (illustrated in figure 2). A fifth group includes bivalent inhibitors that use a combination of one or more of the four preceding binding modes. Lastly, another type of inhibitor comprises the *irreversible* or covalent inhibitors:

- **Type-I:** ATP competitive. They bind to the ATP binding pocket. Target the **active** conformation or "DFG-in" conformation where the Phe is in the hydrophobic regulatory spine and the HRD Asp is facing into the active site **(illustrated in a).**
  Examples**:** Ruxolitinib (JAK2)

- **Type-II:** ATP competitive. They bind to the ATP binding pocket and the DFG pocket. Target the **inactive** conformation or "DFG-out" conformation where the Phe is out of regulatory spine and the HRD Asp is extending outward from the active site. **(illustrated b).**
  Examples: Imatinib (BCR-ABL), NVP-CHZ868 (JAK2), NVP-BBT594 (JAK2)

- **Type-III:** They bind exclusively to an allosteric pocket, located on the kinase domain, close to the ATP binding pocket but does not overlap it **(illustrated in c).**
  Examples: PD184352 (MEK)

- **Type-IV:** They are truly allosteric inhibitors that bind exclusively to an allosteric pocket, distant of the ATP binding pocket **(illustrated d).** Examples: GNF-2 (BCR-ABL)
  They can also bind to other domains of the target protein or to other interaction partners of the kinase **(illustrated in e).**

- **Type-V:** They are bivalent inhibitors that bind to two distinct sites on the kinase. They are composed of an ATP competitors connected to a ligand that target a region remote of the active site.

- **Covalent inhibitors:** They bind irreversibly to the kinase active site by reacting with a highly reactive nucleophilic residue, usually a cysteine, locate in the ATP binding site.
  Examples: Neratinib (ErbB-2), CL-387785 (EGFR)

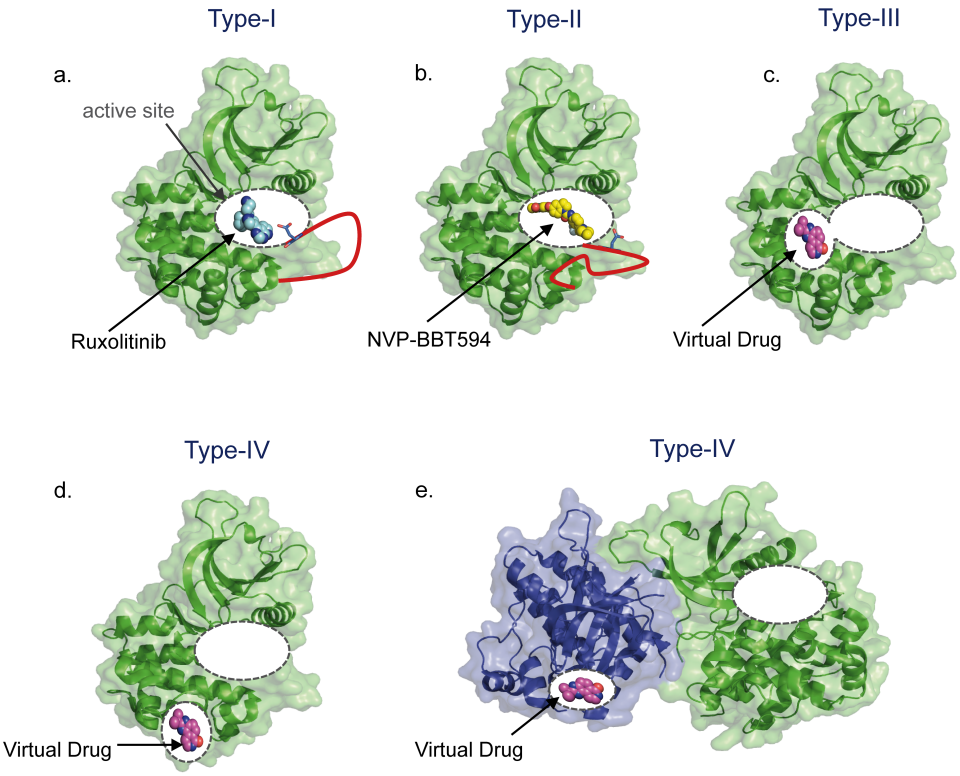

Figure 18. Definition of the different types of kinase inhibitors. The common reversible inhibitors are classified in four different groups from I to IV (illustrated below). The target kinase is represented with green ribbon diagram and transparent surface. The activation loop is represented in red. A fifth group includes bivalent inhibitors that use a combination of one or more of the four preceding binding modes. Lastly, another type of inhibitor comprises the irreversible or covalent inhibitors.

OBJECTIVES

The activating mutation JAK2 V617F was discovered in 2005 and constituted a landmark advancement in the MPN field. However, several important questions regarding the molecular basis of JAK2 V617F-triggered hyperactivation remain unanswered. To date, there is no crystal structure available for the full-length JAK2. Thus, the exact organization of the four main domains has not been characterized. For this reason, the allosteric regulation of JAK2 catalytic activity by the other domains is not completely uncovered. Specifically, the mechanism by which the pseudokinase domain (JH2) mediates regulatory functions on the kinase domain (JH1) is not exactly understood. Similarly, the mechanism by which V617F located in JH2 activates the adjacent JH1 still remains elusive. The discovery of JAK2 V617F mutation has opened the door to drug design and treatment strategies for the MPNs. However, there are no curative treatments available to date. Targeting JAK2 with small molecules inhibitors has been a main focus in the past 10 years. Yet, given the critical role of JAK2 in various biological functions such as the hematopoietic or the immune system, specifically targeting JAK2 V617F over JAK2 WT is of major importance. Efforts to develop such compounds have been hindered by the lack of structural and mechanistic information on JAK2 V617F. How can such specificity be achieved is one of the burning questions. Understand the molecular basis of how JAK2 V617F is hyperactivated would be essential for effective drug design.

In 2010, my host lab reported that the JH2 αC plays a crucial role in triggering the constitutive activity of JAK2 V617F. Indeed, it was shown that JAK2 V617F activation involves a critical stacking interaction between F617 and F594/F595 of the JH2 αC. This work provided the first structural evidence for the molecular basis of JAK2 V617F activation mechanism. In order to peruse this work, I focused my effort on the JH2 αC and hypothesized that it was the first molecular event driving oncogenic activation. Then, I aimed to determine what was the next molecular events driving activation to the kinase domain.

My major focus was to understand how a change in a single residue in the JH2 domain induces activation of the adjacent JH1 domain. For this reason, I wanted to define the molecular interplay between JH2 and JH1 and determine the function of the JH2 domain with special emphasis on its role in the JAK2 V617F activity. That involved getting insights into the biology of pseudokinases and their more general function in signaling.

At the time when I started my project, only a few structural data were available on JAKs as well as on the characterization of the pseudokinase domain and its role in regulating JAK2 activity. To start with, I used a model (described in the **introduction, section 5.3**) illustrating an interface between the pseudokinase and kinase domains to design a mutagenesis strategy. But in the course of my PhD, new structural data and more evolved models on JAKs became available, which made me gradually adapt my project. Based on the available coordinates, I designed a set of mutations that aim to specifically inhibit JAK2 V617F activity but also to map out the residues in JAK2 that are necessary for the oncogenic, but not physiological activation of JAK2.

The specific aims of the study were to: i) Determine the exact role of the JH2 αC in the JAK2 V617F activation, ii) Characterize the residues that are required for V617F-induced *versus* cytokine-induced activation of JAK2, iii) Explore new strategies to specifically inhibit JAK2 V617F based on structure-guided mutagenesis, iv) Characterize new allosteric sites across the JH2-JH1 interface that are important for JAK2 V617F function.
The ultimate goal is to provide new structural and molecular bases concerning JAK2 V617F hyper-activation mechanism, with the hope that they could be used to inform decision in drug design.

RESULTS

ARTICLE 1: Uncoupling JAK2 V617F activation from cytokine-induced signalling by modulation of the JH2 αC helix

Uncoupling JAK2 V617F activation from cytokine-induced signalling by modulation of JH2 αC helix

Emilie Leroy*†, Alexandra Dusa*†, Didier Colau*, Amir Motamedi‡, Xavier Cahu*†, Céline Mouton*†, Lily J. Huang§, Andrew K. Shiau‡ and Stefan N. Constantinescu*†[1]

*Ludwig Institute for Cancer Research, 1200 Brussels, Belgium
†de Duve Institute, Université catholique de Louvain, 1200 Brussels, Belgium
‡Small Molecule Discovery Program, Ludwig Institute for Cancer Research, La Jolla, CA 92093, U.S.A.
§University of Texas Southwestern Medical Center, Dallas, TX 5323, U.S.A.

The mechanisms by which JAK2 is activated by the prevalent pseudokinase (JH2) V617F mutation in blood cancers remain elusive. Via structure-guided mutagenesis and transcriptional and functional assays, we identify a community of residues from the JH2 helix αC, SH2-JH2 linker and JH1 kinase domain that mediate V617F-induced activation. This circuit is broken by altering the charge of residues along the solvent-exposed face of the JH2 αC, which is predicted to interact with the SH2-JH2 linker and JH1. Mutations that remove negative charges or add positive charges, such as E596A/R, do not alter the JH2 V617F fold, as shown by the crystal structure of JH2 V617F E596A. Instead, they prevent kinase domain activation via modulation of the C-terminal residues of the SH2-JH2 linker. These results suggest strategies for selective V617F JAK2 inhibition, with preservation of wild-type function.

Key words: JAK2 V617F, JAK-STAT signalling, inhibitor, kinase, myeloproliferative neoplasm (MPN).

INTRODUCTION

JAK-STAT signalling is essential for development, haematopoiesis and immune responses [1]. Inappropriate signalling, especially the gain-of-function mutations of Janus kinases (JAKs) and cytokine receptors, are linked to multiple human malignancies. JAK2 has a pivotal role in numerous signalling pathways [2], and the unique acquired somatic mutation JAK2 V617F is associated with >65 % of human myeloproliferative neoplasms (MPN) [3]. Considerable interest has emerged toward V617F-specific JAK2 inhibitors since the discovery of the mutation in 2005 [3–6], nonetheless the mechanism of activation of the mutant at the atomic level remains poorly understood. As a consequence, there are no JAK2 inhibitors that can discriminate between the mutant and the wild-type protein. One JAK2 inhibitor has been approved for clinical use in myelofibrosis [7–9], but the effect is not curative and the allele burden of the mutated clone does not appear to decrease. Hence, there is a critical need for novel V617F-targeted therapeutic approaches.

JAK proteins (JAK1–3 and TYK2) include tandem kinase domains: a pseudokinase (JH2) and a canonical tyrosine kinase (JH1) domain. The latter is responsible for the catalytic activity of the protein whereas the function of JH2, where the V617F mutation is located, is still being defined. JH2 exerts an auto-inhibitory role in JAK regulation [10], possibly by restraining JH1 in an inactive conformation in the absence of cytokine receptor activation [11,12]. Whether this inhibition occurs in *cis* or *trans* [13,14] is still unclear, but evidence based on activating/resistance mutations [15] and the recent TYK2 JH1–JH2 crystal structure [12] would suggest a *cis* mechanism. The JAK2 JH2 domain has been crystallized and was found to adopt a protein kinase fold with features typical of tyrosine kinases, including an activation loop (albeit shorter than usual kinases), a G-loop and the critical helix αC [16]. The crystal structures of the individual JH1 and JH2 domains have been solved for every member of the JAK family [12,16–19] with the exception of JAK3, and in addition, a FERM-SH2 structure of TYK2 (tyrosine kinase 2) was recently determined [20]. However, in the absence of a full-length JAK protein structure, the atomic details of how all of these domains work together are still elusive. This clouds our understanding of pseudokinase-mediated auto-inhibition, and hence the basis of V617F constitutive activation. Indeed, despite significant recent insights into this mechanism [11,19], whether the V617F mutation (which is located in JH2) utilizes the same molecular pathway to activate JAK2 as cytokine-induced stimulation is still unknown.

Two JH2 regions in the vicinity of V617F are essential for its activity. First, we previously demonstrated that a stacking interaction between the aromatic rings of F617 and F595 of the JH2 αC is required for constitutive signalling of JAK2 V617F [21]. This interaction mediates a conformational change that has been visualized on the crystal structure of JH2 V617F [16]. Additionally, the JH2 αC of JAK2 was proposed in a molecular dynamics (MD) simulation [11] to be in the JH1/JH2 interface and was later visualized in this interface in the TYK2 JH1/JH2 crystal structure [12]. Attention has lately turned towards a second region, the SH2-JH2 linker, for understanding the mechanism of auto-inhibition of JAK2 [11,12,19]. This linker has been studied for its role in erythropoietin receptor (EpoR) trafficking [22], its importance in controlling JAK2 activity [23] and most recently as a proposed JH1 interaction site by MD simulations [11]. It

Abbreviations: DMEM, Dulbecco's modified Eagle's medium; EpoR, erythropoietin receptor; FACS, fluorescence activated cell sorting; IRES, internal ribosomal entry site; JAK, Janus kinase; JH, JAK homology; MD, molecular dynamics; MPN, myeloproliferative neoplasms; SH, Src homology; STAT, signal transducers and activators of transcription; TCEP, Tris (2-carboxyethyl) phosphine; TpoR, thrombopoietin receptor; TYK2, tyrosine kinase 2.

[1] To whom correspondence should be addressed (email stefan.constantinescu@bru.licr.org).

© 2016 The Author(s). Published by Portland Press Limited on behalf of the Biochemical Society.

also contains the highly conserved F537, which completes the so-called 'F-F-V triad' formed by residues F537, F595 and V617. F537 has been shown to be necessary for JAK2 V617F activity [19].

In the present study, we used a comprehensive structure-guided mutagenesis-based approach to identify additional key residues of the JH2 αC and the SH2-JH2 linker that are required for JAK2 V617F activity. Via these methods, we discovered specific residues that, upon charge negation or reversal, result in inhibition of V617F constitutive activity without impeding cytokine-induced activity. Our results enable us to precisely define a V617F activation circuit involving residues in the JH2 αC and SH2-JH2 linker. Confirming this hypothesis, prominent pathological activating mutations in residues that are not involved in this circuit are not sensitive to charge reversals on JH2 αC. Taken together, our results strongly suggest that wild-type JAK2 and JAK2 V617F activation networks are different. Selective targeting of these novel pathways of inhibition could become a valuable approach leading to mutant-specific inhibition.

EXPERIMENTAL

Vector construction and mutagenesis

Generation of point mutations in JAK2 was achieved by overlap-extension PCR-based mutagenesis using synthetic oligonucleotides containing the specific mutations. The reaction was performed using pfuTurbo (Agilent) following the manufacturer's protocol. All the constructs were subcloned in the bicistronic retroviral vector pMX-IRES-GFP [24], enabling a correlation of the level of expression of the gene cloned upstream of the internal ribosomal entry site (IRES) to the level of expression of the GFP. EpoR is subcloned in the pMX-IRES-CD4 [24]. All the constructs were verified by Sanger sequencing.

Cell lines

γ2A cells are human fibrosarcoma cells that are deficient for JAK2 [25]. 11.1 [26,27] and U4C [28] are TYK2 and JAK1 deficient human fibrosarcoma cell lines respectively. The three cell lines were grown in Dulbecco's modified Eagle's medium (DMEM) with FBS (10 %). BaF3 are murine bone marrow-derived pro-B lymphocytes that are dependent on IL3 for survival [29]. BaF3 are maintained in Gibco® RPMI 1640 medium supplemented by 10 % of FBS and IL-3.

BaF3 transduction

To obtain stable BaF3 expressing EpoR and the JAK2 WT or the JAK2 variants, high-titre helper free retroviruses were generated by transient transfection of BOSC packaging cell line [29]. Supernatant was collected 48 h after transfection and was directly used to infect BaF3 by spin infection for 3 h at 37 °C. GFP for JAK2 and CD4 for EpoR were used as a marker of infections. Populations expressing similar levels of markers were sorted by fluorescence activated cell sorting (FACS).

Dual luciferase assay

STAT5 transcriptional activity of the JAK2 WT and the different mutants was measured in γ2A cells by dual luciferase assays with the reporter gene, Spi_Luc [30]. Cells were seeded overnight in a 48-well plate in DMEM + 10 % FBS. Cells were transiently transfected with EpoR, JAK2, STAT5, Spi_Luc and pRL-TK using Lipofectamine™ 2000 (Invitrogen) with the following ratio: 3:1:1:3:1 in Optimem. Medium was changed 4 h after transfection for DMEM containing or not Epo at 15 unit/ml (Eprex®). The luciferase activity was monitored with the dual Luciferase Reporter Assay System kit (Promega) 24 h after transfection. Emitted light was recorded on a luminescence microplate reader (PerkinElmer).

Proliferation assay

Cells were washed three times and set at a density of 250000 cells/ml in cytokine-free medium. Cells numbers were recorded over a period of six days using either a coulter cell counter or a CellTiter-Glo Luminescent Cell Viability Assay (Promega), where indicated. The later allows quantification of ATP amount within cells, which is directly correlated with the number of living cells per well. Addition of CellTilerGlo® reagents is followed by measurement of the resulting emitted luminescence at 570 nm.

Western blotting

γ2A cells were transfected with cDNAs coding the JAK2 WT or JAK2 mutants and EpoR using FuGene HD (Promega). Cells were plated in 6-well plates the day preceding the transfection in DMEM + 10 % FBS. Forty-eight hours after transfection, medium was changed to DMEM supplemented or not with Epo. Stimulation was performed for 20 min at 37 °C followed by washing cells with PBS. Cells were trypsinized and lysed in 1× Nodinet P-40 (NP40) lysis buffer supplemented with orthovanadate, PMSF and protease inhibitor cocktail (ThermoFischer Scientific). Lysate samples were analysed by SDS/PAGE using a 4–12 % gradient NuPage® NOVEX BisTris Gel (Invitrogen) and transferred to a nitrocellulose membrane. Total JAK2 was detected using Jak2 (D2E12) XP® Rabbit mAb (Cell Signaling Technology #3230) and Phopho-JAK2 with phospho-Jak2 Tyr1007/1008 (C80C3) Rabbit mAb (Cell Signaling Technology #3776). Detection was performed using a peroxidase-conjugated anti-rabbit secondary antibody (GE Healthcare) and images were acquired by Fusion FX7 (Vilber Lourmat).

Flow cytometry and phospho flow analysis

After stimulation, BaF3 cells were fixed with formaldehyde solution (1.6 %, methanol-free, ThermoFisher Scientific) and permeabilized with PermBuffer III (BD Phospflow, BD Biosciences). After washing with PBS FBS 2 %, cells were further stained with pSTAT5-Alexa647 antibody (PY694) (dilution 1:20, BD Biosciences) and phospho-Jak2 (Tyr1007/1008) rabbit antibody (Cell Signaling Technology, dilution 1:400), followed by an anti-rabbit donkey PE antibody (1:400). Flow Cytometry analysis was performed on a BD LSRFortessa cell analyser (BD Biosciences).

Structure determination

The E596A mutation was introduced into a baculovirus expression plasmid encoding the human JAK2 JH2 domain (amino acids 535–812 with a C-terminal thrombin-cleavable His_6-tag) harbouring the V617F and three other mutations (W659A, W777A and F794H) [16], and the resulting mutant protein was expressed in *Spodoptera frugiperda-9* cells as described previously. Cell pellets were resuspended

© 2016 The Author(s). Published by Portland Press Limited on behalf of the Biochemical Society.

in 20 mM Tris (pH 8.5), 500 mM NaCl, 0.5 mM Tris (2-carboxyethyl) phosphine (TCEP), 10 % glycerol, 1 mM sodium orthovanadate and 20 mM imidazole with protease inhibitors (Roche Diagnostics), and lysed using a microfluidizer. After clarification via centrifugation, the lysate was incubated with Ni-NTA Superflow resin (Qiagen), and the bound protein was eluted in 20 mM Tris/HCl, pH 8.5, 500 mM NaCl, 0.5 mM TCEP, 10 % glycerol, 1 mM sodium orthovanadate and 200 mM imidazole. Peak fractions were pooled, diluted 1:11 with 20 mM Tris/HCl, pH 8.5, 0.5 mM TCEP, 10 % glycerol, and flowed through a HiTrap Q HP column. After adding ATP and $MgCl_2$ to 1 and 3 mM respectively, the protein was concentrated to 6.8 mg/ml using Amicon Ultra 3K MWCO concentrators (Millipore).

The protein was crystallized by hanging drop vapour diffusion using a reservoir buffer consisting of 100 mM Tris (pH 8.5), 200 mM sodium acetate, 22 % PEG 4000 at 4 °C. 1.5 μl protein solution was mixed with 1.5 μl reservoir buffer and sealed in a chamber containing 400 μl of reservoir solution. After 1 week, a rod-shaped crystal (~400 μm × 30 μm × 5 μm) was transferred to a cryoprotectant containing 100 mM Tris (pH 8.5), 200 mM sodium acetate, 22 % PEG 4000, 10 % glycerol, 1 mM ATP and 3 mM $MgCl_2$, and flash-frozen in liquid nitrogen.

X-ray diffraction data were measured using NE-CAT beamline 24-ID-C at the Advanced Photon Source at Argonne National Laboratory and processed with XDS [31] and AIMLESS from the CCP4 suite [32]. The structure was determined by molecular replacement using PHASER [33] and a partial model of the wild-type JAK2 JH2 domain (PDB: 4FVP with residues 586–600 and 617 deleted). Refinement was performed using PHENIX [34] interspersed with iterative cycles of rebuilding using Moloc [35].

RESULTS

JAK2 V617F activity requires residue E596 of the helix αC of JH2

Previously, our group showed that the V617F mutation, which lies in the JH2 β4–β5 loop, affects the conformation of the neighbouring helix, αC. Specifically, the substituted F617 side chain interacts with those of two αC aromatic residues, F594 and F595 [21,36], causing a conformational change of this helix [16] that likely nucleates mutant protein activity. In order to determine which residues beyond F594 and F595 might be necessary for V617F activity, we conducted an alanine scan of the entire JH2 αC from R588 to S605 in JAK2 V617F. We then analysed the effect of these substitutions in the context of the mutant JAK2 V617F reconstituted in JAK2-deficient cell line (γ2A) together with the EpoR (Figure 1A). STAT5 transcriptional activity was quantified by a dual luciferase assay using Spi_Luc as the reporter. Expression of JAK2 V617F but not wild-type JAK2 resulted in STAT5 transcriptional activity in the absence of exogenous ligand (Epo), and alanine substitutions of F594 and F595 caused a decrease in this basal activity as previously described [21,36]. In addition to these two already described substitutions, E596A significantly reduced the mutant activity (Figure 1A). The levels of expression of the JAK2 variants were assessed by Western blot, allowing us to conclude that the decreased activity is not due to a reduction of the levels of expression (Figure 1A). Strikingly, E596A in the context on the mutant V617F still permitted response to cytokine, reverting the mutant to a wild-type JAK2 phenotype (Figure 1B). These results were confirmed in a functional assay using the IL-3-dependent haematopoietic cell line BaF3 (Figure 1C). Cells were retrovirally transduced with EpoR and the JAK2 variants for stable expression and sorted for comparable levels of CD4 and GFP respectively. BaF3 expressing JAK2 WT, V617F or V617F/E596A and the parental cell line were grown in the absence of cytokine. Although expression of JAK2 V617F in BaF3 led to factor independent growth of BaF3 cells, the E596A mutation abrogated autonomous proliferation (Figure 1C). We then assessed phosphorylation of STAT5 (Y694) and JAK2 (Y1007/Y1008) before and after stimulation with 50 unit/ml of Epo by phospho-flow cytometry. BaF3 cells expressing JAK2 V617F/E596A only exhibit phosphorylation of the JAK-STAT signalling pathway in response to Epo (Figure 1D).

E596 is located on the face of αC opposite to the one containing F594 and F595 (Figure 1E), and this surface is predicted to face JH1 [11,12]. The JH2 αC harbours other charged amino acids (Supplementary Figure S1); R588 and E592, located on the same helical face, but their substitution to alanine did not lead to any reduction of JAK2 V617F activity (Figure 1A). Further, all possible combinations of alanine mutants of E592, E596 and R588 were generated (Supplementary Figure S1) and only substitution of E596 to alanine reduces the activity of JAK2 V617F. Intriguingly, E596 is necessary for JAK2 V617F oncogenic activation but not for the wild-type activation process, as introduction of this mutation into the wild-type protein did not affect signalling downstream of the kinase (Supplementary Figure S2A).

To begin to determine the mechanism by which E596A affects V617F constitutive activity, we determined the 1.54 Å (1 Å = 0.1 nm) crystal structure of V617F E596A JAK2 JH2 bound to Mg^{2+}-ATP (Figure 1E and Supplementary Table S1) (PDB code: 5I4N). The overall structure of the double mutant domain is highly similar to that of the V617F JAK2 JH2 (PDB: 4FVR; RMSD 0.45 Å; Figure 1D). Remarkably, neither the conformation of F537, F595, F617 nor αC were affected by the E596A mutation. These results led us to surmise that E596A was suppressing the effects of V617F by modulating interactions with other domains of JAK2 such as JH1.

Replacement of residue 596 with a basic residue efficiently inhibits JAK2 V617F constitutive activity without impairing cytokine inducibility

To gain additional insight into the role played by E596 in V617F-mediated activation, we probed the chemical basis of the effects of E596 by mutating it to amino acids with different physical properties. We tested the effect of the E596X mutations in the context of the V617F mutant using transcriptional assays as above (Figure 2A). Unexpectedly, neither replacement of E596 with polar (Q) or large aliphatic (W, L) amino acids significantly decreased constitutive activity, suggesting that the E596A mutation is not disrupting a salt bridge. Of the mutants tested, besides alanine, only basic residue substitutions (E596K and E596R) efficiently inhibited JAK2 V617F without affecting Epo-inducible signalling (Figure 2B). Substitution with arginine was the most potent inhibitory mutation that restored the wild-type phenotype (Figures 2A and 2B). In contrast, the conservative E596D mutation substantially increased the constitutive activity of JAK2 V617F (85 % increase) (Figure 2A). Of interest, this substitution is not activating on its own (Supplementary Figures S2B and S2C). As replacement of the glutamate by a shorter negatively charged residue, aspartate, strongly increased V617F activation, this caused us to hypothesize that a negative charge at position 596 is required to support JAK2 V617F-mediated activation. We then confirmed the behaviour of our mutants in a functional assay. BaF3-EpoR cells were transduced with the set of JAK2 V617F double mutants and sorted for similar levels of GFP.

© 2016 The Author(s). Published by Portland Press Limited on behalf of the Biochemical Society.

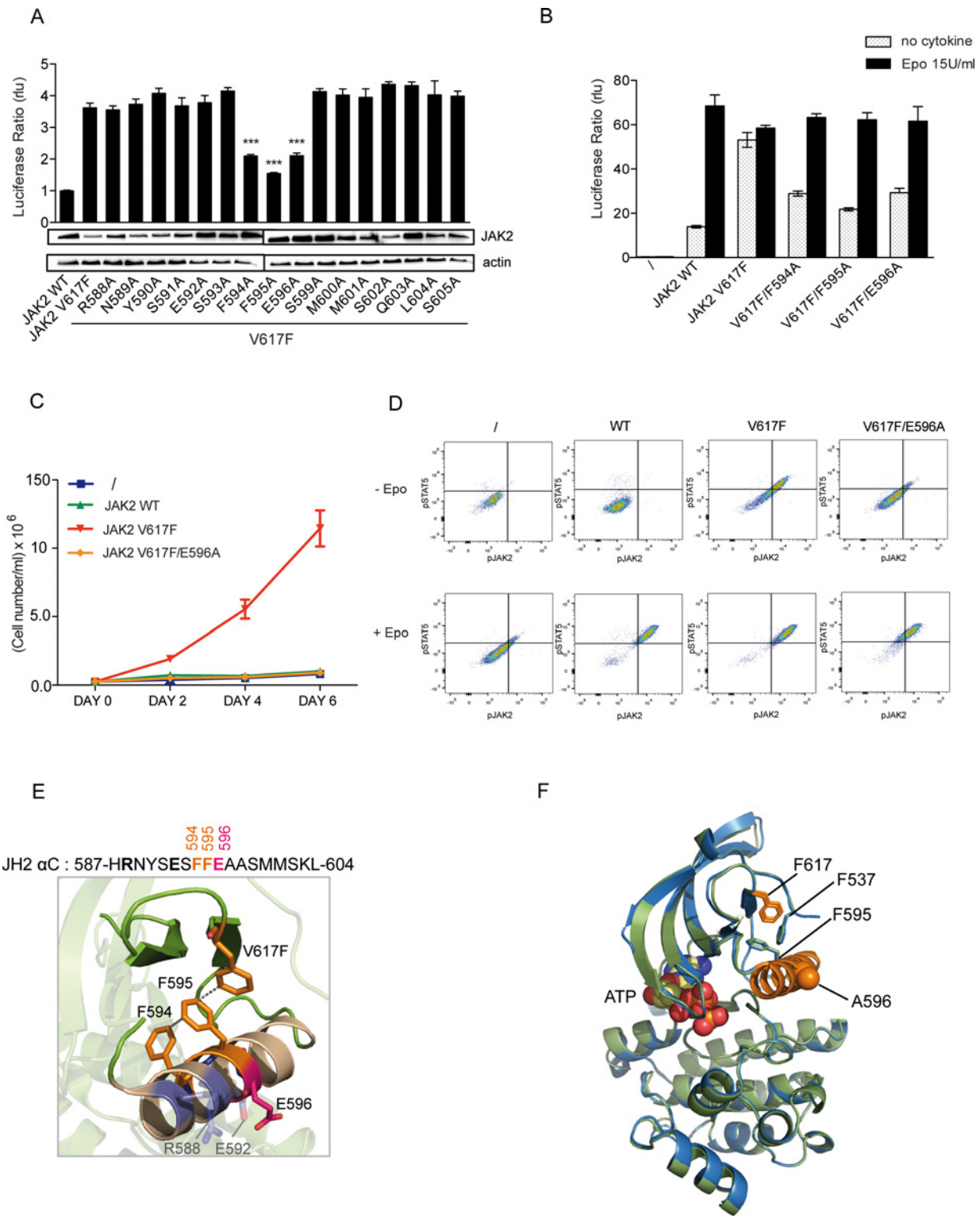

Figure 1 Alanine scanning of the JH2 helix αC of JAK2 V617F

(**A**) γ2A cells were transiently transfected with EpoR, STAT5, pRL-TK, STAT5 luciferase reporter Spi_Luc and the JAK2 variants. Transcriptional activity measurement shows that mutation of F594, F595 and E596 affects the basal activity of JAK2 V617F. Shown are means ± S.E.M. of the mean for three independent experiments done in triplicate (*$P < 0.05$, **$P < 0.01$, ***$P < 0.001$; Dunnett's multiple comparison test). rlu, relative light units. Levels of total JAK2 were analysed in γ2A cells by Western blot. (**B**) Transcriptional activity measurement in the presence of Epo revealed that substitution of E596 still allows normal Epo-induced response similar to JAK2 WT. (**C**) BaF3-EpoR stably expressing JAK2 WT, JAK2 V617F or JAK2 V617F/E596A and the parental cell line were washed and allowed to grow in the absence of cytokine for proliferation assay. Cell numbers were recorded over a period of 6 days with a coulter cell counter (cell numbers = average

© 2016 The Author(s). Published by Portland Press Limited on behalf of the Biochemical Society.

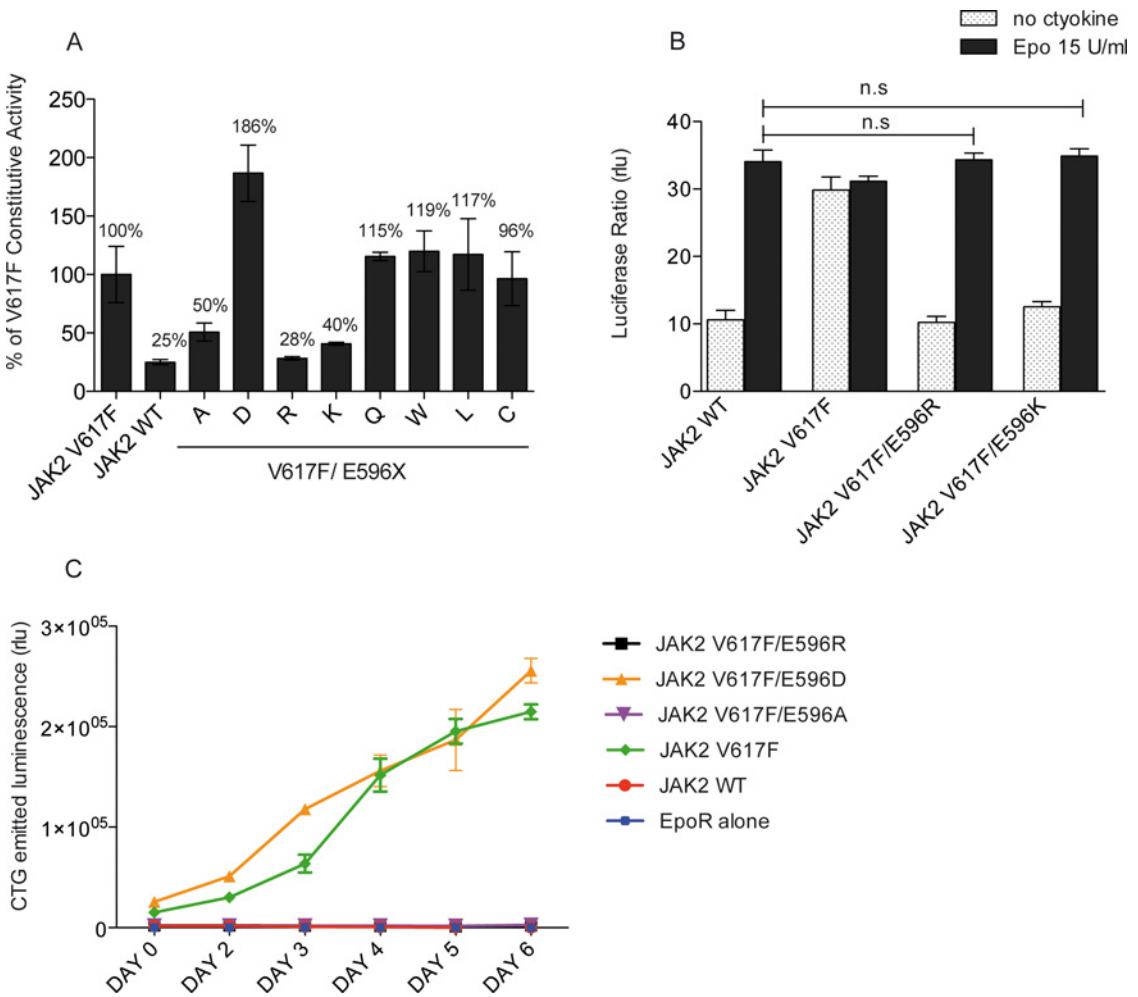

Figure 2 Investigation of the nature of the interaction mediated by E596 in V617F activation

(**A**) STAT5 transcriptional activity was measured in γ2A cells by luciferase assay. Mutation of E596 to either arginine or lysine induces a decrease in constitutive activity of JAK2 V617F up to 71 % and 60 % respectively whereas substitution to aspartate increases the activity of the mutant protein up to 86 %. The activity of the wild-type JAK2 amounted to 25 % of the activity of JAK2 V617F. Shown are means for three independent experiments each performed in triplicate and data were normalized by taking 100 % as the basal activity of JAK2 V617F. (**B**) Substitution of E596 by protonated residues in JAK2 V617F displays an Epo-induced response similar to JAK2 WT. These two mutants behave like the wild-type JAK2. Shown are means $\pm$ S.E.M. for three independent experiments done in triplicate. n.s, not significant. (**C**) BaF3-EpoR stably expressing JAK2 double mutants were starved for 4 h and allow to grow in a cytokine-free media. The number of living cells was evaluated by ATP measurement during 6 days. Only JAK2 V617F and JAK2 V617F/E596D transform the BaF3 into factor-independent cells. Although E596/K and A mutations prevent autonomous grow of JAK2 V617F.

Cells were starved and allowed to grow in cytokine-free medium for 6 days. Only BaF3 cells expressing JAK2 V617F and JAK2 V617F/E596D were able to proliferate, whereas cells expressing V617F/E596A and V617F/E596R were not (Figure 2C). Next, we determined whether the side chain of the E596R mutant inhibits V617F activity by interacting with the nearby carboxylate of E592. This is not the case since the E596R substitution was also able to inhibit JAK2 V617F/E592A (Supplementary Figure S3). In conclusion, we found that besides the substitution of E596 to alanine, positive residues such as arginine or lysine could be placed at position 596 to specifically inhibit the activity of JAK2 V617F without altering the Epo-inducible activity.

Figure 1 Continued

of triplicates $\pm$ S.D.). Although JAK2 V617F gives a proliferative advantage (red line) to the BaF3-EpoR cells, the E596A mutation prevents autonomous growth of the oncogenic JAK2 V617F (orange line). (**D**) The same cell lines were subjected to phospho-flow cytometry to assess the activation of STAT5 and JAK2 in the cells. In the absence of Epo, only BaF3 transfected with JAK2 V617F exhibit phosphorylation of STAT5 and JAK2. The double mutant JAK2 V617F/E596A prevents constitutive activation of STAT5 and JAK2 while triggering good signalling in response to Epo. (**E**) In JAK2 V617F JH2 domain, F595, F594 and F617 (orange) form an aromatic $\pi-\pi$ stacking leading to a change of conformation of JH2 αC responsible for the activation of the kinase domain. E596 (pink) is located on the opposite helical face with two other charged residues R588 and E592 (grey). Position of E596 has been modelled based of the structure of JH2-WT as atoms from its side chain are missing (PDB: 4FVR). (**F**) Crystal structure of JAK2 JH2 V617F/E596A (green) (PDB: 5I4N) overlapped with that of JAK2 V617F (blue) (PDB: 4FVR). ATP is shown in yellow spheres. The conformations of F537, F595 and F617 (stick diagrams) and the αC (orange) are essentially identical in the two structures. The Western blot shown in (**A**) is a representative of three independent experiments. Data presented in (**C**) and (**D**) are representative of two independent experiments.

© 2016 The Author(s). Published by Portland Press Limited on behalf of the Biochemical Society.

Homologous E596R substitutions in JAK1 (E637R) and TYK2 (E657R) decrease constitutive signalling of mutant proteins

Other JAK family members are activated by mutations analogous to V617F, namely V658F in JAK1 and V678F in TYK2 [37]. In addition, the glutamate at position 596 is conserved in all the JAKs (Figure 3A). Substitutions similar to E596R in JAK2 were introduced into JAK1 and TYK2 in order to demonstrate the relevance of this inhibitory mechanism to these proteins. For the JAK1 V658F mutant, we used JAK1-deficient U4C cells [28], where the STAT1/3/5 reporter pGRR5 was transfected along with the JAK1 variants and the chimeric receptor EpoR/gp130 (consisting of the EpoR extracellular domain and gp130 transmembrane and intracellular domain [38]). In U4C cells, co-transfection of EpoR/gp130 with JAK1 restores Epo-mediated activation of STAT5 (Figure 3B) whereas JAK1 V658F drives constitutive STAT5 signalling. Interestingly, JAK1 E637R mutation decreases the constitutive signalling of the mutant as we observed with JAK2 V617F. To test the activity of TYK2 V678F double mutant, we used TYK2-deficient 11.1 cells [26,27]. The STAT3 reporter, pGL3bPpr2_Luc [39] was used to assess the activity of the TYK2 variants co-transfected with the thrombopoietin receptor (TpoR) in 11.1 cells[37] (Figure 3C). Although TYK2 V678F leads to STAT3 signalling in the absence of cytokine, the double mutant V678F/E657R does not, consistent with what we observed for both JAK2 and JAK1. Placement of an arginine at the position analogous to E596 in the JH2 αC can significantly lower the hyperactivity of JAK1 and TYK2 V617F-like mutants to a basal level similar to wild-type protein without compromising cytokine-mediated signalling. Hence, this inhibition approach might also be relevant for JAK1 V658F-drive n adult T-cell lymphoblastic leukaemia (T-ALL) [40,41].

Interfacial placement of arginines along JH2 αC blocks V617F-mediated activation

Based on the preceding findings, we hypothesized that introducing positively charged residues in the vicinity of E596 would be similarly inhibitory. Residues 592, 596 and 600 are located on the same solvent-exposed face of αC, opposite to F595 and proposed to face JH1. After analyses of the available coordinates [11,12] and modelling to visualize where arginines would likely point toward the kinase domain, we also selected position 599. Arginine substitutions of the targeted residues were introduced into JAK2 V617F and the activity of these mutants was assessed by luciferase assays and Western blotting in JAK2 deficient cells (Figures 4A and 4B). Remarkably, arginines placed at positions 592 and 599, like the E596R mutation, could also drastically decrease the pathogenic activation of JAK2 V617F (Figure 4A), whereas the M600R substitution exhibited a more modest effect. Most importantly, all the double mutants were able to induce STAT5 transcriptional activity in response to Epo stimulation to the same extent as the wild-type JAK2 (Figure 4A). Arginine substitutions at positions 592, 599 and 600 also inhibited the hyper-phosphorylation of Y1007/1008 of JAK2 V617F in the absence of Epo (Figure 4B). Phosphorylation of the double mutants was only triggered after Epo stimulation, albeit to varying degrees. We then investigated the effect of arginine substitutions on the activity of the mutant JAK2 V617F in stably expressing BaF3-EpoR and examined the ability of these mutations to reduce the autonomous growth triggered by JAK2 V617F as above (Figure 4C). All the cell lines were able to grow in the presence IL-3 or Epo. After washing, cells were grown in cytokine-free medium for 5 days and counted each day. Cytokine withdrawal led to death of cells expressing either JAK2 WT or

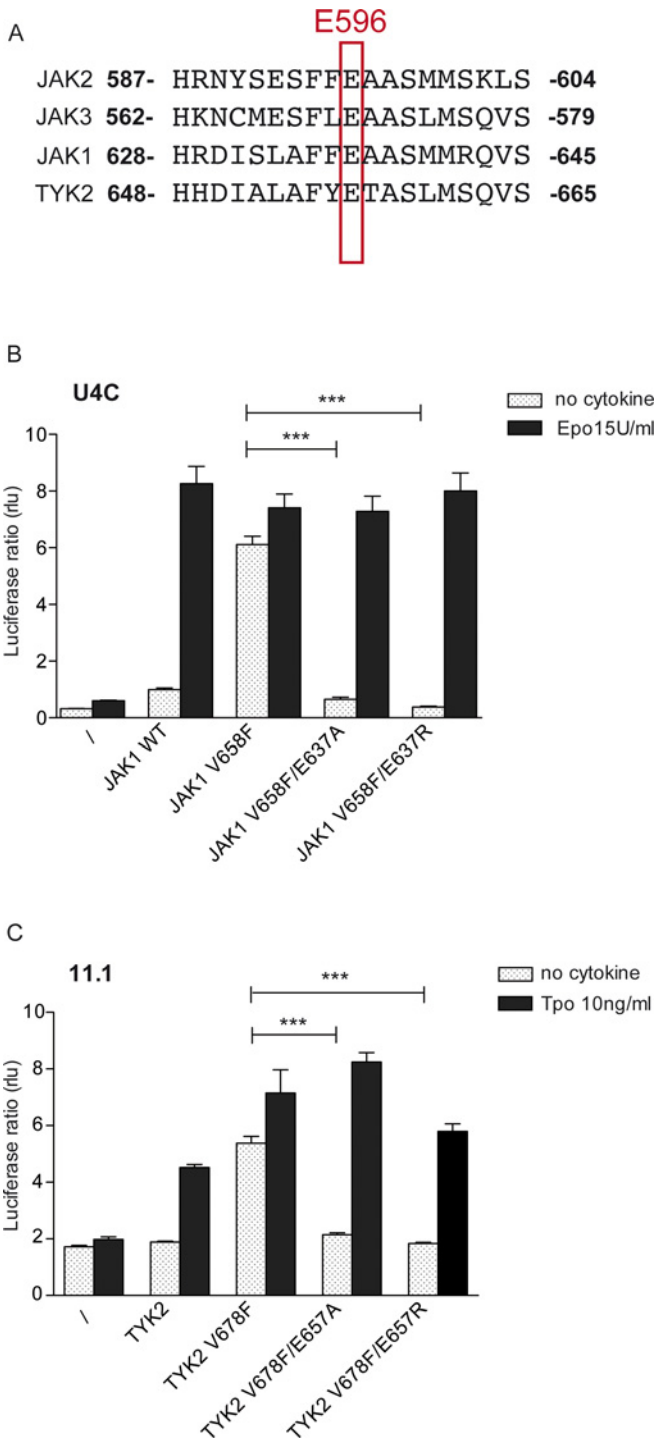

Figure 3 Study of the applicability of the inhibitory substitution to other JAKs

(**A**) Alignment of the JH2 αC sequence of JAKs. A glutamate at position 596 is conserved in other JAK family members. (**B**) JAK1 deficient cells, U4C, were transfected with the JAK1 variants and a chimaeric receptor EpoR/gp130, allowing stimulation by Epo and intracellular binding of two JAK1 molecules signalling in a homodimeric complex. STATs transcriptional activity was measured using pGRR5 reporter. Similarly to JAK2 V617F, its homologous JAK1 V678F could be inhibited by replacement of the glutamate by either alanine or arginine, but still allow normal response to Epo. (**C**) TYK2 deficient cells, 11.1 were transfected with TpoR and the TYK2 variants. STAT3 transcriptional activity was monitored using pGL3bPpr2_Luc reporter. A profound decrease in constitutive activity is observed by substitution of E657 by alanine or arginine. Shown in (**B**) and (**C**) are average units + S.E.M. for three independent experiments performed in triplicate (***$P < 0.0001$, Student's unpaired t test with unequal variance).

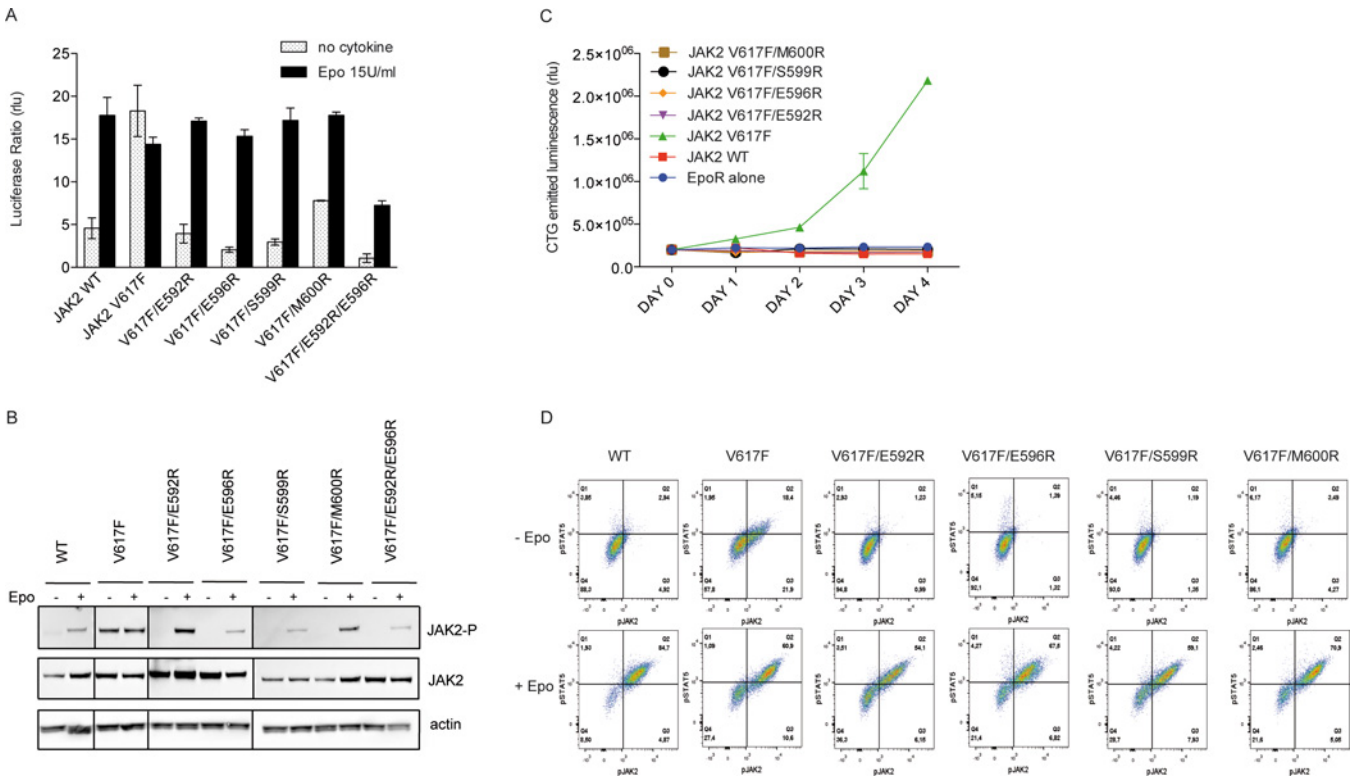

Figure 4 Modulation of JAK2 V617F activity via arginine placement on the JH2 αC

(**A**) Luciferase assay performed in JAK2 deficient cells, γ2A, reveals that arginines placed at either position 592, 596, 599 can achieve significant decrease in the activity of the mutant, whereas a modest decrease is observed with M600R. (**B**) Y2A cells were transiently transfected with EpoR and the JAK2 variants. The whole cell lysate was analysed by Western blot. Analysis of the phosphorylation at Y1007/1008 reveals that arginines placed at different interfacial location suppress V617F-mediated hyperactivation, whereas it allows phosphorylation of JAK2 activation loop after stimulation with Epo. (**C**) BaF3-EpoR cells stably expressing the JAK2 V617F with additional arginine mutation were no longer able to grow in the absence of cytokine. (**D**) Activation of JAK2 and STAT5 was monitored in the BaF3 cell lines by phospho-flow cytometry. JAK2 V617F cells exhibit activation of STAT5 and JAK2 in the absence of cytokine whereas this effect is suppressed by the arginine placement at positions 592, 596, 599 and 600. Cells expressing the JAK2 V617F inhibited forms respond nicely to Epo stimulation. Data presented in (**A**), (**B**) and (**C**) are representative of three independent experiments. Data presented in (**D**) are representative of two independent experiments.

JAK2 double mutants, whereas JAK2 V617F expressing cells survived and proliferated (Figure 4C). In order to verify that the double mutants expressing BaF3 cells respond to Epo simulation, we measured the levels of phosphorylation of STAT5 (Y694) and JAK2 (Y1007/Y1008) before and after stimulation with 50 unit/ml of Epo by flow cytometry (Figure 4D). Although BaF3 JAK2 V617F exhibited phosphorylation of STAT5 and JAK2 in the absence of cytokine, BaF3 JAK2 WT and the E592R, E596R, S599R and M600R JAK2 double mutants did not. In contrast, these cells only displayed STAT5 and JAK2 phosphorylation after Epo stimulation.

JAK2 V617F activity is abolished through modulation of the SH2-JH2 linker C-terminus

The flexible linker between the SH2-like and JH2 domains is involved in the regulation of JAK2 activity [22,23], and was observed to be in the vicinity of V617 and αC by MD simulation [11]. Remodelling of this linker has also been observed in the crystal structure of JAK1 JH2-V658F, where F658 induces a phenylalanine-flipped rearrangement of the linker residue F575 (F537 in JAK2) [19]. Curiously, several residues located in this linker have been associated with clinically observed gain-of-function mutations, namely exon 12 mutations [42]. Hence, we extended our study to the SH2-JH2 linker and screened for residues that are critical for the activity of JAK2 V617F. We used a set of mutants where residues from 501 to 544 in groups of three were substituted with alanine [22] and introduced the mutation V617F. We examined the basal activity of these mutants by Western blot for phosphorylation at Y1007/1008 of JAK2 in transiently transfected γ2A cells (Figure 5A). An absence of phosphorylation was observed for alanine mutants in the N-terminal part of the linker, consistent with previous data obtained in wild-type JAK2 [22]. Indeed, the linker N-terminal fragment was shown to be essential for interaction with the EpoR [22] and it is known that cytokine receptor binding is required for constitutive activation of JAK2 V617F [43,44]. In contrast, the C-terminal part of the linker appears to be specifically required for V617F activity. Mutation of residues from Q534 to L545 significantly reduced JAK2 V617F phosphorylation but not wild type [22]. Next, using structure-guided mutagenesis, we individually mutated residues in the linker C-terminal segment to determine which amino acids are involved in V617F activation process (Supplementary Figure S4A). First, we confirmed that mutation F537A strongly impaired the constitutive activity of the mutant, as has been previously demonstrated [19], without impeding Epo normal response (Figures 5B and 5C). Secondly, we found that mutations K539E and E543/D544 to KK (EDtKK) can also uncouple V617F from cytokine-induced activation, similarly to E596R (Figures 5B and 5C). It was earlier demonstrated that the negatively charged ED motif (E543/D544) was involved in

© 2016 The Author(s). Published by Portland Press Limited on behalf of the Biochemical Society.

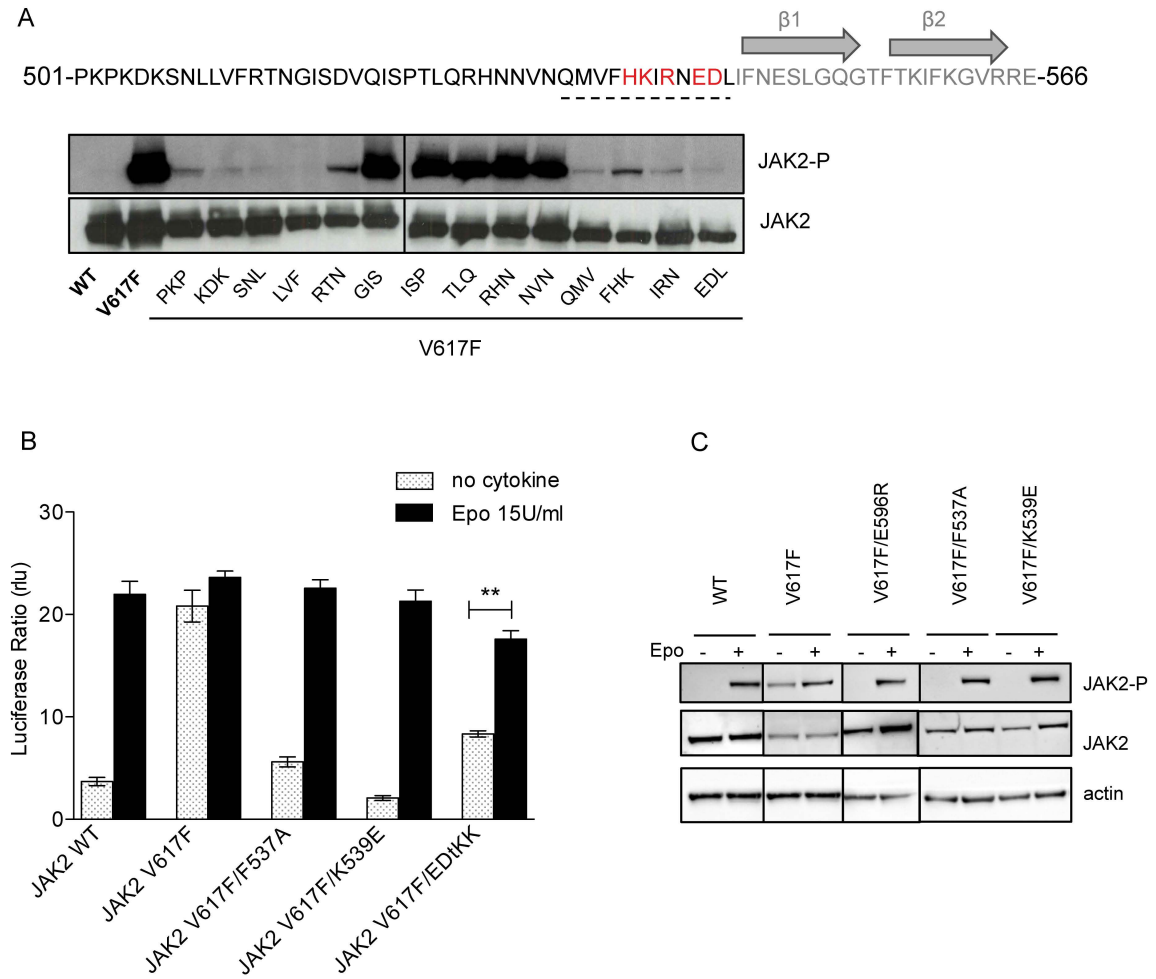

Figure 5 JAK2 V617F-mediated hyperactivation is suppressed by modulation of the SH2-JH2 linker

(**A**) The sequence of the linker between the SH2-like and JH2 is represented above. JAK2 V617F constucts containing alanine-scanning mutations in the SH2-JH2 linker (from PKP/AAA to EDL/AAA) were expressed in JAK2 deficient cells and their levels of activity were assessed by Western blot using anti-phospho JAK2 (Y1007/Y1008) antibodies. JAK2 V617F basal activity is abolished by mutation of the linker N-terminal region and C-terminal region. Mutation of the middle portion sustains phosphorylation of JAK2 V617F. C-terminal region of the linker is important to maintain hyperactivity of JAK2 V617F and contains several charge residues that have been associated with diseases (red). (**B**) STAT5 transcriptional activity measurements by luciferase assay in γ2A show that F537A, K539E strongly decrease V617F, whereas E543/D544KK do so to a lower extent. All the three mutants preserved a normal Epo response. Shown are average units + S.E.M. for three independent experiments performed in triplicate (**$P < 0.01$, Student's unpaired t test with unequal variance). (**C**) Western blot analysis of the three inhibited forms of JAK2 V617F. JAK2 V617F/K539E and JAK2 V617F/F537A were transfected in Y2A and were assessed for activity. Both proteins exhibit a similar decrease in constitutive activity then JAK2 V617F/E596R and a marked response to Epo. Western blots shown in (A) and (C) are representative of three independent experiments.

the auto-inhibitory regulation of JAK2 [22] and its deletion has been associated with MPN [42]. Unexpectedly, mutation of this ED motif can either increase JAK2 WT (Supplementary Figure S4B) or decrease JAK2 V617F basal activity (Figure 5B). Since F537A and K539E preserve the Epo inducibility of JAK2 V617F (Figures 5B and 5C), the inhibition of V617F is not due to a lack of interaction of the JAK with EpoR. Here again, with K539E, we show that a charge inversion can uncouple V617F from cytokine-induced activation of JAK2.

E596R inhibits activation induced by the V617F circuit but not other activating JAK2 mutations relevant for pathology

Our data lead us to hypothesize that the change of conformation of the JH2 αC induced by the mutation V617F rearranges E596, which in turn, triggers a series of activating events via the C-terminal end of the SH2-JH2 linker. Based on inspection of the recently described MD-based model of JAK2 JH1/JH2 [11], we identified several potential networks of residues that could enable inter-domain communication via the SH2-JH2 linker. One of these proposed activation circuits would be switched-on by F537, and would contain E543/D544 (SH2-JH2 linker C-terminal end), D569/Y570 (JH2 N-terminus, β2–β3 loop) and two kinase domain residues K857 (JH1 N-terminus, β1–β2 loop, G-loop) and K883 (JH1 N-terminus, strand-β3) (Figures 6A and 6B). In the context of JAK2 V617F, E596 clashes with the C-terminus of the SH2-JH2 linker, on one hand de-stabilizing the inhibitory JH2–JH1 interface via the E543/D544 and downstream β2–β3 JH2 N-terminus (D569/Y570) and on the other hand allowing F537 (liberated from its interaction with helix αC phenylalanine residues by the V617F mutation [19]) to clash with K857 of JH1 (Supplementary Figure S5C).

Were this activation circuit model to be correct, we would make several predictions: (i) the participants in this circuit, except for the switch F537 would, when appropriately mutated,

© 2016 The Author(s). Published by Portland Press Limited on behalf of the Biochemical Society.

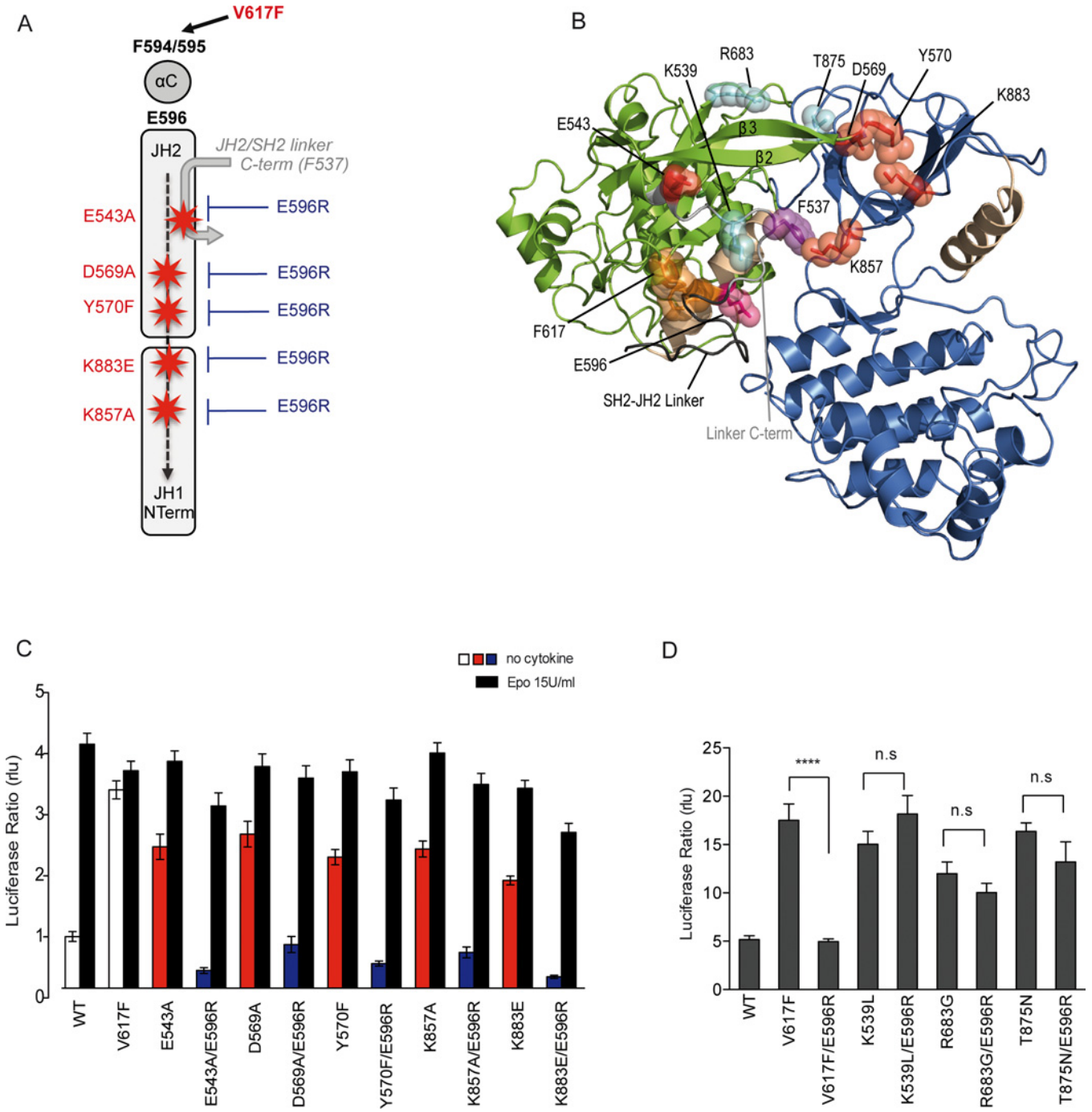

Figure 6 V617F-induced activation circuit

(**A**) Schematic representation the V617F activation circuit. (**B**) Model of the interface between JH1 (blue) and JH2 (green) from MD simulation data (11). E596 (pink) interacts with the C-terminus of the SH2-JH2 linker (grey) and initiates a cascade of activating events involving residues F537 (purple), E543, D569, Y570, K883, K857 (red). (**C**) Y2A cells were transiently transfected with the JAK2 variants and STAT5 transcriptional reporter. E596R mutation decreases the activity of the different hyperactive JAK2 mutants that comprise the V617F activation circuit without impairing Epo normal response. (**D**) Y2A cells were transiently transfected with several JAK2 oncogenic mutants and basal transcriptional activity was measured with STAT5 transcriptional reporter, Spi_Luc. K539L, T875N and R683G all induce constitutive signalling of JAK2. No significant decrease in the constitutive activation of these mutants is observed when substituting E596 with either alanine or arginine. Shown in (C) and (D) are average units + S.E.M. for three independent experiments performed in triplicate (****$P < 0.0001$, n.s, not significant; Dunn's multiple comparison test).

induce constitutive activation; (ii) the E596R mutation would suppress this activation like it suppresses V617F; (iii) activating mutations in JAK2 unrelated to this activating circuit would not be inhibited by the E596R mutation. Indeed, we show that mutants E543A, D569A, Y570F, K857A and K883E predicted by our modelling to be in the V617F circuit, are all constitutively active (Figure 6C). Importantly, this hyperactivity is prevented by the E596R mutation, which is remarkable, especially for the JH1 mutation K857A, which is far away from helix αC (Figures 6B and 6C).

Next, we introduced the E596R mutation in other activated forms of JAK2 previously shown to be active and exhibit

© 2016 The Author(s). Published by Portland Press Limited on behalf of the Biochemical Society.

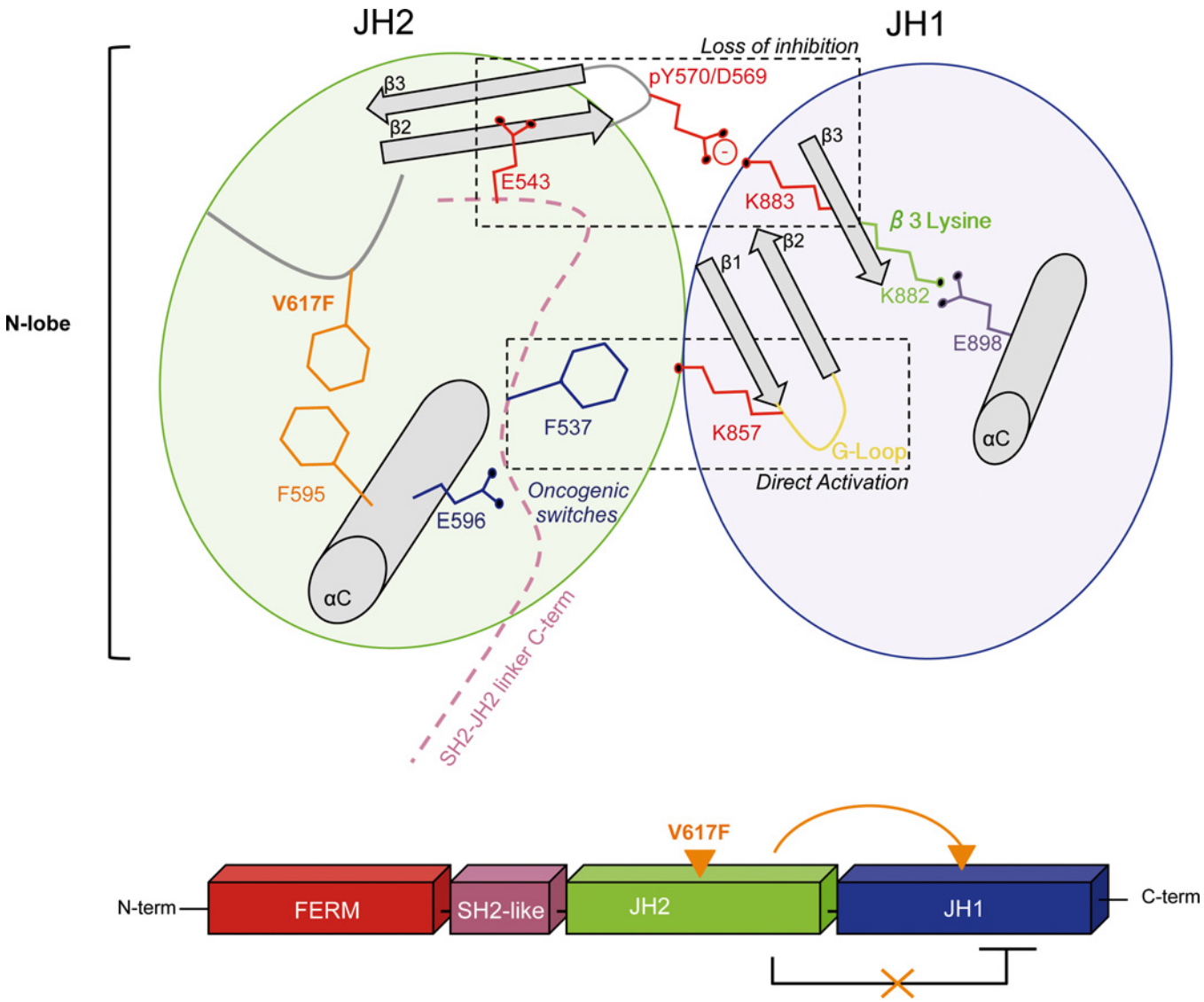

Figure 7 Schematic representation of the V617F-induced activation circuit

Activation of JAK2 V617F is suggested to result from the combination of several activating events that are triggered by the mutation V617F and transmitted through two switch residues E596 and F537. These activating events are part of two different molecular mechanisms that, when combined, will result in the strong activity of the mutant. The first mechanism is the disruption of one of the inhibitory interactions meditated between JH2 and JH1 (pY570-K883) and the second one, is the positive regulatory interaction mediated by F537 (SH2-JH2 linker C-term) on K857 (JH1 N-term).

STAT5 constitutive signalling [45–47], but that are placed outside of the V617F circuit. These mutations include the exon 12 polycythaemia vera (PV) mutation K539L, located in the SH2-JH2 linker of JAK2 [45], as well as the JAK2 R683S mutation, located between the JH2 N- and C-lobes which is found in B-cell acute lymphoblastic leukaemia [47]. We also examined the JAK2 T875N mutant, associated with a megakaryoblastic leukaemia line, located in the $\beta 2$–$\beta 3$ loop of the kinase domain of JAK2 [46] (Figure 6B). All the mutants exhibited STAT5 signalling in the absence of Epo (Figure 6D). Remarkably, E596R exclusively impaired the constitutive activity of V617F and not the activity of the other mutants. Considering the proximity of K539L to V617F (15 Å) (Figure 6B), these results strongly support the specificity of the molecular process involving E596 in the activation process of JAK2 by the V617F mutation.

Overall, our results support the notion that V617F changes the conformation of the αC of JH2 repositioning E596 and leading to changes involving F537, E543/D544 (SH2-JH2 linker C-terminus), D569/Y570 (JH2 N-terminus) and eventually JH1 kinase residues K857/K883 (JH1 N-terminus), which could activate the kinase activity of JH1 (Supplementary Figures S5A–S5C).

DISCUSSION

The prevailing model is that JH2 maintains JAK2 in its auto-inhibited state by restraining JH1, whereas the oncogenic V617F JH2 mutation releases the structural hindrance on JH1 enabling the kinase domain to adopt an active conformation. A second activating event contributes to establish the high and persistent JAK2 V617F activation [11,16,48]. This activation process seems to be first initiated by modulation of the JH2 αC, where the main conformational changes can be detected in the X-ray crystal [16].

© 2016 The Author(s). Published by Portland Press Limited on behalf of the Biochemical Society.

We addressed how the molecular events induced by V617F around JH2 helix C are transmitted to the kinase domain.

Our main findings are that: (i) a glutamic acid (E596) of the JH2 αC is an essential mediator of JAK2 V617F pathogenic activity. This is also the case for JAK1 V658F and TYK2 V678F, suggesting a common activation mechanism by V $\rightarrow$ F mutations in these three proteins. We suggest that E596 participates in the activation of V617F by making a new contact that is only present in the JAK2 V617F conformation, that is likely a steric clash with SH2-JH2 linker C-terminal amino acid backbones; (ii) the V617F mutation causes residues from αC to collaborate with the SH2-JH2 linker to trigger JH1 kinase domain activity and (iii) JAK2 V617F constitutive activity can be uncoupled from cytokine-induced signalling by either placement of positive charges along the JH2 αC or by charge inversion on the SH2-JH2 linker C-terminus, which contributes to activation.

By extensive mutagenesis of the SH2-JH2 linker and of the N-lobes of JH1 and JH2, we propose a defined circuit for JAK2 V617F activation where a sequential set of activating events propagates from JH2 αC to JH1 active site (Figure 6A). We propose that the JAK2 V617F activation derives from the combination of small activating events, which is relevant for the potency of this pathologic mutant. We show that mutations in the nodes of this circuit induce constitutive activation and, importantly, in all cases, the E596R mutation prevents activation. E596R appears to both restore an inhibitory JH2–JH1 interaction and prevent the final step of JH1 activation by V617F. In support of the former, we tested the effect of the E596R mutation on several newly described JH1 activating mutations which break the JH1/JH2 inhibitory interface [11]. E596R could significantly reduce the hyperactivity of such JAK2 mutants, namely K883E and R947E (Supplementary Figure S6A). Since only R947 appears to possibly be in the vicinity of E596 (7 Å), with the K883 residue on JH1 being far from the JH2 αC (28 Å), (Supplementary Figure S6B), the inhibitory effect of E596R is likely mediated by intermediate, possibly SH2-JH2 C-terminus linker residues. Importantly, other activating JAK2 mutations (K539L, R683G, T875N), which affect residues not involved in the V617F-circuit, are not inhibited by the E596R mutation.

Overall, our data indicate that V617F activation results from both loss of the basal auto-inhibition and from a positive regulatory interaction directly mediated by JH1. Indeed, the circuit we identify only partially overlaps with residues that belong to the inhibitory interface previously identified, such as the pair pY570-K883 [11]. In addition, activation involves residue K857 via a different mechanism. We hypothesize that the conformation of K857 in JH1 is influenced by that of the SH2-JH2 linker residue F537. In our model the side chain of F537 comes in close proximity of K857 (Supplementary Figure S5C). This is possible because F537 is liberated from its interaction with F595 by the novel aromatic stacking interaction between F617 and F594/F595 in the V617F context [19]. Mutation of K857 itself leads to activation (Figure 6C). This particular residue is predicted to contribute to the stabilization of the G-loop in an inactive conformation (as is observed in the DFG-out conformation of JH1, PDB: 3UGC; Supplementary Figure S5B). Perturbation of K857 by the linker residue F537 would destabilize the G-loop and favour an active conformation (as is observed in the DFG-in conformation of JH1, PDB: 2B7A; Supplementary Figure S5B). Figure 7 outlines our model of V617F activation circuit. The change of conformation induced in the αC of JH2 by V617F will affect the position of the first oncogenic switch E596, which will clash with the SH2-JH2 linker C-term. The destabilized linker will then trigger two sets of molecular events. The first one will be initiated by a second oncogenic switch, the linker residue F537 (previously described in [19]) that likely contacts K857 in JH1. The second set of events will be initiated by E543 that is predicted to destabilize the position of the JH2 β2–β3 and the inhibitory salt bridge between pY570 and K883 [11] allowing formation of the key salt bridge between K882 (β3 lysine) and the αC glutamate E898 in JH1. Collectively, these conformational changes are suggested to favour an active conformation of JH1.

The αC of JH2 is a typical amphipathic helix where amino acids with hydrophilic side chains extend from one side (R588, E592, E596) whereas hydrophobic side chains of F594 and F595 extend from the opposite side. Since placement of arginines on the same helical face specifically reduced the constitutive activity of JAK2 V617F, it implies that this particular helical interface plays a specific role in mediating V617F activation. Furthermore, the negative E596 seems to play a central role in supporting the activation by V617F as its presence is required for the mutant activity. In JAK2 V617F, the F594/F595/F617 stacking participates in the stabilization of the JH2 αC. However, MD simulations showed that these contacts are only transient [16], so stabilization of this helix seems to require other contacts that might involve SH2-JH2 linker C-terminus residues or intermolecular interactions between two pseudokinase domains as was observed in the non-crystallographic dimer of JAK1-JH2 crystal structure [19].

Our data and others [11,22] established the importance of the SH2-JH2 linker in both JAK2 WT and V617F basal activity. E596A/R mutations are predicted to re-build one of the autoinhibitory JH2/JH1 contacts and to directly suppress the positive regulatory interaction between F537 and K857. Whether the autoinhibitory JH2/JH1 interaction occurs in *cis* or in *trans* has been debated for the past years and lines of evidence supporting both models have been provided [11–14]. Our study supports the *cis* model in which JH2 requires close proximity with the kinase domain to exert an intrinsic auto-inhibition. Nevertheless, we cannot exclude that both inhibitory interfaces might co-exist and represent two levels of auto-inhibition in the JAK2-receptor complex.

One surprising result is that our inhibitory mutations in the JH2 αC do not affect cytokine-induced signalling, which offers intriguing possibilities from a therapeutic perspective. Efforts have been made into the development of allosteric inhibitors [49], however ATP mimicking small molecules prevail in the treatment of cancer. But to date, none of these compounds were able to achieve uncoupling of the oncogenic from the normal activities of the protein kinases such as JAK2. Our results indicate that targeting the region around residue E596 could lead to such effect, thereby avoiding the problematic side effects related to the loss of the normal function of the kinase. Molecules such as α-helix mimetics could be designed to target the JH2 αC face with E596, and introduce a positive charge in the vicinity of the linker and JH1. These compounds would destabilize the activated state of V617F, but would have negligible effects on the wild-type protein. This strategy is not only relevant for JAK2 V617F, but also for the JAK1 V658F mutant associated with adult T-ALL. Such molecules would not affect the wild-type JAK2 allowing to use these molecules at higher doses compared with what is used now in the clinic.

AUTHOR CONTRIBUTION

Stefan Constantinescu and Emilie Leroy conceived and designed the study, interpreted the data and wrote the paper. Emilie Leroy, Alexandra Dusa, Didier Colau and Céline Mouton performed the experiments. Andrew Shiau and Amir Motamedi determined the structure.

© 2016 The Author(s). Published by Portland Press Limited on behalf of the Biochemical Society.

Emilie Leroy, Stefan Constantinescu, Lily Huang and Andrew Shiau analysed the data. Xavier Cahu performed flow cytometry and phospho flow analysis.

ACKNOWLEDGEMENTS

We thank Dr O. Silvennoinen and D. Ungureanu from the University of Tampere, Finland, for providing the pFAST-Bac-JH2 plasmid. Lidvine Genet and Céline Mouton for expert technical assistance. Nicolas Dauguet for expert cell sorting. We thank the Advanced Photon Source NE-CAT (supported by NIH P41 GM103403 and S10 RR029205) for assistance with X-ray data collection.

FUNDING

This work was supported by the Ludwig Institute for Cancer Research, FRS-FNRS [grant number 3.4596.12], the Fondation Salus Sanguinis, Belgium; the Fondation contre le cancer [grant number F/2014/266]; the Actions de Recherche Concertées of the communauté Française de Belgique [grant number ARC10/15-027]; the PAI program Belgian Medical Genetics Initiative [grant number IAP-P7/43]; the FRIA PhD fellowship (to E.L.); and the National Institutes of Health [grant number L089966 (to L.J.H.)].

REFERENCES

1 Akada, H., Akada, S., Hutchison, R.E., Sakamoto, K., Wagner, K.U. and Mohi, G. (2014) Critical role of Jak2 in the maintenance and function of adult hematopoietic stem cells. Stem Cells **32**, 1878–1889 CrossRef PubMed

2 Ghoreschi, K., Laurence, A. and O'Shea, J.J. (2009) Janus kinases in immune cell signaling. Immunol. Rev. **228**, 273–287 CrossRef PubMed

3 James, C., Ugo, V., Le Couedic, J.P., Staerk, J., Delhommeau, F., Lacout, C., Garçon, L., Raslova, H., Berger, R., Bennaceur-Griscelli, A. et al. (2005) A unique clonal JAK2 mutation leading to constitutive signalling causes polycythaemia vera. Nature **434**, 1144–1148 CrossRef PubMed

4 Baxter, E.J., Scott, L.M., Campbell, P.J., East, C., Fourouclas, N., Swanton, S., Vassiliou, G.S., Bench, A.J., Boyd, E.M., Curtin, N. et al. (2005) Acquired mutation of the tyrosine kinase JAK2 in human myeloproliferative disorders. Lancet **365**, 1054–1061 CrossRef PubMed

5 Kralovics, R., Passamonti, F., Buser, A.S., Teo, S.S., Tiedt, R., Passweg, J.R., Tichelli, A., Cazzola, M. and Skoda, R.C. (2005) A gain-of-function mutation of JAK2 in myeloproliferative disorders. N. Engl. J. Med. **352**, 1779–1790 CrossRef PubMed

6 Levine, R.L., Wadleigh, M., Cools, J., Ebert, B.L., Wernig, G., Huntly, B.J., Boggon, T.J., Wlodarska, I., Clark, J.J., Moore, S. et al. (2005) Activating mutation in the tyrosine kinase JAK2 in polycythemia vera, essential thrombocythemia, and myeloid metaplasia with myelofibrosis. Cancer Cell **7**, 387–397 CrossRef PubMed

7 Verstovsek, S., Mesa, R.A., Gotlib, J., Levy, R.S., Gupta, V., DiPersio, J.F., Catalano, J.V., Deininger, M., Miller, C., Silver, R.T. et al. (2012) A double-blind, placebo-controlled trial of ruxolitinib for myelofibrosis. N. Engl. J. Med. **366**, 799–807 CrossRef PubMed

8 Harrison, C., Kiladjian, J.J., Al-Ali, H.K., Gisslinger, H., Waltzman, R., Stalbovskaya, V., McQuitty, M., Hunter, D.S., Levy, R., Knoops, L. et al. (2012) JAK inhibition with ruxolitinib versus best available therapy for myelofibrosis. N. Engl. J. Med. **366**, 787–798 CrossRef PubMed

9 Vannucchi, A.M., Kiladjian, J.J., Griesshammer, M., Masszi, T., Durrant, S., Passamonti, F., Harrison, C.N., Pane, F., Zachee, P., Mesa, R. et al. (2015) Ruxolitinib versus standard therapy for the treatment of polycythemia vera. N. Engl. J. Med. **372**, 426–435 CrossRef PubMed

10 Saharinen, P. and Silvennoinen, O. (2002) The pseudokinase domain is required for suppression of basal activity of Jak2 and Jak3 tyrosine kinases and for cytokine-inducible activation of signal transduction. J. Biol. Chem. **277**, 47954–47963 CrossRef PubMed

11 Shan, Y., Gnanasambandan, K., Ungureanu, D., Kim, E.T., Hammaren, H., Yamashita, K., Silvennoinen, O., Shaw, D.E. and Hubbard, S.R. (2014) Molecular basis for pseudokinase-dependent autoinhibition of JAK2 tyrosine kinase. Nat. Struct. Mol. Biol. **21**, 579–584 CrossRef PubMed

12 Lupardus, P.J., Ultsch, M., Wallweber, H., Bir Kohli, P., Johnson, A.R. and Eigenbrot, C. (2014) Structure of the pseudokinase-kinase domains from protein kinase TYK2 reveals a mechanism for Janus kinase (JAK) autoinhibition. Proc. Natl. Acad. Sci. U.S.A. **111**, 8025–8030 CrossRef PubMed

13 Brooks, A.J., Dai, W., O'Mara, M.L., Abankwa, D., Chhabra, Y., Pelekanos, R.A., Gardon, O., Tunny, K.A., Blucher, K.M., Morton, C.J. et al. (2014) Mechanism of activation of protein kinase JAK2 by the growth hormone receptor. Science **344**, 1249783 CrossRef PubMed

14 Varghese Leila, N., Ungureanu, D., Liau Nicholas, P.D., Young Samuel, N., Laktyushin, A., Hammaren, H., Lucet, I.S., Nicola, N.A., Silvennoinen, O., Babon, J.J. and Murphy, J.M. (2014) Mechanistic insights into activation and SOCS3-mediated inhibition of myeloproliferative neoplasm-associated JAK2 mutants from biochemical and structural analyses. Biochem. J. **458**, 395–405 CrossRef PubMed

15 Springuel, L., Hornakova, T., Losdyck, E., Lambert, F., Leroy, E., Constantinescu, S.N., Flex, E., Tartaglia, M., Knoops, L. and Renauld, J.C. (2014) Cooperating JAK1 and JAK3 mutants increase resistance to JAK inhibitors. Blood **124**, 3924–3931 CrossRef PubMed

16 Bandaranayake, R.M., Ungureanu, D., Shan, Y., Shaw, D.E., Silvennoinen, O. and Hubbard, S.R. (2012) Crystal structures of the JAK2 pseudokinase domain and the pathogenic mutant V617F. Nat. Struct. Mol. Biol. **19**, 754–759 CrossRef PubMed

17 Lucet, I.S., Fantino, E., Styles, M., Bamert, R., Patel, O., Broughton, S.E., Walter, M., Burns, C.J., Treutlein, H., Wilks, A.F. and Rossjohn, J. (2006) The structural basis of Janus kinase 2 inhibition by a potent and specific pan-Janus kinase inhibitor. Blood **107**, 176–183 CrossRef PubMed

18 Kulagowski, J.J., Blair, W., Bull, R.J., Chang, C., Deshmukh, G., Dyke, H.J., Eigenbrot, C., Ghilardi, N., Gibbons, P., Harrison, T.K. et al. (2012) Identification of imidazo-pyrrolopyridines as novel and potent JAK1 inhibitors. J. Med. Chem. **55**, 5901–5921 CrossRef PubMed

19 Toms, A.V., Deshpande, A., McNally, R., Jeong, Y., Rogers, J.M., Kim, C.U., Gruner, S.M., Ficarro, S.B., Marto, J.A., Sattler, M. et al. (2013) Structure of a pseudokinase-domain switch that controls oncogenic activation of Jak kinases. Nat. Struct. Mol. Biol. **20**, 1221–1223 CrossRef PubMed

20 Wallweber, H.J., Tam, C., Franke, Y., Starovasnik, M.A. and Lupardus, P.J. (2014) Structural basis of recognition of interferon-alpha receptor by tyrosine kinase 2. Nat. Struct. Mol. Biol. **21**, 443–448 CrossRef PubMed

21 Dusa, A., Mouton, C., Pecquet, C. and Herman, M. (2010) Constantinescu SN. JAK2 V617F constitutive activation requires JH2 residue F595: a pseudokinase domain target for specific inhibitors. PLoS One **5**, e11157 CrossRef PubMed

22 Zhao, L., Dong, H., Zhang, C.C., Kinch, L., Osawa, M., Iacovino, M., Grishin, N.V., Kyba, M. and Huang, L.J. (2009) A JAK2 interdomain linker relays Epo receptor engagement signals to kinase activation. J. Biol. Chem. **284**, 26988–26998 CrossRef PubMed

23 Sanz Sanz, A., Niranjan, Y., Hammaren, H., Ungureanu, D., Ruijtenbeek, R., Touw, I.P., Silvennoinen, O. and Hilhorst, R. (2014) The JH2 domain and SH2-JH2 linker regulate JAK2 activity: a detailed kinetic analysis of wild type and V617F mutant kinase domains. Biochim. Biophys. Acta **1844**, 1835–1841 CrossRef PubMed

24 Liu, X., Constantinescu, S.N., Sun, Y., Bogan, J.S., Hirsch, D., Weinberg, R.A. and Lodish, H.F. (2000) Generation of mammalian cells stably expressing multiple genes at predetermined levels. Anal. Biochem. **280**, 20–28 CrossRef PubMed

25 Kohlhuber, F., Rogers, N.C., Watling, D., Feng, J., Guschin, D., Briscoe, J., Witthuhn, B.A., Kotenko, S.V., Pestka, S., Stark, G.R. et al. (1997) A JAK1/JAK2 chimera can sustain alpha and gamma interferon responses. Mol. Cell. Biol. **17**, 695–706 CrossRef PubMed

26 Pellegrini, S., John, J., Shearer, M., Kerr, I.M. and Stark, G.R. (1989) Use of a selectable marker regulated by alpha interferon to obtain mutations in the signaling pathway. Mol. Cell. Biol. **9**, 4605–4612 CrossRef PubMed

27 Velazquez, L., Fellous, M., Stark, G.R. and Pellegrini, S. (1992) A protein tyrosine kinase in the interferon alpha/beta signaling pathway. Cell **70**, 313–322 CrossRef PubMed

28 Muller, M., Briscoe, J., Laxton, C., Guschin, D., Ziemiecki, A., Silvennoinen, O., Harpur, A.G., Barbieri, G., Witthuhn, B.A., Schindler, C. et al. (1993) The protein tyrosine kinase JAK1 complements defects in interferon-alpha/beta and -gamma signal transduction. Nature **366**, 129–135 CrossRef PubMed

29 Seubert, N., Royer, Y., Staerk, J., Kubatzky, K.F., Moucadel, V., Krishnakumar, S., Smith, S.O. and Constantinescu, S.N. (2003) Active and inactive orientations of the transmembrane and cytosolic domains of the erythropoietin receptor dimer. Mol. Cell **12**, 1239–1250 CrossRef PubMed

30 Sliva, D., Wood, T.J., Schindler, C., Lobie, P.E. and Norstedt, G. (1994) Growth hormone specifically regulates serine protease inhibitor gene transcription via gamma-activated sequence-like DNA elements. J. Biol. Chem. **269**, 26208–26214 PubMed

31 Kabsch, W. (2010) Xds. Acta Crystallogr. D Biol. Crystallogr. **66** (Pt 2), 125–132 CrossRef PubMed

32 Winn, M.D., Ballard, C.C., Cowtan, K.D., Dodson, E.J., Emsley, P., Evans, P.R., Keegan, R.M., Krissinel, E.B., Leslie, A.G., McCoy, A. et al. (2011) Overview of the CCP4 suite and current developments. Acta Crystallogr. D Biol. Crystallogr. **67** (Pt 4), 235–242 CrossRef PubMed

33 McCoy, A.J., Grosse-Kunstleve, R.W., Adams, P.D., Winn, M.D., Storoni, L.C. and Read, R.J. (2007) Phaser crystallographic software. J. Appl. Crystallogr. **40** (Pt 4), 658–674 CrossRef PubMed

34 Adams, P.D., Afonine, P.V., Bunkoczi, G., Chen, V.B., Davis, I.W., Echols, N., Headd, J.J., Hung, L.W., Kapral, G.J., Grosse-Kunstleve, R.W. et al. (2010) PHENIX: a comprehensive Python-based system for macromolecular structure solution. Acta Crystallogr. D Biol. Crystallogr. **66** (Pt 2), 213–221 CrossRef PubMed

© 2016 The Author(s). Published by Portland Press Limited on behalf of the Biochemical Society.

35 Müller, K., Amman, H.J., Doran, D.M., Gerber, P.R., Gubernator, K. and Schrepfer, G. (1988) MOLOC: a molecular modeling program. Bull. Soc. Chim. Belg. **97**, 655–667

36 Gnanasambandan, K., Magis, A. and Sayeski, P.P. (2010) The constitutive activation of Jak2-V617F is mediated by a pi stacking mechanism involving phenylalanines 595 and 617. Biochemistry **49**, 9972–9984 CrossRef PubMed

37 Staerk, J., Kallin, A., Demoulin, J-B., Vainchenker, W. and Constantinescu, S.N. (2005) JAK1 and Tyk2 activation by the homologous Polycythemia Vera JAK2 V617F mutation: cross-talk with IGF1 receptor. J. Biol. Chem. **280**, 41893–41899 CrossRef PubMed

38 Hemmann, U., Gerhartz, C., Heesel, B., Sasse, J., Kurapkat, G., Grotzinger, J., Wollmer, A., Zhong, Z., Darnell. Jr, J.E., Graeve, L. et al. (1996) Differential activation of acute phase response factor/Stat3 and Stat1 via the cytoplasmic domain of the interleukin 6 signal transducer gp130. II. Src homology SH2 domains define the specificity of stat factor activation. J. Biol. Chem. **271**, 12999–13007 CrossRef PubMed

39 Eyckerman, S., Waelput, W., Verhee, A., Broekaert, D., Vandekerckhove, J. and Tavernier, J. (1999) Analysis of Tyr to Phe and fa/fa leptin receptor mutations in the PC12 cell line. Eur. Cytokine Netw. **10**, 549–556 PubMed

40 Jeong, E.G., Kim, M.S., Nam, H.K., Min, C.K., Lee, S., Chung, Y.J., Yoo, N.J. and Lee, S.H. (2008) Somatic mutations of JAK1 and JAK3 in acute leukemias and solid cancers. Clin Cancer Res. **14**, 3716–3721 CrossRef PubMed

41 Flex, E., Petrangeli, V., Stella, L., Chiaretti, S., Hornakova, T., Knoops, L., Ariola, C., Fodale, V., Clappier, E., Paoloni, F. et al. (2008) Somatically acquired JAK1 mutations in adult acute lymphoblastic leukemia. J. Exp. Med. **205**, 751–758 CrossRef PubMed

42 Ma, W., Kantarjian, H., Zhang, X., Yeh, C.H., Zhang, Z.J., Verstovsek, S and Albitar, M. (2009) Mutation profile of JAK2 transcripts in patients with chronic myeloproliferative neoplasias. J. Mol. Diagn. **11**, 49–53 CrossRef PubMed

43 Lu, X., Levine, R., Tong, W., Wernig, G., Pikman, Y., Zarnegar, S., Gilliland, D.G. and Lodish, H. (2005) Expression of a homodimeric type I cytokine receptor is required for JAK2V617F-mediated transformation. Proc. Natl. Acad. Sci. U.S.A. **102**, 18962–18967 CrossRef PubMed

44 Lu, X., Huang, L.J. and Lodish, H.F. (2008) Dimerization by a cytokine receptor is necessary for constitutive activation of JAK2V617F. J. Biol. Chem. **283**, 5258–5266 CrossRef PubMed

45 Scott, L.M., Tong, W., Levine, R.L., Scott, M.A., Beer, P.A., Stratton, M.R., Futreal, P.A., Erber, W.N., McMullin, M.F., Harrison, C.N. et al. (2007) JAK2 exon 12 mutations in polycythemia vera and idiopathic erythrocytosis. N. Engl. J. Med. **356**, 459–468 CrossRef PubMed

46 Mercher, T., Wernig, G., Moore, S.A., Levine, R.L., Gu, T.L., Frohling, S., Cullen, D., Polakiewicz, R.D., Bernard, O.A., Boggon, T.J. et al. (2006) JAK2T875N is a novel activating mutation that results in myeloproliferative disease with features of megakaryoblastic leukemia in a murine bone marrow transplantation model. Blood **108**, 2770–2779 CrossRef PubMed

47 Mullighan, C.G., Zhang, J., Harvey, R.C., Collins-Underwood, J.R., Schulman, B.A., Phillips, L.A., Tasian, S.K., Loh, M.L., Su, X., Liu, W. et al. (2009) JAK mutations in high-risk childhood acute lymphoblastic leukemia. Proc. Natl. Acad. Sci. U.S.A. **106**, 9414–9418 CrossRef PubMed

48 Constantinescu, S.N., Leroy, E., Gryshkova, V., Pecquet, C. and Dusa, A. (2013) Activating Janus kinase pseudokinase domain mutations in myeloproliferative and other blood cancers. Biochem. Soc. Trans. **41**, 1048–1054 CrossRef PubMed

49 Cowan-Jacob, S.W., Jahnke, W. and Knapp, S. (2014) Novel approaches for targeting kinases: allosteric inhibition, allosteric activation and pseudokinases. Future Med. Chem. **6**, 541–561 CrossRef PubMed

Received 8 February 2016/29 February 2016; accepted 30 March 2016
Accepted Manuscript online 21 April 2016, doi:10.1042/BCJ20160085

© 2016 The Author(s). Published by Portland Press Limited on behalf of the Biochemical Society.

SUPPLEMENTAL INFORMATION

Uncoupling JAK2 V617F activation from cytokine-induced signaling by modulation of JH2 αC helix

Emilie Leroy[1,2], Alexandra Dusa[1,2], Didier Colau[1], Amir Motamedi[3], Xavier Cahu[1,2], Céline Mouton[1,2], Lily J. Huang[4], Andrew K. Shiau[3], Stefan N. Constantinescu[1,2]*

1 Ludwig Institute for Cancer Research, 1200 Brussels, Belgium and

2 de Duve Institute, Université catholique de Louvain, 1200 Brussels, Belgium.

3 Small Molecule Discovery Program, Ludwig Institute for Cancer Research, La Jolla, CA 92093

4 University of Texas Southwestern Medical Center, Dallas, TX

SUPPLEMENTAL FIGURES

Supplementary Figure S1. Effect of combined substitution of the charged amino acids of the JH2 helix αC. JAK2-deficient cells were transfected with the JAK2 variants and STAT5 transcriptional activity was measured in the absence or in the presence of Epo (upper panel). Decrease of JAK2 V617F constitutive activity could only be observed when E596 was substituted to alanine. Although E592 and R588 are located on the same helical face than E596 (lower panel), neither mutation of E592 nor R588 to alanine improved the inhibitory effect of E596A. Only E596 participates in the JAK2 V617F hyperactivity.

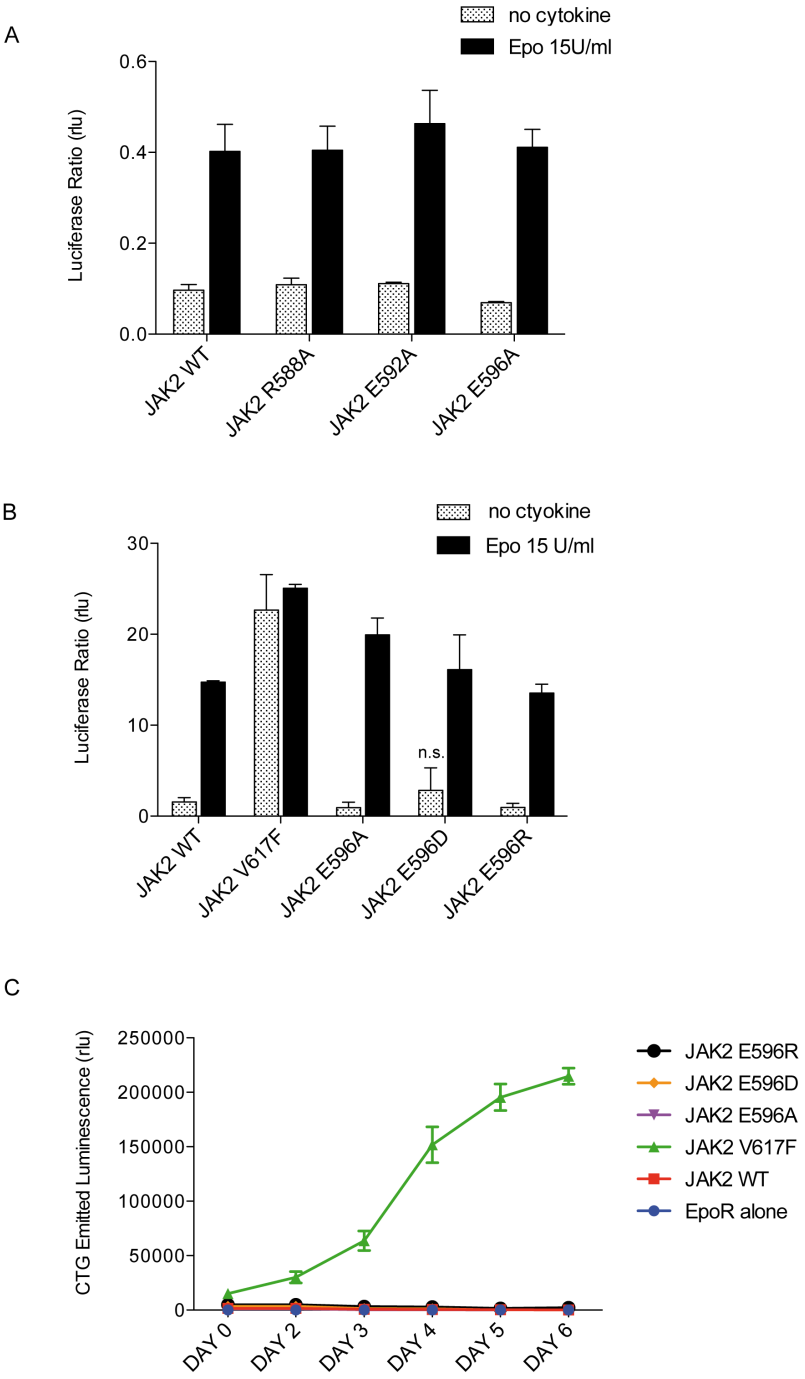

Supplementary Figure S2. Effect of the JH2 helix C substitutions in the wild-type JAK2.

(**A**) STAT5 transcriptional measurement by luciferase assay was performed in JAK2 deficient cell line allow us to support that substitutions of R588, E592 or E596 does not activate JAK2 WT. (**B**) While substitution of E596 by the shorter negative aspartate leads to an increase of the JAK2 V617F hyperactivity, the mutation E596D in the wild-type JAK2 does not lead to constitutive STAT5 transcriptional activity neither to BaF3 independent growth shown in (**C**).

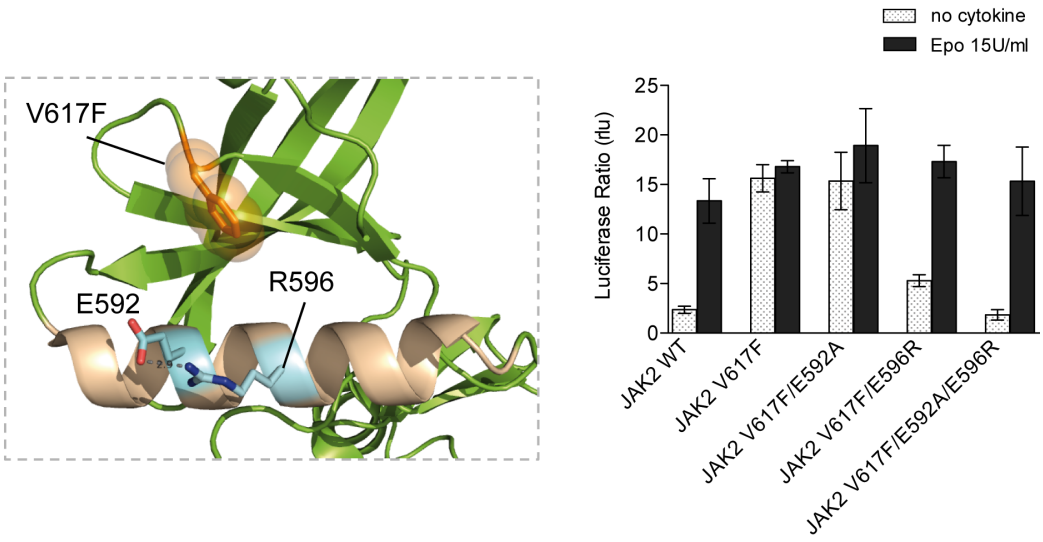

Supplementary Figure S3. E596R does not interact with E592 within the JH2 helix αC.

Left: the possible position of R596 (cyan) has been modeled on the crystal structure of JH2-V617F (PDB: 4FVR) and shows the proximity between E596R and E592 (cyan) in the conformation of the helix αC (brown). Right: However, R596 does not interact with E592 to inhibit JAK2 V617F activity as introduction of E596R in the background of JAK2 V617F/E592A could still inhibit JAK2 hyperactivity, as shown by STAT5 transcriptional activity measurement.

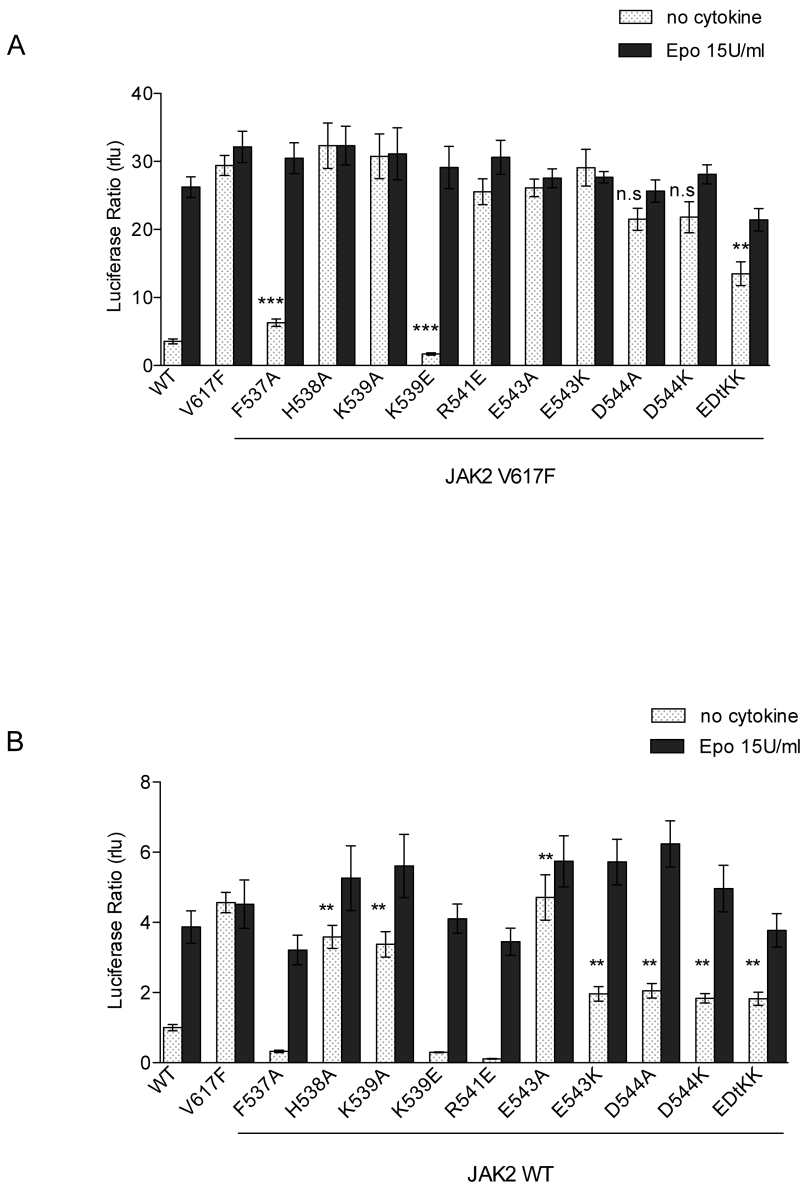

Supplementary Figure S4. Activating mutation in the SH2-JH2 linker.

C-terminus residues were mutagenized individually in JAK2 V617F (**A**) or in JAK2 WT (**B**) and activity of these JAK2 variants were assessed by Luciferase in Y2A. (**A**) Mutation F535A was already shown to decrease V617F-mediated activation and was used here as a control. Mutation K539E extensively decreases hyperactivation when compare with V617F, while E543/D544KK at a smaller extent. (**B**) The C-terminal portion of the SH2-JH2 linker harbors several strong activating mutations such as H538A, K539A and E543A; and weaker activating mutations such as E543K, D544A, D544K and E543/E544/KK. Shown are average units + SEM of three independent experiment performed in triplicate. (*p<0.05, **p<0.01, ***p<0.001; Dunnett's Multiple comparison test).

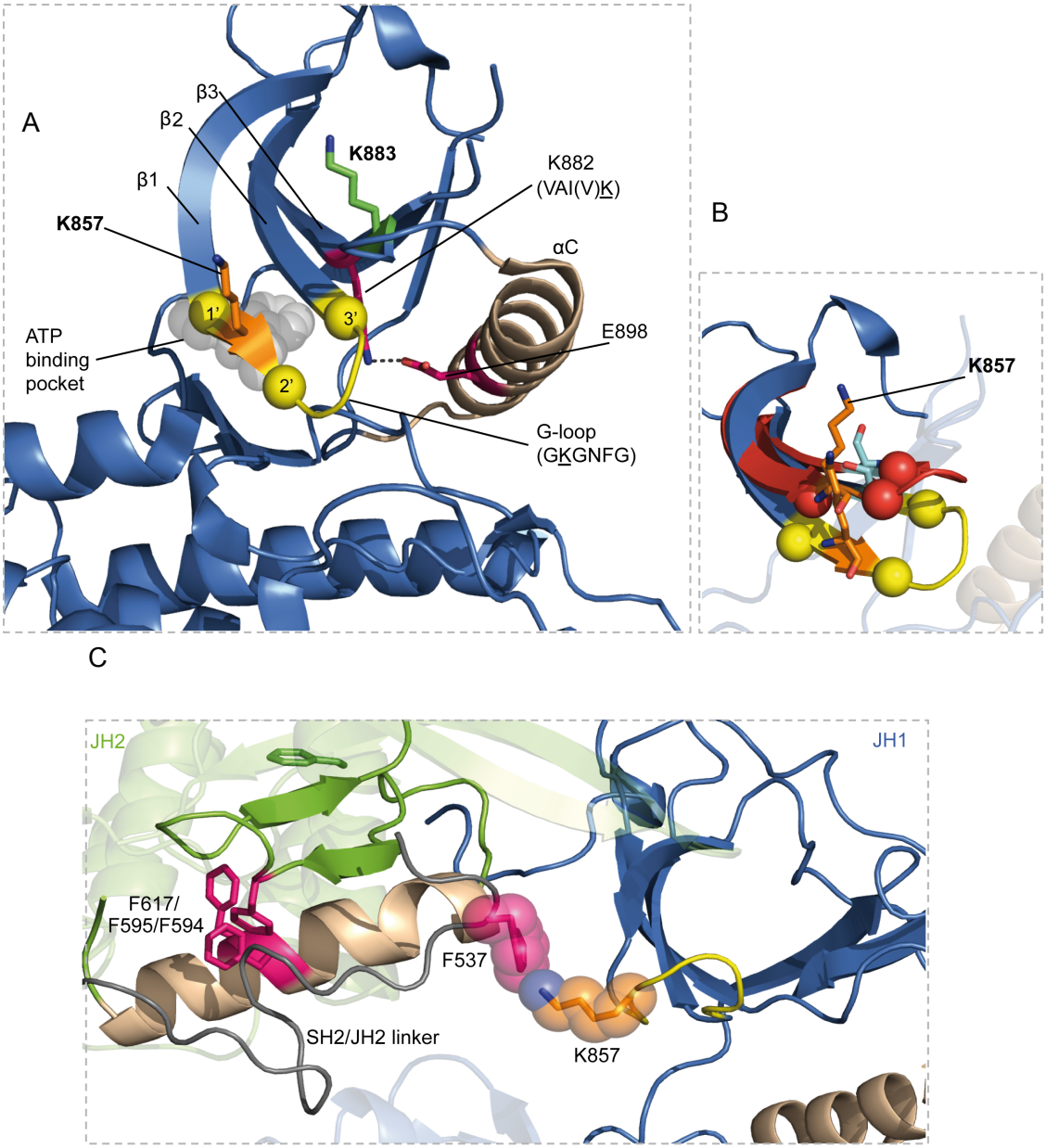
A
β3
β2
β1
K883
K882
(VAI(V)K)
K857
αC
1'
3'
2'
ATP
binding
pocket
E898
G-loop
(GKGNFG)
B
K857
C
JH2
JH1
F617/
F595/F594
F537
SH2/JH2 linker
K857

Supplementary Figure S5. JAK2 V617F activation circuit

JAK2 V617F activation process likely involves activating molecular events propagating from the αC of JH2 to JH1 through modulation of the SH2-JH2 linker, which can be blocked by the E596R inhibitory mutation. V617F triggers a series of activating events involving F537, E543/D544 (SH2-JH2 linker C-term), D569/Y570 (JH2 N-term) and finally K857/K883 (JH1 N-term). The activation circuit converges to JH1 N-lobe composed of β-strands, where the consensus motifs necessary for kinase activity lie. (**A**). K857 (orange) is part of the glycine-rich-loop (G-loop) (yellow) of JH1 and is located between the first and second glycine (small spheres). (**B**) The G-loop is the most dynamic structure of the kinase core that covers and anchors the non-transferable ATP phosphates within the catalytic site (1). Superposition of JH1 in the two states (inactive and active) highlights the dynamics of this loop, which adopts two different configurations in the active state (closed conformation / yellow) and in the inactive state (opened conformation / red). Our structure-guided modeling indicates that K857 participates in the control of the G-loop position and maintains it in an “opened” /inactive conformation by interacting with a distal segment. (**C**) In the mutant conformation, the SH2-JH2 linker F537 residue was shown to undergo a flipped-out rearrangement, away from the aromatic interactions formed between F594, F595 and F617 in the presence of F617 (2). Our modeling indicates that during the V617F activation, the flipped-F537 contacts K857 on JH1, rendering it unable to maintain the opened/inactive conformation of the G-loop. Shown in A and B are the electron density maps of active JH1 (PDB: 2B7A) and inactive JH1 (PDB: 3UGC). Shown in C is the modeling of the JH1/JH2-interface (3), where position of F617 has been artificially modeled.

A

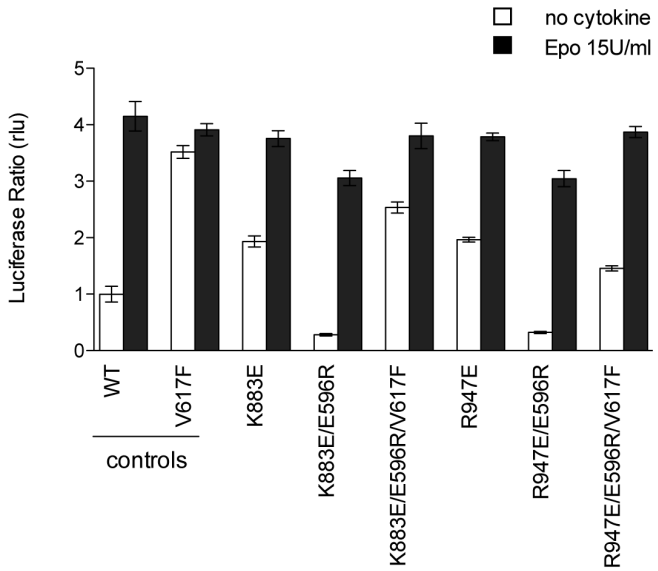
no cytokine
Epo 15U/ml
Luciferase Ratio (rlu)
0
1
2
3
4
5
WT
V617F
controls
K883E
K883E/E596R
K883E/E596R/V617F
R947E
R947E/E596R
R947E/E596R/V617F

B

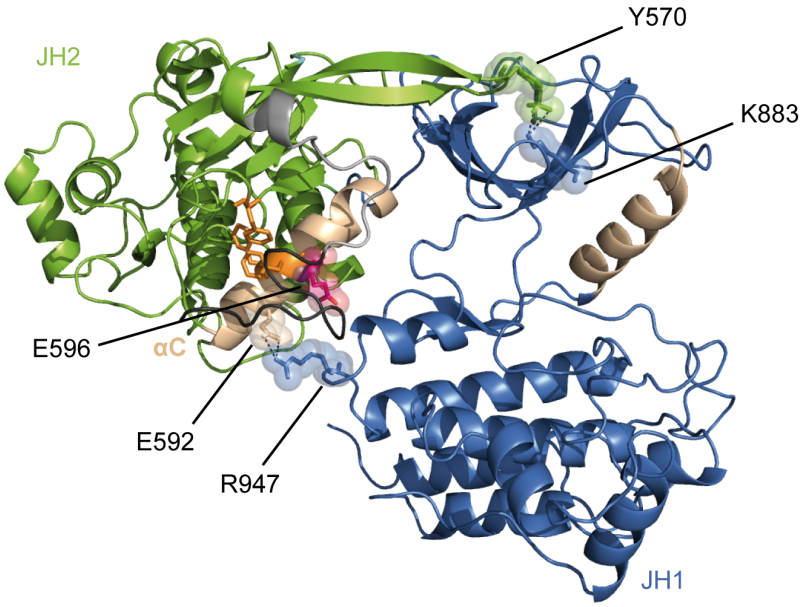
JH2
Y570
K883
E596
αC
E592
R947
JH1

Supplementary Figure S6. Activating mutation in JH1 (K883E and R947E) can be suppressed by E596R.

(**A**) The two JH1 activating mutations, K882E and R947E, are believed to participate in maintaining the inhibitory interplay between JH1 and JH2. The hyperactivity of these two JH1 mutants could be suppressed by E596R. STAT5 transcriptional measurement was by luciferase assay in γ2A cells that has no endogenous JAK2. Shown are average units + SEM of three independent experiment performed in triplicate. (**B**) While R947, located in JH1 αD-αE loop, could potentially be in contact with E596R (pink), the residue K883, located in JH1 β3 sheet, is very distant from E596R. Direct contact between E596R and K883E is to exclude. Shown are coordinates of the model from MD of JAK2 JH1/JH2(3) where JH2 is colored in green and JH1 is colored in blue. The JH2 αC is colored in light brown and shows the position of E596R (pink).

SUPPLEMENTAL TABLES

Data collection	ATP – JAK2 JH2 (E596A/V617F)
Resolution (Å)	114.87 – 1.54
	(1.62 – 1.54)
Space Group	$P2_12_12_1$
Unit Cell Dimensions (a, b, c) Å	53.43, 56.97, 114.9
Unit cell Angles (α,β,γ) °	90, 90, 90
I/σ (last shell)	16.4 (1.9)
[1]R_{sym} (last shell)	0.063 (0.940)
[2]R_{meas} (last shell)	0.069 (1.030)
[3]$CC_{1/2}$ (last shell)	0.998 (0.696)
Completeness (last shell) %	99.7 (99.7)
Number of reflections	332947
unique	52561
Multiplicity (last shell)	6.3 (6.1)
Refinement	
Resolution (Å)	48.45 – 1.54
	(1.58 – 1.54)
No. of reflections	
working	50493
free	1991
[4]R_{work} (%)	17.36
[4]R_{free} (%)	19.29
Structure/Stereochemistry	
No. of atoms	
protein	4426
solvent	57
ligand	186
r.m.s.d. bond lengths (Å)	0.010
r.m.s.d. bond angles (°)	1.371
Average B-Factor	33
Protein Data Bank ID	5I4N

Supplementary Table S1. Data collection and refinement statistics

1Rsym = ∑∑j|Ij – ⟨I⟩|/∑Ij, where Ij is the intensity measurement for reflection j and ⟨I⟩ is the mean intensity for multiply recorded reflections. 2Rmeas = ∑h [√(n/(n-1)) ∑j [Ihj - ⟨Ih⟩] / ∑hj ⟨Ih⟩, where Ihj is a single intensity measurement for reflection h, ⟨Ih⟩ is the average intensity measurement for multiply recorded reflections, and n is the number of observations of reflection h. 3CC1/2 is the Pearson correlation coefficient between the average measured intensities of two randomly-assigned half-sets of the measurements of each unique reflectionkar (4). 4Rwork, free = ∑||Fobs| – |Fcalc||/|Fobs|, where the working and free R-factors are calculated using the working and free reflection sets, respectively. Coordinates and structure factors have been deposited with the Protein Data Bank (http://www.pdb.org) with the noted accession codes.

SUPPLEMENTAL REFERENCES

1. Kornev AP, Taylor SS. Dynamics-Driven Allostery in Protein Kinases. Trends Biochem Sci. 2015;40(11):628-47.

2. Toms AV, Deshpande A, McNally R, Jeong Y, Rogers JM, Kim CU, et al. Structure of a pseudokinase-domain switch that controls oncogenic activation of Jak kinases. Nat Struct Mol Biol. 2013;20(10):1221-3.

3. Shan Y, Gnanasambandan K, Ungureanu D, Kim ET, Hammar√©n H, Yamashita K, et al. Molecular basis for pseudokinase-dependent autoinhibition of JAK2 tyrosine kinase. Nature Structural & Molecular Biology. 2014;21(7):579-84.

4. Karplus PA, Diederichs K. Linking crystallographic model and data quality. Science. 2012;336(6084):1030-3.

Addendum_unpublished data.

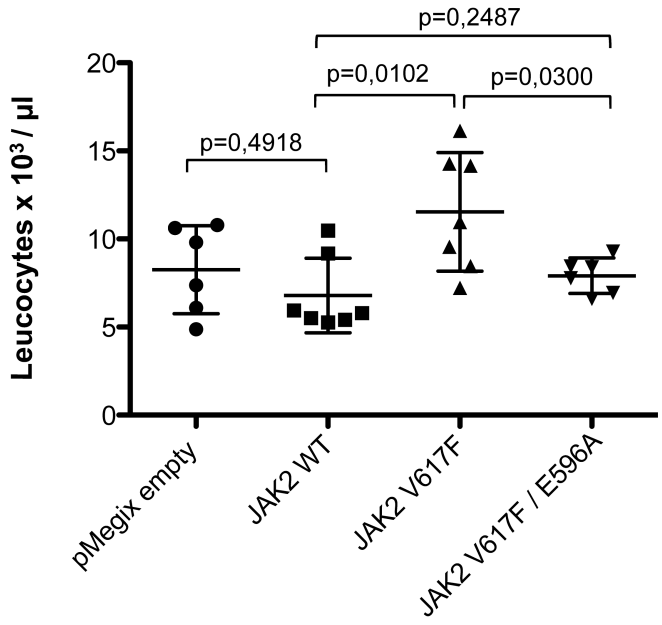

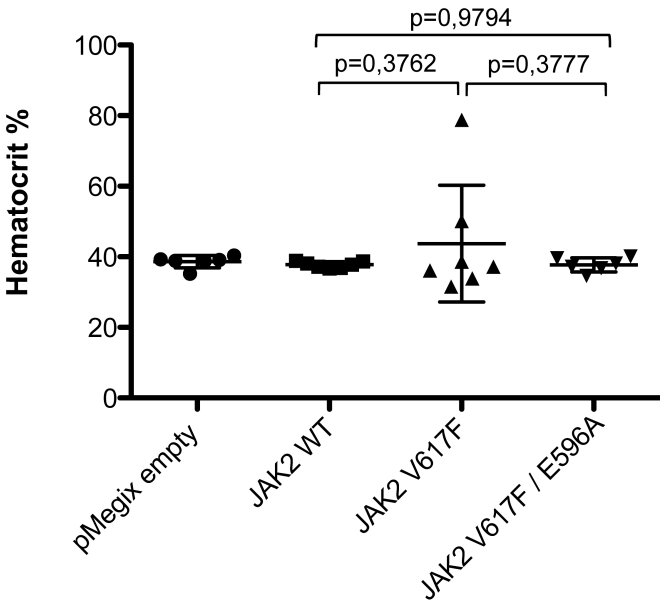

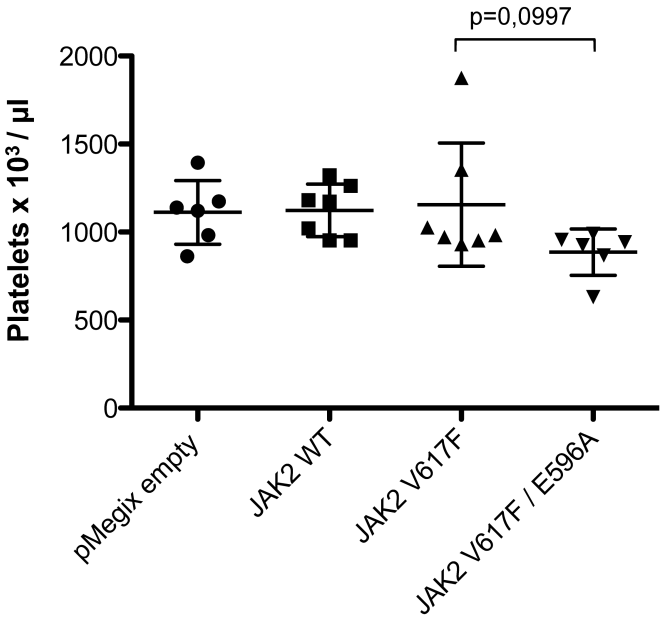

In Vivo effects of mutation E596A on the hyperactivity of JAK2 V617F.
Peripheral blood counts of mice that received a transplant of bone marrow cells expressing the indicated JAK2 variants or the empty vectors (pMegix) 3 months after reconstitution. All mice presented more than 25 % GFP-positive cells at 3 months after reconstitution. The inhibitory effect of the mutation E596A seems to be reproduced in vivo. The change in the leucocytes counts between V617F and V617F/E596A is statistically different.

Material and methods:

Bone marrow reconstitution assays

Murine JAK2 WT, JAK2 V617F and JAK2 V617F/E596A were cloned into pMegix-IRES-GFP (pMegix) retroviral vector, which contains, as a provirus, a MESV long terminal repeat driving the expression of the JAK2 genes (cap-dependent) and the GFP reporter gene (encephalo-myocarditis virus (ECMV)-derived IRES-dependent). The empty vector was used as control. Viruses were produced in the 293-EBNA cells. Bone marrow cells were collected from C57BL/6 mice 3 days after 5-fluorouracil (5-FU) injection and infected for 3 days with the viral particles. Retrovirally transduced cells (10^6) were then injected into 6-8 week old C57BL/6 lethally irradiated (950 rad) mice (1). Peripheral blood was examined for GFP expression 3 months after transplantation. Peripheral blood cell counts were performed using a Melet Schloessing MS9-3 cell counter (2).

Contributions

I generated the constructs and produced the viral particles. Dr. C. Pecquet performed the reconstitution and blood counts.

References:

1. James C, Ugo V, Le Couedic JP, Staerk J, Delhommeau F, Lacout C, et al. A unique clonal JAK2 mutation leading to constitutive signalling causes polycythaemia vera. Nature. 2005;434(7037):1144-8.

2. Pecquet C, Staerk J, Chaligne R, Goss V, Lee KA, Zhang X, et al. Induction of myeloproliferative disorder and myelofibrosis by thrombopoietin receptor W515 mutants is mediated by cytosolic tyrosine 112 of the receptor. Blood. 2010;115(5):1037-48.

ARTICLE 2. Inhibition of JAK2 V617F by Targeting the Aromatic Interactions Around F617

Inhibition of JAK2 V617F by Targeting the Aromatic Interactions Around F617

Leroy Emilie[1,2], Dusa Alexandra[1,2], Pecquet Christian[1,2], Mouton Céline[1,2], Colau Didier[1,2], Ungureanu Daniela[3], Silvennoinen Olli[3], Constantinescu Stefan[1,2].

1 Ludwig Institute for Cancer Research, 1200 Brussels, Belgium and
2 de Duve Institute, Université catholique de Louvain, 1200 Brussels, Belgium.
3 School of Medicine, University of Tampere, FI-33014 Tampere, Finland

ABSTRACT

Deregulation of JAK2 signaling is associated with hematopoietic malignancies. Indeed, the JAK2 V617F mutation, which constitutively activates JAK2, is found in over 95% of Polycythemia Vera patients. Understanding the mechanism of activation of V617F at an atomic level has always been a challenge since JAK2 was proposed as a target for treating theses diseases. JAK2 has a pivotal role in triggering several signaling pathways; therefore specific targeting of the mutant protein is absolutely required. Currently, no drug can discriminate between the mutant and the wild-type protein, necessitating novel therapeutic approaches. We have previously shown that one of the V617F-induced molecular effects involves the F595 residue of the α helix C of JH2 where an aromatic stacking interaction between F617 and F595 is required for constitutive signaling of JAK2 V617F. Here, we report that mutations strategically localizing around this aromatic interaction, and disrupting it with other aromatic residues, are able to preferentially inhibit JAK2 V617F over wild type JAK2. This open new perspective to design allosteric site targeting inhibitors.

INTRODUCTION

V617F is the most common JAK2 substitution in myeloproliferative diseases (MPN) (2-5). Other activation mutations at V617 exist in patients, such as V617I, but they are very rare and significantly weaker (7). V617FI can be associated with hereditary thrombocytosis (8, 9). The discovery of JAK2 V617F as the major driver mutation in patients with MPNs provided the first insight into JAK2 biology and MPN pathogenesis. Yet, the mechanism by which V617F, located on the pseudokinase domain (JH2) of JAK2 promotes the kinase activity of the adjacent kinase domain (JH1) is not clear. The recent crystal structure of both TYK2 tandem kinase domains (11), as well as a model of JAK2 JH1-JH2 derived from MD simulations studies (1) provided new lines of evidence on the interface between the two domains and the inhibitory role exerted by JH2 on JH1.

JAKs (JAK1-JAK3 and TYK2) consist of four different domains (FERM, SH2-like, pseudokinase/JH2 and the kinase/JH1). No three-dimensional structure exists for a full-JAK length protein. The regulatory mechanisms exerted by the different domains on the kinase domain, and the relative dispositions of the domains in receptor complexes are just beginning to be studied. Each domain could have a particular role in regulating the activity of JAK2 in the cytokine receptor-JAK complex.

The comparison of the crystal structures of JAK2 JH2 WT and JAK2 JH2 V617F indicates that the αC changes conformation upon the valine to phenylalanine substitution (12). The αC in the mutant structure displays a more rigid configuration and an additional N-terminal turn (12), likely due to an aromatic interaction between phenylalanines residues. In fact, the three residues, F594, F595 from the αC and F617, are involved in a double T-shaped π-π stacking interaction where F595 plays a pivotal role in maintaining these interactions. This is supported by previous mutagenesis data that showed that the two phenylalanines from JH2 αC are specifically necessary for the hyperactivity of JAK2 V617F as their substitutions to alanine suppressed the activity of the mutant without altering cytokine inducibility (10, 13). Of interest, F595 normally appears to interact with a phenylalanine residue from the SH2-

JH2 linker F537. One activation model posits that the aromatic interaction between F617 and F595 liberates F537, which along with a re-configuration of the SH2-JH2 leads to activation of the kinase domain (6, 14). This is supported by inhibition of JAK2 V617F kinase activity by F537A mutant (14).

Current JAK2 inhibitors exclusively consist of ATP mimicking compounds targeting the active site of the JH1 kinase domain (15). Nevertheless their effects are not curative and their potency is limited. Compounds such as Ruxolitinib exhibit limitation in the selectivity for JAK2 against the other JAKs resulting in immunosuppressive sides effects (16). Moreover, to date no compound can distinguish between wild type JAK2 and the mutant V617F. Given the position of this mutation in a domain adjacent to the kinase domain, we suggest that targeting sites remote from the kinase active site could constitute a new strategy in order to inhibit the hyperactivity of JAK2 V617F. Discovery of new allosteric sites would generate opportunities for the identification of novel compounds with better specificity and/or potency.
Allosteric sites have been progressively identified in various enzymes, which paved the way for the development of a new type of pharmaceuticals. One example is the development of the BCR-ABL allosteric inhibitor GNF-2, which binds to the myristate pocket within the kinase C-lobe and induces inhibition (17). Not only this compound could overcome the effect of resistant mutations (18), but also exhibited enhanced potency when used in combination with classical ATP competitive inhibitors (19). We hypothesized that the change of conformation of the JH2 αC is first molecular event leading to the activation of JH1. Therefore, we sought to find ways to displace the position of the αC in the mutant conformation in order to disrupt the V617F activation process. Using the coordinates of the solved structures of JH2 WT and JH2 V617F, we explored the hydrophobic environment around the αC through structure-guided mutagenesis. Disruption of the π-π stacking interaction could achieve preferential inhibition of the mutant JAK2 V617F, suggesting new potential site to target with small molecules. We found that major changes in the hydrophobic environment of the αC can decrease the hyperactivity of JAK2 V617F thereby underlying the importance of the position of the αC in the oncogenic activation of JAK2.

MATERIAL AND METHODS:

cDNA

JAK2 (and JAK1) is subcloned in the pMX-IRES-GFP and EpoR in the pMX-IRES-CD4 (20). JAK2 JH2 domain (amino acids 535-812) was subcloned in the pFast-Bac1 vector (Life Technologies) and contains a C-terminal thrombin-cleavable His_6-tag (12). Site-directed mutagenesis was achieved by the overlapping-extension PCR amplification method using primers containing the desired single point mutation. The reaction was performed using 1 µl of pfuTurbo DNA polymerase 2.5 U/µl following the manufacturer's protocol. The coding region of each construct was verified by Sanger sequencing.

Cell cultures

γ2A are JAK2 deficient human fibrosarcoma cells (21) and U4C are JAK1 fibrosarcoma cells (22) maintained in DMEM and 10% FBS. Pro-B IL-3 (interleukin 3) dependent hematopoietic BaF3 cells were maintained in RPMI 1640 and 10% FBS (fetal calf serum) supplemented with WEHI cell supernatant as a source of IL-3 (23). Autonomous cells expressing JAK2 V617F were cultured without IL-3.

Retroviral transduction and generation of cell lines

High-titer ectopic retroviruses were generated by transient transfection of BOSC packaging cells with the bicistronic pMX-IRES-GFP encoding the JAK2 variants and GFP as a marker of infection (24). Retroviruses-containing supernatant was collected 48 hours after transfection. BaF3-EpoR cells were infected by spin infection in medium containing the packaged retroviruses and 4 µg/ml of polybrene (Sigma) during 4 hours at 37°C. GFP was used as a marker of infection. Cell pools expressing equivalent levels of GFP (above 25%) were isolated by flow cytometry cell sorting.

Proliferation assay
BaF3-EpoR cells expressing the different JAK2 variants were washed three times in PBS and suspended in RPMI +10% FBS free of cytokine. Cell numbers were recorded after seven days or over a period of five days.

Dual luciferase Assay
Transcriptional activity of STAT5 was assessed by measuring luciferase activity in JAK2 deficient cells (γ2A) or JAK1 deficient cells (U4C) transfected with the pGRR5-luciferase reporter containing five copies of STAT responsive elements of the IFNγ responsive region (GRR) of the high affinity receptor for IgG1 (25). pRL-TK vector containing the thymidine kinase promoter upstream of the renilla luciferase reporter gene was used as an internal control (Promega). pGRR5, pRL-TK, JAK2, STAT5 and receptor chains cDNA were transfected by lipofectamine 2000 (Invitrogen). For erythropoietin stimulations, epoetin alfa (Eprex®) was added at 25 U/ml 4 hours after transfection. Cells were lysed 24 hours after transfection and luciferase assays were performed using the dual reporter assay kit (Promega). Each experiment was performed three times in triplicate.

Western blots
$1x10^6$ γ2A were plated in each well of a 6-well plates the day preceding the transfection in DMEM + 10% FBS. cDNAs coding the EpoR and the JAK2 variants were transfected in a ratio 1:1 using FuGene 6 (Promega). 48 hours after transfection, medium was changed to DMEM supplemented or not with Epo 15 U/ml. Cells were stimulation during 20 min at 37°C. Cells were trypsinized and lysed in 1X Nodinet P-40 (NP40) lysis buffer containing orhtovanadate, MPSF and protease inhibitor cocktail (ThermoFisher Scientific). Samples were analysed by SDS-PAGE 4-12% gradient NuPAGE® BisTris Gel (Invitrogen) and transferred to nitrocellulose membrane. Phosph-JAK2 (Y1007/1008) and total-JAK2 were detected using Rabbit mAb C80C3 (Cell Signaling Technologies #3776) and Rabbit mAb D2E12 XP® (Cell Signaling Technologies #3230), respectively. HRP (Horseradish peroxidase)-linked secondary rabbit antibody (Cell Signaling Technologies #7074) was used to detect the signal. Images were acquired by Fusion FX7 (Vilber Lourmat).

Protein production
His-tagged JAK2 JH2 recombinant proteins were expressed in *Spodoptera frugiperda-9* cells (Sf9). After cell collection, proteins were purified using Ni-NTA affinity and anion-exchange chromatography as previously described (12, 26). Proteins were concentrated to 2 mg/ml or higher, snap-frozen in liquid N2 and stored at – 80°C. Protein concentrations were estimated on the basis of absorbance at 280 nm and the calculated molar absorption coefficients (27).

Thermal shift assay
Thermal shift assay was performed as previously described (27). Typically, a Corbett Real Time PCR machine was used to perform the assay. The reaction was performed in a 25 µl reaction mix containing the proteins diluted at 2 µM in 1 mM MgCl, 20 mM Tris/HCl (pH 8.0), 500 mM NaCl, 20% glycerol and 100- 400 µM ATP. SYPRO orange (Molecular Probes) was used as a probe with fluorescence detected at 530 nm. The melting curves were calculated based on 1°C increase/min from 4°C to 95°C and fluorescence readings were taken at each interval. Values were normalized using a non-protein control sample (DMSO). The melting temperature (Tm) and ΔTm were calculated using Bolzman equation (Prism Software). Tm corresponds to the midpoint for the protein unfolding transition and ΔTm corresponds to the changes in the unfolding transition temperature compared with the control curve. A minimum of two independent experiments was performed in duplicate for each protein and representative data are shown for each.

Structural modelling
The coordinates for the JAK2 JH2 V617F were obtained from the PDB database (accession code: 4FVR). PyMOL Molecular Graphics System (Version 1.8 Schrödinger, LLC) was used to model the position of the phenylalanine substitutions.

RESULTS

1. Specific phenylalanines substitutions on the JH2 αC diminish V617F activity.

We hypothesized that the aromatic interaction between F594, F595 and F617 forms the basis for the constitutive activation of JAK2 V617F. In order to block JAK2 activation by the V617F mutation, we aim to interrupt this non-covalent contact by placing phenylalanine residues in the vicinity of the middle αC. After structural analysis of JH2 V617F (PDB: 4FVR), we selected positions 597 and 598 to substitute for phenylalanines and the two different JAK2 V617F/double mutants were generated in the bicistronic vector, pMX-IRES-GFP. Stable hematopoietic BaF3 cell lines were generated to express the different JAK2 variants and the erythropoietin receptor (EpoR) subcloned in the pMX-IRES-CD4. These cells depend on IL-3 and Epo for survival, thus in the absence of cytokine, only BaF3 cells expressing an oncogene grow autonomously. This was the case for BaF3 expressing JAK2 V617F and JAK2 V617F/A597V (**Figure 1 A, B**). BaF3 cells expressing JAK2 V617F/A597F and JAK2 V617F/A598F could not grow in the absence of cytokine (**Figure 1 A, B**). Hence, the mutations A597F and A598F could suppress the V617F-mediated transformation of BaF3-EpoR. The inhibitory effect of A597F and A598F is likely due to the aromatic moiety of the phenylalanine residues. Indeed, substitution of A597 by another non-aromatic aliphatic residue such as valine (A598V) did not inhibit the activity of JAK2 V617F (**Figure 1A**).

We also used this transient system to confirm the results obtained with JAK2 mutants in BaF3 cells. STAT5 transcriptional activity was then measured in JAK2-deficient cell lines (γ2A) after transfection of the JAK2 variants along with EpoR (**Figure 1C**). Interestingly, A598F diminished, but did not completely abolish, the constitutive activity of JAK2 V617F without altering the cytokine inducibility. The difference between complete inhibition in BaF3 cells and only partial inhibition in the transient γ2A system might be due to the overexpression conditions of the latter.

Interestingly the A597F mutant did not support constitutive or ligand-induced activity. Modeling of the A597F mutation (**Figure S.1**) indicates that the ring of F597 might contact and change position of the DPG motif (consensus DFG) of JH2. D699 (from DPG) forms an ion pair with the β3 lysine K581, thereby substituting the canonical β3 lysine – αC glutamate ion pair necessary for proper ATP binding (12). Mutations of both K581 and D699 to alanine were shown to abolish hyperactivity of JAK2 V617F similarly to A597F (28). These data also support the previous finding that ATP binding is critical for the hyperactivity of JAK2 V617F. Along the same lines, A597F mutation did not significantly affect the Epo-induced activation of JAK2 wild type (**Figure S.1**), as it was observed for D699A and K581A (28).

γ2A cells were then transfected with EpoR and JAK2 variants having the inhibitory mutation A598F in either JAK2 WT or JAK2 V617F. JAK2 and STAT5 phosphorylation were analyzed by western blot before and after stimulation by Epo (**Figure 1E**). A598F did not affect the Epo-induced response of JAK2 WT and the downstream STAT5 transcriptional activity. In addition, A598F even suppressed the basal phosphorylation of STAT5 (left panel). A598F decreased the basal phosphorylation of JAK2 V617F and the downstream STAT5, but did not affect Epo-induced activation (right panel). A880F mutation was used as a kinase-dead mutant control (KD). Residue A880 belongs to the hydrophobic residues part of the so-called "catalytic spine" typically found in active kinases that is completed by the adenine ring of ATP (29, 30). It was shown in other kinases that replacement of the small alanine by a bulky hydrophobic residue such as phenylalanine could prevent ATP binding and stabilize the closed/active conformation of the kinase by completing the catalytic spine (31).

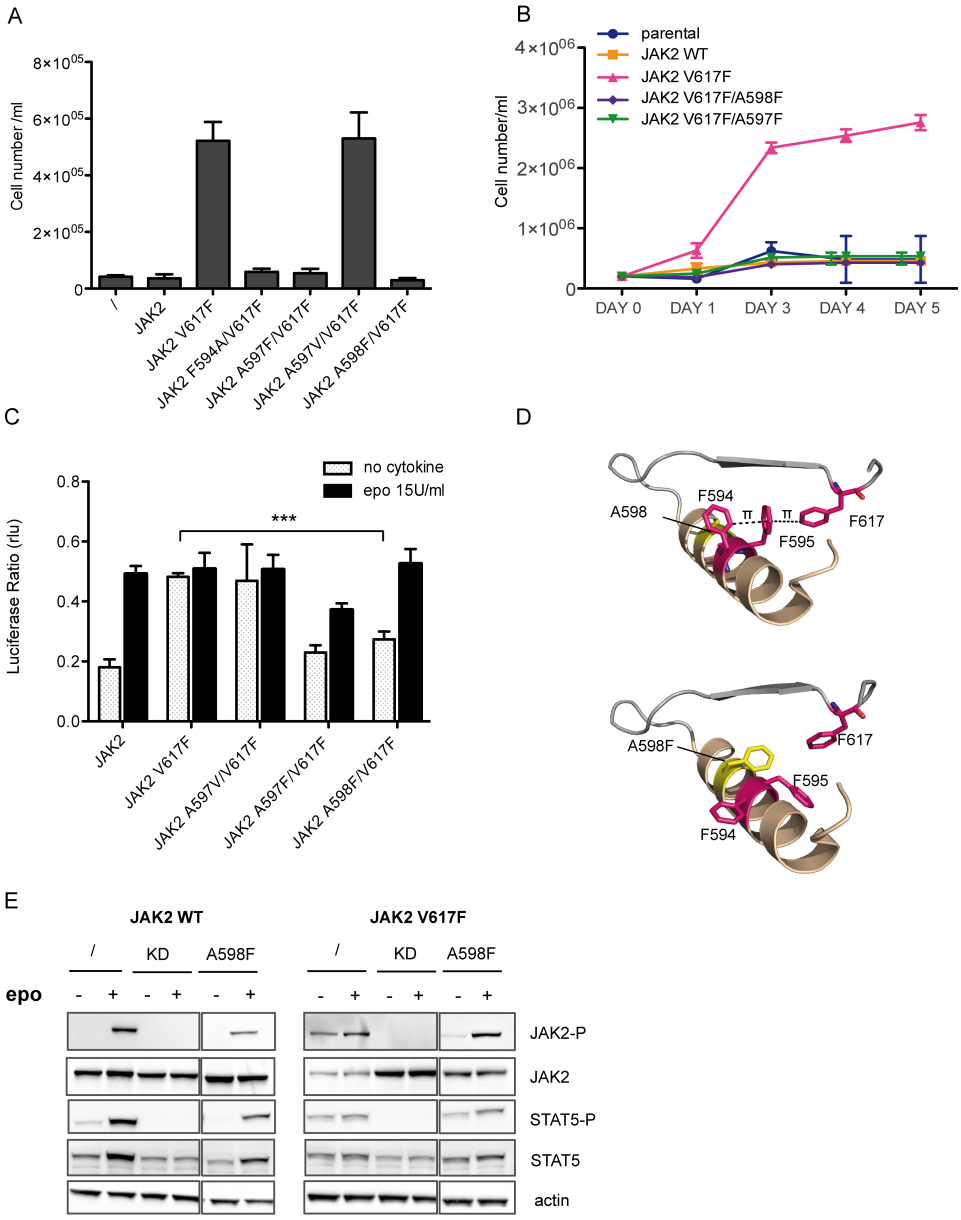

Figure 1. Effect of phenylalanines introductions in the JH2 αC on the JAK2 V617F hyperactivity. a. Hematopoietic BaF3-EpoR cells stably expressing JAK2 V617F with a secondary site mutation have been set for proliferation assay in cytokine-free medium. Cells were count after 5 days. Only cells expressing JAK2 V617F and JAK2 V617F/A597V were able to proliferate in the absence of cytokine. A597F and A597F suppressed BaF3-EpoR JAK2 V617F autonomous growth. Shown are average + S.D. of one representative experiment out of three independent experiments done in triplicate. **b.** Proliferation of BaF3-EpoR cells expressing the JAK2 variants was assessed during a period of 5 days. From day 3, only cells expressing JAK2 V617F survived and proliferate in the absence of cytokine. Shown are average +/- S.D. of one representative experiment out of three independent experiments done in triplicate **c.** STAT5 transcriptional activity measured by dual luciferase assay in JAK2-deficient cells (γ2A). Cells were transiently transfected with EpoR and the various JAK2 constructs in addition to pRL-TK, pGRR5 and STAT5. Both A597F and A598F blocked JAK2 V617F constitutive transcriptional activity. JAK2 V617F/A598F triggered STAT5 transcriptional activity in response to Epo (15U/ml) similarly to JAK2 WT, while JAK2 V617F/A597F did not. Show are average units + S.E.M of three independent experiments done in triplicate (*** P < 0,001, Mann Whitney test). **d.** Modeling of substitution A598F on the αC of JH2-V617F (PDB: 4FVR) and the putative break of the aromatic interaction between F617-F595-F594. **e.** Immunoblot analysis of JAK2 deficient cells (γ2A) co-transfected with the different JAK2 variants and EpoR. A598F suppressed the constitutive phosphorylation of JAK2 V617F and STAT5 but still allow phosphorylation after Epo stimulation (right panel). A598F do not affect the Epo-induced JAK2 and STAT5 phosphorylation triggered by JAK2 WT (left panel). KD = kinase dead JAK2 (with the A880F) mutation blocks the activities of both JAK2 WT and JAK2 V617F.

This mutant is catalytically dead, presumably because the phenylalanine ring fills the ATP adenine pocket. The lack of phosphorylation on JAK2 and STAT5 after Epo stimulation (**Figure 1E**) indicates that A880F abolishes both JAK2 and JAK2 V617F-mediated signaling, by creating a catalytically dead JAK2. This is in contrast with what has been observed with the homologous mutations in CRAF (A373F), BRAF (A471F) and KSR1 (A587F), where the mutation that blocks ATP binding still allowed dimerization and downstream signaling with other partners, in our case possibly other JAKs, which was not the case as our reporters would read general STAT5/3/1 activity (31). We interpret the result that the A598F mutation diminishes JAK2 V617F hyperactivity by interrupting the aromatic π-π stacking interaction mediated between F594, F595 and the abnormal F617 (**Figure 1D**).

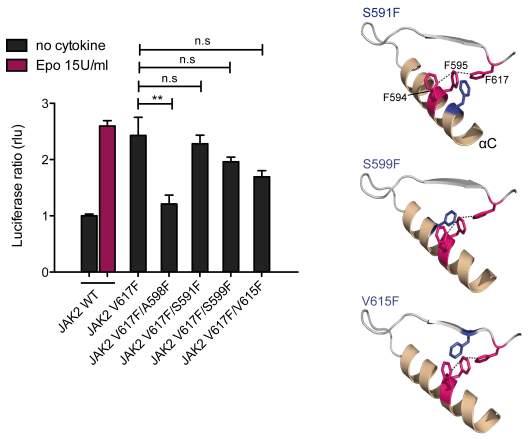

Figure 2. Position A598 on the JH2 αC is highly specific. Left panel, STAT5 transcriptional activity of JAK2 V617F variants were assessed in JAK2 deficient cells by dual luciferase assay. Only substitution of residue A598 to phenylalanine could suppress the constitutive activity of JAK2 V617F. Substitutions of other residues found in the vicinity of V617F (S591, S599, V615) to phenylalanines did not block JAK2 V617F hyperactivity. Right panel, modeling of the other putative sites where substitution to phenylalanine could possibly contact F617 side chain and affect the activity of JAK2 V617F. Shown are average units + S.E.M of three independent experiments done in triplicate (** $P < 0.01$, n.s, not significant, Kruskal-Wallis with Dunn's post test).

Structural analysis of JAK2 JH2 V617F guided us to substitute other residues in the vicinity of the aromatic interaction as modeled on **Figure 2**. The position A598 appears to be highly specific, as substituting phenylalanines at other positions along the JH2 αC did not reach inhibition of JAK2 V617F (**Figure 2**). This highlights the relevance of position 598 on JH2 αC for the placement of JAK2 V617F inhibitory bulky hydrophobic mutation.

2. The mutant protein JAK1 V658F can be inhibited by homologous A598F mutation (A639F) in both homodimeric and heterodimeric cytokine receptor complexes.

To test the functional conservation of A598F inhibitory mutation, we performed similar studies in JAK1 (**Figure 3)**. JAK1 can be activated by a mutation analogous to V617F (32), JAK1 V658F, which can be associated with T-cell lymphoblastic leukemia (T-ALL), as other JAK1 and JAK3 mutations (33, 34). Similarly to what it was observed with JAK2 V617F, homologous A598F substitution in JAK1 (A639F) decreases constitutive signaling of the hyperactive mutant when coexpressed with the chimeric receptor EpoR/gp130 (comprising the EpoR extracellular domain and gp130 transmembrane and intracellular domain binding to JAK1 (35)) in JAK1 deficient cells, U4C (**Figure 3A**). The inhibitory effect of A598F can be translated to hyperactive JAK1 V658F mutant in an artificial homodimeric complex. Interestingly, A639F mutations could also inhibit the hyperactivity of JAK1 V658F mutant in a heterodimeric complex when co-expressed with IL-9R and JAK3 (**Figure 3B**)

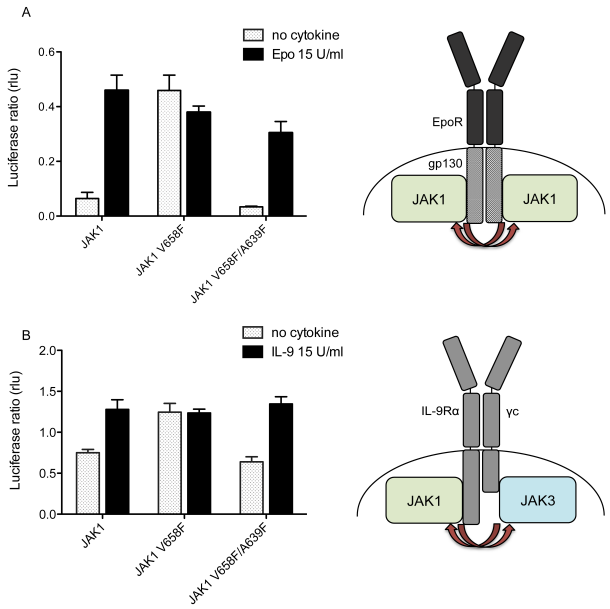

Figure 3. The homologous mutation in JAK1, A639F, also blocks hyperactivity of JAK2 V658F in homodimeric and heterodimeric complexes. JAK1 deficient cells (U4C) were transfected with the JAK1 mutants and STAT5 transcriptional activity was assessed by dual luciferase assay. **a.** JAK1 constructs were co transfected with chimeric receptors EpoR/gp130 enabling homodimerization of two JAK1 molecules. A639F suppressed the constitutive activity of JAK1 V658F without altering the cytokine-induced signal. **b.** JAK1 variants were co-transfected with IL9R, γc and JAK3. A639F was also able to supress the oncogenic activity o JAK1 V658F in the heterodimeric complex context. Show in (A) and (B) are average units + S.E.M of three independent experiments done in triplicate.

3. A598F mutation preserves cytokine inducibility of JAK2

Next, we asked whether the inhibitory mutation A598F affects the ability of JAK2 V617F or JAK2 WT to respond to cytokine. As shown in **Figure 4A**, A598F does not seem to influence to Epo-activated signaling of JAK2 V617F (**Figure 4A**). A598F in the context of JAK2 WT exhibited a small inhibition of response to lower concentrations of Epo (**Figure 4A**), but not to higher Epo doses (**Figure 4 A, B**). Thus, A598F only marginally affects the low Epo inducibility in JAK2 WT, but not in the V617F context. Importantly, A598F does not induce constitutive activity of JAK2 but in contrast, lower the basal activity of JAK2 WT (**Figure 4B**). Altogether, our data indicate that A598F decrease the constitutive activation of JAK2 V617F without altering its responsiveness to different cytokine stimulations.

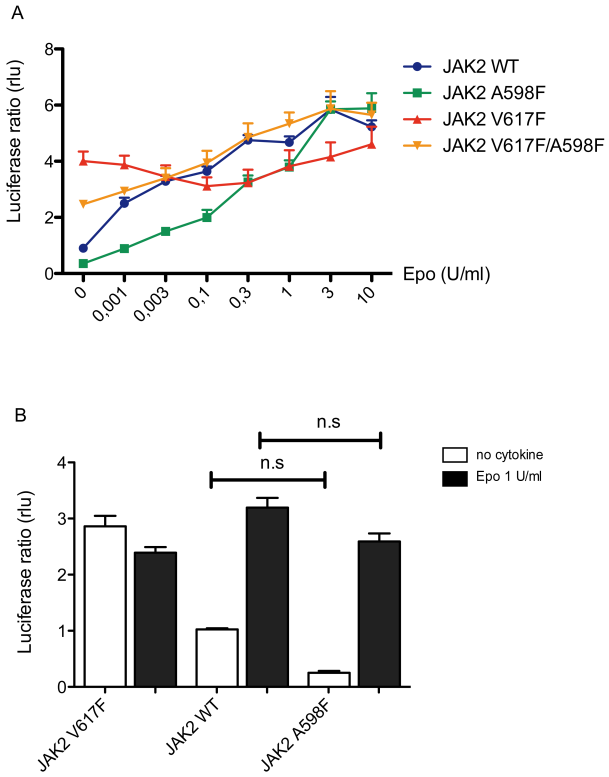

Figure 4. A598F does not affect cytokine inducibility of mutant and wild type JAK2. a. The effect of the inhibitory mutation A598F on the cytokine sensitivity of JAK2 WT and JAK2 V617F was measured by dual luciferase assay in γ2A cells. After transfection, medium containing several concentrations of Epo was added, as indicated. A598F restores normal Epo responsiveness in JAK2 V617F similar to JAK2 WT. A598F affected the Epo responsiveness of JAK2 WT at submolecular concentrations (0,001 - 1 U/ml) but not higher concentrations (3 – 10 U/ml). Shown are average units + S.E.M of two independent experiments done in triplicate. **b.** At 1U/ml the difference between JAK2 WT and JAK2 A598F is not statistically different. The basal level of activation of JAK2 WT is not affected by the mutation A598F in contrary to the basal level of JAK2 V617F. Shown are average units + S.E.M of four independent experiments done in triplicate (n.s, not significant; Mann Whitney test).

4. A598F decreases the activity of other clinically relevant JAK2 mutants

We assessed the effect of the inhibitory mutation A598F on other activated forms of JAK2 including R683G, T875N and K539L. K539L is one of the so-called “exon 12 mutations” associated with polycythaemia vera (PV) (36). K539L is located in the linker between the SH2-like and the pseudokinase domain. R683G is located at the tip of β6 strand in the inter-lobe region on JH2 and is found in B-cell acute lymphoblastic leukaemia (37). T875N lies in the β2-β3 loop of the kinase domain and was described in a megakaryoblastic leukaemia cell line (38). Similarly to JAK2 V617F, these three mutants displayed constitutive STAT5 transcriptional activity when transfected in γ2A cells along with the EpoR (**Figure 5**). Interestingly, A598F decreased the hyperactivity of R683G and T875N mutants, but not of K539L. These data suggest that R683G and T875N require a stable JH2 helix αC for their hyperactivity, while K539L located in the SH2-JH2 linker, directly activates JH1 without passing through the JH2 αC. K539L is model for the exon 12 mutations associated with a fraction of PV patients that exhibit mainly erythrocytosis, without major involvement of other lineages. Molecular dynamic simulation indicated that both R683G and T875N are located in the inhibitory JH1/JH2 interface, which also encompasses the JH2 αC(1). Hence, the hyperactivity of R683G and T875N is presumably occurring through destabilization of JH2 αC and the JH1/JH2 inhibitory interface, while K539L hyperactivity occurs through a different mechanism not including changes of the JH2 αC.

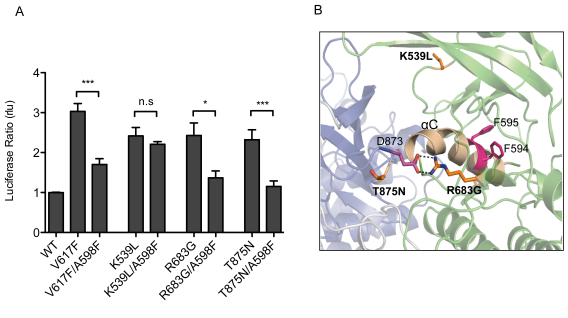

C

Mutation	Gene	Domain	Disease
V617F	Exon 14	JH2	PV, ET, PM, HES, CMML, SM, CNL,JMML, RARS,RA RCMD, RAEB,AML, IE, RARS-T, MDS/ MPN-U,MPN-U
K539L	Exon 12	SH2-JH2 linker	PV, IE
R683S	Exon 16	JH2	DS-B-ALL, B-ALL
T875N	Exon 20	JH1	AMKL-cell line

Figure 5. The mutation A598F has an inhibitory effect on the hyperactivity of some, but not all, disease associated JAK2 mutants. a. The disease-associated JAK2 mutants K539L, R683G and T875N all induce constitutive STAT5 transcriptional activity similar to JAK2 V617F. A598F decreased the activity of R683G and T875N but not K539L. Shown are means +/ − S.E.M. of three independent experiments done in triplicate. (***P < 0.001, * P < 0.05, n.s, not significant; Mann Whitney test). **b.** Spatial position of three oncogenic JAK2 mutants. K539L lies in the SH2-JH2 linker and is distant from the JH2 αC. T875N is located in the kinase domain (JH1) but close to the JH2 αC in the model of the JH1/JH2 complex (1). R683G localizes in JH2, close to the αC, and forms electrostatic interactions with D873 from JH1 across the JH1/JH2 interface. **c.** The four JAK2 oncogenic mutants are associated with numerous blood disorders. *Abbreviations,* PV: Polycythemia Vera, ET: essential thrombocythemia, PM: primary myelofibrosis, HES: hypereosinophilic syndrome, CMML: Chronic Myelomonocytic Leukemia, SM: systemic mastocytosis, CNL: chronic neutrophilic leukaemia, JMML: juvenile myelomonocytic leukaemia, RARS: refractory anaemia with ringed sideroblasts, RA: refractory anaemia, RCMD: refractory cytopenia with multilineage dysplasia, RAEB: refractory anaemia with excess of blasts, AML: acute myeloid leukaemia, IE: idiopathic erythrocytosis, RARS-T: refractory anaemia with ringed sideroblasts with thrombocytosis, MDS/MPN-U: unclassifiable Myelodysplastic syndrome/myeloproliferative neoplasms, MNP-U: unclassifiable or atypical myeloproliferative neoplasms, DS-B-ALL: Down Syndrom - B-ALL, B-ALL: B cell precursor ALL, AMKL: acute megakaryoblastic; leukaemia

5. A598F substitution exerts only a very weak destabilizing effect on the structure of JH2, but still allows ATP binding.

JAK2 JH2 exhibits a non-canonical ATP binding pocket that was shown to be accessible to ATP and Mg^{++}(12). We used thermal shift assay (TSA) to examine the effect of the A598F mutation on nucleotide binding and stability of the JAK2 pseudokinase domain *in vitro* (27). We produced different recombinant JAK2 JH2 proteins (12) bearing inhibitory mutations in addition to V617F and performed thermal shift assay (TSA) in the absence or the presence of various concentrations of ATP (**Figure 6**). E596A was previously shown to efficiently uncouple JAK2 V617F from cytokine-induced activity of JAK2 (6) and this mutation does not seem to structurally destabilize JH2. F595A was originally shown to inhibit JAK2 V617F hyperactivity without altering cytokine inducibility (10).

However, F595A induced a significant effect on the melting temperature (Tm) of JAK2 V617F (**Figure 6**) suggesting that it exerts a destabilizing effect on JH2. This finding is supported by long-scale molecular dynamic simulations performed on JH2 V617F/F595A, indicating that F595A induces a reversion of the αC stability of JH2 V617F back to a level lower than the JAK2 WT (12). A598F mutation only marginally affected the Tm of JAK2 V617F, especially when compared to F595A. Thus, the A598F mutation efficiently inhibits the activity of JAK2 V617F, without a major effect on folding of JH2 and without altering ATP binding.

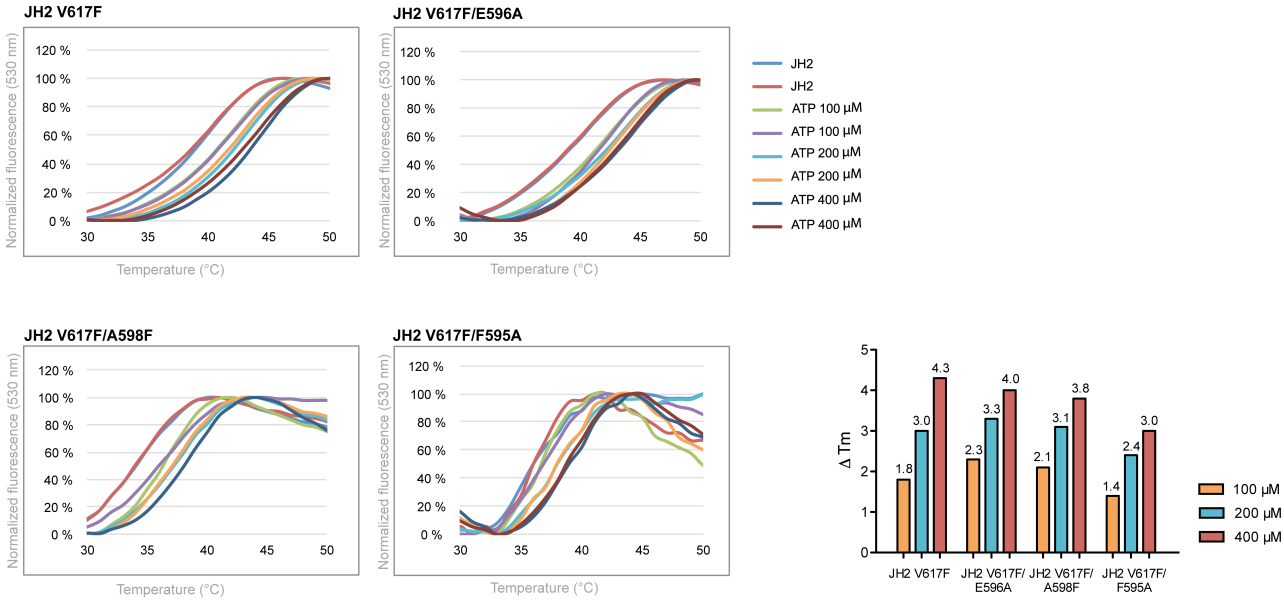

Figure 6. Effect of the inhibitory mutation A598F on the structural stability of JH2 V617F. Thermal denaturation curves of JAK2 JH2 domains (left panel) with the corresponding histograms depicting the Δ Tm values in each condition (right panel). Thermal denaturation of JAK2-JH2 V617F is not affected by the inhibitory mutation E596A (6) and slightly affected by the inhibitory mutation A598F. In contrary, the inhibitory mutation F595A (10) strongly alter the thermal denaturation of JAK2-JH2 V617F.

DISCUSSION

As an allosteric regulator of the JH1 kinase domain, JH2 can adopt an active conformation, which can no longer maintain inhibition on JH1 during activation by either cytokine stimulation or activating mutation of JH2, such as V617F. In the presence of V617F, the JH2 αC undergoes a change of configuration responsible for the constitutive activation of JAK2. This change of conformation is due to the formation of a π-π stacking interaction between the β4-β5 loop V617F and the αC F594/F595 of JH2. We investigated potential -ways to disturb this key contact only present in the active form of JAK2 V617F.
By strategically introducing bulky hydrophobic residue such as phenylalanine in the vicinity of the π-π stacking interaction, we aimed to turn off the hyperactivity of JAK2 V617F. We engineered a double mutant, namely JAK2 V617F/A598F that exhibited a basal activity close to that of the JAK2 WT. Thus, we described an inhibitory mutation A598F for JAK2 V617F hyperactivity. More interestingly this inhibitory mutation is preferential for JAK2 V617F and does not inhibit the cytokine activation of JAK2. The A598F mutation exerts its inhibitory function better in conditions of low physiologic expression than when the protein is overexpressed, suggesting that in latter conditions the F617-F595 aromatic interaction can reform even in the presence of A598F. In addition, we also shown that this inhibitory effect can be translated to homologous JAK1 V658F mutant associated with ALL. We hope that this new finding will facilitate inhibitor design strategies that target this key aromatic interaction only present in the mutant form of JAK2 V617F.

The inhibitory effect of A598F seems to be very similar to the effect of F595A previously described in that it affect the same molecular interaction necessary for the activity of JAK2 V617F. We previously showed that JAK2 V617F induces activation of JAK2 irrespectively of the dimeric conformation adopted by the cytokine receptor (10) and that the inhibitory mutation F595A, which decreases JAK2 V617F hyperactivity, causes the JAK2 V617F/F595A to lose its ability to signal from any dimeric conformations. Similarly, A598F could restore to JAK2 V617F the requirement for a particular EpoR dimeric configuration as shown by assessing JAK2 V617F/A598F in the presence of differently oriented EpoR dimers (**Figure S3**). This indicates that affecting the aromatic molecular interaction between F617 and F594/F595 from within the aromatic partners (F595A) or from the outside (A598F) leads to the similar inhibition of activation. However, the latter seems to be less aggressive on the JH2 structure than the former, as indicated by thermal shift assay.

JH2 seems to require ATP binding, but not phosphoryl transfer, in order to enable JH1 to adopt the correct conformation for its complete activation. Indeed, only JH2 of JAK2 was reported to possess a weak kinase activity (26), while JH2 domains of JAK1 and TYK2 were shown to bind ATP. It is highly likely that JH2 fulfills similar regulatory functions in all the JAKs family members.

Targeting the phenylalanines of the JH2 helix C such as F595 could also inhibit other JAK2 mutants. Indeed, Dusa et al (10) proposed that F595A mutation also affected the activity of other activated forms of JAK2, such as exon12 mutation (K539L).
JH1 cannot serve as scaffold for the other partner JAK JH1 domains during trans phosphorylation of the JAK2 molecules. We confirm that a mutation stabilizing the catalytic spine in a closed conformation is catalytically inactive. Furthermore, in the case of JAK2, this catalytic spine mutation cannot activate the kinase domain of the other JAK molecule through allosteric mechanisms, like it was reported for other kinases.

One major concern for the feasibility of an inhibition mechanism targeting the aromatic interaction could be the accessibility of the F-F-F aromatic interaction in the full-length three-dimensional structure of mutant JAK2. Molecular dynamic simulations of the JH1-JH2 complex of JAK2 (1) and structural data on the JH1-JH2 of TYK2 (11) indicate that the JH2 αC is located in the JH1-JH2 interface and which possibly hinders its accessibility to small molecules. However, the two models that were proposed were those of the inhibited form of JAKs. Indeed, Shan and colleagues ran simulations on JH1 and JH2 domains possessing two inhibitory sites that were phosphorylated (S523-P and Y570-P), while Lupardus and colleagues obtained the

X-ray crystal structure of the JH1-JH2 complex by expressing a kinase-inactive (D1023N) form of TYK2. In the conformation of JAK2 V617F, it is likely that the JH1-JH2 interface might differ therefore exposing the JH2 αC triple aromatic rings pocket that would become accessible to small disruptive molecules.

Our current studies placed bulky Phe residues in the vicinity of the π-π stacking interaction of F595 and F617. The inhibitory effect of A598F suggests that this approach might also be useful using exogenous molecules able to affect π-π stacking interactions. Such molecules would have the advantage that they will not be substituting residues possibly required for folding or dimerization of JAKs in active or inactive conformations. To this end we will start using a set of molecules, previously known to be involved in aromatic interactions. These molecules will be tested directly on JH2 V617F to assess their effects on JH2 folding and ATP binding by TSA. In the same time, we will test these molecules in functional assays to assess whether they affect signaling induced by JAK2 and JAK2 V617F basally, and in the presence of cytokines. Finally, we will test also wild type JAK1 and the constitutively active JAK1 V658F mutant in the settings of homodimeric and heterodimeric receptor complexes.

REFERENCES

1. Shan Y, Gnanasambandan K, Ungureanu D, Kim ET, Hammaren H, Yamashita K, et al. Molecular basis for pseudokinase-dependent autoinhibition of JAK2 tyrosine kinase. Nat Struct Mol Biol. 2014;21(7):579-84.
2. Baxter EJ, Scott LM, Campbell PJ, East C, Fourouclas N, Swanton S, et al. Acquired mutation of the tyrosine kinase JAK2 in human myeloproliferative disorders. Lancet. 2005;365(9464):1054-61.
3. James C, Ugo V, Le Couedic JP, Staerk J, Delhommeau F, Lacout C, et al. A unique clonal JAK2 mutation leading to constitutive signalling causes polycythaemia vera. Nature. 2005;434(7037):1144-8.
4. Levine RL, Wadleigh M, Cools J, Ebert BL, Wernig G, Huntly BJ, et al. Activating mutation in the tyrosine kinase JAK2 in polycythemia vera, essential thrombocythemia, and myeloid metaplasia with myelofibrosis. Cancer Cell. 2005;7(4):387-97.
5. Kralovics R, Passamonti F, Buser AS, Teo SS, Tiedt R, Passweg JR, et al. A gain-of-function mutation of JAK2 in myeloproliferative disorders. N Engl J Med. 2005;352(17):1779-90.
6. Leroy E, Dusa A, Colau D, Motamedi A, Cahu X, Mouton C, et al. Uncoupling JAK2 V617F activation from cytokine-induced signalling by modulation of JH2 alphaC helix. Biochem J. 2016;473(11):1579-91.
7. Ma W, Kantarjian H, Zhang X, Yeh CH, Zhang ZJ, Verstovsek S, et al. Mutation profile of JAK2 transcripts in patients with chronic myeloproliferative neoplasias. J Mol Diagn. 2009;11(1):49-53.
8. Mead AJ, Chowdhury O, Pecquet C, Dusa A, Woll P, Atkinson D, et al. Impact of isolated germline JAK2V617I mutation on human hematopoiesis. Blood. 2013;121(20):4156-65.
9. Mead AJ, Rugless MJ, Jacobsen SE, Schuh A. Germline JAK2 mutation in a family with hereditary thrombocytosis. N Engl J Med. 2012;366(10):967-9.
10. Dusa A, Mouton C, Pecquet C, Herman M, Constantinescu SN. JAK2 V617F constitutive activation requires JH2 residue F595: a pseudokinase domain target for specific inhibitors. PLoS One. 2010;5(6):e11157.
11. Lupardus PJ, Ultsch M, Wallweber H, Bir Kohli P, Johnson AR, Eigenbrot C. Structure of the pseudokinase-kinase domains from protein kinase TYK2 reveals a mechanism for Janus kinase (JAK) autoinhibition. Proc Natl Acad Sci U S A. 2014;111(22):8025-30.
12. Bandaranayake RM, Ungureanu D, Shan Y, Shaw DE, Silvennoinen O, Hubbard SR. Crystal structures of the JAK2 pseudokinase domain and the pathogenic mutant V617F. Nat Struct Mol Biol. 2012;19(8):754-9.
13. Gnanasambandan K, Magis A, Sayeski PP. The constitutive activation of Jak2-V617F is mediated by a pi stacking mechanism involving phenylalanines 595 and 617. Biochemistry. 2010;49(46):9972-84.
14. Toms AV, Deshpande A, McNally R, Jeong Y, Rogers JM, Kim CU, et al. Structure of a pseudokinase-domain switch that controls oncogenic activation of Jak kinases. Nat Struct Mol Biol. 2013;20(10):1221-3.
15. Patel AB, Vellore NA, Deininger MW. New Strategies in Myeloproliferative Neoplasms: The Evolving Genetic and Therapeutic Landscape. Clin Cancer Res. 2016;22(5):1037-47.
16. Heine A, Brossart P, Wolf D. Ruxolitinib is a potent immunosuppressive compound: is it time for anti-infective prophylaxis? Blood. 2013;122(23):3843-4.
17. Adrian FJ, Ding Q, Sim T, Velentza A, Sloan C, Liu Y, et al. Allosteric inhibitors of Bcr-abl-dependent cell proliferation. Nat Chem Biol. 2006;2(2):95-102.

18. Khateb M, Ruimi N, Khamisie H, Najajreh Y, Mian A, Metodieva A, et al. Overcoming Bcr-Abl T315I mutation by combination of GNF-2 and ATP competitors in an Abl-independent mechanism. BMC Cancer. 2012;12:563.
19. Zhang J, Adrian FJ, Jahnke W, Cowan-Jacob SW, Li AG, Iacob RE, et al. Targeting Bcr-Abl by combining allosteric with ATP-binding-site inhibitors. Nature. 2010;463(7280):501-6.
20. Liu X, Constantinescu SN, Sun Y, Bogan JS, Hirsch D, Weinberg RA, et al. Generation of mammalian cells stably expressing multiple genes at predetermined levels. Anal Biochem. 2000;280:20-8.
21. Kohlhuber F, Rogers NC, Watling D, Feng J, Guschin D, Briscoe J, et al. A JAK1/JAK2 chimera can sustain alpha and gamma interferon responses. Mol Cell Biol. 1997;17(2):695-706.
22. Muller M, Briscoe J, Laxton C, Guschin D, Ziemiecki A, Silvennoinen O, et al. The protein tyrosine kinase JAK1 complements defects in interferon-alpha/beta and -gamma signal transduction. Nature. 1993;366(6451):129-35.
23. Seubert N, Royer Y, Staerk J, Kubatzky KF, Moucadel V, Krishnakumar S, et al. Active and inactive orientations of the transmembrane and cytosolic domains of the erythropoietin receptor dimer. Mol cell. 2003;12(5):1239-50.
24. Pear WS, Nolan GP, Scott ML, Baltimore D. Production of high-titer helper-free retroviruses by transient transfection. Proc Natl Acad Sci U S A. 1993;90(18):8392-6.
25. Dumoutier L, Van Roost E, Colau D, Renauld JC. Human interleukin-10-related T cell-derived inducible factor: molecular cloning and functional characterization as an hepatocyte-stimulating factor. Proc Natl Acad Sci U S A. 2000;97(18):10144-9.
26. Ungureanu D, Wu J, Pekkala T, Niranjan Y, Young C, Jensen ON, et al. The pseudokinase domain of JAK2 is a dual-specificity protein kinase that negatively regulates cytokine signaling. Nat Struct Mol Biol. 2011;18(9):971-6.
27. Murphy JM, Zhang Q, Young SN, Reese ML, Bailey FP, Eyers PA, et al. A robust methodology to subclassify pseudokinases based on their nucleotide-binding properties. Biochem J. 2014;457(2):323-34.
28. Hammaren HM, Ungureanu D, Grisouard J, Skoda RC, Hubbard SR, Silvennoinen O. ATP binding to the pseudokinase domain of JAK2 is critical for pathogenic activation. Proc Natl Acad Sci U S A. 2015;112(15):4642-7.
29. Kornev AP, Haste NM, Taylor SS, Eyck LF. Surface comparison of active and inactive protein kinases identifies a conserved activation mechanism. Proc Natl Acad Sci U S A. 2006;103(47):17783-8.
30. Kornev AP, Taylor SS, Ten Eyck LF. A helix scaffold for the assembly of active protein kinases. Proc Natl Acad Sci U S A. 2008;105(38):14377-82.
31. Hu J, Yu H, Kornev AP, Zhao J, Filbert EL, Taylor SS, et al. Mutation that blocks ATP binding creates a pseudokinase stabilizing the scaffolding function of kinase suppressor of Ras, CRAF and BRAF. Proc Natl Acad Sci U S A. 2011;108(15):6067-72.
32. Staerk J, Kallin A, Demoulin J-B, Vainchenker W, Constantinescu SN. JAK1 and Tyk2 activation by the homologous Polycythemia Vera JAK2 V617F mutation: cross-talk with IGF1 receptor. J Biol Chem. 2005;280:41893-9.
33. Flex E, Petrangeli V, Stella L, Chiaretti S, Hornakova T, Knoops L, et al. Somatically acquired JAK1 mutations in adult acute lymphoblastic leukemia. J Exp Med. 2008;205(4):751-8.
34. Jeong EG, Kim MS, Nam HK, Min CK, Lee S, Chung YJ, et al. Somatic mutations of JAK1 and JAK3 in acute leukemias and solid cancers. Clin Cancer Res. 2008;14(12):3716-21.
35. Hemmann U, Gerhartz C, Heesel B, Sasse J, Kurapkat G, Grotzinger J, et al. Differential activation of acute phase response factor/Stat3 and Stat1 via the cytoplasmic domain of the interleukin 6 signal transducer gp130. II. Src homology SH2 domains define the specificity of stat factor activation. J Biol Chem. 1996;271(22):12999-3007.
36. Scott LM, Tong W, Levine RL, Scott MA, Beer PA, Stratton MR, et al. JAK2 exon 12 mutations in polycythemia vera and idiopathic erythrocytosis. N Engl J Med. 2007;356(5):459-68.
37. Mullighan CG, Zhang J, Harvey RC, Collins-Underwood JR, Schulman BA, Phillips LA, et al. JAK mutations in high-risk childhood acute lymphoblastic leukemia. Proc Natl Acad Sci U S A. 2009;106(23):9414-8.
38. Mercher T, Wernig G, Moore SA, Levine RL, Gu TL, Frohling S, et al. JAK2T875N is a novel activating mutation that results in myeloproliferative disease with features of megakaryoblastic leukemia in a murine bone marrow transplantation model. Blood. 2006;108(8):2770-9.

SUPPLEMENTAL INFORMATION

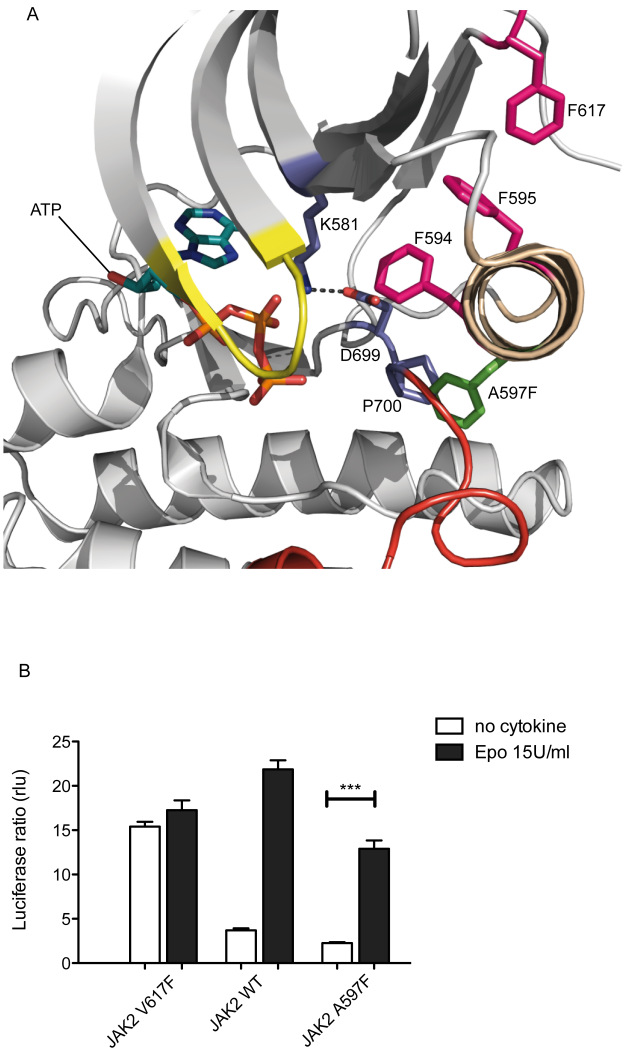

Figure S.1

a. Ribbon diagram of the crystal structure of JAK2-JH2 V617F (PDB: 4FVR). The αC is colored in wheat and the ATP binding loop in yellow. ATP molecule is depicted behind the ATP binding loop. The three phenylalanines residues involved in the aromatic interaction are shown in pink (F617, F595 and F594). The mutation A597F has been modeled on the diagram (green) and the F597 side chain could possibly contact P700 from the DPG (consensus DFG) motif, which might also alter the position of the D699 that forms a salt bridge with the β3 lysine (K581). This salt bridge is necessary for proper ATP binding and for JAK2 V617F activity but not JAK2 WT activity (28). **b.** STAT5 transcriptional activity of JAK2 WT with the point mutation A597F was measured in JAK2 deficient cells. While A598F prevents cytokine-induced signaling of JAK2 V617F, it allows Epo stimulation of JAK2 WT.

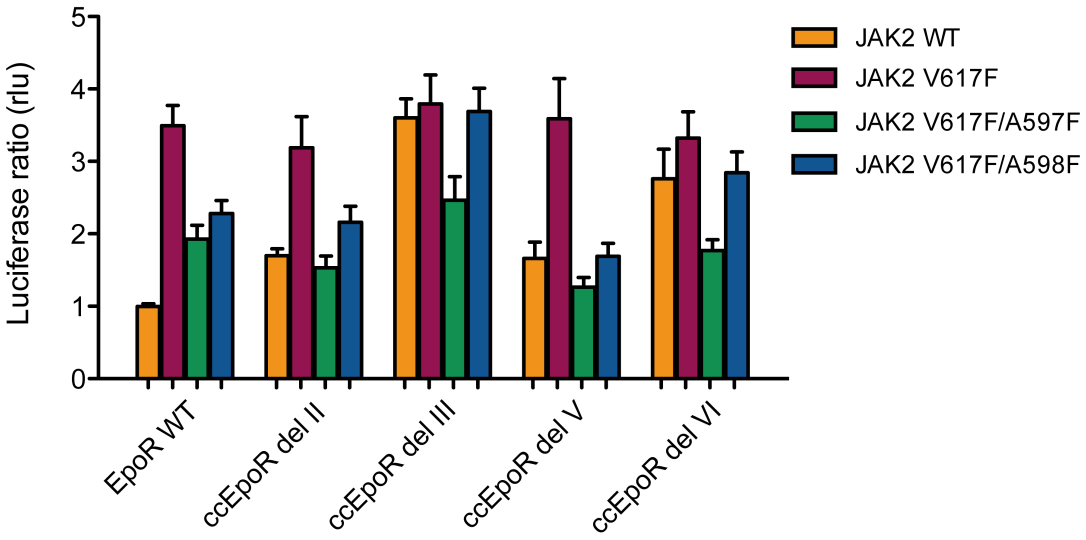

Figure S.2

STAT5 transcriptional activity of JAK2 V617F inhibited forms in the presence of differently oriented dimeric EpoR. JAK2 deficient cells we co-transfected with the JAK2 variants and chimeric EpoR receptors (ccEpoR del II, ccEpoR del III, ccEpoR del V, cc EpoR del VI) previously engineered by replacing the EpoR extracellular domain by a coiled-coil domain imposing different dimeric interfaces to the receptors downstream (23). JAK2 V617F can induce constitutive signaling regardless of the dimeric conformation of the bound receptor, while JAK2 WT requires specific orientations likely corresponding to the ligand-activated EpoR conformations (cc EpoR del III and cc EpoR VI) (10). JAK2 V617F/A598F lost the ability to signal constitutively from any dimeric conformations and behaves like JAK2 WT. In contrary, JAK2 V617F/A597F cannot trigger signaling from none of the inactive (cc EpoR del II, cc EpoR V) nor active (cc EpoR del III, cc EpoR del VI) conformation, suggesting the A597F alter catalytic function of JAK2 V617F.

DISCUSSION

1. Physiological activation of JAK2 by cytokine receptor

Homodimeric type-I cytokine receptors such as TpoR or EpoR are able to activate two JAK2 molecules that are non-covalently pre-bound to their cytosolic tails. Cytokine binding is thought to induce either conformational changes of the dimeric receptors or dimerization (or oligomerization) of the receptors. Consequently, this brings together the receptor-associated JAK2 molecules into a position conducive for cross-phosphorylation, which will then trigger signaling cascades. While the extracellular domains of some of these receptors are well characterized, little is known about their intracellular domains and how they behave following activation. In addition, the exact mechanisms underlying JAK2 cross-activation is poorly understood and the precise molecular interplay between two JAK2 molecules has yet to be elucidated. The only undeniable fact is that, following activation of the receptors, the two JH1 domains need to be in close proximity and oriented in a conformation suitable for cross-phosphorylation. Also, the role played by JH2 during this process is still unclear. It is of critical importance to understand how JH2 is functioning in the activation process, since the JH2 active site has been recently considered as a pharmacologically target.

1.1 Function of the pseudokinase domain during JAK2 activation: *cis* versus *trans* auto-inhibition

A central idea in the field is that JH2 negatively regulates JAK2 activity. This has been supported by the fact that numerous mutations located in the JH2 domain induce activation of the adjacent kinase domain, thus implying that such mutations abrogate the inhibitory effect exerted by JH2 on JH1. JH2 is thought to maintain suppression of JH1's kinase activity by an auto-

inhibitory action through interdomain contacts between JH1 and JH2. However, since cytokine receptors complexes include two JAK molecules, there are currently two prevailing models for regulation of JAK kinase activity by the JH2 domain: either JH2 inhibits JH1 within the same molecule via an "*in cis*" mechanism, or JH2 inhibits the JH1 domain of the other molecule via an "*in trans*" mechanism (**Figure 19**).

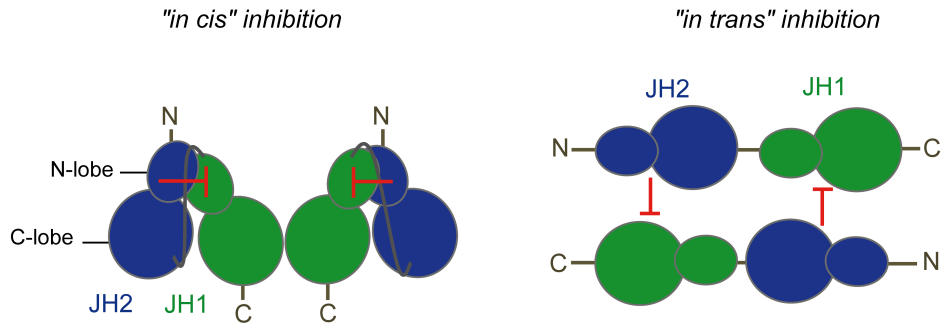

Figure 19. Two models have been proposed for regulation of JAK kinase domain by the pseudokinase domain. Left: in the *in cis* inhibition, JH2 binds and inhibits the kinase domain within the same JAK2 monomer, which suppresses JAK2 kinase activity. Right: the *in trans* model suggests that JH2 binds and inhibits the kinase domain of another JAK2 monomer within the same receptor-JAK complex to suppress the kinase activity of JAK2. Reorientation of the JAKs in both models is believed to facilitate the correct alignment and final trans-phosphorylation of the kinase domains that will activate the JAKs.

Several conflicting studies on how the JH2-mediated inhibition might occur have been recently published. Firstly, Brooks and colleagues suggested a model for JAK2 activation by the growth hormone receptor (GHR) supporting the *in trans* auto-inhibitory mechanism (98). By using FRET (fluorescence resonance energy transfer), they showed that the GHR mainly exist as a pre-dimerized receptor. They proposed that cytokine binding induces a rearrangement of the transmembrane helices leading to separation of the membrane proximal region of the receptor including box1. This separation is thought to pull apart the two JH2 domains,

whilst bringing the two JH1s in close proximity (**Figure 19, right**). Secondly, SAXS (small angle X-ray scattering) studies demonstrated that in solution, JAK2 JH2-JH1 domains exist in an elongated configuration with no evidence for interaction between JH1 and JH2 within the same molecule (266) (**Figure 19, right**). However, it should be noted that the JAK2 JH2-JH1 proteins were purified in an activated state, thus the observed configuration might not be relevant for an inhibited state of JAK2.

Third, in contrast with the two previous studies, a recent long time-scale molecular dynamic simulation of JAK2 JH2-JH1 provided the first structural model for the auto-inhibitory interaction between the two domains supporting an *in cis* mechanism (209)(described in **the introduction, section 5.3, Figure 14**). At the same time, the structure of TYK2 JH2-JH1 was solved and highly resembles to the JAK2 model (208). The TYK2 structure also supports an inhibitory mechanism occurring *in cis* (**Figure 19, left**). The two models describe an interacting interface predominantly mediated by the N-lobes of each domain (**Figure 19, left**). Because the length of linker between the two domains is quite short (40 amino acids in JAK2), it does not allow JH1 to wander too far. Thus, it supports the notion that the observed interface in both studies is an *in cis* rather than an *in trans* interface. Given the difficulty in purifying kinases in an inactivated state, it is not absolutely certain whether the observed *in cis* auto-inhibitory interface is the correct one. In fact, molecular dynamic simulations (209) were run using JAK2 JH2 (PDB: 4FVQ) and an activated form of JH1 (PDB: 3KRR) where the activation loop has been expelled out of the kinase active site. Whether by using the inactivated form of JAK2 JH1, such as the one bound to the type-II inhibitor NVP-BBT594 (PDB: 3UGC) (**Table 2**) (218), the *in cis* auto-inhibitory interface would have been the same is questionable. In addition, although the crystallographic data of TYK2 JH2-JH1 (208) were obtained using a kinase-dead mutant (D1023N), JH1 still exhibits an activation loop with an open-conformation implying that TYK2 JH1 is active, thereby raising the possibility of misrepresenting the inhibitory interface.

The fact that JAK2 auto-inhibition only relies on an *in trans* inhibitory mechanism is doubtful considering that EpoR exhibits several inactive interfaces (96). Indeed, it is unlikely that several *in-trans* inhibitory interfaces coexist within the receptor-JAK complex.

While supporting evidence for each model have been shown, our study supports an *in cis* auto-inhibitory mechanism, in which activating mutations occurring in the vicinity of the interface abrogates the JH2-mediated inhibition leading to JAK2 activation. However, it is highly conceivable that multiple levels of auto-inhibition might occur in JAKs. Indeed, a straightforward "on/off" system is not relevant for JAKs regulation, as multiple transient inhibitory states likely exist in receptors and JAKs. Proteins are in perpetual motion and oscillate between different conformational states. Cytokine binding must stabilize on activated state of the receptor that position the JAKs in an orientation compatible for kinase domain cross-phosphorylation.

Hopefully, by solving the full-length structure of JAK2, the regulatory mechanisms will start to be understood. However, when alone in solution, the JAK2 molecule might not behave the same as when it is bound to receptor. JAK2 full-length structure should be studied in a broader context. Indeed, the binding to the receptor cytosolic tail as well as the membrane environment must be taken into consideration when studying JAK2 configuration. For instance, single particle imaging of the gp130/IL-6/IL-6R/JAK1 holocomplex showed that JAK1 association with gp130 is enhanced by the presence of the lipidic membrane environment (267). Hence, both the membrane and the receptor cytokine tail must play a role in the final and productive configuration of JAK2 during activation. Activating mutations or cytokine binding seem to destabilize the *in cis* inhibitory interface, which in turn liberate the kinase domain from its steric constraint. The kinase domain is therefore free to phosphorylate the other JAK2 molecule that is in close proximity. While the intra-molecular interaction is beginning to be uncovered, the molecular basis of the inter-domain communication has yet to be elucidated.

1.2 Function of the pseudokinase domain in the inter-molecular interface.

Our study was based on the *in cis* inhibitory mechanism, in which V617F triggers a series of activating events across the JH2-JH1 interface, destabilizing the inhibitory effect exerted by JH2 on JH1. Both cytokine binding and activating mutations weaken this interface, thereby giving three-dimensional freedom to JH1 to activate the other JH1 domain. However, it seems that receptor-JAK2 complexes require a second molecular event to properly trigger signaling. The second event is likely induced by conformational change of the receptor and the subsequent rearrangement of the appended JAKS. This is supported by the finding that JAK2 V617F oncogenic effects are not triggered unless homodimeric receptors, such as EpoR or TpoR, are present. Hence, it implies that this second molecular event must occur likely through dimerization of the receptor or configurational change of dimerized receptors. While the role of the JH1 domain in the inter-molecular confrontation is evident (cross-phosphorylation), the function of the JH2 domain is less clear. Three theoretical models can be proposed to sketch the interaction between two JAK2 monomers within the receptor-JAK complex (**Figure 20**).

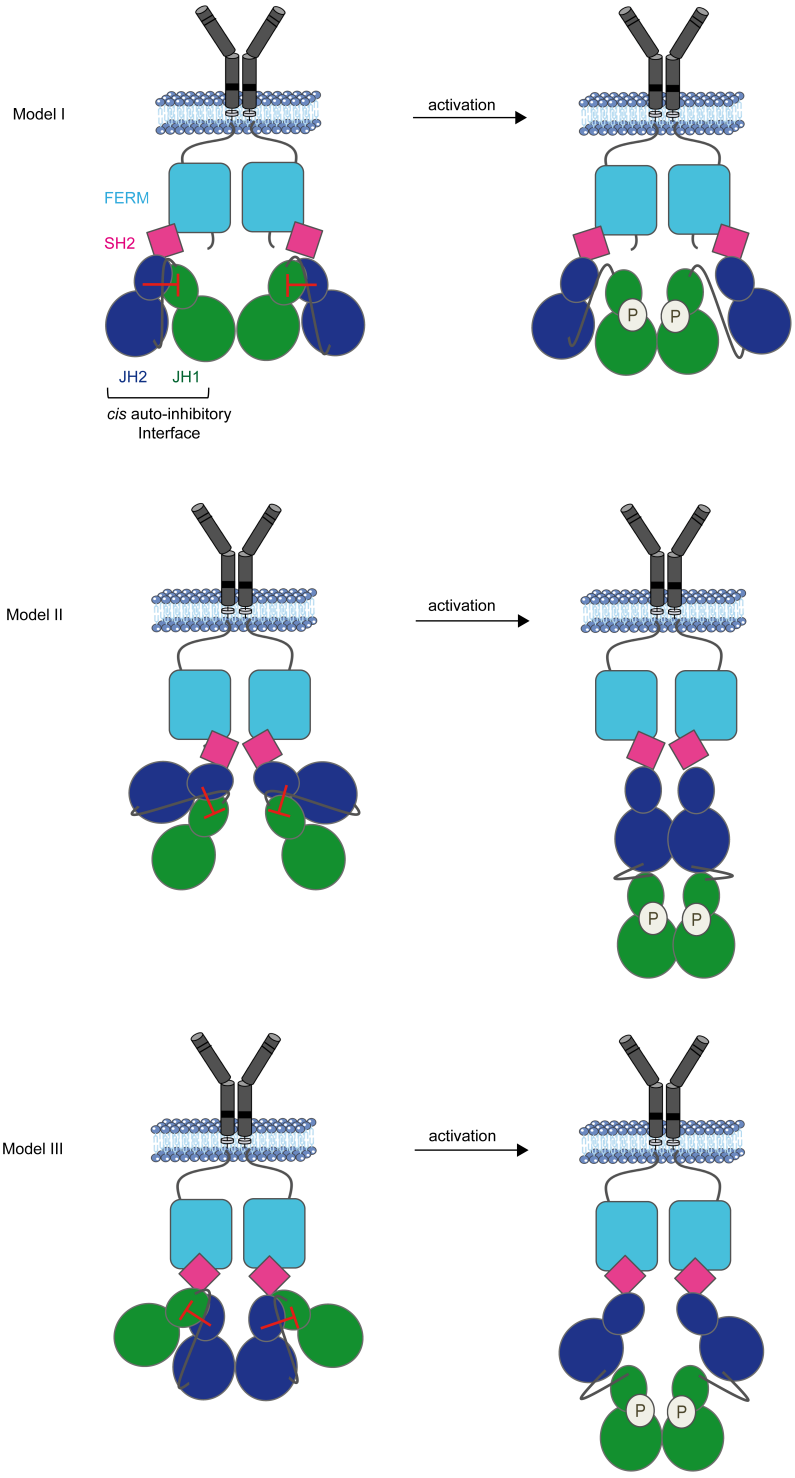
Model I
activation
FERM
SH2
JH2
JH1
cis auto-inhibitory
Interface
P
P
Model II
activation
P
P
Model III
activation
P
P

Figure 20. Theoretical models of the inter-molecular interplay between two JAK2 molecules and the role of JH2 in the process.
Model I: Single role of JH2. In this model, no additional event to the release of the *in cis* auto-inhibitory interface is required for activation. The two JH1 domains are already well positioned in the inter-domain interface to cross-phosphorylate each other.

Model II: Dual /opposite roles of JH2. In this second model, JH2 has the *in cis* auto-inhibitory function. In addition, JH2 plays a positive role as a steric scaffold bringing the two JH1 together in the activated state.
During activation, rearrangement and association of the two JH2 domains will guide the two JH1 to come in close proximity. This model suggests the existence of a positive inter-molecular JH2 interface in the activated state.

Model III: Dual/combined roles of JH2. In this third model, in addition to the *in cis* auto-inhibitory function, JH2 plays a second negative role as a steric spacer preventing the two JH1 from coming into close proximity in the inactivated state.
During activation, rearrangement and separation of the two JH2 domains will induce more three-dimensional freedom to the JH1 domains allowing them to come into close proximity. This model suggests the existence of a negative inter-molecular JH2 interface in the inactivated state.

Our data can only account for the *in cis* auto-inhibitory interface and cannot support one or the other models. However, the existence of a JH2 dimer is highly suggested from structural data analyses. In fact, several JH2 dimers can be suggested by examining the crystal packing of several JH2 structures including JAK1 (PDB: 4L00) and TYK2 (PDB: 5C01 and 4WOV). The JAK1 JH2 dimer interface is supported by mutagenesis data (210), whereas the more recent TYK2 JH2 dimer interface has yet to be investigated. The existence of a JH2 dimer interface would exclude the first model. Moreover, the kinase domains seem to be prone to movement during activation, as demonstrated by Brooks and colleagues with the GHR (98) who were able to measure the kinase domains convergence by FRET during GRH activation. This supports either the second or the third model. A combination of mutagenesis and protein-protein interaction-based techniques will be required to determine the second role of JH2 during the process of activation of JAK2. It is essential to determine the exact function of JH2 during this process in order to anticipate the effect of small molecules binding the JH2 active site. Indeed, such compounds could either stabilize or destabilize a probable JH2 dimer that will either induce activation or inactivation of the signaling complex.

2. Pathological activation of JAK2 by the mutation V617F

More than 10 years after the discovery of the mutation JAK2 V617F, the exact mechanism by which the mutation V617F activates JAK2 is still unclear. However, some lines of evidence on the structural and molecular levels have started to unveil molecular machinery triggering constitutive kinase activity. It is now well accepted that the key player in this activation cascade is the JH2 αC helix. This concept is now corroborated by analysis of the solved crystal structure of JAK2 JH2 V617F. Reconfiguration of the JH2 αC is thought to trigger a molecular signaling cascade leading to activation of JH1. The mechanism by which V617F activates JH2 through disruption an auto-inhibitory interaction between JH2 and JH1 is largely based on the *in cis* model. The work described in this thesis suggests that, similarly to a domino chain reaction, V617F triggers a series of activating events,

which eventually causes kinase domain activation (**Figure 21**). When valine 617 is mutated to phenylalanine in JH2, a region remote from the active site, information is transferred through the protein to JH1 via a sequential set of events propagating linearly from an allosteric site (JH2 αC) to the kinase active site. The set of events inducing V617F-mediated activation can be divided in two types of molecular events (blue and red residues on the figure): First, *the oncogenic switches* (F595, E596 and F537 in blue) are residues transmitting the conformational changes. When they are mutated to alanine, they suppress the oncogenic activation without altering the normal activation of JAK2. Second, *the activating events* (E543, D569, Y570, K857, K883 in red) are residues that indirectly (E543, D569, Y570) or directly (K857, K883) participate in controlling the catalytic activity of the kinase domain. When they are mutated to alanine, they induce activation of JAK2 (**Figure 21**).

Figure 21. The domino model illustrates the sequential set of events propagating from the V617F site to the kinase active site. The oncogenic switches are colored in blue, while the direct activating events that are part of the molecular path are colored in red. The chain reaction is triggered in JH2 by V617F and is then transmitted via the SH2-JH2 linker to the JH2 N-lobe and finally to the JH1 N-lobe.

The oncogenic switches transmit activation from the V617F mutation, triggering the domino chain reaction

The role of F595 has already been described in the introduction (**Figure 15**). It participates in the aromatic interaction with V617F that is responsible for the change in conformation of the JH2 αC. E596 side chain is believed to alter its orientation due to the conformational change of the JH2 αC (**Figure 22**) and then, to contact and clash with residues from the SH2-JH2 linker C-terminal region. This linker, which participates to the auto-inhibitory interface between JH1 and JH2, undertakes remodeling and destabilizes the inhibitory interplay. F537 is part of a highly conserved F-F-V triad (F537-F595-V617). When the V is mutated to F (like in V617F), it displaces F537 from its original position in the triad, rearranging the SH2-JH2 linker. F537 is kicked-out of the triad and likely contact residues in JH1 involved in catalytic activity, such as residues of the G-loop.

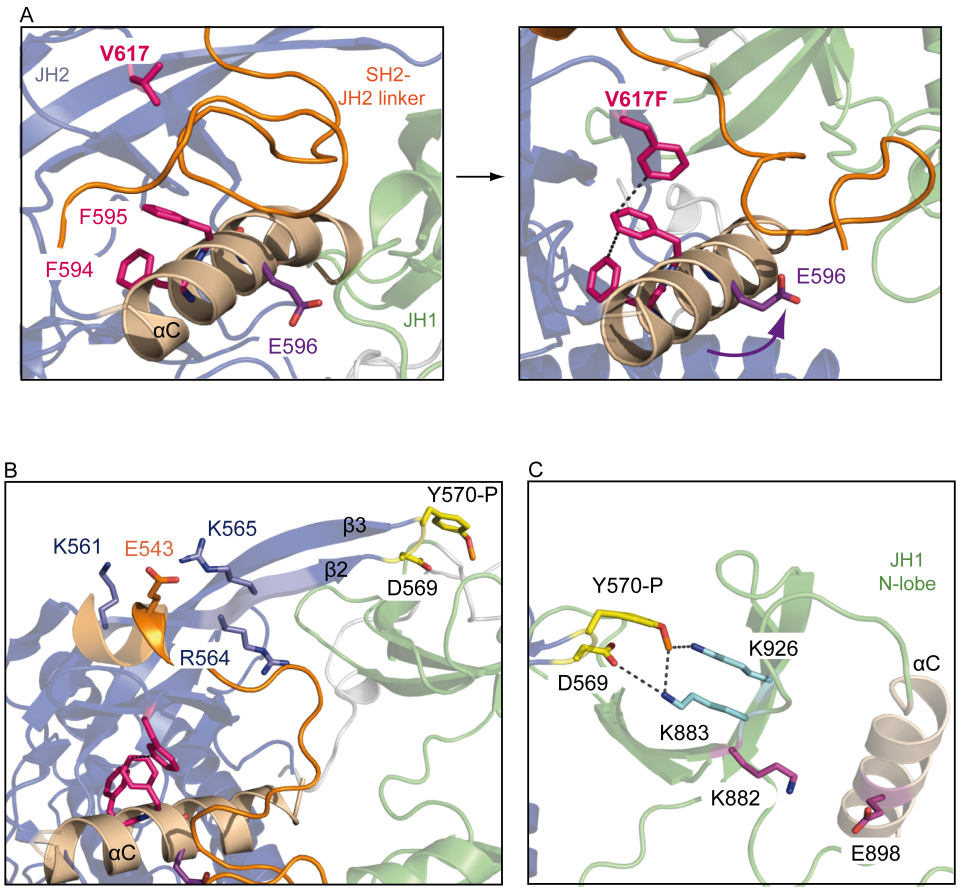

Figure 22. Modeling of the structural changes induced by V617F mutation from the JH2 αC helix to the N-lobe of JH1. a. In the wild type conformation, the position of E596 is thought not to contact the SH2-JH2 linker that stabilizes the JH2-JH2 inhibitory interface. Upon V617F mutation, the JH2 αC changes configuration that will alter the position of E596 (arrow). E596 clashes with the SH2-JH2 linker. **b.** The tip of the linker contains E543. Rearrangement of the linker will interrupt the contact between E543 and the β2 strand residues leading the destabilization of the β2- β3 loop containing Y570 and D569. **c.** Ion pairs between JH2 N-lobe residues and JH1-N-lobe residues are broken, which leads to the activation of JH1. Coordinates of the JAK2 JH2-JH1 modeling have been used to illustrate the changes (202).

The activating events are part of the domino chain reaction leading to JH1 activation

E543 is located in the SH2-JH2 linker and its deletion has been already associated with MPNs (46). Thus, it is not surprising that mutating this glutamate to an alanine leads to constitutive activation of JAK2. E543K is not an activating mutation (**Supplemental Fig 4, Paper 1**), which implies that E543 is involved in hydrogen bonding formation. Structural analysis of the JH2-JH1 model indicates that E543 could potentially contact polar residues from JH2 β2 strand (**Figure 22**). Loss of the polar side chain at position 543 induces loss of interactions between the SH2-JH2 liker and the β2 strand, leading to structural destabilization of the β2-β3 loop where Y570 and D569 are positioned. When phosphorylated, Y570 was shown by MD simulation to form a salt bridge with K883 on JH1 (209), while D569 is thought to mediate a hydrogen bond with E864 on JH1 (**Figure 22**). Loss of these two inter-domain contacts is believed to enable formation of the critical salt bridge between the VAIK lysine (K883) and the αC glutamate (E864) described in the **introduction, section 4.3**. Finally, K857 is involved in controlling the position of the JH1 P-loop as its position is likely affected by the movement of F537. When F537 is liberated from the F-F-V triad, it is though to clash with the K857 side chain.

The SH2-JH2 linker plays a pivotal role in the activation of JAK2 V617F

The SH2-JH2 linker is a highly flexibly region. However, in the basal state, its C-terminal region is stabilized within the JH2-JH1 auto-inhibitory interface. Our data showed that this portion is actually necessary for the constitutive activation of JAK2 V617F. This region seems to play a critical role in transmitting the V617F effects from JH2 to JH1, thereby underlying the positive regulatory function exerted by JH2 on JH1. Curiously, numerous MPN and hematological disease-linked mutations and deletions cluster in this linker region (46, 236), regrouped under the name of "exon 12 mutations". Thus, activation can also be triggered directly from this region to JH1 by a still undefined molecular mechanism. Interestingly, this portion consists of several amino acids with charged side chains likely to be involved in polar or electrostatic interactions with either JH1 or JH2 N-lobes. This could give a rationale for the activation mechanism of exon 12 mutations since they mostly involve substitutions or deletions of charged residues (**Annex 7**). The SH2-JH2 linker is suggested to be a key player in both normal and pathological activation of JAK2. Although it forms contacts with both JH2 and JH1 to bridge the two domains in the basal state, it is yet to be confirmed if these interactions remain in the full-length context. However, the concept that the linker mainly interacts with N-lobe and the hinge region of JH1 is supported by kinetic analyses on recombinant proteins demonstrating its role in regulating the JH1 affinity for ATP (233). Thus, the linker functions to allosterically stabilize the active conformation of the JH1 tyrosine kinase through modulation of the catalytic motif.

V617F promotes JH2-mediated positive interaction

V617F activation has always been thought to be the result of a loss of the inhibitory effect exerted by JH2 on JH1. Indeed, V617F destabilizes the inhibitory molecular interplay between these two domains. However, we believe that V617F phenotype results from a combination of *loss of auto-inhibition* and an additional *direct activation mechanism*. While, the former is starting to be better understood, thanks to mutagenesis studies (**Article 1**)

and MD simulation (209), the latter has drawn less attention and is still largely unexamined. Our data and modeling suggest that this activation process would involve the SH2-JH2 linker contacting new residues in JH1 in the mutant conformation. It is probable that this additional mechanism stabilizes a positive regulatory interaction mediated by JH2, the molecular details of which are still under investigation.

What is clear is that V617F must drive the formation of the active conformation of JH1 through remodeling of the molecular interplay between JH1 and JH2. Given that the final step of activation of a kinase is the correct alignment of the motifs involved in catalytic activity, we believe that V617F influences the position of these motifs through an allosteric mechanism that is starting to be understood in part. Kinase activation is triggered by changes in the positioning of the catalytic motifs. In the case of JAK2 V617F, it seems that modulation of the P-loop and the VAIK lysine might be part of the activation process. In contrast, movement of the JH1 αC helix does not appear to be involved in V617F-mediated activation of JAK2, nor in cytokine-induced activation. In fact, structural comparison between the active (PDB: 2B7A) and the inactive conformation (PDB: 3UGC) of JH1 shows that the αC remains in the same position in both activation states. In addition, the crystal structure of TYK2 JH2-JH1 (208) and model of JAK2 JH2-JH1 (209) show a kinase domain with the activation loop expelled from the active site, despite the use of a kinase-dead mutant for TYK2 (D1023N) and an auto-inhibited form of JAK2 for the modeling (with inhibitory sites Y570 and S523 that are phosphorylated). Thus, release of the activation segment does not seem to be part of the activation process of JAK2 WT nor V617F. This current model is far from the initial one in which the activation segment of JH1 was maintained open by direct contact with the loop containing V617.

Undoubtedly, the crystal structure of the full-length JAK2 is required to fully explain the mechanism of activation of JAK2 V617F at the molecular level. Furthermore, whether V617F promotes a JH2-mediated positive interaction that is normally induced by cytokine has still to be elucidated. Nevertheless, we postulate that V617F activation does not use the same molecular pathway to activate JH1 as cytokine-induced activation. This is supported by the description of five inhibitory mutations that are able to uncouple V617F-from cytokine induced activation (see following section).

The activation mechanism of V617F in JAK2 can be translated to others JAKs

JAK1 and TYK2 can be activated by a similar mutation to V617F (38). Valine 617 is not conserved in JAK3 (M592) and JAK3 cannot be activated by a similar substitution to V617F. JAK3 M592F does not induce constitutive activation of JAK3 probably due to the non-conservation of an aromatic residue at in the middle αC at position similar to F595 (replaced by a leucine in JAK3, L570). The inhibitory effects of F595A, E596A and A598F have been shown to be applicable to JAK1 V658F. Given the spatial conservation of most of the residues involved in the V617F-mediated activation across the JAKs (**Table 3**), it is likely that comparable activation mechanisms occur in JAK1 and TYK2 upon mutation of the residues homologous to V617. The electrostatic network across the JH2-JH1 interface displays great similarities between JAK1, JAK2 and TYK2 (208, 209). However, as JAK2 is the only JAK that signals through homodimeric complex formation in cells, it cannot be excluded that JAK2 possesses its own regulatory mechanisms necessary to maintain stronger autoinhibition between two JAK2 molecules. This can be supported by the fact that JAK1 exhibits a lower basal activation level than JAK2. In addition, the effects of the inhibitory mutations (E596A and A598F) are more potent in JAK1 V658F than in JAK2 V617F, suggesting that JAK1 is more prone to inhibition than JAK2. JAK2 seems to possess a general higher activation level that requires additional *intramolecular* negative regulatory mechanisms such as phosphorylation of residues (Y570 and S523). V617F and homologous mutations probably trigger a corresponding molecular cascade in other JAKs leading to activation of JH1.

JAK2	JAK3	JAK1	TYK2	Spatial location
V617	M592	V658	V678	JH2, β4-β5 loop
F594	F569	F635	F655	JH2, αC
F595	L570	F636	Y656	JH2, αC
E596	E571	E637	E657	JH2, αC
F537	F513	F575	F581	SH2-JH2 linker
E543	D519	D582	E588	SH2-JH2 linker
D569	D545	D608	D622/D623	JH2, β2-β3 loop
Y570	E547	E609	E624	JH2, β2-β3 loop
K883	Q856	S909	A931	JH1, β3 strand
E864	E837	K888	K910	JH1, β2 strand
K857	K830	E883	E905	JH1, G-loop

Table 3 Conservation of the residues involved in V617F-mediated activation across JAKs. The residues that are not conserved are colored in red. E864 and K857 are both replaced by an amino acid of opposite charge in JAK1 and TYK2.

3. Development of inhibitors specific for JAK2 V617F

3.1 Novel allosteric sites in the pseudokinase/kinase interface of JAK2.

Regulation of JAK2 activity occurs through different levels of coordination between the different domains of the same protein, or between JAK2 and other molecules. Understanding the regulatory mechanism at the molecular level will be useful in the development of novel allosteric inhibitors. To do so, identification of druggable pockets on the surface of JAK2 that are distant from the kinase domain active site is necessary. The JH2 domain displays several cavities and pockets (**Figure 23**) that could be investigated.

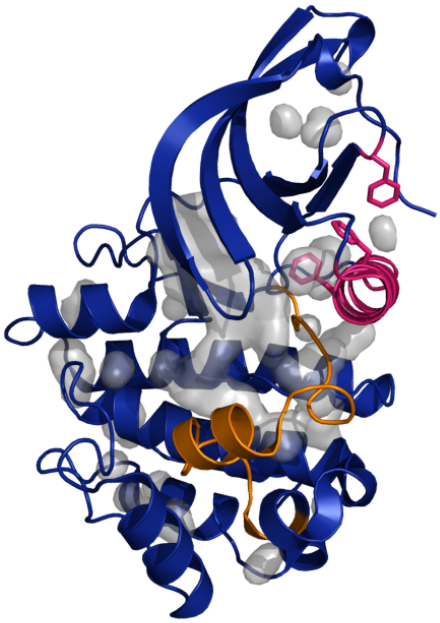

Figure 23. Representation of the pockets and cavities in JAK2 JH2 V617F. The pseudokinase domain of JAK2 displays several cavities and pockets (grey) that could potentially be accessible by small molecules. The largest pocket between the two lobes is the ATP binding pocket. The αC is colored in pink and the activation loop in orange. (PDB: 4FVR). Cavities and pockets are depicted using PyMol.

Given the latest advances in the structural biology of JAKs (all JAKs domains structures, except for JAK3, are solved; see table 2) combined with the major progress in molecular dynamics (MD) simulation, the feasibility of the task is improving. MD can be used to predict protein structure and the assembly of the different domains; such it has been done for JAK2 JH2-JH1 (209). It can also be used to study the interaction between a protein and other molecules, such as in ligand docking. Protein-ligand docking is a method used to predict the preferred orientation of a given molecule to bind a target protein of known 3D structure, in order to form a stable complex (268). This method has become a useful tool in various drug discovery programs. Five mutations have been shown to be able to uncouple V617F from cytokine-induced activation of JAK2, 3 from the JH2 αC: F595A, E596A/R and A598F as well as 2 from the SH2/JH2 linker: F537A and K539E summarized in **Figure 24**.

Our data could appreciably inform the design and development of next-generation inhibitors. Indeed, targeting these allosteric sites, if located in an accessible cavity or pocket, could possibly achieve potent and specific inhibition of JAK2 V617F. In addition to this, based on the recent findings in the field of JAKs biology, I endeavored to summarize the possible novel strategies in the review presented in the **perspectives, page 126**.

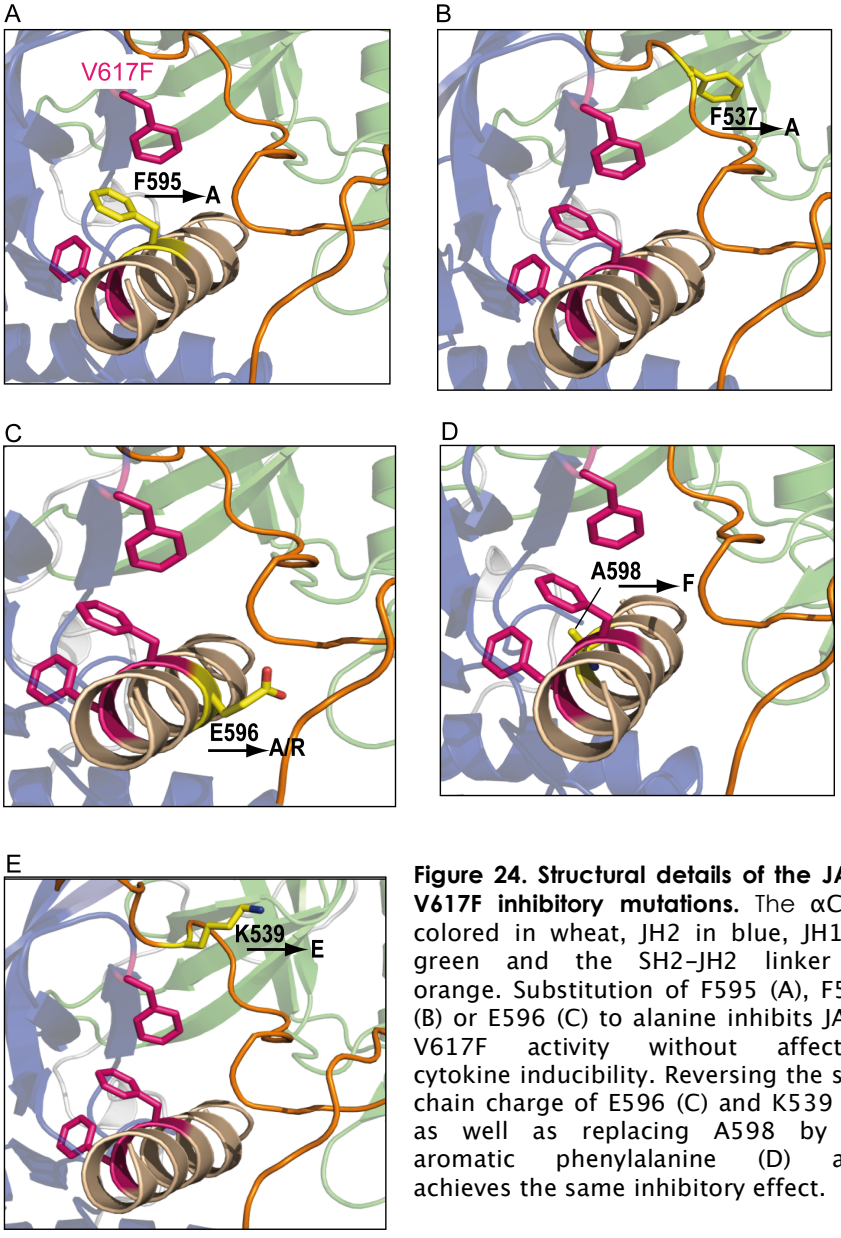

Figure 24. Structural details of the JAK2 V617F inhibitory mutations. The αC is colored in wheat, JH2 in blue, JH1 in green and the SH2–JH2 linker in orange. Substitution of F595 (A), F537 (B) or E596 (C) to alanine inhibits JAK2 V617F activity without affecting cytokine inducibility. Reversing the side chain charge of E596 (C) and K539 (E), as well as replacing A598 by an aromatic phenylalanine (D) also achieves the same inhibitory effect.

3.2 *Ab initio* modeling of small molecules specific for JAK2 V617F.

The identification of allosteric sites that only affect the V617F-mediated activity of JAK2 is a godsend for pharmacological development. Investigation of these allosteric sites by analyzing the available X-ray crystal structures has given a detailed view of the molecular mechanism of inhibition occurring at these sites. One strategy for the pharmacological restraint of JAK2 V617F would be the *ab initio* design of compounds that would achieve the same effects as the inhibitory mutations defining the allosteric sites. A hydrophobic pocket around residue E596 was detected in the JAK2-JH2 V617F X-ray structure (PDB: 4FVR) (**Figure 25**). Our hypothesis is that targeting this pocket with a compound that could react and neutralize E596 would achieve inhibition of JAK2 V617F. Whether this pocket is still accessible in the context of the full-length protein will have to be determined. **Figure 25** sketches the effect of a virtual compound binding to the pocket around E596.

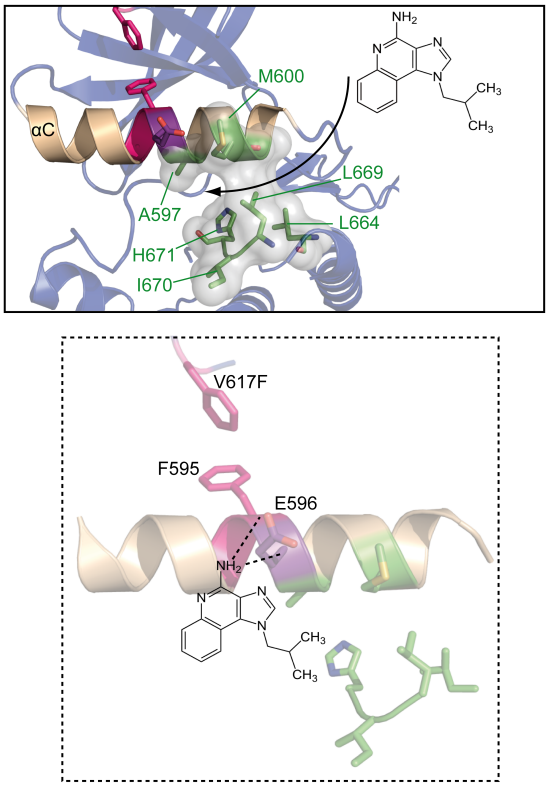

Figure 25 Location of a hydrophobic pocket underneath the JH2 αC and close to residue E596. The pocket was identified on the X-ray crystal structure of JAK2 JH2-V617F (PDB: 4FVR) using the PyMol plugin PocketPicker. This hydrophobic pocket is made of residues A597 and M600 from the αC; L699, I670 and H671 from the catalytic loop and L664 from αE. The compound shown here is virtual and displays two amines that could potentially neutralize the glutamate at position E596.

Our data with the double mutant JAK2 V617F-A598F also indicated that disruption of the π-stacking between F617 and F595 specifically inhibits the hyperactivity of JAK2 V617F. Thus, we propose that small molecules able to interrupt this aromatic interaction in the same way as A598F does would be a potential inhibitory strategy. Compounds with chemical scaffolds such as nitrobenzene, fluorenone or pyridinium could target and disrupt the interaction between F617 and F595 (**Figure 26**). The possible structural effect of the inhibitory mutation A598F on the JAK2 V617F αC (**Article 2**), suggests that small compounds inducing the same structural disturbance would achieve specific inhibition of JAK2 V617F.

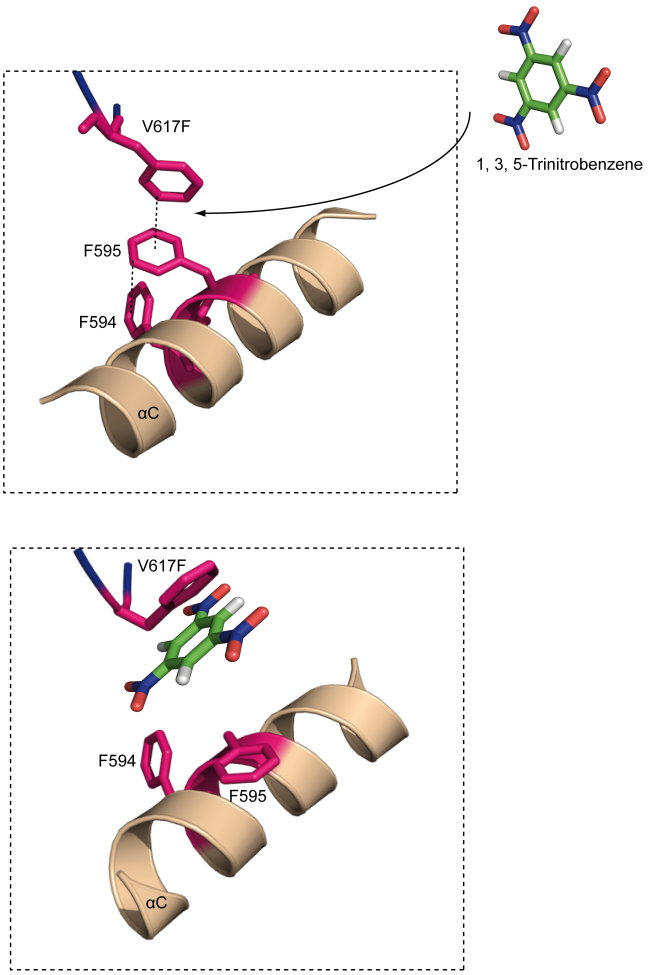

Figure 26.
Putative aromatic π-stacking disruptive chemicals. The JH2 αC of JAK2 V617F is shown with the three phenylalanines involved in the aromatic π-stacking interaction. Chemicals shown of the right are proposed to interact and disrupt this interaction in the same way as A598F.

CONCLUSION

The probability of success of JAK2 inhibitors to cure MPNs has always been problematic. The available JAK2 targeting compounds are aimed at inhibiting the kinase domain and have shown variable dose-dependent toxicities and emerging resistance. The growing arsenal of ATP-competitive inhibitors might not be sufficient in treating JAK2 V617F-positive MPN patients. For this reason, we believe that allosteric regulation should be considered when developing new JAK2 inhibitory strategies. JAK2 and the JAK-STAT pathway are necessary for the hematopoietic development and immune system, thus JAK2 inhibitors cannot be used at high doses. For JAK2 inhibitors, besides a strong catalytic inhibition, molecules must possess a high selectivity for JAK2 amongst the other JAKs and ultimately for JAK2 mutants such as JAK2 V617F versus the native form. A detailed understanding of the structural features regulating both normal and pathological JAK2 activities is required. Our general understanding of how cytokine receptors activate JAK2 is poor compared to other systems such as tyrosine kinase receptors or GPCRs. In addition, JAK2 has the peculiarity to comprise tandem kinases domains, JH1 and JH2. The JAK2 JH2 is a hotspot for mutation associated with hematological diseases and the exact regulatory function of this domain in both normal and pathological activation of JAK2 is still unclear.

We identified novel allosteric sites predominantly in JH2 of JAK2 V617F and the mechanisms by which allosteric inhibition occur at these sites have been investigated. The inhibitory mutations at these sites distant from JH1 were also informative for pathological activation, as well as for the normal regulation of the protein. We have added to the evidence that the JH2 αC is a key element in triggering JAK2 V617F hyperactivity and showed that it is possible to uncouple V617F from cytokine-induced activation by modulating sites around the JH2 αC. In addition, we identified a community of residues across the SH2-JH2 linker, JH2 and JH1 that mediate V617F-activation.

The three-dimensional structure of full-length JAK2 will be necessary to fully understand the regulation of kinase activity by the other domains as well as to answer more of the pertinent questions on the exact molecular effects induced by activating mutations in JAKs. In the meantime, this study shed a light on possible allosteric sites involved in the hyperactivity of JAK2 V617F that offer great potential to be exploited in the design of future JAK2 inhibitors.

PERSPECTIVES

Rethinking JAK2 inhibition: towards novel strategies of more specific and versatile Janus kinase inhibition

Janus kinases (JAKs) are required for cytokine receptor signaling. Since the discovery of the highly prevalent JAK2 V617F mutation in myeloproliferative neoplasms (MPNs), JAK2 became a prime target for inhibition. Only one approved JAK2 inhibitor exists, with positive, but not curative effects in MPNs, and promising effects in autoimmune diseases and cancer. Based on recent advances in the structural features regulating both normal and mutant JAKs, as well as in small-molecule targeting, we review the current state of JAK2 inhibitor development and present novel avenues of selecting JAK2 inhibitors, with broad and narrow specificities and extend these approaches to other JAKs.

1. Allosteric inhibitors

Allosteric inhibitors can present significant advantages compared to ATP-site binders. An allosteric site is defined as a region distinct from the kinase active site and where ligand binding can either positively or negatively regulate the enzyme activity (269). This holds the potential of higher selectivity because every kinase possesses specific regulatory mechanisms. Moreover, targeting regions outside of the ATP binding site will allow the development of compounds with different and improved physiochemical properties (270), unlike the hydrophobicity and poor solubility of molecules targeting the ATP-binding site. Another asset of allosteric inhibitors would be the possibility to overcome drug resistance by targeting two different sites in combination, as drug resistance usually emerges when mutations arise to prevent the compound from binding to one site (262).

Indirect targeting of the catalytic function of kinases has already been investigated for some kinases. For instance, the compound GNF-2 was shown to inhibit Bcr-Abl by binding to the C-terminal myristoyl pocket of Abl kinase domain (271).
Allosteric inhibitors that are defined as molecules binding to a region on the kinase that does not overlap with the ATP binding site are also referred as type-III inhibitors (262) (**see introduction, Figure 18, page 64**). To date no such molecules have been clearly identified for JAK2. Two molecules, LS104 and ON044580 were described as allosteric inhibitors of JAK2 (263-265) and demonstrated inhibitory activity against native JAK2 and JAK2 V617F. However, their allosteric mechanism was never confirmed, and their development was not continued. At present, structural and mechanistic studies (210, 211, 221, 238) indicate that allosteric inhibition of JAK2 could be achieved by targeting other domains of JAK2, distinct from the kinase domain. This new class of compounds, sometimes referred as type-IV inhibitors (262) (**See introduction, Figure 18, page 64**), could be possibly developed in order to achieve JAK2 V617F specific inhibition.

Targeting the pseudokinase ATP binding site

JAKs are intriguing proteins, as they possess both a pseudokinase and an active kinase domain in their C-terminal part (**Figure 27**). Together with GCN2 (general control nonderepressible-2), they are the unique proteins to share this feature within the kinome. The pseudokinase domain (JH2) exhibits important regulatory functions in JAKs, playing key roles in both activation and inhibition of the kinase domain (204, 205, 235, 272). An inhibitory function of the JH2 domain in JAKs was indicated by early studies and by recent molecular dynamic simulation (for JAK2) and structural x-ray structure determination (for TYK2) (208, 209). The lab of S. Hubbard solved for the first time the atomic details of JH2 in both WT and V617F-mutated forms and found that it adopts a typical protein kinase fold (206). Interestingly, JH2 was shown to bind ATP (175) in a non-canonical way (206); however, the high affinity binding and weak hydrolysis of ATP implies a structural rather than catalytic role of JH2 nucleotide binding (211). Indeed, ATP seems to act as a pseudokinase stabilizer though which it mediates auto-inhibition in the absence of stimulation.

Results from structure-guided mutagenesis and biochemical studies indicate that ATP binding to JH2 is critical for hyperactivity of JAK2 mutants, and apparently to a lesser extent for the activity of JAK2 WT (211). Hence, abrogating ATP binding on JH2 with the use of nucleotide mimicking inhibitors might be a good approach in order to reach mutant-specific inhibition. To our knowledge, no ATP competitors were discovered to bind JH2 and modulate the activity of JAK2, but the pseudokinase domains of TYK2 and JAK1 have been described to bind such compounds (223, 273). In addition, a co–crystal structure of TYK2 JH2 with a pyrazine compound confirmed that the non-canonical ATP binding pocket of the pseudokinase domain is actually accessible to ATP competitors (207), but whether this would lead to inhibition has to be clarified. Tokarski and colleagues provided the first evidence that signaling inhibition can be reached by pharmacologically targeting TYK2 JH2 (223). It is not clear whether this approach could be translated to the other JAK family members, especially JAK2.

The latter functions in homodimeric receptor complexes, and also contains two unique autoinhibitory phosphorylation sites such as S523 and Y570 (175). Since abrogating auto-phosphorylation sites in JH2 leads to weak basal activation of the JAK2 kinase domain (175), JH2 targeting could also raise the basal kinase level constitutively, while inhibiting mutant JAKs. The development of JH2 binders, along with our increasing comprehension of the mechanistic role of JH2 might bring new inhibition strategies for JAK2.

Targeting specific allosteric sites involved in V617F-activation mechanism

The V617F mutation is located in the loop connecting β4 to β5 strand in the N-lobe of JH2 (**Figure 27**). It induces activation of the kinase domain of JAK2, so in one sense itself is an allosteric regulator of the JH1 kinase domain. Guided by the discovery that a large hydrophobic residue was required at position 617 to cause JAK2 activation (53) and inspection of available kinases structures, it was suggested that F617 could possibly interact with the middle αC helix phenylalanines, F545 and F595.

It was established that these two residues are necessary for the activation by V617F and suggested that the three aromatic residues are involved in a π-π stacking interaction which impact the conformation of the αC helix of JH2 (238). This change of conformation was visualized by the X-ray crystal structure of the pseudokinase domain containing V617F (274). Small molecules able to disrupt the π-π stacking interaction that only exist in the mutant conformation would represent a valuable approach in order to achieve mutant-specific inhibition.

Another key element of V617F-mediated activation is an absolute requirement for the negative charge of the face of helix C opposite to F594/F595 and facing JH1 and the SH2-JH2 linker. (221). Reversing the charge of this face or of one residue, E596, via an E596R/K mutation restores wild type phenotype to JAK2, absent constitutive activity and normal response to cytokine stimulation. Further structure-guided modeling and mutagenesis indicated that V617F activates JAK2 through a community of residues across JAK2. Mutations along this circuit activate on their own and can be inhibited, like V617F by E596R. Strikingly identical circuits exist for active JAK1 and TYK2 homologous mutants. These data indicate that mutant-specific inhibition can be achieved by modulating a region remote from the JAK2 active site. Small molecules interfering with the aromatic π-π stacking or neutralizing the charge at 596 should be explored.

V617F was shown to induce a rearrangement of the SH2-JH2 linker (**Figure 27**), repositioning the highly conserved linker residue F537 (210). F537 was found to be necessary for the hyperactivity of V617F (210), but not for the normal cytokine-induced activation of JAK2 (221). Yet, targeting this linker appears difficult due to its high flexibility and its potential to induce activation of JAK2 (209, 210, 221, 236).

Potential new allosteric sites in the mutant JAK2 V617F are summarized in **Figure 27**. Whether these regions correspond to druggable pockets on the protein surface still has to be investigated. Future efforts will focus these allosteric sites and the development of compounds able to shift the regulatory interactions toward auto-inhibition in the case of mutant JAK2.

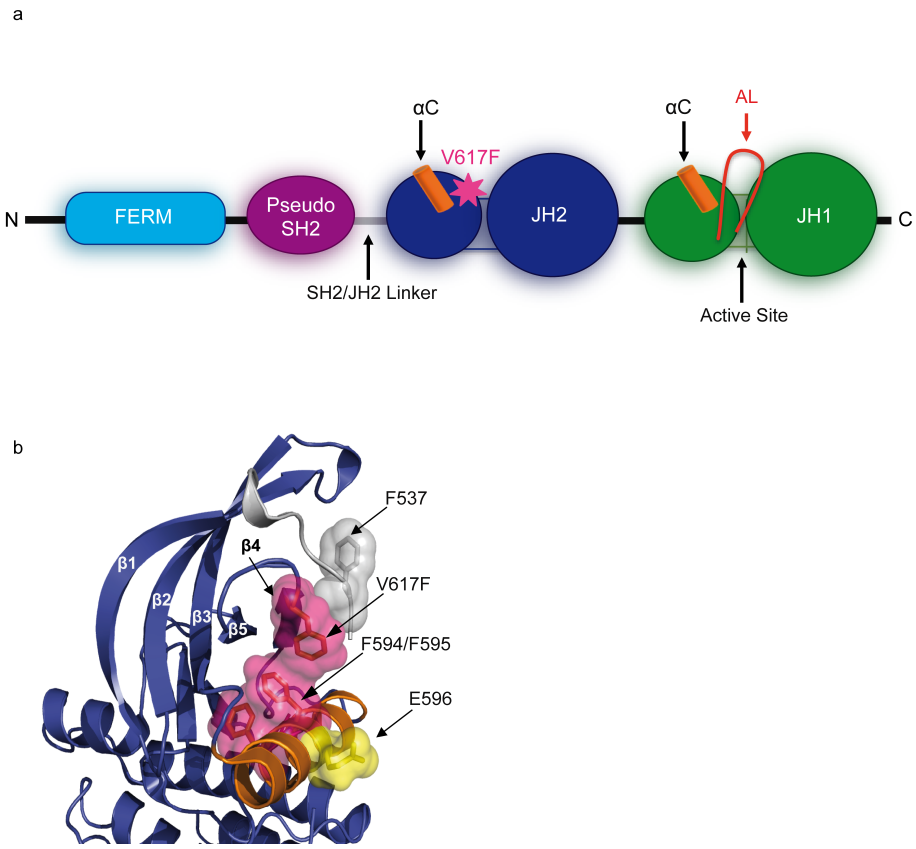

Figure 27. JAK2 structures and the possible allosteric sites. a. Representation of the primary domain structure of JAK2 **b.** The N-term lobe of JH2 is shown in blue ribbon diagram (PDB 4FVR). The αC is shown in orange. The three possible allosteric sites of JH2 are represented by sticks and surface in three different colors. The first allosteric site, shown in grey, is the region around F537 located on the SH2/JH2 linker. The second one, shown in pink, is the phenylalanine triad maintained by an aromatic stacking. F594 and F595 from the αC interact with V617F located in the β4-β5 turn. A third possible site, shown in yellow, is the glutamate 596 located on the opposite face of αC than F594 and F595. The side chain position of E596 and F537 were artificially modeled on the structure.

2. Covalent inhibitors

Another class of inhibitors has been designed by structure-guided integration of electrophilic moiety into compounds already possessing certain binding affinity for the kinase (**see introduction, Figure 18, page 64**). These covalent inhibitors are usually developed to target a nucleophilic cysteine lying in the active site of the kinase, where it will irreversibly bind through the formation of a covalent bond (275). While cysteine residues are not conserved in kinase active site, some kinases serendipitously possess this residue in or around their ATP binding site. In fact, there are 211 kinases that have at least one cysteine residue in their ATP binding site disseminated in 27 positions (276).

JAK3 kinase domain possesses a unique cysteine in its active site, C909, which has been exploited by covalent inhibitor for specific targeting (224, 277). This cysteine is shared by 11 kinases such as EGFR, HER2, HER3 or BTK and was previously used for covalent inhibitors development guided against EGFR (Neratinib, HIK-272) (278), which would easily justify its clinical development. While this cysteine is not conserved in the kinase domain of the other JAK isoforms, the pseudokinase domain of JAK1-2 and TYK2 share a cysteine around the ATP binding site in the pseudo catalytic loop at position 675 in JAK2 (**Figure 28**). Of note, this cysteine is also conserved in three other pseudokinases SgK223/pragmin, SCYL1 and SCYL3 (276), also able to bind ATP. The co-crystal structure of TYK2 JH2 with a ligand (207) showed the proximity of the piperidine group of this compound with the cysteine 736 (homologous to C675 in JAK2) suggesting that an electrophilic moiety added at this position would potentially react with the cysteine (**Figure 28**). The accessibility to the cysteine thiol group lying in JAKs JH2 should be examined. Finally, a combination of JH2 covalent inhibitors and JH1 classical inhibitors could possibly achieve high specificity and potency.

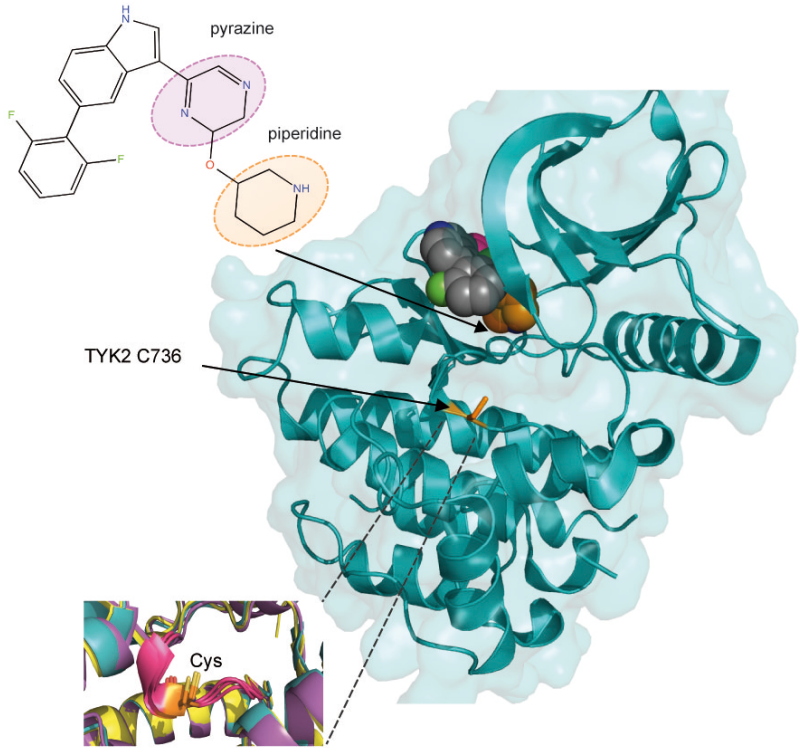


```
JAK2   671 HGNVCAKN 678  .....  933 PLGSLRDY 940
JAK1   712 HGNVCTKN 719  .....  960 PSGSLKEY 967
TYK2   732 HGNVCGRN 739  .....  982 PYGSLRDY 989
JAK3   645 HGNVSARK 652  .....  906 PSGCLRDF 913
           JH2                     JH1
```

Figure 28. Possible strategy for the development of covalent allosteric inhibitors. Shown in the main panel is the co-crystal structure of TYK2-JH2 (cyan ribbon and surface) bound to a ligand that contains pyrazine (pink) and piperidine (orange) moieties linked by an ether group (PDB: 5C01). A cysteine residue colored as orange stick, C736, is located in the ATP binding region of TYK2-JH2 not far from the piperidine moiety of the compound. Modification of the piperidine group can potentially lead to covalent binding to C736. This cysteine residue is conserved in the pseudokinase domains of JAK1 and JAK2 but not JAK3; see sequence alignment. The small square represents the structural alignment of TYK2-JH2, JAK2-JH2 and JAK1-JH2 that highlights the conserved position of this cysteine residue. While JAK3 does not carry this cysteine in JH2, it possess a unique cysteine in its JH1 active site used for the development of specific JAK3 covalent inhibitors

3. Tuning JAK2 signaling from the outside.

Cytokine receptors serve as scaffold for JAK2 molecules and thus, are essential for JAK2 to transmit signaling (**Figure 29**). JAK2 V617F-driven transformation necessarily requires homodimeric cytokine receptors such as EpoR or TpoR (35, 36). Orientation specific signaling has been demonstrated for TpoR (90, 279), EpoR (96), where inactive and active conformations of the dimeric receptors could be determined. However, in contrast to JAK2 WT, JAK2 V617F could signal regardless of the orientation imposed by the upstream receptor (238). This assumes that larger changes of the receptor dimer topology might be required to efficiently reduce activated JAK2 signaling. The team of K. C. Garcia used diabodies (small recombinant bispecific antibody-derived fragments) to neutralize EpoR/JAK2 V617F ligand-independent signaling (95). These substitute ligands can reorient the receptor-JAK2 complex geometry in an inactive conformation, presumably by imposing a physical separation between the two JAK2 molecules large enough to prevent trans-phosphorylation of the cytosolic kinases.
Aside from the inter-subunit distance within dimers, it appears that JAK2 V617F is free to signal whatever receptor dimeric geometry is imposed to EpoR (238). Thus, rotation alone will not suffice, in contrast to inducing separation of dimers (95).

4. Targeting cytokine receptor-JAK2 interaction.

Receptor-JAK2 interactions are crucial for cytokine signaling, in that cytokine binding to the extracellular receptor domains transmits a conformational change to the cytosolic domain, and to the JAK2 molecules that are attached to this region. JAK2 contains in its N-terminal end a FERM domain (four-point-one/ezrin/radixin/moesin) and a pseudo SH2 domain (**Figure 27**). This FERM-SH2 segment mediates non-covalent interactions with the receptor cytosolic tail (78, 79). Cytokine receptors possess specific motifs, the membrane proximal Pro-rich box1 and the downstream hydrophobic box2, which are required for these interactions. The FERM domain is also crucial for discriminating between the large repertoires of cell surface cytokine receptors (76, 77, 200, 280).

Interestingly, the FERM domain was shown to positively regulate JAK2 V617F (34), while negatively regulating JAK2 WT (198). Thus, targeting the specific receptor-JAK2 interface has always been a tantalizing approach. Lack of structural information has hindered this quest.

Due to the advances made by the group of P. Lupardus, the first structural understanding of JAK-cytokine receptor recognition could be provided, where tandem FERM and SH2 domains participate in the binding interface with the receptor (78, 79). In a first study, the solved structure of TYK2 FERM-SH2 domain in complex with the box2 of IFNR1 (Interferon α receptor 1) revealed a central and unexpected role of the atypical JAK SH2 domain in receptor interaction (78). The SH2 domain binds to the receptor around a glutamate residue in box2 that mimics phosphotyrosine-binding site for classical SH2 domain. In a second study, structures of JAK1 FERM-SH2 in complex with peptides derived from either IFN-λ or IL-10 receptors were solved. JAK1 principally binds to these receptors through a well-defined box1, while box2 only stabilizes this interaction (79). The structure of JAK2 FERM-SH2 was solved and identified potential receptor-binding sites that might contribute to the specificity of receptor engagement (194).
The compatible topology between the different such structure offers a picture of how box1 and box2 sequences of one receptor can bind independently to one JAK molecule.

These advances pave the way for the generation of small molecules or therapeutics that would induce disruption of receptor-JAK association. Indeed, exploring targetable pockets around the defined interface between the FERM-SH2 domain and the cytosolic receptor portions, avoiding conserved/identical regions, could be an avenue for achieving inhibition of specific receptor-JAK complexes. In addition these structures explain why point mutations in the FERM domain exerted such spectacular inhibitory effects on JAK function: mutations in Y114 in JAK2, or equivalents in other JAKs (76, 89, 281), likely misfolded the entire JAK FERM domain.

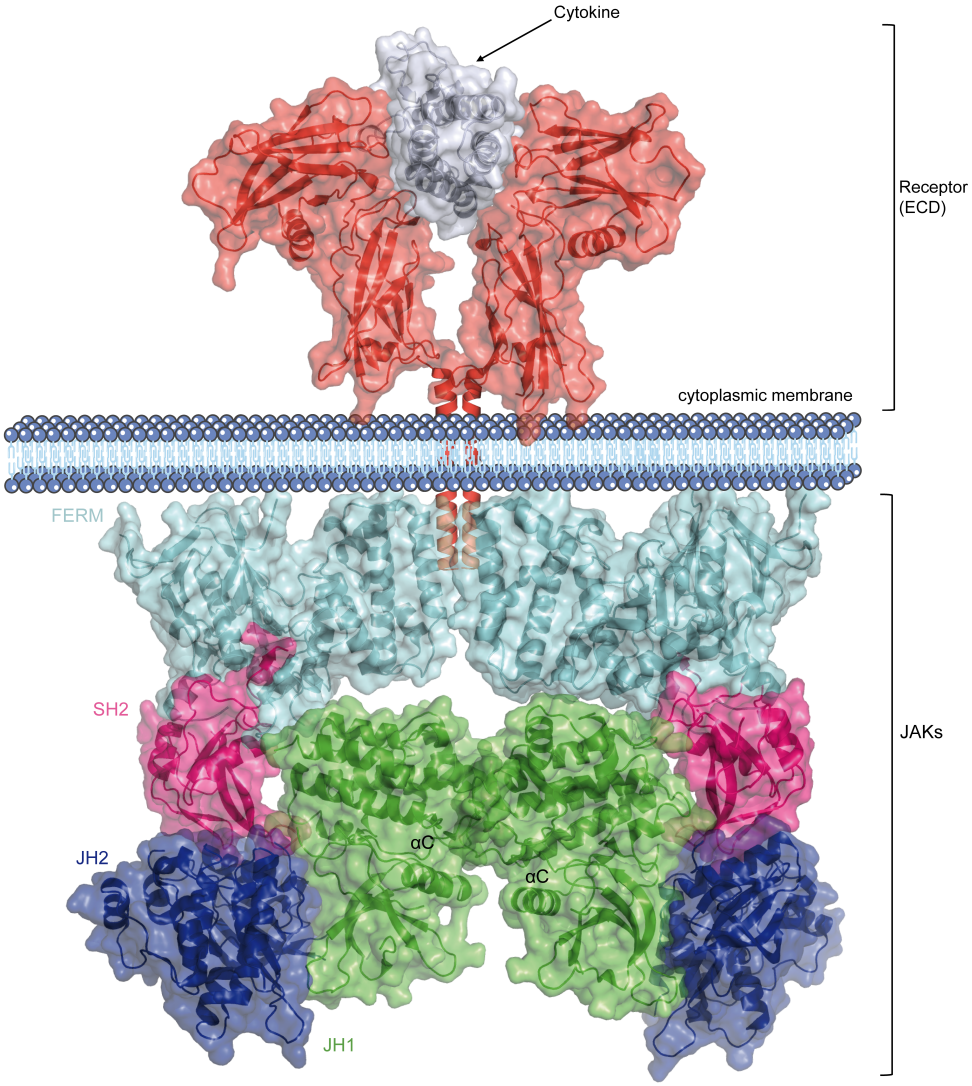

Figure 29. Model of the cytokine-receptor-JAK complex. The cytosolic domains of cytokine receptors and the two appended JAKs form functional units that together, control and trigger signaling. Shown here is the EpoR-JAK2 complex. Over the cytoplasmic membrane is shown the crystal structure of extracellular domains of EpoR dimer bound to Epo (PDB: 1EER)(94). Under the cytoplasmic membrane are ribbon diagrams of the crystal structure of JAK2-FERM-SH2 (PDB: 4Z32) (194) arbitrarily assembled to the JH2-JH1 coordinates derived from molecular dynamic simulations using JH1 (PDB: 3KRR) and JH2 (PDB: 4FVQ)(209). The two JAK2 molecules are shown to scale the size of the receptor.

5. Conclusion

Current JAK2 inhibitors are type-I ATP competitors targeting the ATP-pocket of the JH1 kinase. Using the major current structural and biochemical advances, a number of new strategies are available for obtaining novel, more potent and more specific inhibitors and for overcoming some of the major challenges of JAK2 inhibition: i) to achieve potent catalytic inhibition without off-target effects; ii) to reach high degree of selectivity for JAK2 against the other JAKs; iii) to specifically or preferentially target mutated forms against JAK2 WT, thus directly targeting the clone and sparing the normal hematopoiesis; iv) to specifically disrupt JAK2 function in define cytokine receptor complexes. We believe that this selectivity could be achieved by developing allosteric inhibitors targeting sites outside of the active site. JAK2 activity is controlled through diverse levels of regulation across its different protein domains and through the receptors, which offers several possible drug-targetable sites. Taking advantage of the non-catalytic functions of kinases, which are less conserved within the kinome, would have better chance to have specific outcomes.

Since JAK2 activation by the pseudokinase V617F mutation seems to be mediated through a community of specific residues across JAK2 (221), exploiting these interactions have the potential to provide drugs with specificity against mutant JAK2 exclusively. All results for JAK2 V617f could be validated also for JAK1 and TYK2 homologous mutants, suggesting results on JAK2 will be useful for activating mutants of JAK1 and TYK2.

The therapeutic potential of JAK2 inhibitors has emerged throughout the past decade in MPNs (282), autoimmune diseases (283), and possibly solid tumors (284, 285). In that sense JAKs are in a situation comparable to EGF receptors several years ago for a variety of pathologies.

REFERENCES

1. Hoang T. The origin of hematopoietic cell type diversity. Oncogene. 2004;23(43):7188-98.
2. Fey MF. Normal and malignant hematopoiesis. Ann Oncol. 2007;18 Suppl 1:i9-i13.
3. Dameshek W. Some speculations on the myeloproliferative syndromes. Blood. 1951;6(4):372-5.
4. Tefferi A, Vardiman JW. Classification and diagnosis of myeloproliferative neoplasms: the 2008 World Health Organization criteria and point-of-care diagnostic algorithms. Leukemia. 2008;22(1):14-22.
5. Tefferi A. Myeloproliferative neoplasms: A decade of discoveries and treatment advances. Am J Hematol. 2016;91(1):50-8.
6. Tefferi A, Guglielmelli P, Larson DR, Finke C, Wassie EA, Pieri L, et al. Long-term survival and blast transformation in molecularly annotated essential thrombocythemia, polycythemia vera, and myelofibrosis. Blood. 2014;124(16):2507-13; quiz 615.
7. Verstovsek S, Passamonti F, Rambaldi A, Barosi G, Rosen PJ, Rumi E, et al. A phase 2 study of ruxolitinib, an oral JAK1 and JAK2 Inhibitor, in patients with advanced polycythemia vera who are refractory or intolerant to hydroxyurea. Cancer. 2014;120(4):513-20.
8. Harrison C, Kiladjian JJ, Al-Ali HK, Gisslinger H, Waltzman R, Stalbovskaya V, et al. JAK inhibition with ruxolitinib versus best available therapy for myelofibrosis. N Engl J Med. 2012;366(9):787-98.
9. Verstovsek S, Mesa RA, Gotlib J, Levy RS, Gupta V, DiPersio JF, et al. A double-blind, placebo-controlled trial of ruxolitinib for myelofibrosis. N Engl J Med. 2012;366(9):799-807.
10. Cervantes F, Arellano-Rodrigo E, Alvarez-Larran A. Blood cell activation in myeloproliferative neoplasms. Haematologica. 2009;94(11):1484-8.
11. Rampal R, Ahn J, Abdel-Wahab O, Nahas M, Wang K, Lipson D, et al. Genomic and functional analysis of leukemic transformation of myeloproliferative neoplasms. Proc Natl Acad Sci U S A. 2014;111(50):E5401-10.

12. Nangalia J, Massie CE, Baxter EJ, Nice FL, Gundem G, Wedge DC, et al. Somatic CALR mutations in myeloproliferative neoplasms with nonmutated JAK2. N Engl J Med. 2013;369(25):2391-405.
13. Klampfl T, Gisslinger H, Harutyunyan AS, Nivarthi H, Rumi E, Milosevic JD, et al. Somatic mutations of calreticulin in myeloproliferative neoplasms. N Engl J Med. 2013;369(25):2379-90.
14. Tapper W, Jones AV, Kralovics R, Harutyunyan AS, Zoi K, Leung W, et al. Genetic variation at MECOM, TERT, JAK2 and HBS1L-MYB predisposes to myeloproliferative neoplasms. Nat Commun. 2015;6:6691.
15. Oh ST, Simonds EF, Jones C, Hale MB, Goltsev Y, Gibbs KD, Jr., et al. Novel mutations in the inhibitory adaptor protein LNK drive JAK-STAT signaling in patients with myeloproliferative neoplasms. Blood. 2010;116(6):988-92.
16. Lasho TL, Pardanani A, Tefferi A. LNK mutations in JAK2 mutation-negative erythrocytosis. N Engl J Med. 2010;363(12):1189-90.
17. Suessmuth Y, Elliott J, Percy MJ, Inami M, Attal H, Harrison CN, et al. A new polycythaemia vera-associated SOCS3 SH2 mutant (SOCS3F136L) cannot regulate erythropoietin responses. Br J Haematol. 2009;147(4):450-8.
18. Velazquez L, Cheng AM, Fleming HE, Furlonger C, Vesely S, Bernstein A, et al. Cytokine signaling and hematopoietic homeostasis are disrupted in Lnk-deficient mice. J Exp Med. 2002;195(12):1599-611.
19. Takaki S, Morita H, Tezuka Y, Takatsu K. Enhanced hematopoiesis by hematopoietic progenitor cells lacking intracellular adaptor protein, Lnk. J Exp Med. 2002;195(2):151-60.
20. Teofili L, Martini M, Cenci T, Guidi F, Torti L, Giona F, et al. Epigenetic alteration of SOCS family members is a possible pathogenetic mechanism in JAK2 wild type myeloproliferative diseases. Int J Cancer. 2008;123(7):1586-92.
21. Vannucchi AM, Lasho TL, Guglielmelli P, Biamonte F, Pardanani A, Pereira A, et al. Mutations and prognosis in primary myelofibrosis. Leukemia. 2013;27(9):1861-9.
22. Delhommeau F, Dupont S, Della Valle V, James C, Trannoy S, Masse A, et al. Mutation in TET2 in myeloid cancers. N Engl J Med. 2009;360(22):2289-301.

23. Ortmann CA, Kent DG, Nangalia J, Silber Y, Wedge DC, Grinfeld J, et al. Effect of mutation order on myeloproliferative neoplasms. N Engl J Med. 2015;372(7):601-12.
24. Saint-Martin C, Leroy G, Delhommeau F, Panelatti G, Dupont S, James C, et al. Analysis of the ten-eleven translocation 2 (TET2) gene in familial myeloproliferative neoplasms. Blood. 2009;114(8):1628-32.
25. Baxter EJ, Scott LM, Campbell PJ, East C, Fourouclas N, Swanton S, et al. Acquired mutation of the tyrosine kinase JAK2 in human myeloproliferative disorders. Lancet. 2005;365(9464):1054-61.
26. James C, Ugo V, Le Couedic JP, Staerk J, Delhommeau F, Lacout C, et al. A unique clonal JAK2 mutation leading to constitutive signalling causes polycythaemia vera. Nature. 2005;434(7037):1144-8.
27. Kralovics R, Passamonti F, Buser AS, Teo SS, Tiedt R, Passweg JR, et al. A gain-of-function mutation of JAK2 in myeloproliferative disorders. N Engl J Med. 2005;352(17):1779-90.
28. Levine RL, Wadleigh M, Cools J, Ebert BL, Wernig G, Huntly BJ, et al. Activating mutation in the tyrosine kinase JAK2 in polycythemia vera, essential thrombocythemia, and myeloid metaplasia with myelofibrosis. Cancer Cell. 2005;7(4):387-97.
29. Jamieson CH, Gotlib J, Durocher JA, Chao MP, Mariappan MR, Lay M, et al. The JAK2 V617F mutation occurs in hematopoietic stem cells in polycythemia vera and predisposes toward erythroid differentiation. Proc Natl Acad Sci U S A. 2006;103(16):6224-9.
30. Delhommeau F. Effect of mutation order on myeloproliferative neoplasms. N Engl J Med. 2015;372(19):1865.
31. Tiedt R, Hao-Shen H, Sobas MA, Looser R, Dirnhofer S, Schwaller J, et al. Ratio of mutant JAK2-V617F to wild-type Jak2 determines the MPD phenotypes in transgenic mice. Blood. 2008;111(8):3931-40.
32. Moliterno AR, Williams DM, Rogers O, Isaacs MA, Spivak JL. Phenotypic variability within the JAK2 V617F-positive MPD: roles of progenitor cell and neutrophil allele burdens. Exp Hematol. 2008;36(11):1480-6.
33. Kralovics R, Guan Y, Prchal JT. Acquired uniparental disomy of chromosome 9p is a frequent stem cell defect in polycythemia vera. Exp Hematol. 2002;30(3):229-36.

34. Wernig G, Gonneville JR, Crowley BJ, Rodrigues MS, Reddy MM, Hudon HE, et al. The Jak2V617F oncogene associated with myeloproliferative diseases requires a functional FERM domain for transformation and for expression of the Myc and Pim proto-oncogenes. Blood. 2008;111(7):3751-9.
35. Lu X, Huang LJ, Lodish HF. Dimerization by a cytokine receptor is necessary for constitutive activation of JAK2V617F. J Biol Chem. 2008;283(9):5258-66.
36. Lu X, Levine R, Tong W, Wernig G, Pikman Y, Zarnegar S, et al. Expression of a homodimeric type I cytokine receptor is required for JAK2V617F-mediated transformation. Proc Natl Acad Sci USA. 2005;102(52):18962-7.
37. Li J, Spensberger D, Ahn JS, Anand S, Beer PA, Ghevaert C, et al. JAK2 V617F impairs hematopoietic stem cell function in a conditional knock-in mouse model of JAK2 V617F-positive essential thrombocythemia. Blood. 2010;116(9):1528-38.
38. Staerk J, Kallin A, Demoulin J-B, Vainchenker W, Constantinescu SN. JAK1 and Tyk2 activation by the homologous Polycythemia Vera JAK2 V617F mutation: cross-talk with IGF1 receptor. J Biol Chem. 2005;280:41893-9.
39. Jeong EG, Kim MS, Nam HK, Min CK, Lee S, Chung YJ, et al. Somatic mutations of JAK1 and JAK3 in acute leukemias and solid cancers. Clin Cancer Res. 2008;14(12):3716-21.
40. Flex E, Petrangeli V, Stella L, Chiaretti S, Hornakova T, Knoops L, et al. Somatically acquired JAK1 mutations in adult acute lymphoblastic leukemia. J Exp Med. 2008;205(4):751-8.
41. Ma W, Kantarjian H, Zhang X, Yeh CH, Zhang ZJ, Verstovsek S, et al. Mutation profile of JAK2 transcripts in patients with chronic myeloproliferative neoplasias. J Mol Diagn. 2009;11(1):49-53.
42. Yoo JH, Park TS, Maeng HY, Sun YK, Kim YA, Kie JH, et al. JAK2 V617F/C618R mutation in a patient with polycythemia vera: a case study and review of the literature. Cancer Genet Cytogenet. 2009;189(1):43-7.
43. Schnittger S, Bacher U, Kern W, Schroder M, Haferlach T, Schoch C. Report on two novel nucleotide exchanges in the JAK2 pseudokinase domain: D620E and E627E. Leukemia. 2006;20(12):2195-7.

44. Grunebach F, Bross-Bach U, Kanz L, Brossart P. Detection of a new JAK2 D620E mutation in addition to V617F in a patient with polycythemia vera. Leukemia. 2006;20(12):2210-1.
45. Zhang SJ, Li JY, Li WD, Song JH, Xu W, Qiu HX. The investigation of JAK2 mutation in Chinese myeloproliferative diseases-identification of a novel C616Y point mutation in a PV patient. Int J Lab Hematol. 2007;29(1):71-2.
46. Scott LM, Tong W, Levine RL, Scott MA, Beer PA, Stratton MR, et al. JAK2 exon 12 mutations in polycythemia vera and idiopathic erythrocytosis. N Engl J Med. 2007;356(5):459-68.
47. Percy MJ, Scott LM, Erber WN, Harrison CN, Reilly JT, Jones FG, et al. The frequency of JAK2 exon 12 mutations in idiopathic erythrocytosis patients with low serum erythropoietin levels. Haematologica. 2007;92(12):1607-14.
48. Grisouard J, Li S, Kubovcakova L, Rao TN, Meyer SC, Lundberg P, et al. JAK2 exon 12 mutant mice display isolated erythrocytosis and changes in iron metabolism favoring increased erythropoiesis. Blood. 2016;128(6):839-51.
49. Etheridge SL, Cosgrove ME, Sangkhae V, Corbo LM, Roh ME, Seeliger MA, et al. A novel activating, germline JAK2 mutation, JAK2R564Q, causes familial essential thrombocytosis. Blood. 2014;123(7):1059-68.
50. Marty C, Saint-Martin C, Pecquet C, Grosjean S, Saliba J, Mouton C, et al. Germ-line JAK2 mutations in the kinase domain are responsible for hereditary thrombocytosis and are resistant to JAK2 and HSP90 inhibitors. Blood. 2014;123(9):1372-83.
51. Milosevic Feenstra JD, Nivarthi H, Gisslinger H, Leroy E, Rumi E, Chachoua I, et al. Whole-exome sequencing identifies novel MPL and JAK2 mutations in triple-negative myeloproliferative neoplasms. Blood. 2016;127(3):325-32.
52. Mead AJ, Rugless MJ, Jacobsen SE, Schuh A. Germline JAK2 mutation in a family with hereditary thrombocytosis. N Engl J Med. 2012;366(10):967-9.
53. Dusa A, Staerk J, Elliott J, Pecquet C, Poirel HA, Johnston JA, et al. Substitution of pseudokinase domain residue Val-617 by large non-polar amino acids causes activation of JAK2. J Biol Chem. 2008;283(19):12941-8.

54. Mead AJ, Chowdhury O, Pecquet C, Dusa A, Woll P, Atkinson D, et al. Impact of isolated germline JAK2V617I mutation on human hematopoiesis. Blood. 2013;121(20):4156-65.
55. Chen E, Staudt LM, Green AR. Janus kinase deregulation in leukemia and lymphoma. Immunity. 2012;36(4):529-41.
56. Duek A, Lundberg P, Shimizu T, Grisouard J, Karow A, Kubovcakova L, et al. Loss of Stat1 decreases megakaryopoiesis and favors erythropoiesis in a JAK2-V617F-driven mouse model of MPNs. Blood. 2014;123(25):3943-50.
57. Staerk J, Lacout C, Sato T, Smith SO, Vainchenker W, Constantinescu SN. An amphipathic motif at the transmembrane-cytoplasmic junction prevents autonomous activation of the thrombopoietin receptor. Blood. 2006;107(5):1864-71.
58. Defour JP, Itaya M, Gryshkova V, Brett IC, Pecquet C, Sato T, et al. Tryptophan at the transmembrane-cytosolic junction modulates thrombopoietin receptor dimerization and activation. Proc Natl Acad Sci U S A. 2013;110(7):2540-5.
59. Chaligne R, James C, Tonetti C, Besancenot R, Le Couedic JP, Fava F, et al. Evidence for MPL W515L/K mutations in hematopoietic stem cells in primitive myelofibrosis. Blood. 2007;110(10):3735-43.
60. Pardanani AD, Levine RL, Lasho T, Pikman Y, Mesa RA, Wadleigh M, et al. MPL515 mutations in myeloproliferative and other myeloid disorders: a study of 1182 patients. Blood. 2006;108(10):3472-6.
61. Ma W, Zhang X, Wang X, Zhang Z, Yeh CH, Uyeji J, et al. MPL mutation profile in JAK2 mutation-negative patients with myeloproliferative disorders. Diagn Mol Pathol. 2011;20(1):34-9.
62. Beer PA, Campbell PJ, Scott LM, Bench AJ, Erber WN, Bareford D, et al. MPL mutations in myeloproliferative disorders: analysis of the PT-1 cohort. Blood. 2008;112(1):141-9.
63. Pardanani A, Guglielmelli P, Lasho TL, Pancrazzi A, Finke CM, Vannucchi AM, et al. Primary myelofibrosis with or without mutant MPL: comparison of survival and clinical features involving 603 patients. Leukemia. 2011;25(12):1834-9.
64. Defour JP, Chachoua I, Pecquet C, Constantinescu SN. Oncogenic activation of MPL/thrombopoietin receptor by 17 mutations at W515: implications for myeloproliferative neoplasms. Leukemia. 2016;30(5):1214-6.

65. Pecquet C, Staerk J, Chaligne R, Goss V, Lee KA, Zhang X, et al. Induction of myeloproliferative disorder and myelofibrosis by thrombopoietin receptor W515 mutants is mediated by cytosolic tyrosine 112 of the receptor. Blood. 2010;115(5):1037-48.
66. Ding J, Komatsu H, Wakita A, Kato-Uranishi M, Ito M, Satoh A, et al. Familial essential thrombocythemia associated with a dominant-positive activating mutation of the c-MPL gene, which encodes for the receptor for thrombopoietin. Blood. 2004;103(11):4198-200.
67. Onishi M, Mui AL, Morikawa Y, Cho L, Kinoshita S, Nolan GP, et al. Identification of an oncogenic form of the thrombopoietin receptor MPL using retrovirus-mediated gene transfer. Blood. 1996;88(4):1399-406.
68. Ding J, Komatsu H, Iida S, Yano H, Kusumoto S, Inagaki A, et al. The Asn505 mutation of the c-MPL gene, which causes familial essential thrombocythemia, induces autonomous homodimerization of the c-Mpl protein due to strong amino acid polarity. Blood. 2009;114(15):3325-8.
69. Zhang JX, Braakman I, Matlack KE, Helenius A. Quality control in the secretory pathway: the role of calreticulin, calnexin and BiP in the retention of glycoproteins with C-terminal truncations. Mol Biol Cell. 1997;8(10):1943-54.
70. Marty C, Pecquet C, Nivarthi H, El-Khoury M, Chachoua I, Tulliez M, et al. Calreticulin mutants in mice induce an MPL-dependent thrombocytosis with frequent progression to myelofibrosis. Blood. 2016;127(10):1317-24.
71. Chachoua I, Pecquet C, El-Khoury M, Nivarthi H, Albu RI, Marty C, et al. Thrombopoietin receptor activation by myeloproliferative neoplasm associated calreticulin mutants. Blood. 2016;127(10):1325-35.
72. Robb L. Cytokine receptors and hematopoietic differentiation. Oncogene. 2007;26(47):6715-23.
73. Miranda MB, Johnson DE. Signal transduction pathways that contribute to myeloid differentiation. Leukemia. 2007;21(7):1363-77.
74. Nicola NA, Hilton DJ. General classes and functions of four-helix bundle cytokines. Adv Protein Chem. 1998;52:1-65.
75. Miura O, Cleveland JL, Ihle JN. Inactivation of erythropoietin receptor function by point mutations in a region having homology with other cytokine receptors. Mol Cell Biol. 1993;13(3):1788-95.

76. Haan C, Is'harc H, Hermanns HM, Schmitz-Van De Leur H, Kerr IM, Heinrich PC, et al. Mapping of a region within the N terminus of Jak1 involved in cytokine receptor interaction. J Biol Chem. 2001;276(40):37451-8.
77. Zhao Y, Wagner F, Frank SJ, Kraft AS. The amino-terminal portion of the JAK2 protein kinase is necessary for binding and phosphorylation of the granulocyte-macrophage colony-stimulating factor receptor beta c chain. J Biol Chem. 1995;270(23):13814-8.
78. Wallweber HJ, Tam C, Franke Y, Starovasnik MA, Lupardus PJ. Structural basis of recognition of interferon-alpha receptor by tyrosine kinase 2. Nat Struct Mol Biol. 2014;21(5):443-8.
79. Ferrao R, Wallweber HJ, Ho H, Tam C, Franke Y, Quinn J, et al. The Structural Basis for Class II Cytokine Receptor Recognition by JAK1. Structure. 2016.
80. Bagley CJ, Woodcock JM, Stomski FC, Lopez AF. The structural and functional basis of cytokine receptor activation: lessons from the common beta subunit of the granulocyte-macrophage colony-stimulating factor, interleukin-3 (IL-3), and IL-5 receptors. Blood. 1997;89(5):1471-82.
81. Tanner JW, Chen W, Young RL, Longmore GD, Shaw AS. The conserved box 1 motif of cytokine receptors is required for association with JAK kinases. J Biol Chem. 1995;270(12):6523-30.
82. de Sauvage FJ, Hass PE, Spencer SD, Malloy BE, Gurney AL, Spencer SA, et al. Stimulation of megakaryocytopoiesis and thrombopoiesis by the c-Mpl ligand. Nature. 1994;369(6481):533-8.
83. Solar GP, Kerr WG, Zeigler FC, Hess D, Donahue C, de Sauvage FJ, et al. Role of c-mpl in early hematopoiesis. Blood. 1998;92(1):4-10.
84. Qian H, Buza-Vidas N, Hyland CD, Jensen CT, Antonchuk J, Mansson R, et al. Critical role of thrombopoietin in maintaining adult quiescent hematopoietic stem cells. Cell Stem Cell. 2007;1(6):671-84.
85. Alexander WS, Roberts AW, Nicola NA, Li R, Metcalf D. Deficiencies in progenitor cells of multiple hematopoietic lineages and defective megakaryocytopoiesis in mice lacking the thrombopoietic receptor c-Mpl. Blood. 1996;87(6):2162-70.
86. Sabath DF, Kaushansky K, Broudy VC. Deletion of the extracellular membrane-distal cytokine receptor homology module of Mpl results in constitutive cell growth and loss of thrombopoietin binding. Blood. 1999;94(1):365-7.

87. Sattler M, Durstin MA, Frank DA, Okuda K, Kaushansky K, Salgia R, et al. The thrombopoietin receptor c-MPL activates JAK2 and TYK2 tyrosine kinases. Exp Hematol. 1995;23(9):1040-8.
88. Drachman JG, Millett KM, Kaushansky K. Thrombopoietin signal transduction requires functional JAK2, not TYK2. J Biol Chem. 1999;274(19):13480-4.
89. Royer Y, Staerk J, Costuleanu M, Courtoy PJ, Constantinescu SN. Janus kinases affect thrombopoietin receptor cell surface localization and stability. J Biol Chem. 2005;280(29):27251-61.
90. Staerk J, Defour JP, Pecquet C, Leroy E, Antoine-Poirel H, Brett I, et al. Orientation-specific signalling by thrombopoietin receptor dimers. EMBO J. 2011;30(21):4398-413.
91. Constantinescu SN, Huang LJ, Nam H, Lodish HF. The erythropoietin receptor cytosolic juxtamembrane domain contains an essential, precisely oriented, hydrophobic motif. Mol Cell. 2001;7(2):377-85.
92. Constantinescu SN, Keren T, Socolovsky M, Nam H, Henis YI, Lodish HF. Ligand-independent oligomerization of cell-surface erythropoietin receptor is mediated by the transmembrane domain. Proc Natl Acad Sci U S A. 2001;98(8):4379-84.
93. Livnah O, Stura EA, Middleton SA, Johnson DL, Jolliffe LK, Wilson IA. Crystallographic evidence for preformed dimers of erythropoietin receptor before ligand activation. Science. 1999;283(5404):987-90.
94. Syed RS, Reid SW, Li C, Cheetham JC, Aoki KH, Liu B, et al. Efficiency of signalling through cytokine receptors depends critically on receptor orientation. Nature. 1998;395(6701):511-6.
95. Moraga I, Wernig G, Wilmes S, Gryshkova V, Richter CP, Hong WJ, et al. Tuning cytokine receptor signaling by re-orienting dimer geometry with surrogate ligands. Cell. 2015;160(6):1196-208.
96. Seubert N, Royer Y, Staerk J, Kubatzky KF, Moucadel V, Krishnakumar S, et al. Active and inactive orientations of the transmembrane and cytosolic domains of the erythropoietin receptor dimer. Mol Cell. 2003;12(5):1239-50.
97. Livnah O, Johnson DL, Stura EA, Farrell FX, Barbone FP, You Y, et al. An antagonist peptide-EPO receptor complex suggests that receptor dimerization is not sufficient for activation. Nat Struct Biol. 1998;5(11):993-1004.

98. Brooks AJ, Dai W, O'Mara ML, Abankwa D, Chhabra Y, Pelekanos RA, et al. Mechanism of activation of protein kinase JAK2 by the growth hormone receptor. Science. 2014;344(6185):1249783.
99. Yang N, Wang X, Jiang J, Frank SJ. Role of the growth hormone (GH) receptor transmembrane domain in receptor predimerization and GH-induced activation. Mol Endocrinol. 2007;21(7):1642-55.
100. Qazi AM, Tsai-Morris CH, Dufau ML. Ligand-independent homo- and heterodimerization of human prolactin receptor variants: inhibitory action of the short forms by heterodimerization. Mol Endocrinol. 2006;20(8):1912-23.
101. Tenhumberg S, Schuster B, Zhu L, Kovaleva M, Scheller J, Kallen KJ, et al. gp130 dimerization in the absence of ligand: preformed cytokine receptor complexes. Biochem Biophys Res Commun. 2006;346(3):649-57.
102. Constantinescu SN, Leroy E, Gryshkova V, Pecquet C, Dusa A. Activating Janus kinase pseudokinase domain mutations in myeloproliferative and other blood cancers. Biochem Soc Trans. 2013;41(4):1048-54.
103. Eckhart W, Hutchinson MA, Hunter T. An activity phosphorylating tyrosine in polyoma T antigen immunoprecipitates. Cell. 1979;18(4):925-33.
104. Hunter T, Sefton BM. Transforming gene product of Rous sarcoma virus phosphorylates tyrosine. Proc Natl Acad Sci U S A. 1980;77(3):1311-5.
105. Baker SJ, Rane SG, Reddy EP. Hematopoietic cytokine receptor signaling. Oncogene. 2007;26(47):6724-37.
106. Constantinescu SN, Vainchenker W. JAK/STA signalling and haematological malignancies. eLS John Wiley @ Sons. 2015.
107. Drachman JG, Kaushansky K. Dissecting the thrombopoietin receptor: functional elements of the Mpl cytoplasmic domain. Proc Natl Acad Sci U S A. 1997;94(6):2350-5.
108. Quelle FW, Wang D, Nosaka T, Thierfelder WE, Stravopodis D, Weinstein Y, et al. Erythropoietin induces activation of Stat5 through association with specific tyrosines on the receptor that are not required for a mitogenic response. Mol Cell Biol. 1996;16(4):1622-31.
109. Gobert S, Chretien S, Gouilleux F, Muller O, Pallard C, Dusanter-Fourt I, et al. Identification of tyrosine residues within the intracellular domain of the erythropoietin receptor crucial for STAT5 activation. EMBO J. 1996;15(10):2434-41.

110. Darnell JE, Jr., Kerr IM, Stark GR. Jak-STAT pathways and transcriptional activation in response to IFNs and other extracellular signaling proteins. Science. 1994;264(5164):1415-21.
111. Penta K, Sawyer ST. Erythropoietin induces the tyrosine phosphorylation, nuclear translocation, and DNA binding of STAT1 and STAT5 in erythroid cells. J Biol Chem. 1995;270(52):31282-7.
112. Kirito K, Uchida M, Yamada M, Miura Y, Komatsu N. A distinct function of STAT proteins in erythropoietin signal transduction. J Biol Chem. 1997;272(26):16507-13.
113. Halupa A, Bailey ML, Huang K, Iscove NN, Levy DE, Barber DL. A novel role for STAT1 in regulating murine erythropoiesis: deletion of STAT1 results in overall reduction of erythroid progenitors and alters their distribution. Blood. 2005;105(2):552-61.
114. Schulze H, Ballmaier M, Welte K, Germeshausen M. Thrombopoietin induces the generation of distinct Stat1, Stat3, Stat5a and Stat5b homo- and heterodimeric complexes with different kinetics in human platelets. Exp Hematol. 2000;28(3):294-304.
115. Rawlings JS, Rosler KM, Harrison DA. The JAK/STAT signaling pathway. J Cell Sci. 2004;117(Pt 8):1281-3.
116. Rodig SJ, Meraz MA, White JM, Lampe PA, Riley JK, Arthur CD, et al. Disruption of the Jak1 gene demonstrates obligatory and nonredundant roles of the Jaks in cytokine-induced biologic responses. Cell. 1998;93(3):373-83.
117. Neubauer H, Cumano A, Muller M, Wu H, Huffstadt U, Pfeffer K. Jak2 deficiency defines an essential developmental checkpoint in definitive hematopoiesis. Cell. 1998;93(3):397-409.
118. Parganas E, Wang D, Stravopodis D, Topham DJ, Marine JC, Teglund S, et al. Jak2 is essential for signaling through a variety of cytokine receptors. Cell. 1998;93(3):385-95.
119. Karaghiosoff M, Neubauer H, Lassnig C, Kovarik P, Schindler H, Pircher H, et al. Partial impairment of cytokine responses in Tyk2-deficient mice. Immunity. 2000;13(4):549-60.
120. Shimoda K, Kato K, Aoki K, Matsuda T, Miyamoto A, Shibamori M, et al. Tyk2 plays a restricted role in IFN alpha signaling, although it is required for IL-12-mediated T cell function. Immunity. 2000;13(4):561-71.

121. Baird AM, Lucas JA, Berg LJ. A profound deficiency in thymic progenitor cells in mice lacking Jak3. J Immunol. 2000;165(7):3680-8.
122. Darnell JE. Validating Stat3 in cancer therapy. Nat Med. 2005;11(6):595-6.
123. Haddad BR, Gu L, Mirtti T, Dagvadorj A, Vogiatzi P, Hoang DT, et al. STAT5A/B gene locus undergoes amplification during human prostate cancer progression. Am J Pathol. 2013;182(6):2264-75.
124. Caffarel MM, Zaragoza R, Pensa S, Li J, Green AR, Watson CJ. Constitutive activation of JAK2 in mammary epithelium elevates Stat5 signalling, promotes alveologenesis and resistance to cell death, and contributes to tumourigenesis. Cell Death Differ. 2012;19(3):511-22.
125. Seavey MM, Dobrzanski P. The many faces of Janus kinase. Biochem Pharmacol. 2012;83(9):1136-45.
126. Neel BG, Gu H, Pao L. The 'Shp'ing news: SH2 domain-containing tyrosine phosphatases in cell signaling. Trends Biochem Sci. 2003;28(6):284-93.
127. Saur SJ, Sangkhae V, Geddis AE, Kaushansky K, Hitchcock IS. Ubiquitination and degradation of the thrombopoietin receptor c-Mpl. Blood. 2010;115(6):1254-63.
128. Ungureanu D, Saharinen P, Junttila I, Hilton DJ, Silvennoinen O. Regulation of Jak2 through the ubiquitin-proteasome pathway involves phosphorylation of Jak2 on Y1007 and interaction with SOCS-1. Mol Cell Biol. 2002;22(10):3316-26.
129. Kershaw NJ, Murphy JM, Liau NP, Varghese LN, Laktyushin A, Whitlock EL, et al. SOCS3 binds specific receptor-JAK complexes to control cytokine signaling by direct kinase inhibition. Nat Struct Mol Biol. 2013;20(4):469-76.
130. Chung CD, Liao J, Liu B, Rao X, Jay P, Berta P, et al. Specific inhibition of Stat3 signal transduction by PIAS3. Science. 1997;278(5344):1803-5.
131. Liu B, Liao J, Rao X, Kushner SA, Chung CD, Chang DD, et al. Inhibition of Stat1-mediated gene activation by PIAS1. Proc Natl Acad Sci U S A. 1998;95(18):10626-31.
132. Tong W, Lodish HF. Lnk inhibits Tpo-mpl signaling and Tpo-mediated megakaryocytopoiesis. J Exp Med. 2004;200(5):569-80.

133. Tong W, Zhang J, Lodish HF. Lnk inhibits erythropoiesis and Epo-dependent JAK2 activation and downstream signaling pathways. Blood. 2005;105(12):4604-12.
134. Ha JS, Jeon DS. Possible new LNK mutations in myeloproliferative neoplasms. Am J Hematol. 2011;86(10):866-8.
135. Zhang J, Ding L, Holmfeldt L, Wu G, Heatley SL, Payne-Turner D, et al. The genetic basis of early T-cell precursor acute lymphoblastic leukaemia. Nature. 2012;481(7380):157-63.
136. Hookham MB, Elliott J, Suessmuth Y, Staerk J, Ward AC, Vainchenker W, et al. The myeloproliferative disorder-associated JAK2 V617F mutant escapes negative regulation by suppressor of cytokine signaling 3. Blood. 2007;109(11):4924-9.
137. Hanks SK, Hunter T. Protein kinases 6. The eukaryotic protein kinase superfamily: kinase (catalytic) domain structure and classification. FASEB J. 1995;9(8):576-96.
138. Manning G, Whyte DB, Martinez R, Hunter T, Sudarsanam S. The protein kinase complement of the human genome. Science. 2002;298(5600):1912-34.
139. Sutherland EW, Jr., Wosilait WD. Inactivation and activation of liver phosphorylase. Nature. 1955;175(4447):169-70.
140. Neet K, Hunter T. Vertebrate non-receptor protein-tyrosine kinase families. Genes Cells. 1996;1(2):147-69.
141. Knighton DR, Zheng JH, Ten Eyck LF, Xuong NH, Taylor SS, Sowadski JM. Structure of a peptide inhibitor bound to the catalytic subunit of cyclic adenosine monophosphate-dependent protein kinase. Science. 1991;253(5018):414-20.
142. Cowan-Jacob SW. Structural biology of protein tyrosine kinases. Cell Mol Life Sci. 2006;63(22):2608-25.
143. Kannan N, Neuwald AF. Did protein kinase regulatory mechanisms evolve through elaboration of a simple structural component? J Mol Biol. 2005;351(5):956-72.
144. Kornev AP, Haste NM, Taylor SS, Eyck LF. Surface comparison of active and inactive protein kinases identifies a conserved activation mechanism. Proc Natl Acad Sci U S A. 2006;103(47):17783-8.

145. Nolen B, Taylor S, Ghosh G. Regulation of protein kinases; controlling activity through activation segment conformation. Mol Cell. 2004;15(5):661-75.
146. Gibbs CS, Zoller MJ. Rational scanning mutagenesis of a protein kinase identifies functional regions involved in catalysis and substrate interactions. J Biol Chem. 1991;266(14):8923-31.
147. Adams JA, Taylor SS. Divalent metal ions influence catalysis and active-site accessibility in the cAMP-dependent protein kinase. Protein Sci. 1993;2(12):2177-86.
148. Kornev AP, Taylor SS, Ten Eyck LF. A helix scaffold for the assembly of active protein kinases. Proc Natl Acad Sci U S A. 2008;105(38):14377-82.
149. Johnson LN, Noble ME, Owen DJ. Active and inactive protein kinases: structural basis for regulation. Cell. 1996;85(2):149-58.
150. Endicott JA, Noble ME, Johnson LN. The structural basis for control of eukaryotic protein kinases. Annu Rev Biochem. 2012;81:587-613.
151. Kornev AP, Taylor SS. Dynamics-Driven Allostery in Protein Kinases. Trends Biochem Sci. 2015;40(11):628-47.
152. Weigert O, Lane AA, Bird L, Kopp N, Chapuy B, van Bodegom D, et al. Genetic resistance to JAK2 enzymatic inhibitors is overcome by HSP90 inhibition. J Exp Med. 2012;209(2):259-73.
153. Bailey FP, Andreev VI, Eyers PA. The resistance tetrad: amino acid hotspots for kinome-wide exploitation of drug-resistant protein kinase alleles. Methods Enzymol. 2014;548:117-46.
154. Iyer GH, Moore MJ, Taylor SS. Consequences of lysine 72 mutation on the phosphorylation and activation state of cAMP-dependent kinase. J Biol Chem. 2005;280(10):8800-7.
155. Boyken SE, Chopra N, Xie Q, Joseph RE, Wales TE, Fulton DB, et al. A conserved isoleucine maintains the inactive state of Bruton's tyrosine kinase. J Mol Biol. 2014;426(21):3656-69.
156. Rodriguez-Viciana P, Tetsu O, Tidyman WE, Estep AL, Conger BA, Cruz MS, et al. Germline mutations in genes within the MAPK pathway cause cardio-facio-cutaneous syndrome. Science. 2006;311(5765):1287-90.
157. Losdyck E, Hornakova T, Springuel L, Degryse S, Gielen O, Cools J, et al. Distinct Acute Lymphoblastic Leukemia (ALL)-associated Janus Kinase 3 (JAK3) Mutants Exhibit Different Cytokine-Receptor Requirements and JAK Inhibitor Specificities. J Biol Chem. 2015;290(48):29022-34.

158. Lucet IS, Fantino E, Styles M, Bamert R, Patel O, Broughton SE, et al. The structural basis of Janus kinase 2 inhibition by a potent and specific pan-Janus kinase inhibitor. Blood. 2006;107(1):176-83.
159. Taylor SS, Shaw AS, Kannan N, Kornev AP. Integration of signaling in the kinome: Architecture and regulation of the alphaC Helix. Biochim Biophys Acta. 2015;1854(10 Pt B):1567-74.
160. Ruan Z, Kannan N. Mechanistic Insights into R776H Mediated Activation of Epidermal Growth Factor Receptor Kinase. Biochemistry. 2015;54(27):4216-25.
161. Rajakulendran T, Sahmi M, Lefrancois M, Sicheri F, Therrien M. A dimerization-dependent mechanism drives RAF catalytic activation. Nature. 2009;461(7263):542-5.
162. Lee JW, Kim YG, Soung YH, Han KJ, Kim SY, Rhim HS, et al. The JAK2 V617F mutation in de novo acute myelogenous leukemias. Oncogene. 2006;25(9):1434-6.
163. Hu J, Ahuja LG, Meharena HS, Kannan N, Kornev AP, Taylor SS, et al. Kinase regulation by hydrophobic spine assembly in cancer. Mol Cell Biol. 2015;35(1):264-76.
164. Kornev AP, Taylor SS. Defining the conserved internal architecture of a protein kinase. Biochim Biophys Acta. 2010;1804(3):440-4.
165. Brown NR, Noble ME, Endicott JA, Johnson LN. The structural basis for specificity of substrate and recruitment peptides for cyclin-dependent kinases. Nat Cell Biol. 1999;1(7):438-43.
166. De Bondt HL, Rosenblatt J, Jancarik J, Jones HD, Morgan DO, Kim SH. Crystal structure of cyclin-dependent kinase 2. Nature. 1993;363(6430):595-602.
167. Sicheri F, Moarefi I, Kuriyan J. Crystal structure of the Src family tyrosine kinase Hck. Nature. 1997;385(6617):602-9.
168. Xu W, Harrison SC, Eck MJ. Three-dimensional structure of the tyrosine kinase c-Src. Nature. 1997;385(6617):595-602.
169. Zeqiraj E, van Aalten DM. Pseudokinases-remnants of evolution or key allosteric regulators? Curr Opin Struct Biol. 2010;20(6):772-81.
170. Boudeau J, Miranda-Saavedra D, Barton GJ, Alessi DR. Emerging roles of pseudokinases. Trends Cell Biol. 2006;16(9):443-52.
171. Tanaka H, Iguchi N, Nakamura Y, Kohroki J, de Carvalho CE, Nishimune Y. Cloning and characterization of human haspin gene

encoding haploid germ cell-specific nuclear protein kinase. Mol Hum Reprod. 2001;7(3):211-8.
172. Brennan DF, Dar AC, Hertz NT, Chao WC, Burlingame AL, Shokat KM, et al. A Raf-induced allosteric transition of KSR stimulates phosphorylation of MEK. Nature. 2011;472(7343):366-9.
173. Shi F, Telesco SE, Liu Y, Radhakrishnan R, Lemmon MA. ErbB3/HER3 intracellular domain is competent to bind ATP and catalyze autophosphorylation. Proc Natl Acad Sci U S A. 2010;107(17):7692-7.
174. Mukherjee K, Sharma M, Urlaub H, Bourenkov GP, Jahn R, Sudhof TC, et al. CASK Functions as a Mg2+-independent neurexin kinase. Cell. 2008;133(2):328-39.
175. Ungureanu D, Wu J, Pekkala T, Niranjan Y, Young C, Jensen ON, et al. The pseudokinase domain of JAK2 is a dual-specificity protein kinase that negatively regulates cytokine signaling. Nat Struct Mol Biol. 2011;18(9):971-6.
176. Murphy JM, Zhang Q, Young SN, Reese ML, Bailey FP, Eyers PA, et al. A robust methodology to subclassify pseudokinases based on their nucleotide-binding properties. Biochem J. 2014;457(2):323-34.
177. Hammaren HM, Virtanen AT, Silvennoinen O. Nucleotide-binding mechanisms in pseudokinases. Biosci Rep. 2016;36(1):e00282.
178. Zhang H, Photiou A, Grothey A, Stebbing J, Giamas G. The role of pseudokinases in cancer. Cell Signal. 2012;24(6):1173-84.
179. Reiterer V, Eyers PA, Farhan H. Day of the dead: pseudokinases and pseudophosphatases in physiology and disease. Trends Cell Biol. 2014;24(9):489-505.
180. Bailey FP, Byrne DP, McSkimming D, Kannan N, Eyers PA. Going for broke: targeting the human cancer pseudokinome. Biochem J. 2015;465(2):195-211.
181. Claus J, Cameron AJ, Parker PJ. Pseudokinase drug intervention: a potentially poisoned chalice. Biochem Soc Trans. 2013;41(4):1083-8.
182. Wilks AF. Two putative protein-tyrosine kinases identified by application of the polymerase chain reaction. Proc Natl Acad Sci U S A. 1989;86(5):1603-7.
183. Wilks AF, Harpur AG, Kurban RR, Ralph SJ, Zurcher G, Ziemiecki A. Two novel protein-tyrosine kinases, each with a second phosphotransferase-related catalytic domain, define a new class of protein kinase. Mol Cell Biol. 1991;11(4):2057-65.

184. Harpur AG, Andres AC, Ziemiecki A, Aston RR, Wilks AF. JAK2, a third member of the JAK family of protein tyrosine kinases. Oncogene. 1992;7(7):1347-53.
185. Yeh TC, Pellegrini S. The Janus kinase family of protein tyrosine kinases and their role in signaling. Cell Mol Life Sci. 1999;55(12):1523-34.
186. Conway G, Margoliath A, Wong-Madden S, Roberts RJ, Gilbert W. Jak1 kinase is required for cell migrations and anterior specification in zebrafish embryos. Proc Natl Acad Sci U S A. 1997;94(7):3082-7.
187. Binari R, Perrimon N. Stripe-specific regulation of pair-rule genes by hopscotch, a putative Jak family tyrosine kinase in Drosophila. Genes Dev. 1994;8(3):300-12.
188. Perrimon N, Mahowald AP. l(1)hopscotch, A larval-pupal zygotic lethal with a specific maternal effect on segmentation in Drosophila. Dev Biol. 1986;118(1):28-41.
189. Gu J, Wang Y, Gu X. Evolutionary analysis for functional divergence of Jak protein kinase domains and tissue-specific genes. J Mol Evol. 2002;54(6):725-33.
190. Yamaoka K, Saharinen P, Pesu M, Holt VE, 3rd, Silvennoinen O, O'Shea JJ. The Janus kinases (Jaks). Genome Biol. 2004;5(12):253.
191. Watowich SS, Wu H, Socolovsky M, Klingmuller U, Constantinescu SN, Lodish HF. Cytokine receptor signal transduction and the control of hematopoietic cell development. Annu Rev Cell Dev Biol. 1996;12:91-128.
192. Huang LJ, Constantinescu SN, Lodish HF. The N-terminal domain of Janus kinase 2 is required for Golgi processing and cell surface expression of erythropoietin receptor. Mol Cell. 2001;8(6):1327-38.
193. Ceccarelli DF, Song HK, Poy F, Schaller MD, Eck MJ. Crystal structure of the FERM domain of focal adhesion kinase. J Biol Chem. 2006;281(1):252-9.
194. McNally R, Toms AV, Eck MJ. Crystal Structure of the FERM-SH2 Module of Human Jak2. PLoS One. 2016;11(5):e0156218.
195. Funakoshi-Tago M, Pelletier S, Matsuda T, Parganas E, Ihle JN. Receptor specific downregulation of cytokine signaling by autophosphorylation in the FERM domain of Jak2. EMBO J. 2006;25(20):4763-72.

196. Funakoshi-Tago M, Pelletier S, Moritake H, Parganas E, Ihle JN. Jak2 FERM domain interaction with the erythropoietin receptor regulates Jak2 kinase activity. Mol Cell Biol. 2008;28(5):1792-801.
197. Zhou YJ, Chen M, Cusack NA, Kimmel LH, Magnuson KS, Boyd JG, et al. Unexpected effects of FERM domain mutations on catalytic activity of Jak3: structural implication for Janus kinases. Mol Cell. 2001;8(5):959-69.
198. Zhao L, Ma Y, Seemann J, Huang LJ. A regulating role of the JAK2 FERM domain in hyperactivation of JAK2(V617F). Biochem J. 2010;426(1):91-8.
199. Radtke S, Haan S, Jorissen A, Hermanns HM, Diefenbach S, Smyczek T, et al. The Jak1 SH2 domain does not fulfill a classical SH2 function in Jak/STAT signaling but plays a structural role for receptor interaction and up-regulation of receptor surface expression. J Biol Chem. 2005;280(27):25760-8.
200. Kohlhuber F, Rogers NC, Watling D, Feng J, Guschin D, Briscoe J, et al. A JAK1/JAK2 chimera can sustain alpha and gamma interferon responses. Mol Cell Biol. 1997;17(2):695-706.
201. Gorantla SP, Dechow TN, Grundler R, Illert AL, Zum Buschenfelde CM, Kremer M, et al. Oncogenic JAK2V617F requires an intact SH2-like domain for constitutive activation and induction of a myeloproliferative disease in mice. Blood. 2010;116(22):4600-11.
202. Luo H, Hanratty WP, Dearolf CR. An amino acid substitution in the Drosophila hopTum-l Jak kinase causes leukemia-like hematopoietic defects. EMBO J. 1995;14(7):1412-20.
203. Luo H, Rose P, Barber D, Hanratty WP, Lee S, Roberts TM, et al. Mutation in the Jak kinase JH2 domain hyperactivates Drosophila and mammalian Jak-Stat pathways. Mol Cell Biol. 1997;17(3):1562-71.
204. Saharinen P, Silvennoinen O. The pseudokinase domain is required for suppression of basal activity of Jak2 and Jak3 tyrosine kinases and for cytokine-inducible activation of signal transduction. J Biol Chem. 2002;277(49):47954-63.
205. Saharinen P, Takaluoma K, Silvennoinen O. Regulation of the Jak2 tyrosine kinase by its pseudokinase domain. Mol Cell Biol. 2000;20(10):3387-95.
206. Bandaranayake RM, Ungureanu D, Shan Y, Shaw DE, Silvennoinen O, Hubbard SR. Crystal structures of the JAK2 pseudokinase domain and the pathogenic mutant V617F. Nat Struct Mol Biol. 2012;19(8):754-9.

207. Min X, Ungureanu D, Maxwell S, Hammaren H, Thibault S, Hillert EK, et al. Structural and Functional Characterization of the JH2 Pseudokinase Domain of JAK Family Tyrosine Kinase 2 (TYK2). J Biol Chem. 2015;290(45):27261-70.
208. Lupardus PJ, Ultsch M, Wallweber H, Bir Kohli P, Johnson AR, Eigenbrot C. Structure of the pseudokinase-kinase domains from protein kinase TYK2 reveals a mechanism for Janus kinase (JAK) autoinhibition. Proc Natl Acad Sci U S A. 2014;111(22):8025-30.
209. Shan Y, Gnanasambandan K, Ungureanu D, Kim ET, Hammaren H, Yamashita K, et al. Molecular basis for pseudokinase-dependent autoinhibition of JAK2 tyrosine kinase. Nat Struct Mol Biol. 2014;21(7):579-84.
210. Toms AV, Deshpande A, McNally R, Jeong Y, Rogers JM, Kim CU, et al. Structure of a pseudokinase-domain switch that controls oncogenic activation of Jak kinases. Nat Struct Mol Biol. 2013;20(10):1221-3.
211. Hammaren HM, Ungureanu D, Grisouard J, Skoda RC, Hubbard SR, Silvennoinen O. ATP binding to the pseudokinase domain of JAK2 is critical for pathogenic activation. Proc Natl Acad Sci U S A. 2015;112(15):4642-7.
212. Briscoe J, Rogers NC, Witthuhn BA, Watling D, Harpur AG, Wilks AF, et al. Kinase-negative mutants of JAK1 can sustain interferon-gamma-inducible gene expression but not an antiviral state. EMBO J. 1996;15(4):799-809.
213. Feng J, Witthuhn BA, Matsuda T, Kohlhuber F, Kerr IM, Ihle JN. Activation of Jak2 catalytic activity requires phosphorylation of Y1007 in the kinase activation loop. Mol Cell Biol. 1997;17(5):2497-501.
214. Gauzzi MC, Velazquez L, McKendry R, Mogensen KE, Fellous M, Pellegrini S. Interferon-alpha-dependent activation of Tyk2 requires phosphorylation of positive regulatory tyrosines by another kinase. J Biol Chem. 1996;271(34):20494-500.
215. Liu KD, Gaffen SL, Goldsmith MA, Greene WC. Janus kinases in interleukin-2-mediated signaling: JAK1 and JAK3 are differentially regulated by tyrosine phosphorylation. Curr Biol. 1997;7(11):817-26.
216. Boggon TJ, Li Y, Manley PW, Eck MJ. Crystal structure of the Jak3 kinase domain in complex with a staurosporine analog. Blood. 2005;106(3):996-1002.

217. Haan C, Kroy DC, Wuller S, Sommer U, Nocker T, Rolvering C, et al. An unusual insertion in Jak2 is crucial for kinase activity and differentially affects cytokine responses. J Immunol. 2009;182(5):2969-77.
218. Andraos R, Qian Z, Bonenfant D, Rubert J, Vangrevelinghe E, Scheufler C, et al. Modulation of activation-loop phosphorylation by JAK inhibitors is binding mode dependent. Cancer discovery. 2012;2(6):512-23.
219. Williams NK, Bamert RS, Patel O, Wang C, Walden PM, Wilks AF, et al. Dissecting specificity in the Janus kinases: the structures of JAK-specific inhibitors complexed to the JAK1 and JAK2 protein tyrosine kinase domains. J Mol Biol. 2009;387(1):219-32.
220. Baffert F, Regnier CH, De Pover A, Pissot-Soldermann C, Tavares GA, Blasco F, et al. Potent and selective inhibition of polycythemia by the quinoxaline JAK2 inhibitor NVP-BSK805. Mol Cancer Ther. 2010;9(7):1945-55.
221. Leroy E, Dusa A, Colau D, Motamedi A, Cahu X, Mouton C, et al. Uncoupling JAK2 V617F activation from cytokine-induced signalling by modulation of JH2 alphaC helix. Biochem J. 2016;473(11):1579-91.
222. Liang J, Tsui V, Van Abbema A, Bao L, Barrett K, Beresini M, et al. Lead identification of novel and selective TYK2 inhibitors. Eur J Med Chem. 2013;67:175-87.
223. Tokarski JS, Zupa-Fernandez A, Tredup JA, Pike K, Chang C, Xie D, et al. Tyrosine Kinase 2-mediated Signal Transduction in T Lymphocytes Is Blocked by Pharmacological Stabilization of Its Pseudokinase Domain. J Biol Chem. 2015;290(17):11061-74.
224. Tan L, Akahane K, McNally R, Reyskens KM, Ficarro SB, Liu S, et al. Development of Selective Covalent Janus Kinase 3 Inhibitors. J Med Chem. 2015;58(16):6589-606.
225. Godeny MD, Sayyah J, VonDerLinden D, Johns M, Ostrov DA, Caldwell-Busby J, et al. The N-terminal SH2 domain of the tyrosine phosphatase, SHP-2, is essential for Jak2-dependent signaling via the angiotensin II type AT1 receptor. Cell Signal. 2007;19(3):600-9.
226. Ferrand A, Kowalski-Chauvel A, Bertrand C, Escrieut C, Mathieu A, Portolan G, et al. A novel mechanism for JAK2 activation by a G protein-coupled receptor, the CCK2R: implication of this signaling pathway in pancreatic tumor models. J Biol Chem. 2005;280(11):10710-5.
227. Laurence A, Pesu M, Silvennoinen O, O'Shea J. JAK Kinases in Health and Disease: An Update. Open Rheumatol J. 2012;6:232-44.

228. Ishida-Takahashi R, Rosario F, Gong Y, Kopp K, Stancheva Z, Chen X, et al. Phosphorylation of Jak2 on Ser(523) inhibits Jak2-dependent leptin receptor signaling. Mol Cell Biol. 2006;26(11):4063-73.
229. Mazurkiewicz-Munoz AM, Argetsinger LS, Kouadio JL, Stensballe A, Jensen ON, Cline JM, et al. Phosphorylation of JAK2 at serine 523: a negative regulator of JAK2 that is stimulated by growth hormone and epidermal growth factor. Mol Cell Biol. 2006;26(11):4052-62.
230. Kurzer JH, Argetsinger LS, Zhou YJ, Kouadio JL, O'Shea JJ, Carter-Su C. Tyrosine 813 is a site of JAK2 autophosphorylation critical for activation of JAK2 by SH2-B beta. Mol Cell Biol. 2004;24(10):4557-70.
231. Carpino N, Kobayashi R, Zang H, Takahashi Y, Jou ST, Feng J, et al. Identification, cDNA cloning, and targeted deletion of p70, a novel, ubiquitously expressed SH3 domain-containing protein. Mol Cell Biol. 2002;22(21):7491-500.
232. Saharinen P, Vihinen M, Silvennoinen O. Autoinhibition of Jak2 tyrosine kinase is dependent on specific regions in its pseudokinase domain. Mol Biol Cell. 2003;14(4):1448-59.
233. Sanz Sanz A, Niranjan Y, Hammaren H, Ungureanu D, Ruijtenbeek R, Touw IP, et al. The JH2 domain and SH2-JH2 linker regulate JAK2 activity: A detailed kinetic analysis of wild type and V617F mutant kinase domains. Biochim Biophys Acta. 2014;1844(10):1835-41.
234. Russell SM, Tayebi N, Nakajima H, Riedy MC, Roberts JL, Aman MJ, et al. Mutation of Jak3 in a patient with SCID: essential role of Jak3 in lymphoid development. Science. 1995;270(5237):797-800.
235. Yeh TC, Dondi E, Uze G, Pellegrini S. A dual role for the kinase-like domain of the tyrosine kinase Tyk2 in interferon-alpha signaling. Proc Natl Acad Sci U S A. 2000;97(16):8991-6.
236. Zhao L, Dong H, Zhang CC, Kinch L, Osawa M, Iacovino M, et al. A JAK2 interdomain linker relays Epo receptor engagement signals to kinase activation. J Biol Chem. 2009;284(39):26988-98.
237. Sanz A, Ungureanu D, Pekkala T, Ruijtenbeek R, Touw IP, Hilhorst R, et al. Analysis of Jak2 catalytic function by peptide microarrays: the role of the JH2 domain and V617F mutation. PLoS One. 2011;6(4):e18522.
238. Dusa A, Mouton C, Pecquet C, Herman M, Constantinescu SN. JAK2 V617F constitutive activation requires JH2 residue F595: a pseudokinase domain target for specific inhibitors. PLoS One. 2010;5(6):e11157.

239. Visser O, Trama A, Maynadie M, Stiller C, Marcos-Gragera R, De Angelis R, et al. Incidence, survival and prevalence of myeloid malignancies in Europe. Eur J Cancer. 2012;48(17):3257-66.
240. Pietra D, Brisci A, Rumi E, Boggi S, Elena C, Pietrelli A, et al. Deep sequencing reveals double mutations in cis of MPL exon 10 in myeloproliferative neoplasms. Haematologica. 2011;96(4):607-11.
241. Rampal R, Al-Shahrour F, Abdel-Wahab O, Patel JP, Brunel JP, Mermel CH, et al. Integrated genomic analysis illustrates the central role of JAK-STAT pathway activation in myeloproliferative neoplasm pathogenesis. Blood. 2014;123(22):e123-33.
242. Passamonti F, Caramazza D, Maffioli M. JAK inhibitor in CALR-mutant myelofibrosis. N Engl J Med. 2014;370(12):1168-9.
243. Guglielmelli P, Biamonte F, Rotunno G, Artusi V, Artuso L, Bernardis I, et al. Impact of mutational status on outcomes in myelofibrosis patients treated with ruxolitinib in the COMFORT-II study. Blood. 2014;123(14):2157-60.
244. Stein BL, Gotlib J, Arcasoy M, Nguyen MH, Shah N, Moliterno A, et al. Historical views, conventional approaches, and evolving management strategies for myeloproliferative neoplasms. J Natl Compr Canc Netw. 2015;13(4):424-34.
245. Badrinarayan P, Sastry GN. Rational approaches towards lead optimization of kinase inhibitors: the issue of specificity. Curr Pharm Des. 2013;19(26):4714-38.
246. Vannucchi AM. Ruxolitinib versus standard therapy for the treatment of polycythemia vera. N Engl J Med. 2015;372(17):1670-1.
247. Verstovsek S, Kantarjian H, Mesa RA, Pardanani AD, Cortes-Franco J, Thomas DA, et al. Safety and efficacy of INCB018424, a JAK1 and JAK2 inhibitor, in myelofibrosis. N Engl J Med. 2010;363(12):1117-27.
248. Nakaya Y, Shide K, Naito H, Niwa T, Horio T, Miyake J, et al. Effect of NS-018, a selective JAK2V617F inhibitor, in a murine model of myelofibrosis. Blood Cancer J. 2014;4:e174.
249. Ma L, Clayton JR, Walgren RA, Zhao B, Evans RJ, Smith MC, et al. Discovery and characterization of LY2784544, a small-molecule tyrosine kinase inhibitor of JAK2V617F. Blood Cancer J. 2013;3:e109.
250. Pratilas CA, Taylor BS, Ye Q, Viale A, Sander C, Solit DB, et al. (V600E)BRAF is associated with disabled feedback inhibition of RAF-MEK

signaling and elevated transcriptional output of the pathway. Proc Natl Acad Sci U S A. 2009;106(11):4519-24.
251. Hatzivassiliou G, Song K, Yen I, Brandhuber BJ, Anderson DJ, Alvarado R, et al. RAF inhibitors prime wild-type RAF to activate the MAPK pathway and enhance growth. Nature. 2010;464(7287):431-5.
252. Han EK, Leverson JD, McGonigal T, Shah OJ, Woods KW, Hunter T, et al. Akt inhibitor A-443654 induces rapid Akt Ser-473 phosphorylation independent of mTORC1 inhibition. Oncogene. 2007;26(38):5655-61.
253. Hornakova T, Springuel L, Devreux J, Dusa A, Constantinescu SN, Knoops L, et al. Oncogenic JAK1 and JAK2-activating mutations resistant to ATP-competitive inhibitors. Haematologica. 2011;96(6):845-53.
254. Deshpande A, Reddy MM, Schade GO, Ray A, Chowdary TK, Griffin JD, et al. Kinase domain mutations confer resistance to novel inhibitors targeting JAK2V617F in myeloproliferative neoplasms. Leukemia. 2011.
255. Marit MR, Chohan M, Matthew N, Huang K, Kuntz DA, Rose DR, et al. Random mutagenesis reveals residues of JAK2 critical in evading inhibition by a tyrosine kinase inhibitor. PLoS One. 2012;7(8):e43437.
256. Koppikar P, Bhagwat N, Kilpivaara O, Manshouri T, Adli M, Hricik T, et al. Heterodimeric JAK-STAT activation as a mechanism of persistence to JAK2 inhibitor therapy. Nature. 2012;489(7414):155-9.
257. Meyer SC, Keller MD, Chiu S, Koppikar P, Guryanova OA, Rapaport F, et al. CHZ868, a Type II JAK2 Inhibitor, Reverses Type I JAK Inhibitor Persistence and Demonstrates Efficacy in Myeloproliferative Neoplasms. Cancer Cell. 2015;28(1):15-28.
258. Liu Y, Gray NS. Rational design of inhibitors that bind to inactive kinase conformations. Nat Chem Biol. 2006;2(7):358-64.
259. Nagar B, Bornmann WG, Pellicena P, Schindler T, Veach DR, Miller WT, et al. Crystal structures of the kinase domain of c-Abl in complex with the small molecule inhibitors PD173955 and imatinib (STI-571). Cancer Res. 2002;62(15):4236-43.
260. Wu SC, Li LS, Kopp N, Montero J, Chapuy B, Yoda A, et al. Activity of the Type II JAK2 Inhibitor CHZ868 in B Cell Acute Lymphoblastic Leukemia. Cancer Cell. 2015;28(1):29-41.
261. Manley PW, Bruggen J, Floersheimer A, Furet P, Jensen MR, Mestan J, et al. Chimia. 2008;62(579).

262. Cowan-Jacob SW, Jahnke W, Knapp S. Novel approaches for targeting kinases: allosteric inhibition, allosteric activation and pseudokinases. Future Med Chem. 2014;6(5):541-61.
263. Jatiani SS, Cosenza SC, Reddy MV, Ha JH, Baker SJ, Samanta AK, et al. A Non-ATP-Competitive Dual Inhibitor of JAK2 and BCR-ABL Kinases: Elucidation of a Novel Therapeutic Spectrum Based on Substrate Competitive Inhibition. Genes Cancer. 2010;1(4):331-45.
264. Lipka DB, Hoffmann LS, Heidel F, Markova B, Blum MC, Breitenbuecher F, et al. LS104, a non-ATP-competitive small-molecule inhibitor of JAK2, is potently inducing apoptosis in JAK2V617F-positive cells. Mol Cancer Ther. 2008;7(5):1176-84.
265. Samanta AK, Chakraborty SN, Wang Y, Schlette E, Reddy EP, Arlinghaus RB. Destabilization of Bcr-Abl/Jak2 Network by a Jak2/Abl Kinase Inhibitor ON044580 Overcomes Drug Resistance in Blast Crisis Chronic Myelogenous Leukemia (CML). Genes Cancer. 2010;1(4):346-59.
266. Varghese LN, Ungureanu D, Liau NP, Young SN, Laktyushin A, Hammaren H, et al. Mechanistic insights into activation and SOCS3-mediated inhibition of myeloproliferative neoplasm-associated JAK2 mutants from biochemical and structural analyses. Biochem J. 2014;458(2):395-405.
267. Lupardus PJ, Skiniotis G, Rice AJ, Thomas C, Fischer S, Walz T, et al. Structural snapshots of full-length Jak1, a transmembrane gp130/IL-6/IL-6Ralpha cytokine receptor complex, and the receptor-Jak1 holocomplex. Structure. 2011;19(1):45-55.
268. Sousa SF, Fernandes PA, Ramos MJ. Protein-ligand docking: current status and future challenges. Proteins. 2006;65(1):15-26.
269. Zhang J, Yang PL, Gray NS. Targeting cancer with small molecule kinase inhibitors. Nat Rev Cancer. 2009;9(1):28-39.
270. Cowan-Jacob SW, Mobitz H, Fabbro D. Structural biology contributions to tyrosine kinase drug discovery. Curr Opin Cell Biol. 2009;21(2):280-7.
271. Adrian FJ, Ding Q, Sim T, Velentza A, Sloan C, Liu Y, et al. Allosteric inhibitors of Bcr-abl-dependent cell proliferation. Nat Chem Biol. 2006;2(2):95-102.
272. Chen M, Cheng A, Candotti F, Zhou YJ, Hymel A, Fasth A, et al. Complex effects of naturally occurring mutations in the JAK3 pseudokinase

domain: evidence for interactions between the kinase and pseudokinase domains. Mol Cell Biol. 2000;20(3):947-56.
273. Davis MI, Hunt JP, Herrgard S, Ciceri P, Wodicka LM, Pallares G, et al. Comprehensive analysis of kinase inhibitor selectivity. Nat Biotechnol. 2011;29(11):1046-51.
274. Bandaranayake RM, Ungureanu D, Shan Y, Shaw DE, Silvennoinen O, Hubbard SR. Crystal structures of the JAK2 pseudokinase domain and the pathogenic mutant V617F. Nature structural & molecular biology. 2012;19(8):754-9.
275. Liu Q, Sabnis Y, Zhao Z, Zhang T, Buhrlage SJ, Jones LH, et al. Developing irreversible inhibitors of the protein kinase cysteinome. Chem Biol. 2013;20(2):146-59.
276. Leproult E, Barluenga S, Moras D, Wurtz JM, Winssinger N. Cysteine mapping in conformationally distinct kinase nucleotide binding sites: application to the design of selective covalent inhibitors. J Med Chem. 2011;54(5):1347-55.
277. Goedken ER, Argiriadi MA, Banach DL, Fiamengo BA, Foley SE, Frank KE, et al. Tricyclic covalent inhibitors selectively target Jak3 through an active site thiol. J Biol Chem. 2015;290(8):4573-89.
278. Yun CH, Mengwasser KE, Toms AV, Woo MS, Greulich H, Wong KK, et al. The T790M mutation in EGFR kinase causes drug resistance by increasing the affinity for ATP. Proc Natl Acad Sci U S A. 2008;105(6):2070-5.
279. Matthews EE, Thevenin D, Rogers JM, Gotow L, Lira PD, Reiter LA, et al. Thrombopoietin receptor activation: transmembrane helix dimerization, rotation, and allosteric modulation. FASEB J. 2011;25(7):2234-44.
280. Frank SJ, Yi W, Zhao Y, Goldsmith JF, Gilliland G, Jiang J, et al. Regions of the JAK2 tyrosine kinase required for coupling to the growth hormone receptor. J Biol Chem. 1995;270(24):14776-85.
281. Cacalano NA, Migone TS, Bazan F, Hanson EP, Chen M, Candotti F, et al. Autosomal SCID caused by a point mutation in the N-terminus of Jak3: mapping of the Jak3-receptor interaction domain. EMBO J. 1999;18(6):1549-58.
282. O'Sullivan JM, McLornan DP, Harrison CN. Safety considerations when treating myelofibrosis. Expert Opinion On Drug Safety. 2016([Epub ahead of print]).

283. Genovese MC, Kremer J, Zamani O, Ludivico C, Krogulec M, Xie L, et al. Baricitinib in Patients with Refractory Rheumatoid Arthritis. N Engl J Med. 2016;374(13):1243-52.
284. Plimack ER, Lorusso PM, McCoon P, Tang W, Krebs AD, Curt G, et al. AZD1480: a phase I study of a novel JAK2 inhibitor in solid tumors. Oncologist. 2013;18(7):819-20.
285. Seavey MM, Lu LD, Stump KL, Wallace NH, Hockeimer W, O'Kane TM, et al. Therapeutic efficacy of CEP-33779, a novel selective JAK2 inhibitor, in a mouse model of colitis-induced colorectal cancer. Mol Cancer Ther. 2012;11(4):984-93.

Annex

Germ-line *JAK2* mutations in the kinase domain are responsible for hereditary thrombocytosis and are resistant to JAK2 and HSP90 inhibitors

Caroline Marty,[1,2,3] Cécile Saint-Martin,[1,4] Christian Pecquet,[5,6] Sarah Grosjean,[1,4] Joseph Saliba,[1,2,3] Céline Mouton,[5,6] Emilie Leroy,[5,6] Ashot S. Harutyunyan,[7] Jean-François Abgrall,[8] Rémi Favier,[1,9] Aurélie Toussaint,[10] Eric Solary,[1,2,3] Robert Kralovics,[7,11] Stefan N. Constantinescu,[5,6] Albert Najman,[12] William Vainchenker,[1,2,3] Isabelle Plo,[1,2,3] and Christine Bellanné-Chantelot[1,4]

[1]Institut National de la Santé et de la Recherche Médicale, Unité Mixte de Recherche 1009, Laboratory of Excellence GR-Ex, Villejuif, France; [2]Université Paris XI, Unité Mixte de Recherche 1009, Institut Gustave Roussy, Villejuif, France; [3]Institut Gustave Roussy, Villejuif, France; [4]Assistance Publique-Hôpitaux de Paris, Département de Génétique, Hôpital Pitié-Salpêtrière, Université Pierre et Marie Curie, Paris, France; [5]Ludwig Institute for Cancer Research, Brussels, Belgium; [6]de Duve Institute, Université Catholique de Louvain, Brussels, Belgium; [7]Research Center for Molecular Medicine of the Austrian Academy of Sciences, Vienna, Austria; [8]Centre hospitalier universitaire de Brest, Service d'Hématologie, Brest, France; [9]Assistance Publique-Hôpitaux de Paris, Service d'Hématologie Biologique, Le Centre de Référence des Pathologies Plaquettaires, Hôpital Armand Trousseau, Paris, France; [10]Assistance Publique-Hôpitaux de Paris, Service de Biochimie et Génétique Moléculaire, Groupe Hospitalier Cochin, Paris, France; [11]Division of Hematology and Blood Coagulation, Department of Internal Medicine I, Medical University of Vienna, Vienna, Austria; and [12]Assistance Publique-Hôpitaux de Paris, Service des Maladies du Sang et de Thérapie Cellulaire, Hôpital Saint-Antoine, Université Pierre et Marie Curie, Paris, France

Key Points

- New germ-line mutations of *JAK2* in the kinase domain were identified.
- Specificity for MPL and resistance to JAK2 and HSP90 inhibitors was determined.

The main molecular basis of essential thrombocythemia and hereditary thrombocytosis is acquired, and germ-line–activating mutations affect the thrombopoietin signaling axis. We have identified 2 families with hereditary thrombocytosis presenting novel heterozygous germ-line mutations of *JAK2*. One family carries the *JAK2* R867Q mutation located in the kinase domain, whereas the other presents 2 *JAK2* mutations, S755R/R938Q, located in *cis* in both the pseudokinase and kinase domains. Expression of Janus kinase 2 (JAK2) R867Q and S755R/R938Q induced spontaneous growth of Ba/F3-thrombopoietin receptor (MPL) but not of Ba/F3–human receptor of erythropoietin cells. Interestingly, both Ba/F3-MPL cells expressing the mutants and platelets from patients displayed thrombopoietin-independent phosphorylation of signal transducer and activator of transcription 1. The JAK2 R867Q and S755R/R938Q proteins had significantly longer half-lives compared with JAK2 V617F. The longer half-lives correlated with increased binding to the heat shock protein 90 (HSP90) chaperone and with higher MPL cell-surface expression. Moreover, these mutants were less sensitive to JAK2 and HSP90 inhibitors than JAK2 V617F. Our results suggest that the mutations in the kinase domain of JAK2 may confer a weak activation of signaling specifically dependent on MPL while inducing a decreased sensitivity to clinically available JAK2 inhibitors. (*Blood*. 2014;123(9):1372-1383)

Introduction

Thrombocytosis is a rare entity characterized by an abnormal proliferation of the megakaryocytic lineage resulting in overproduction of platelets (>450 × 10^9/L in adults). The overproduction of platelets is related to the activation of the thrombopoietin (TPO)/TPO receptor (MPL) axis that signals through several pathways, which include Janus kinase 2 (JAK2)/signal transducer and activator of transcription (STAT) 1-3-5, phosphatidylinositol 3-kinase (PI3K)/AKT, and mitogen-activated protein kinase.[1,2]

Familial thrombocytosis involves heterogeneous disorders that can be subdivided into true myeloproliferative neoplasms (MPNs) transmitted by autosomal inheritance with incomplete penetrance, and hereditary thrombocytosis with an autosomal dominant pattern and an early onset (complete penetrance) of the hematologic abnormalities.[3,4] The latter are considered as nonmalignant diseases because of the polyclonal nature of hematopoiesis.

To date, germ-line mutations that have been identified in familial thrombocytosis all affect genes involved in TPO/MPL signaling. The genes targeted by germ-line mutations in familial thrombocytosis are often the same as sporadic mutations in MPNs, but the mutations disrupt different residues in the proteins. They include *MPL* S505N and *MPL* P106L, leading to the constitutive activation of the receptor and to a presumptive defect of TPO binding, respectively.[5-7] An *MPL* W515R mutation, which is rare in sporadic MPNs compared with *MPL* W515L or W515K, has also recently been identified in familial thrombocytosis.[8] Likewise, 2 germ-line mutations, *JAK2* V617I (different from the V617F substitution classically found in 60% of

Submitted May 23, 2013; accepted December 26, 2013. Prepublished online as *Blood* First Edition paper, January 7, 2014; DOI 10.1182/blood-2013-05-504555.

I.P. and C.B.-C. contributed equally to this study.

The online version of this article contains a data supplement.

The publication costs of this article were defrayed in part by page charge payment. Therefore, and solely to indicate this fact, this article is hereby marked "advertisement" in accordance with 18 USC section 1734.

© 2014 by The American Society of Hematology

From www.bloodjournal.org by guest on June 27, 2016. For personal use only.

sporadic essential thrombocythemias [ETs]) and *JAK2* R564Q (never observed in sporadic MPNs), have been reported.[9-11] Several mutations in the *TPO* gene that lead to increased TPO translation have also been described in families with a thrombocytosis.[12-15]

Here, we report 2 families with hereditary thrombocytosis carrying so far unidentified heterozygous germ-line mutations in *JAK2*.

Methods

Materials

Human recombinant erythropoietin (EPO) and interleukin 3 (IL-3) were generous gifts from Amgen (Neuilly, France). Stem cell factor (SCF) was from Biovitrum AB (Stockholm, Sweden), and recombinant TPO was a generous gift from Kirin (Tokyo, Japan). Restriction enzymes were purchased from Fermentas (St. Leon-Rot, Germany).

Patients and cell purification

Pedigrees of hereditary thrombocytosis registered in the French national collection of MPNs (DC 2009-957) were analyzed. All participants gave their written informed consent. Clinical and biological annotations were recorded in an Access database approved by the Commission Nationale de l'informatique et des Libertés (#815419). This study was conducted in accordance with the Declaration of Helsinki. Thrombocytosis was defined by a platelet count $>450 \times 10^9$/L in patients who had no evidence for reactive thrombocytosis and no World Health Organization criteria for ET.[16] Peripheral blood from patients was collected in sterile citrated tubes. Platelet-rich plasma was obtained by centrifugation at 180*g* for 15 minutes at 20°C. Platelet-rich plasma was mixed with acid citrate dextrose at a 9:1 ratio and centrifuged at 1500*g* for 15 minutes at 20°C. Platelet pellet was carefully resuspended in phosphate-buffered saline with 0.1% ethylenediaminetetraacetic acid. Blood mononuclear cells (BMCs) were plated in 6-well plates for 1 hour to remove monocytes and then seeded in semisolid cultures, or they were used to sort $CD34^+$ and $CD3^+$ cells by flow cytometry.

Quantification of clonogenic progenitors in semisolid cultures

BMCs were plated in methylcellulose, and burst-forming unit–erythroid (BFU-E) and colony-forming unit (CFU)–granulo-monocytic progenitors were counted 14 days later. BMCs were evaluated in serum-free fibrin clot assays to quantify CFU-megakaryocyte (MK) progenitor–derived colonies at day 10 by an indirect immuno–alkaline phosphatase staining technique using an anti-CD41a monoclonal antibody (clone HIP8; Becton Dickinson) as previously described.[17,18]

JAK2 molecular analysis

Amplification of the 25 exons and intron-exon boundaries of *JAK2* (NM_004972.3) was performed in the probands on genomic DNA extracted from BMCs. Purified polymerase chain reaction products were sequenced in both directions using the BigDye Terminator chemistry (Life Technologies, Saint-Aubin, France) on an ABI3730 Genetic Analyzer.

DNA manipulations, production of retroviruses

The 2265T>A (S755R), 2600G>A (R867Q), and 2813G>A (R938Q) point mutations were introduced into the MIGR1-human JAK2 WT-IRES-GFP plasmid by the QuikChange site-directed mutagenesis method using the PfuUltra high-fidelity DNA polymerase (Stratagene, Amsterdam, The Netherlands). Full-length *JAK2* mutant complementary DNAs were verified by sequencing. Vesicular stomatitis virus glycoprotein–pseudotyped viral particles were produced into 293EBNA cells.

Cell lines

The murine pro-B Ba/F3 cells were grown in Dulbecco's modified Eagle medium supplemented with 10% fetal bovine serum (Stem Cell Technologies, Grenoble, France) and 5% conditioned medium from WEHI-3B cells as a source of murine IL-3. Ba/F3 cells were retrovirally transduced with MIGR1-IRES-CD4 to stably express the human receptor of EPO (EPOR) or TPO (MPL) harboring an N-terminal FLAG tag and maintained in the presence of 1 U/mL EPO and 5% WEHI, respectively. Ba/F3-EPOR and Ba/F3-MPL cell lines expressing the various JAK2 mutants were generated after transduction and subsequent green fluorescent protein (GFP)–positive cell sorting by flow cytometry (MoFlo; Beckman-Coulter, Villepinte, France).

Proliferation assays

The premixed WST-1 (5-[2,4-disulfophenyl]-2H-tetrazolium, monosodium salt) cell proliferation assay system was carried out according to the manufacturer's instructions (Takara Bio Europe, Clontech, Saint-Germain-en-Laye, France). Experiments were done in triplicate. For inhibitor treatments, values were transformed to percent inhibition relative to vehicle-treated (dimethylsulfoxide) cells, and sigmoidal curves were fitted according to nonlinear regression analysis of the data using GraphPad PRISM software to calculate 50% inhibitory concentration. Dose-response curves to EPO and TPO were expressed as percent of viability of the maximal response.

Western blot analysis and coimmunoprecipitation

Signaling studies were performed on platelets and Ba/F3 cell lines by western blot analysis using polyclonal antibodies against the phosphorylated forms of JAK2 (Tyr 1007/1008), STAT1 (Tyr 701), STAT3 (Tyr 705), STAT5 (Tyr 694), extracellular signal-regulated kinase (ERK) 1/2 (Thr 202/Tyr 204), and AKT (Thr 308) and against the pan proteins (Cell Signaling Technology [Ozyme]). Heat shock cognate 70 (HSC70) (Stressgen, Victoria, Canada) or β-actin (Sigma, Saint Quentin Fallavier, France) were used as loading controls. For coimmunoprecipitation experiments, cells lysates were incubated with anti-JAK2 antibody (Ozyme) and A/G agarose beads. HSP90 and MPL were revealed with antibodies from Ozyme and Upstate (Millipore, Molsheim, France), respectively.

Cell-surface expression of FLAG-tagged MPL

Expression of MPL at the surface of Ba/F3 cells was examined by flow cytometry with 10 μg/mL monoclonal anti-FLAG M2 antibody (Sigma-Aldrich) followed with 1:400 diluted phycoerythrin (PE)–conjugated anti-mouse IgG(H+L) from Jackson ImmunoResearch Laboratories (Interchim, Montluçon, France).

Dual luciferase transcriptional assays

Transcriptional activation of STAT5, STAT3, and STAT1 was analyzed in γ2A JAK2-deficient cells using the dual pGRR5 firefly luciferase reporter (responding to STATs) and pRL-TK-driven renilla luciferase system. γ2A cells were transiently transfected using Lipofectamine reagent with complementary DNAs coding for JAK2 (or mutants thereof), MPL, and either STAT5, STAT3, or STAT1 as described.[19] A Perkin-Elmer Victor X Light analyzer was used for detecting luminescence in cell lysates.

Modeling of mutation effects in JAK2 JH2 and JH1

The inactive and active crystal structures of JH1 (kinase domain)[20] and the crystal structure of the JH2 (pseudokinase domain)[21] were superimposed by Dr Andrew Shaw (Ludwig Institute for Cancer Research, San Diego, CA). Mutagenesis and effects on known salt bridges and intramolecular interactions were examined by the PyMol program.

Results

Identification of new germ-line *JAK2* mutations

We performed a genome-wide single-nucleotide polymorphism (SNP) analysis of a large pedigree (family 1) with 7 affected members (individuals 1-7) showing only *JAK2* V617F–negative thrombocytosis

From www.bloodjournal.org by guest on June 27, 2016. For personal use only.

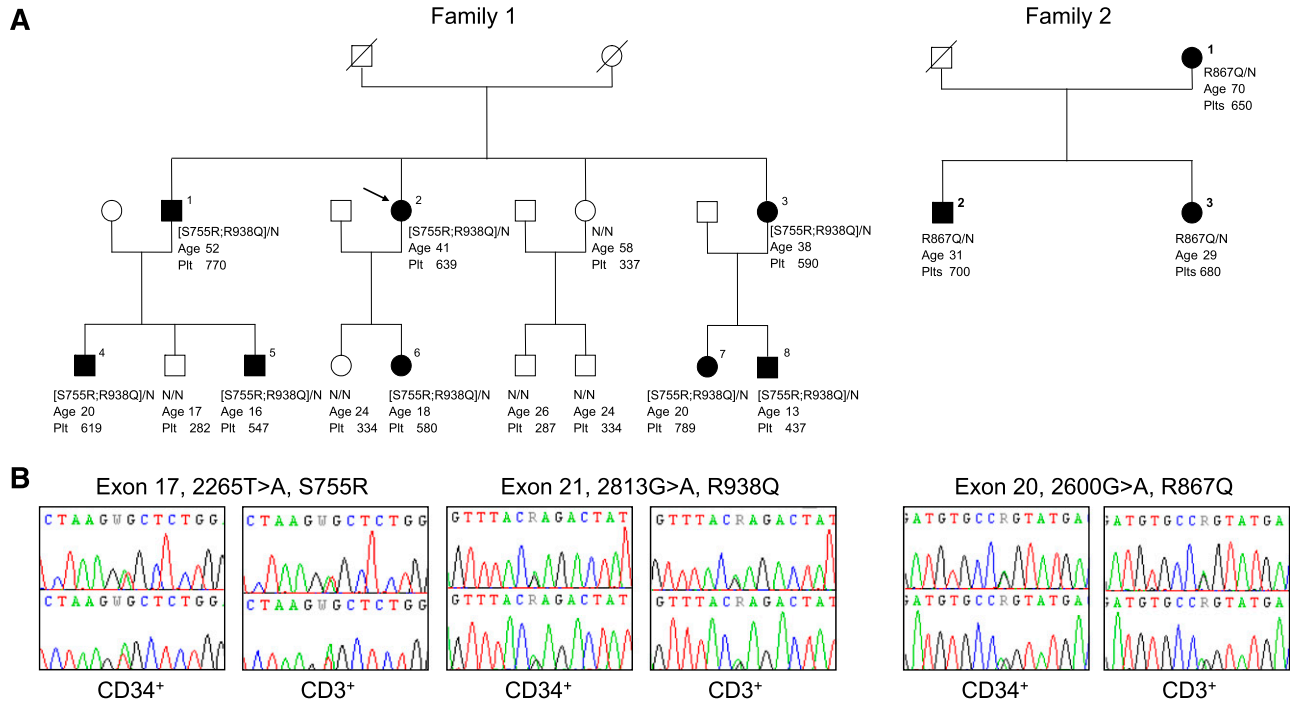

Figure 1. Clinical and molecular features of 2 pedigrees with hereditary thrombocytosis. (A) Filled symbols represent individuals with *JAK2* germ-line mutations. Below each symbol is reported the *JAK2* genotype with "N" indicating a normal allele, the age (years) at diagnosis for affected individuals or the age at last examination for asymptomatic relatives, and the platelet level ($\times 10^9$/L). (B) Sequence electropherograms of the germ-line *JAK2* mutations.

(Figure 1A). We genotyped the affected individuals using the Affymetrix 6.0 SNP array (906 622 SNPs) and determined 9 chromosomal regions with SNP alleles shared by all of them. One was located on chromosome 9 and encompassed the *JAK2* locus (supplemental Table 1, available on the *Blood* Web site). Sequencing of the entire *JAK2* gene identified 2 heterozygous *JAK2* mutations, that is, c.2265T>A (S755R) and c.2813G>A (R938Q). Segregation analysis showed that both mutations were located on the same allele (Figure 1A). Subsequently, we analyzed 5 other families characterized by isolated elevated platelet counts ranging from 470×10^9/L to 1900×10^9/L, the absence of *JAK2* V617F, an age at onset <40 years in at least 1 affected case, and a family history compatible with an autosomal dominant inheritance. They were sequenced for *JAK2*, and a new single heterozygous *JAK2* mutation, c.2600G>A (R867Q), was found in family 2 (Figure 1A-B). Sequence analysis for 7 affected individuals from the 2 families confirmed the presence of the *JAK2* mutations at heterozygous state in $CD34^+$ and $CD3^+$ cells. In both families, all members carrying these mutations suffer from thrombocytosis except 1 young relative of family 1 with a platelet count (437×10^9/L) close to the normal upper limit (subject 8). Their detailed hematologic and clinical characteristics are shown in supplemental Table 2.

The identified mutations are novel *JAK2* missense mutations that have not been reported in genomic databases. The S755R mutation is located in the pseudokinase domain (JH2), whereas R867Q and R938Q mutations are situated in the kinase domain (JH1) of the protein (Figure 2A). These mutations affect amino acids that are highly conserved across species, and in silico analysis of the potential impact of these substitutions predicted a pathogenic effect on JAK2 function (supplemental Table 3). More specifically, the R867Q mutation in JH1 was predicted to abolish a salt bridge (between R867 and D869), which is present in the inactive JH1 and is lost upon activation.[20] Thus, the R867Q mutation would result in an active state in the region around β sheets 2 and 3 (Figure 2B). The S755R mutation was predicted to interfere with another important salt bridge (between D635 from α helix D and K752 in the region linking α helix D to α helix G) with the bulky positive R755 triggering a steric clash (Figure 2B).[21] The loss of this salt bridge may destabilize the network of α helices at the C terminus of JH2 by pushing away helix G. This network of helices has previously been shown to exert inhibitory effects on JH1.[22] The R938Q is located in a sensitive region of the JH1, not far from the adenosine triphosphate (ATP) loop and substrate access site (Figure 2B).

To determine the clonality of hematopoieisis of these *JAK2*-mutated patients, we carried out methylation-sensitive polymerase chain reaction assays using the *HUMARA* and *PCSK1N* loci on granulocytes and $CD3^+$ cells of 3 affected women (subjects 3 and 7 of family 1 and subject 3 of family 2).[23] Results were in favor of a polyclonal hematopoiesis as opposed to a *JAK2* V617F–positive patient with polycythemia vera who displayed a complete X inactivation in agreement with a clonal hematopoiesis (supplemental Table 4).

Finally, we verified that the TPO/MPL axis controlling platelet production was not affected besides the mutations of *JAK2*, by sequencing *MPL* and assessing TPO levels in plasma for these 2 families. No mutation was identified in *MPL* for patient 2 of family 1 and patient 3 of family 2, and TPO levels were inside the normal range (<30 pg/mL) (supplemental Table 2).

JAK2 R867Q and *JAK2* S755R/R938Q are gain-of-function mutations that induce spontaneous growth and constitutive signaling of MPL-expressing cells

We modeled the *JAK2* mutations in Ba/F3 cells lines expressing either MPL (Ba/F3-MPL) or EPOR (Ba/F3-EPOR). Ba/F3-MPL and Ba/F3-EPOR expressing JAK2 V617F or JAK2 WT were used as controls. We measured cellular proliferation in response to cytokines using WST-1 assays. None of the JAK2 mutants, except JAK2

From www.bloodjournal.org by guest on June 27, 2016. For personal use only.

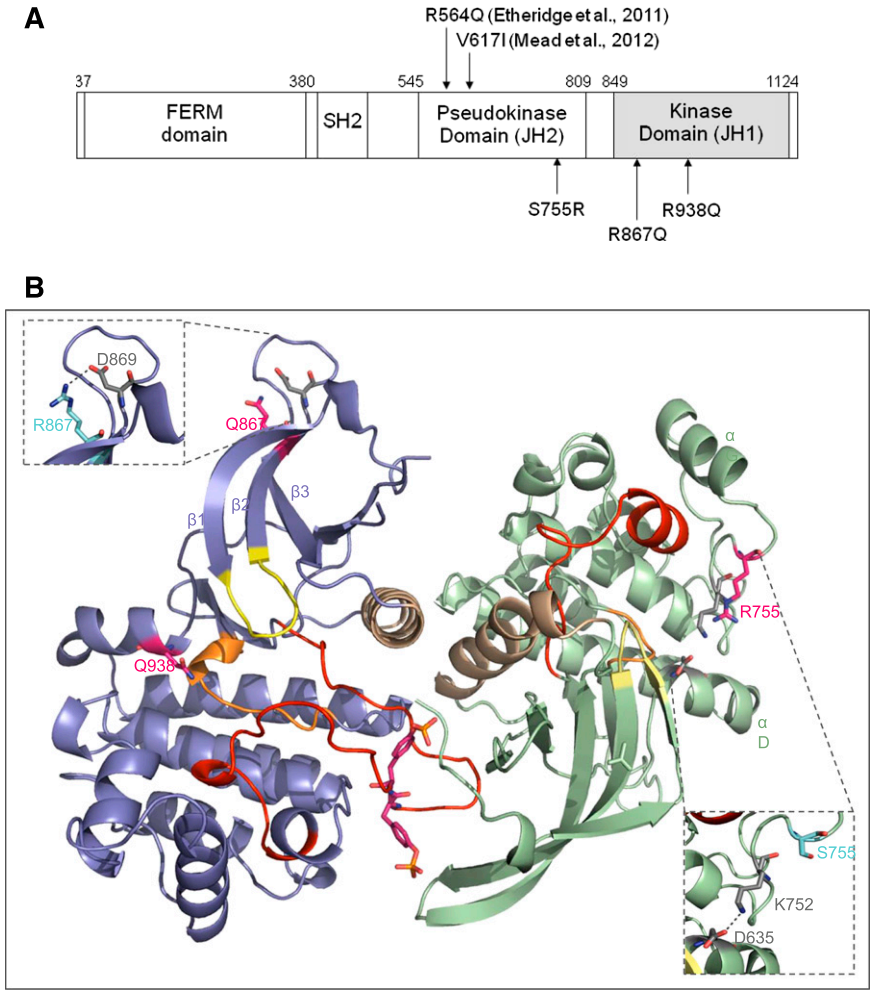

Figure 2. Scheme and in silico modeling of the JAK2 mutants. (A) Scheme and location of germ-line *JAK2* mutations. (B) Superimposition of the crystal structures of the active JH1 kinase and JH2 pseudokinase domains of JAK2 wild type (WT) based on 2 radiograph crystal structure studies.[20,21] On the left in blue: coordinate of active JH1 (protein data bank [PDB] code: 2B7A). On the right in green: coordinate of active JH2 (PDB code: 4FVQ). Two of the mutations, R938Q and R867Q, are located in the JH1, whereas the S755R mutation is located in the JH2 (pink residues). The germ-line *JAK2* S755R/R938Q mutant therefore contains mutations in both JH2 and JH1. The activation loop is represented in red in both JH1 and JH2. The glycine-rich loop is in yellow, and the catalytic loop is in orange. The salt bridge between D869 and R867 is only formed in the inactive JH1, which is the coordinate represented on the small square on the left. The coordinate of inactive JH1 is PDB code 3UGC. The salt bridge between K752 and D635 is formed in active JH2 (WT and V617F). The coordinate shown here in the small square on the right is the active JH2 WT (PDB code: 4FVQ).

V617F, conferred hypersensitivity to EPO to the Ba/F3-EPOR cell line (Figure 3A). In contrast, the Ba/F3-MPL cells expressing either of the JAK2 mutants, except for JAK2 S755R, could be maintained in a cytokine-deprived condition (>3 weeks). Independency to TPO was confirmed using a WST-1 assay (Figure 3B). TPO induced a sigmoidal dose-response curve in the Ba/F3-MPL cell line (Figure 3B, "endogenous"). As previously described for JAK2 WT and JAK2 V617F,[24,25] overexpression of the JAK2 mutants resulted in TPO-induced bell curves with a peak at 0.05 ng/mL and reduced cell viability at higher doses (Figure 3B-C). Of note, JAK2 S755R did not confer TPO independency to the cells. However, at high doses of TPO, the decreased viability of Ba/F3-MPL cells in the presence of JAK2 S755R was attenuated compared with JAK2 WT and JAK2 R938Q (Figure 3B-C). These data suggest that the R938Q mutation drives the TPO-independent proliferation of the double mutant JAK2 S755R/R938Q. The S755R mutation might be involved in maintaining basal growth in the presence of high doses of TPO as seen with JAK2 V617F.

As expected, overexpression of JAK2 V617F in Ba/F3-EPOR cells induced a constitutive phosphorylation of all signaling pathways tested (STAT5, AKT, and ERK) (Figure 4A). Although the levels of expression of the JAK2 mutants in Ba/F3-EPOR cells were similar to JAK2 WT or JAK2 V617F, we observed a weak phosphorylation of ERK in the presence of all the mutants except JAK2 R938Q, and a detectable phosphorylation of AKT in presence of JAK2 S755R and JAK2 S755R/R938Q (Figure 4A). However, there was no distinct phosphorylation of STAT5 in absence of EPO, as shown by the P-STAT5/HSC70 ratios that remain below the level induced by JAK2 V617F.

In Ba/F3-MPL cells, overexpression of JAK2 V617F induced constitutive phosphorylation of STAT3/5, AKT, and ERK as expected (Figure 4B). R867Q, R938Q alone, and S755R/R938Q JAK2 mutants induced constitutive signaling of the same pathways. Noticeably, in the presence of R867Q and S755R/R938Q JAK2 mutants, we detected a spontaneous activation of STAT1. JAK2 S755R alone did not induce any constitutive phosphorylation besides a weak activation of STAT5 (Figure 4B). This last result implies that the S755R mutation compared with the R938Q mutation might play a lesser role in the constitutive signaling of JAK2 S755R/R938Q.

We then cotransfected JAK2 V617F, R867Q, or S755R/R938Q mutant in JAK2-deficient γ2A cells in the presence of a similar amount of JAK2 WT to mimic the heterozygous state of the mutations found in patients. The effect of these mutants combined with MPL on STAT1, STAT3, or STAT5 activation was measured by luciferase assays. Figure 4C shows that mutants of JAK2 induced constitutive signaling primarily via STAT1 and, to a lesser extent, STAT3 in MPL-expressing cells and under conditions of heterozygosity. Of note, JAK2 S755R had no effect on basal STAT activation (supplemental Figure 1). Activation of the STATs was dependent on MPL (supplemental Figure 2A). In addition, we used a battery of 6 coiled-coil MPL dimeric fusion proteins,

From www.bloodjournal.org by guest on June 27, 2016. For personal use only.

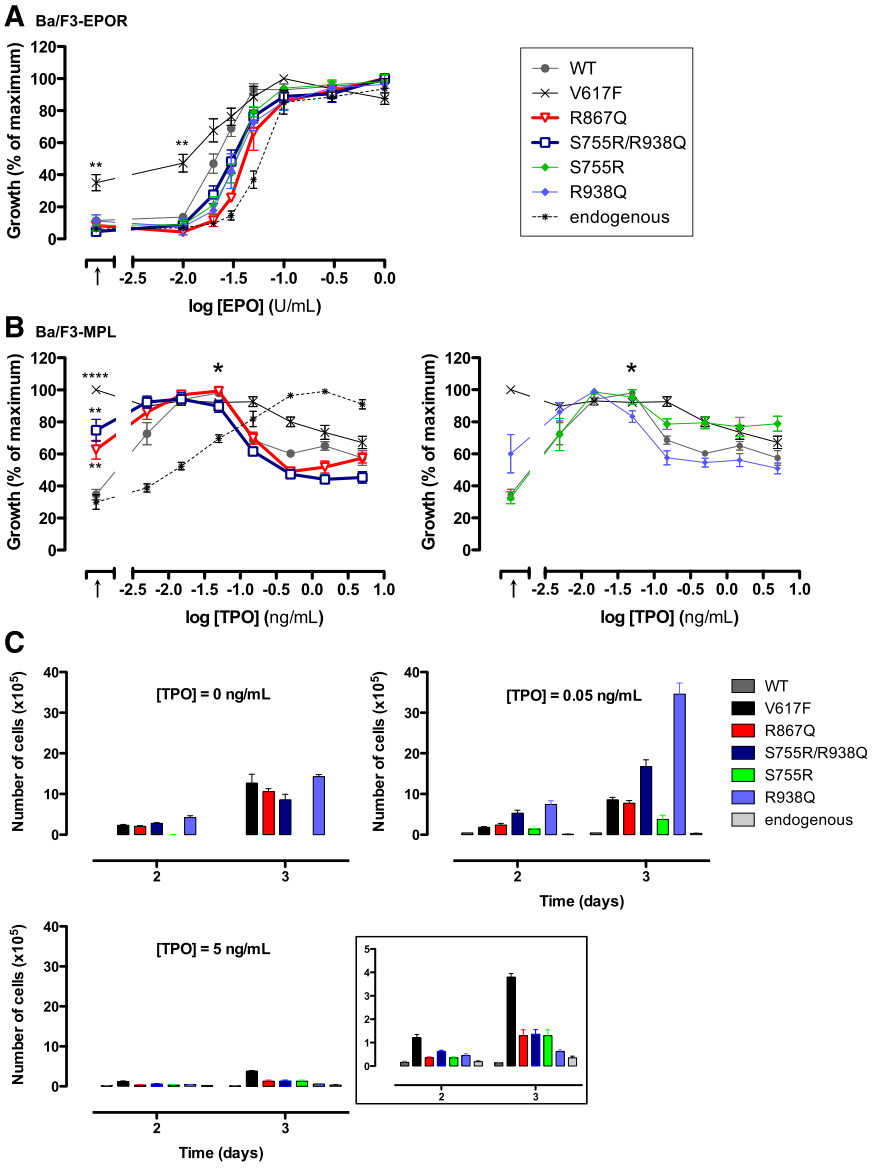

Figure 3. Sensitivities to EPO and TPO of Ba/F3-EPOR and Ba/F3-MPL cells. (A) Ba/F3-EPOR cells expressing each of the JAK2 forms were cultured for 48 hours either in the absence of cytokine (black arrow, x-axis) or in the presence of increasing doses of EPO (0.01, 0.02, 0.03, 0.05, 0.1, 0.3, and 1 U/mL). Viable cells were quantified by WST-1 proliferation assay. Dose-response curves are means expressed in percentages of maximum growth value ± standard error of the mean (SEM; n = 4 in triplicate). (B) Proliferation was assayed 48 hours after culturing Ba/F3-MPL cells expressing each of the JAK2 forms in the absence of cytokine (black arrow, x-axis) or in the presence of increasing doses of TPO (0.005, 0.015, 0.05, 0.15, 0.5, 1.5, and 5 ng/mL). The asterisk indicates 0.05 ng/mL TPO. Data are means ± SEM (n = 4 independent experiments performed in triplicate). Two-tailed Student *t* test: $^{**}P < .01$; $^{****}P < .0001$. (C) Ba/F3-MPL cell lines were plated at 30 000 cells and cultured over a period of 72 hours in the absence or presence of either 0.05 ng/mL or 5 ng/mL TPO and numbered. Curves show cumulative cell number ± standard deviation of a typical experiment out of 3 performed in triplicate. Insert represents data at 5 ng/mL TPO with an adapted y-axis scale.

with different orientations.[26] The 2 new JAK2 mutants were consistently weaker than JAK2 V617F and mostly induced STAT-dependent signaling only in the presence of active or partially active MPL dimeric orientations, and they were less active in the presence of cc-MPL-II (supplemental Figure 2B).

Taken together, these results show that the constitutive signaling of JAK2 R867Q, R938Q, and S755R/R938Q is dependent on the presence of MPL and leads to growth-factor independency and hypersensitivity to TPO.

JAK2 mutants are less sensitive than JAK2 V617F to classical JAK2 inhibitors and an HSP90 inhibitor in Ba/F3 cell lines

Randomly generated point mutations in the kinase domain of JAK2 V617F have been shown to be resistant to JAK2 inhibitors while still sensitive to inhibition of HSP90, a chaperone for JAK2.[27,28] Therefore, we tested the impact of the R867Q and S755R/R938Q mutations on the sensitivity of these mutated kinases to JAK2 inhibitors (INCB018424, TG101348, CYT-387, and AZ960) and to an HSP90 inhibitor (AUY922) by WST-1 assays. Autonomous Ba/F3-MPL cell lines (growing without cytokines for at least 3 weeks) expressing either JAK2 R867Q, JAK2 S755R/R938Q, or JAK2 V617F displayed constitutive phosphorylation of JAK2 and STAT5 (Figure 5A). JAK2 R867Q was reproducibly found to be more phosphorylated than JAK2 S755R/R938Q and JAK2 V617F. Cells were treated with increasing doses of inhibitors. Interestingly, the JAK2 R867Q–expressing and JAK2 S755R/R938Q–expressing cells were 5- to 15-fold less sensitive than their JAK2 WT and V617F counterparts to classical JAK2 inhibitors currently used in clinics and clinical trials such as TG101348 (SAR302503) and INCB018424 (ruxolitinib), AZ960, and CYT-387. Whereas high doses of TG101348 and AZ960 (>1 μM) prevented growth of all 3 mutated cell lines, equivalent doses of INCB018424 and CYT-387 failed to completely inhibit the proliferation of the cells expressing JAK2 R867Q and JAK2 S755R/R938Q (Figures 5B,E).

The R867Q and S755R/R938Q JAK2 mutants presented similar sensitivity as JAK2 V617F to a PI3K inhibitor (LY-294002) (Figure 5C), suggesting that the 3 JAK2 mutants (R867Q, S755R/R938Q, and V617F) require downstream PI3K for Ba/F3-MPL cell proliferation. However, they were less sensitive than JAK2 V617F to an HSP90

From www.bloodjournal.org by guest on June 27, 2016. For personal use only.

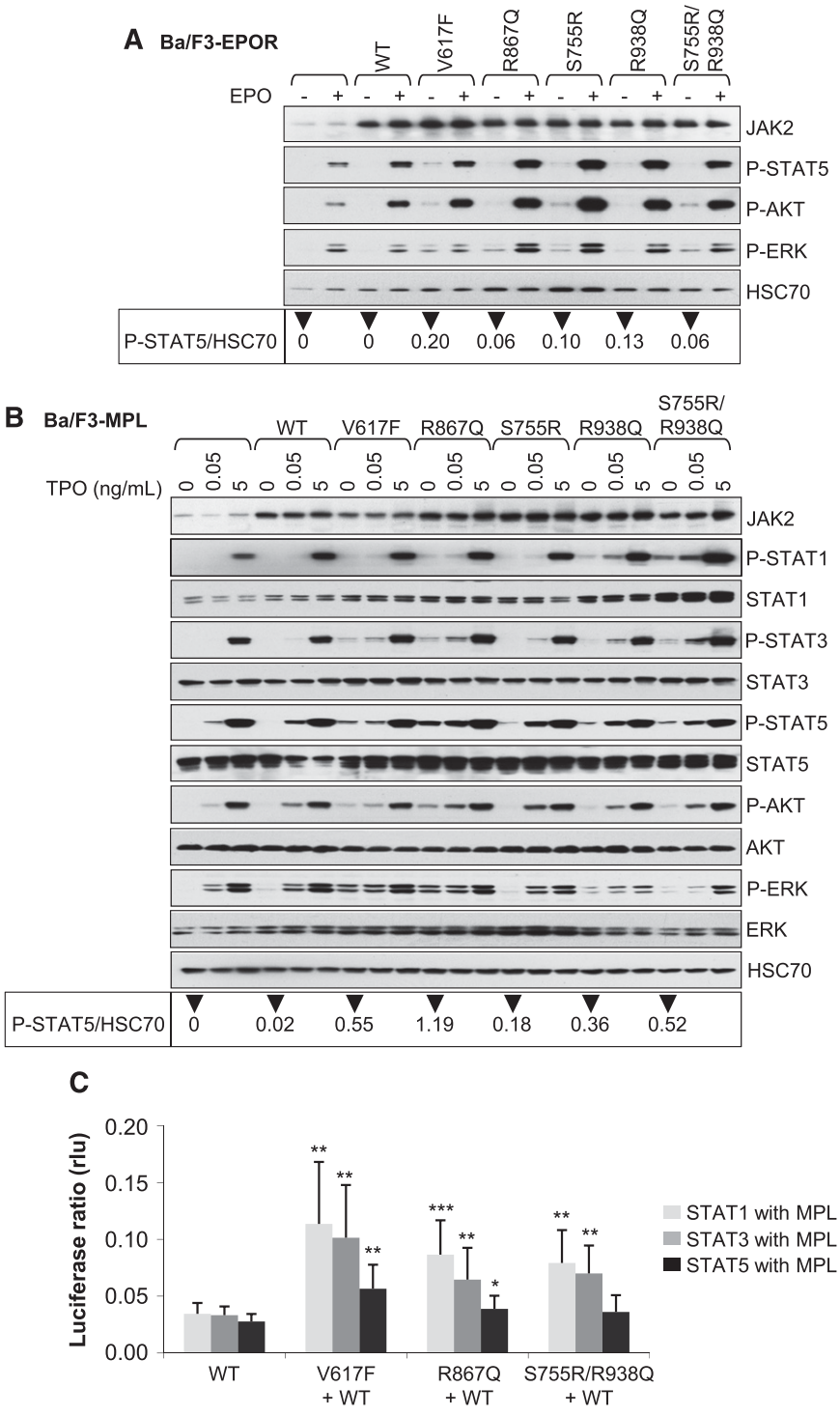

Figure 4. Signaling studies in Ba/F3-EPOR and Ba/F3-MPL cells and STAT activities in γ2A cells. (A) Ba/F3-EPOR or (B) Ba/F3-MPL cells expressing the different JAK2 constructs were serum- and cytokine-starved for 6 hours prior to a 15-minute stimulation with (A) 1 U/mL EPO and (B) 0.05 and 5 ng/mL TPO at 37°C, as indicated. Cells were lysed, and the phosphorylation status of STAT1, STAT3, STAT5, AKT, and ERK1/2 was examined by western blotting with the respective anti-phospho specific antibodies, as indicated. Expression of HSC70 in the samples was used as loading control and was consistent with expression of total AKT, ERK1/2, and the individual STAT isoforms. Blots shown were reproduced in 2 independent experiments. The quantification of the phospho-STAT5 (P-STAT5) blots for unstimulated Ba/F3-EPOR and Ba/F3-MPL were shown as P-STAT5/HSC70 ratios (arbitrary units [AU]) and displayed below the figures. (C) JAK2-deficient γ2A cells were transfected to express the various JAK2 mutants in the presence of equal amounts of JAK2 WT and MPL. STAT1-, STAT3-, or STAT5-dependent transcriptional activity was measured 24 hours after transfection by the dual firefly (pGRR5 reporter responding to STATs) and renilla (pRL-TK reporter with constitutive expression) luciferase system. Shown are averages ± SEM of 9 experiments in triplicate. Two-tailed Student *t* test: $^{*}P < .05$; $^{**}P < .01$; $^{***}P < .001$.

inhibitor (AUY922), even at high doses (Figure 5D). Accordingly, HSP90 coimmunoprecipitated to a greater extent with JAK2 mutants (R867Q, S755R/R938Q) than with JAK2 V617F and WT (Figure 5F).

Altogether, these results show that the new JAK2 mutants are less sensitive than JAK2 V617F to both JAK2 and HSP90 inhibitors.

Effects of JAK2 mutants on MPL stability and MPL cell-surface localization

To understand the properties of these JAK2 mutants, we assessed their stability. We treated the different Ba/F3-MPL cell lines with cycloheximide (CHX) and performed a western blot analysis with anti-JAK2 and anti-MPL antibodies (Figure 6A). JAK2 S755R/R938Q mutant was twofold more stable than JAK2 WT, whereas JAK2 V617F was twofold less stable than JAK2 WT. JAK2 R867Q was found to be as stable as JAK2 WT. Moreover, JAK2 S755R/R938Q significantly increased the stability of cell-surface MPL compared with the other JAK2.

We next assessed the level of cell-surface MPL in the presence of the JAK2 mutants by flow cytometry using an anti-FLAG antibody. As previously described,[25] overexpression of JAK2 WT led to

From www.bloodjournal.org by guest on June 27, 2016. For personal use only.

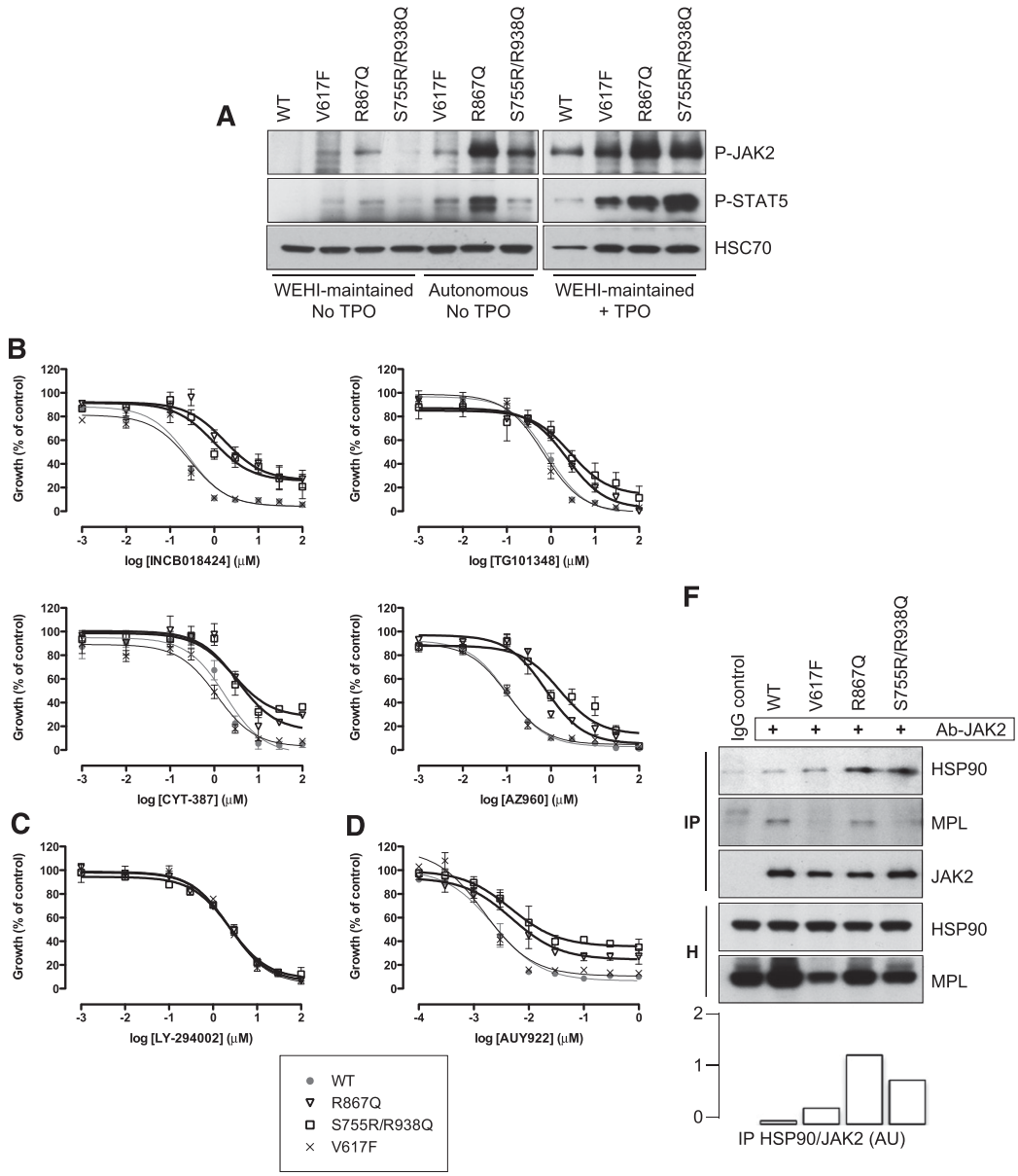

E

IC50 (μM)	INCB018424	CYT-387	TG101348	AZ960	AUY922
WT	0.2623	1.7930	0.8451	0.1032	0.002288
R867Q	1.7600	3.4100	2.3470	0.7586	0.004930
S755R/R938Q	0.9744	2.7380	2.7610	1.5710	0.004727
V617F	0.2799	1.1440	0.6858	0.1019	0.001557

Figure 5. Sensitivity of JAK2 R867Q and JAK2 S755R/R938Q mutants to JAK2 and HSP90 inhibitors. (A) Ba/F3-MPL cells expressing either JAK2 R867Q, JAK2 S755R/R938Q, or JAK2 V617F could be maintained in WEHI-supplemented medium but also exhibited cytokine-independent growth (Autonomous). Autonomous or WEHI-maintained cells were serum-starved for 6 hours and stimulated, or not (no TPO), with 5 ng/mL TPO for 15 minutes (+TPO). The constitutive phosphorylation level of each of the JAK2 constructs was analyzed by western blotting. The level of P-STAT5 was also detected, and expression of HSC70 served as a loading control. Blots are representative of a typical experiment. (B) Growth of autonomous Ba/F3-MPL cells expressing JAK2 V617F (×), R867Q (▽), and S755R/R938Q mutants (□), as well as WEHI-dependent Ba/F3-MPL expressing JAK2 WT (gray circle), was determined in response to treatment with various concentrations of INCB018424, TG101348, CYT-387, AZ960, (C) the PI3K inhibitor LY-294002, or (D) AUY922. A WST-1 proliferation assay was performed after 72 hours of exposure to the inhibitors, in the presence of 5 ng/mL TPO. Data (means ± SEM) were calculated as percentages of vehicle-treated cells and were conducted in duplicate in 4 independent experiments. Significant differences for R867Q and S755R/R938Q mutants compared with JAK2 WT were found for all inhibitors except for LY-294002 ($P < .05$ using the 2-tailed Student t test). (E) The 50% inhibitory concentration (IC50) values of cytokine-independent Ba/F3-MPL cells exposed to inhibitors for 72 hours were calculated using GraphPad PRISM software. (F) Coimmunoprecipitation (IP) was performed in Ba/F3-MPL cells using an anti-JAK2 antibody and blotted for the presence of HSP90 and MPL. Cell homogenates (H) show the amount of proteins before the IP. A quantification of both HSP90 and JAK2 in the IP fractions using ImageJ software (National Institutes of Health) was performed, and the histogram represents the HSP90/JAK2 ratios in AU. Blots shown were reproduced in 2 independent experiments.

increased MPL cell-surface expression, whereas JAK2 V617F induced its decrease. In good agreement with their stabilities, JAK2 S755R/R938Q allowed a twofold augmentation of MPL cell-surface expression, while JAK2 R867Q behaved similarly as JAK2 WT (Figure 6B-C). Thus, the half-life of the JAK2 mutants directly correlated with their ability to promote cell-surface localization of MPL.

From www.bloodjournal.org by guest on June 27, 2016. For personal use only.

In patients, JAK2 mutants specifically act on the megakaryocytic lineage

Four patients of family 1 displaying the *JAK2* S755R/R938Q mutation (P1, P3, P7, and P8) and 2 patients of family 2 with the *JAK2* R867Q mutation (P′2, P′3) were studied for hematopoietic progenitors and compared with control donors (n = 5). Clonogenic assays showed no growth of endogenous erythroid colonies or MK colonies in SCF plus IL-3 or SCF alone, respectively. There was no statistical difference compared with controls in the frequency of circulating BFU-E and CFU–granulocyte macrophage progenitors (Figure 7A-B). However, there was a slight but significant increase in CFU-MK colony frequency (Figure 7C-G) combined with larger colony size (number of MKs per colony) especially in the family with *JAK2* S755R/R938Q (Figure 7H-I).

Finally, signaling studies on platelets were performed by western blot analysis. TPO induced the phosphorylation of JAK2, STAT1, STAT3, STAT5, AKT, and ERK (Figure 7J-K). As expected from Ba/F3-MPL cell lines, we observed a weak spontaneous phosphorylation of STAT1 in *JAK2* S755R/R938Q patients (Figure 7J and supplemental Figure 3). Moreover, TPO-induced phosphorylation of STAT3 and STAT5 was reduced in the *JAK2* R867Q patients compared with the control, whereas STAT1 phosphorylation was stimulated by TPO equally well in patients and in the control (Figure 7K).

Altogether, these results show that JAK2 R867Q and JAK2 S755R/R938Q both stimulate moderately but specifically MK proliferation, which correlates with STAT1-mediated signaling.

Discussion

In this study, we identified 2 families with hereditary thrombocytosis carrying 3 so far unidentified heterozygous *JAK2* germ-line mutations in the kinase and pseudokinase domains. One family displayed a single point mutation in the JAK2 kinase domain (R867Q), and the other one 2 mutations in the same *JAK2* allele affecting the pseudokinase (S755R) and the kinase (R938Q) domains. This is the first report of inherited mutations in the kinase domain of JAK2 associated with a thrombocytosis phenotype, while *JAK2* R867Q was initially identified in a pediatric acute lymphoblastic leukemia.[29] Two novel germ-line mutations in the pseudokinase domain of JAK2 (V617I and R564Q) have recently been observed in hereditary thrombocytosis.[9,11] Thrombotic complications appear to be rare in the patients of these 2 families, suggesting that familial thrombocytosis related to these molecular variants could be underestimated.

JAK2 R867Q and *JAK2* S755R/R938Q are gain-of-function mutations with weak activities compared with JAK2 V617F and are specifically dependent on the presence of MPL in both families, as demonstrated using the Ba/F3-MPL cell line and primary cells from patients. JAK2 R867Q or JAK2 S755R/R938Q overexpression induces TPO independency and a spontaneous phosphorylation of signaling molecules such as STAT1, STAT3, STAT5, ERK, and AKT in Ba/F3-MPL cells, whereas no or little effect was found in Ba/F3-EPOR cells. Both the absence of spontaneous CFU-MK in primary cells from patients and the preferential use of MPL to induce constitutive signaling suggest that the 2 new JAK2 mutants have a significantly weaker constitutive activity than JAK2 V617F. This is reminiscent of JAK2 V617I mutant shown to be weaker than JAK2 V617F on the growth of cytokine-independent progenitors.[10,11,19] Signaling induced by JAK2 S755R/R938Q may result from the unusually long half-life of this mutant correlating with MPL cell-surface expression and stability. One major difference between MPL and EPOR is the extended stability of the mature cell-surface MPL, whereas EPOR is highly unstable.[30] We suppose that the high stability of both MPL and the new JAK2 S755R/R938Q mutant induces a weak but persistent signal that will be sufficient to promote thrombocytosis, but not erythrocytosis. On the other hand, our results suggest a different mechanism for the constitutive activation of JAK2 R867Q. Significantly increased levels of autophosphorylation of this JAK2 mutant were detected compared with the other JAK2 mutants, possibly indicating an impaired regulation by phosphatases.

Interestingly, detailed studies in γ2A cells where we examined the ability of JAK2 mutants to activate STAT1, STAT3, and STAT5 via MPL in heterozygous situations showed that they essentially activate STAT1. These results are in line with the observation that these mutations specifically activate STAT1 in platelets from patients and in Ba/F3-MPL cells. A previous study showed that the JAK2 V617F–induced high phosphorylation level of STAT1 is associated with an ET-like phenotype without change in the number of red cells.[31] In the Ba/F3-MPL cell model, overexpression of JAK2 V617F mimics the homozygous state of the mutation, characteristic of polycythemia vera, and did not induce spontaneous STAT1 phosphorylation. In contrast, the MPL-expressing γ2A cell model in which JAK2 V617F and JAK2 WT were cotransfected reproduces the heterozygous *JAK2* V617F configuration found in ET patients, and JAK2 V617F stimulated the TPO-independent phosphorylation of STAT1.

Finally, we studied the respective functions of the individual JAK2 S755R and JAK2 R938Q mutants in Ba/F3 cells. We found that JAK2 R938Q was the key activating mutation because it induced constitutive signaling and the growth of Ba/F3-MPL cells like JAK2 S755R/R938Q. In contrast, JAK2 S755R activity was comparable to JAK2 WT except at high doses of TPO. This subtle difference might be important for the double mutant to escape a senescence-like phenotype because JAK2 WT was shown to induce senescence and antiproliferative effects at high levels of TPO.[24,25] Presumably, the heterozygous expression of JAK2 R938Q in patients might not be sufficient to induce a thrombocytosis, whereas R938Q may synergize with S755R in the double JAK2 mutant. In favor of this hypothesis, we found that none of the single mutants were able to clearly increase MPL cell-surface expression in contrast to JAK2 S755R/R938Q (Figure 6B).

The R867Q and S755R/R938Q mutations conferred resistance to several JAK2 enzymatic inhibitors such as ruxolitinib, TG101348, CYT-387, and AZ960. In particular, ruxolitinib and CYT-387 failed to induce a complete inhibition of Ba/F3-MPL cell growth at high doses. It was reported that synthetic mutants of the kinase domain of JAK2 V617F, generated by random mutagenesis, were less sensitive to these inhibitors.[27,28] The resistance of JAK2 R867Q and S755R/R938Q mutants to type I ATP-competitive inhibitors of JAK2 is likely to reflect allosteric effects on the ATP-binding pocket induced by the disruption of kinase domain and pseudokinase domain salt bridges (R867-D869 and D635-K752). Furthermore, R867Q and R938Q mutations are in proximity of residues that were previously shown to generate resistant mutants (E864K and Y931C), thus indicating that the allosteric effects on the ATP-binding pocket can be induced by several mutations in those regions.[27,28,32]

Recently, some studies have focused their interest on HSP90, an essential chaperone for JAK2 stability. Inhibition of HSP90 promotes the degradation of both JAK2 WT and JAK2 V617F. Weigert et al

From www.bloodjournal.org by guest on June 27, 2016. For personal use only.

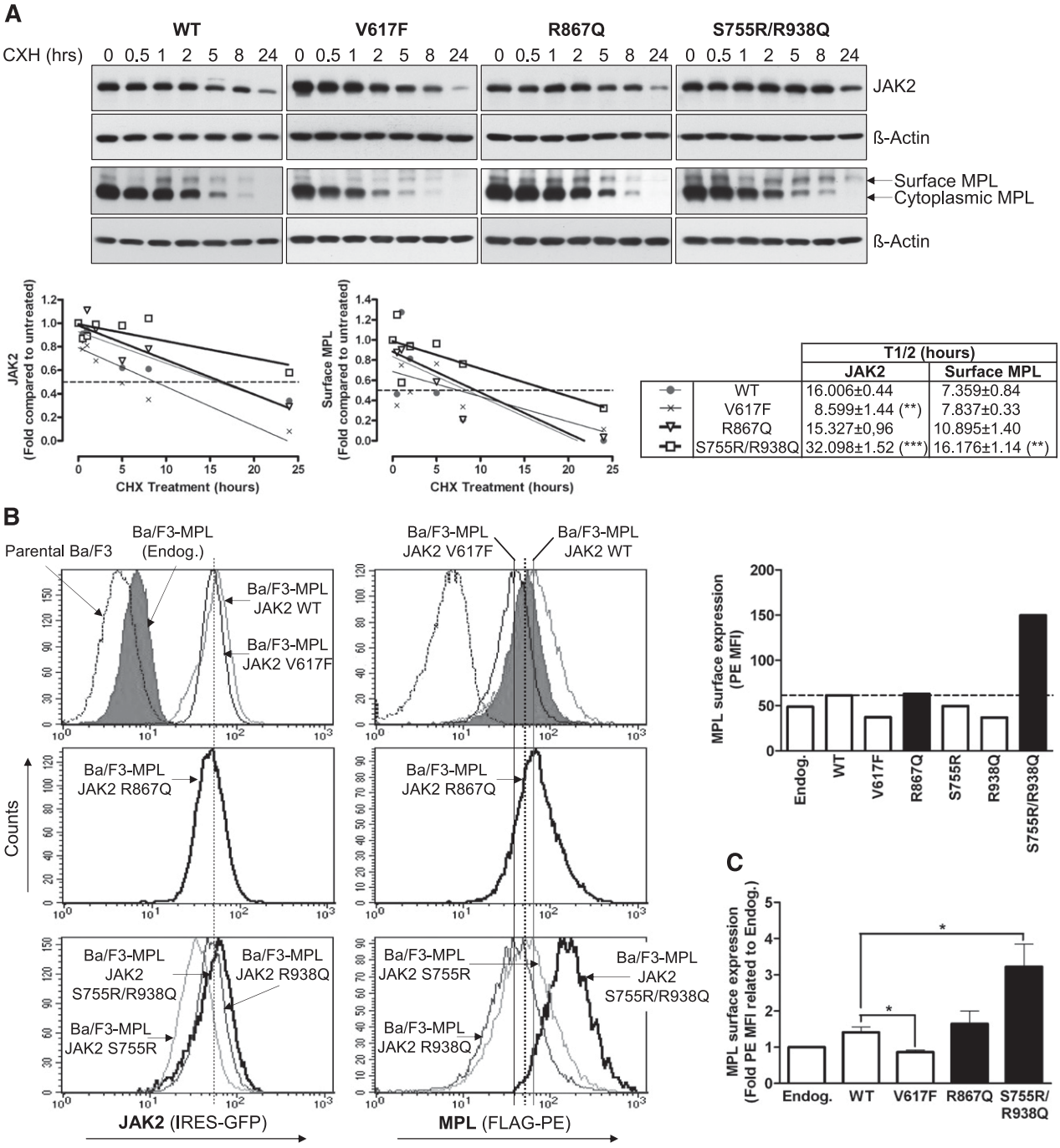

		T1/2 (hours)	
		JAK2	Surface MPL
●	WT	16.006±0.44	7.359±0.84
×	V617F	8.599±1.44 (**)	7.837±0.33
▼	R867Q	15.327±0,96	10.895±1.40
□	S755R/R938Q	32.098±1.52 (***)	16.176±1.14 (**)

Figure 6. Effect of JAK2 mutations on protein stability and chaperone function for MPL cell-surface expression. (A) Ba/F3-MPL cells expressing either JAK2 WT, V617F, R867Q, or S755R/R938Q and maintained in WEHI-supplemented medium were treated with CHX (50 μg/mL) for 0, 0.5, 1, 2, 5, 8, and 24 hours. Levels of both total JAK2 and MPL proteins were examined by western blotting, and β-actin serves as loading control. Table shows means ± SEM of the half-lives (T1/2) of JAK2 WT and mutants and mature cell-surface MPL interpolated from y = 0.5 on the curves corresponding to half of the protein remaining in CHX-treated cells compared with CHX-untreated cells (n = 3). Significance compared with JAK2 WT T1/2 or cell-surface MPL T1/2 in presence of JAK2 WT was assessed using the 2-tailed Student *t* test. **P* < .05; ***P* < .01; ****P* < .001. (B) Ba/F3 cells expressing the FLAG-tagged MPL and transduced with the bicistronic retroviral pMIGR-IRES-GFP vector encoding either JAK2 WT, V617F, R867Q, S755R/R938Q, S755R, or R938Q were sorted for equal GFP levels and maintained in IL-3–supplemented medium. GFP expression allowed monitoring of JAK2 level in the various cell lines, and MPL cell-surface expression was assessed by flow cytometry using PE fluorescence labeling of the extracellular FLAG tag. Histogram shows the mean fluorescence intensities (MFIs) of PE-labeled cell-surface MPL. (C) Histogram shows means ± SEM of PE MFI in fold related to Ba/F3-MPL cells with no overexpression of JAK2 (Endog.) (n = 3). Significance compared with the Ba/F3–MPL–JAK2 WT condition was calculated using the 2-tailed Student *t* test. **P* < .05.

reported that their synthetic mutants of JAK2, which were resistant to JAK2 inhibitors, remained sensitive to HSP90 inhibition.[28] In contrast, our data showed that JAK2 R867Q–expressing and JAK2 S755R/R938Q–expressing Ba/F3-MPL cells were also less sensitive to the HSP90 inhibitor AUY922 than cells harboring JAK2 V617F. Resistance to AUY922 is probably attributable to a more stable interaction between HSP90 and JAK2 S755R/R938Q or R867Q. JAK2 V617F was the least stable mutant and also the best target for both ATP-competitive JAK2 inhibitors and HSP90 inhibitors. These natural mutants of JAK2 that are less sensitive to the current JAK2

From www.bloodjournal.org by guest on June 27, 2016. For personal use only.

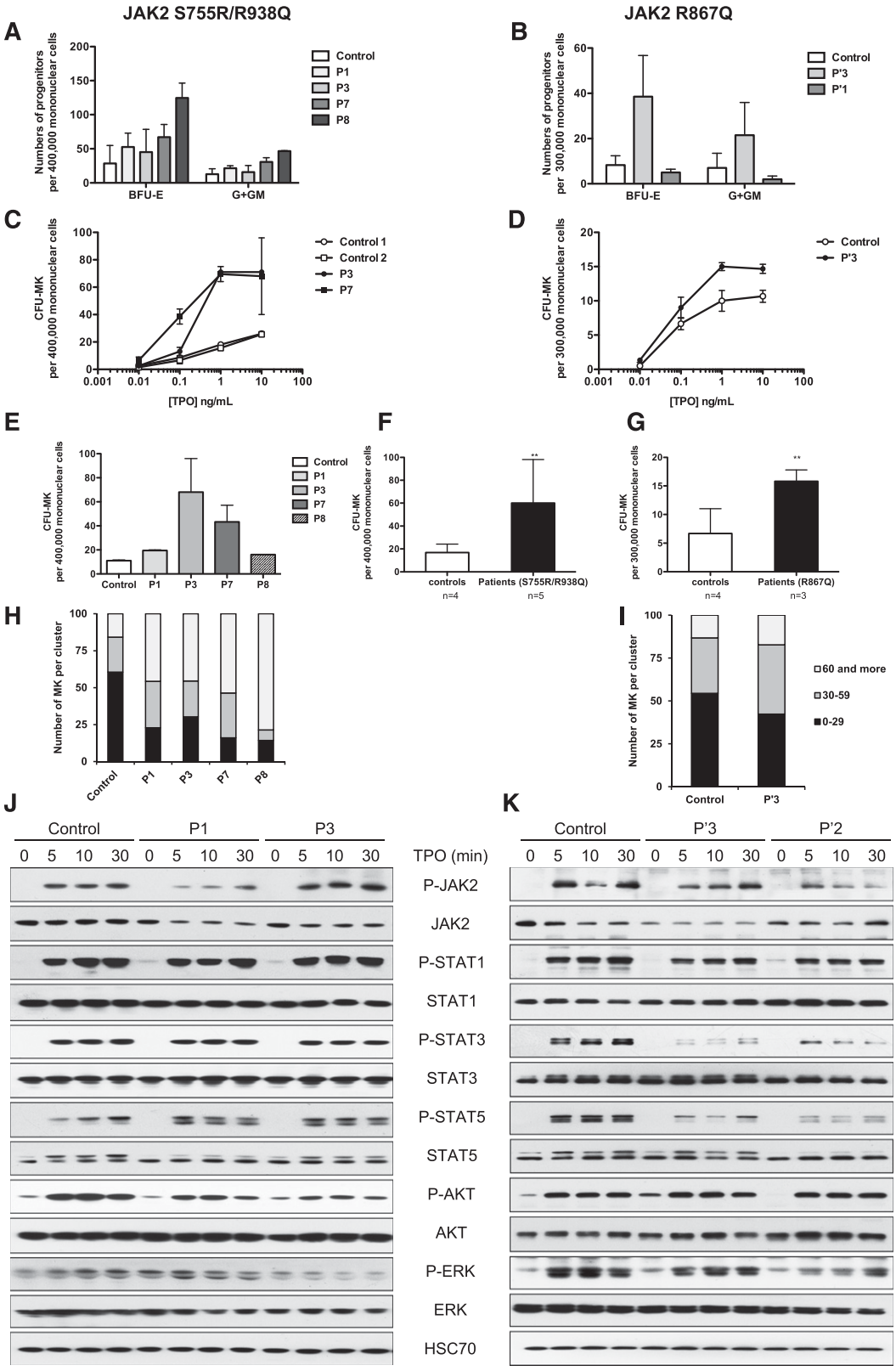

Figure 7. Assessment of myeloid progenitor amplification and signaling in platelets from JAK2-mutated patients from families 1 and 2. Mononuclear cells from R867Q (n = 2) patients, S755R/R938Q (n = 4) patients, or control donors (n = 5) were purified and plated (A-B) in methylcellulose with SCF/IL-3/EPO to study BFU-E progenitors or (C-D) in serum-free fibrin clot with SCF and increasing doses of TPO, (E) with 10 ng/mL TPO to study CFU-MK progenitors. Data represent means ± standard deviation for each patient plated in triplicate. (F-G) Histograms represent the means ± SEM of CFU-MK progenitors in the presence of SCF and TPO (10 ng/mL) for patients (n = 5 for S755R/938Q, n = 3 for R867Q) and controls (n = 4). Two-tailed Student *t* test: $^{**}P < .01$. (H-I) The numbers of MKs per cluster were counted. (J-K) Platelets were isolated from R867Q (n = 2) patients, S755R/R938Q (n = 4) patients, or control donors (n = 3); washed in phosphate-buffered saline; and stimulated or not with TPO (5 ng/mL). Platelets were lysed, and the phosphorylation status of JAK2, STAT1, STAT3, STAT5, AKT, and ERK1/2 was examined by western blotting with the respective anti-phospho specific antibodies, as indicated. Expressions of HSC70 and of total STAT proteins, AKT, and ERK in the samples were used as loading controls. Blots show representative results in 2 S755R/R938Q patients (P1, P3) (J) and 2 R867Q patients (P′2, P′3) (K).

From www.bloodjournal.org by guest on June 27, 2016. For personal use only.

and HSP90 inhibitors could be used as models to screen new small molecules that could benefit MPN patients.

Acknowledgments

We thank the physicians, Michel Blanc, Selim Corm, Valérie Ugo, and Unité de Recherche Clinique de l'est Parisien who contributed to the recruitment of patients and to the collection of biological samples. We wish to gratefully acknowledge the 2 families for participating in the study. We thank Gwendoline Leroy.

This work was supported by grants from Ligue Nationale Contre le Cancer "Equipe labellisée 2012," Association pour la Recherche sur le Cancer (projet libre), Agence Nationale de la Recherche (thrombocytose), Agence Nationale de la Recherche, programme Jeunes Chercheuses et Jeunes Chercheurs, Programme Hospitalier de Recherche Clinique (AOR07014) (S.G.), Association pour la Recherche sur la Moelle Osseuse, and Institut National de la Santé et de la Recherche Médicale. C. Marty was funded by a postdoctoral fellowship from Agence Nationale de la Recherche Blanc and supported by a Laboratory of Excellence Globule Rouge-Excellence fellowship. R.K. received funding from the Austrian Science Fund (P23257-B12) and the MPN Research Foundation. Laboratory of Excellence Globule Rouge-Excellence (I.P., W.V.) is funded by the program "Investissements d'avenir." Support to S.N.C. is acknowledged from the Fonds de la Recherche Scientifique-Fonds National de Recherche Scientifique and Fonds de la Recherche Scientifique Médicale, the Salus Sanguinis Foundation, the Association pour la Recherche sur le Cancer MEXP31C1 and Agence pour la Recherche sur le Cancer 10/15-027 program of the Université Catholique de Louvain, the Fondation contre le Cancer, the Belgium Interuniversity Attraction Poles Program, the St Luc Foundation, and the Ludwig Institute for Cancer Research. C.P. was supported by Fonds de la Recherche Scientifique-Fonds National de Recherche Scientifique, and E.L. by Industrial and Agricultural Research Fund's PhD fellowship of the FRS-FNRS Belgium.

Authorship

Contribution: I.P. and C.B.-C. designed and performed research, analyzed data, prepared figures, and wrote the paper; W.V. conducted research, analyzed data, and wrote the paper; C. Marty performed research, analyzed data, prepared figures, and wrote the paper; C.S.-M. performed research and analyzed data; A.N. conducted the study; S.N.C. conducted the study (luciferase tests, in silico modeling) and gave intellectual input; R.K. conducted the study on allele-sharing SNP genotyping analysis (SEGEX) analysis; A.S.H. performed allele-sharing SNP genotyping analysis analysis; E.L., C. Mouton, and C.P. performed experiments (luciferase tests, in silico modeling); E.S. discussed data and wrote the manuscript; R.F. did the MPL sequencing and TPO measurements; J.-F.A. was the clinician in charge of the families; J.S. performed semisolid experiments on primary cells; S.G. performed molecular biology and signaling studies; A.T. performed clonality analysis; and all authors contributed to writing and editing the manuscript.

Conflict-of-interest disclosure: The authors declare no competing financial interests.

Correspondence: Christine Bellanné-Chantelot, Hôpital Pitié-Salpétrière, 47/83 Bd de l'Hôpital, 75013 Paris, France; e-mail: christine.bellanne-chantelot@psl.aphp.fr; and Isabelle Plo, INSERM UMR1009, Institut Gustave Roussy, 114 rue Edouard Vaillant, 94805 Villejuif, France; e-mail: isabelle.plo@igr.fr.

References

1. Chang Y, Bluteau D, Debili N, Vainchenker W. From hematopoietic stem cells to platelets. *J Thromb Haemost.* 2007;5(suppl 1):318-327.
2. Skoda RC. Thrombocytosis. *Hematology Am Soc Hematol Educ Program.* 2009(1):159-167.
3. Bellanné-Chantelot C, Chaumarel I, Labopin M, et al. Genetic and clinical implications of the Val617Phe JAK2 mutation in 72 families with myeloproliferative disorders. *Blood.* 2006;108(1): 346-352.
4. Saint-Martin C, Leroy G, Delhommeau F, et al; French Group of Familial Myeloproliferative Disorders. Analysis of the ten-eleven translocation 2 (TET2) gene in familial myeloproliferative neoplasms. *Blood.* 2009;114(8):1628-1632.
5. Beer PA, Campbell PJ, Scott LM, et al. MPL mutations in myeloproliferative disorders: analysis of the PT-1 cohort. *Blood.* 2008;112(1):141-149.
6. Ding J, Komatsu H, Wakita A, et al. Familial essential thrombocythemia associated with a dominant-positive activating mutation of the c-MPL gene, which encodes for the receptor for thrombopoietin. *Blood.* 2004;103(11): 4198-4200.
7. El-Harith EA, Roesl C, Ballmaier M, et al. Familial thrombocytosis caused by the novel germ-line mutation p.Pro106Leu in the MPL gene. *Br J Haematol.* 2009;144(2):185-194.
8. Vilaine M, Gourain V, Cleyrat C, et al. Germline MPLW515R mutation in a family with isolated thrombocytosis [abstract]. *Blood.* 2012;120(21). Abstract 1764.
9. Etheridge L, Corbo LM, Kaushansky K, Chan E, Hitchcock IS. A novel activating JAK2 mutation, JAK2R564Q, causes familial essential thrombocytosis (fET) via mechanisms distinct from JAK2V617F [abstract]. *Blood.* 2011;118(21). Abstract 123.
10. Mead AJ, Chowdhury O, Pecquet C, et al. Impact of isolated germline JAK2V617I mutation on human hematopoiesis. *Blood.* 2013;121(20): 4156-4165.
11. Mead AJ, Rugless MJ, Jacobsen SE, Schuh A. Germline JAK2 mutation in a family with hereditary thrombocytosis. *N Engl J Med.* 2012; 366(10):967-969.
12. Ghilardi N, Skoda RC. A single-base deletion in the thrombopoietin (TPO) gene causes familial essential thrombocythemia through a mechanism of more efficient translation of TPO mRNA. *Blood.* 1999;94(4):1480-1482.
13. Ghilardi N, Wiestner A, Kikuchi M, Ohsaka A, Skoda RC. Hereditary thrombocythaemia in a Japanese family is caused by a novel point mutation in the thrombopoietin gene. *Br J Haematol.* 1999;107(2):310-316.
14. Kondo T, Okabe M, Sanada M, et al. Familial essential thrombocythemia associated with one-base deletion in the 5′-untranslated region of the thrombopoietin gene. *Blood.* 1998;92(4):1091-1096.
15. Wiestner A, Padosch SA, Ghilardi N, et al. Hereditary thrombocythaemia is a genetically heterogeneous disorder: exclusion of TPO and MPL in two families with hereditary thrombocythaemia. *Br J Haematol.* 2000;110(1): 104-109.
16. Tefferi A, Vardiman JW. Classification and diagnosis of myeloproliferative neoplasms: the 2008 World Health Organization criteria and point-of-care diagnostic algorithms. *Leukemia.* 2008; 22(1):14-22.
17. Debili N, Coulombel L, Croisille L, et al. Characterization of a bipotent erythro-megakaryocytic progenitor in human bone marrow. *Blood.* 1996;88(4):1284-1296.
18. Norol F, Vitrat N, Cramer E, et al. Effects of cytokines on platelet production from blood and marrow CD34+ cells. *Blood.* 1998;91(3): 830-843.
19. James C, Ugo V, Le Couédic JP, et al. A unique clonal JAK2 mutation leading to constitutive signalling causes polycythaemia vera. *Nature.* 2005;434(7037):1144-1148.
20. Lucet IS, Fantino E, Styles M, et al. The structural basis of Janus kinase 2 inhibition by a potent and specific pan-Janus kinase inhibitor. *Blood.* 2006; 107(1):176-183.
21. Bandaranayake RM, Ungureanu D, Shan Y, Shaw DE, Silvennoinen O, Hubbard SR. Crystal structures of the JAK2 pseudokinase domain and the pathogenic mutant V617F. *Nat Struct Mol Biol.* 2012;19(8):754-759.
22. Saharinen P, Vihinen M, Silvennoinen O. Autoinhibition of Jak2 tyrosine kinase is dependent on specific regions in its pseudokinase domain. *Mol Biol Cell.* 2003;14(4):1448-1459.
23. Bertelsen B, Tümer Z, Ravn K. Three new loci for determining X chromosome inactivation patterns. *J Mol Diagn.* 2011;13(5):537-540.

From www.bloodjournal.org by guest on June 27, 2016. For personal use only.

24. Besancenot R, Chaligné R, Tonetti C, et al. A senescence-like cell-cycle arrest occurs during megakaryocytic maturation: implications for physiological and pathological megakaryocytic proliferation. *PLoS Biol.* 2010;8(9):e1000476.

25. Pecquet C, Diaconu CC, Staerk J, et al. Thrombopoietin receptor down-modulation by JAK2 V617F: restoration of receptor levels by inhibitors of pathologic JAK2 signaling and of proteasomes. *Blood.* 2012;119(20):4625-4635.

26. Staerk J, Defour JP, Pecquet C, et al. Orientation-specific signalling by thrombopoietin receptor dimers. *EMBO J.* 2011;30(21):4398-4413.

27. Deshpande A, Reddy MM, Schade GO, et al. Kinase domain mutations confer resistance to novel inhibitors targeting JAK2V617F in myeloproliferative neoplasms. *Leukemia.* 2012; 26(4):708-715.

28. Weigert O, Lane AA, Bird L, et al. Genetic resistance to JAK2 enzymatic inhibitors is overcome by HSP90 inhibition. *J Exp Med.* 2012; 209(2):259-273.

29. Mullighan CG, Zhang J, Harvey RC, et al. JAK mutations in high-risk childhood acute lymphoblastic leukemia. *Proc Natl Acad Sci USA.* 2009;106(23):9414-9418.

30. Royer Y, Staerk J, Costuleanu M, Courtoy PJ, Constantinescu SN. Janus kinases affect thrombopoietin receptor cell surface localization and stability. *J Biol Chem.* 2005;280(29): 27251-27261.

31. Chen E, Beer PA, Godfrey AL, et al. Distinct clinical phenotypes associated with JAK2V617F reflect differential STAT1 signaling. *Cancer Cell.* 2010;18(5):524-535.

32. Hornakova T, Springuel L, Devreux J, et al. Oncogenic JAK1 and JAK2-activating mutations resistant to ATP-competitive inhibitors. *Haematologica.* 2011;96(6):845-853.

MYELOID NEOPLASIA

Annex 2

Whole-exome sequencing identifies novel *MPL* and *JAK2* mutations in triple-negative myeloproliferative neoplasms

Jelena D. Milosevic Feenstra,[1] Harini Nivarthi,[1] Heinz Gisslinger,[2] Emilie Leroy,[3,4] Elisa Rumi,[5] Ilyas Chachoua,[3,4] Klaudia Bagienski,[1] Blanka Kubesova,[1,6] Daniela Pietra,[5] Bettina Gisslinger,[2] Chiara Milanesi,[5] Roland Jäger,[1] Doris Chen,[1] Tiina Berg,[1] Martin Schalling,[2] Michael Schuster,[1] Christoph Bock,[1] Stefan N. Constantinescu,[3,4] Mario Cazzola,[5,7] and Robert Kralovics[1,2]

[1]CeMM Research Center for Molecular Medicine of the Austrian Academy of Sciences, Vienna, Austria; [2]Department of Internal Medicine I, Division of Hematology and Blood Coagulation, Medical University of Vienna, Vienna, Austria; [3]Ludwig Institute for Cancer Research, Brussels, Belgium; [4]de Duve Institute, Université Catholique de Louvain, Brussels, Belgium; [5]Department of Hematology Oncology, Fondazione Istituto di Ricovero e Cura a Carattere Scientifico (IRCCS) Policlinico San Matteo, Pavia, Italy; [6]Center of Molecular Biology and Gene Therapy, Department of Internal Medicine–Hematology and Oncology, University Hospital Brno and Medical Faculty Masaryk University, Brno, Czech Republic; and [7]Department of Molecular Medicine, University of Pavia, Pavia, Italy

Key Points

- Activating mutations outside exon 10 of *MPL* were identified in 10% (7 of 69) of triple-negative cases of ET and PMF.
- *JAK2*-V625F and *JAK2*-F556V were identified in 2 triple-negative cases of ET and were shown to activate JAK-STAT5 signaling.

Essential thrombocythemia (ET) and primary myelofibrosis (PMF) are chronic diseases characterized by clonal hematopoiesis and hyperproliferation of terminally differentiated myeloid cells. The disease is driven by somatic mutations in exon 9 of *CALR* or exon 10 of *MPL* or *JAK2*-V617F in >90% of the cases, whereas the remaining cases are termed "triple negative." We aimed to identify the disease-causing mutations in the triple-negative cases of ET and PMF by applying whole-exome sequencing (WES) on paired tumor and control samples from 8 patients. We found evidence of clonal hematopoiesis in 5 of 8 studied cases based on clonality analysis and presence of somatic genetic aberrations. WES identified somatic mutations in 3 of 8 cases. We did not detect any novel recurrent somatic mutations. In 3 patients with clonal hematopoiesis analyzed by WES, we identified a somatic *MPL*-S204P, a germline *MPL*-V285E mutation, and a germline *JAK2*-G571S variant. We performed Sanger sequencing of the entire coding region of *MPL* in 62, and of *JAK2* in 49 additional triple-negative cases of ET or PMF. New somatic (T119I, S204F, E230G, Y591D) and 1 germline (R321W) *MPL* mutation were detected. All of the identified *MPL* mutations were gain-of-function when analyzed in functional assays. *JAK2* variants were identified in 5 of 57 triple-negative cases analyzed by WES and Sanger sequencing combined. We could demonstrate that *JAK2*-V625F and *JAK2*-F556V are gain-of-function mutations. Our results suggest that triple-negative cases of ET and PMF do not represent a homogenous disease entity. Cases with polyclonal hematopoiesis might represent hereditary disorders. (*Blood*. 2016;127(3):325-332)

Introduction

Essential thrombocythemia (ET), primary myelofibrosis (PMF), and polycythemia vera (PV) are the classical *BCR-ABL*–negative myeloproliferative neoplasms (MPNs). They are chronic diseases, characterized by clonal expansion of differentiated myeloid cells driven by somatic mutations. Most of the cases are sporadic, however, familial clustering has also been observed. In 95% of PV cases and 50% to 60% of ET and PMF cases the disease is driven by an acquired mutation in the *JAK2* gene V617F.[1-4] *JAK2*-V617F leads to the constitutive activation of the Janus kinase 2 (JAK2) and subsequently the JAK-signal transducer and activator of transcription (STAT) signaling pathway. The remaining cases of PV carry mutations in exon 12 of *JAK2*. Although *JAK2* mutations in MPNs are acquired, in recent years several families with hereditary thrombocytosis (HT) have been described to have germline *JAK2* mutations.[5-7] The second most commonly mutated gene in ET and PMF is *CALR* encoding calreticulin. Mutations in exon 9 of *CALR* have been described in 25% and 35% of patients with ET and PMF, respectively.[8,9] There are over 40 different *CALR* mutation types reported in the literature and they all result in a frameshift into alternative reading frame 1 of the last exon of the *CALR* gene and hence the acquisition of a novel peptide at the C terminus of the mutant protein.[8,9] The functional consequence of *CALR* mutations is not yet well understood, but the available data suggest that similar to *JAK2* mutations, *CALR* mutations also lead to the activation of the JAK-STAT signaling pathway.[8] Besides *JAK2* and *CALR*, a small proportion (5%-10%) of ET and PMF patients carry somatic mutations in exon 10 of *MPL*, encoding the thrombopoietin receptor (MPL).[10,11] The most common mutation is W515L, however, W515K, W515A, W515S, and others have been reported.[11,12] The mutations cluster in the intracellular

Submitted July 31, 2015; accepted September 13, 2015. Prepublished online as *Blood* First Edition paper, September 30, 2015; DOI 10.1182/blood-2015-07-661835.

The data reported in this article have been deposited in the ArrayExpress database (accession number E-MTAB-3778).

The online version of this article contains a data supplement.

There is an Inside *Blood* Commentary on this article in this issue.

The publication costs of this article were defrayed in part by page charge payment. Therefore, and solely to indicate this fact, this article is hereby marked "advertisement" in accordance with 18 USC section 1734.

© 2016 by The American Society of Hematology

From www.bloodjournal.org by guest on June 3, 2016. For personal use only.

juxtamembrane domain of the receptor, which prevents its activation in the absence of the ligand.[13] Germline mutations in *MPL* have been associated with cases of HT. *MPL*-S505N in exon 10 was found in 1 family, although it was also reported as somatic in sporadic cases of ET.[12,14] Mutations in *JAK2*, *CALR*, and *MPL* are usually mutually exclusive and account for >90% of ET and PMF cases.[8] However, in 12% of ET and 5% of PMF cases the disease driver is currently unknown and this group of patients is referred to as the triple negative. In clinical practice, the diagnostic workup of these patients is limited to analyzing exon 14 of *JAK2*, exon 10 of *MPL*, and exon 9 of *CALR* for the presence of mutations. Mutations in other genes such as *TET2*, *ASXL1*, and *CBL* have been described in all MPN patients, however, they co-occur with *JAK2*, *MPL*, and *CALR* mutations and are found across a variety of myeloid malignancies.[15-18] Most of these mutations were shown to be involved in establishing clonal hematopoiesis or disease progression.

In this study, we aimed to identify the disease-causing mutation in triple-negative cases of ET and PMF by applying whole-exome sequencing (WES) primarily for the purpose of identifying somatic mutations. In cases where somatic mutations could not be identified, we looked for germline mutations that might be relevant for the phenotype. Finally, we aimed to assess the functional consequence of identified mutations.

Methods

Patient samples

The study included 79 patients diagnosed with ET (N = 67) or PMF (N = 12), followed at the Department of Hematology Oncology, Fondazione Istituto di Ricovero e Cura a Carattere Scientifico (IRCCS) Policlinico San Matteo (Pavia, Italy) and the Medical University of Vienna (Vienna, Austria). All patients provided written informed consent in accordance with the Declaration of Helsinki and the study was approved by local ethics committees. Diagnostic criteria were applied as previously reported and later revised.[3,19,20] Genomic DNA was isolated according to standard procedures from peripheral blood granulocytes, whole-blood samples, and immunomagnetically purified circulating T cells. *JAK2*, *MPL*, and *CALR* mutation analyses were performed as previously described, and presence of these mutations was excluded in all patients included in the study.[8]

Microarray analysis

DNA samples were processed according to the manufacturer's instructions and hybridized to Genome-Wide Human SNP 6.0 arrays (Affymetrix). The data were analyzed using Genotyping Console version 3.0.2 software (Affymetrix), by applying previously reported criteria for annotation.[21]

WES and Sanger sequencing

DNA libraries were generated from genomic DNA isolated from granulocytes and $CD3^+$ T lymphocytes using the TruSeq DNA Sample Prep kit (version 2; Illumina) with the TruSeq Exome Enrichment kit (Illumina) and the Nextera Rapid Capture Exome kit (Illumina) according to the manufacturer's instructions. Sequencing was performed using the Illumina HiSeq 2000 platform, the 51-bp or 100-bp paired-end configuration, and Illumina version 3 reagents. Data analysis is described in supplemental Methods (see supplemental Data available at the *Blood* Web site).

Sanger sequencing was performed as described previously.[8] Details and primer sequences are listed in supplemental Methods.

X-inactivation–based clonality assay

Clonal analysis of hematopoietic cells was performed through the study of methylation pattern and allelic expression of *HUMARA*, *PGK*, and *IDS* genes on peripheral blood granulocytes, whereas T lymphocytes were used as a control tissue, as previously described.[22]

Functional analysis of identified mutations

Methods used for generation of DNA constructs, virus production and transduction, cell proliferation and viability assays performed in Ba/F3 cells, and western blotting are described in supplemental Methods. Details of the luciferase assay performed in γ2A cells are also described in supplemental Methods.

Results

WES identifies novel mutations in triple-negative PMF and ET

To identify disease-driving mutations in triple-negative MPN, we selected 4 cases of ET and 4 cases of PMF in which mutations in *MPL* exon 10, *CALR* exon 9, and *JAK2*-V617F were excluded, as previously reported.[8] WES was performed, in all 8 cases, on the DNA samples from granulocytes and T cells, which were considered as the tumor and the control tissue, respectively. The median number of 104 713 153 unique reads per sample was obtained, which resulted in median coverage of 110× across all target regions. The variants identified in the tumor tissue were annotated for functional consequence and several filtering criteria were applied, including subtraction of variants present in the control tissue, in order to detect potential somatic mutations (supplemental Methods). Candidate somatic mutations were validated using Sanger sequencing on samples from both tissues, to exclude false positive and insufficiently covered germline variants. Using this approach, we identified somatic mutations in 3 of 8 patients. Two patients diagnosed with PMF carried 10 somatic mutations each, whereas 2 somatic mutations were found in 1 patient with ET (Figure 1A). In both PMF patients, we identified mutations in genes known to be relevant for myeloid malignancies, *CBL*, *TET2*, *ASXL1*, *SRSF2*, including a somatic mutation affecting the thrombopoietin receptor *MPL*-S204P. We did not detect any recurrent novel somatic mutations in the 8 studied patients.

As in 5 of 8 patients we did not detect a single somatic mutation by WES; we analyzed the WES data for the presence of germline mutations in genes involved in MPN pathogenesis by applying the same filtering criteria as described for analysis of somatic mutations, except for the subtraction of variants present in the control tissue (supplemental Methods). In 1 PMF patient, we identified a germline mutation in *MPL*-V285E and validated it by Sanger sequencing. In the ET patient with 2 identified somatic mutations, we detected and validated a germline variant in *JAK2*-G571S (Figure 1A). The germline mutations in *MPL* and *JAK2* were not annotated as common variants in any of the databases we used for the analysis of the WES data.

Granulocyte DNA samples of the 8 selected patients were, in addition to WES, analyzed for acquired chromosomal copy number alterations and uniparental disomies (UPDs) using genome-wide single-nucleotide polymorphism microarrays. Due to DNA quality, the data were obtained for 7 of 8 cases. We identified a somatic UPD of chromosome 6p in 1 patient with PMF (supplemental Figure 1) and a gain on chromosome 4q in a patient with ET. The patient with 6p UPD carried a germline *MPL*-V285E mutation and no detectable somatic mutations, whereas the ET patient with 4q gain carried the 2 validated somatic mutations in *ITGAV* and *WBSCR28* (Figure 1A).

Chromosomal aberrations often target genomic regions that carry the genes relevant for the disease. We integrated the microarray data from an additional 20 triple-negative MPN patients, with the microarray and WES data from the 8 patients described previously; however, we

From www.bloodjournal.org by guest on June 3, 2016. For personal use only.

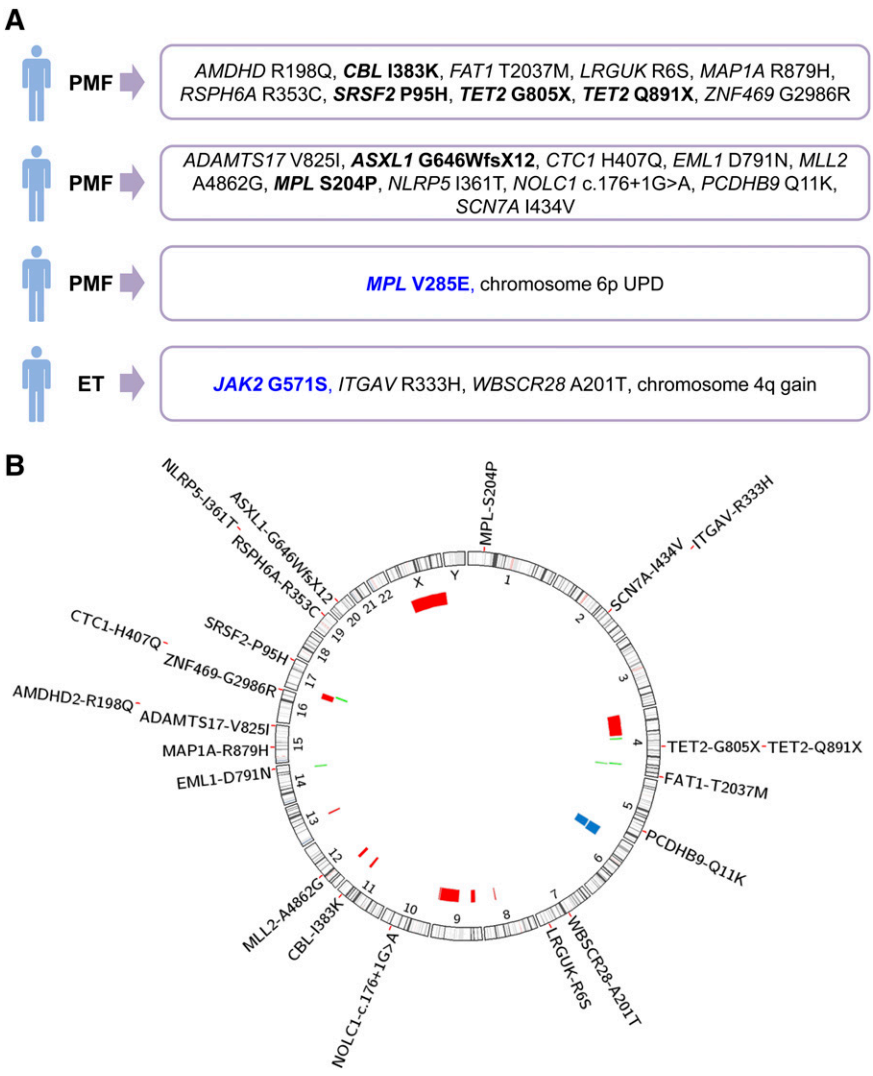

Figure 1. Overview of genetic aberrations identified in 28 patients with triple-negative ET or PMF. (A) Genetic findings from 4 of 8 studied patients, in which somatic genetic aberrations were identified using WES or microarray analysis. Somatic mutations are marked in black and germline mutations in blue. (B) Genomic overview of somatic mutations identified in 8 patients analyzed by WES and chromosomal aberrations found in 27 patients, detected with Affymetrix Genome-Wide Human SNP 6.0 microarrays. The position and size of the colored bars indicate the chromosomal aberrations. Red bars depict deletions, blue bars depict UPDs, and green bars depict gains.

did not identify any somatic mutations in the regions affected with chromosomal aberrations (Figure 1B). Chromosomal aberrations were detected in 7 of 27 cases, suggesting that the disease is clonal in at least 25.9% of the cases. UPD of chromosome 6p was observed in 2 cases, however, the target gene remains unknown.

As 3 of 8 patients studied by WES and microarrays were female, we performed X-inactivation–based clonality analysis. Clonal hematopoiesis was observed in 1 PMF case and polyclonal pattern in 1 ET case, whereas in the second case of ET the patient was not informative at the analyzed loci. Taking the results of WES, microarray analysis, and clonality assay in consideration, we have found evidence of clonal hematopoiesis in 5 of 8 triple-negative MPN patients (4 of 4 with PMF and 1 of 4 with ET) included in the study, suggesting that the disease might be polyclonal in the other 3 cases. Two triple-negative MPN patients carried mutations affecting the extracellular domain of the thrombopoietin receptor, in contrast to the previously reported mutations, which cluster in the juxtamembrane domain encoded by exon 10 of the *MPL* gene.

Targeted sequencing of all coding exons of *MPL* and *JAK2* genes

To determine the frequency of the *MPL* mutations outside of exon 10, in triple-negative MPN patients, we performed Sanger sequencing of all coding exons of *MPL* on samples from 61 triple-negative MPN cases (53 patients with ET and 8 patients with PMF), in addition to the 8 cases who were subject to WES. Variants outside exon 10 of *MPL* were identified in 5 of 61 cases. The control tissue was available for 4 patients and we could determine the origin of identified mutations. *MPL*-T119I, *MPL*-S204F, and *MPL*-E230G were somatic mutations (Figure 2A), whereas *MPL*-R321W was germline (Figure 2B). We identified a second triple-negative case with the *MPL*-S204P mutation and diagnosis of ET, however, the control tissue was not available. The same mutation was confirmed to be somatic in the PMF case subjected to WES (Figure 2A). We also detected a variant R321Q in 1 case of triple-negative ET, however, this variant was reported with a variant frequency of 3% in an East Asian population in the 1000 Genomes Project, and therefore was not considered further for functional analysis.

Mutations outside exon 10 of *MPL* were identified in 7 of 69 cases of triple-negative MPNs analyzed by WES (N = 8) and Sanger sequencing (N = 61) (Figure 2A-B, supplemental Table 3). All mutations affect the extracellular domain of the thrombopoietin receptor (Figure 2D).

In addition to these 69 cases, we performed targeted sequencing of all coding exons of *MPL* in a case of ET, which was initially diagnosed as *JAK2* and *MPL*-negative, but developed a *JAK2*-V617F positivity 5.5 years following the diagnosis. We tested the diagnostic sample for *CALR* mutations, however, it was negative. When we sequenced the entire coding region of *MPL*, we identified a somatic *MPL*-Y591D mutation in the

From www.bloodjournal.org by guest on June 3, 2016. For personal use only.

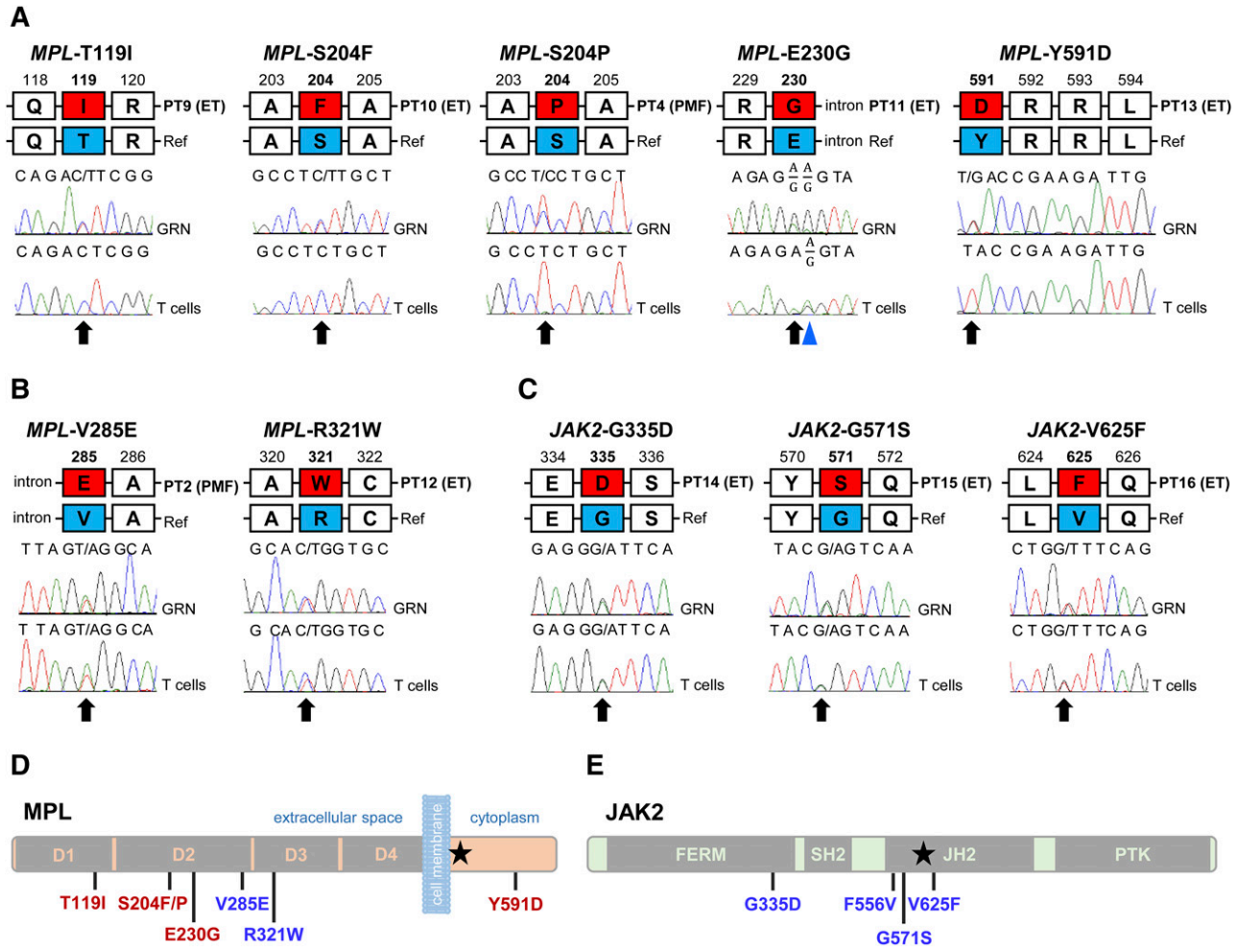

Figure 2. Mutations outside exon 10 of *MPL* and exons 12 and 14 of *JAK2* identified in triple-negative ET and PMF. (A) Somatic mutations in *MPL* identified in 4 cases of ET and 1 case of PMF. A common polymorphism is marked with the blue triangle. (B) Germline mutations in *MPL* identified in single cases of ET and PMF. (C) Germline *JAK2* mutations found in 3 cases of triple-negative ET. Red boxes in panels A-C represent the amino acid change; black arrows indicate mutated bases. GRN, granulocyte; PT, patient; Ref, reference. (D) Schematic representation of the thrombopoietin receptor and the positions of mutations identified in triple-negative ET and PMF. Somatic mutations are indicated in red. (E) Schematic representation of the JAK2 kinase and the mutations found in ET. Black stars (★) in panels D and E indicate positions of MPL-W515K and JAK2-V617F, respectively.

diagnostic sample (Figure 2A), which remained throughout the 5.5 years follow-up. Because the clinical data indicate that the *MPL*-Y591D mutation was sufficient to cause the phenotype at diagnosis, we included this mutation for the functional validations.

As WES revealed a germline *JAK2*-G571S mutation in 1 of 8 triple-negative MPN patients, we performed Sanger sequencing for all coding exons of *JAK2* on DNA samples from additional 49 triple-negative MPN patients (41 patients with ET and 8 with PMF) which were also analyzed for mutations in *MPL* (supplemental Table 3). We identified variants in *JAK2* in 4 of 49 analyzed cases. All patients with *JAK2* variants were diagnosed with ET. *JAK2*-G335D and *JAK2*-V625F were confirmed as germline mutations, whereas the control tissue was not available from patients with *JAK2*-F556V and a second case of *JAK2*-G571S (Figure 2C,E). Mutations affecting exons 8, 13, and 15 of the *JAK2* gene were identified in a total of 5 of 57 triple-negative MPN cases.

Clonality analysis was performed for 23 of 39 female patients included for targeted sequencing of both *MPL* and *JAK2*. Clonal hematopoiesis was revealed in 3 cases, whereas 10 cases were polyclonal and 10 cases were either noninformative or showed an ambiguous result of the analysis. In regard to patients with germline mutations, the patient carrying *JAK2*-V625F was not informative, whereas the patient with *MPL*-R321W had clonal hematopoiesis. Other patients with germline mutations (*JAK2*-G335D, *JAK2*-G571S, and *MPL*-V285E) were male. All the patients with germline *MPL* and *JAK2* mutations where considered as sporadic as the family history was either negative for the presence of MPN phenotype in family members or unavailable. Overview of molecular data and results of clonality analyses performed for all the patients included in the study, is listed in supplemental Table 3.

Functional analysis of identified *MPL* and *JAK2* mutations

We next performed functional assays to determine whether the identified MPL mutants were able to induce ligand-independent JAK-STAT signaling, similar to other pathogenic mutants such as S505N and W515.[23] We used a luciferase reporter assay in JAK2-deficient γ2A cells where we transiently expressed the complementary DNAs for wild-type or mutant MPL, JAK2, STAT5, the STAT5 reporter Spi-Luc, and pRL-TK for transfection control.[23] As shown in Figure 3A, expression of MPL mutants supported cytokine-independent JAK2-STAT5 signaling. Of interest, detection of activity required longer times (48 hours) than for the usual pathogenic mutants W515K or S505N, which exhibit constitutive activity at 24 hours posttransfection.[23] These data suggest that the identified mutations have a milder effect compared with the common W515K mutant.

From www.bloodjournal.org by guest on June 3, 2016. For personal use only.

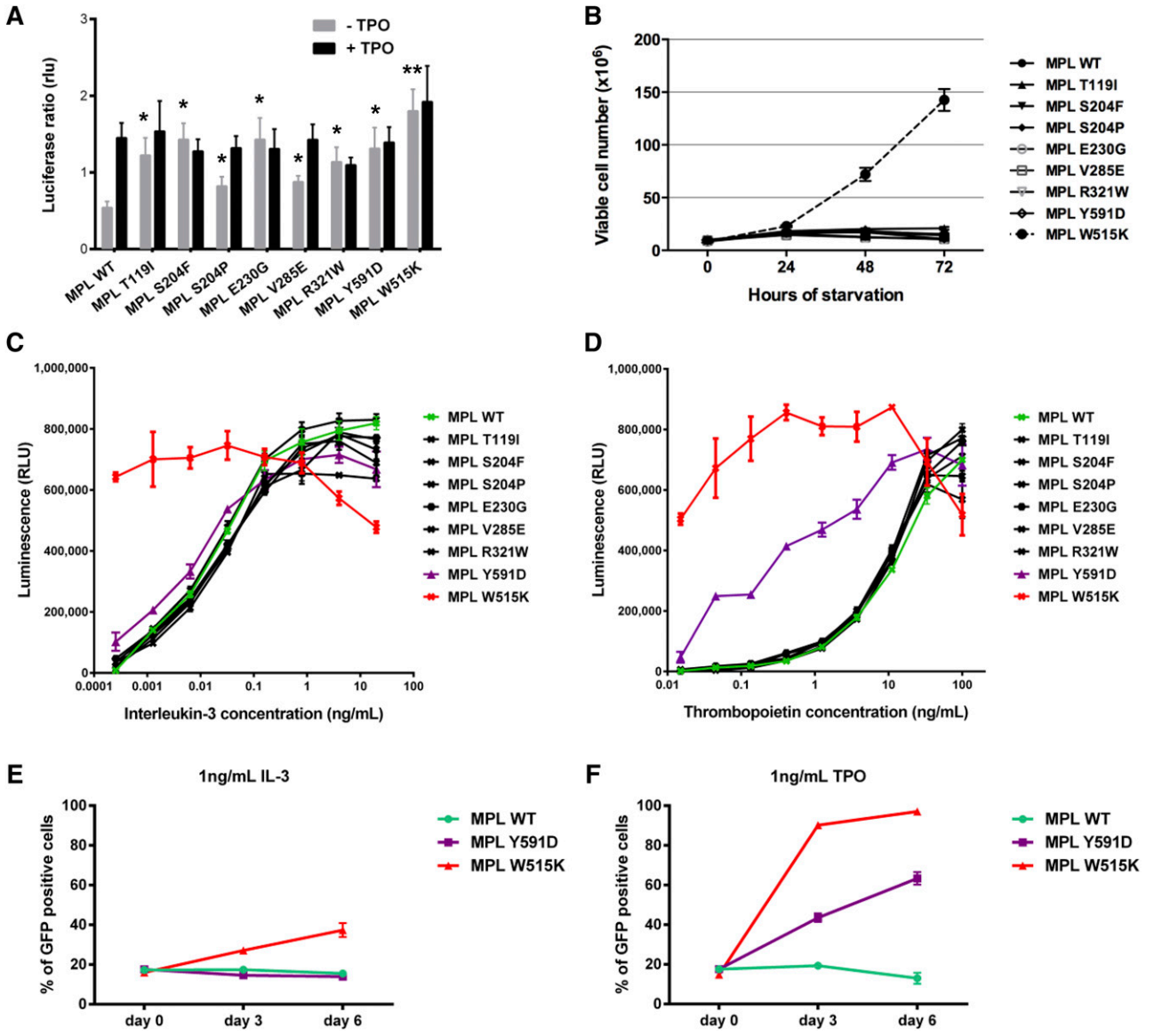

Figure 3. Functional analysis of MPL mutants. (A) STAT-dependent transcriptional activity induced by wild-type MPL or mutants of MPL. γ2A cells which are JAK2-deficient were transiently transfected with wild-type MPL (or mutants), JAK2, STAT5, and with Firefly STAT5 luciferase reporter spi-Luc and pRL-TK vector coding for Renilla luciferase. Luminescence was measured 48 hours after transfection. After transfection, medium was changed after 5 hours and replaced either with culture medium or medium supplemented with TPO (10 ng/mL). Shown are average units + SEM of 1 representative experiment performed in triplicate out of 3. $^{**}P < .001$; $^{*}P < .05$. (B) Number of viable Ba/F3 cells expressing wild-type MPL or different MPL mutants, in the absence of IL-3, was measured every 24 hours for 72 hours. The data are shown as the average of 2 biological replicates performed each in triplicate ± SEM. (C-D) The viability of Ba/F3 cells expressing wild-type MPL or different mutants was assessed after 72 hours in the presence of increasing concentrations of IL-3 (C) and TPO (D). Error bars represent SEM. (E-F) Ba/F3 cells expressing wild-type MPL (MPL wt-puro) but not GFP were mixed with Ba/F3 cells expressing either wild-type MPL (MPL wt-GFP), MPL Y591D (MPL Y591D-GFP), or MPL W515K (MPL W515K-GFP) and GFP in a 4:1 ratio and cultured in the presence of 1 ng/mL IL-3 (E) or 1 ng/mL TPO (F). The GFP positivity of the mixed culture was assessed every 72 hours by flow cytometric analysis. The experiment was performed in triplicate, with error bars representing SEM. SEM, standard error of the mean.

To further study the functional consequence of MPL mutations, we expressed the MPL wild-type or mutants in the interleukin-3 (IL-3)-dependent murine cell line Ba/F3. To test how the expression of MPL mutants affects proliferation of Ba/F3 cells, we performed a starvation assay for 72 hours (Figure 3B). None of the mutants conferred cytokine-independent growth of Ba/F3 cells or hypersensitivity to IL-3, except for the W515K which was used as a positive control (Figure 3B-C; supplemental Figure 2A). Because most of the mutations clustered in the extracellular domain of the thrombopoietin receptor, we tested the cell viability in the dilution series of thrombopoietin (TPO) to determine whether the mutations confer hypersensitivity to TPO (Figure 3D; supplemental Figure 2B). We did not observe a difference between the cells expressing the mutants affecting the extracellular domain of MPL compared with the wild type. However, Ba/F3 cells expressing MPL-Y591D showed marked hypersensitivity to TPO. To confirm that the MPL-Y591D mutation gives proliferative advantage to the Ba/F3 cells, we performed a competition assay in which the cells expressing MPL wild type (pMSCV-HA-MPLwt-puro) were mixed in 4:1 ratio with cells expressing MPL-Y591D and green fluorescent protein (GFP) (pMx-IRES-HA-MPLY591D-GFP). We assessed the GFP positivity by flow cytometry analysis at days 0, 3, and 6. In 2 independent biological replicates we could show that the GFP positivity of mixed culture reaches 60% in the presence of 1 ng/mL TPO in 6 days, meaning that expression of MPL-Y591D confers

From www.bloodjournal.org by guest on June 3, 2016. For personal use only.

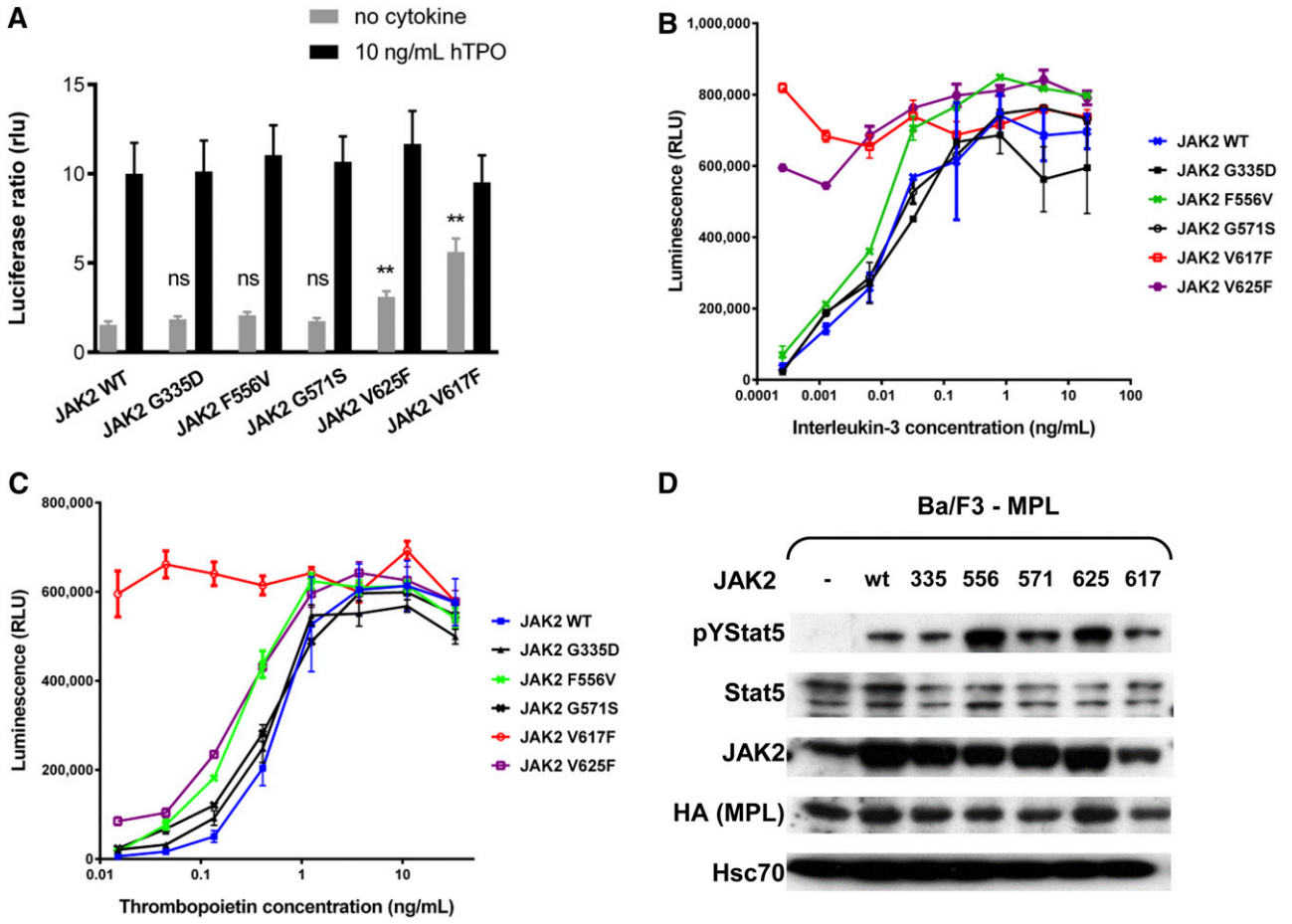

Figure 4. Functional analysis of JAK2 mutants. (A) STAT-dependent transcriptional activity induced by wild-type JAK2 or mutants of JAK2. γ2A cells which are JAK2-deficient were transiently transfected with wild-type JAK2 (or wild-type JAK2 and mutant JAK2 at a 1:1 ratio to represent heterozygous condition), MPL, STAT5, and with Firefly STAT5 luciferase reporter spi-Luc and pRL-TK vector coding for Renilla luciferase. Luminescence was measured 24 hours after transfection. After transfection, medium was changed after 5 hours and replaced either with culture medium or medium supplemented with TPO (10 ng/mL). Shown are means ± SEM of 3 independent experiments done in triplicate. $^{**}P < .001$; $^{*}P < .05$. (B-C) The viability of Ba/F3 cells expressing wild-type MPL together with wild-type JAK2 or different mutants was assessed after 72 hours in the presence of increasing concentrations of IL-3 (B) and TPO (C). Error bars represent SEM. (D) The activation of STAT5 in starving condition. Ba/F3 cells expressing the wild-type MPL only, or together with wild-type JAK2 or JAK2 mutants were cultured for 48 hours on TPO (1 ng/mL) and then starved for 4 hours in serum-free medium without TPO. Western blot was performed on the cell lysates with antibodies against pYSTAT5, STAT5, hemagglutinin-tag (HA), and JAK2. An antibody against Hsc70 was used as loading control.

proliferative advantage in vitro (Figure 3F; supplemental Figure 2D). The effect on proliferation was lower than the one observed for MPL-W515K, and also absent when the cells were cultured in the presence of IL-3 (Figure 3E; supplemental Figure 2C).

The functional data suggest that all identified MPL mutations are gain-of-function mutations, leading to the activation of JAK2-STAT5 signaling. MPL-Y591D is the only mutation which gives an obvious but mild proliferative advantage to the cells in vitro.

We used the luciferase reporter assay in JAK2-deficient γ2A cells to assess the ligand-independent JAK-STAT5 signaling activation of identified JAK2 mutants in the presence of MPL (Figure 4A) and erythropoietin receptor (supplemental Figure 3A).[23] Only the expression of JAK2-V625F supported cytokine-independent JAK2-STAT5 signaling in the presence of MPL, whereas no difference was observed for other mutants compared with the wild type. Upon expressing all of the JAK2 mutants or the wild type in Ba/F3-MPL cells, we tested the cell viability in the serial dilution of IL-3 and TPO concentrations. The cells expressing JAK2-V625F showed hypersensitivity to both IL-3 and TPO (Figure 4B-C; supplemental Figure 3B-C), whereas for JAK2-F556V–expressing cells we could also observe hypersensitivity to TPO. In addition, we examined the phosphorylation of STAT5 in the absence of cytokine in the transfected cell lines. We detected increased phosphorylation of STAT5 in the absence of cytokines in the cells expressing JAK2-V625F and JAK2-F556V (Figure 4D). Thus, increased activation of JAK-STAT signaling is likely responsible for the hypersensitivity to TPO observed for the 2 mutants.

Discussion

We identified somatic and germline mutations outside exon 10 of *MPL* in 10.1% of cases (7 of 69) of triple-negative ET and PMF. Somatic mutations of MPL at positions T119I, S204F, S204P, and E230G were detected in exons 3, 4, and 5, respectively, whereas germline mutations V285E and R321W were affecting exon 6 of *MPL*. In 1 additional triple-negative case of ET, we identified a somatic mutation in exon 12 of *MPL*, *MPL*-Y591D, at diagnosis, however, the patient became *JAK2*-V617F positive in a 5.5-year follow-up. Germline mutations of the JAK2 at positions G335D, G571S, and V625F, and mutation of unknown origin F556V in exons 8, 13, and 15 of *JAK2* were found in 8.8% (5 of 57) cases

From www.bloodjournal.org by guest on June 3, 2016. For personal use only.

of triple-negative ET and PMF. All mutations were heterozygous. Taken together, noncanonical mutations (outside of exons usually examined for diagnostic purposes) of *MPL* and *JAK2* are present in about 18.9% of triple-negative MPN cases. We could demonstrate that all identified MPL mutations lead to constitutive activation of JAK-STAT5 signaling, and that MPL-Y591D provides proliferative advantage to Ba/F3 cells. We could demonstrate that *JAK2*-V625F is a gain-of-function mutation, whereas for F556V we found evidence of constitutive activation of JAK-STAT5 signaling by Western immunodetection. However, the other JAK2 mutants do not significantly influence the JAK-STAT5 signaling in the presence of erythropoietin receptor or MPL in vitro.

Mutations outside exon 10 of *MPL* have previously been reported in the literature, but their origin was not determined, mainly due to lack of control tissue availability. *MPL*-S204F mutation associated with chromosome 1p UPD and heterozygous *MPL*-S204P mutation have previously been identified in 2 *JAK2*-V617F–negative PMF cases,[24,25] whereas *MPL*-Y591D was reported in a *JAK2*-V617F–positive PV patient with chromosome 1p UPD.[24] In all 3 cases, the control tissue was not available, and the functional relevance of the mutations was not shown. We could demonstrate that somatic *MPL*-Y591D mutation was present at diagnosis in a triple-negative ET patient who, during follow-up, acquired *JAK2*-V617F. Hitchcock et al have shown that MPL-Y591 is a part of the YRRL motif (Figure 2A), which, through interaction with AP2, regulates surface expression and degradation of MPL upon stimulation.[26] In the same study, the authors showed that cells expressing MPL-Y591F have a proliferation advantage and an increased JAK2, STAT5, and AKT activation upon stimulation.[26] It is unclear why *MPL*-Y591D is found together with *JAK2*-V617F. Further studies will be necessary to determine whether combination of these mutations has a specific effect on the patient's phenotype.

Germline *MPL* mutations have been reported in cases of HT. Clinical features of ET and HT are similar and that is why some of the HT cases could be diagnosed as sporadic ET, especially if the family history is unknown or absent. The differences in the biology of the 2 diseases are mainly that HT exhibit polyclonal hematopoiesis, lack somatic mutations, and have generally better prognosis without disease progression.[27] The first germline *MPL* mutation associated with HT was S505N in exon 10, which was also reported as somatic in sporadic ET.[12,14] *MPL*-Y252H mutation was reported in a pediatric case of ET with clonal hematopoiesis without evidence of the mutation origin,[28] whereas P106L was reported as homozygous in several Arabic families with HT.[29] In our cohort, 2 activating germline mutations were identified in cases initially diagnosed as PMF (V285E) and ET (R321W). We cannot exclude the possibility that these mutations could have been acquired in common progenitors, as the only available germline control was DNA isolated from T cells. Both patients had clonal hematopoiesis, as detected by presence of acquired UPD of chromosome 6 in a patient with PMF (supplemental Figure 1) and the X-inactivation–based clonality assay in the patient with ET. We can only speculate that *MPL*-V285E and *MPL*-R321W are either not sufficient to cause the observed phenotypes and that an additional event is necessary, likely the target of 6p aberration in the case with PMF, as we did not detect any other somatic mutations in this patient, or that the 6p aberration and presence of clonal hematopoiesis are associated with disease progression.

The 4 somatic mutations we identified were affecting the extracellular ligand binding domain of the MPL,[30,31] whereas the 2 germline mutations affected the membrane proximal extracellular domain which appears to play a role in negative regulation of receptor activation. We initially hypothesized that the mutations might affect the affinity to TPO, however, the luciferase assay we performed in γ2A cells showed that all identified mutants activated STAT5-induced transcription in the absence of stimulation with TPO.

Triple-negative status of patients with PMF was shown to associate with inferior overall and leukemia-free survival,[32] however, in 2 of 12 triple-negative PMF patients with novel mutations identified in our study, *MPL*-S204P and *MPL*-V285E, we did not observe disease progression or leukemic transformation in a 12-year and 6-year follow-up, respectively. Although the number of patients is too low to perform statistical analyses, the clinical data indicate that these patients might have a better clinical course, in accordance with our molecular and functional findings. Analysis of larger patient cohorts will be necessary to confirm the effect of noncanonical *MPL* mutations on patients' prognosis.

Germline *JAK2* mutations clustering in the pseudokinase or kinase domain have been reported in several families with HT.[5-7] In all cases, they were weak gain-of-function mutations. Here, we reported 4 different *JAK2* mutations in 5 triple-negative ET cases. For JAK2-V625F and JAK2-F556V, we could demonstrate that they are gain-of-function mutations leading to increased phosphorylation of STAT5 and hypersensitivity to TPO. *JAK2*-G571S was found in 2 patients. In 1 case, we had evidence for presence of somatic mutations identified by WES and a gain of chromosome 4q, indicating a clonal disease. *JAK2*-G571S was previously reported in a *CALR*-positive patient with ET, and the lack of any hematologic phenotype in family members carrying *JAK2*-G571S indicated that this mutation might be a polymorphism not relevant for the disease.[33] We did not find evidence for G571S and G335D mutations altering the function of JAK2. These *JAK2* variants either do not play a role in the disease pathogenesis or require additional genetic events to exert a phenotype.

We cannot exclude that some of the patients with wild-type *MPL* and *JAK2*, as determined by Sanger sequencing, might carry low burden mutations in these genes, as sensitivity of this method is estimated to ≥10%. Our data indicate that inclusion of all coding exons of *JAK2* and *MPL* in the targeted sequencing panels designed for next-generation sequencing–based approaches for detection of mutations, which are likely to enter the clinical practice in near future, is recommended. Analysis of bigger patient cohorts using such panels will provide more accurate estimation of the frequency of the noncanonical *MPL* and *JAK2* mutations in triple-negative MPN, and their relevance for diagnostic purposes.

In the rest of the cases studied by WES, we did not identify a causative mutation due to absence of recurrent mutations. Similar results were obtained by other groups,[34,35] who reported clonal hematopoiesis in 10 of 17 cases, similar to our study (evidence of clonality in 5 of 8 patients). The cases with polyclonal hematopoiesis are likely to be hereditary MPN-like disorders. The lack of recurrency (and the fact that in 1 female PMF patient with clonal hematopoiesis, we did not identify any somatic mutations) can be attributed to the limitations of the WES approach, which can only detect mutations in the coding exons of genes. RNA sequencing for detection of fusion oncogenes and whole-genome sequencing for covering the regulatory sequences in the genome might provide an answer to which mutations drive the disease in the remaining triple-negative MPN cases and whether they represent a heterogeneous disease entity.

Acknowledgments

The authors thank the Biomedical Sequencing Facility at CeMM and Edith Bogner for their technical assistance.

The grants Sonderforschungsbereich (SFB) from the Austrian Science Fund (FWF): F2812-B20 and F4702-B20, are acknowledged for their generous support to R.K. and H.N. J.D.M.F. acknowledges support from L'ORÉAL Österreich, For Women in

From www.bloodjournal.org by guest on June 3, 2016. For personal use only.

Science Fellowship. Studies performed at the Department of Hematology Oncology, Fondazione IRCCS Policlinico San Matteo and University of Pavia were supported by grants from Associazione Italiana per la Ricerca sul Cancro (AIRC) and Ministero dell'Istruzione, dell'Università e della Ricerca (MIUR; PRIN 2010-2011) to M.C., and from the Italian Ministry of Health (GR-2009-1580521) and AIRC (MFAG-2014-15672) to E.R. In particular, M.C. acknowledges funding from the AIRC Special Program "Molecular Clinical Oncology 5 per mille" (AIRC Gruppo Italiano Malattie Mieloproliferative [AGIMM], project #1005). S.N.C was supported by the Ludwig Institute for Cancer Research, FNRS (FRSM), Belgium, the Salus Sanguinis Foundation, the Action de Recherche Concertée projects MEXP31C1 and ARC10/15-027 of the University Catholique de Louvain, the Fondation Contre le Cancer, Brussels, the PAI Programs BCHM61B5 and Belgian Medical Genetics Initiative BeMGI, Belgium. E.L. and I.C. received fellowships from FRIA and Télévie, Belgium. B.K. was supported by MUNI/A/1180/2014 and MH CZ-DRO (FNBr, 65269705).

Authorship

Contribution: J.D.M.F. and R.K. conceived and designed the experiments and wrote the paper; J.D.M.F., H.N., E.L., I.C., K.B., B.K., D.P., C.M., R.J., T.B., and M. Schalling performed the experiments; J.D.M.F., H.N., E.L., E.R., I.C., D.P., C.M., D.C., M. Schuster, C.B., S.N.C., and R.K. analyzed and interpreted the data; H.G., E.R., B.G., C.B., S.N.C., M.C., and R.K. contributed reagents/materials/analysis tools; and all authors contributed to the final version of the manuscript.

Conflict-of-interest disclosure: The authors declare no competing financial interests.

Correspondence: Robert Kralovics, CeMM Research Center for Molecular Medicine of the Austrian Academy of Sciences, Lazarettgasse 14, AKH BT25.3, 1090 Vienna, Austria; e-mail: robert.kralovics@cemm.oeaw.ac.at.

References

1. Baxter EJ, Scott LM, Campbell PJ, et al; Cancer Genome Project. Acquired mutation of the tyrosine kinase JAK2 in human myeloproliferative disorders. *Lancet.* 2005;365(9464):1054-1061.
2. James C, Ugo V, Le Couédic JP, et al. A unique clonal JAK2 mutation leading to constitutive signalling causes polycythaemia vera. *Nature.* 2005;434(7037):1144-1148.
3. Kralovics R, Passamonti F, Buser AS, et al. A gain-of-function mutation of JAK2 in myeloproliferative disorders. *N Engl J Med.* 2005;352(17):1779-1790.
4. Levine RL, Wadleigh M, Cools J, et al. Activating mutation in the tyrosine kinase JAK2 in polycythemia vera, essential thrombocythemia, and myeloid metaplasia with myelofibrosis. *Cancer Cell.* 2005;7(4):387-397.
5. Etheridge SL, Cosgrove ME, Sangkhae V, et al. A novel activating, germline JAK2 mutation, JAK2R564Q, causes familial essential thrombocytosis. *Blood.* 2014;123(7):1059-1068.
6. Mead AJ, Rugless MJ, Jacobsen SE, Schuh A. Germline JAK2 mutation in a family with hereditary thrombocytosis. *N Engl J Med.* 2012;366(10):967-969.
7. Rumi E, Harutyunyan AS, Casetti I, et al. A novel germline JAK2 mutation in familial myeloproliferative neoplasms. *Am J Hematol.* 2014;89(1):117-118.
8. Klampfl T, Gisslinger H, Harutyunyan AS, et al. Somatic mutations of calreticulin in myeloproliferative neoplasms. *N Engl J Med.* 2013;369(25):2379-2390.
9. Nangalia J, Massie CE, Baxter EJ, et al. Somatic CALR mutations in myeloproliferative neoplasms with nonmutated JAK2. *N Engl J Med.* 2013;369(25):2391-2405.
10. Pikman Y, Lee BH, Mercher T, et al. MPLW515L is a novel somatic activating mutation in myelofibrosis with myeloid metaplasia. *PLoS Med.* 2006;3(7):e270.
11. Pardanani AD, Levine RL, Lasho T, et al. MPL515 mutations in myeloproliferative and other myeloid disorders: a study of 1182 patients. *Blood.* 2006;108(10):3472-3476.
12. Beer PA, Campbell PJ, Scott LM, et al. MPL mutations in myeloproliferative disorders: analysis of the PT-1 cohort. *Blood.* 2008;112(1):141-149.
13. Staerk J, Lacout C, Sato T, Smith SO, Vainchenker W, Constantinescu SN. An amphipathic motif at the transmembrane-cytoplasmic junction prevents autonomous activation of the thrombopoietin receptor. *Blood.* 2006;107(5):1864-1871.
14. Ding J, Komatsu H, Wakita A, et al. Familial essential thrombocythemia associated with a dominant-positive activating mutation of the c-MPL gene, which encodes for the receptor for thrombopoietin. *Blood.* 2004;103(11):4198-4200.
15. Abdel-Wahab O, Manshouri T, Patel J, et al. Genetic analysis of transforming events that convert chronic myeloproliferative neoplasms to leukemias. *Cancer Res.* 2010;70(2):447-452.
16. Delhommeau F, Dupont S, Della Valle V, et al. Mutation in TET2 in myeloid cancers. *N Engl J Med.* 2009;360(22):2289-2301.
17. Grand FH, Hidalgo-Curtis CE, Ernst T, et al. Frequent CBL mutations associated with 11q acquired uniparental disomy in myeloproliferative neoplasms. *Blood.* 2009;113(24):6182-6192.
18. Zhang SJ, Rampal R, Manshouri T, et al. Genetic analysis of patients with leukemic transformation of myeloproliferative neoplasms shows recurrent SRSF2 mutations that are associated with adverse outcome. *Blood.* 2012;119(19):4480-4485.
19. Swerdlow S, Campo E, Harris NL, et al. WHO Classification of Tumours of Haematopoietic and Lymphoid Tissues. Lyon, France: International Agency for Research on Cancer; 2008.
20. Vardiman JW, Thiele J, Arber DA, et al. The 2008 revision of the World Health Organization (WHO) classification of myeloid neoplasms and acute leukemia: rationale and important changes. *Blood.* 2009;114(5):937-951.
21. Milosevic JD, Puda A, Malcovati L, et al. Clinical significance of genetic aberrations in secondary acute myeloid leukemia. *Am J Hematol.* 2012;87(11):1010-1016.
22. Malcovati L, Della Porta MG, Pietra D, et al. Molecular and clinical features of refractory anemia with ringed sideroblasts associated with marked thrombocytosis. *Blood.* 2009;114(17):3538-3545.
23. Defour JP, Itaya M, Gryshkova V, et al. Tryptophan at the transmembrane-cytosolic junction modulates thrombopoietin receptor dimerization and activation. *Proc Natl Acad Sci USA.* 2013;110(7):2540-2545.
24. Kawamata N, Ogawa S, Yamamoto G, et al. Genetic profiling of myeloproliferative disorders by single-nucleotide polymorphism oligonucleotide microarray. *Exp Hematol.* 2008;36(11):1471-1479.
25. Williams DM, Kim AH, Rogers O, Spivak JL, Moliterno AR. Phenotypic variations and new mutations in JAK2 V617F-negative polycythemia vera, erythrocytosis, and idiopathic myelofibrosis. *Exp Hematol.* 2007;35(11):1641-1646.
26. Hitchcock IS, Chen MM, King JR, Kaushansky K. YRRL motifs in the cytoplasmic domain of the thrombopoietin receptor regulate receptor internalization and degradation. *Blood.* 2008;112(6):2222-2231.
27. Harutyunyan AS, Kralovics R. Role of germline genetic factors in MPN pathogenesis. *Hematol Oncol Clin North Am.* 2012;26(5):1037-1051.
28. Lambert MP, Jiang J, Batra V, Wu C, Tong W. A novel mutation in MPL (Y252H) results in increased thrombopoietin sensitivity in essential thrombocythemia. *Am J Hematol.* 2012;87(5):532-534.
29. El-Harith HA, Roesl C, Ballmaier M, et al. Familial thrombocytosis caused by the novel germ-line mutation p.Pro106Leu in the MPL gene. *Br J Haematol.* 2009;144(2):185-194.
30. Feese MD, Tamada T, Kato Y, et al. Structure of the receptor-binding domain of human thrombopoietin determined by complexation with a neutralizing antibody fragment. *Proc Natl Acad Sci USA.* 2004;101(7):1816-1821.
31. Chen WM, Yu B, Zhang Q, Xu P. Identification of the residues in the extracellular domain of thrombopoietin receptor involved in the binding of thrombopoietin and a nuclear distribution protein (human NUDC). *J Biol Chem.* 2010;285(34):26697-26709.
32. Tefferi A, Lasho TL, Finke CM, et al. CALR vs JAK2 vs MPL-mutated or triple-negative myelofibrosis: clinical, cytogenetic and molecular comparisons. *Leukemia.* 2014;28(7):1472-1477.
33. Panovska-Stavridis I, Eftimov A, Pivkova-Veljanovska A, Ivanovski M, Cevreska L, Dimovski AJ. Familiar JAK2 G571S variant not linked with essential trombocythemia [abstract]. *Blood.* 2014;124(21):5585.
34. Campregher PV, Helman R, Pereira WO, et al. Genomic profile of patients with triple negative (JAK2, CALR and MPL) essential thrombocythemia and primary myelofibrosis [abstract]. *Blood.* 2014;124(21). Abstract 4589.
35. Cabagnols X, Ianotto JC, Bluteau O, et al. Mutational profile in essential thrombocytemia (Et) "negative" for Jak2 and Mpl [abstract]. *Haematologica.* 2014;99(6)(suppl 1):515. Abstract 1328.

THE JOURNAL OF BIOLOGICAL CHEMISTRY VOL. 291, NO. 6, pp. 2974–2987, February 5, 2016
© 2016 by The American Society for Biochemistry and Molecular Biology, Inc. Published in the U.S.A.

Annex 3

His[499] Regulates Dimerization and Prevents Oncogenic Activation by Asparagine Mutations of the Human Thrombopoietin Receptor*

Received for publication, October 4, 2015, and in revised form, November 27, 2015 Published, JBC Papers in Press, December 1, 2015, DOI 10.1074/jbc.M115.696534

Emilie Leroy[‡1,2], Jean-Philippe Defour[‡1,3], Takeshi Sato[§], Sharmila Dass[¶], Vitalina Gryshkova[‡4], Myat M. Shwe[‡5], Judith Staerk[‖], Stefan N. Constantinescu[‡6], and Steven O. Smith[¶7]

From the [‡]Ludwig Institute for Cancer Research, 1200 Brussels, Belgium de Duve Institute, Université catholique de Louvain, 1200 Brussels, Belgium, [§]Institute for Protein Research, Osaka University, 3-2 Yamadaoka, Suita, Osaka 565-0871, Japan, [¶]Department of Biochemistry and Cell Biology, Stony Brook University, Stony Brook, New York 11794-5215, and [‖]Stem Cell Group, Nordic European Molecular Biology Laboratory Partnership and Center for Molecular Medicine, 0318 Oslo, Norway

Ligand binding to the extracellular domain of the thrombopoietin receptor (TpoR) imparts a specific orientation on the transmembrane (TM) and intracellular domains of the receptors that is required for physiologic activation via receptor dimerization. To map the inactive and active dimeric orientations of the TM helices, we performed asparagine (Asn)-scanning mutagenesis of the TM domains of the murine and human TpoR. Substitution of Asn at only one position (S505N) activated the human receptor, whereas Asn substitutions at several positions activated the murine receptor. Second site mutational studies indicate that His[499] near the N terminus of the TM domain is responsible for protecting the human receptor from activation by Asn mutations. Structural studies reveal that the sequence preceding His[499] is helical in the murine receptor but non-helical in peptides corresponding to the TM domain of the inactive human receptor. The activating S505N mutation and the small molecule agonist eltrombopag both induce helix in this region of the TM domain and are associated with dimerization and activation of the human receptor. Thus, His[499] regulates the activation of human TpoR and provides additional protection against activating mutations, such as oncogenic Asn mutations in the TM domain.

The thrombopoietin (Tpo)[8] or Mpl receptor regulates megakaryocyte development and supports hematopoietic stem cell survival (1). The Tpo receptor (TpoR) shares general homology with other members of the cytokine receptor family, including the erythropoietin and granulocyte colony-stimulating factor receptors (2). These receptors contain a large extracellular domain that binds signaling hormones in a 2:1 ratio of receptor to hormone (3–5) along with a single membrane-spanning helix and an intracellular domain that associates non-covalently with a tyrosine kinase.

The minimal functional region of the intracellular domain stretches from the boundary of the transmembrane (TM) domain and includes three regions with limited sequence homology: a conserved switch region, Box 1, and Box 2. The switch region contains a hydrophobic motif whose orientation is required for signaling (6, 7). Box 1 is characterized by a proline-rich motif (P*XX*P*X*P) that is crucial for cytokine receptors to bind and activate their cognate Janus kinases (8–10). Box 2 is loosely defined as a motif with acidic and hydrophobic residues and is required for maximal cell growth in response to cytokines.

The TpoR has several unique features. First, the extracellular domain is duplicated, and deletion of the membrane-distal domain causes constitutive activation (11). Second, there are 5 amino acids (RWQFP) inserted directly C-terminal to the TM domain whose deletion or mutation causes ligand-independent receptor activation (12). Finally, clinically relevant mutations have been identified that induce constitutive receptor activity in the extracellular juxtamembrane (JM) region (T487A (13)), the TM domain (S505N (14, 15)), and the intracellular RWQFP motif (W515K/L/A (12, 16–19)). The fact that these are clustered in and around the TM domain reflects the importance of this region in the regulation of receptor activation.

It is generally accepted that the active signaling form of cytokine receptors is a dimer, but whether the inactive state is dimeric or monomeric is unknown. Several lines of evidence

* This work was supported in part by National Institutes of Health-National Science Foundation Instrumentation Grants S10 RR13889 and DBI-9977553 and National Institutes of Health Grant GM-46732 (to S. O. S.). The authors declare that they have no conflicts of interest with the contents of this article. The content is solely the responsibility of the authors and does not necessarily represent the official views of the National Institutes of Health.

[1] Both authors contributed equally to this work.

[2] Supported by a Fonds pour la formation à la Recherche dans l'Industrie et dans l'Agriculture (FRIA) Ph.D. fellowship.
[3] Supported by a FRIA Ph.D. fellowship and the Cliniques universitaires St. Luc.
[4] Supported by a de Duve Institute postdoctoral fellowship and a Belspo Interuniversity Attraction Poles fellowship.
[5] Supported by an Erasmus Mundus Panacea fellowship.
[6] Supported by Ludwig Cancer Research, Fonds de la Recherche Scientifique-Fonds National de la Recherche Scientifique, Salus Sanguinis, Fondation contre le cancer, Project Action de Recherche Concertée of the Université catholique de Louvain (Grant ARC10/15-027), and the PAI program Belgian Medical Genetics Initiative. To whom correspondence may be addressed. Tel.: 322-764-7540; Fax: 322-764-6566; E-mail: stefan.constantinescu@bru.licr.org.

[7] To whom correspondence may be addressed. Tel.: 631-632-1210; Fax: 631-632-8575; E-mail: steven.o.smith@stonybrook.edu.

[8] The abbreviations used are: Tpo, thrombopoietin; TpoR, Tpo receptor; EpoR, erythropoietin receptor; ATR, attenuated total reflection; hTpoR, human thrombopoietin receptor; JM, juxtamembrane; mTpoR, murine thrombopoietin receptor; Mpl, myeloproliferative leukemia; TM, transmembrane; EndoH, endoglycosidase H; hGluc, *Gaussia* luciferase fragment; MAS, magic angle spinning; IC, intracellular.

Downloaded from http://www.jbc.org/ at UNIVERSITE CATHOLIQUE LOUVAIN on June 27, 2016

exist to suggest that the erythropoietin receptor (EpoR), one of the most extensively studied cytokine receptors, exists as a preformed dimer, and activation is induced by structural reorganization of the dimer after hormone binding. Crystallographic studies of the EpoR extracellular domain in the presence and absence of ligand suggest that the full-length inactive receptor is dimeric, and hormone binding causes subunit rotation for activation (4, 20). A similar model has been proposed for the structurally related growth hormone receptor (21–23). The first evidence that the TM domain contributes to dimerization of the inactive EpoR came from co-patching measurements using chimeras of the prolactin and erythropoietin receptors in HEK293-derived BOSC cells (24). These studies found the TM domain of the EpoR to be both necessary and sufficient for receptor dimerization in the context of the full-length receptor. This conclusion is supported by biophysical measurements showing that the isolated TM domain of the murine EpoR associates as a dimer (25). However, unlike the TpoR, the TM domain of the EpoR is not a hot spot for activating mutations.

Much less is known about whether the TpoR forms an inactive dimer that changes orientation upon ligand binding. Studies using coiled coil fusions to the TM-cytosolic domain of the murine TpoR showed that one dimeric interface is inactive, one interface mimics the physiologic functions of TpoR, and several orientations induce partial levels of activation *in vitro* and in bone marrow transplantation experiments *in vivo* in mice (26). However, these studies use an artificial receptor where the large, native extracellular domain dimer (preformed or ligand-bound) is replaced with a short, tightly associated coiled coil that forces symmetric dimerization. Biophysical studies on the association of the human TpoR TM domain using cysteine mutagenesis and the TOXCAT reporter assay indicate that the wild-type TM sequence (residues 491–515) associates as a dimer (27). However, we have recently shown that the 5-amino acid (RWQFP) insert at the intracellular TM-JM boundary of the TpoR impairs dimerization of the upstream TpoR TM helix (28). We further showed that mutation of Trp^{515} within this motif leads to dimerization of the TM-JM region of TpoR by changing the orientation of the TM helix relative to the membrane bilayer normal (28). Although the studies on isolated TM-JM regions of TpoR reveal that they have a propensity to dimerize, it remains an open question as to whether the full-length receptor is primarily dimeric or monomeric or exists in a monomer-dimer equilibrium.

In this study, asparagine-scanning mutagenesis of the murine TpoR (mTpoR) and human TpoR (hTpoR) was used to modulate the orientation and dimerization of the TM domain of the receptor. The asparagine mutations provide an alternative to the coiled coil dimerization sequences we have previously used to engineer TpoR dimers (26). Asparagine is able to mediate dimerization of TM helices through strong hydrogen bonding interactions and often does so in a sequence-independent fashion (29–31). Moreover, asparagine-scanning mutagenesis addresses the question of whether the clinically observed S505N mutation in humans is unique or just one of many mutations that lead to constitutive activation. We made use of full-length receptors, truncated receptors, and peptides corresponding to only the TM-JM domain for comparative studies between the murine and human receptors. Together, our results provide the structural basis for why the hTpoR cannot be activated by asparagine mutations that readily activate the mTpoR, suggesting an evolutionary mechanism that results in resistance to oncogenic activation of hTpoR.

Experimental Procedures

cDNA Constructs and Cells—Mouse and human TpoR cDNAs cloned in the pMX-IRES-GFP bicistronic vector contained a hemagglutinin (HA) tag at the N terminus. Site-directed mutagenesis was achieved by the overlapping-extension PCR amplification method. The PCR was performed using 1 μl of PfuTurbo DNA polymerase (2.5 units/μl) following the protocol in the QuikChange XL site-directed mutagenesis kit (Stratagene, Santa Clara, CA) as described (28). Sanger sequencing of the entire coding region was used for each construct.

Cell Proliferation Assay—Pro-B interleukin 3 (IL-3)-dependent Ba/F3 cells were maintained in RPMI 1640 medium and 10% fetal calf serum using WEHI cell supernatant as a source of IL-3. TpoR Asn variants subcloned in the pMX-IRES-GFP were used for packaging ectopic retrovirus in BOSC cells. Cells were infected in medium containing Polybrene with packaged retrovirus, and cell pools expressing similar levels (top 15%) of green fluorescent protein (GFP) coded by the bicistronic retroviral vectors were isolated using flow cytometry cell sorting. Cell surface TpoR was assessed by staining with anti-HA antibodies (Covance, Princeton, NJ; 10 μg/ml) and phycoerythrin-conjugated donkey anti-mouse IgG secondary antibodies (28). The levels of TpoR total protein expression were determined by Western blotting using anti-HA antibodies (Roche Applied Science). For determining the maturation state of the *N*-glycosylated TpoR mutants, we used digestion with endoglycosidase H (EndoH) for 4 h followed by Western blotting with anti-HA antibodies as described (6). Cell proliferation in the presence or absence of cytokines was measured using the CellTiter-Glo luminescent cell viability assay (Promega, Madison, WI).

Dual-Luciferase Transcriptional Assay of STAT Activation—Transcriptional activation of STAT3 and STAT5 downstream TpoR variants was assessed in γ-2A cells (Janus kinase 2-deficient cells reconstituted with Janus kinase 2) using the Dual-Luciferase assay kit (Promega, Madison, WI). The assay measures luciferase luminescence after transient transfection of the pGRR5 reporter containing the firefly luciferase and STAT3/STAT5 binding sites and a control reporter (pRL-TK) containing *Renilla* luciferase. The luminescence ratio of these two luciferases provides a measure of STAT activation (26, 32). Luminescence was detected in cell lysates with a PerkinElmer Life Sciences Victor-X light analyzer.

Split Luciferase Complementation Assay of Receptor Dimerization—TpoR dimerization was measured using a complementation assay in which two halves of *Gaussia princeps* luciferase were attached separately to the C terminus of TpoR. The cDNA of TpoR was inserted between the NotI and ClaI restriction sites of the pcDNA3.1/Zeo vector upstream of either the hGluc fragment coding amino acids 1–93 (hGluc1) or the fragment coding amino acids 94–169 (hGluc2) of *G. princeps* luciferase (33). BOSC cells plated on 24-well plates were co-transfected with the plasmids (coding hGluc1and hGluc2) using

Downloaded from http://www.jbc.org/ at UNIVERSITE CATHOLIQUE LOUVAIN on June 27, 2016

206

Lipofectamine (Invitrogen). Twenty-four hours after transfection cells were trypsinized and resuspended in 150 μl of DMEM/F-12 without phenol red (Gibco). Cell samples were flash frozen on dry ice for 10 min and thawed in a water bath at 37 °C for 10 min (cycle was repeated twice). After centrifugation (10,000 × *g*, 5 min), the supernatants were collected and aliquoted (100 μl/well) in 96-well white plates (Nunc, Thermo Fisher Scientific) to measure the luciferase activity. Native coelenterazine (NanoLight Technology) was reconstituted as a stock solution (1 mg/ml in methanol) and diluted to a final concentration of 20 μM in DMEM/F-12 at room temperature for injection (100 μl). Signal intensities (integrated over 10 s with an injection delay of 2 s) were read on a Victor-X light analyzer. Aliquots of the supernatants were also used to detect the proteins on Western blots (33).

Membrane Reconstitution of TM-JM Peptides for Biophysical Studies—Peptides (40 residues in length) corresponding to the TM domain and JM regions of hTpoR (TRVETATETAWISLVTALHLVLGLSAVLGLLLLRWQFPAH) and mTpoR (ARVSTGSETAWITLVTALLLVLSLSALLGLLLLKWQFPAH) were synthesized using solid-phase methods. Deuterated (5,5,5-d_3) leucine and deuterium-free water were purchased from Cambridge Isotope Laboratories (Andover, MA). Other amino acids and octyl β-glucoside were obtained from Sigma. The crude peptide (5–15 mg) was purified by reverse-phase HPLC on a C_4 column using gradient elution. Purified TpoR peptides were reconstituted by detergent dialysis using 1,2-dimyristoyl-*sn*-glycero-3-phosphocholine and 1,2-dimyristoyl-*sn*-glycero-3-phosphoglycerol (10:3) and a ~1:60 peptide-to-lipid ratio. Lipids were obtained from Avanti Polar Lipids (Alabaster, AL) as lyophilized powders and used without further purification. The lipid, detergent, and peptide were dissolved in organic solvent (*e.g.* hexafluoro-2-propanol or trifluoroethanol). The mixture of lipid, detergent, and peptide in organic solvent was incubated at 37 °C for over 2 h, the solvent was removed by evaporation using a stream of argon gas, and then the sample was placed under vacuum. The dry mixture was rehydrated with phosphate buffer (10 mM phosphate and 50 mM NaCl, pH 7.4) such that the final concentration of octyl β-glucoside was 5–10% (w/v). The rehydrated sample was then stirred slowly for at least 6 h, and the octyl β-glucoside was removed by dialysis using Spectra-Por dialysis tubing (3500 molecular weight cutoff) for 24 h against phosphate buffer at 37 °C. To confirm that the membrane-reconstituted peptides did not aggregate during dialysis, the samples were loaded onto 10–40% (w/v) sucrose gradients and purified. Samples for IR spectroscopy were dialyzed a second time to remove sucrose. The dichroic ratios were compared before and after dialysis. Samples for NMR spectroscopy were pelleted by ultracentrifugation and, if needed, washed twice to remove sucrose. The pelleted samples were lyophilized, rehydrated with deuterium-depleted water (50 ± 5% weight), and incubated at 37 °C for 24 h before loading into NMR rotors.

Polarized IR Spectroscopy—Polarized attenuated total reflection (ATR) Fourier transform infrared (FTIR) spectra were obtained on a Bruker IFS 66V/S spectrometer. Reconstituted hTpoR and mTpoR TM-JM peptides (50–100 μg) were layered onto a germanium internal reflection element using a slow flow of air or argon gas directed at an oblique angle to the ATR plate to form an oriented multilamellar lipid-peptide film. IR spectra were obtained using light having either parallel or perpendicular polarization relative to the surface of the germanium plate. The dichroic ratio (R_{ATR}) is defined as the ratio between the absorption of parallel ($A_{\parallel}$) and perpendicular ($A_{\perp}$) polarized light. The frequency of the amide I vibration is sensitive to the global secondary structure of the protein, and the dichroic ratio of the amide I band provides information on the orientation of TM helices relative to the plane of the membrane (34). A detailed analysis has been described previously (34). 1000 scans were acquired and averaged for each sample at a resolution of 4 cm^{-1}. The calculation of the helix tilt angles from the observed dichroic ratios was based on a value of the transition moment angle (α) of 39.5° and a maximum membrane order parameter (S_{mem}) of 0.85 (34). The use of the values of α and S_{mem} is based on measurements of bacteriorhodopsin, an integral membrane protein with seven transmembrane helices of known structure that forms well ordered, two-dimensional membrane arrays. We do not independently know the disorder of the reconstituted TM helices in our samples. Consequently, we assume that the maximum order obtained is equal to that of bacteriorhodopsin obtained from diffraction measurements (35). This results in a lower estimate for the helix tilt angles reported in Table 1 (*i.e.* greater disorder in our membrane reconstitutions than that found for bacteriorhodopsin would correspond to lower actual tilt angles for an ideal sample with no disorder).

Solid-state NMR Spectroscopy—Deuterium NMR spectra were obtained at a ^2H frequency of 55.2 MHz on a Bruker Avance NMR spectrometer using a 4-mm magic angle spinning (MAS) probe. A MAS frequency of 3 kHz was used to increase the number of spinning side bands. Single pulse excitation was utilized using a 4–7.5-μs 90° pulse followed by a 4.5-μs delay before data acquisition. The repetition delay was 0.25 s. A total of 600,000–1,500,000 transients were averaged for each spectrum and processed using a 100-Hz exponential line broadening function. Spectra were obtained at 25 °C.

Two-dimensional dipolar assisted rotational resonance NMR experiments (36) were performed at a ^{13}C frequency of 125 MHz on a Bruker Avance spectrometer. The MAS spinning rate was set in the range of 9–11 KHz ± 5 Hz. The ramped amplitude cross-polarization contact time was 2 ms. Two-pulse phase-modulated decoupling was used during the evolution and acquisition periods. The radiofrequency field strength was 80 kHz. Internuclear $^{13}C\ldots{}^{13}C$ distance constraints were obtained using a mixing time of 600 ms. The sample temperature was maintained at −50 ± 2 °C. All ^{13}C solid-state MAS NMR spectra were externally referenced to the ^{13}C resonance of neat tetramethylsilane at 0 ppm at room temperature. Using tetramethylsilane as the external reference, we calibrated the carbonyl resonance of solid glycine at 176.46 ppm. The chemical shift difference between ^{13}C of 4,4-dimethyl-4-silapentane-1-sulfonic acid in D_2O relative to neat tetramethylsilane is 2.01 ppm.

Results

Asparagine Mutations in the Transmembrane Domain of the Human and Murine TpoR Induce Different Effects—The TM sequences of human and murine receptors are shown in Fig. 1*A*

Downloaded from http://www.jbc.org/ at UNIVERSITE CATHOLIQUE LOUVAIN on June 27, 2016

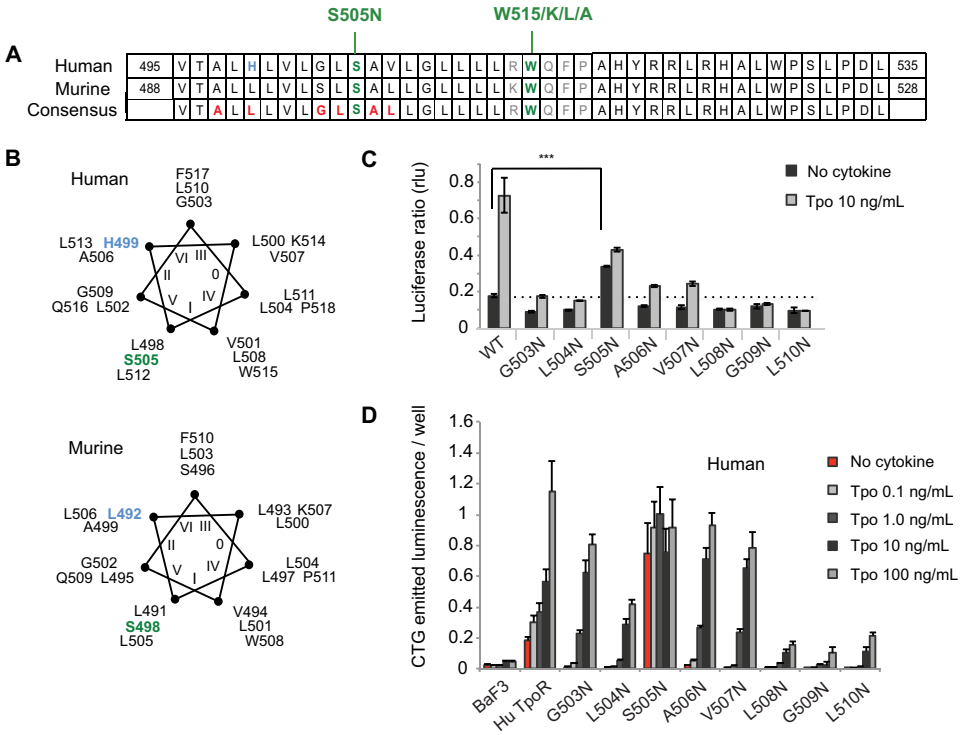

FIGURE 1. **Asparagine substitutions in the transmembrane domain of the human TpoR lead to activation of only one dimeric interface.** *A*, TM sequences of hTpoR (*upper*) and mTpoR (*middle*) showing the position of His^{499} and the intracellular (R/K)WQFP motif. A consensus sequence (*bottom*) of 50 different mammalian TpoRs highlights (*red*) the positions with sequence identity of <90%. Four of these residues bracket Ser^{498} (murine) and Ser^{505} (human), which is highly conserved. *B*, helical wheel diagrams of hTpoR (*left*) and mTpoR (*right*) showing the dimer interfaces that would be predicted for interacting helices in a left-handed coiled coil geometry. *C*, transcriptional activation of hTpoR after substitution of Gly^{503}–Leu^{510} with asparagine. γ2A cells were transiently transfected with Janus kinase 2 and the wild-type TpoR or the different TpoR mutants, and the activity of these receptors was assessed by measuring luciferase luminescence (in relative luciferase units (*rlu*)) in the absence or presence of 50 ng/ml Tpo as indicated. Only the S505N mutation triggers ligand-independent dimerization and signaling. *D*, BaF3 cells stably expressing the hTpoR (*hu TpoR*) variants were grown in the absence of cytokine or in the presence of different concentrations of Tpo as indicated. Only TpoR-S505N induced BaF3 autonomous growth. The presented values are averages of triplicates ±S.D. (*error bars*) for one representative experiment of at least three. ***, $p < 0.001$, one-way analysis of variance.

along with a consensus sequence for mammalian TpoRs. Across a wide range of species, the TM domain is relatively well conserved. Ser^{505} and Trp^{515} both have a sequence identity of ~96%. The S505N is associated with familial forms of thrombocytosis, whereas the W515K/L/A mutations are associated with essential thrombocythemia and primary myelofibrosis. There are only a few residues with less than 90% identity (shown in *red*). There are four differences between human and mouse in the TM-JM sequence shown. Based on sequence comparison between TpoRs from 50 species, leucine at positions 492 and 500 in the mouse and glycine and arginine at positions 503 and 514, respectively, in the human are the consensus residues.

Asparagine, the residue that leads to constitutive activation upon mutation at Ser^{505} (human), is able to mediate dimerization of TM helices as left-handed coiled coils. The early studies of leucine zippers involved Asn residues at the "a" position in the heptad repeat characteristic of a left-handed coiled coil (37, 38). The crystal structure of the GCN4 transcription factor shows that the amide side chain of Asn forms an asymmetric hydrogen bond across the dimer interface (38), and dimerization studies showed that this contributes about −2 kcal/mol of binding energy (39).

Helical wheel diagrams illustrate the possible dimer interfaces in hTpoR and mTpoR (Fig. 1, *A* and *B*). Such dimeric interfaces are imposed when the coiled coil domain of Put3 is fused at consecutive positions to the TM domain of mTpoR, thus replacing the extracellular domain (26). There are seven possible symmetric interfaces that might mediate dimerization in the native receptor and that were created by progressive deletion of residues from the N-terminal end of the TM domain after fusion with the Put3 coiled coil (26). These are designated cc-TpoR-0 through cc-TpoR-VI. The cc-TpoR-II interface was found to be inactive, whereas the other interfaces exhibited various degrees of activity.

To investigate whether the full-length TpoR can be activated by asparagine mutations on different TM helix interfaces, TM residues 503–510 were individually substituted with asparagine in the hTpoR, and the receptor activity was monitored using a luciferase assay that reports on STAT5 transcriptional activation (see "Experimental Procedures"). Substitution with Asn only at a single position (S505N) leads to ligand-independent activation of the hTpoR (Fig. 1*C*). This position is the same as that detected in clinical studies showing only a single site (Ser^{505}) where an Asn mutation leads to disease. The results on STAT5 transcriptional activity were confirmed with cell proliferation assays in stable Ba/F3 transduced cells (Fig. 1*D*). For these measurements, each receptor mutant was retrovirally transduced into Ba/F3 cells and sorted using flow cytometry for similar levels of expression. Only the S505N mutant led to cytokine-independent cell proliferation. Importantly, several substitutions (L508N, G509N, and L510N) led to receptors that

Downloaded from http://www.jbc.org/ at UNIVERSITE CATHOLIQUE LOUVAIN on June 27, 2016

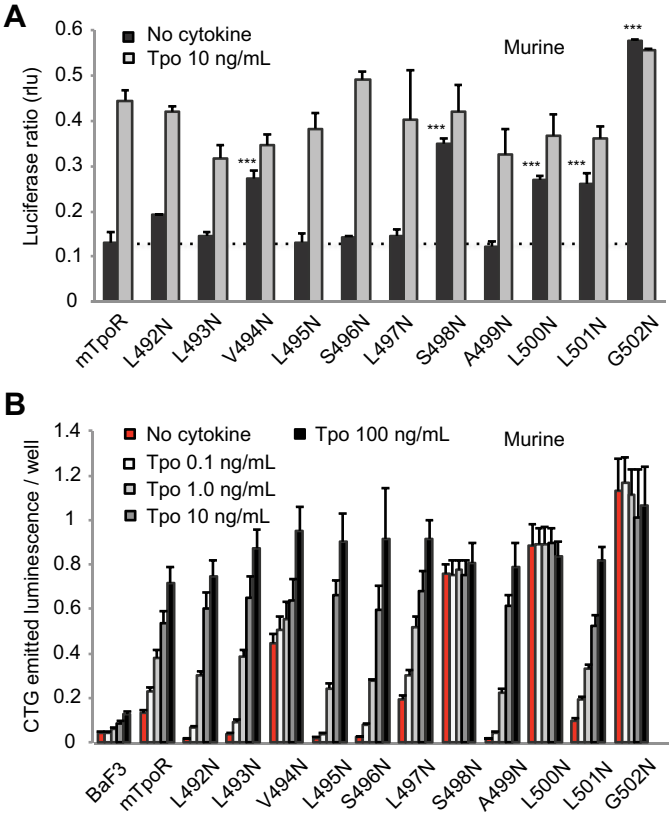

FIGURE 2. **Asparagine substitutions in the transmembrane domain of the murine TpoR lead to activation of several dimeric interfaces.** Leu^{492}–Gly^{502} were substituted with asparagine, and these mutant receptors were assessed for their ability to signal in the absence of cytokine. *A*, γ2A cells were transiently transfected with the constructs, and the transcriptional activation of STAT5 was measured by luciferase luminescence (in relative luciferase units (*rlu*)). V494N, S498N, L500N, L501N, and G502N triggered signaling in the absence of stimulation. *B*, BaF3 cells stably expressing the different constructs were grown, and cell viability was measured in the absence or presence of the different concentrations of Tpo ligand as indicated. V494N, S498N, L500N, and G502N allow proliferation of BaF3 in the absence of cytokine. The values presented are averages of triplicates ± S.D. (*error bars*) for one representative experiment of at least three. ***, $p < 0.001$, one-way analysis of variance between the wild type and each mutant in the absence of cytokine. *CTG*, *CellTiter-Glo*.

were unable to traffic to the cell surface and were, as a consequence, inactive when Tpo was added.

Asparagine-scanning measurements of STAT5 transcriptional activation of the mTpoR reveal a very different picture (Fig. 2*A*). In contrast to hTpoR, asparagine substitutions at positions 494, 498, 500, 501, and 502 in mTpoR stabilize active receptors in the absence of ligand. These results were confirmed by cell proliferation assays in Ba/F3 cells for positions 494, 498, 500, and 502 (Fig. 2*B*). Asn substitutions at four different positions of the mTpoR clearly lead to activation, whereas only S505N (equivalent to S498N in the mouse) activates the hTpoR.

Mutation of His^{499} to Leucine Leads to Increased Cell Surface Localization and Signaling by the hTpoR-G509N Mutant—One of the largest sequence differences in the TM and JM regions between the murine and human receptors is at position 499 where histidine in human (His^{499}) is replaced by leucine in mouse (Leu^{492}). This TM residue is unique to TpoR and granulocyte colony-stimulating factor receptor within the family of type I cytokine receptors and only appeared later in species evolution. The histidine in the human receptor has previously been shown to bind eltrombopag, a small molecule agonist of hTpoR, leading to receptor activation (40). In this section, we explore the influence on activation of the H499L and L492H mutants in the context of the human and murine receptors, respectively, and show how these mutations influence the ability of Asn substitutions within the TM domain to activate TpoR. STAT5 activation and cell proliferation were measured using the Dual-Luciferase and cell viability assays, respectively, on the murine (Fig. 3*A*) and human (Fig. 3*B*) receptors with swapped residues (*i.e.* H499L and L492H). Several conclusions can be drawn.

First, mTpoR-G502N (the most strongly activating single Asn mutant) is not active in the context of the mTpoR-G502N/L492H double mutant. Indeed, placement of histidine at position 492 in the mTpoR-G502N mutant abolished the activity of the mutant in the absence and the presence of ligand, yielding the same phenotype as the human receptor with the corresponding G509N substitution.

Second, the mTpoR is not sensitive to eltrombopag, whereas substitution of L492H in the mTpoR imparts sensitivity to eltrombopag as observed previously (40). This confirms that eltrombopag binding requires the presence of histidine in the TM sequence. In contrast, removal of histidine at position 499 in the hTpoR-G509N mutant could restore the activity of this mutant in the presence and absence of ligand. As a control, the human receptor lacking His^{499} could no longer respond to eltrombopag.

Third, the hTpoR-G509N mutant (equivalent to mTpoR-G502N) does not traffic to the plasma membrane. The hTpoR-G509N mutant is retained intracellularly in an EndoH-sensitive form (Fig. 4), indicating that it contains high mannose *N*-glycosylation, characteristic of immature receptor retained in the endoplasmic reticulum, or possibly a receptor that cannot progress past the *cis*-Golgi. In contrast, the double mutation (H499L/G509N) allows the receptor to traffic to the plasma membrane (Fig. 4) and to induce STAT5 activation and autonomous proliferation in Ba/F3 cells (Fig. 3*C*). H499L appears to also rescue activity for additional Asn mutants in the hTpoR. For example, V507N is partially rescued by the H499L mutation and exhibits weak activity (data not shown). Rescued receptors become EndoH-resistant and are localized at the cell surface (Fig. 4). In the background of the mouse TpoR, the L492H mutation inactivates the Asn mutants and impairs their ability to traffic to the cell surface (data not shown).

Dimerization of hTpoR Causes Straightening of the TM Helix Near His^{499}—The structural basis underlying the mechanism by which His^{499} influences receptor activation and cell surface expression is a challenge to study in full-length Tpo receptors. However, the original studies describing the influence of Asn mutations on TM helix dimerization were undertaken on isolated TM domains that independently fold into helical secondary structure when reconstituted into membrane bilayers (29–31). Indeed, we have previously shown that the activating S505N and W515K mutations in the context of TM-JM peptides of the human TpoR lead to a change of the tilt angle of the TM helix and induce dimerization, consistent with measure-

Downloaded from http://www.jbc.org/ at UNIVERSITE CATHOLIQUE LOUVAIN on June 27, 2016

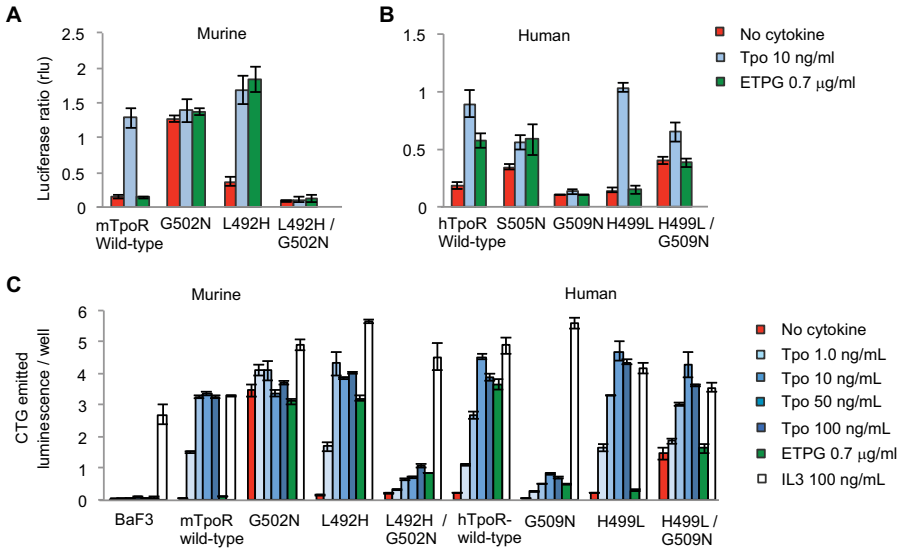

FIGURE 3. **Addition or removal of the TM histidine modifies the activity of the Asn mutants.** *A*, introduction of His instead of Leu at the homologous position in the murine receptor abrogated the activity of the G502N mutant as indicated on the Dual-Luciferase assay performed in transiently transfected γ2A cells. As a control, eltrombopag (*ETPG*) was added and was able to activate the L492H receptor. *B*, substitution of His^{499} by leucine restored the activity of the G509N mutant. Eltrombopag was no longer able to activate the receptor lacking His^{499}. *C*, BaF3 cells stably expressing the TpoR variants were assessed for their ability to grow in the absence of cytokine (*red*) or in the presence of different concentrations of Tpo (gradient of *blue*; 1, 10, 50, and 100 ng/ml) and eltrombopag (*green*; 0.7 μg/ml). Cells were all able to growth in the presence of IL-3 (*white*). The human double mutant G509N/H499L and its murine homolog G502N were able to induce BaF3 autonomous growth in the absence of cytokine. Histograms are averages of triplicates ±S.D. (*error bars*) for one representative experiment of at least three. *CTG*, *CellTiter-Glo; rlu,* relative luciferase units.

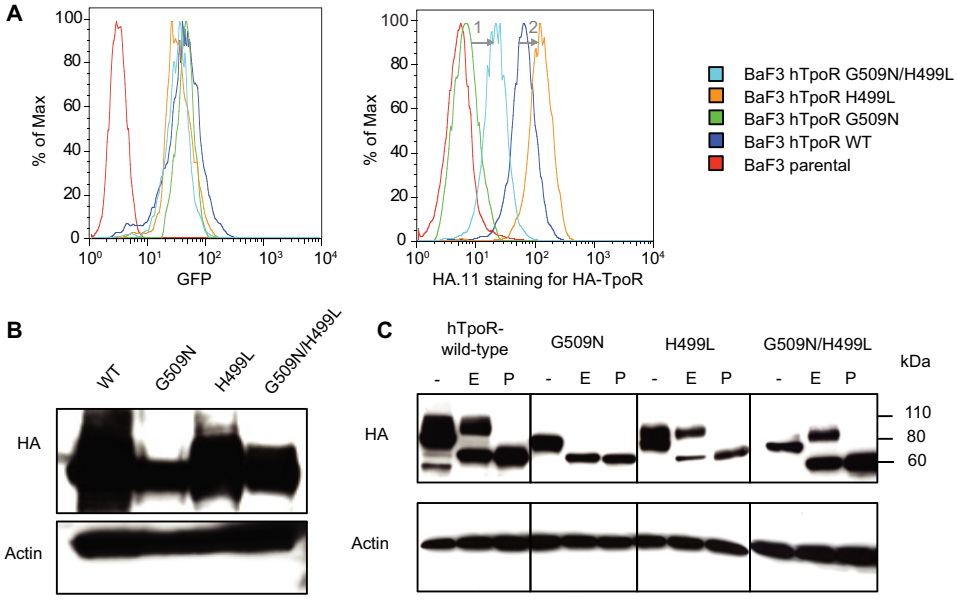

FIGURE 4. **TpoR-G509N is not expressed at the cell surface.** *A*, cell surface expression of HA-tagged TpoR was assessed by FACS using an anti-HA.11 antibody. *B*, BaF3 cells were sorted for the same level of GFP. *C*, the total level of TpoR protein was assessed by Western blotting with Np40 cell extracts using an anti-HA antibody. *D*, EndoH and peptide-*N*-glycosidase F treatment of stable BaF3 cell lines. Sorted BaF3 cells stably expressing the TpoR asparagine variants were treated with EndoH (*E*) or peptide-*N*-glycosidase F (*P*) or not treated (−), and the total level of TpoR protein was assessed using an anti-HA antibody by Western blotting. All the receptors except G509N mutant were resistant to EndoH treatment, revealing that the proteins are mature. The G509N mutant, which was fully degraded by EndoH, is likely immature and does not proceed to the cell surface because of some misfolding that blocks it at the rough endoplasmic reticulum-Golgi transport system. All the receptors depend on *N*-glycosylation for processing as revealed by the peptide-*N*-glycosidase F treatment.

ments on the full-length receptor using the split luciferase assay (28). Here, we extend these studies to the G509N and H499L mutants in hTpoR and to the G502N and L492H mutants in mTpoR (Table 1).

Polarized FTIR spectroscopy provides information on the global secondary structure and orientation of membrane-reconstituted TM-JM peptides. Typically, these peptides fold into α-helical secondary structure that gives rise to an amide I vibrational band at ~1655 cm^{-1} in the IR spectrum. The orientation of the TM helix (*i.e.* the helix tilt angle relative to the bilayer normal; see "Experimental Procedures") is probed in polarized IR spectra by measurements of the dichroic ratio (R_{ATR}). Hydrophobic peptides (20–24 residues in length) typically exhibit dichroic ratios of >3.0, corresponding to a maximum

Downloaded from http://www.jbc.org/ at UNIVERSITE CATHOLIQUE LOUVAIN on June 27, 2016

TABLE 1
Orientation, secondary structure, and association of hTpoR-WT, mTpoR-WT, and their mutants

Sequence	Dichroic ratio[a]	Helix tilt angle (°)	Leu^{494}–Ala^{497} structure	Leu^{494}, Val^{495} $^{13}C{=}O$ shift	Association
hTpoR-WT	2.7 ± 0.1	35	Extended	172.3, 172.3	Monomer
S505N	3.4 ± 0.1	17	Helix	175.9, 175.9	Dimer
G509N	2.5 ± 0.2	40	Extended	172.3, 172.3	Dimer
H499L	3.2 ± 0.1	23	Helix	176.1, 176.1	Dimer
hTpoR-WT + eltrombopag	3.0 ± 0.1	28	Helix	175.3, 175.3	Dimer
mTpoR-WT	3.3 ± 0.1	20	Helix	176.3, 176.3	Dimer
S498N	3.3 ± 0.1	20	Helix	177.2, 177.2	Dimer
G502N	3.2 ± 0.1	25	Helix	176.6, 176.6	Dimer
L492H	2.6 ± 0.2	38	Extended	173.1, 173.1	Monomer

[a] The error in the dichroic ratio corresponds to the standard deviation in three replicate runs.

helix tilt of ~28°. Lower dichroic ratios indicate something unusual in the TM sequence (or simply reflect poor membrane reconstitutions). Our previous FTIR studies on hTpoR TM-JM peptides revealed dichroic ratios of ≤2.8 (28). In Fig. 5, *A* and *B*, we show using parallel reconstitutions that mTpoR-WT peptides exhibit a striking increase in the dichroic ratio compared with hTpoR-WT, corresponding to a decrease in the helix tilt angle from 35 to 20°. This change in orientation can be mimicked in the hTpoR by the H499L mutation, which exhibits the same dichroic ratio (3.2) within error as the mTpoR (Table 1).

A second mechanism for increasing the dichroic ratio of the hTpoR-WT TM helix is incorporation of the S505N mutation. The hTpoR-S505N dichroic ratio (3.4) is closer to that of mTpoR-WT (3.3) than to that of hTpoR-WT (2.7). We attribute this increase to a shift in the monomer-dimer equilibrium toward dimer in the S505N mutant (28). The mTpoR-S498N and hTpoR-S505N peptides exhibit similar dichroic ratios (3.3 *versus* 3.4), suggesting that they adopt similar active orientations.

We also compared the homologous hTpoR-G509N and mTpoR-G502N mutants. The mTpoR-G502N peptide has a much higher dichroic ratio (3.2) than hTpoR-G509N (2.5), consistent with the higher activity of the full-length mTpoR-G502N mutant. The dichroic ratio of hTpoR-G509N is slightly lower than that of hTpoR-WT (2.7). The presence of two polar residues (His^{499} and Asn^{509}) appears to alter the orientation of the TM helix in the membrane and may be associated with the poor ability of the G509N mutant to traffic. Similarly, introducing a histidine (at the equivalent His^{499} position) in the murine coiled coil constructs induces TpoR protein instability as observed by loss of activity and protein expression at the cell surface (data not shown).

Previous NMR studies on the structure and orientation of the TM helix of hTpoR found that there was a break in helical secondary structure near Ala^{497}, one turn before His^{499} (41). The low dichroic ratio of the amide I band observed in FTIR spectra of wild-type hTpoR would be consistent with this observation. To directly probe the helical secondary structure in this region of the peptide in mTpoR and hTpoR, we made use of intramolecular distance measurements using two-dimensional ^{13}C NMR spectroscopy with MAS (36).

Two-dimensional ^{13}C NMR spectra were obtained on the hTpoR and mTpoR TM sequences isotopically labeled with [1-^{13}C]Leu^{494} or [1-^{13}C]Leu^{487}, [1-^{13}C]Val^{495} or [1-^{13}C]Val^{488}, and [3-^{13}C]Ala^{497} or [3-^{13}C]Ala^{490}. These positions just precede His^{499} and Leu^{492} in the hTpoR and mTpoR sequences, respectively. In the two-dimensional NMR spectra, intramolecular cross-peaks are observed between ^{13}C sites with a through space separation of ≤6 Å. For example, in mTpoR, the 3-^{13}C carbon of Ala^{490} is in close proximity to the $^{13}C{=}O$ groups of Leu^{487} (4.3 Å) and Val^{488} (5.4 Å) in α-helical secondary structure, and cross-peaks between these ^{13}C resonances are observed in the two-dimensional NMR spectrum. Fig. 5*C* shows the full two-dimensional dipolar assisted rotational resonance spectrum of mTpoR-WT where a distinct cross-peak is observed between [3-^{13}C]Ala^{490} and either [1-^{13}C]Leu^{487} and/or [1-^{13}C]Val^{488} whose resonances are not resolved. The cross-peak (highlighted in Fig. 5*E*) confirms that this region of mTpoR-WT is α-helical. In contrast, this cross-peak is absent in hTpoR (Fig. 5*D*), revealing that this region does not adopt helical secondary structure.

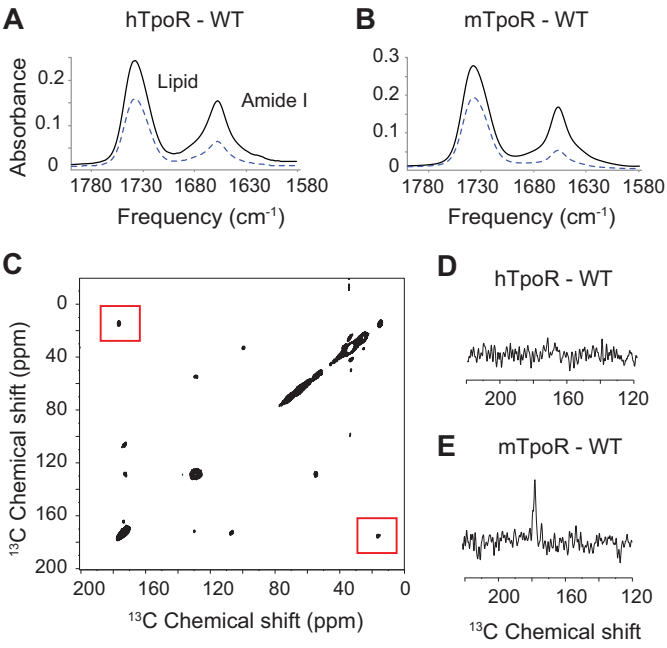

FIGURE 5. **Comparison reveals differences in the secondary structure and orientation of hTpoR and mTpoR TM peptides.** *A* and *B*, polarized IR spectra of hTpoR-WT and mTpoR-WT. *C*, two-dimensional dipolar assisted rotational resonance NMR of mTpoR-WT using TM peptides isotopically labeled at [1-^{13}C]Leu^{487}, [1-^{13}C]Val^{488}, and [3-^{13}C]Ala^{490}. The cross-peak (*boxed*) between the [3-^{13}C]Ala^{490} and the 1-^{13}C resonances of Leu^{487} and/or Val^{488} is consistent with α-helical secondary structure in this region of the TM-JM peptide. *D*, row through the [3-^{13}C]Ala^{497} resonance of hTpoR showing the absence of a cross-peak to either Leu^{494} or Val^{495}, which is consistent with a kink or break in helical secondary structure in this region of the TM-JM peptide. *E*, row through the [3-^{13}C]Ala^{490} resonance of mTpoR showing a strong cross-peak to Leu^{487} and/or Val^{488}.

In addition to the observation of intrahelical cross-peaks in mTpoR, there are distinct changes in chemical shifts of the

Downloaded from http://www.jbc.org/ at UNIVERSITE CATHOLIQUE LOUVAIN on June 27, 2016

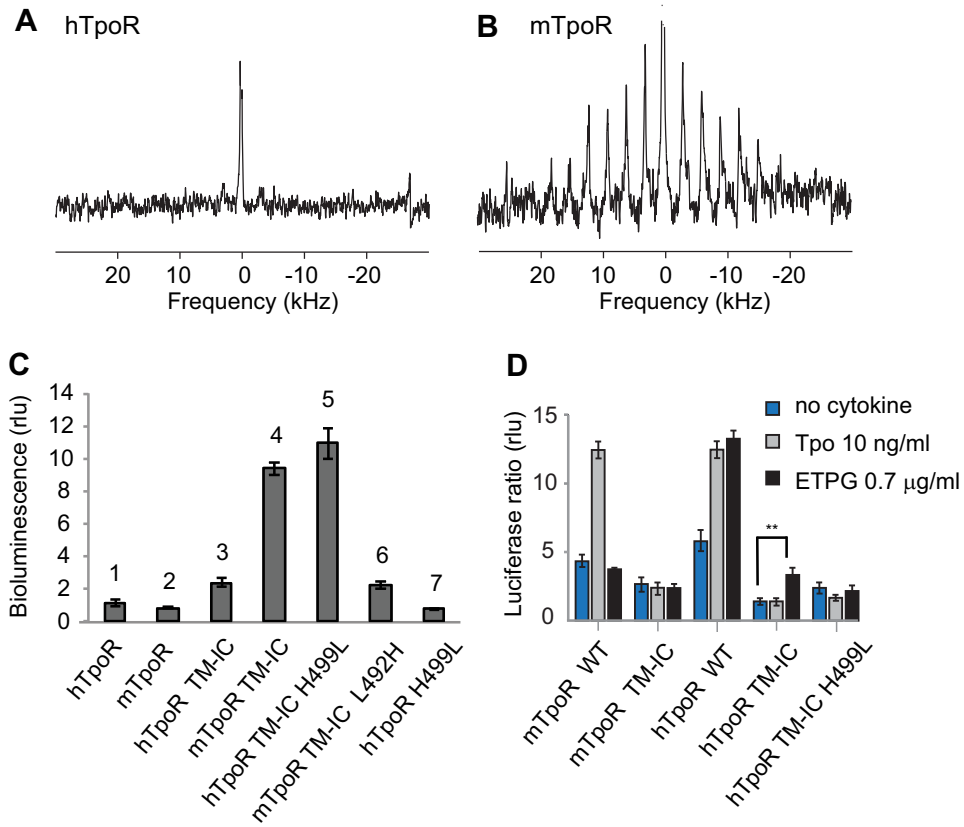

FIGURE 6. **Comparison reveals differences in dimerization of the hTpoR and mTpoR TM peptides.** Deuterium MAS NMR spectra of hTpoR-WT (*A*) and mTpoR-WT (*B*) are shown. The peptides contained deuterated leucine at position 512 (hTpoR) or 505 (mTpoR). *C*, dimerization of full-length hTpoR and mTpoR. Dimerization was detected using the split luciferase assay in cell lysates. hGluc-tagged full-length or TM-IC forms of TpoR as well as mutant hTpoR TM-IC-H499L were co-expressed in BOSC cells, and luciferase activity was measured after cell lysis. *D*, STAT5 transcriptional activity as measured by the split luciferase assay. Histograms are means ± S.D. (*error bars*) of four independent experiments. **, $p < 0.001$, one-way analysis of variance. *ETPG*, eltrombopag; *rlu,* relative luciferase units.

$^{13}C{=}O$ resonances between the hTpoR and mTpoR sequences (Table 1). The $^{13}C{=}O$ chemical shifts above ~174 ppm in the mTpoR-WT peptide are consistent with a helical geometry, whereas chemical shifts below ~174 ppm are consistent with unraveling of the helix just N-terminal to His^{499}.

Table 1 summarizes the polarized IR and NMR measurements on hTpoR-WT, mTpoR-WT, and several mutants. There is a general correlation between the dichroic ratio and the presence of helical secondary structure above Leu^{492} (mTpoR) and His^{499} (hTpoR). That is, the TM helices adopt a more parallel orientation (low tilt) when helical structure is observed around Leu^{492} or His^{499}. In the section below, we show that these changes are associated with the ability of the TM helix to dimerize. The comparisons suggest that hTpoR-H499L is structurally similar to mTpoR-WT and that mTpoR-L492H is structurally similar to hTpoR-WT.

The TM Domain of mTpoR Has a Stronger Propensity to Dimerize than hTpoR—In the wild-type and mutant TpoR peptides, dimerization can be estimated from deuterium MAS NMR spectra (28). In these experiments, the peptides are deuterated at Leu^{512} (hTpoR) or Leu^{505} (mTpoR). Comparison of the deuterium MAS NMR spectra of hTpoR-WT and mTpoR-WT reveals a large difference in the MAS spectra (Fig. 6, *A* and *B*). We have previously shown that fast rotational diffusion of the hTpoR monomer results in the loss of the side band pattern and that mutations in the TM and JM regions that lead to dimerization restore the MAS rotational side bands (28). On the basis of the observed side band pattern, we conclude that the monomer-dimer equilibrium in mTpoR-WT is shifted toward dimer compared with hTpoR-WT. The deuterium side band pattern characteristic of dimerization is observed for the activating mutants of hTpoR (S505N and G509N) (Table 1). TM dimerization is also observed for the activating mutants of mTpoR (S498N, G502N, and W508K).

The *G. princeps* luciferase complementation assay (28, 33) was used to assess the dimerization status of the full-length as well as of truncated mouse and human TpoRs containing TM/intracellular (IC) domains. In this assay, two proteins of interest are fused to complementary fragments of *G. princeps* luciferase, denoted hGluc1 and hGluc2. If the proteins interact, luciferase fragments are brought together and fold into their native structure, and the reconstituted luciferase enzyme catalyzes the oxidation of the substrate coelenterazine, which can be detected and quantified using luminescence readers.

The C terminus of murine or human TpoR was fused to complementary fragments of *G. princeps* luciferase (hGluc1 and hGluc2) and transiently co-expressed in BOSC cells where their expression levels were comparable and could be assessed by Western blotting (data not shown). The expression of these constructs individually as expected did not result in reconstitu-

Downloaded from http://www.jbc.org/ at UNIVERSITE CATHOLIQUE LOUVAIN on June 27, 2016

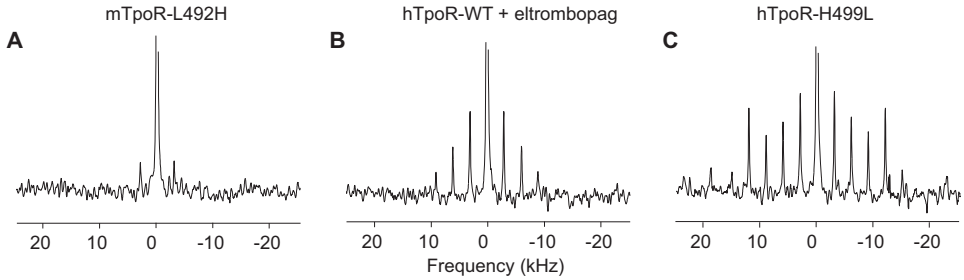

FIGURE 7. **Influence of His^{499} and eltrombopag on TM dimerization.** Deuterium NMR spectra of mTpoR-L492H (*A*), hTpoR-WT with eltrombopag (*B*), and hTpoR-H499L (*C*) are shown. The absence of side bands in the MAS spectra of mTpoR-L492H reflects rapid axial rotation of the peptide in the membrane bilayers. Dimerization induced in the hTpoR-WT peptide by eltrombopag and by the H499L mutation reduces axial diffusion rate and leads to increased intensity in the MAS side bands.

tion of luciferase activity (28). The complementation of hGluc-tagged murine and human full-length TpoR was relatively low and appeared to be at similar levels (Fig. 6*C*, conditions 1 and 2), indicating that the level of preformed dimers detected by proximity of cytosolic domains is low. Importantly, removal of the extracellular domain resulted in significantly higher dimerization of the mTpoR (condition 4) but not of the hTpoR (condition 3) whose dimerization remained the same compared with the full-length receptor. Thus, the hTpoR TM-IC segment possesses an additional mechanism to prevent its self-dimerization that could be ascribed to His^{499}. Indeed, substitution of His^{499} to leucine allows dimerization of the TM-IC form of hTpoR (condition 5), whereas substitution of Leu^{492} to histidine in the TM-IC form of the mTpoR dramatically decreased dimerization as assayed by luciferase complementation (condition 6).

The results in Fig. 6*C* for the TM-IC constructs are consistent with the NMR analysis of the TM-JM peptides, namely that His^{499} prevents dimerization of the TM domain of hTpoR in the context of a truncated TpoR lacking the extracellular domain. Using the Dual-Luciferase assay to monitor receptor activity, we show in Fig. 6*D* that the TM-IC constructs of mTpoR are inactive despite increased dimerization. In the hTpoR constructs, truncation of the extracellular domain abolishes Tpo-dependent activity but still allows activation upon the addition of eltrombopag. This activation is not detected in the H499L mutant.

Eltrombopag Induces Dimerization of hTpoR TM Helix Peptides—Comparison of the hTpoR and mTpoR TM-JM peptides shows that the monomer-dimer equilibrium is shifted toward monomer in hTpoR-WT compared with mTpoR-WT (Fig. 6, *A* and *B*). Binding of the small molecule agonist eltrombopag induces receptor activation and requires the presence of His^{499} (40). In the absence of activation, His^{499} was previously shown to cause a kink in the TM helix (41). We asked whether this structure changes in the presence of eltrombopag and whether eltrombopag influences dimerization of the hTpoR TM domains. Comparison of hTpoR-WT peptides without (Fig. 6*A*) and with eltrombopag (Fig. 7*B*) shows a slight increase in the intensity of the deuterium MAS side bands, consistent with a shift toward the peptide dimer. Furthermore, the secondary structure around His^{499} becomes helical in the hTpoR-WT peptide in the presence of eltrombopag (Table 1). Increased dimerization agrees with the studies on the TM-IC constructs containing the full IC domain that exhibit an increase in activity upon eltrombopag binding (Fig. 6*D*). We also asked whether substituting His^{499} with leucine, the corresponding residue in mTpoR, would influence dimerization. Indeed, hTpoR-H499L also becomes more dimeric compared with hTpoR-WT (Fig. 7*C*), consistent with an observed increase in the dichroic ratio from polarized IR measurements (Table 1), whereas the mTpoR-L492H peptide becomes more monomeric compared with mTpoR-WT (Fig. 7*A*). The dimeric interfaces in Fig. 7, *B* and *C*, are predicted to be different between the inactive dimeric and active dimeric states of hTpoR (see below).

Rotational Orientation of TM Helices in Inactive and Active Dimers—Interhelical NMR measurements of specifically labeled 41-residue mTpoR peptides (Glu^{481}–Ser^{524}) allow us to probe the interface that mediates dimerization. In these experiments, two mTpoR peptides with complementary ^{13}C labeling were reconstituted together into 1,2-dimyristoyl-*sn*-glycero-3-phosphocholine/*1,2-dimyristoyl-sn-glycero-3-phosphoglycerol* bilayers at a peptide:lipid molar ratio of 1:60. The positions of the labels were selected on the basis of our previous engineered Put3 constructs that defined the inactive and active interfaces.

To probe the inactive dimer interface, two-dimensional ^{13}C NMR spectra were obtained on mTpoR-WT peptides containing ^{13}C-labeled Ala^{499} and Gly^{502}. One peptide was labeled with [3-^{13}C]Ala^{499} and [1-^{13}C]Gly^{502}, and the other was labeled with [1-^{13}C]Ala^{499} and [2-^{13}C]Gly^{502}. Ala^{499} is predicted to be in the inactive interface, whereas Gly^{502} is at the boundary between inactive and active interfaces. We observe a cross-peak between the diagonal 3-^{13}C and 1-^{13}C resonances of Ala^{499} (Fig. 8*A*) and between the diagonal 2-^{13}C and 1-^{13}C resonances of Gly^{502} (Fig. 8*B*). These ^{13}C-labeled carbons are on different peptides, and the cross-peak intensities are consistent with an interhelical [3-^{13}C]Ala^{499} to ^{13}C=O distance of ~5.4 Å and an interhelical [2-^{13}C]Gly^{502} to C=O distance of ~5.2 Å. An intrahelical cross-peak is also observed between the [2-^{13}C]Gly^{502} resonance and the [1-^{13}C]Ala^{499} resonance. These ^{13}C labels are on the same peptide and are estimated to be ~4.4 Å apart in an α-helical geometry. An intrahelical cross-peak between the [3-^{13}C]Ala^{499} and [1-^{13}C]Gly^{502} resonances was not observed as the distance between ^{13}C sites is >6 Å in an α-helix.

To probe the potential active interface(s), parallel two-dimensional NMR experiments were undertaken on mTpoR-S498N (Fig. 8, *C* and *D*). In contrast to the results above, we do not observe interhelical Ala^{499}-Ala^{499} or Gly^{502}-Gly^{502} cross-peaks in peptides containing this activating mutation, confirm-

Downloaded from http://www.jbc.org/ at UNIVERSITE CATHOLIQUE LOUVAIN on June 27, 2016

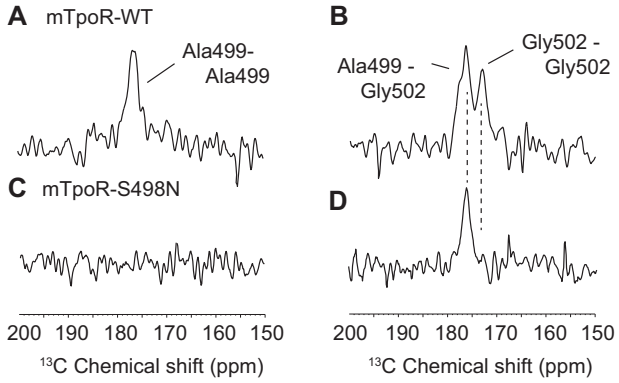

FIGURE 8. **Interhelical NMR measurements of mTpoR peptides (Glu^{481}–Ser^{524}).** *A*, row through the diagonal resonance of the [3-^{13}C]Ala^{499} carbon reveals a cross-peak with the [1-^{13}C]Ala^{499} C=O resonance. In an inactive dimer, the interhelical [3-^{13}C]Ala^{499} to [1-^{13}C]Ala^{499} distance is predicted to be ~5.4 Å. *B*, row through the diagonal resonance of [2-^{13}C]Gly^{502} reveals a cross-peak with the [1-^{13}C]Gly^{502} resonance where the predicted interhelical distance is ~5.2 Å. In this sample, an intrahelical cross-peak is also observed between [2-^{13}C]Gly^{502} and [1-^{13}C]Ala^{499}. *C* and *D*, dipolar assisted rotational resonance NMR experiments were undertaken on mTpoR-S498N using the same labeling strategy as in *A* and *B*. We do not observe Ala^{499}-Ala^{499} or Gly^{502}-Gly^{502} cross-peaks in peptides containing this activating mutation.

ing that we lose the inactive interface. The absence of contacts between these residues is consistent with a shift in the dimer interface to either the active cc-TpoR-I or cc-TpoR-V interfaces defined by engineered Put3 dimers, both of which contain Ser^{498} in the interface.

Models of the TM domain of the hTpoR in inactive and active orientations are shown in Fig. 9*A*. The inactive receptor exists in a monomer-dimer equilibrium. The split luciferase measurements of the full-length receptor along with deuterium NMR measurements of the hTpoR-WT TM-JM peptides indicate that the equilibrium is shifted toward monomer. His^{499} induces a break in the TM helix. The side chain of His^{499} is predicted to reside within the headgroup region of phospholipids on the extracellular side of the bilayer. Given the bilayer thickness, this requires the RWQFP motif to partition into the headgroup region of the phospholipids on the intracellular side of the bilayer. The active orientation is modeled as a dimer (Fig. 9*A*, *right*). In the wild-type full-length receptor, ligand binding drives a shift of the receptor dimer to an active orientation with Ser^{505} in the interface. Dimerization is also mediated by hydrogen bonding interactions involving the Asn side chains in the S505N mutant (Fig. 9*A*, *right*). In the TM-JM peptides, dimerization induces helical secondary structure in the region just N-terminal to His^{499} and reduces the overall dichroic ratio (helix tilt angle).

The inactive mTpoR also exists in a monomer-dimer equilibrium (Fig. 9*B*). In the absence of the extracellular domain, the equilibrium shifts toward dimer. The interface mediating the inactive dimer in TM-JM peptides involves packing of Ala^{499} and Gly^{502}. This interface is the same as that found in the engineered Put3 constructs (26). In the wild-type full-length receptor, ligand binding also drives a shift of the receptor dimer to an active orientation with Ser^{498} in the interface. Hydrogen bonding interactions involving Asn side chains stabilize this orientation in the S498N mutant (Fig. 9*B*, *right*).

Discussion

We show that several asparagine mutations in the TM domain of the mTpoR activate signaling, whereas only one asparagine substitution (S505N) does so for the hTpoR. Thus, human TpoR appears to be largely protected from oncogenic activation by Asn mutations. This major difference can be abolished if His^{499} in the hTpoR is substituted by leucine, the homologous residue in the mTpoR. We further show that His^{499} locally influences the structure and orientation of the TM helix, and this change influences the ability of receptors with specific TM asparagine mutations to traffic to the cell surface.

Receptor Dimerization in TpoR Signaling—Dimerization of the cytokine receptors is required for activation. The EpoR (24), prolactin receptor (42), and growth hormone receptor (22, 23) have been found to associate as preformed (inactive) dimers mediated by TM domain interactions. The implication is that there is a change in TM helix interfaces upon ligand binding and that this change is relayed to the intracellular domain to allow receptor activation.

Our previous studies indicated that, upon ligand binding or in the constitutively active S505N and W515K mutants, the monomer-dimer equilibrium shifts toward the active dimer (28). We extend these results here using the split luciferase assay to show that both the full-length hTpoR and mTpoR exist at a low level as preformed dimers with the majority of chains detected as monomers. Interestingly, removal of the extracellular domain induces receptor dimerization in the mTpoR but not the hTpoR.

The model that emerges is one where ligand binding triggers a conformational change in the extracellular domain that allows receptor dimerization in an active conformation. Using structural approaches, we are able to mimic the dimerization behavior of the murine and human receptors when the extracellular domain is removed (*i.e.* the TM-JM peptides and the TM-IC constructs are largely monomeric for hTpoR and dimeric for mTpoR). This observation indicates that the extracellular domain blocks the ability of the TM helices to directly interact in the mTpoR. In the hTpoR, there is an additional mechanism that blocks helix association, namely the change in the helix conformation induced by His^{499}. The H499L mutation induces constitutive dimerization of hTpoR in the absence of the extracellular domain in both the TM-IC constructs and the TM-JM peptides. In both the wild-type hTpoR receptor constructs and the TM-JM peptides, the ability of the activating Asn mutations and eltrombopag (for hTpoR) to induce dimerization strongly suggests that helix association is a key element of the activation mechanism.

The comparative studies on dimerization using the split luciferase assay between the full-length WT TpoRs and the corresponding truncated TM-IC constructs show large differences in receptor dimerization. We have previously compared dimerization for hTpoR-WT and murine EpoR-WT using the split luciferase assay and observed a 2-fold difference in bioluminescence, indicating that both the hTpoR and murine EpoR receptors exist in a monomer-dimer equilibrium with murine EpoR shifted more toward the receptor dimer (28). The subpopulation of preformed dimers may be the relevant form for

Downloaded from http://www.jbc.org/ at UNIVERSITE CATHOLIQUE LOUVAIN on June 27, 2016

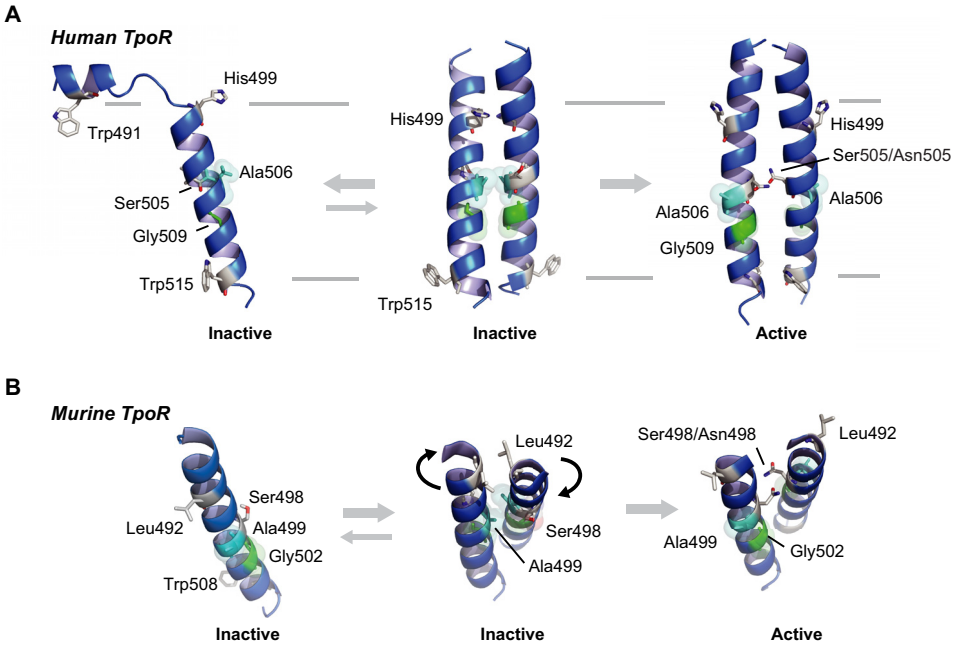

FIGURE 9. **Models of the monomeric and dimeric TM domains of the hTpoR and mTpoR.** *A*, human TpoR. FTIR and NMR measurements on the TM-JM domain of hTpoR show that the wild-type peptide is primarily monomer (*left*) with a break in helical secondary structure in the region N-terminal to His^{499}. In the S505N mutant of the hTpoR TM-JM domain (*right*), an increase in the dichroic ratio of the amide I vibration indicates that the TM helix is oriented closer to the bilayer normal, whereas the NMR measurements indicate that helix is induced in the region N-terminal to His^{499}. In the full-length receptor, we propose that the monomer and inactive dimer (*middle*) are in equilibrium and that either ligand binding or the S505N mutation shifts the equilibrium to the active dimer with either Ser^{505} (WT) or Asn^{505} (mutant) in the dimer interface. *B*, murine TpoR. FTIR and NMR measurements on the TM-JM domain of mTpoR show that the wild-type peptide is primarily dimer (*middle*) in which dimerization is mediated by close packing of Ala^{499} and Gly^{502}. *D*, in the full-length receptor, we propose that the monomer (*right*) and inactive dimer are in equilibrium and that either ligand binding or the S498N mutation shifts the equilibrium to the active dimer with either Ser^{498} (WT) or Asn^{498} (mutant) in the dimer interface. The dimer structures of hTpoR-S505N, mTpoR-WT, and mTpoR-S505N were taken from computational searches using the program CHI (52, 53) as described previously (26). These low energy structures correspond to the average of several structures in the searches that form clusters and best reproduce the experimental data presented here.

rapid signaling by TpoR. Although our studies reveal clear differences in dimerization in comparisons of (for *e.g.*) the full-length hTpoR and hTpoR TM-IC-H499L, they open up the question as to how different cell types or membrane environments influence the monomer-dimer equilibrium. For example, there may be differences in the monomer-dimer equilibrium (and hence the level of preformed dimers) between TpoR-expressing cells, namely hematopoietic stem cells and megakaryocyte progenitors, or there may be a shift in equilibrium if the membrane environment changes, such as incorporation of receptors into lipid rafts. The ability of the cell to modulate the monomer-dimer equilibrium would provide an additional control mechanism for receptor activation.

TM Helix Orientation in TpoR Signaling—The orientation of the TM and intracellular domains within dimers of single TM receptors is generally important for activation. In both the EpoR (32) and TpoR (26), we have shown using Put3 coiled coil constructs that receptor activity is dependent on the orientation of the TM helix. For mTpoR, only one dimeric interface (cc-TpoR-II) is inactive. The cc-TpoR-II interface is lined with leucines and an A*XX*G motif and ends with Gln^{509} within the (K/R)WQFP motif, corresponding to Gln^{516} in the hTpoR. The A*XX*G sequence has similarities with the G*XXX*G sequences known to mediate TM dimerization (43, 44). The close packing of the TM helices due to these small side chains places Gln^{509} of mTpoR in a position where it can mediate interhelical hydrogen bonding and stabilize dimerization. We ascribe this inactive interface to the same interface that mediates dimerization of the inactive TM-IC constructs of mTpoR. Moreover, we show with NMR (Fig. 8) that the TM-JM peptides (also lacking a large extracellular domain and hence similar to the TM-IC constructs) dimerize via the same interface as in the inactive cc-TpoR-II construct.

In contrast, several interfaces in the Put3 coiled coil constructs have previously been shown to exhibit various levels of activity (26). cc-TpoR-I induced high numbers of platelets without other cytological features of myeloproliferation in bone marrow, and cc-TpoR-V induced a myeloproliferative phenotype with small red blood cells and variable levels of thrombocytosis (26). Thus, the active helix interfaces identified in the Put3 experiments are consistent with the Asn substitutions reported here, at least for the mTpoR. That is, the cc-TpoR-I and cc-TpoR-V interfaces involve the residues where asparagine mutations lead to the strongest activity (V494N, S498N, L501N, and G502N). In cc-TpoR-V, the dimer interface is mediated by an S*XXX*G sequence, which again allows close helix packing. In our NMR studies, the S498N mutation induces a change in the conformation of the mTpoR peptide dimer, and we lose the contacts between Ala^{499} and Gly^{502} characteristic of the inactive dimer (Fig. 8). The low energy structure shown in Fig. 9*B* corresponds to cc-TpoR-I in which Asn^{498} forms interhelical hydrogen bonds.

Eltrombopag Drives Dimerization of hTpoR-WT—Eltrombopag is a Food and Drug Administration-approved drug used

Downloaded from http://www.jbc.org/ at UNIVERSITE CATHOLIQUE LOUVAIN on June 27, 2016

for the treatment of thrombocytopenia (low platelet numbers). Previous studies have found that eltrombopag can activate hTpoR but not mTpoR (40). Eltrombopag and related small molecule agonists have been found to interact with His^{499} (41). We find that this transmembrane-acting compound increases the dichroic ratio in FTIR measurements, induces helix in the Leu^{494}–Ala^{497} sequence in the TM domain, and leads to receptor dimerization as assayed by deuterium NMR line shapes. The changes in dimerization induced by eltrombopag (Fig. 7*B*) are weaker than those observed for the H499L mutant (Fig. 7*C*). Nevertheless, eltrombopag appears to induce receptor activation in a similar manner as the S505N mutation; namely, both overcome the ability of His^{499} to inhibit TM dimerization.

Multiple Levels of Regulation Involving the TM and JM Regions of TpoR—The wild-type hTpoR has several mechanisms for regulating dimerization of the TM region of the receptor. These involve the extracellular domain, the TM His^{499} residue, and the intracellular RWQFP insert. Removal of the extracellular domain or the H499L mutation alone does not induce dimerization. Both are required in the same construct. Ligand binding within the extracellular domain or mutations of Trp^{515} within the RWQFP insert can both overcome these mechanisms, leading to an active receptor conformation. In the mTpoR, removal of the extracellular domain induces dimerization in an inactive conformation. Dual-Luciferase measurements of receptor activation show that the TM-IC constructs of mTpoR are inactive. Thus, dimerization *per se* does not suffice for activation. Interestingly, the TM-IC constructs differ from the viral Mpl protein of the myeloproliferative leukemia virus by the presence of an extracellular domain of 109 amino acids comprising 43 from the original murine sequence and 66 from the Friend murine leukemia virus. This suggests that the extracellular amino acids in the v-Mpl are able to stabilize the TM-IC portion of the receptor in an active orientation.

Our results reveal that the TM helices in TpoR are not passive elements in ligand-induced dimerization. The TM helices have a stronger propensity to form dimers or higher order oligomers than to remain in a monomeric state. The extracellular, juxtamembrane, and intracellular domains all contribute to modulating TM association. This observation may generally hold for ligand-induced activation of single TM receptors. For example, the TM helices in the *ErbB* family of receptor tyrosine kinases all have a strong propensity to dimerize (45), and removal of the extracellular domain can lead to active dimers (46, 47) or can trigger intramembrane proteolysis (48, 49). In these receptors, the juxtamembrane sequences play an influential role in dimerization and activation (50). Mutation of Val^{664} to Gln in the TM sequence of the *ErbB2-Neu* receptor can induce dimerization and constitutive receptor activation in a manner similar to the S505N mutation in hTpoR (51).

The additional layer of activity control exerted by His^{499} in hTpoR may reflect the central role that this receptor plays in hematopoiesis. TpoR not only regulates megakaryocyte/platelet development but also contributes to the survival of hematopoietic stem cells, which give rise to all other blood cells. The acquisition of histidine at position 499 during evolution protects the hTpoR from the transforming effect of several Asn TM mutations that are activating in the mTpoR.

Author Contributions—S. O. S. and S. N. C. conceived and designed the study, interpreted the data, and wrote the paper. E. L. and J.-P. D. designed and performed experiments (γ2A luciferase assays, Ba/F3 cell retroviral transduction, sorting, cell surface labeling, and proliferation), analyzed the data, prepared the figures, and wrote the paper. J. S. designed and performed experiments (γ2A luciferase assays, Ba/F3 cell retroviral transduction, sorting, cell surface labeling, and proliferation). S. M. M. performed cloning and expression of TpoR constructs. E. L. performed intracellular TpoR metabolism studies. T. S. synthesized and purified the TM peptides. S. D. carried out membrane reconstitutions and FTIR studies. V. G. performed the *Gaussia* luciferase experiments.

Acknowledgments—We are grateful to Dr. Martine Ziliox for assistance with the NMR experiments. We also thank Drs. Ian Brett and Miki Itaya for preliminary experiments that formed the basis for the studies described here, Céline Mouton for expert technical support, and Dr. Nicolas Dauguet for flow cytometry and cell sorting. We gratefully acknowledge the W. M. Keck Foundation for support of the NMR facilities in the Center of Structural Biology at Stony Brook.

References

1. Geddis, A. E., Linden, H. M., and Kaushansky, K. (2002) Thrombopoietin: a pan-hematopoietic cytokine. *Cytokine Growth Factor Rev.* **13,** 61–73
2. Vigon, I., Mornon, J. P., Cocault, L., Mitjavila, M. T., Tambourin, P., Gisselbrecht, S., and Souyri, M. (1992) Molecular-cloning and characterization of Mpl, the human homolog of the v-mpl oncogene—identification of a member of the hematopoietic growth-factor receptor superfamily. *Proc. Natl. Acad. Sci. U.S.A.* **89,** 5640–5644
3. Watowich, S. S., Yoshimura, A., Longmore, G. D., Hilton, D. J., Yoshimura, Y., and Lodish, H. F. (1992) Homodimerization and constitutive activation of the erythropoietin receptor. *Proc. Natl. Acad. Sci. U.S.A.* **89,** 2140–2144
4. Syed, R. S., Reid, S. W., Li, C., Cheetham, J. C., Aoki, K. H., Liu, B., Zhan, H., Osslund, T. D., Chirino, A. J., Zhang, J., Finer-Moore, J., Elliott, S., Sitney, K., Katz, B. A., Matthews, D. J., Wendoloski, J. J., Egrie, J., and Stroud, R. M. (1998) Efficiency of signalling through cytokine receptors depends critically on receptor orientation. *Nature* **395,** 511–516
5. de Vos, A. M., Ultsch, M., and Kossiakoff, A. A. (1992) Human growth-hormone and extracellular domain of its receptor: crystal structure of the complex. *Science* **255,** 306–312
6. Royer, Y., Staerk, J., Costuleanu, M., Courtoy, P. J., and Constantinescu, S. N. (2005) Janus kinases affect thrombopoietin receptor cell surface localization and stability. *J. Biol. Chem.* **280,** 27251–27261
7. Constantinescu, S. N., Huang, L. J., Nam, H., and Lodish, H. F. (2001) The erythropoietin receptor cytosolic juxtamembrane domain contains an essential, precisely oriented, hydrophobic motif. *Mol. Cell* **7,** 377–385
8. Tanner, J. W., Chen, W., Young, R. L., Longmore, G. D., and Shaw, A. S. (1995) The conserved box-1 motif of cytokine receptors is required for association with JAK kinases. *J. Biol. Chem.* **270,** 6523–6530
9. Quelle, F. W., Sato, N., Witthuhn, B. A., Inhorn, R. C., Eder, M., Miyajima, A., Griffin, J. D., and Ihle, J. N. (1994) Jak2 associates with the β_C chain of the receptor far granulocyte-macrophage colony-stimulating factor, and Its activation requires the membrane-proximal region. *Mol. Cell. Biol.* **14,** 4335–4341
10. Tong, W., Sulahian, R., Gross, A. W., Hendon, N., Lodish, H. F., and Huang, L. J. (2006) The membrane-proximal region of the thrombopoietin receptor confers its high surface expression by JAK2-dependent and -independent mechanisms. *J. Biol. Chem.* **281,** 38930–38940
11. Sabath, D. F., Kaushansky, K., and Broudy, V. C. (1999) Deletion of the extracellular membrane-distal cytokine receptor homology module of Mpl results in constitutive cell growth and loss of thrombopoietin binding. *Blood* **94,** 365–367
12. Staerk, J., Lacout, C., Sato, T., Smith, S. O., Vainchenker, W., and Constantinescu, S. N. (2006) An amphipathic motif at the transmembrane-cytoplasmic junction prevents autonomous activation of the thrombopoi-

Downloaded from http://www.jbc.org/ at UNIVERSITE CATHOLIQUE LOUVAIN on June 27, 2016

216

etin receptor. *Blood* **107,** 1864–1871
13. Malinge, S., Ragu, C., Della-Valle, V., Pisani, D., Constantinescu, S. N., Perez, C., Villeval, J. L., Reinhardt, D., Landman-Parker, J., Michaux, L., Dastugue, N., Baruchel, A., Vainchenker, W., Bourquin, J. P., Penard-Lacronique, V., and Bernard, O. A. (2008) Activating mutations in human acute megakaryoblastic leukemia. *Blood* **112,** 4220–4226
14. Ding, J., Komatsu, H., Wakita, A., Kato-Uranishi, M., Ito, M., Satoh, A., Tsuboi, K., Nitta, M., Miyazaki, H., Iida, S., and Ueda, R. (2004) Familial essential thrombocythemia associated with a dominant-positive activating mutation of the c-MPL gene, which encodes for the receptor for thrombopoietin. *Blood* **103,** 4198–4200
15. Onishi, M., Mui, A. L., Morikawa, Y., Cho, L., Kinoshita, S., Nolan, G. P., Gorman, D. M., Miyajima, A., and Kitamura, T. (1996) Identification of an oncogenic form of the thrombopoietin receptor MPL using retrovirus-mediated gene transfer. *Blood* **88,** 1399–1406
16. Marty, C., Chaligné, R., Lacout, C., Constantinescu, S. N., Vainchenker, W., and Villeval, J. L. (2009) Ligand-independent thrombopoietin mutant receptor requires cell surface localization for endogenous activity. *J. Biol. Chem.* **284,** 11781–11791
17. Pecquet, C., Staerk, J., Chaligné, R., Goss, V., Lee, K. A., Zhang, X., Rush, J., Van Hees, J., Poirel, H. A., Scheiff, J. M., Vainchenker, W., Giraudier, S., Polakiewicz, R. D., and Constantinescu, S. N. (2010) Induction of myeloproliferative disorder and myelofibrosis by thrombopoietin receptor W515 mutants is mediated by cytosolic tyrosine 112 of the receptor. *Blood* **115,** 1037–1048
18. Pardanani, A. D., Levine, R. L., Lasho, T., Pikman, Y., Mesa, R. A., Wadleigh, M., Steensma, D. P., Elliott, M. A., Wolanskyj, A. P., Hogan, W. J., McClure, R. F., Litzow, M. R., Gilliland, D. G., and Tefferi, A. (2006) MPL515 mutations in myeloproliferative and other myeloid disorders: a study of 1182 patients. *Blood* **108,** 3472–3476
19. Pikman, Y., Lee, B. H., Mercher, T., McDowell, E., Ebert, B. L., Gozo, M., Cuker, A., Wernig, G., Moore, S., Galinsky, I., DeAngelo, D. J., Clark, J. J., Lee, S. J., Golub, T. R., Wadleigh, M., Gilliland, D. G., and Levine, R. L. (2006) MPLW515L is a novel somatic activating mutation in myelofibrosis with myeloid metaplasia. *PLoS Med.* **3,** e270
20. Livnah, O., Stura, E. A., Middleton, S. A., Johnson, D. L., Jolliffe, L. K., and Wilson, I. A. (1999) Crystallographic evidence for preformed dimers of erythropoietin receptor before ligand activation. *Science* **283,** 987–990
21. Brown, R. J., Adams, J. J., Pelekanos, R. A., Wan, Y., McKinstry, W. J., Palethorpe, K., Seeber, R. M., Monks, T. A., Eidne, K. A., Parker, M. W., and Waters, M. J. (2005) Model for growth hormone receptor activation based on subunit rotation within a receptor dimer. *Nat. Struct. Mol. Biol.* **12,** 814–821
22. Brooks, A. J., Chhabra, Y., Abankwa, D., O'Mara, M., Dai, W., Gardon, O., Tunny, K. A., Blucher, K. M., Morton, C. J., Parker, M. W., Sierecki, E., Gambin, Y., Gomez, G. A., Alexandrov, K. K., Doxastakis, M., Mark, A. E., and Waters, M. J. (2014) A new cytokine receptor activation paradigm: activation of JAK2 by the growth hormone receptor. *Cytokine* **70,** 22
23. Brooks, A. J., Dai, W., O'Mara, M. L., Abankwa, D., Chhabra, Y., Pelekanos, R. A., Gardon, O., Tunny, K. A., Blucher, K. M., Morton, C. J., Parker, M. W., Sierecki, E., Gambin, Y., Gomez, G. A., Alexandrov, K., Wilson, I. A., Doxastakis, M., Mark, A. E., and Waters, M. J. (2014) Mechanism of activation of protein kinase JAK2 by the growth hormone receptor. *Science* **344,** 1249783
24. Constantinescu, S. N., Keren, T., Socolovsky, M., Nam, H., Henis, Y. I., and Lodish, H. F. (2001) Ligand-independent oligomerization of cell-surface erythropoietin receptor is mediated by the transmembrane domain. *Proc. Natl. Acad. Sci. U.S.A.* **98,** 4379–4384
25. Ebie, A. Z., and Fleming, K. G. (2007) Dimerization of the erythropoietin receptor transmembrane domain in micelles. *J. Mol. Biol.* **366,** 517–524
26. Staerk, J., Defour, J.-P., Pecquet, C., Leroy, E., Antoine-Poirel, H., Brett, I., Itaya, M., Smith, S. O., Vainchenker, W., and Constantinescu, S. N. (2011) Orientation-specific signalling by thrombopoietin receptor dimers. *EMBO J.* **30,** 4398–4413
27. Matthews, E. E., Thévenin, D., Rogers, J. M., Gotow, L., Lira, P. D., Reiter, L. A., Brissette, W. H., and Engelman, D. M. (2011) Thrombopoietin receptor activation: transmembrane helix dimerization, rotation, and allosteric modulation. *FASEB J.* **25,** 2234–2244
28. Defour, J.-P., Itaya, M., Gryshkova, V., Brett, I. C., Pecquet, C., Sato, T., Smith, S. O., and Constantinescu, S. N. (2013) Tryptophan at the transmembrane-cytosolic junction modulates thrombopoietin receptor dimerization and activation. *Proc. Natl. Acad. Sci. U.S.A.* **110,** 2540–2545
29. Zhou, F. X., Cocco, M. J., Russ, W. P., Brunger, A. T., and Engelman, D. M. (2000) Interhelical hydrogen bonding drives strong interactions in membrane proteins. *Nat. Struct. Biol.* **7,** 154–160
30. Zhou, F. X., Merianos, H. J., Brunger, A. T., and Engelman, D. M. (2001) Polar residues drive association of polyleucine transmembrane helices. *Proc. Natl. Acad. Sci. U.S.A.* **98,** 2250–2255
31. Choma, C., Gratkowski, H., Lear, J. D., and DeGrado, W. F. (2000) Asparagine-mediated self-association of a model transmembrane helix. *Nat. Struct. Biol.* **7,** 161–166
32. Seubert, N., Royer, Y., Staerk, J., Kubatzky, K. F., Moucadel, V., Krishnakumar, S., Smith, S. O., and Constantinescu, S. N. (2003) Active and inactive orientations of the transmembrane and cytosolic domains of the erythropoietin receptor dimer. *Mol. Cell* **12,** 1239–1250
33. Remy, I., and Michnick, S. W. (2006) A highly sensitive protein-protein interaction assay based on *Gaussia* luciferase. *Nat. Methods* **3,** 977–979
34. Liu, W., Crocker, E., Constantinescu, S. N., and Smith, S. O. (2005) Helix packing and orientation in the transmembrane dimer of gp55-P of the spleen focus forming virus. *Biophys. J.* **89,** 1194–1202
35. Rothschild, K. J., and Clark, N. A. (1979) Polarized infrared spectroscopy of oriented purple membrane. *Biophys. J.* **25,** 473–487
36. Takegoshi, K., Nakamura, S., and Terao, T. (2001) ^{13}C-^{1}H dipolar-assisted rotational resonance in magic-angle spinning NMR. *Chem. Phys. Lett.* **344,** 631–637
37. Landschulz, W. H., Johnson, P. F., and McKnight, S. L. (1988) The leucine zipper: a hypothetical structure common to a new class of DNA binding proteins. *Science* **240,** 1759–1764
38. O'Shea, E. K., Klemm, J. D., Kim, P. S., and Alber, T. (1991) X-ray structure of the GCN4 leucine zipper, a two-stranded, parallel coiled coil. *Science* **254,** 539–544
39. Lear, J. D., Gratkowski, H., Adamian, L., Liang, J., and DeGrado, W. F. (2003) Position-dependence of stabilizing polar interactions of asparagine in transmembrane helical bundles. *Biochemistry* **42,** 6400–6407
40. Nakamura, T., Miyakawa, Y., Miyamura, A., Yamane, A., Suzuki, H., Ito, M., Ohnishi, Y., Ishiwata, N., Ikeda, Y., and Tsuruzoe, N. (2006) A novel nonpeptidyl human c-Mpl activator stimulates human megakaryopoiesis and thrombopoiesis. *Blood* **107,** 4300–4307
41. Kim, M. J., Park, S. H., Opella, S. J., Marsilje, T. H., Michellys, P. Y., Seidel, H. M., and Tian, S. S. (2007) NMR structural studies of interactions of a small, nonpeptidyl Tpo mimic with the thrombopoietin receptor extracellular juxtamembrane and transmembrane domains. *J. Biol. Chem.* **282,** 14253–14261
42. Gadd, S. L., and Clevenger, C. V. (2006) Ligand-independent dimerization of the human prolactin receptor isoforms: functional implications. *Mol. Endocrinol.* **20,** 2734–2746
43. MacKenzie, K. R., and Engelman, D. M. (1998) Structure-based prediction of the stability of transmembrane helix-helix interactions: the sequence dependence of glycophorin A dimerization. *Proc. Natl. Acad. Sci. U.S.A.* **95,** 3583–3590
44. Russ, W. P., and Engelman, D. M. (1999) TOXCAT: a measure of transmembrane helix association in a biological membrane. *Proc. Natl. Acad. Sci. U.S.A.* **96,** 863–868
45. Mendrola, J. M., Berger, M. B., King, M. C., and Lemmon, M. A. (2002) The single transmembrane domains of ErbB receptors self-associate in cell membranes. *J. Biol. Chem.* **277,** 4704–4712
46. Downward, J., Yarden, Y., Mayes, E., Scrace, G., Totty, N., Stockwell, P., Ullrich, A., Schlessinger, J., and Waterfield, M. D. (1984) Close similarity of epidermal growth-factor receptor and V-Erb-B oncogene protein sequences. *Nature* **307,** 521–527
47. Matsushime, H., Wang, L. H., and Shibuya, M. (1986) Human c-ros-1 gene homologous to the v-ros sequence of UR2 sarcoma virus encodes for a transmembrane receptorlike molecule. *Mol. Cell. Biol.* **6,** 3000–3004
48. Lee, H. J., Jung, K. M., Huang, Y. Z., Bennett, L. B., Lee, J. S., Mei, L., and Kim, T. W. (2002) Presenilin-dependent γ-secretase-like intramembrane cleavage of ErbB4. *J. Biol. Chem.* **277,** 6318–6323

Downloaded from http://www.jbc.org/ at UNIVERSITE CATHOLIQUE LOUVAIN on June 27, 2016

49. Vidal, G. A., Naresh, A., Marrero, L., and Jones, F. E. (2005) Presenilin-dependent γ-secretase processing regulates multiple ERBB4/HER4 activities. *J. Biol. Chem.* **280,** 19777–19783
50. Hubbard, S. R. (2004) Juxtamembrane autoinhibition in receptor tyrosine kinases. *Nat. Rev. Mol. Cell Biol.* **5,** 464–471
51. Bargmann, C. I., and Weinberg, R. A. (1988) Oncogenic activation of the *neu*-encoded receptor protein by point mutation and deletion. *EMBO J.* **7,** 2043–2052
52. Arkin, I. T., Adams, P. D., MacKenzie, K. R., Lemmon, M. A., Brünger, A. T., and Engelman, D. M. (1994) Structural organization of the pentameric transmembrane α-helices of phospholamban, a cardiac ion channel. *EMBO J.* **13,** 4757–4764
53. Adams, P. D., Arkin, I. T., Engelman, D. M., and Brünger, A. T. (1995) Computational searching and mutagenesis suggest a structure for the pentameric transmembrane domain of phospholamban. *Nat. Struct. Biol.* **2,** 154–162

Downloaded from http://www.jbc.org/ at UNIVERSITE CATHOLIQUE LOUVAIN on June 27, 2016

The EMBO Journal (2011) 30, 4398–4413 | © 2011 European Molecular Biology Organization | All Rights Reserved 0261-4189/11
www.embojournal.org

THE EMBO JOURNAL

Annex 4

Orientation-specific signalling by thrombopoietin receptor dimers

Judith Staerk[1,2,6,7], Jean-Philippe Defour[1,2,6], Christian Pecquet[1,2], Emilie Leroy[1,2], Hélène Antoine-Poirel[3], Ian Brett[4], Miki Itaya[4], Steven O Smith[4], William Vainchenker[5] and Stefan N Constantinescu[1,2,*]

[1]Ludwig Institute for Cancer Research, Brussels, Belgium, [2]de Duve Institute, Université Catholique de Louvain, Brussels, Belgium, [3]Cliniques Universitaires St-Luc, Université Catholique de Louvain, Brussels, Belgium, [4]Center for Structural Biology, Department of Biochemistry and Cell Biology, Stony Brook University, Stony Brook, NY, USA and [5]INSERM, U1009, Université Paris-Sud, Institut Gustave Roussy, Villejuif Cedex, France

Ligand binding to the thrombopoietin receptor is thought to stabilize an active receptor dimer that regulates megakaryocyte differentiation and platelet formation, as well as haematopoietic stem cell renewal. By fusing a dimeric coiled coil in all seven possible orientations to the thrombopoietin receptor transmembrane (TM)–cytoplasmic domains, we show that specific biological effects and *in vivo* phenotypes are imparted by distinct dimeric orientations, which can be visualized by cysteine mutagenesis and crosslinking. Using functional assays and computational searches, we identify one orientation that represents the inactive dimeric state and another similar to a physiologically activated receptor. Several other dimeric orientations are identified that induce proliferation and *in vivo* myeloproliferative and myelodysplastic disorders, indicating the receptor can signal from several dimeric interfaces. The set of dimeric thrombopoietin receptors with different TM orientations may offer new insights into the activation of distinct signalling pathways by a single receptor and suggests that subtle differences in cytokine receptor dimerization provide a new layer of signalling regulation that is relevant for disease.

The EMBO Journal (2011) **30,** 4398–4413. doi:10.1038/emboj.2011.315; Published online 2 September 2011
Subject Categories: signal transduction
Keywords: dimerization; hematopoiesis; JAK2; myeloproliferation; TpoR

*Corresponding author. Ludwig Institute for Cancer Research, Avenue Hippocrate 74, UCL 7459, Brussels 1200, Belgium. Tel.: +32 2 764 7540; Fax: +32 2 764 6566; E-mail: stefan.constantinescu@bru.licr.org
[6]These authors are co-first authors
[7]Present address: Whitehead Institute for Biomedical Research, Cambridge, MA 02142, USA

Received: 4 November 2010; accepted: 4 August 2011; published online: 2 September 2011

Introduction

The thrombopoietin (Tpo) receptor (TpoR, c-Mpl) is a key regulator of megakaryopoiesis (de Sauvage *et al*, 1994; Kaushansky, 1997), and of haematopoietic stem cell (HSC) renewal (Solar *et al*, 1998) and quiescence (Qian *et al*, 2007; Yoshihara *et al*, 2007). Binding of Tpo induces a conformational change of the receptor (Alexander *et al*, 1995), resulting in activation of the tyrosine kinases JAK2 and TYK2 (Drachman *et al*, 1995, 1999; Miyakawa *et al*, 1995; Watowich *et al*, 1996; Royer *et al*, 2005). Activated Janus kinases (JAKs) in turn phosphorylate tyrosine residues within the TpoR cytosolic domain that function as binding sites for downstream signalling molecules such as STAT3, STAT5 (the signal transducers and activators of transcription 3 and 5) and adaptors triggering phosphatydylinositol-3-kinase (PI-3-kinase) or Mitogen Activated Protein (MAP)-kinase activation (Miyakawa *et al*, 1995, 1996, 2001; Oda *et al*, 1996; Onishi *et al*, 1996; Drachman and Kaushansky, 1997).

Mutations that activate TpoR signalling in the absence of its ligand include single amino-acid substitutions by cysteine or asparagine in the extracellular and transmembrane (TM) domains, respectively (Alexander *et al*, 1995; Onishi *et al*, 1996; Ding *et al*, 2004), as well as mutations in the juxtamembrane (JM) region, on both the extracellular and intracellular sides (Pardanani *et al*, 2006; Pikman *et al*, 2006; Staerk *et al*, 2006; Malinge *et al*, 2008). Furthermore, truncation of part of the extracellular domain and fusion on the amino-terminus with a viral-derived sequence also activates TpoR signalling (Souyri *et al*, 1990). All these mutant receptors trigger cytokine-independent cell proliferation and induce myeloproliferative disorders presumably by ligand-independent dimerization in conformations productive for signalling (Alexander *et al*, 1995; Onishi *et al*, 1996; Ding *et al*, 2009). The precise dimeric interface(s) adopted by these active TpoR mutants remain however unknown.

Among cytokine receptors, TpoR is special as it plays essential roles at different stages of haematopoiesis. To carry out its multiple functions, different ligands and distinct cell types might induce changes in the active dimeric state of the receptor and its interaction with other cellular proteins. It is known that TpoR can respond to at least two ligands, Tpo (Kaushansky, 1997) and a human homologue of a fungal nuclear migration protein (hNUDC) (Chen *et al*, 2010). Very little is known about the dimeric structure of the activated TpoR TM and cytoplasmic domains. Whether the dimeric orientations adopted by ligand-activated TpoR differ in various cell types, megakaryocyte progenitors versus HSCs remains unclear. Different biologic effects of activated TpoR might result from interactions with other receptors or signalling proteins, which may be cell type specific. One hypothesis would posit that TpoR interacts with cell type-specific receptors and signalling proteins through different conformations of the TM and cytoplasmic domains of TpoR. This proposed mechanism for activation is quite different from that of

 ©2011 European Molecular Biology Organization

the erythropoietin receptor (EpoR), where essentially one dimeric conformation appears to be required for promoting erythroid cell formation (Seubert *et al*, 2003).

To test whether the TpoR requires a specific dimeric conformation for signalling or whether it signals from many different dimeric conformations, we replaced the extracellular domain of the TpoR by a dimeric coiled coil. By engineering the junction of the coiled coil to the TpoR TM domain, we were able to impose the seven possible relative orientations on the TM and cytoplasmic domains of the TpoR. In this approach, we obtain seven individual dimers that adopt different interfaces in the TM and intracellular JM domains, which are due to the register of the coiled coil. The JM cytosolic region of cytokine receptors was suggested to be rigid by both functional assays (Constantinescu *et al*, 2001; Huang *et al*, 2001) and by single particle electron microscopy (Skiniotis *et al*, 2008; Lupardus *et al*, 2011). The different orientations of the TM–JM region are thus likely to be transmitted to the cytosolic domain and influence signalling. Furthermore, in the case of the growth hormone receptor, subunit rotation in a receptor dimer was shown to suffice for activation (Brown *et al*, 2005). To show that the rotation induced by the coiled coil is transmitted, as predicted, to the JM region, we used two approaches, cysteine mutagenesis in combination with crosslinking and alanine insertions at the intracellular boundary.

We tested the biologic effects of the seven possible TpoR dimers in cell lines and *in vivo* in mouse bone marrow reconstitution experiments. This allowed us to use functional blood formation as a read-out in order to identify the precise dimer conformation that most faithfully resembles the effect of Tpo on platelet formation (*cc-TpoR*-I). To our surprise, five other dimeric conformations of the TpoR also led to proliferation of cytokine-dependent cells, with differences in cell morphology and signalling. *In vivo*, these orientations induce different effects, with two being associated with mixed myelodysplastic/myeloproliferative phenotypes, and others with myeloproliferation. We propose the model that different dimeric TpoR interfaces induce different biological outcomes and that different dimeric receptors could possibly favour different myeloproliferative and myelodysplastic disorders. Importantly, we show that this orientation-dependent signalling specificity requires the KWQFP motif in the JM region, which maintains the unliganded TpoR inactive (Staerk *et al*, 2006).

Results

Fusion of the Put3 coiled coil to the TpoR TM and cytosolic domains

The C-terminal 28 amino acids of Put3, a soluble transcriptional activator protein from *Saccharomyces cerevisiae*, associate in a stable left-handed coiled-coil dimer (Swaminathan *et al*, 1997; Walters *et al*, 1997). Fusion of the C-terminal residue of the Put3 sequence to the N-terminal residue of the TM sequence of the TpoR induces dimerization of the TpoR TM domain, which is known to be α-helical through F510 based on polarized infrared spectroscopy of membrane reconstituted peptides corresponding to the TM and JM domains (Supplementary Figure S1). Fusion of the Put3 coiled-coil domain imposes its structure on the α-helical residues downstream in the TM domain and enables us to identify the amino acids that are present in the interface of the active TpoR dimer (Figure 1A and B; Swaminathan *et al*, 1997; Walters *et al*, 1997). Position of heptad repeats characteristic of left-handed coiled coils are denoted *a*–*g* or *a*′–*g*′. The last residue of the Put3 coiled coil is in a *b* position. As a result, the first fused residue of the TpoR TM domain is in a *c* position (Figure 1B). By designing seven different junctions between the coiled coil and the TpoR TM domain, all possible dimeric receptor orientations can be imposed (Mattoon *et al*, 2001; Seubert *et al*, 2003), due to the registry and tight dimerization of the 28 amino acid Put3 coiled coil (Swaminathan *et al*, 1997; Walters *et al*, 1997).

We constructed seven TpoR fusion proteins where the Put3 coiled coil was fused to the TM and cytoplasmic domains of the TpoR, denoted *cc-TpoR*-0–VI. By varying the junction between the Put3 coiled coil and the TpoR TM and cytoplasmic sequences, all seven possible registers could be obtained (Figures 1A, B and 7A). All fusion proteins were expressed at the expected size of 27 kDa in Ba/F3 cells. In order to confirm the orientation of our *cc-TpoR* fusion proteins, we introduced a cysteine residue at position 505 (L505C) for crosslinking studies and eliminated all other cysteine residues by truncation of the cytosolic domain at position 553 in all *cc-TpoRs*. All the truncated fusion proteins were expressed in BOSC cells at the expected size of 12 kDa. Consistent with our hypothesis that only *cc-TpoR*-I, *cc-TpoR*-II and *cc-TpoR*-V should have L505C in the dimeric interface, we only visualized formation of *N*,*N*′-1,2-phenylenedimaleimide (o-PDM) crosslinked dimers for those three receptors (Figure 1C). Indeed, treatment of cells with o-PDM enables formation of intermolecular bonds maintaining stable dimers in denaturing conditions. Crosslinking on live cells, therefore, validates the orientation imposed by the coiled coil up to the outset of the cytosolic JM domain.

Cell surface expression levels of the *cc-TpoR*-0–VI proteins were measured by flow cytometry using an anti-HA tag antibody. Levels of *cc-TpoR* cell surface localization were between 20 and 40%, as compared with the wtTpoR levels, which were taken as 100% for the same level of GFP (Figure 1D).

Proliferation mediated by the cc-TpoR-0–VI fusion proteins

Ba/F3 cells were infected with retroviruses coding for the seven *cc-TpoR* fusion proteins and sorted for equal GFP levels. Cells were washed, grown in the absence of any cytokines and monitored by cell counting at different intervals. Four out of six active conformations induced maximal proliferation, *cc-TpoR*-0, -I, -III and -IV, while two, *cc-TpoR*-V and -VI, were able to promote growth of Ba/F3 cells, but to a lower extent (Figure 2A). *cc-TpoR*-II was inactive.

We next ensured that dimerization of the TpoR TM and cytoplasmic domains mediated by the Put3 coiled-coil fusion was required for the proliferative effects of the *cc-TpoR*-0–VI fusion proteins. We, therefore, substituted the lysine at position 86 within the Put3 amino-acid sequence by a proline (KtP). This mutation has been shown to block dimerization of the Put3 coiled coil (Swaminathan *et al*, 1997). The Put3-KtP substitution disabled cytokine-independent growth mediated by the *cc-TpoR* fusion proteins (Figure 2B), showing that dimerization mediated by the coiled-coil Put3 was crucial for the activity of *cc-TpoR* fusion proteins.

©2011 European Molecular Biology Organization

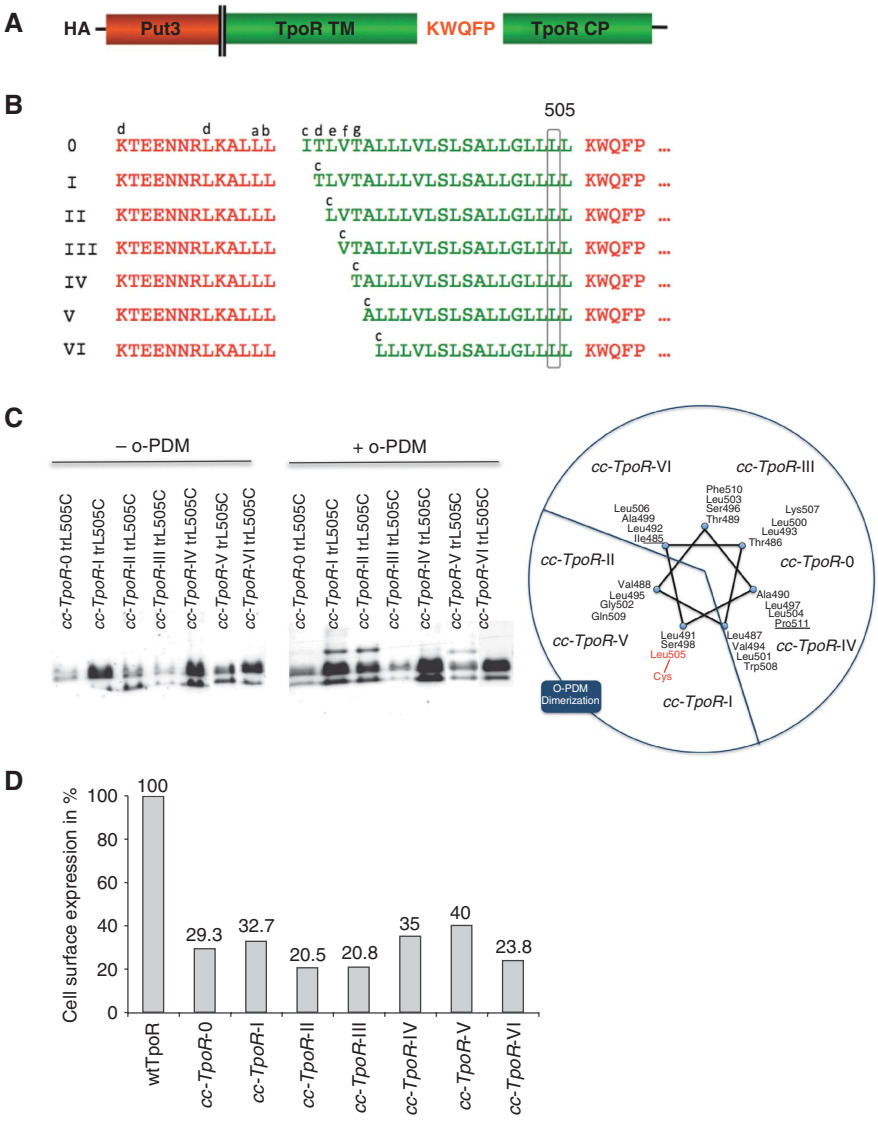

Figure 1 Design, validation and expression of seven fusion proteins that contain the Put3 coiled coil fused in all possible orientations to the TpoR TM–cytoplasmic domains. (**A**) Design of the *cc-TpoR* fusion proteins. The coiled-coil segment of Put3 was fused to the TM and cytoplasmic domains of TpoR. (**B**) By varying the junction between the Put3 coiled coil and the downstream TpoR TM α-helical domain, all seven possible registers could be imposed. All fusion proteins contain an HA tag at their N-terminus. The position of heptad repeats characteristic of coiled coils is denoted *a*–*g* or *a*′–*g*′. The last residue of the Put3 coiled-coil is in a *b* position, while the first fused residue will be in a *c* position. The dimeric interface contains the *a*, *d*, *d*′ and *a*′ positions. (**C**) Crosslinking studies on live cells. *Left panel*: BOSC cells were transiently transfected with cDNA coding for seven truncated coiled-coil TpoR cysteine mutants (L505C). Cells were lysed after crosslinking with *N*,*N*′-1,2-phenylenedimaleimide (+ o-PDM), or in the absence of crosslinking (− o-PDM). Lysates were analysed on 12–14% Bis-Tris Gel followed by immunoblotting with an anti-HA antibody. *Right panel:* Helical representation of the different *cc-TpoR* interfaces and the putative localization of the Cys505 residue. (**D**) HA staining for cell surface expression of the *cc-TpoR* fusion proteins. The wtTpoR cell surface expression was set as 100%. Percent expression of the *cc-TpoR* fusion proteins was related to that of the wtTpoR. Shown is one experiment with data collected for 10 000 cells of three independent determinations; variations were <10%.

Ba/F3 cells expressing the active *cc-TpoR* fusion proteins showed remarkable differences in their morphology. When cells expressed *cc-TpoR*-IV, large clusters were observed (Figure 2C). In contrast, cells that expressed *cc-TpoR*-I or *cc-TpoR*-III did not induce such strong cell-to-cell interactions, although they induced proliferation at similar levels (Figure 2A). Interestingly, *cc-TpoR*-IV induced cell-to-cell adhesion in many cell lines and in primary bone marrow haematopoietic progenitors, both in suspension and in methylcellulose assays (not shown). To examine the ability of the wtTpoR to induce such cell-to-cell interactions, we stimulated wtTpoR expressing Ba/F3 cells (Ba/F3-TpoR) using Tpo concentrations between 5 and 500 ng/ml. Ba/F3-wtTpoR stimulated with extremely high Tpo concentrations (500 ng/ml) formed the same cell clusters (Figure 2C, right panel), as observed with *cc-TpoR*-IV, whereas at lower doses (5 ng/ml) only small clusters could be seen (Figure 2C, left panel). Thus, in the dimeric conformation adopted by *cc-TpoR*-IV, signalling events appear to be similar to those induced by very high Tpo levels via the wtTpoR. Such high levels may be attained in the bone marrow endosteal niches, close to HSC reservoirs.

Our results using the seven *cc-TpoR* fusion proteins suggest that the TpoR can signal from multiple dimeric conforma-

©2011 European Molecular Biology Organization

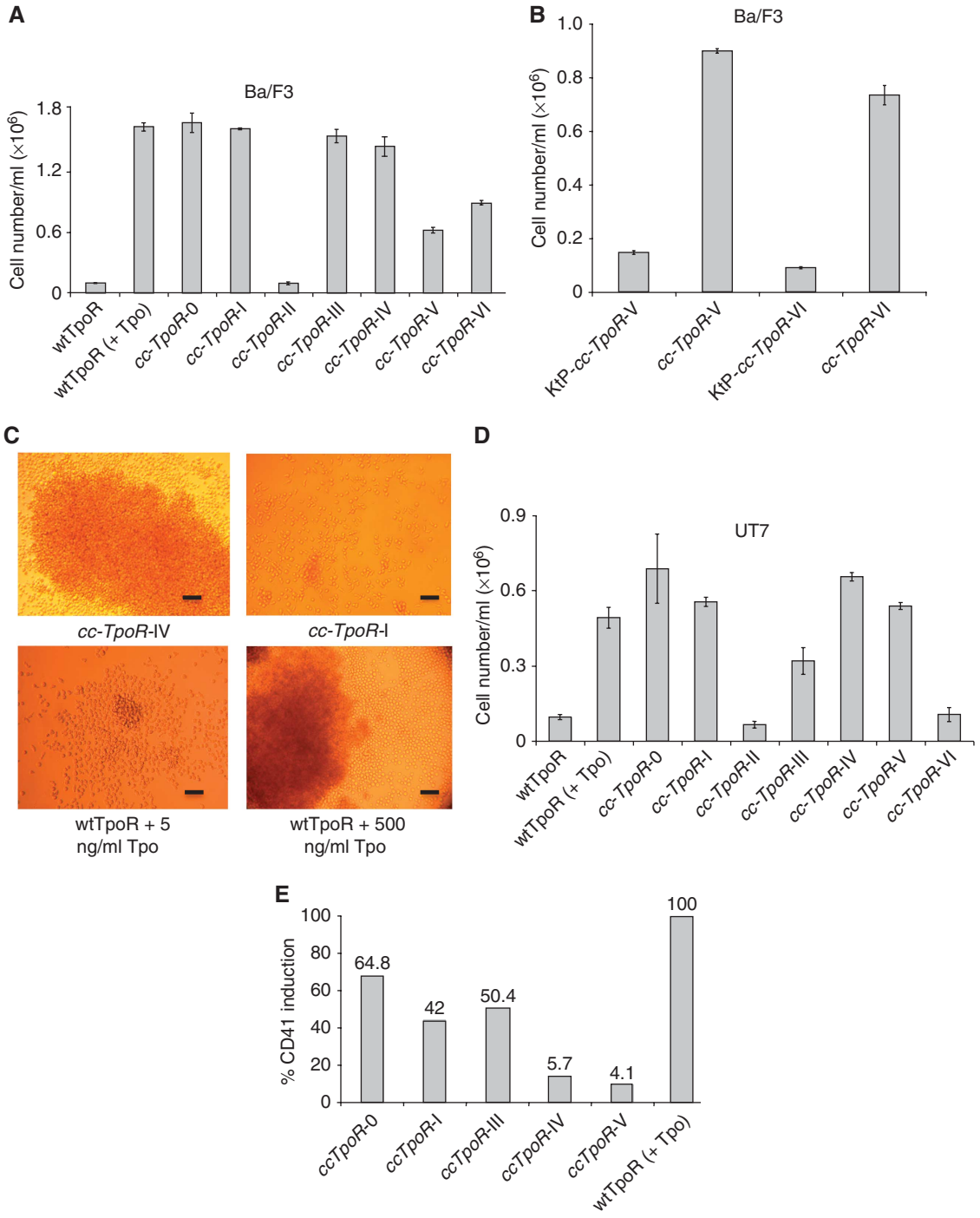

Figure 2 Cell proliferation induced by the seven *cc-TpoR* fusion proteins. (**A**, **B**) Proliferation assays were performed with Ba/F3 cells expressing the wtTpoR or the indicated *cc-TpoR*-0–VI fusion proteins (**A**), or K86P (KtoP) mutants thereof (**B**) at equal GFP levels in the absence of any cytokines or stimulated with 5 ng/ml Tpo as indicated. Cell numbers (averages of triplicates ± s.d.) were counted at day 6. One representative experiment out of four is shown. (**C**) Morphology of Ba/F3 cells expressing *cc-TpoR*-IV or *cc-TpoR*-I. Only *cc-TpoR*-IV induced cell-to-cell adhesion that lead to tight clusters (upper panel). Ba/F3 cells expressing the wtTpoR were stimulated with 5 or 500 ng/ml Tpo. At very high Tpo concentrations, cells formed clusters similar to those induced by *cc-TpoR*-IV (lower panel). Scale bar, 50 μm. (**D**) Proliferation assays were performed with UT7 cells expressing the wtTpoR or the *cc-TpoR*-0–VI fusion proteins at equal infection efficiency (GFP levels) in the absence of any cytokines or stimulated with 5 ng/ml Tpo, as indicated. Cell numbers were counted at day 8 and shown are averages of triplicates ± s.d. (**E**) Induction of CD41 expression of UT7 retrovirally transduced with the seven *cc-TpoR* fusion proteins or with the wtTpoR. Initiation of megakaryocyte differentiation of UT7 cells was assayed by flow cytometry analysis of the induction of cell surface CD41. The induction of CD41 cell surface localization by 5 ng/ml Tpo on cells expressing the wtTpoR was taken as 100%.

tions (except for that of *cc-TpoR*-II, and in certain cells of *cc-TpoR*-VI), but that different orientations induce different effects. We took advantage of the UT7 cell line (Komatsu *et al*, 1991), first to test whether *cc-TpoR* fusion proteins induce similar proliferative effects as in Ba/F3 cells, and second, to explore the abilities of the *cc-TpoR* proteins to

©2011 European Molecular Biology Organization

222

promote commitment towards the megakaryocyte lineage. UT7 cells are strictly dependent on GM-CSF or Epo for growth (Komatsu *et al*, 1991). We introduced all seven TpoR fusion proteins in parental UT7 cells maintained in GM-CSF, sorted for equivalent GFP expression and then tested proliferation after withdrawal of GM-CSF (Figure 2D). One of these weaker conformations in Ba/F3 cells, *cc-TpoR*-VI, was not able to mediate growth of UT7 cells, similarly to *cc-TpoR*-II, which was inactive in both cell lines (Figure 2A and D). Whereas UT7 cells that expressed *cc-TpoR*-II and -VI did not survive or proliferate in the absence of ligand, UT7 cells expressing *cc-TpoR*-III proliferated to a lower extent compared with the proliferation level in Ba/F3 cells (Figure 2A and D). One explanation for this observation is that *cc-TpoR*-III induces senescence, as it was recently shown for late megakaryocytes and UT7-Mpl cell lines treated with Tpo (Besancenot *et al*, 2010); another possibility is that *cc-TpoR*-III induces higher levels of megakaryocyte commitment.

Stably transfected UT7-TpoR cells respond to Tpo by induction of the expression of the megakaryocyte-specific differentiation antigen CD41 (gpIIb) (Porteu *et al*, 1996), and such cells have been the standard for exploring signals leading to megakaryocyte commitment. We then selected stably transduced UT7 cells for growth factor-independent proliferation. We analysed the expression of the CD41 in these cells and found that *cc-TpoR*-0 and -III, as well as *cc-TpoR*-I, were able to induce CD41 expression, while *cc-TpoR*-IV and -V were very weak inducers of CD41 expression (Figure 2E). On the basis of these data, we predict that one or several of the *cc-TpoR* fusion proteins that induce CD41 expression in UT7 cells might induce *in vivo* physiologic platelet formation.

Transcriptional activity mediated by the cc-TpoR fusion proteins

We examined the transcriptional activity in Ba/F3 and in JAK2-deficient γ2A cells (Kohlhuber *et al*, 1997) expressing the different coiled-coil fusion proteins using the reporter genes for STAT5, STAT3, MAP-kinase, PI-3-kinase, as described in Materials and methods. For all pathways tested, *cc-TpoR*-0, -I and -IV activated signalling via STAT5, STAT3 and MAP-kinase very strongly (Figure 3A and B). As expected, signalling via PI-3-kinase resulted in inhibition of transcriptional activity of the 6xDBE-Luc FoxO reporter, with *cc-TpoR*-0, -I and -IV being strong activators of this pathway (Supplementary Figure S2). Since *cc-TpoR*-I was one of the active orientations not promoting cell-to-cell adhesion, these results rule out the possibility that formation of cell clusters is simply a consequence of the quantitative level of signalling activation and suggests that different dimeric orientations may attract different adaptors or signalling proteins. While in Ba/F3 cells, *cc-TpoR*-III mediates proliferation to the same extent as *cc-TpoR*-0 and -IV, *cc-TpoR*-III induces a slightly lower level of STAT5 and STAT3 activity, when compared with *cc-TpoR*-0, -I, -IV and it only weakly induces MAP-kinase activation (Figure 3A and B). While *cc-TpoR*-III and -V displayed a very weak MAP-kinase activity, *cc-TpoR*-II and -VI failed to induce any detectable MAP-kinase response. Noteworthy cc-*TpoR*-II, -V, and -VI are located on the same face in the helical representation (Figure 1C) and correspond to a low JAK/STAT, low MAP-kinase, and low PI-3-kinase interface (Supplementary Figure S4). On the opposite face, *cc-TpoR*-0, -I, -IV activate very strongly JAK/STAT, MAP-kinase and PI-3-kinase (Figure 1C; Supplementary Figures S2 and S4; Table I).

Orientation-dependent activation of JAK2 and TYK2 signalling

Tpo binding to TpoR leads to activation of two members of the JAK family, JAK2 and TYK2. These kinases exhibit similar potency to promote traffic stability of TpoR at the cell surface (Royer *et al*, 2005). JAK2, however, is much more potent to mediate downstream signalling (Drachman *et al*, 1999; Royer *et al*, 2005). We asked whether differently oriented TpoR dimers would preferentially signal via JAK2 versus TYK2. To this end, we compared STAT5 or STAT3 transcriptional activity of *cc-TpoR* fusion proteins in JAK2-deficient γ2A cells in the presence of JAK2 or TYK2 (Royer *et al*, 2005). As shown in Figure 3B (left panel), *cc-TpoR*-0, -I and -IV induced strong STAT5 signalling in the presence of JAK2. In contrast, in the presence of TYK2 (right panel), *cc-TpoR*-III and cc-*TpoR*-VI induced the highest STAT5 and STAT3 activation. Thus, signalling via JAK2 and TYK2 may be induced via different interfaces (with cc-*TpoR*-VI being specific for TYK2 and cc-*TpoR*-III supporting both JAK2 and TYK2 activations; Table I). Further studies are required to determine whether, in blood progenitors, TpoR could signal via JAK2–TYK2 heterodimers, and whether a dimeric interface, such as that of cc-*TpoR*-III, could actually assemble such JAK2–TYK2 heterodimers.

We then asked whether the differences observed in transcriptional activities of *cc-TpoRs* could also be obtained if rotations were introduced at the end of the TM domain. As a proof of principle, insertions of one or more alanines after the TM domain of *cc-TpoR*s rotate the receptor clockwise. Addition of two alanines to the strongest coiled coil via JAK2 (*cc-TpoR*-IV + 2A) diminished the STAT transcriptional activity, rendering *cc-TpoR-IV* similar to *cc-TpoR*-II, as predicted. Addition of one alanine to the weakest coiled coil via JAK2 (*cc-TpoR*-II + 1A) enhanced the STAT transcriptional activity, to the levels of cc-*TpoR*-I, as predicted (Figure 3C). This rotational effect can also be demonstrated by measuring the signalling downstream TYK2 with cc-*TpoR*-V + 2A being a phenocopy of the powerful cc-*TpoR*-III via TYK2 (Figure 3D). These results indicate that the TM α-helix is a continuum and that rotations at the C-terminus are transmitted to the JM domain in the same manner as those induced by the coiled coil at the N-terminus.

Early downstream signalling and traffic of cc-TpoR fusion proteins

Having determined the biologic activities of *cc-TpoR*s in Ba/F3 cells, and their transcriptional activities, we aimed to determine the immediate signalling events at the receptor cytosolic domain. We immunoprecipitated the receptors and tested the phosphorylation level of the main signalling tyrosine residue, Y626 (Drachman and Kaushansky, 1997), using an antibody specifically recognizing this phosphorylated residue (Pecquet *et al*, 2010). *cc-TpoR*-V, -VI and -II presented very low phosphorylation levels of Y626 compared with *cc-TpoR*-0, -I, -III and -IV (Figure 4A). We validated these results by analysing the activity of some downstream pathways, like STAT1 or STAT3. Indeed, *cc-TpoR*-II shows no activation of these pathways (Figure 4B). *cc-TpoR*-V and -VI

©2011 European Molecular Biology Organization

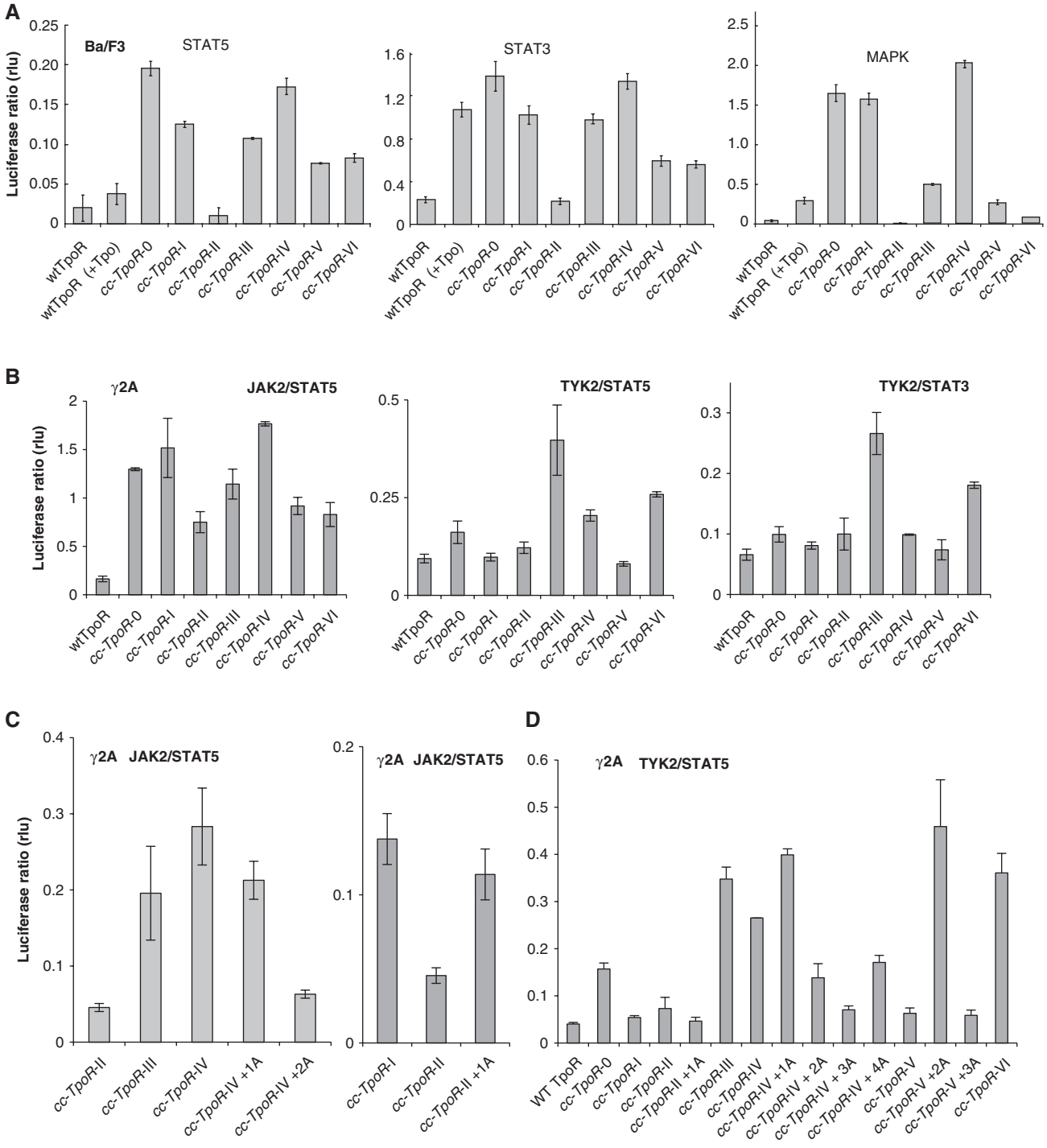

Figure 3 Transcriptional activity mediated by the wild-type (wt) TpoR or *cc-TpoR*-0–VI with and without alanine insertions. (**A**) Ba/F3 cells were selected in Tpo or without cytokines and starved overnight in RPMI/1 mg/ml BSA. To measure the transcriptional activity of STAT5 (left panel), STAT3 (middle) or MAP-kinase (MAPK) (right panel) pLHRE-luc, pGL3bPpr2-luc and pSRE-luc were used, respectively. pRL-TK encoding the renilla luciferase was co-electroporated for normalization of luciferase values. Cells were stimulated with 50 ng/ml Tpo or mock treated, as indicated. The results shown reflect averages of triplicate values ± s.d. Similar results were obtained performing three independent experiments. (**B**) γ2A cells were transfected with cDNAs coding for the *cc-TpoR* fusion proteins, JAK2 (left panel) or TYK2 (right panel), STAT5/STAT3 pGRR5-luc luciferase reporter and pRL-TK. The results represent averages of triplicate values ± s.d. of one representative experiment out of at least three. (**C**, **D**) γ2A cells were co-transfected with pGRR5-luc and pRL-TK luciferase reporter along with cDNAs coding for *cc-TpoR*s in which alanines were inserted at the end of the TM region, as indicated, and for JAK2 (**C**) or TYK2 (**D**).

presented low activation of STAT1 while *cc-TpoR*-0, -I, -III and -IV were fully active (Figure 4B). Thus, the strength of signalling and biologic effects appear to correlate with levels of Y626 phosphorylation.

We next analysed the internalization rate of the fusion proteins as well as their recycling. Cell surface biotinylation followed by cell surface immunoprecipitation enables us to assess the internalization over a certain period of time, but

©2011 European Molecular Biology Organization

Table I Summary of biologic effects and signalling of *cc-TpoR* fusion proteins in Ba/F3 cells

	Proliferation	Cell clustering	JAK2/STATs activation	TYK2/STATs activation	MAP-kinase activation	PI-3-K/AKT activation
cc-TpoR-0	+ + +	–	+ + +	–	+ + +	+ +
cc-TpoR-I	+ + +	+	+ + +	–	+ + +	+ +
cc-TpoR-II	–	–	–	–	–	–
cc-TpoR-III	+ + +	–	+ +	+ + +	+	+
cc-TpoR-IV	+ + +	+ + +	+ + +	+	+ + +	+ +
cc-TpoR-V	+	+	+ +	–	+	+
cc-TpoR-VI	+/–	–	+	+ +	–	+

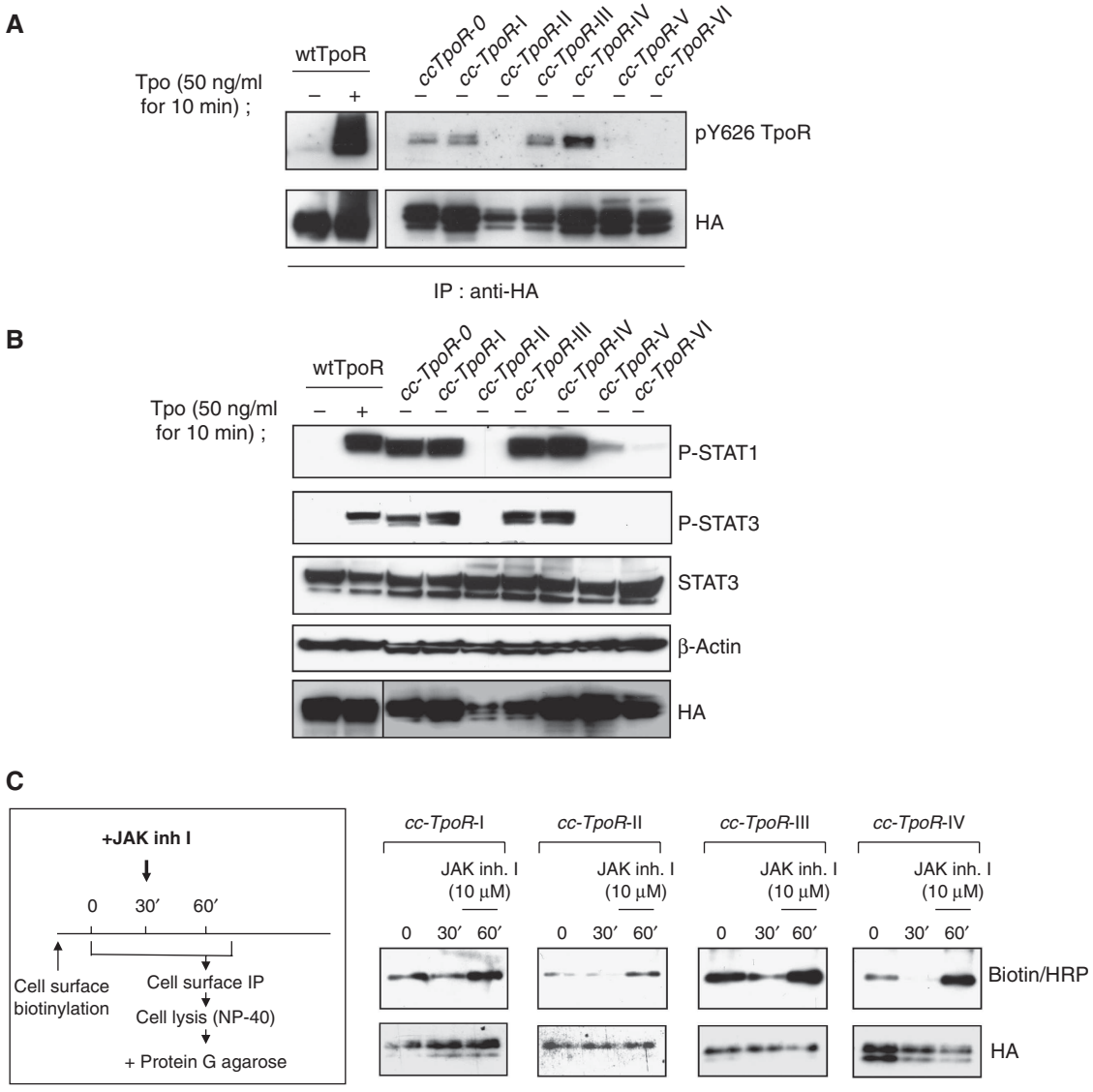

Figure 4 Early signalling and traffic of *cc-TpoR* fusion proteins. (**A**) Immunoprecipitation of the indicated fusion proteins. Induction of phosphorylation of cytosolic Y626 was assessed using an anti-pY626 TpoR antibody. The anti-HA antibody was used to analyse the expression level of the *cc-TpoR* fusion protein. (**B**) Western blot analysis performed on Ba/F3 cells expressing the fusion proteins by using the indicated antibodies. (**C**) Recycling assay on Ba/F3 cells expressing *cc-TpoR*-I, *cc-TpoR*-II, *cc-TpoR*-III or *cc-TpoR*-IV. Cells were subjected to cell surface biotinylation, allowed to internalize the receptor, and then were maintained in culture in presence of JAK inhibitor I, in order to block JAK2 signalling, for the indicated time. Cell surface immunoprecipitation was performed on the cells followed by lysis in NP-40 buffer. Immunoprecipitates were analysed by immunoblot with an anti-biotin/HRP and an anti-HA.

also the recycling. For the latter, we blocked the activity of the receptors with a JAK2 inhibitor, JAK inhibitor I (Thompson *et al*, 2002). All fusion proteins tested (*cc-TpoR*-I, -II, -III or -IV) were internalized after 30 min in Ba/F3 cells, with higher levels of internalization being correlated with signalling strength. Importantly, after treatment with JAK inhibitor I, recycling was observed for the tested fusion proteins, *cc-TpoR*-I, -II, -III or -IV (Figure 4C), suggesting that traffic

©2011 European Molecular Biology Organization

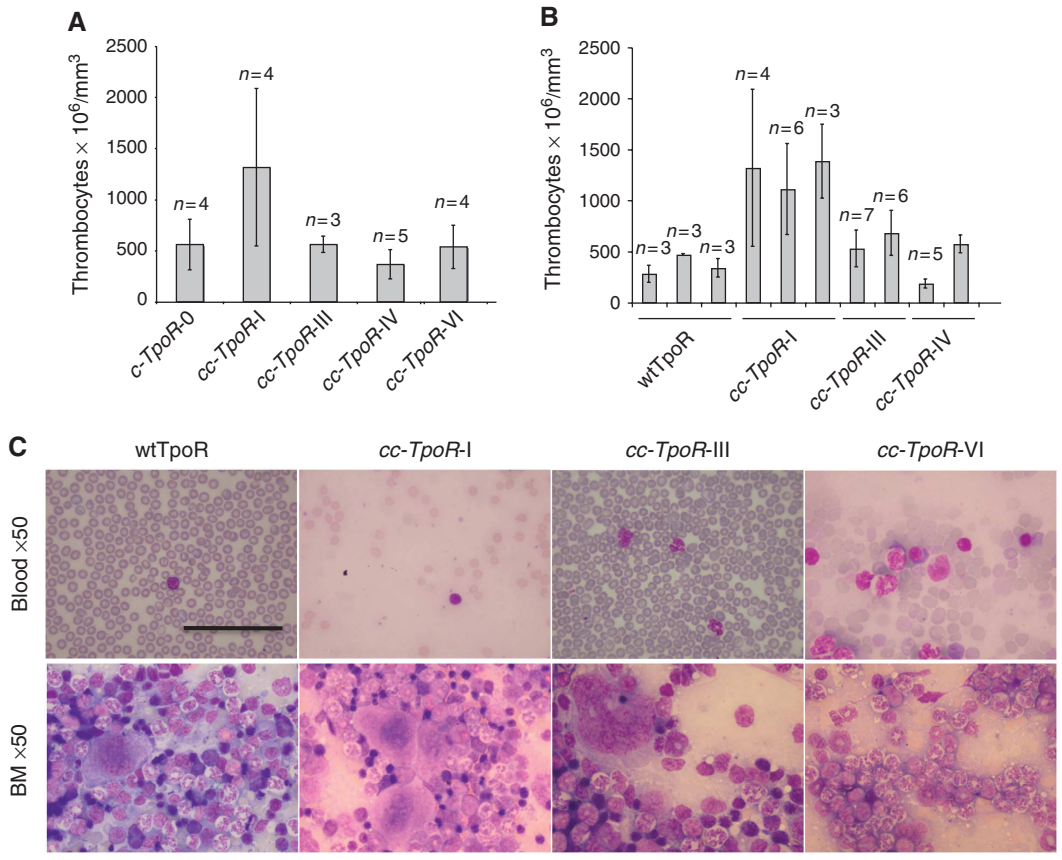

Figure 5 *In vivo* expression of *cc-TpoR* fusion proteins. (**A**, **B**) Mice were reconstituted with bone marrow cells retrovirally transduced with the indicated *cc-TpoR* fusion proteins. Peripheral blood counts were measured 6–8 weeks after reconstitution. (**A**) Platelets counts are the average + s.d. of six mice per construct. (**B**) The peripheral number of platelets is shown for the indicated *cc-TpoR* fusion proteins; *n*, number of mice. Three independent reconstitutions are shown for TpoR wt, *cc-TpoR*-I and *cc-TpoR*-V, and two independent reconstitutions are shown for *cc-TpoR*-III and *cc-TpoR*-IV. (**C**) Peripheral blood was isolated from GFP-positive mice 6 weeks after reconstitution and blood smears were performed. Cover slides were stained using a May-Grunwald stain and analysed for qualitative or quantitative abnormalities in the blood. Bone marrow cytologic examination was performed after May Grunwald staining. The magnification was × 50. Scale bar, 50 μm.

and especially recycling are not the determinants of their different biologic activities.

Expression of different TpoR fusion proteins in bone marrow progenitors induced specific myeloid disorders in bone marrow transplanted mice

We next investigated the *in vivo* effects of the *cc-TpoR*-0–VI fusion proteins. Bone marrow cells from 6- to 8-week-old C57/B6 mice were isolated and infected with retroviruses encoding the wtTpoR or the active *cc-TpoR* fusion proteins. In all, 0.5×10^6 cells were injected intravenously into lethally irradiated mice. Peripheral blood examined 3 weeks after reconstitution by FACS analyses showed that >90% of peripheral blood cells were GFP positive. A high level of platelet formation was induced *in vivo* by *cc-TpoR*-I (Figure 5A and B). Cytology examination on May-Grunwald-Giemsa stained bone marrow showed normal cellularity, with correct maturation of the myeloid lineages and excess of megakaryocytes of small to normal size that did not exhibit phenotypic changes of the myeloproliferative disorders. Interestingly, the *cc-TpoR*-I conformation has S498 (equivalent to S505 in human TpoR) in the interface (Figure 7A), suggesting that this particular orientation might reflect the active wtTpoR interface. Another fusion protein that contains S498 in the interface, *cc-TpoR*-V (Figure 7A), induced a different phenotype with circulating erythroblasts, and dyserythropoietic picture with microcytic red cells overlapping in size with platelets, which gave an artificially high count for platelets. In the marrow, *cc-TpoR*-V induced a picture of dysplasia of the erythroid and granulocytic lineages (not shown). Adopting a different orientation (Figure 7A), *cc-TpoR*-III induced granulocytosis with normal platelet counts, 2% erythroblast peripheral counts with normal red blood cell counts, while in the marrow cytologic examination showed large megakaryocytes with emperipolesis (dysmegakaryopoiesis), dyserythropoiesis and enhanced granulocytopoiesis (Figure 5). *cc-TpoR*-IV is the one orientation that induced strong clustering activity in cell lines and primary bone marrow cells (Figure 2C), which led to variable levels of reconstitution (not shown); this made the analysis difficult. An inducible system would be necessary to avoid factoring in the effects of adhesion during bone marrow reconstitution. Mice reconstituted with *cc-TpoR*-VI (adopting a conformation resembling that of *cc-TpoR*-III; Figure 7A) had a high degree of granulocytosis, at higher levels than *cc-TpoR*-III, with also immature granulocytic precursors in the peripheral blood, high levels of erythroblasts (15%), reticulocytosis and normal platelets. In the marrow, *cc-TpoR*-VI induced a major increase in the granulocytic lineage (very high granuloerythropoietic ratio),

©2011 European Molecular Biology Organization

226

with decreased megakaryocyte numbers and dysmegakaryopoiesis.

No orientation-dependent signalling is induced by the Δ5cc-TpoR fusion proteins

In all of our *cc-TpoR* fusion proteins, the JM KWQFP motif is present at the junction between the TpoR TM and cytosolic domains. This domain, in particular the Trp residue, is required to maintain the unliganded TpoR inactive (Staerk *et al*, 2006). Amino-acid substitutions of W515 result in oncogenic receptors, and are the basis of a fraction of human myeloproliferative neoplasms (MPNs) (Pardanani *et al*, 2006; Pikman *et al*, 2006; Pecquet *et al*, 2010). We, therefore, addressed whether this motif affects signalling by the different dimeric conformations of the TpoR. Ba/F3 or UT7 cells were infected with retroviruses coding for the seven Δ*5cc-TpoR* fusion proteins (Figure 6A) and sorted for equal GFP levels as described above.

Strikingly, when the KWQFP motif was deleted, all seven Δ*5cc-TpoR* fusion proteins promoted maximal proliferation of Ba/F3 or UT7 cells (Figure 6B and C). These results indicate that the KWQFP motif played an important role in orientation-dependent proliferation obtained by the wtTpoR. None of the Δ*5cc-TpoR* fusion proteins could induce formation of cell-to-cell adhesion or cell clusters (Figure 6D, compared with Figure 2C). Furthermore, the inhibitory conformation induced by *cc-TpoR*-II was changed by the deletion of the KWQFP motif and the Δ*5cc-TpoR*-II became active (Figure 6B and C). The specificity of TYK2 activation by only *cc-TpoR*-III and -VI fusion proteins was lost, with all Δ*5cc-TpoR* fusion proteins activating TYK2 (Figure 6E) and JAK2 (not shown) to the same high extent.

Reconstitution of mice with Δ*5cc-TpoR* fusion proteins showed in general a uniform increase in granulocytes and platelets in peripheral blood, without the specific effects seen for the *cc-TpoR* fusion proteins (Figure 6F). For Δ*5cc-TpoR*-I, -III and -VI all three had granulocytosis, while that was not the case for *cc-TpoR*-I. Platelet numbers were increased for Δ*5cc-TpoR*-I, -III, and for the latter this was in direct contrast with *cc-TpoR*-III. Functionally, Δ*5cc-TpoR*-VI resembles the most its *cc-TpoR*-VI counterpart, especially also showing erythroblastosis (10%); however, the platelet numbers increased, which was not the case for *cc-TpoR*-VI. Overall, the differences noted between individual *cc-TpoR* fusion proteins were mostly lost for the Δ*5cc-TpoR* counterparts, with the exception of the erythroblastosis for Δ*5cc-TpoR*-VI.

Introduction of the equivalent of the W515K mutation in the *cc-TpoR* fusion proteins (W508C for the murine TpoR sequence) led to active proteins for all orientations, when signalling was tested via JAK2. This included the inactive *cc-TpoR*-II, which became active upon W508K mutation (Supplementary Figure S3). These results are in agreement with the activating effect induced by deletion of the KWQFP motif.

Computational searches of the TpoR TM dimer interface

The *cc-TpoR* fusion proteins identify several orientations for the TM helices of the TpoR that induce strong receptor activity, as well as orientations that inhibit receptor activity. The choice of Put3 as a fusion partner was dictated by its ability to function as an extracellular domain, and importantly that it forms a left-handed (LHCC) dimeric coiled coil. Structural studies using solid-state NMR spectroscopy on membrane reconstituted peptides that include the TM and JM sequence of the TpoR up to the Box 1 region show that the sequence up to F510 is helical (Staerk *et al*, 2006; Supplementary Figure S1).

The helical wheel diagrams for dimers packing with an LHCC geometry have a spacing of 3.5 residues-per-turn. The heptad repeat is formed by two helical turns. The positions of amino acids relative to the dimer interface are denoted *a*–*g* with the *a* and *d* positions corresponding to those residues that are directly in the dimer interface. The diagrams for the seven Put3 coiled-coil dimers are shown in Figure 7A. In order to evaluate which of these orientations may correspond to low-energy dimer conformations, computational searches were performed using the program CHI (Adams *et al*, 1996; see Materials and methods). For the EpoR TM domain (Seubert *et al*, 2003), using this approach, we were able to identify two stable dimer conformations that corresponded well with active and inactive orientations imposed by the Put3 coiled coil. For the murine TpoR, computational searches were carried out on residues I485–L506 corresponding to the TM domain, and on residues I485–P511 corresponding to the TM domain with the KWQFP motif.

Figure 7B presents the results of a typical computational search on the TpoR TM domain (residues I485–L506) where possible dimer structures are generated by rotating each helix through rotation angles φ1 and φ2 from 0° to 360° with a sampling size of 45° and performing molecular dynamics simulations for each orientation. Favourable orientations are identified by structures that fall into a 'cluster', where a cluster is defined as a minimum of five structures with a root mean square (r.m.s.) deviation of 1 Å or less. An average molecular structure is calculated and the energy is minimized for each cluster. The clusters with the lowest energy are shown for each search.

There are three clusters of structures located along the diagonal of the search plot in Figure 7B. Since symmetric orientations of the TM helices (where $\varphi 1 = \varphi 2$) are induced by the Put3 constructs, these are the clusters of interest that represent the natural tendencies of the TM residues to assume symmetric dimers. The two lowest energy clusters found in the searches correspond to *cc-TpoR*-II and *cc-TpoR*-VI. *cc-TpoR*-II is inactive in both Ba/F3 and UT7 cells. *cc-TpoR*-VI is generated by a 50° counterclockwise rotation from *cc-TpoR*-II. *cc-TpoR*-VI is inactive in UT7 cells and is the least active of the dimers other than *cc-TpoR*-II in Ba/F3 cells. These results suggest that ligand-independent dimerization of the wild-type TpoR via TM domain interactions would result in an inactive receptor. The lowest energy active dimeric orientation that results in cell proliferation in both Ba/F3 and UT7 cells is *cc-TpoR*-V. For this structure, the TM dimer is stabilized by interhelical hydrogen bonding of S498. Higher energy dimer structures are found for the other *cc-TpoR* orientations in the computational searches, including *cc-TpoR*-I.

Computational searches of TM domain along with the five residues KWQFP insert typically yield clusters of *cc-TpoR*-II, *cc-TpoR*-IV and *cc-TpoR*-V. The average molecular structures of the clusters corresponding to the *cc-TpoR*-II and the *cc-TpoR*-V dimers are shown in Figure 7C and D, respectively. In the *cc-TpoR*-II dimer, K507 and W508 are oriented away from the dimer interface. The dimer structure is largely

 ©2011 European Molecular Biology Organization

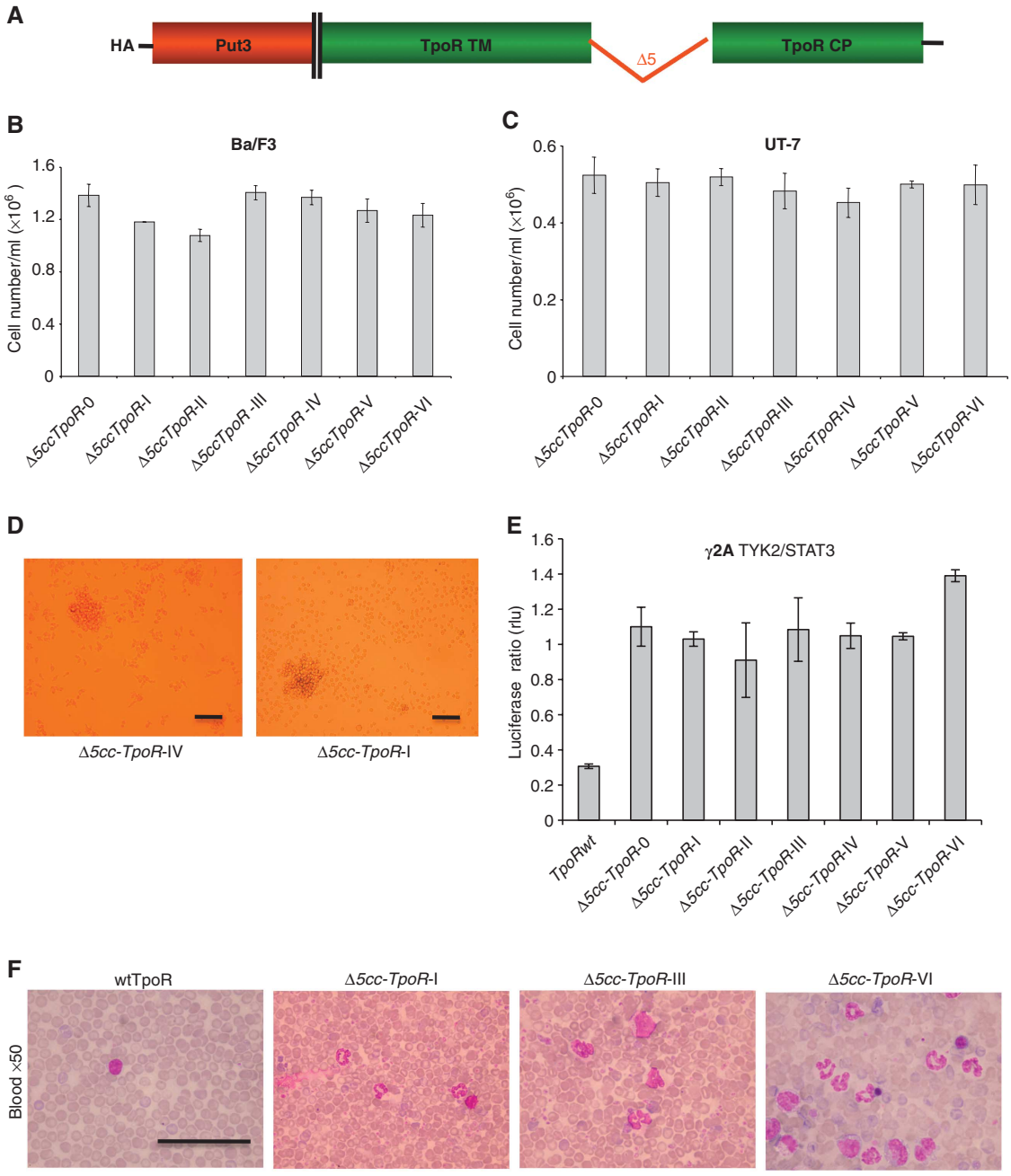

Figure 6 Deletion of the juxtamembrane KWQFP motif eliminates differences in biologic effects between the seven *cc-TpoR* dimers. (**A**) Design of the *cc-TpoR* and Δ*5cc-TpoR* fusion proteins. The coiled-coil segment of Put3 was fused to the TM and cytoplasmic (CP) domains of the wtTpoR or the Δ5TpoR. (**B**, **C**) Proliferation assays were performed with Ba/F3 (**A**) and UT7 (**B**) cells expressing the *cc-TpoR* fusion proteins where the KWQFP motif was deleted (Δ*5cc-TpoR*-0–VI). Cell numbers (averages of triplicates ± s.d.) were counted at day 6 (**A**, **B**). (**D**) Cell morphology of Ba/F3 cells expressing Δ*5cc-TpoR*-IV or Δ*5cc-TpoR*-I. No clusters were induced by Δ*5cc-TpoR*-IV, which lacks the KWQFP motif. For all pictures shown, Ba/F3 cells were plated in 24-well plates and pictures were taken at day 4. (**E**) γ2A cells were transfected with cDNAs coding for the Δ*5cc-TpoR* fusion proteins, and TYK2, STAT3 and STAT5/STAT3 pGRR5-luc luciferase reporter and pRL-TK. The results represent averages of triplicate values ± s.d. of one representative experiment out of at least three. (**F**) Peripheral blood and bone marrow were isolated from mice expressing the indicated Δ*5cc-TpoR* fusion proteins. Coverslides were stained using a May-Grunwald stain and analysed for qualitative or quantitative abnormalities in the blood. Bone marrow was examined by haematoxylin–eosin staining. The magnification was × 50. Scale bar, 50 μm.

stabilized by an interhelical hydrogen bond between the side chain amide of Q509 and the backbone carbonyl of Q509 on the opposing helix. van der Waals interactions between V488, L492, L498, A499, G502 and L506 also contribute to stabilizing this orientation of the TM helices.

One major question we asked was whether the *cc-TpoR*-I conformation (the fully active conformation) could be adopted spontaneously by the TpoR TM domain having the KWQFP JM insert. In our searches with the KWQFP insert, tryptophan at position 508 prevented dimer formation for

©2011 European Molecular Biology Organization

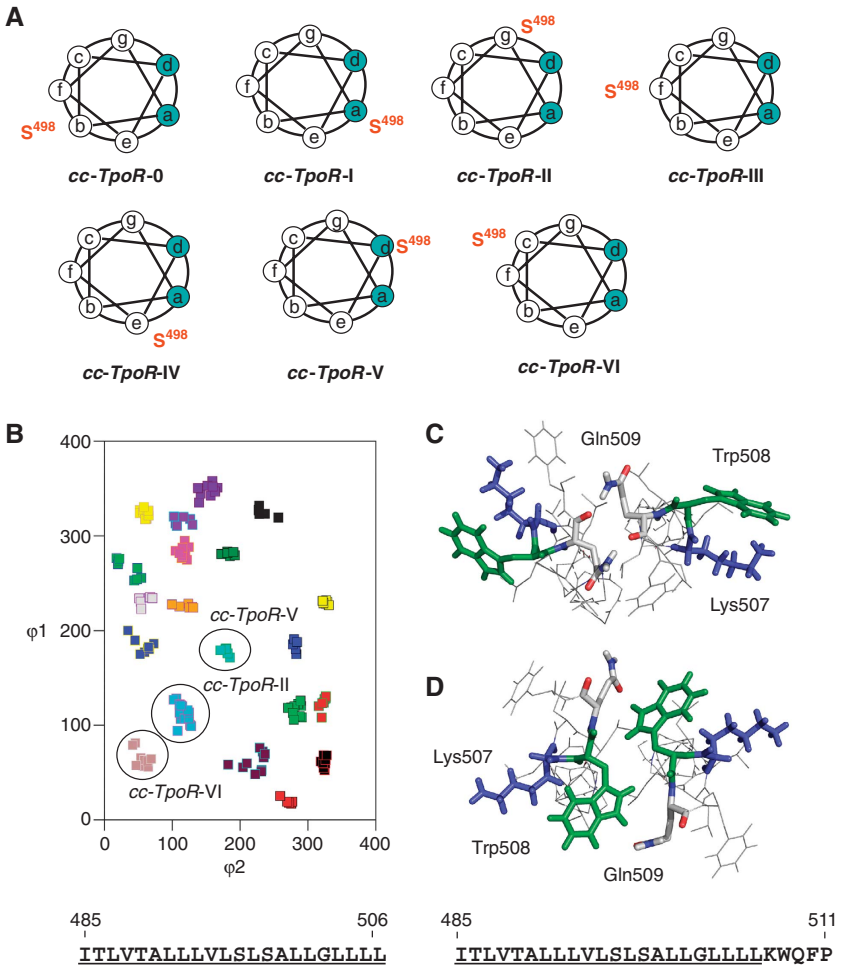

Figure 7 Computational searches of the TpoR transmembrane dimer. (**A**) Helical wheel predictions of the seven dimeric interfaces of the TM domain of the TpoR imposed by the Put3 coiled-coil fusion. Residue S498 of the TM domain is placed in the interface in *cc-TpoR*-I and *cc-TpoR*-V. (**B**) Computational search using the TpoR TM sequence from I485 to L506. The axial separation between the TM helices was set to be 10 Å. Computational searches with axial separations of 9.5–10.5 Å gave similar results. (**C**, **D**) Average molecular structures of the helix dimer corresponding to *cc-TpoR*-II and *cc-TpoR*-V. The helices have left-handed crossing angles and the dimer is viewed down the helix axis from the C-terminal end of the dimer. In *cc-TpoR*-II (**C**), the hydrogen bonding of Q509 stabilizes the helix dimer. The side chain of K509 contacts the aromatic ring of W508 characteristic of a stabilizing cation-π interaction. In *cc-TpoR*-V (**D**), the TM helices have rotated 50° counterclockwise, and hydrogen bonds form between indole NH of W508 and the amide side chain of Q509. The active *cc-TpoR*-I fusion protein adopts a conformation rotated by another 50° from *cc-TpoR*-V, where W508 residues would be predicted to clash.

orientations of TM helices corresponding to *cc-TpoR*-I. One can easily visualize the steric clash of W508 that would occur in *cc-TpoR*-I by rotating the helices in Figure 7D counterclockwise by 50°. A 50° rotation converts the *cc-TpoR*-V structure shown in Figure 7D into *cc-TpoR*-I, with both dimers having S498 in the interface (Figure 7A). This might explain why the KWQFP motif impairs activation of TpoR in the absence of Tpo (Staerk *et al*, 2006), and why adopting this structure needs either coiled-coil fusion or ligand binding to the extracellular domain of the receptor, both events requiring strong conformational changes.

Discussion

Our main observation is that the TpoR can signal from six out of seven possible symmetric dimeric orientations (Table I) leading to cell proliferation and different differentiation outputs, such as different abilities to promote megakaryocyte differentiation, cell-to-cell adhesion and myeloproliferative and myelodysplasia phenotypes *in vivo*. These results are relevant for the mechanisms by which TpoR can function at different stages of differentiation from HSCs to mature platelets in the course of physiologic haematopoiesis. Besides its ligand Tpo, the extracellular domain of TpoR was recently shown to bind a human homologue of a fungal nuclear migration protein (hNUDC) (Chen *et al*, 2010), a novel regulator of haematopoiesis (Miller *et al*, 1999; Gocke *et al*, 2000). It is, thus, conceivable that subtle differences in dimeric conformations are induced by different ligands or by the same ligand in different cell types. On the other hand, our data indicate that signalling by differently oriented TpoR dimers induces *in vivo* myeloproliferative and myelodysplastic disorders. While TpoR has already been discovered to be mutated in Essential Thrombocythemia and Myelofibrosis neoplasms (Pardanani *et al*, 2006; Pikman *et al*, 2006), it is not yet known whether it plays a role in myelodysplasia or mixed myelodysplasia/myeloproliferative disorders. TpoR is one of the three receptors that bind to JAK2 V617F, a mutant

©2011 European Molecular Biology Organization

associated with the vast majority of BCR-ABL-negative MPNs (Vainchenker *et al*, 2008). The basis for the observed orientation-dependent signalling of TpoR is represented by the recently identified JM KWQFP motif, which contains the W515, the very residue that maintains the unliganded TpoR inactive (Staerk *et al*, 2006) and which is mutated to Leu, Lys, Ala residues in MPNs (Pardanani *et al*, 2006; Pikman *et al*, 2006; Pecquet *et al*, 2010).

In addition to the W515 mutations in MPNs, several activating mutations in the TM and JM domains of TpoR signalling have been described in patients or cell lines from leukaemia patients (Onishi *et al*, 1996; Malinge *et al*, 2008). Substitutions of serine at position 498 (mouse) or 505 (human) by asparagine activate TpoR signalling in the absence of the ligand (Onishi *et al*, 1996; Ding *et al*, 2004). This residue is in the interface of *cc-TpoR*-I and *cc-TpoR*-V (Figure 7A); however, the phenotype induced by these two fusion proteins *in vivo* was remarkably different. *cc-TpoR*-I induced high numbers of platelets, without cytological features of myeloproliferation in the marrow, and *cc-TpoR*-V induced a picture of myelodysplasia, with small red blood cells and variable levels of thrombocytosis (Figure 5C). Again, subtle differences in dimeric conformation are translated into important differences in biologic effects.

We investigated the orientation requirements for TpoR-mediated signalling and identified several fusion proteins (*cc-TpoR*-0, -I, and -IV) that induced maximal proliferation of Ba/F3 and UT7 cells, two fusion proteins that supported weaker proliferation and one conformation that was inactive (*cc-TpoR*-II). This situation is different from that of the EpoR where essentially one dimeric orientation is permissive for signalling (Seubert *et al*, 2003). Self-association and packing density of TM sequences were shown to promote signalling by the active EpoR dimeric interface (Kubatzky *et al*, 2001, 2005; Becker *et al*, 2008). That EpoR activation is stringently controlled by dimeric orientation is also supported by the report that only rare anti-EpoR monoclonal antibodies are agonistic (Elliott *et al*, 1996). In contrast, tagged versions of TpoR can be activated by treatment with anti-tag antibodies (Millot *et al*, 2004). While antibodies and other small molecules may activate TpoR signalling in cell lines, our data suggest that careful studies would be necessary in order to establish exactly which biologic function of the TpoR would be induced by agonistic molecules.

Although six out of seven *cc-TpoR* fusion proteins induced cell proliferation, they induced unique effects depending on their dimeric conformation (Figures 2 and 5; Supplementary Figure S4; Table I). *cc-TpoR*-IV induced strong cell-to-cell adhesion (clusters), but was not permissive to induce commitment to the megakaryocyte lineage, as measured by CD41 expression in UT7 cells (Figure 2E). *cc-TpoR*-IV-induced clustering is reminiscent of the effects of high levels of Tpo ligand in TpoR expressing Ba/F3 cells (Figure 2D) or in UT-7-TpoR cells. High local levels of Tpo might exist in niches, such as the osteoblastic niche, where Tpo was reported to maintain quiescence of HSCs (Qian *et al*, 2007; Yoshihara *et al*, 2007). On the other hand, the effect of Tpo was initially described to induce HSC renewal (Alexander *et al*, 1996b) and early haematopoiesis (Solar *et al*, 1998), or to amplify the immediate progenies of HSCs (Abkowitz and Chen, 2007). More recently, we described a senescence-inducing effect of Tpo in late-stage post-mitotic megakaryocytes (Besancenot *et al*, 2010). Such distinct and apparently opposed actions of TpoR might be the result of different dimeric orientations adopted by the receptor in response to various ligand levels, ligand presentation or cell type. Signalling by TpoR was previously shown to require phosphorylation of Y626, which couples the receptor to several signalling pathways, especially to the STAT5/3 and MAP-kinase pathways (Gurney *et al*, 1995; Alexander *et al*, 1996a; Drachman and Kaushansky, 1997; Pecquet *et al*, 2010). The same TpoR cytosolic Y626 residue is absolutely required for induction of myeloproliferative disorder by the TpoR W515A mutant via excessive activation of the STAT3 and MAP-kinase pathways. The strength of signalling by *cc-TpoR* fusion proteins also appears to correlate with levels of phosphorylation of Y626 (Figure 4A). The *in vivo* phenotype induced by *cc-TpoRs* is milder than that of TpoR W515 mutants (Pecquet *et al*, 2010). It will be of interest to determine the precise adaptors associated with phosphorylated Y626, as a function of dimeric orientation (*cc-TpoRs*) or in the case of TpoR W515 mutants.

Transplantation assays in mice with bone marrow cells expressing the active *cc-TpoR* fusion proteins confirmed our hypothesis that different dimeric orientations induce effects that resemble the physiological function of TpoR (*cc-TpoR*-I), or that induce different degrees of myeloproliferative and myelodysplasia disorders (*cc-TpoR*-III, *cc-TpoR*-VI and *cc-TpoR*-V; Figure 5). All seven fusion proteins were equally able to support cell proliferation but lost orientation-specific signalling upon deletion of the KWQFP motif (Δ5*cc-TpoR* fusion proteins). For example, Δ5*cc-TpoR*-II was active after deletion of the KWQFP motif, while *cc-TpoR*-II was not. In addition, Δ5*cc-TpoR*-IV did not induce cell-to-cell adhesion.

These data support our hypothesis that the TpoR could indeed signal through various orientations. One possible explanation for TpoR signalling from multiple dimeric interfaces is the utilization of two JAKs for signal transmission: JAK2 and TYK2. Expression of TYK2 alone, in the absence of JAK2, allows only *cc-TpoR*-III and *cc-TpoR*-VI to activate STAT5 and STAT3 signalling, while expression of JAK2 promotes STAT signalling via multiple interfaces, represented by *cc-TpoR*-0, -I, -III, and -IV (Figure 3). It needs to be further investigated whether the TpoR is signalling *in vivo* via heteromeric JAK2–TYK2 complexes. Of interest, *cc-TpoR*-III and *cc-TpoR*-VI have some common signalling and biologic features: (i) activation of TYK2 signalling in addition to JAK2, (ii) induction of granulocytosis and of different degrees of erythroid and megakaryocytic dysplasia, (iii) lower levels of MAP-kinase activation. A tight control and limitation of the levels of MAP-kinase activation were described to be necessary for normal granulocyte differentiation and maintenance of granulocytic progenitors (Baumann *et al*, 2005; Geest *et al*, 2009).

Coiled coils are symmetric dimers and the models that emerge after the use of coiled-coil fusion proteins have a bias towards symmetric left-handed parallel dimers of α-helices, while membrane proteins may also adopt asymmetric geometries. Further structural studies are required to establish whether the TpoR dimer is symmetric or asymmetric. Cysteine crosslinking (Figure 1C) and alanine insertion mutagenesis (Figure 3C and D) confirmed that the coiled-coil fusion to successive TM residues at the N-terminus of the TM domain enables to dial-in the predicted dimeric

©2011 European Molecular Biology Organization

conformations at the outset of the JM cytosolic domain. To gain insight into the dimerization mechanism(s) of the TpoR, we performed computational searches of the TM and JM sequences. In this approach, stable dimer conformations are observed as clusters of structures. A comparison of the computational searches in Figure 7B–D shows that the orientation of the TM helices in *cc-TpoR*-II generates a stable structure. This construct has the only orientation that results in an inactive TpoR dimer. Thus, the natural tendency of the TpoR TM dimer is to adopt the inactive conformation. In this inactive structure, K507 and W508 are oriented as far as possible away from the dimer interface. Rotation of the TM helices in either direction by 50° (leading to *cc-TpoR*-V or *cc-TpoR*-VI) results in partial activity. Functional data indicate that *cc-TpoR*-I represents the closest conformation to the physiologically activated TpoR by Tpo. Although dimeric clusters representing *cc-TpoR*-I are identified by our searches, they are among the higher energy dimer structures (less stable). Thus, this dimeric orientation is unlikely to be adopted spontaneously. Interestingly, in the computational search that includes the KWQFP motif, we could not identify a cluster corresponding to *cc-TpoR*-I. Therefore, it is very likely that the KWQFP motif actively prevents the formation of a dimer corresponding to the *cc-TpoR*-I, and is doing so via a clash between interfacially oriented W508 residues (W515 in the human TpoR). Taken together, functional and computational data indicate that the W508 of the KWQFP motif is crucial for preventing TpoR activation and is required for orientation-specific signalling. Noteworthy, the TM domain of the human TpoR, in the absence of the JM RWQFP motif, was found by bacterial TOXCAT and cysteine cross-linking assays to promote dimerization in three rotationally related orientations, possibly corresponding to inactive, active and partially active states of the receptor (Matthews *et al*, 2011). The proposed interfaces correspond to our coiled coil-induced inactive *cc-TpoR*-II and active orientations.

In conclusion, our data show that several dimeric conformations of the TpoR can support cell proliferation and that specific dimeric orientations imposed by the KWQFP JM motif differ in their signalling output and biologic effects. While one dimeric orientation having S498 in the interface emerges as the best model for the physiologically activated TpoR, and a different one corresponds to the inactive dimer, other orientations induce different degrees of myeloproliferative and myelodysplastic disorders. The system of differently dimerized TpoRs may offer new insights with respect to apportioning a particular signalling pathway to a biologic effect, such as megakaryocytic differentiation or the establishment of myeloid disorders.

Materials and methods

cDNA constructs

The wtTpoR and mutants thereof (TpoR mutants where the KWQFP insert was deleted (Δ5) or mutated (W508K), the *cc-TpoR* fusion proteins (*cc-TpoR*-0-VI) and the *cc-TpoR* fusion proteins where the KWQFP insert was deleted (Δ*5cc-TpoR*-0-VI)) were subcloned in pMX-IRES-GFP and MSCV-IRES-GFP vectors, as described previously (Staerk *et al*, 2006). All TpoRs and *cc-TpoRs* contain an HA tag at the amino-terminus, after the cleavage site of the signal peptidase (Huang *et al*, 2001). For the crosslinking experiment, the seven cysteine-free coiled-coil receptor backbones were created by introducing a stop codon after amino acid 553, and Leu505 was mutated into Cys. To alter the helical register of the seven murine *cc-TpoR* fusion proteins and as a proof of principle, alanines were inserted at the end of the TM region. We also mutated Trp508 (mouse equivalent of Trp515 in the human TpoR) into Lys, introducing in the seven *cc-TpoRs*, the pathological W515K mutation found in MPN patients. All constructs were verified by sequencing.

Crosslinking studies

Six-well plates of human BOSC cells were transfected (Lipofectamine™ 2000, Invitrogen, Carlsbad, CA) with cDNAs encoding the seven cysteine *cc-TpoR* mutants. Cells were harvested 24 h after transfection and checked for GFP expression prior to crosslinking experiments.

Cells were washed with phosphate-buffered saline and resuspended in 1 ml of phosphate-buffered saline containing 1 mM $MgCl_2$ and 0.1 mM $CaCl_2$. Crosslinking was then performed for 10 min at room temperature with a final concentration of the crosslinker *N*,*N*′-1,2-phenylenedimaleimide (o-PDM) dissolved in DMSO of 100 μM. Cells were lysed with 1 × NP-40 lysis buffer containing 2% of β-mercaptoethanol in order to quench excess crosslinker (Kubatzky *et al*, 2005). Lysate samples were analysed by SDS–PAGE using a 4–12% gradient NuPage® NOVEX Bis-Tris Gel (Invitrogen) and then transferred onto nitrocellulose membrane. After blocking with 1% milk PBS, membranes were incubated with a 1:500 diluted mouse anti-HA antibody (HA.11, Covance, Berkeley, CA) followed by a 1:2500 diluted peroxidase-conjugated anti-mouse antibody (GE Healthcare UK Ltd, Buckingham, UK). Detection was then performed using enhanced chemiluminescence.

Generation of cell lines

Ba/F3 and UT7 cell lines were transduced with *cc-TpoR* constructs using ecotropic (Liu *et al*, 2000) or amphotropic viral supernatant, respectively (Chagraoui *et al*, 2002; Staerk *et al*, 2006). Cell populations were sorted for equal GFP expression.

Assay for Tpo-independent growth

Transduced and sorted Ba/F3 cells were expanded in IL-3, washed and subsequently placed in RPMI 10% fetal bovine serum without cytokines or Tpo as indicated. UT7 cells expressing the *cc-TpoR* constructs were washed with α-MEM medium (Invitrogen) to remove GM-CSF and placed in cytokine-free α-MEM medium containing 10% FBS or in α-MEM medium containing 10% FBS and Tpo as specified. Cell numbers were counted at the indicated time points.

Immunoprecipitation and immunoblots

Ba/F3 cells were washed with PBS and starved for 2 h in RMPI with 0.1% BSA. Cells were stimulated with 50 ng/ml rmTpo (R&D) or PBS and lysed in NP-40 buffer as described previously (Staerk *et al*, 2006; Pecquet *et al*, 2010). Immunoprecipitation was performed with anti-HA antibodies (Roche Diagnostics, Indianapolis, IN), incubated with protein G agarose (Invitrogen) overnight. Samples were analysed by western blot using anti-pY626 TpoR (Cell Signaling Technology, Danvers, MA) and anti-HA.

Activation of downstream signalling pathways was analysed using anti-p-STAT1, anti-STAT1, anti-p-STAT3, anti-STAT3, or anti-p-Erk1,2, anti-Erk1,2 (Cell Signaling Technology), anti-β-actin (Sigma, St Louis, MO) and anti-HA antibodies (Roche Diagnostics), as described previously (Pecquet *et al*, 2010).

Receptor-recycling assay and cell surface biotinylation

In all, 3×10^7 Ba/F3 cells expressing the indicated *cc-TpoRs* were incubated with 10 mg/ml EZ link sulfo-NHS-Biotin (Thermo Scientific, Rockford, IL) at 4°C for 2 h. Cells were washed in 100 mM glycine-PBS solution to remove excess biotinylation reagent. After biotinylation, cells were maintained in culture for 30 min and then treated or not with 10 μM JAK inhibitor I (Calbiochem, La Jolla, CA) for additional 30 min. For cell surface immunoprecipitation, cells were incubated with anti-HA antibodies (Roche Diagnostics) for 1 h at 4°C. Cells were then lysed in 1% NP-40 buffer as previously described and lysates were incubated overnight with protein G agarose at 4°C. The beads were washed in lysis buffer and subjected to western blotting by using an anti-biotin/HRP (New England Biolabs, Beverly, MA) and anti-HA antibodies (Roche Diagnostics).

©2011 European Molecular Biology Organization

Dual luciferase assays

Activation of STAT5 and STAT3 was analysed by assaying for luciferase production in cells transfected with pLHRE-Luc (Sotiropoulos *et al*, 1995; Storz *et al*, 1999), pGL3bPpr2 (Eyckerman *et al*, 1999) or pGRR5 constructs (Dumoutier *et al*, 2000). To assess MAPK activation we used the pSRE-luc construct (Treisman, 1995). The PI-3-kinase/Akt pathway negatively affects FoxO activity. PI-3-kinase/Akt activation was, therefore, indirectly measured using a $6\times$ DBE-Luc reporter, which is activated by FoxO family members (Kuiperij *et al*, 2005). The pRL-TK vector (Promega, Madison, WI) containing the renilla luciferase gene under control of the TK promoter was used as internal control. Ba/F3 cells expressing TpoR proteins were starved for 3 h in RPMI/1 mg/ml BSA, Luciferase assays were performed as described (Seubert *et al*, 2003). JAK2-deficient γ2A fibrosarcoma cells (Kohlhuber *et al*, 1997) were transiently transfected with TpoR proteins and signalling proteins as described (Royer *et al*, 2005). Luminescence was recorded in cell lysates 24 h after using a Perkin-Elmer Victor X Light analyzer.

Surface expression of HA-tagged TpoR and HA-tagged cc-TpoR fusion proteins

Surface expression of HA-TpoR and HA-tagged *cc-TpoR* fusion proteins was measured by flow cytometry as described (Huang *et al*, 2001; Pecquet *et al*, 2010).

Bone marrow reconstitutions

Bone marrow was isolated from mice 72 h after 5-fluorouracil injection (Chagraoui *et al*, 2002; Pecquet *et al*, 2010). In all, 1×10^6 bone marrow cells transduced with *cc-TpoRs* or TpoR were injected into lethally irradiated, 6–8-week-old C57Bl6 mice. Reconstitution was assessed by GFP expression in peripheral blood cells using flow cytometry 3 weeks after transplantation. Peripheral blood cell numbers were counted using Melet Schloessing MS9-3. Histopathology analysis and blood smears were performed as described (Pecquet *et al*, 2010).

Computational searches

Low-energy dimer structures of the TM sequence of the TpoR were identified computationally using the program CHI (Adams *et al*, 1996). The program generates canonical helices from the TpoR sequence and constructs a matrix of helix dimers in which each helix is rotated through all possible orientations between 0° and 360° with a sampling size of 45°. For each starting structure, MD simulations with simulated annealing and energy minimization were performed within CHI using the program X-PLOR. The X-PLOR force field uses the TOPH19 and PARAM19 parameters sets with all polar hydrogens included. A non-bonded cutoff of 13 Å is set with a switching function between 10 and 12 Å for the van der Waals and electrostatic terms. Distance constraints are applied between the backbone O_i and N_{i+4} atoms to maintain an α-helical conformation and between the helix directors to maintain a fixed axial separation. Different computational searches were performed for axial distances of 9.5, 10 and 10.5 Å, and for helices starting with left- and right-handed crossing angles. Both the helix rotation and the crossing angles are allowed to vary during the simulations, and the results are plotted as a function of the angles φ1 and φ2, corresponding to rotational orientation of each helix in the dimer. The dimer structures migrate from their initial geometry and cluster into low-energy conformations. All calculations were performed *in vacuo*, approximating the low dielectric environment of the membrane. Separate computational searches were performed for TpoR sequence without (I485–L506) and without (I485–P511) the KWQFP insert.

Supplementary data

Supplementary data are available at *The EMBO Journal* Online (http://www.embojournal.org).

Acknowledgements

We thank Dr Jean-Marie Scheiff for histopathology diagnosis, Céline Mouton for expert technical assistance, André Tonon for expert flow cytometry expertise, Yan Yin and Julie Klein for technical and graphics assistance. This work was supported by grants from *La Ligue Nationale contre le Cancer* (*équipe labellisée* 2010, WV), by NIH grant (GM-46732) to SOS, the *Fondation contre le Cancer*, the de Hovre Foundation, the Salus Sanguinis Foundation, the *Action de Recherche Concertée* MEXP31C1 of the *Université catholique de Louvain*, the PAI Program BCHM61B5, Belgium and the Atlantic Philanthropies, New York, and the FNRS (*Mandat d'impulsion*), Belgium (to SNC). JS was supported by fellowships from Daimler-Benz, Exchange Marie Curie, Télévie and Salus Sanguinis Foundations. J-PD is supported by an FRIA PhD fellowship of the FRS-FNRS Belgium. CP was supported by a postdoctoral fellowship of the de Duve Institute, by the PAI Program BCHM61B5 and by the FRS-FNRS. WV is supported by an interface contract between INSERM and IGR. SNC is a Research Associate of the FNRS.

Author contributions: JS, J-PD and SNC planned and performed experiments, interpreted data and wrote paper; CP, EL and IB performed experiments and interpreted data; SOS and WV planned experiments and interpreted data; MI and SOS performed molecular dynamics simulations; HAP interpreted data.

Conflict of interest

The authors declare that they have no conflict of interest.

References

Abkowitz JL, Chen J (2007) Studies of c-Mpl function distinguish the replication of hematopoietic stem cells from the expansion of differentiating clones. *Blood* **109:** 5186–5190

Adams PD, Engelman DM, Brunger AT (1996) Improved prediction for the structure of the dimeric transmembrane domain of glycophorin A obtained through global searching. *Proteins* **26:** 257–261

Alexander WS, Maurer AB, Novak U, Harrison-Smith M (1996a) Tyrosine-599 of the c-Mpl receptor is required for Shc phosphorylation and the induction of cellular differentiation. *EMBO J* **15:** 6531–6540

Alexander WS, Metcalf D, Dunn AR (1995) Point mutations within a dimer interface homology domain of c-Mpl induce constitutive receptor activity and tumorigenicity. *EMBO J* **14:** 5569–5578

Alexander WS, Roberts AW, Nicola NA, Li R, Metcalf D (1996b) Deficiencies in progenitor cells of multiple hematopoietic lineages and defective megakaryocytopoiesis in mice lacking the thrombopoietic receptor c-Mpl. *Blood* **87:** 2162–2170

Baumann M, Frye T, Naqvi T, Gomez-Cambronero J (2005) Normal neutrophil maturation is associated with selective loss of MAP kinase activation by G-CSF. *Leuk Res* **29:** 73–78

Becker V, Sengupta D, Ketteler R, Ullmann GM, Smith JC, Klingmuller U (2008) Packing density of the erythropoietin receptor transmembrane domain correlates with amplification of biological responses. *Biochemistry* **47:** 11771–11782

Besancenot R, Chaligne R, Tonetti C, Pasquier F, Marty C, Lecluse Y, Vainchenker W, Constantinescu SN, Giraudier S (2010) A senescence-like cell-cycle arrest occurs during megakaryocytic maturation: implications for physiological and pathological megakaryocytic proliferation. *PLoS Biol* **8:** e1000476

Brown RJ, Adams JJ, Pelekanos RA, Wan Y, McKinstry WJ, Palethorpe K, Seeber RM, Monks TA, Eidne KA, Parker MW, Waters MJ (2005) Model for growth hormone receptor activation based on subunit rotation within a receptor dimer. *Nat Struct Mol Biol* **12:** 814–821

Chagraoui H, Komura E, Tulliez M, Giraudier S, Vainchenker W, Wendling F (2002) Prominent role of TGF-beta 1 in thrombopoietin-induced myelofibrosis in mice. *Blood* **100:** 3495–3503

Chen WM, Yu B, Zhang Q, Xu P (2010) Identification of the residues in the extracellular domain of thrombopoietin receptor involved in the binding of thrombopoietin and a nuclear distribution protein (human NUDC). *J Biol Chem* **285:** 26697–26709

Constantinescu SN, Huang LJ, Nam H, Lodish HF (2001) The erythropoietin receptor cytosolic juxtamembrane domain con-

©2011 European Molecular Biology Organization

tains an essential, precisely oriented, hydrophobic motif. *Mol Cell* **7:** 377–385

de Sauvage FJ, Hass PE, Spencer SD, Malloy BE, Gurney AL, Spencer SA, Darbonne WC, Henzel WJ, Wong SC, Kuang WJ, Oles KJ, Hultgren B, Solberg Jr LA, Goeddel DV, Eaton DL (1994) Stimulation of megakaryocytopoiesis and thrombopoiesis by the c-Mpl ligand. *Nature* **369:** 533–538

Ding J, Komatsu H, Iida S, Yano H, Kusumoto S, Inagaki A, Mori F, Ri M, Ito A, Wakita A, Ishida T, Nitta M, Ueda R (2009) The Asn505 mutation of the c-MPL gene, which causes familial essential thrombocythemia, induces autonomous homodimerization of the c-Mpl protein due to strong amino acid polarity. *Blood* **114:** 3325–3328

Ding J, Komatsu H, Wakita A, Kato-Uranishi M, Ito M, Satoh A, Tsuboi K, Nitta M, Miyazaki H, Iida S, Ueda R (2004) Familial essential thrombocythemia associated with a dominant-positive activating mutation of the c-MPL gene, which encodes for the receptor for thrombopoietin. *Blood* **103:** 4198–4200

Drachman JG, Griffin JD, Kaushansky K (1995) The c-Mpl ligand (thrombopoietin) stimulates tyrosine phosphorylation of Jak2, Shc, and c-Mpl. *J Biol Chem* **270:** 4979–4982

Drachman JG, Kaushansky K (1997) Dissecting the thrombopoietin receptor: functional elements of the Mpl cytoplasmic domain. *Proc Natl Acad Sci USA* **94:** 2350–2355

Drachman JG, Millett KM, Kaushansky K (1999) Thrombopoietin signal transduction requires functional JAK2, not TYK2. *J Biol Chem* **274:** 13480–13484

Dumoutier L, Van Roost E, Colau D, Renauld JC (2000) Human interleukin-10-related T cell-derived inducible factor: molecular cloning and functional characterization as an hepatocyte-stimulating factor. *Proc Natl Acad Sci USA* **97:** 10144–10149

Elliott S, Lorenzini T, Yanagihara D, Chang D, Elliott G (1996) Activation of the erythropoietin (EPO) receptor by bivalent anti-EPO receptor antibodies. *J Biol Chem* **271:** 24691–24697

Eyckerman S, Waelput W, Verhee A, Broekaert D, Vandekerckhove J, Tavernier J (1999) Analysis of Tyr to Phe and fa/fa leptin receptor mutations in the PC12 cell line. *Eur Cytokine Netw* **10:** 549–556

Geest CR, Buitenhuis M, Groot Koerkamp MJ, Holstege FC, Vellenga E, Coffer PJ (2009) Tight control of MEK-ERK activation is essential in regulating proliferation, survival, and cytokine production of CD34 + -derived neutrophil progenitors. *Blood* **114:** 3402–3412

Gocke CD, Reaman GH, Stine C, Zhang MY, Osmani SA, Miller BA (2000) The nuclear migration gene NudC and human hematopoiesis. *Leuk Lymphoma* **39:** 447–454

Gurney AL, Wong SC, Henzel WJ, de Sauvage FJ (1995) Distinct regions of c-Mpl cytoplasmic domain are coupled to the JAK-STAT signal transduction pathway and Shc phosphorylation. *Proc Natl Acad Sci USA* **92:** 5292–5296

Huang LJ, Constantinescu SN, Lodish HF (2001) The N-terminal domain of Janus kinase 2 is required for Golgi processing and cell surface expression of erythropoietin receptor. *Mol Cell* **8:** 1327–1338

Kaushansky K (1997) Thrombopoietin: more than a lineage-specific megakaryocyte growth factor. *Stem Cells* **15** (Suppl 1)**:** 97–102; discussion 102–103

Kohlhuber F, Rogers NC, Watling D, Feng J, Guschin D, Briscoe J, Witthuhn BA, Kotenko SV, Pestka S, Stark GR, Ihle JN, Kerr IM (1997) A JAK1/JAK2 chimera can sustain alpha and gamma interferon responses. *Mol Cell Biol* **17:** 695–706

Komatsu N, Nakauchi H, Miwa A, Ishihara T, Eguchi M, Moroi M, Okada M, Sato Y, Wada H, Yawata Y, Suda T, Miura Y (1991) Establishment and characterization of a human leukemic cell line with megakaryocytic features: dependency on granulocyte-macrophage colony-stimulating factor, interleukin 3, or erythropoietin for growth and survival. *Cancer Res* **51:** 341–348

Kubatzky KF, Liu W, Goldgraben K, Simmerling C, Smith SO, Constantinescu SN (2005) Structural requirements of the extracellular to transmembrane domain junction for erythropoietin receptor function. *J Biol Chem* **280:** 14844–14854

Kubatzky KF, Ruan W, Gurezka R, Cohen J, Ketteler R, Watowich SS, Neumann D, Langosch D, Klingmuller U (2001) Self assembly of the transmembrane domain promotes signal transduction through the erythropoietin receptor. *Curr Biol* **11:** 110–115

Kuiperij HB, van der Horst A, Raaijmakers J, Weijzen S, Medema RH, Bos JL, Burgering BM, Zwartkruis FJ (2005) Activation of FoxO transcription factors contributes to the antiproliferative effect of cAMP. *Oncogene* **24:** 2087–2095

Liu X, Constantinescu SN, Sun Y, Bogan JS, Hirsch D, Weinberg RA, Lodish HF (2000) Generation of mammalian cells stably expressing multiple genes at predetermined levels. *Anal Biochem* **280:** 20–28

Lupardus PJ, Skiniotis G, Rice AJ, Thomas C, Fischer S, Walz T, Garcia KC (2011) Structural snapshots of full-length Jak1, a transmembrane gp130/IL-6/IL-6Ralpha cytokine receptor complex, and the receptor-Jak1 holocomplex. *Structure* **19:** 45–55

Malinge S, Ragu C, Della-Valle V, Pisani D, Constantinescu SN, Perez C, Villeval JL, Reinhardt D, Landman-Parker J, Michaux L, Dastugue N, Baruchel A, Vainchenker W, Bourquin JP, Penard-Lacronique V, Bernard OA (2008) Activating mutations in human acute megakaryoblastic leukemia. *Blood* **112:** 4220–4226

Matthews EE, Thévenin D, Rogers JM, Gotow L, Lira PD, Reiter LA, Brissette WH, Engelman DM (2011) Thrombopoietin receptor activation: transmembrane helix dimerization, rotation and allosteric modulation. *FASEB J* **25:** 2234–2244

Mattoon D, Gupta K, Doyon J, Loll PJ, DiMaio D (2001) Identification of the transmembrane dimer interface of the bovine papillomavirus E5 protein. *Oncogene* **20:** 3824–3834

Miller BA, Zhang MY, Gocke CD, De Souza C, Osmani AH, Lynch C, Davies J, Bell L, Osmani SA (1999) A homolog of the fungal nuclear migration gene nudC is involved in normal and malignant human hematopoiesis. *Exp Hematol* **27:** 742–750

Millot GA, Vainchenker W, Dumenil D, Svinarchuk F (2004) Differential signalling of NH2-terminal flag-labelled thrombopoietin receptor activated by TPO or anti-FLAG antibodies. *Cell Signal* **16:** 355–363

Miyakawa Y, Oda A, Druker BJ, Kato T, Miyazaki H, Handa M, Ikeda Y (1995) Recombinant thrombopoietin induces rapid protein tyrosine phosphorylation of Janus kinase 2 and Shc in human blood platelets. *Blood* **86:** 23–27

Miyakawa Y, Oda A, Druker BJ, Miyazaki H, Handa M, Ohashi H, Ikeda Y (1996) Thrombopoietin induces tyrosine phosphorylation of Stat3 and Stat5 in human blood platelets. *Blood* **87:** 439–446

Miyakawa Y, Rojnuckarin P, Habib T, Kaushansky K (2001) Thrombopoietin induces phosphoinositol 3-kinase activation through SHP2, Gab, and insulin receptor substrate proteins in BAF3 cells and primary murine megakaryocytes. *J Biol Chem* **276:** 2494–2502

Oda A, Miyakawa Y, Druker BJ, Ishida A, Ozaki K, Ohashi H, Wakui M, Handa M, Watanabe K, Okamoto S, Ikeda Y (1996) Crkl is constitutively tyrosine phosphorylated in platelets from chronic myelogenous leukemia patients and inducibly phosphorylated in normal platelets stimulated by thrombopoietin. *Blood* **88:** 4304–4313

Onishi M, Mui AL, Morikawa Y, Cho L, Kinoshita S, Nolan GP, Gorman DM, Miyajima A, Kitamura T (1996) Identification of an oncogenic form of the thrombopoietin receptor MPL using retrovirus-mediated gene transfer. *Blood* **88:** 1399–1406

Pardanani AD, Levine RL, Lasho T, Pikman Y, Mesa RA, Wadleigh M, Steensma DP, Elliott MA, Wolanskyj AP, Hogan WJ, McClure RF, Litzow MR, Gilliland DG, Tefferi A (2006) MPL515 mutations in myeloproliferative and other myeloid disorders: a study of 1182 patients. *Blood* **108:** 3472–3476

Pecquet C, Staerk J, Chaligne R, Goss V, Lee KA, Zhang X, Rush J, Van Hees J, Poirel HA, Scheiff JM, Vainchenker W, Giraudier S, Polakiewicz RD, Constantinescu SN (2010) Induction of myeloproliferative disorder and myelofibrosis by thrombopoietin receptor W515 mutants is mediated by cytosolic tyrosine 112 of the receptor. *Blood* **115:** 1037–1048

Pikman Y, Lee BH, Mercher T, McDowell E, Ebert BL, Gozo M, Cuker A, Wernig G, Moore S, Galinsky I, Deangelo DJ, Clark JJ, Lee SJ, Golub TR, Wadleigh M, Gilliland DG, Levine RL (2006) MPLW515L is a novel somatic activating mutation in myelofibrosis with myeloid metaplasia. *PLoS Med* **3:** e270

Porteu F, Rouyez MC, Cocault L, Benit L, Charon M, Picard F, Gisselbrecht S, Souyri M, Dusanter-Fourt I (1996) Functional regions of the mouse thrombopoietin receptor cytoplasmic domain: evidence for a critical region which is involved in differentiation and can be complemented by erythropoietin. *Mol Cell Biol* **16:** 2473–2482

 ©2011 European Molecular Biology Organization

Qian H, Buza-Vidas N, Hyland CD, Jensen CT, Antonchuk J, Mansson R, Thoren LA, Ekblom M, Alexander WS, Jacobsen SE (2007) Critical role of thrombopoietin in maintaining adult quiescent hematopoietic stem cells. *Cell Stem Cell* **1:** 671–684

Royer Y, Staerk J, Costuleanu M, Courtoy PJ, Constantinescu SN (2005) Janus kinases affect thrombopoietin receptor cell surface localization and stability. *J Biol Chem* **280:** 27251–27261

Seubert N, Royer Y, Staerk J, Kubatzky KF, Moucadel V, Krishnakumar S, Smith SO, Constantinescu SN (2003) Active and inactive orientations of the transmembrane and cytosolic domains of the erythropoietin receptor dimer. *Mol Cell* **12:** 1239–1250

Skiniotis G, Lupardus PJ, Martick M, Walz T, Garcia KC (2008) Structural organization of a full-length gp130/LIF-R cytokine receptor transmembrane complex. *Mol Cell* **31:** 737–748

Solar GP, Kerr WG, Zeigler FC, Hess D, Donahue C, de Sauvage FJ, Eaton DL (1998) Role of c-mpl in early hematopoiesis. *Blood* **92:** 4–10

Sotiropoulos A, Moutoussamy S, Binart N, Kelly PA, Finidori J (1995) The membrane proximal region of the cytoplasmic domain of the growth hormone receptor is involved in the activation of Stat 3. *FEBS Lett* **369:** 169–172

Souyri M, Vigon I, Penciolelli JF, Heard JM, Tambourin P, Wendling F (1990) A putative truncated cytokine receptor gene transduced by the myeloproliferative leukemia virus immortalizes hematopoietic progenitors. *Cell* **63:** 1137–1147

Staerk J, Lacout C, Smith SO, Vainchenker W, Constantinescu SN (2006) An amphipathic motif at the transmembrane-cytoplasmic junction prevents autonomous activation of the thrombopoietin receptor. *Blood* **107:** 1864–1871

Storz P, Doppler H, Horn-Muller J, Groner B, Pfizenmaier K, Muller G (1999) A cellular reporter assay to monitor insulin receptor kinase activity based on STAT 5-dependent luciferase gene expression. *Anal Biochem* **276:** 97–104

Swaminathan K, Flynn P, Reece RJ, Marmorstein R (1997) Crystal structure of a PUT3-DNA complex reveals a novel mechanism for DNA recognition by a protein containing a Zn2Cys6 binuclear cluster. *Nat Struct Biol* **4:** 751–759

Thompson JE, Cubbon RM, Cummings RT, Wicker LS, Frankshun R, Cunningham BR, Cameron PM, Meinke PT, Liverton N, Weng Y, DeMartino JA (2002) Photochemical preparation of a pyridone containing tetracycle: a Jak protein kinase inhibitor. *Bioorg Med Chem Lett* **12:** 1219–1223

Treisman R (1995) Journey to the surface of the cell: Fos regulation and the SRE. *EMBO J* **14:** 4905–4913

Vainchenker W, Dusa A, Constantinescu SN (2008) JAKs in pathology: role of Janus kinases in hematopoietic malignancies and immunodeficiencies. *Semin Cell Dev Biol* **19:** 385–393

Walters KJ, Dayie KT, Reece RJ, Ptashne M, Wagner G (1997) Structure and mobility of the PUT3 dimer. *Nat Struct Biol* **4:** 744–750

Watowich SS, Wu H, Socolovsky M, Klingmuller U, Constantinescu SN, Lodish HF (1996) Cytokine receptor signal transduction and the control of hematopoietic cell development. *Annu Rev Cell Dev Biol* **12:** 91–128

Yoshihara H, Arai F, Hosokawa K, Hagiwara T, Takubo K, Nakamura Y, Gomei Y, Iwasaki H, Matsuoka S, Miyamoto K, Miyazaki H, Takahashi T, Suda T (2007) Thrombopoietin/MPL signaling regulates hematopoietic stem cell quiescence and interaction with the osteoblastic niche. *Cell Stem Cell* **1:** 685–697

©2011 European Molecular Biology Organization

Annex 5

Activating Janus kinase pseudokinase domain mutations in myeloproliferative and other blood cancers

Stefan N. Constantinescu[1], Emilie Leroy, Vitalina Gryshkova, Christian Pecquet and Alexandra Dusa
Ludwig Institute for Cancer Research and Université Catholique de Louvain, de Duve Institute, Brussels B1200, Belgium

Abstract

The discovery of the highly prevalent activating JAK (Janus kinase) 2 V617F mutation in myeloproliferative neoplasms, and of other pseudokinase domain-activating mutations in JAK2, JAK1 and JAK3 in blood cancers, prompted great interest in understanding how pseudokinase domains regulate kinase domains in JAKs. Recent functional and mutagenesis studies identified residues required for the V617F mutation to induce activation. Several X-ray crystal structures of either kinase or pseudokinase domains including the V617F mutant of JAK2 pseudokinase domains are now available, and a picture has emerged whereby the V617F mutation induces a defined conformational change around helix C of JH (JAK homology) 2. Effects of mutations on JAK2 can be extrapolated to JAK1 and TYK2 (tyrosine kinase 2), whereas JAK3 appears to be different. More structural information of the full-length JAK coupled to cytokine receptors might be required in order to define the structural basis of JH1 activation by JH2 mutants and eventually obtain mutant-specific inhibitors.

Introduction: the JAK family and their functions

The human genome codes for four JAKs (Janus kinases, although JAK initially stood for 'just another kinase') [1]. They contain homologous domains, denoted JH (JAK homology) domains, which are, from the C-terminus to the N-terminus: JH1 (kinase domain), JH2 (pseudokinase domain), JH3–(part of) JH4 [SH2 (Src homology 2) domain] and (part of JH4)–JH7 [N-terminal FERM (band 4.1/ezrin/radixin/moesin domain], that is required for attachment of JAKs to the cytosolic domains of cytokine receptors (Figure 1a) [2–4].

The N-terminal FERM–SH2 fragments of JAKs were shown to chaperone and stabilize receptors at the cell surface [4–6] (Figure 1b). In the absence of ligand, receptor–JAK complexes are inactive. Binding of cytokines to their receptors triggers a conformational change of usually pre-formed dimers [7,8] that are transmitted to the cytosolic domains, which leads to cross-phosphorylation and activation of JAKs that phosphorylate tyrosine residues on the cytosolic domains of receptors. These then recruit signalling proteins that become substrates of JAKs [8–11]. The STAT (signal transducer and activator of transcription) [12] along with Ras/MAPK (mitogen-activated protein kinase) and PI3K (phosphoinositide 3-kinase)/Akt/mTOR (mammalian target of rapamycin) pathways then transmit the signal to the nucleus.

In the blood myeloid lineages, Epo (erythropoietin) controls erythroid differentiation, Tpo (thrombopoietin) controls megakaryocytic differentiation, whereas G-CSF (granulocyte colony-stimulating factor) regulates granulocyte formation. The three receptors, i.e. EpoR (Epo receptor), TpoR (Tpo receptor) (c-MPL) and G-CSFR (G-CSF receptor), utilize JAK2 [9,13].

There is evidence for both positive and negative roles of pseudokinase (JH2) domains on JH1 kinase activity. A positive role was shown by the Pellegrini laboratory for TYK2 (tyrosine kinase 2) with JH2 mutations that completely (E782K) [14] or partially (I684S, P1104A) [15] inactivate TYK2 JH1 kinase. Inhibitory JH2 mutations were also described in JAK3 [16]. On the other hand, biochemical studies from the Silvennoinen laboratory showed that the pseudokinase domain inhibits basal kinase activity of the kinase domain, suggesting a negative role of JH2 on JH1 activity [17,18].

JH2 binds ATP and possesses weak kinase activity, phosphorylating *in cis* Ser^{523} (in the SH2–JH2 linker) and *in trans* Tyr^{570} (in JH2) [19,20], that are negative regulatory sites [21,22]. The precise residues targeted by phosphorylated Ser^{523} and Tyr^{570} and the mechanism of JH1 inhibition remain unknown.

Physiological activation of JAKs by cytokine-activated receptors requires JAK dimerization and close proximity,

Key words: blood cancer, Janus kinase (JAK), myeloproliferative disorder, pseudokinase domain.
Abbreviations used: APL, acute promyelocytic leukaemia; DHFR, dihydrofolate reductase; Epo, erythropoietin; EpoR, Epo receptor; FERM, band 4.1/ezrin/radixin/moesin; G-CSF, granulocyte colony-stimulating factor; G-CSFR, G-CSF receptor; JAK, Janus kinase; JH, JAK homology; PML, promyelocytic leukaemia; RARα, retinoic acid receptor α; SH2, Src homology 2; STAT, signal transducer and activator of transcription; Tpo, thrombopoietin; TpoR, Tpo receptor; TYK2, tyrosine kinase 2.
[1] To whom correspondence should be addressed (email stefan.constantinescu@bru.licr.org).

©The Authors Journal compilation ©2013 Biochemical Society

Figure 1 | **JAK2 segment structure and interaction with cytokine receptors**

(**a**) Representation of JAK2 primary structure that consists of seven JH domains. The point mutation V617F is located in the pseudokinase domain and is found in >95 % of patients with polycythaemia vera. (**b**) Schematic illustration of intracellular type I cytokine receptor trafficking to the cell surface. JAK2, via its FERM domain, promotes cell-surface localization and stabilization of cytokine receptors, such as EpoR and TpoR.

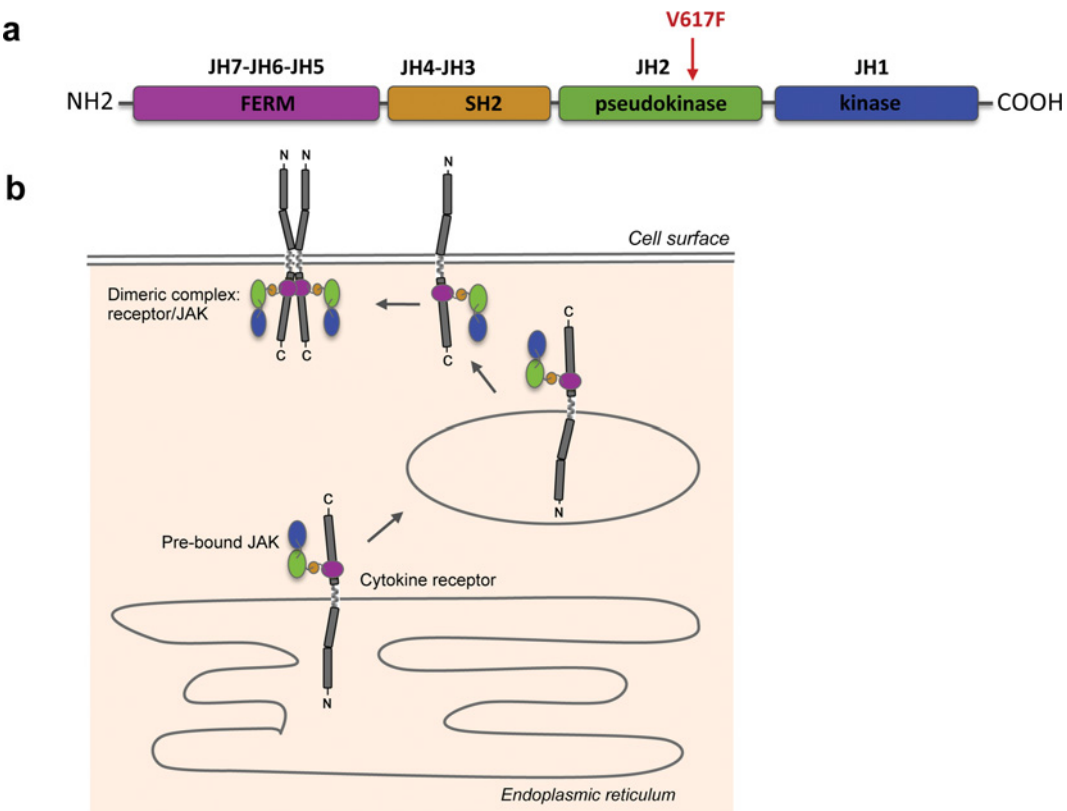

so that the activation loop residue Tyr^{1007} becomes phosphorylated [23]. Protein fragment complementation using JAK2 fused at the C-terminus to complementing fragments of DHFR (dihydrofolate reductase), showed that in cells transfected with EpoR, Epo treatment for 30 min led to DHFR reconstitution [24]. Thus, upon cytokine addition, the C-terminal ends of JAK2 come into close proximity.

JAK2 V617F in myeloid cancers

A major interest was elicited in pseudokinase JAK domains when an activating mutation was discovered in a group of human blood cancers: MPNs (myeloproliferative neoplasms) [25]. The unique acquired somatic JAK2 V617F mutation is associated with >98 % of polycythaemia vera and >50 % of essential thrombocythaemia and myelofibrosis patients [25–28].

The V617F mutation leads to constitutive JAK2 signalling, via STAT5, STAT3, ERK (extracellular-signal-regulated kinase) 1/2 and Akt [25]. For activation, a cytokine receptor must be co-expressed [29], and the FERM domain of JAK2 V617F must be intact [30]. The three dimeric myeloid receptors, i.e. EpoR, TpoR and G-CSFR, form complexes with JAK2 V617F, and they signal constitutively.

Saturation mutagenesis at Val^{617} showed that tryptophan, leucine, isoleucine and methionine were also activating mutations. V617Y does not induce activation [31], suggesting that the hydroxy group of tyrosine prevents activation.

V617W showed the strongest activity, followed by V617F and then V617I, V617L or V617M were weaker [31]. However, for obtaining V617W or V617M, three or two nucleotides should be mutated respectively, whereas JAK2 V617F is obtained by one nucleotide change. V617I can be obtained by one base pair change, and it can be detected in rare myelofibrosis patients [32]. The same mutation has been discovered in a family with hereditary thrombocytosis [33]. Weaker than JAK2 V617F, JAK2 V617I signals in association only with TpoR, and not with other receptors, thus explaining the thrombocytosis phenotype [34].

©The Authors Journal compilation ©2013 Biochemical Society

Mechanisms of activation by V617F at the structural level

Several studies have converged on the important role of one phenylalanine residue, Phe^{595} of helix C, in supporting the activation by V617F. By aligning JH2 with other kinases, by assuming that JH2 also is folded like a kinase domain and by comparing the X-ray crystal structures of those kinase domains, the closest residue in space [<4 Å (1 Å = 0.1 nm)] to Phe^{617} was shown to be Phe^{595} [35]. Mutations of Phe^{595} to several aliphatic residues (F595A, F595I, F595L, F595K) inhibited the constitutive activity of JAK2 V617F, but did not affect its ability to be activated when cells were treated with Epo (for EpoR cells) [35]. Mutations of Phe^{595} to aromatic residues (F595W or F595Y) supported constitutive V617F activity. Thus an aromatic stacking interaction is necessary for constitutive V617F activity. Another study, utilizing cytokine receptors other than EpoR or TpoR, also detected an important role for Phe^{595} in JAK2 V617F activity [36].

A major advance was represented by the X-ray crystal structure of the JAK2 JH2 domain with or without V617F that was solved by the Hubbard laboratory in a collaborative effort with the Silvennoinen laboratory [20]. The X-ray crystal structures showed that JH2 bound ATP in a non-conventional manner, that it adopted an active kinase fold and that the V617F mutation rigidified, and extended by one turn, the helix C of JH2, via an aromatic stacking between Phe^{617}, Phe^{595} and Phe^{594} (Figure 2), which comes into this aromatic network only in the V617F mutant [20]. Computational approaches that succeeded in microsecond simulations by David Shaw's group showed that the stability of helix C of JH2 is actually increased by the V617F mutation, and decreased by the F595A mutation [20].

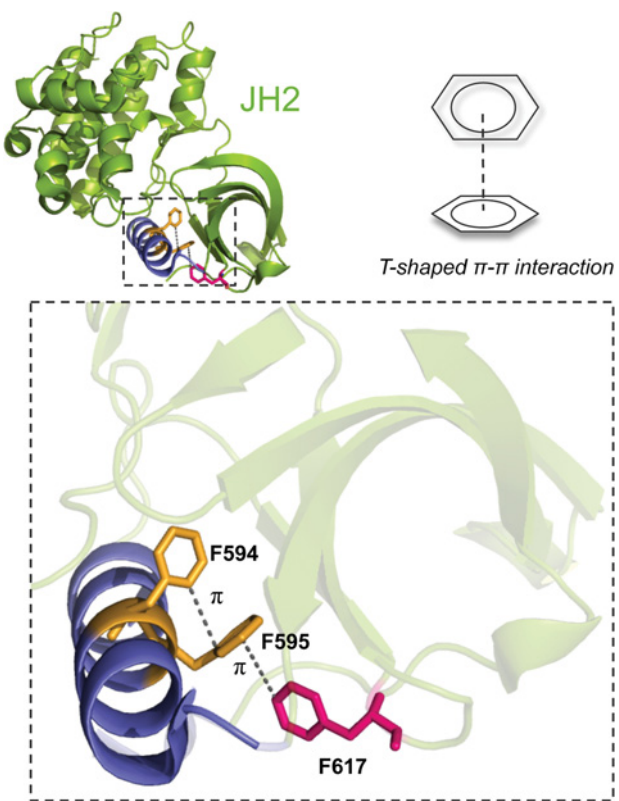

Figure 2 | Structural features of the JAK2 V617F α-helix C

In the mutant JAK2 V617F (PDB code 4FVR), the three aromatic residues Phe^{594}, Phe^{595} and Phe^{617} are involved in a double T-shaped π–π stacking interaction where Phe^{595} plays a pivotal role in maintaining the non-covalent interaction leading to a change of conformation of JH2 α-helix C, which is presumed to be responsible for the activation of the kinase domain. The X-ray crystal structure of JH2 V617F displays a more rigid and longer JH2 α-helix C due to the aromatic interplay. In the mutant protein, substitution of Phe^{595} by a non-aromatic residue produces a kinase, which responds to stimuli in a similar manner to wild-type JAK2.

Models for activation

It is not known at the moment how the kinase domains are regulated by JH2 or by JH2 V617F. The F739R mutation in helix F of the C-terminal lobe, which is predicted to disorganize the fold of the C-terminal lobe of JH2 only led to levels of activation that were much lower than those induced by the V617F mutation [20]. These data indicate that the V617F mutation activates JH1, and does not only remove the JH2 inhibition on JH1. JH2 domains might form heteromeric dimers with JH1 domains (*in cis* or *in trans*), or with themselves, and this could change between inactive and active states.

Two major theoretical models have been used to explore effects of V617F. One is the Lindauer–Kroemer model [37,38]. It was based on a dimer seen in the X-ray crystal structure of the FGFR1 (fibroblast growth factor receptor 1) kinase [39]. This is an antiparallel symmetric (anti-symmetrical) JH1–JH2 interaction in the inactive state (also having JH2 as an inactive kinase) and defined two interfaces, one between helices C of JH2 and JH1 and the other between the Val^{617}-containing loop and residues of JH1. In the active state of JH1, its activation loop was predicted to clash with residues around position 617. Amazingly, this 2001 model proposed that residues 617 and 618 might be mutated in active JAK2 mutants [37]. Molecular dynamics simulations based on this model suggested that Phe^{595} prevents activation normally, and forms an aromatic stacking interaction with Phe^{617} in V617F, thus preventing JH1 inhibition by JH2 [40]. However, single Phe^{595} mutations are not activating [35].

The second is an asymmetric model [41,42], whereby the N-terminal lobe of JH2 binds to the C-terminal lobe of JH1, possibly inhibiting JH1. This model is based on the mechanism of activation described for EGFR (epidermal growth factor receptor) kinase in a dimer where one kinase is the 'activator' and the other kinase binding with its N-terminal lobe being the 'receiver' [43,44]. The V617F mutation is presumed to alter this arrangement and subsequently to favour a dimer of JH1 kinases that leads to activation. Several interface residues were described between JH2 and JH1 interacting in the initial antiparallel symmetric

©The Authors Journal compilation ©2013 Biochemical Society

Figure 3 | **The cytokine receptor–JAK2 complex**

JAK2 is 1132 amino acids long, whereas the length of type I cytokine cytosolic domains vary between 122 (TpoR) or 236 (EpoR) amino acids. The prediction is that cytokine receptor cytosolic domains form functional units with the appended JAKs.

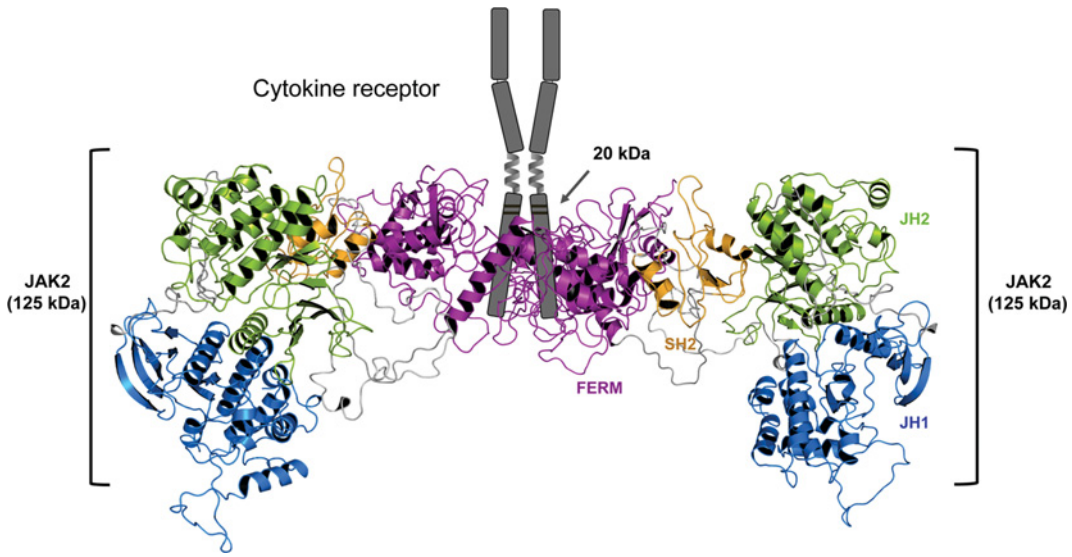

Kroemer model configuration or between JH2 and JH1 interacting in an intermediate conformation between the symmetric and asymmetric models (JH2 helix C binding to the activation loop of JH1) [42]. On the basis of mutagenesis data, it is thought that V617F-induced activation of JAK2 requires intramolecular effects along the full-length JAK2 [30,45,46].

Furthermore, cytosolic tails of cytokine receptors might be crucial for JAK2 V617F activation, both as scaffolds, and by promoting dimerization of JAK2 V617F (or other mutants) in preformed oligomeric receptor complexes [7,8,29,47,48]. Receptors have been notoriously difficult to crystallize, possibly because cytosolic distal regions might be largely non-structured. It was proposed that juxtamembrane regions are helical up until Box 1 and that they are rigid and their conformation is controlled by the transmembrane helix [8,10]. Single-particle electron microscopy on an IL-6 (interleukin 6) receptor by the Garcia group in Stanford showed that these regions are rigid and closely packed in the full-length receptor that binds JAKs [49]. Given that JAKs are 4–6-fold larger than the average cytosolic domains of receptors (Figure 3), it is likely that receptors and JAKs form functional units. Thus a structure of the entire receptor–JAK complex would be necessary. Interestingly, a negative regulator, SOCS3 (suppressor of cytokine signalling 3), has been shown to target specific receptor–JAK2 complexes by simultaneously binding the JAK2 kinase domain and the receptor cytosolic domain [50].

A provocative possibility is that the V617F mutation somehow promotes the formation of the regulatory hydrophobic spine, aligning in an active conformation four non-polar residues located on β4 and αC in the N-terminal lobe and the phenylalanine and tyrosine residues of the DFG (Asp-Phe-Gly) and Y/HRD (Tyr/His-Arg-Asp) motifs [51]. During activation, the phenylalanine residue from the activation loop DFG moves into the spine (DFG-in conformation), pushing out the activation loop and allowing its activation. V617F might alter the spine of JH2, and this might promote formation of the hydrophobic spine of JH1, eventually achieving its activation. Further studies are required to verify this hypothesis.

V617F homologous JAK1 and TYK2 mutations

The V617F homologous mutations activate JAK1 (V658F) and TYK2 (V678F), but not JAK3 [52]. A methionine residue is present at the homologous 617 position in JAK3, and methionine is already activating for JAK2 [31], indicating that activating conformations for JAK3 differ from the other JAKs. JAK1 V658F was found in a fraction of acute adult T-ALL (T-lymphoblastoid leukaemia) and in several other leukaemic conditions [53–55].

In a mouse model of APL (acute promyelocytic leukaemia)-M3, expression of the PML (promyelocytic leukaemia)–RARα (retinoic acid receptor α) fusion protein induced leukemia in mice after 8 months. In those leukaemia blasts, one recurrent acquired mutation was JAK1 V658F [56]. Co-expression of PML–RARα and JAK1 V658F led to rapid APL-M3 in mice [56]. Thus acquisition of JAK mutations precisely at the V617F homologous position seems to be a common event in experimental leukaemia.

©The Authors Journal compilation ©2013 Biochemical Society

Other JAK pseudokinase domain mutations

In JAK2, exon 12 mutations around Lys^{539} in the linker between the SH2 and JH2 domains are strongly activating and associate with 2% of polycythaemia vera cases [57]. A salt bridge between Asp^{620} and Lys^{539} is predicted to prevent a tight contact between Val^{617} and the helix C of JH2 [57,58]. However, Lys^{539} is missing from the JH2 crystal [20]. Interrupting this salt bridge might change the conformation of the Val^{617} loop in such a way [57,58] that it might somehow induce effects similar to those of bulky residues at Val^{617} [31]. Recent molecular dynamics simulations indicate that the SH2–JH2 linker stabilizes the conformation induced by V617F [42].

A deletion of $I^{682}REED^{686}$ in JAK2 was first shown to be associated with Down's syndrome B-cell precursor lymphoblastoid leukaemia [59]. The arginine residue (Arg^{683}) in the IREED sequence (located in the hinge between the JH2 N- and C-terminal lobes) was then found to be mutated to serine and glycine in paediatric lymphoblastic leukaemia [54,60].

Several studies selecting in culture for active JAK2 and JAK1 mutations showed that most of such mutations were in the JH2 and SH2–JH2 linker. Certain active mutations were in JH1, and some were JAK2-inhibitor resistant [45,48,61]. A simple model where mutations in JH2 would only alleviate the inhibitory effect of JH2 on JH1 would imply that also mutations on the JH1 site of the interface should be frequently detected, which was not the case.

Finally, a number of activating mutations have been identified in JAK3 with some being in the helix C of the pseudokinase domain. One mutation (A572V) was associated with megakaryoblastic leukaemia [62]. A similar mutation in JAK2 is not activating (A. Dusa, E. Leroy, C. Pecquet, C. Mouton and S.N. Constantinescu, unpublished work), again pointing to differences between JAK3 and other JAKs.

Conclusion

An emerging principle is that, in several pathologies, mutations in the pseudokinase domain of JAKs activate their kinase domain. Whereas the conformational change locally in JH2 induced by the prevalent V617F mutation has been visualized by X-ray crystal structure studies, the mechanism by which mutated JH2 domains activate JH1 domains remains unknown. Structural and biophysical studies are required for understanding how transmembrane cytokine receptors interact with JAKs, and how cytokine binding or mutations in JAKs lead to JH1 kinase domain activation.

Funding

Grant support from FRS-FNRS (Fonds de la Recherche Scientifique), Salus Sanguinis Foundation, Fondation contre le Cancer, Belgium, Ludwig Institute for Cancer Research, de Duve Institute, Action de Recherche Concertée of Université Catholique de Louvain [grant number ARC10/15-027] and the Interuniversity Attraction Pole (IAP) of Belgium is acknowledged. V.G. and E.L. were supported by de Duve Institute Delori postdoctoral fellowship and by a Fonds pour la formation à la Recherche dans l'Industrie et dans l'Agriculture (FRIA) PhD fellowship respectively. S.N.C. is a senior research associate of FRS-FNRS, Belgium.

References

1 Ziemiecki, A., Harpur, A.G. and Wilks, A.F. (1994) JAK protein tyrosine kinases: their role in cytokine signalling. Trends Cell Biol. **4**, 207–212
2 Hilkens, C.M., Is'harc, H., Lillemeier, B.F., Strobl, B., Bates, P.A., Behrmann, I. and Kerr, I.M. (2001) A region encompassing the FERM domain of Jak1 is necessary for binding to the cytokine receptor gp130. FEBS Lett. **505**, 87–91
3 Haan, C., Is'harc, H., Hermanns, H.M., Schmitz-Van De Leur, H., Kerr, I.M., Heinrich, P.C., Grotzinger, J. and Behrmann, I. (2001) Mapping of a region within the N terminus of Jak1 involved in cytokine receptor interaction. J. Biol. Chem. **276**, 37451–37458
4 Huang, L.J., Constantinescu, S.N. and Lodish, H.F. (2001) The N-terminal domain of Janus kinase 2 is required for Golgi processing and cell surface expression of erythropoietin receptor. Mol. Cell **8**, 1327–1338
5 Radtke, S., Hermanns, H.M., Haan, C., Schmitz-Van De Leur, H., Gascan, H., Heinrich, P.C. and Behrmann, I. (2002) Novel role for Janus kinase 1 in the regulation of oncostatin M receptor surface expression. J. Biol. Chem. **277**, 11297–11305
6 Ragimbeau, J., Dondi, E., Alcover, A., Eid, P., Uze, G. and Pellegrini, S. (2003) The tyrosine kinase Tyk2 controls IFNAR1 cell surface expression. EMBO J. **22**, 537–547
7 Constantinescu, S.N., Keren, T., Socolovsky, M., Nam, H., Henis, Y.I. and Lodish, H.F. (2001) Ligand-independent oligomerization of cell-surface erythropoietin receptor is mediated by the transmembrane domain. Proc. Natl. Acad. Sci. U.S.A. **98**, 4379–4384
8 Brown, R.J., Adams, J.J., Pelekanos, R.A., Wan, Y., McKinstry, W.J., Palethorpe, K., Seeber, R.M., Monks, T.A., Eidne, K.A., Parker, M.W. and Waters, M.J. (2005) Model for growth hormone receptor activation based on subunit rotation within a receptor dimer. Nat. Struct. Mol. Biol. **12**, 814–821
9 Haan, C., Kreis, S., Margue, C. and Behrmann, I. (2006) Jaks and cytokine receptors: an intimate relationship. Biochem. Pharmacol. **72**, 1538–1546
10 Seubert, N., Royer, Y., Staerk, J., Kubatzky, K.F., Moucadel, V., Krishnakumar, S., Smith, S.O. and Constantinescu, S.N. (2003) Active and inactive orientations of the transmembrane and cytosolic domains of the erythropoietin receptor dimer. Mol. Cell **12**, 1239–1250
11 Witthuhn, B.A., Quelle, F.W., Silvennoinen, O., Yi, T., Tang, B., Miura, O. and Ihle, J.N. (1993) JAK2 associates with the erythropoietin receptor and is tyrosine phosphorylated and activated following stimulation with erythropoietin. Cell **74**, 227–236
12 Darnell, Jr, J.E., Kerr, I.M. and Stark, G.R. (1994) Jak–STAT pathways and transcriptional activation in response to IFNs and other extracellular signaling proteins. Science **264**, 1415–1421
13 Vainchenker, W., Dusa, A. and Constantinescu, S.N. (2008) JAKs in pathology: role of Janus kinases in hematopoietic malignancies and immunodeficiencies. Semin. Cell Dev. Biol. **19**, 385–393
14 Shaw, M.H., Boyartchuk, V., Wong, S., Karaghiosoff, M., Ragimbeau, J., Pellegrini, S., Muller, M., Dietrich, W.F. and Yap, G.S. (2003) A natural mutation in the Tyk2 pseudokinase domain underlies altered susceptibility of B10.Q/J mice to infection and autoimmunity. Proc. Natl. Acad. Sci. U.S.A. **100**, 11594–11599
15 Li, Z., Gakovic, M., Ragimbeau, J., Eloranta, M.L., Ronnblom, L., Michel, F. and Pellegrini, S. (2013) Two rare disease-associated Tyk2 variants are catalytically impaired but signaling competent. J. Immunol. **190**, 2335–2344
16 Russell, S.M., Tayebi, N., Nakajima, H., Riedy, M.C., Roberts, J.L., Aman, M.J., Migone, T.S., Noguchi, M., Markert, M.L., Buckley, R.H. et al. (1995) Mutation of Jak3 in a patient with SCID: essential role of Jak3 in lymphoid development. Science **270**, 797–800
17 Saharinen, P. and Silvennoinen, O. (2002) The pseudokinase domain is required for suppression of basal activity of Jak2 and Jak3 tyrosine kinases and for cytokine-inducible activation of signal transduction. J. Biol. Chem. **277**, 47954–47963
18 Saharinen, P., Takaluoma, K. and Silvennoinen, O. (2000) Regulation of the Jak2 tyrosine kinase by its pseudokinase domain. Mol. Cell. Biol. **20**, 3387–3395

©The Authors Journal compilation ©2013 Biochemical Society

19 Ungureanu, D., Wu, J., Pekkala, T., Niranjan, Y., Young, C., Jensen, O.N., Xu, C.F., Neubert, T.A., Skoda, R.C., Hubbard, S.R. and Silvennoinen, O. (2011) The pseudokinase domain of JAK2 is a dual-specificity protein kinase that negatively regulates cytokine signaling. Nat. Struct. Mol. Biol. **18**, 971–976

20 Bandaranayake, R.M., Ungureanu, D., Shan, Y., Shaw, D.E., Silvennoinen, O. and Hubbard, S.R. (2012) Crystal structures of the JAK2 pseudokinase domain and the pathogenic mutant V617F. Nat. Struct. Mol. Biol. **19**, 754–759

21 Ishida-Takahashi, R., Rosario, F., Gong, Y., Kopp, K., Stancheva, Z., Chen, X., Feener, E.P. and Myers, Jr, M.G. (2006) Phosphorylation of Jak2 on Ser^{523} inhibits Jak2-dependent leptin receptor signaling. Mol. Cell. Biol. **26**, 4063–4073

22 Argetsinger, L.S., Kouadio, J.L., Steen, H., Stensballe, A., Jensen, O.N. and Carter-Su, C. (2004) Autophosphorylation of JAK2 on tyrosines 221 and 570 regulates its activity. Mol. Cell. Biol. **24**, 4955–4967

23 Feng, J., Witthuhn, B.A., Matsuda, T., Kohlhuber, F., Kerr, I.M. and Ihle, J.N. (1997) Activation of Jak2 catalytic activity requires phosphorylation of Y1007 in the kinase activation loop. Mol. Cell. Biol. **17**, 2497–2501

24 Remy, I., Wilson, I.A. and Michnick, S.W. (1999) Erythropoietin receptor activation by a ligand-induced conformation change. Science **283**, 990–993

25 James, C., Ugo, V., Le Couedic, J.P., Staerk, J., Delhommeau, F., Lacout, C., Garcon, L., Raslova, H., Berger, R., Bennaceur-Griscelli, A. et al. (2005) A unique clonal JAK2 mutation leading to constitutive signalling causes polycythaemia vera. Nature **434**, 1144–1148

26 Baxter, E.J., Scott, L.M., Campbell, P.J., East, C., Fourouclas, N., Swanton, S., Vassiliou, G.S., Bench, A.J., Boyd, E.M., Curtin, N. et al. (2005) Acquired mutation of the tyrosine kinase JAK2 in human myeloproliferative disorders. Lancet **365**, 1054–1061

27 Levine, R.L., Wadleigh, M., Cools, J., Ebert, B.L., Wernig, G., Huntly, B.J., Boggon, T.J., Wlodarska, I., Clark, J.J., Moore, S. et al. (2005) Activating mutation in the tyrosine kinase JAK2 in polycythemia vera, essential thrombocythemia, and myeloid metaplasia with myelofibrosis. Cancer Cell **7**, 387–397

28 Kralovics, R., Passamonti, F., Buser, A.S., Teo, S.S., Tiedt, R., Passweg, J.R., Tichelli, A., Cazzola, M. and Skoda, R.C. (2005) A gain-of-function mutation of JAK2 in myeloproliferative disorders. N. Engl. J. Med. **352**, 1779–1790

29 Lu, X., Huang, L.J. and Lodish, H.F. (2008) Dimerization by a cytokine receptor is necessary for constitutive activation of JAK2V617F. J. Biol. Chem. **283**, 5258–5266

30 Wernig, G., Gonneville, J.R., Crowley, B.J., Rodrigues, M.S., Reddy, M.M., Hudon, H.E., Walz, C., Reiter, A., Podar, K., Royer, Y. et al. (2008) The Jak2V617F oncogene associated with myeloproliferative diseases requires a functional FERM domain for transformation and for expression of the Myc and Pim proto-oncogenes. Blood **111**, 3751–3759

31 Dusa, A., Staerk, J., Elliott, J., Pecquet, C., Poirel, H.A., Johnston, J.A. and Constantinescu, S.N. (2008) Substitution of pseudokinase domain residue Val-617 by large non-polar amino acids causes activation of JAK2. J. Biol. Chem. **283**, 12941–12948

32 Ma, W., Kantarjian, H., Zhang, X., Yeh, C.H., Zhang, Z.J., Verstovsek, S. and Albitar, M. (2009) Mutation profile of JAK2 transcripts in patients with chronic myeloproliferative neoplasias. J. Mol. Diagn. **11**, 49–53

33 Mead, A.J., Rugless, M.J., Jacobsen, S.E. and Schuh, A. (2012) Germline JAK2 mutation in a family with hereditary thrombocytosis. N. Engl. J. Med. **366**, 967–969

34 Mead, A.J., Chowdhury, O., Pecquet, C., Dusa, A., Woll, P., Atkinson, D., Burns, A., Score, J., Rugless, M., Clifford, R. et al. (2013) Impact of isolated germline JAK2V617I mutation on human hematopoiesis. Blood **121**, 4156–4165

35 Dusa, A., Mouton, C., Pecquet, C., Herman, M. and Constantinescu, S.N. (2010) JAK2 V617F constitutive activation requires JH2 residue F595: a pseudokinase domain target for specific inhibitors. PLoS ONE **5**, e11157

36 Gnanasambandan, K., Magis, A. and Sayeski, P.P. (2010) The constitutive activation of Jak2-V617F is mediated by a pi stacking mechanism involving phenylalanines 595 and 617. Biochemistry **49**, 9972–9984

37 Lindauer, K., Loerting, T., Liedl, K.R. and Kroemer, R.T. (2001) Prediction of the structure of human Janus kinase 2 (JAK2) comprising the two carboxy-terminal domains reveals a mechanism for autoregulation. Protein Eng. **14**, 27–37

38 Giordanetto, F. and Kroemer, R.T. (2002) Prediction of the structure of human Janus kinase 2 (JAK2) comprising JAK homology domains 1 through 7. Protein Eng. **15**, 727–737

39 Mohammadi, M., Schlessinger, J. and Hubbard, S.R. (1996) Structure of the FGF receptor tyrosine kinase domain reveals a novel autoinhibitory mechanism. Cell **86**, 577–587

40 Lee, T.S., Ma, W., Zhang, X., Giles, F., Kantarjian, H. and Albitar, M. (2009) Mechanisms of constitutive activation of Janus kinase 2-V617F revealed at the atomic level through molecular dynamics simulations. Cancer **115**, 1692–1700

41 Wan, S. and Coveney, P.V. (2012) Regulation of JAK2 activation by Janus homology 2: evidence from molecular dynamics simulations. J. Chem. Inf. Model. **52**, 2992–3000

42 Wan, X., Ma, Y., McClendon, C.L., Huang, L.J. and Huang, N. (2013) *Ab initio* modeling and experimental assessment of Janus kinase 2 (JAK2) kinase–pseudokinase complex structure. PLoS Comput. Biol. **9**, e1003022

43 Jura, N., Shan, Y., Cao, X., Shaw, D.E. and Kuriyan, J. (2009) Structural analysis of the catalytically inactive kinase domain of the human EGF receptor 3. Proc. Natl. Acad. Sci. U.S.A. **106**, 21608–21613

44 Shan, Y., Arkhipov, A., Kim, E.T., Pan, A.C. and Shaw, D.E. (2013) Transitions to catalytically inactive conformations in EGFR kinase. Proc. Natl. Acad. Sci. U.S.A. **110**, 7270–7275

45 Zhao, L., Dong, H., Zhang, C.C., Kinch, L., Osawa, M., Iacovino, M., Grishin, N.V., Kyba, M. and Huang, L.J. (2009) A JAK2 interdomain linker relays Epo receptor engagement signals to kinase activation. J. Biol. Chem. **284**, 26988–26998

46 Gorantla, S.P., Dechow, T.N., Grundler, R., Illert, A.L., Zum Buschenfelde, C.M., Kremer, M., Peschel, C. and Duyster, J. (2010) Oncogenic JAK2V617F requires an intact SH2-like domain for constitutive activation and induction of a myeloproliferative disease in mice. Blood **116**, 4600–4611

47 Malka, Y., Hornakova, T., Royer, Y., Knoops, L., Renauld, J.C., Constantinescu, S.N. and Henis, Y.I. (2008) Ligand-independent homomeric and heteromeric complexes between interleukin-2 or -9 receptor subunits and the γ chain. J. Biol. Chem. **283**, 33569–33577

48 Hornakova, T., Staerk, J., Royer, Y., Flex, E., Tartaglia, M., Constantinescu, S.N., Knoops, L. and Renauld, J.C. (2009) Acute lymphoblastic leukemia-associated JAK1 mutants activate the Janus kinase/STAT pathway via interleukin-9 receptor α homodimers. J. Biol. Chem. **284**, 6773–6781

49 Lupardus, P.J., Skiniotis, G., Rice, A.J., Thomas, C., Fischer, S., Walz, T. and Garcia, K.C. (2011) Structural snapshots of full-length Jak1, a transmembrane gp130/IL-6/IL-6Rα cytokine receptor complex, and the receptor–Jak1 holocomplex. Structure **19**, 45–55

50 Kershaw, N.J., Murphy, J.M., Liau, N.P., Varghese, L.N., Laktyushin, A., Whitlock, E.L., Lucet, I.S., Nicola, N.A. and Babon, J.J. (2013) SOCS3 binds specific receptor–JAK complexes to control cytokine signaling by direct kinase inhibition. Nat. Struct. Mol. Biol. **20**, 469–476

51 Kornev, A.P., Haste, N.M., Taylor, S.S. and Eyck, L.F. (2006) Surface comparison of active and inactive protein kinases identifies a conserved activation mechanism. Proc. Natl. Acad. Sci. U.S.A. **103**, 17783–17788

52 Staerk, J., Kallin, A., Demoulin, J.-B., Vainchenker, W. and Constantinescu, S.N. (2005) JAK1 and Tyk2 activation by the homologous polycythemia vera JAK2 V617F mutation: cross-talk with IGF1 receptor. J. Biol. Chem. **280**, 41893–41899

53 Flex, E., Petrangeli, V., Stella, L., Chiaretti, S., Hornakova, T., Knoops, L., Ariola, C., Fodale, V., Clappier, E., Paoloni, F. et al. (2008) Somatically acquired JAK1 mutations in adult acute lymphoblastic leukemia. J. Exp. Med. **205**, 751–758

54 Mullighan, C.G., Zhang, J., Harvey, R.C., Collins-Underwood, J.R., Schulman, B.A., Phillips, L.A., Tasian, S.K., Loh, M.L., Su, X., Liu, W. et al. (2009) JAK mutations in high-risk childhood acute lymphoblastic leukemia. Proc. Natl. Acad. Sci. U.S.A. **106**, 9414–9418

55 Jeong, E.G., Kim, M.S., Nam, H.K., Min, C.K., Lee, S., Chung, Y.J., Yoo, N.J. and Lee, S.H. (2008) Somatic mutations of JAK1 and JAK3 in acute leukemias and solid cancers. Clin. Cancer Res. **14**, 3716–3721

56 Wartman, L.D., Larson, D.E., Xiang, Z., Ding, L., Chen, K., Lin, L., Cahan, P., Klco, J.M., Welch, J.S., Li, C. et al. (2011) Sequencing a mouse acute promyelocytic leukemia genome reveals genetic events relevant for disease progression. J. Clin. Invest. **121**, 1445–1455

57 Scott, L.M., Tong, W., Levine, R.L., Scott, M.A., Beer, P.A., Stratton, M.R., Futreal, P.A., Erber, W.N., McMullin, M.F., Harrison, C.N. et al. (2007) JAK2 exon 12 mutations in polycythemia vera and idiopathic erythrocytosis. N. Engl. J. Med. **356**, 459–468

©The Authors Journal compilation ©2013 Biochemical Society

58 Gnanasambandan, K., Magis, A.T. and Sayeski, P.P. (2012) A shift in the salt bridge interaction of residues D620 and E621 mediates the constitutive activation of Jak2-H538Q/K539L. Mol. Cell. Biochem. **367**, 125–140
59 Malinge, S., Ben-Abdelali, R., Settegrana, C., Radford-Weiss, I., Debre, M., Beldjord, K., Macintyre, E.A., Villeval, J.L., Vainchenker, W., Berger, R. et al. (2007) Novel activating JAK2 mutation in a patient with Down syndrome and B-cell precursor acute lymphoblastic leukemia. Blood **109**, 2202–2204
60 Bercovich, D., Ganmore, I., Scott, L.M., Wainreb, G., Birger, Y., Elimelech, A., Shochat, C., Cazzaniga, G., Biondi, A., Basso, G. et al. (2008) Mutations of JAK2 in acute lymphoblastic leukaemias associated with Down's syndrome. Lancet **372**, 1484–1492
61 Weigert, O., Lane, A.A., Bird, L., Kopp, N., Chapuy, B., van Bodegom, D., Toms, A.V., Marubayashi, S., Christie, A.L., McKeown, M. et al. (2012) Genetic resistance to JAK2 enzymatic inhibitors is overcome by HSP90 inhibition. J. Exp. Med. **209**, 259–273
62 Walters, D.K., Mercher, T., Gu, T.L., O'Hare, T., Tyner, J.W., Loriaux, M., Goss, V.L., Lee, K.A., Eide, C.A., Wong, M.J. et al. (2006) Activating alleles of JAK3 in acute megakaryoblastic leukemia. Cancer Cell **10**, 65–75

Received 20 May 2013
doi:10.1042/BST20130084

©The Authors Journal compilation ©2013 Biochemical Society

From www.bloodjournal.org by guest on October 11, 2016. For personal use only.

Brief Report

blood

MYELOID NEOPLASIA

Annex 6

Cooperation of germ line JAK2 mutations E846D and R1063H in hereditary erythrocytosis with megakaryocytic atypia

Katarina Kapralova,[1-3,*] Monika Horvathova,[1,*] Christian Pecquet,[2,3,*] Jana Fialova Kucerova,[1] Dagmar Pospisilova,[4] Emilie Leroy,[2,3] Barbora Kralova,[1] Jelena D. Milosevic Feenstra,[5] Fiorella Schischlik,[5] Robert Kralovics,[5] Stefan N. Constantinescu,[2,3] and Vladimir Divoky[1]

[1]Department of Biology, Faculty of Medicine and Dentistry, Palacký University, Olomouc, Czech Republic; [2]Signal Transduction and Molecular Hematology Unit, Ludwig Institute for Cancer Research, Brussels, Belgium; [3]de Duve Institute, Université catholique de Louvain, Brussels, Belgium; [4]Department of Pediatrics, University Hospital and Faculty of Medicine and Dentistry, Olomouc, Czech Republic; and [5]CeMM Research Center for Molecular Medicine of the Austrian Academy of Sciences, Vienna, Austria

Key Points

- Cells expressing JAK2 E846D or R1063H exhibit pathologic STAT5 activation in the specific context of EPOR.
- Cooperation of germ line JAK2 mutations E846D and R1063H defines a JAK2-signaling threshold for induction of erythrocytosis.

The role of somatic *JAK2* mutations in clonal myeloproliferative neoplasms (MPNs) is well established. Recently, germ line *JAK2* mutations were associated with polyclonal hereditary thrombocytosis and triple-negative MPNs. We studied a patient who inherited 2 heterozygous JAK2 mutations, E846D from the mother and R1063H from the father, and exhibited erythrocytosis and megakaryocytic atypia but normal platelet number. Culture of erythroid progenitors from the patient and his parents revealed hypersensitivity to erythropoietin (EPO). Using cellular models, we show that both E846D and R1063H variants lead to constitutive signaling (albeit much weaker than JAK2 V617F), and both weakly hyperactivate JAK2/STAT5 signaling only in the specific context of the EPO receptor (EPOR). JAK2 E846D exhibited slightly stronger effects than JAK2 R1063H and caused prolonged EPO-induced phosphorylation of JAK2/STAT5 via EPOR. We propose that JAK2 E846D predominantly contributes to erythrocytosis, but is not sufficient for the full pathological phenotype to develop. JAK2 R1063H, with very weak effect on JAK2/STAT5 signaling, is necessary to augment JAK2 activity caused by E846D above a threshold level leading to erythrocytosis with megakaryocyte abnormalities. Both mutations were detected in the germ line of rare polycythemia vera, as well as certain leukemia patients, suggesting that they might predispose to hematological malignancy. (*Blood*. 2016;128(10):1418-1423)

Introduction

Somatic *JAK2* mutations are the most common disease-causing event in patients with myeloproliferative neoplasms (MPNs). In the majority of MPN patients, an acquired gain-of-function V617F JAK2 mutation leads to constitutive activation of the JAK2 kinase and subsequently to excessive activation of JAK/STAT signaling.[1-4] Recently, germ line *JAK2* mutations (different from V617F substitution) have been described in cases with familial MPNs exhibiting hereditary polyclonal thrombocytosis[5-7] and triple-negative MPNs.[8] All of these inherited *JAK2* mutations, localized in the kinase and pseudokinase domain of JAK2, signal through the thrombopoietin receptor (MPL) rather than the erythropoietin (EPO) receptor (EPOR), explaining the phenotype of the polyclonal disease. It is proposed that differential signaling of STATs leads to different clinical phenotypes associated with different activating *JAK2* mutations: essential thrombocythemia and hereditary thrombocytosis being promoted by MPL/STAT1 signaling; STAT5 activation resulting in excessive erythroid proliferation and polycythemia vera (PV).[6,9]

Here, we studied a patient who inherited 2 *JAK2* mutations and presented with erythrocytosis and abnormal megakaryopoiesis in the bone marrow (BM), partially resembling PV cases with *JAK2* exon 12 mutations.[10] Thus, in contrast to previously studied germ line *JAK2* mutations, which were all heterozygous, here mutations on both *JAK2* alleles are present. We show that both of these mutations are activating in the context of EPOR, but with different characteristics. Functional analyses of the 2 germ line *JAK2* mutations suggested the threshold of JAK2 activity necessary for induction of erythrocytosis.

Study design

Descriptions of assays and tests performed on patient's samples can be found in supplemental Materials and methods (available on the *Blood* Web site).

Ba/F3-EPOR[11] JAK2 stable transfectants or γ-2A cells were used in viability and proliferation assays, analyses of JAK2 signal transduction, and dual-luciferase assays for STAT transcriptional activities. Retrovirally transduced mouse BM cells were used for in vitro colony assay. Analysis of x-ray crystallography data was performed using PyMOL software. For detailed descriptions of individual procedures, see supplemental Materials and methods.

Submitted February 10, 2016; accepted June 30, 2016. Prepublished online as *Blood* First Edition paper, July 7, 2016; DOI 10.1182/blood-2016-02-698951.

*K.K., M.H., and C.P. contributed equally to this work.

The online version of this article contains a data supplement.

The publication costs of this article were defrayed in part by page charge payment. Therefore, and solely to indicate this fact, this article is hereby marked "advertisement" in accordance with 18 USC section 1734.

© 2016 by The American Society of Hematology

From www.bloodjournal.org by guest on October 11, 2016. For personal use only.

A

Hematological data and clinical characteristics of the whole family.

	Patient *(Normal values)*	Mother *(Normal values)*	Father *(Normal values)*	Brother *(Normal values)*
Age at diagnosis (years)	15	44	47	24
Sex	male	female	male	male
Red blood cell count (x10^{12}/L)	5.6 ± 0.2 *(4.5-5.3)*	5.0 *(3.8-4.9)*	5.1 *(4.3-5.7)*	5.0 *(4.3-5.7)*
Hemoglobin level (g/dL)	17.2 ± 0.5 *(13.0-16.0)*	14.9 *(12.0-16.0)*	16.2 *(13.0-18.0)*	15.6 *(13.0-18.0)*
Hematocrit (%)	49 ± 1.0 *(37.0-49.0)*	45 *(37.0-47.0)*	47 *(42.0-52.0)*	43 *(42.0-52.0)*
Red cell mass (mL/kg)	32.1 *(24.0 – 32.0)*	ND	ND	ND
Erythropoietin (IU/L)	8.9 ± 1.8 *(4.3-29.0)*	8.7 *(4.3-29.0)*	4.7 *(4.3-29.0)*	17.0 *(4.3-29.0)*
Clinical signs	Plethora, splenomegaly	None	None	None

B

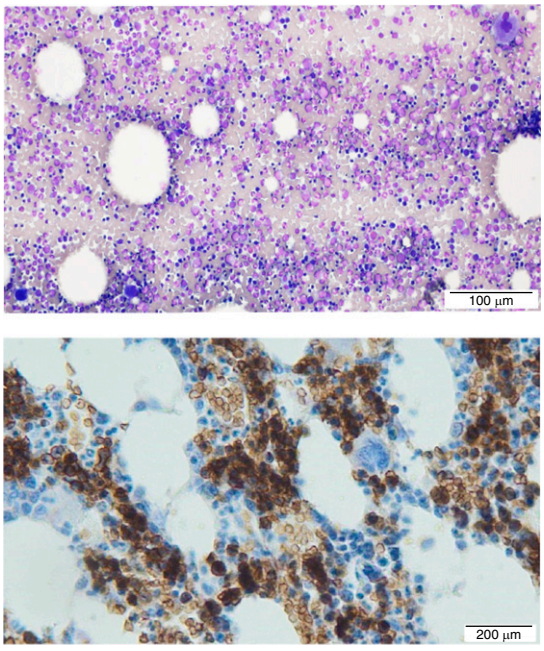

C

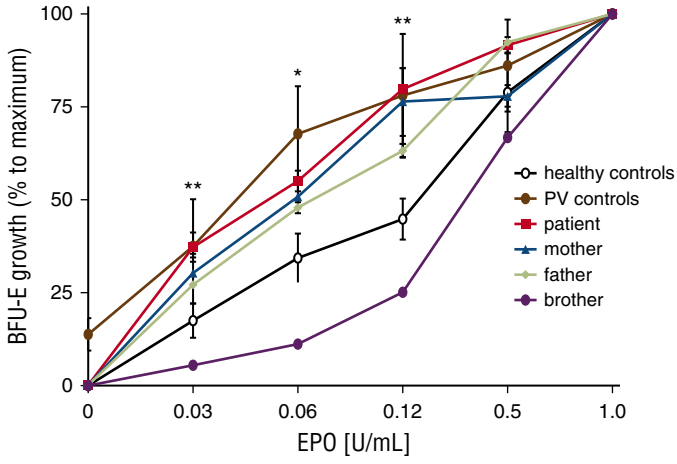

EPO [U/mL]	Patient *P value*	Mother *P value*	Father *P value*	PV *P value*
0.0	*NS*	*NS*	*NS*	**.00002**
0.03	**.00847**	**.03445**	*NS*	**.03115**
0.06	**.01636**	**.03039**	*NS*	**.00698**
0.12	**.00103**	**.00496**	**.011**	**.00424**
0.5	*NS*	*NS*	*NS*	*NS*

Figure 1. Hematological parameters, clinical data, BM evaluation, and in vitro sensitivity assay of erythroid progenitors to EPO. (A) Hematological and clinical analysis of the propositus and his family members revealed erythrocytosis, plethora, and palpable spleen (splenic length of 12 cm based on ultrasound measurement) in the patient. ND, not done. (B) Patient's BM aspirate (May-Grünwald-Giemsa staining, top) and BM biopsy (glycophorin C staining specific for erythroid lineage, brown color, bottom) showed hypercellularity, erythroid hyperplasia, normal granulopoiesis, and abnormal megakaryopoiesis (for details, see supplemental Figure 1). The images were visualized with an Olympus BX41 light microscope (Hamburg, Germany) and acquired with an Olympus DP73 camera driven by CellSens Entry software. Images were labeled using Adobe Photoshop software (Adobe Systems, San Jose, CA). Top: magnification, ×100; scale bar, 100 μm. Bottom: magnification, ×200; scale bar, 200 μm. (C) The EPO dose-response curves derived from the patient, patient's brother, patient's parents, normal controls, and PV patients. The growth of BFU-E colonies at the indicated concentrations of EPO was expressed as a percentage of maximal EPO stimulation (represented by EPO concentration of 1 U/mL). Erythroid progenitors from the patient (red curve) were hypersensitive to EPO; there was a relatively higher number of BFU-E colonies in comparison with healthy controls (black curve) in low EPO concentrations. The in vitro growth of the erythroid progenitors of both of the patient's parents (blue and green curve, respectively) also showed slightly increased sensitivity to EPO when compared with normal controls (black curve). The progenitors of the patient's brother (purple curve) showed normal growth. Two PV patients, positive for the V617F mutation (brown curve), were used as positive controls for hypersensitivity and formation of EPO-independent colonies (EECs). The table below the graph shows statistical evaluation of the BFU-E colony number at individual concentrations with respect to normal controls. *P* values were calculated using Origin 6.1 software (OriginLab Corporation, Norhampton, MA, USA). *$P < .05$; **$P < .01$. NS, not significant.

From www.bloodjournal.org by guest on October 11, 2016. For personal use only.

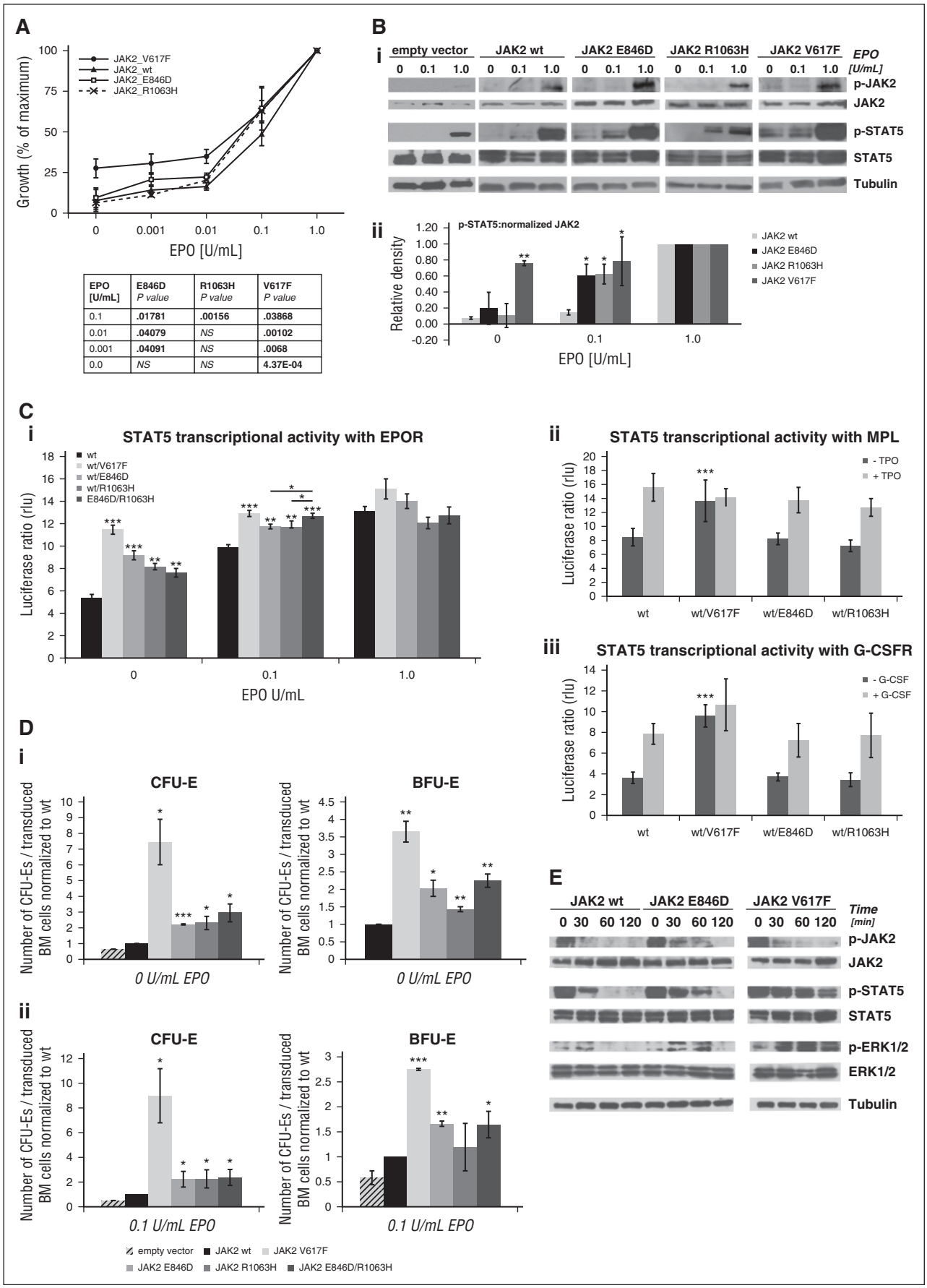

EPO [U/mL]	E846D *P value*	R1063H *P value*	V617F *P value*
0.1	**.01781**	**.00156**	**.03868**
0.01	**.04079**	*NS*	**.00102**
0.001	**.04091**	*NS*	**.0068**
0.0	*NS*	*NS*	**4.37E-04**

Figure 2.

From www.bloodjournal.org by guest on October 11, 2016. For personal use only.

Results and discussion

Case presentation, EPO hypersensitivity of erythroid progenitors, and mutational analyses

The diagnosis of polycythemia in a 15-year-old boy was based on the hematological and clinical data summarized in Figure 1A. The patient had increased hemoglobin/hematocrit level, higher red blood cell count, plethora, palpable spleen, and normal EPO level. Although the white blood cell differential and platelet count were normal (supplemental Table 1), the BM aspirate and BM biopsy showed hypercellularity, erythroid hyperplasia, and atypical, enlarged, and immature megakaryocytes, likely resulting from the stimulation of the megakaryocytic lineage (Figure 1B; supplemental Figure 1). The iron status parameters were normal (supplemental Table 2). The in vitro colony assay revealed hypersensitivity of the patient's burst-forming unit-erythroid (BFU-E) progenitors to EPO (Figure 1C), a feature characteristic for primary polycythemia states.[12] Both parents and the patient's brother were clinically normal, with normal EPO levels and hematological (Figure 1A) and iron status parameters, with the exception of elevated ferritin in the father and brother likely due to infection (supplemental Table 2). Nevertheless, the sensitivity of BFU-E progenitors to EPO was significantly increased in the mother and slightly also in the father compared with healthy controls and the patient's brother (Figure 1C). In addition, the colony assay revealed significantly increased numbers of circulating BFU-E progenitors in the patient and his parents compared with healthy controls (supplemental Figure 2A). These results suggested the hereditary nature of the propositus's erythrocytosis. No somatic mutations or chromosomal aberrations were uncovered by either whole-exome sequencing or microarray analysis (supplemental Table 3i-ii), suggesting that the hematopoiesis was likely polyclonal. Targeted mutational screening (see supplemental Materials and methods) and search for germ line variants using whole-exome sequencing revealed a E846D substitution in JAK2 in a heterozygous state in the propositus and his mother and JAK2 R1063H in the propositus and his father (supplemental Results; supplemental Figure 2B); both variants were reported as polymorphisms with very low frequencies (supplemental Table 4). Subsequent screening of a cohort of 99 subjects (including healthy controls, MPN patients, and pediatric patients with essential thrombocythemia or hereditary erythrocytosis) detected JAK2 E846D substitution in 1 $CALR^+/V617F^+$ MPN patient and JAK2 R1063H in 1 $V617F^+$ PV patient (supplemental Table 5) and in 1 triple-negative MPN patient (J.D.M.F. and R.K., unpublished data, August 29, 2015). The E846D substitution was previously reported in normal-karyotype acute myeloid leukemia[13] and the JEG-3 cancer cell line[14]; R1063H was reported in 3 JAK2 $V617F^+$ PV patients,[2] as well as in acute myeloid leukemia[13] and B-cell acute lymphoblastic leukemia cases.[15] Altogether, these data suggest a much higher frequency of these 2 variants in MPN patients than in normal individuals.

JAK2 E846D and R1063H promote survival at low EPO concentrations by increasing EPO-induced phosphorylation of STAT5

Because the germ line *JAK2* mutations emerged as the main disease-causing event in our patient, we created a cellular model: Ba/F3-EPOR cells expressing JAK2_E846D and JAK2_R1063H. Ba/F3-EPOR cells transfected with the wild-type human JAK2 (JAK2_wt) and V617F JAK2 were used as a negative and positive control, respectively.[16] As expected, the JAK2_V617F transfectants exhibited survival advantage and supported constitutive proliferation in EPO-free or EPO-limiting conditions[1,4,17] (supplemental Figure 3A; Figure 2A). The viability of JAK2_E846D and JAK2_R1063H transfectants in EPO-free medium was comparable to the JAK2_wt transfectants (supplemental Figure 3A); neither these transfectants expressing individual JAK2 genetic variants nor double transfectants with both E846D and R1063H (not shown) became growth factor independent. Nevertheless, JAK2_E846D–expressing cells showed significantly increased proliferation in EPO-limiting conditions compared with

Figure 2. Proliferation assay in cytokine-limiting conditions, immunoblot analysis of JAK2 signal transduction, luciferase assay, and colony assay of retrovirally transduced BM cells. (A) MTT (3-[4,5-dimethylthiazol-2-yl]-2,5-diphenyltetrazolium bromide) test in Ba/F3-EPOR-IL-3–dependent cells stably transfected with different JAK2 vectors. The percentage of proliferating cells was calculated as the percentage of the maximal cell growth observed at EPO concentration of 1.0 U/mL. The transfectants were starved for 12 hours in IL-3–free media and then incubated for 48 hours in the media with different EPO concentration. Results are shown as the mean ± standard deviation (SD) (n = at least 4 tests performed in triplicates). The table below the graph shows statistical evaluation of the growth of individual Ba/F3 transfectants at tested EPO concentrations compared with cell-expressing JAK2 wt. *P* values were calculated using Origin 6.1 software (OriginLab Corporation). (B) JAK2 downstream signaling in stable Ba/F3-EPOR-IL-3–dependent transfectants. The cells were starved in IL-3–free media for 12 hours and then stimulated with indicated concentrations of EPO for 15 minutes. JAK2_V617F–expressing cells served as a positive control and showed constitutive activation of STAT5 (i-ii). Immunoblot and subsequent densitometry analysis revealed that JAK2_E846D transfectants and also R1063H-expressing cells showed increase in STAT5 activation (i-ii). Each bar represents the ratio of the density of phosphorylated STAT5 (p-STAT5) to the density of normalized total JAK2 and is presented as fold change against the ratio calculated for 1.0 U/mL EPO. For detailed information on JAK2 normalization, see supplemental Materials and methods. Activation of JAK2 and its targets was determined by antibodies recognizing specific phosphorylation sites (as detailed in supplemental Materials and methods); tubulin antibody was used as a loading control. (C) STAT5 transcriptional activity in JAK2-deficient γ-2A cells transfected with various JAK2 complementary DNAs (cDNAs) in the presence of EPOR, MPL, and G-CSF receptor (G-CSFR). The heterozygous configuration was mimicked by cotransfection of JAK2 wt cDNA with JAK2 V617F, JAK2 E846D, or JAK2 R1063H. Four hours after transfection, the cells were stimulated with different concentrations of EPO (i) or stimulated with 10 ng/mL thrombopoietin (ii) or 10 ng/mL G-CSF (iii) and luminescence was detected in cell lysates 24 hours (ii-iii) or 48 hours (i) after transfection using a PerkinElmer Victor X Light analyzer. (i) STAT5 transcriptional activity downstream of JAK2 E846D and R1063H was significantly increased in both EPO-free and EPO-limiting condition in comparison with JAK2 wt in the presence of EPOR; the double mutants expressing both JAK2 E846D and R1063H mutants showed increased STAT5 transcriptional activity over the single mutants in low EPO concentration. (ii-iii) Only JAK2 V617F significantly increased STAT5 transcriptional activity in the presence of MPL and G-CSFR. STAT5 transcriptional activity of JAK2 E846D and JAK2 R1063H cells was comparable to wt cells. The panels show the average of 3 independent experiment ± standard error of the mean (SEM). *$P < .05$, **$P < .01$, ***$P < .001$ using the 2-tailed Student *t* test. rlu, relative light unit. (D) In vitro colony growth of transduced murine BM. Murine BM cells were infected with retroviruses coding for murine JAK2 wt, V617F, E846D, or R1063H for single mutant configuration and with E846D and R1063H retroviral particles for double mutant configuration. Infected murine BM cells were then plated on methylcellulose media in the absence of EPO (i) or in the presence of 0.1 U/mL EPO (ii). After 2 and 7 days, the plates were evaluated for the formation of CFU-E and BFU-E, respectively. The BM cells infected with the virus containing the empty pMEGIX vector were used as a control. JAK2_E846D and JAK2_E846D/R1063H BM cells have significantly higher numbers of CFU-E and BFU-E colonies in both EPO-free and low EPO conditions when compared with JAK2_wt cells. Cells with JAK2_R1063H mutation had significantly increased CFU-E, but not BFU-E colony formation. The highest number of erythroid colonies was detected in the sample derived from JAK2_V617F positive control. Congruent results were obtained by determination of the replating capacity of primary human cells naturally harboring the JAK2 E846D and R1063H mutations (supplemental Figure 6). The panels show the average of 3 independent experiments. The BFU-E and CFU-E colony numbers are expressed as the number of colonies per transduced cells and are normalized to wt values ± SD. *P* values were calculated using Origin 6.1 software. *$P < .05$, **$P < .01$, ***$P < .001$. (E) Immunoblot analysis of prolonged activity of E846D-mutant JAK2 kinase. The JAK2 transfectants were after IL-3 starvation stimulated with 20 U/mL EPO for 15 minutes and then incubated in base Iscove modified Dulbecco medium (IMDM) with no additives for indicated periods of time. JAK2_E846D–expressing cells showed prolonged activation of STAT5 and EKR1/2 similarly to JAK2_V617F transfectants as predicted by in silico modeling (supplemental Figure 7).

From www.bloodjournal.org by guest on October 11, 2016. For personal use only.

JAK2_wt (Figure 2A). Improved proliferation for JAK2_R1063H transfectants was observed only in 0.1 U/mL EPO concentration (Figure 2A). These results suggested that E846D and R1063H substitutions have a weaker effect on the survival and proliferation capacity of cells than the oncogenic V617F mutation, which is consistent with their germ line transmission and with nonclonal hematopoiesis observed in the JAK2 E846D$^+$ mother (described in supplemental Materials and methods). This also showed a stronger effect of E846D substitution on improved proliferation in EPO-limiting conditions compared with R1063H.

We then focused on JAK2 downstream signal transduction pathways. Upon interleukin-3 (IL-3) starvation and short incubation in IL-3–free EPO-containing medium, JAK2_E846D– and JAK2_R1063H–expressing cells showed increased STAT5 phosphorylation (Figure 2B). Weak activation of STAT1 was also observed for both mutants (supplemental Figure 3B).

JAK2 E846D and R1063H activate STAT5 transcriptional activity specifically through EPOR

Next, we tested the effect of our JAK2 mutants on STAT transcriptional activity by dual-reporter luciferase assay in JAK2-deficient γ-2A cells.[18] Figure 2Ci shows that JAK2 E846D and R1063H significantly increased STAT5 transcriptional activity in EPO-free and low EPO conditions in the presence of EPOR when compared with cells expressing JAK2 wt. In EPO-limiting conditions, the coexpression of these 2 JAK2 mutants further improved STAT5 transcriptional activity compared with cells expressing a single JAK2 mutant (E846D or R1063H). No effect of JAK2 E846D and R1063H was observed on basal STAT5 activation via MPL or the granulocyte colony-stimulating factor (G-CSF) receptor (Figure 2Cii-iii) or on the activation of other STAT members (supplemental Figure 4). This was in agreement with increased STAT5 phosphorylation in the patient's BM detected by immunohistochemical analysis of STAT5 (supplemental Figure 5) and is consistent with the erythroid phenotype in our patient.

JAK2 E846D–transduced murine BM cells show increased capacity for CFU-E and BFU-E formation whereas JAK2 R1063H increases only CFU-E formation

To assess the effect of JAK2 mutants on primary cells, BM cells from C57BL/6 mice were retrovirally transduced with murine JAK2 expression vectors and used for in vitro colony assay. The cells expressing the E846D mutant formed significantly increased numbers of colony forming unit-erythroid (CFU-E) and BFU-E, when compared with cells with JAK2 wt in EPO-free or EPO-limiting conditions (Figure 2D). The observation that the R1063H mutant induced CFU-E rather than BFU-E colony growth (see also primary father's progenitors in supplemental Figure 6) is reminiscent of the weak activation of EPOR by the anemic strain of the Friend virus complex gp55 envelope protein (gp55-A), which also specifically supported CFU-E formation.[19,20] For the EPO-free condition, the co-occurrence of the 2 mutations was slightly more effective in colony growth than the single mutants alone (Figure 2D). This assay indicated that JAK2 E846D and R1063H mutations facilitate hypersensitive response of erythroid progenitors from the patient or patient's parents to EPO.

In silico analysis predicted increased activity of JAK2 R1063H–mutant kinase and prolonged activation of JAK2 E846D–mutant kinase after cytokine stimulation

In silico modeling using the x-ray structures of the inactive and active JH1 domain of JAK2[21,22] suggested that the R1063H mutation would be presumed to facilitate the active conformation of JH1, whereas the JAK2 E846D mutant would show slower return to the ground state after cytokine stimulation (supplemental Figure 7). The effect of E846D substitution was confirmed by immunoblots analysis in which IL-3–starved JAK2_E846D transfectants showed prolonged activation of STAT5 and extracellular signal-regulated kinase 1/2 (ERK1/2) compared with JAK2_wt after high-dose EPO stimulation and subsequent EPO withdrawal (Figure 2E) resembling signaling downstream EPOR gain-of-function mutants.[23] The prolonged STAT5 and ERK1/2 activation downstream JAK2_E846D can be effectively reduced by JAK2 inhibitors, ruxolitinib or AZ-960, but not by wortmannin, a phosphoinositide-3-kinase inhibitor (supplemental Figure 8).

In summary, we establish that E846D and R1063H are weakly activating mutations and conclude that the cooperation of these activating *JAK2* mutations causes a polyclonal hereditary erythrocytosis with megakaryocytic atypia, clinically resembling JAK2 exon 12–positive PV.

Acknowledgments

The authors thank Michael Schuster and Donat Alpar (the Biomedical Sequencing Facility at CeMM) as well as Martin Tichy and Anna Lapcikova (University Hospital and Faculty of Medicine and Dentistry in Olomouc) for their technical assistance, and Srdan Verstovsek (MD Anderson, Houston, TX) for critical reading of the paper and discussions.

This work was supported by Czech Science Foundation Project P301/12/1503 (V.D.). J.F.K. was supported by CZ.1.07/2.3.00/30.0041. Support to S.N.C. was from the Fonds de la Recherche Scientifique–Fonds National de la Recherche Scientifique, Belgium, the Salus Sanguinis Foundation, the Action de Recherche Concertée projects MEXP31C1 and ARC10/15-027 of the University catholique de Louvain, Brussels, the Fondation contre le Cancer, Brussels, the Pôle d'Attraction Interuniversitaire Programs BCHM61B5, and Belgian Medical Genetics Initiative (BeMG). E.L. was supported by a Fonds pour la formation à la Recherche dans l'Industrie et dans l'Agriculture PhD fellowship. The Sonderforschungsbereich grant from the Austrian Science Fund F4702-B20 is acknowledged for its generous support to R.K. J.D.M.F. acknowledges support from L'ORÉAL Österreich, For Women in Science Fellowship.

Authorship

Contribution: K.K. and M.H. designed and performed research, analyzed data, and wrote the paper; C.P. designed and performed research, analyzed data, and reviewed the paper; J.F.K. performed research, analyzed data, and reviewed the paper; D.P. recruited the patient and contributed to the editing of the paper; E.L. performed research and contributed to the writing of the paper; B.K. performed research and analyzed data; J.D.M.F. designed and performed research and analyzed data; F.S. analyzed data; R.K. contributed to study design, analyzed data, reviewed the paper, and provided financial support; S.N.C. contributed to study design, analyzed data, wrote the paper, and provided financial support; and V.D. designed the study, analyzed data, wrote the paper, and provided financial support.

Conflict-of-interest disclosure: The authors declare no competing financial interests.

ORCID profiles: J.F.K., 0000-0002-8808-9411; J.D.M.F., 0000-0001-7420-3298; R.K., 0000-0002-6997-8539.

From www.bloodjournal.org by guest on October 11, 2016. For personal use only.

Correspondence: Vladimir Divoky, Department of Biology, Faculty of Medicine and Dentistry, Palacký University, Hnevotinska 3, Olomouc, 775 15, Czech Republic; e-mail: vladimir.divoky@upol.cz; or Stefan N. Constantinescu, Signal Transduction and Molecular Hematology Unit, Ludwig Institute for Cancer Research and de Duve Institute, Université catholique de Louvain, Avenue Hippocrate 74, UCL 75-4, Brussels B-1200, Belgium; e-mail: stefan.constantinescu@bru.licr.org.

References

1. James C, Ugo V, Le Couédic JP, et al. A unique clonal JAK2 mutation leading to constitutive signalling causes polycythaemia vera. *Nature.* 2005;434(7037):1144-1148.
2. Levine RL, Wadleigh M, Cools J, et al. Activating mutation in the tyrosine kinase JAK2 in polycythemia vera, essential thrombocythemia, and myeloid metaplasia with myelofibrosis. *Cancer Cell.* 2005;7(4):387-397.
3. Funakoshi-Tago M, Tago K, Abe M, Sonoda Y, Kasahara T. STAT5 activation is critical for the transformation mediated by myeloproliferative disorder-associated JAK2 V617F mutant. *J Biol Chem.* 2010;285(8):5296-5307.
4. Dusa A, Mouton C, Pecquet C, Herman M, Constantinescu SN. JAK2 V617F constitutive activation requires JH2 residue F595: a pseudokinase domain target for specific inhibitors. *PLoS One.* 2010;5(6):e11157.
5. Mead AJ, Chowdhury O, Pecquet C, et al. Impact of isolated germline JAK2V617I mutation on human hematopoiesis. *Blood.* 2013;121(20):4156-4165.
6. Marty C, Saint-Martin C, Pecquet C, et al. Germline JAK2 mutations in the kinase domain are responsible for hereditary thrombocytosis and are resistant to JAK2 and HSP90 inhibitors. *Blood.* 2014;123(9):1372-1383.
7. Etheridge SL, Cosgrove ME, Sangkhae V, et al. A novel activating, germline JAK2 mutation, JAK2R564Q, causes familial essential thrombocytosis. *Blood.* 2014;123(7):1059-1068.
8. Milosevic Feenstra JD, Nivarthi H, Gisslinger H, et al. Whole-exome sequencing identifies novel MPL and JAK2 mutations in triple-negative myeloproliferative neoplasms. *Blood.* 2016;127(3):325-332.
9. Chen E, Beer PA, Godfrey AL, et al. Distinct clinical phenotypes associated with JAK2V617F reflect differential STAT1 signaling. *Cancer Cell.* 2010;18(5):524-535.
10. Lakey MA, Pardanani A, Hoyer JD, et al. Bone marrow morphologic features in polycythemia vera with JAK2 exon 12 mutations. *Am J Clin Pathol.* 2010;133(6):942-948.
11. D'Andrea AD, Yoshimura A, Youssoufian H, Zon LI, Koo JW, Lodish HF. The cytoplasmic region of the erythropoietin receptor contains nonoverlapping positive and negative growth-regulatory domains. *Mol Cell Biol.* 1991;11(4):1980-1987.
12. Prchal JT. Primary and secondary polycythemias (erythrocytosis). In: Kaushansky K, Lichtman MA, Beutler E, Kipps TJ, Seligsohn U, Prchal JT, eds. Williams Hematology. 8th ed. New York, NY: McGraw Hill; 2010:823-838.
13. Schnittger S, Bonin M, Schroeder C, et al. Development of an oligonucleotide resequencing array for rapid mutation analysis in acute myeloid leukemia with normal karyotype [abstract] *Blood.* 2009;114(22). Abstract 705.
14. Matthews DJ, Gerritsen ME. Tumor associated mutations in JAK2. In: Matthews DJ, Gerritsen ME, eds. Targeting Protein Kinases for Cancer Therapy. Hoboken, NJ: John Wiley & Sons, Inc; 2010.
15. Sadras T, Heatley S, Nievergall E, et al. JAK2 mutations are highly enriched in CRLF2-rearranged B-ALL cases with a Ph-like gene signature [abstract]. *Haematologica.* 2015;100(s1):199. Abstract P524.
16. Baxter EJ, Scott LM, Campbell PJ, et al; Cancer Genome Project. Acquired mutation of the tyrosine kinase JAK2 in human myeloproliferative disorders. *Lancet.* 2005;365(9464):1054-1061.
17. Staerk J, Kallin A, Demoulin JB, Vainchenker W, Constantinescu SN. JAK1 and Tyk2 activation by the homologous polycythemia vera JAK2 V617F mutation: cross-talk with IGF1 receptor. *J Biol Chem.* 2005;280(51):41893-41899.
18. Kohlhuber F, Rogers NC, Watling D, et al. A JAK1/JAK2 chimera can sustain alpha and gamma interferon responses. *Mol Cell Biol.* 1997;17(2):695-706.
19. Wendling F, Tambourin P, Gallien-Lartigue O, Charon M. Comparative differentiation and numeration of CFUs from mice infected either by the anemia- or polycythemia-inducing strains of Friend viruses. *Int J Cancer.* 1974;13(4):454-462.
20. Constantinescu SN, Wu H, Liu X, Beyer W, Fallon A, Lodish HF. The anemic Friend virus gp55 envelope protein induces erythroid differentiation in fetal liver colony-forming units-erythroid. *Blood.* 1998;91(4):1163-1172.
21. Andraos R, Qian Z, Bonenfant D, et al. Modulation of activation-loop phosphorylation by JAK inhibitors is binding mode dependent. *Cancer Discov.* 2012;2(6):512-523.
22. Lucet IS, Fantino E, Styles M, et al. The structural basis of Janus kinase 2 inhibition by a potent and specific pan-Janus kinase inhibitor. *Blood.* 2006;107(1):176-183.
23. Divoky V, Song J, Horvathova M, et al. Delayed hemoglobin switching and perinatal neocytolysis in mice with gain-of-function erythropoietin receptor. *J Mol Med (Berl).* 2016;94(5):597-608.

Mutations in Janus kinases associated with hematological malignancies

Domain	Mutation	Validated effect		Disease	Corresponding mutants in other JAKs
		Proliferation	Signaling		
JAK1					
FERM	I62V[1]	ni	ni	B-ALL, T-ALL	------
	K204M[1]	ni	ni	B-ALL	------
	R360W[1]	ni	ni	T-ALL	------
SH2	T478S[2-3]	--	+	AML	------
	S512L[1]	ni	ni	T-ALL	------
Pseudokinase	V623A[2-3]	--	+	AML	------
	L624_R629>W[4-5]	ni	ni	ch-B-ALL	------
	D625R[6]	ni	ni	DS-AMKL	------
	A634D[1]	+	+	B-ALL, T-ALL	------
	S646F[4]	+	+	ch-B-ALL	------
	V651M[5-6]	ni	ni	DS-B-ALL	------
	L653F[1]	ni	ni	ch-T-ALL	------
	V658F[4-5, 7-9]	+	+	ch-B-ALL, DS-B-ALL, T-ALL, AML	JAK2 V617
	R724H[1]	+	+	B-ALL, T-ALL	JAK2 R683 + JAK3 R657
	L783F[9]	ni	ni	T-ALL	------
Kinase	R879C[1]	--	--	T-ALL	------
	R879H[1]	ni	ni	T-ALL	------
	R879S[1]	ni	ni	T-ALL	------
JAK2					
FERM	G335D[63]	-	-	MPN	-----
SH2-pseudokinase linker					
exon12	T514M[10]	ni	ni	MPN	------
exon12	N533Y[10]	ni	ni	MPN	------
exon12	M535I[11-12]	+	-	ch-AMKL	JAK3 M511
exon12	F537I[13]	ni	ni	PV	------
exon12	H538del[10]	ni	ni	MPN	------
exon12	K539L + L545V[10]	ni	ni	MPN	------
exon12	K539L[14-16]	+	+	PV, IE	------
exon12	K539E[17]	ni	ni	PV	------
exon12	F537-K539delinsK[10]	ni	ni	MPN	------
exon12	F537-K539delinsL[10, 14-16, 18-19]	+	+	PV, IE	------
exon12	H538-K539delinsL[10, 19-20]	ni	ni	PV, IE	------
exon12	H538Q + K539L[15-16]	+	+	PV, IE	------
exon12	F533I + K539L[21]	ni	ni	MPN	------
exon12	F537I + K539L[21]	ni	ni	MPN	------
exon12	H538D +K539L + I540S[16]	ni	ni	PV	------
exon12	H538-K539del[10, 16]	ni	ni	PV	------

exon12	V536-F547dup[10, 16]	ni	ni	PV	------
exon12	V537-F547dup[22]	ni	ni	PV	------
exon12	V536-I546dup11[19]	ni	ni	PV, IE	------
exon12	F537-I546dup10 + F547L[19]	ni	ni	PV, IE	------
exon12	I540-E543delinsMK[19, 23]	ni	ni	PV, IE	------
exon12	I540-D544delinsMK[10]	ni	ni	MPN	------
exon12	I540-E543delinsKK[24]	ni	ni	PV	------
exon12	I540-N542delinsK[25]	ni	ni	PV	------
exon12	R541-E543delinsK[19-20, 23]	ni	ni	PV, IE	------
exon12	N542-E543del[10, 14-16, 18-20]	+	+	PV, IE	------
exon12	N542-D544delinsN[10]	ni	ni	MPN	------
exon12	N542S[17]	ni	ni	PV	------
exon12	E543-D544del[10, 14, 16, 19, 26]	ni	ni	PV, IE	------
exon12	D544-L545del[16]	ni	ni	PV	------
exon12	D544G[17]	ni	ni	PV	------
exon12	L545S[17]	ni	ni	PV	------
exon12	I546-F547ins11[25]	ni	ni	PV	------
exon12	F547L[10]	ni	ni	MPN	------
exon12	F547V[21]	ni	ni	MPN	------
Pseudokinase					
exon13	F556V[63]	+	+	MPN	------
exon13	G571S[10,63]	-	-	DS-B-ALL, MPN	------
exon14	K607N[27]	ni	ni	AML	------
exon14	H608Q[10]	ni	ni	MPN	------
exon14	H608Y[10]	ni	ni	MPN	------
exon14	L611S[12, 28-29]	+	+	ch-B-ALL	------
exon14	C616Y + V617F[30]	ni	ni	PV	------
exon14	V617F[12, 20, 27, 31-42]	+	+	PV, ET, PM, HES, CMML, SM, CNL, JMML, RARS, RA RCMD, RAEB, AML, IE, RARS-T, MDS/MPN-U, MPN-U	JAK1 V658
exon14	V617F + C618R[43-44]	ni	ni	PV	JAK3 A593
exon14	C618R[10]	ni	ni	MPN	------
exon14	D620E[45-46]	ni	ni	PV	------
	L624P[10]	ni	ni	MPN	------
	V625F[63]	+	+	MPN	------
	Δexon15+16 (ΔN622-D710)[47]	ni	ni	MDS/ MPN-U	------
exon16	L681-I682delinsTPYEGMPGH[48]	ni	ni	DS-B-ALL	------
exon16	I682F[4-5, 49-50]	+	+	ch-B-ALL, MHH-CALL-4 cell line	------

				(ch-B-ALL)	
exon16	I682AQG[4]	ni	ni	DS-B-ALL	------
exon16	IR682RQ[7]	ni	ni	DS-B-ALL	------
exon16	I682-D686del (ΔIREED)[51]	+	+	DS-B-ALL	------
exon16	I682delinsMPAP[48]	ni	ni	DS-B-ALL	------
exon16	R683G[4-7, 48-50, 52-55]	+	+	DS-B-ALL, ad-B-ALL, ch-B-ALL, MUTZ5 cell line (ch-B-ALL)	JAK1 R724 + JAK3 R657
exon16	R683S[4-5, 7, 12, 48-50, 52-54]	+	+	DS-B-ALL, ad-B-ALL, ch-B-ALL	JAK1 R724 + JAK3 R657
exon16	R683T[7, 52, 54]	ni	ni	DS-B-ALL, ad-B-ALL	JAK1 R724 + JAK3 R657
exon16	R683K[7, 48-49]	+	+	DS-B-ALL, ch-B-ALL	JAK1 R724 + JAK3 R657
exon16	QGinsR683[5]	ni	ni	DS-B-ALL	------
exon16	R683insGGCCCCATC[6]	ni	ni	DS-B-ALL	------
	F694L[55,we]	ni	ni	DS-B-ALL, ch-B-ALL	------
Kinase	Y813D[22]	ni	ni	IMF	------
	G861W[7]	ni	ni	ch-B-ALL	------
	R867Q[4-5]	+	+	ch-B-ALL MPN	------
	D873N[4-5]	+	+	ch-B-ALL	------
	T875N[7, 56]	+	+	ch-B-ALL, CHRF-288-11 cell line (AMKL)	------
	P933R[4-5]	+	+	ch-B-ALL	------
	R938Q/S755R[4]	+	+	MPN	
	N1108S[22]	ni	ni	PV	
JAK3					
FERM	I87T[57-58]	+	+	TMD	------
	P132T[2, 59]	+	+	AMKL, AML	------
	P151R + 2851-3442DEL592[60]	ni	ni	DS-TMD	------
	SpliceΔexon2-5, Δexon3-5[60]	ni	ni	DS-TMD	------
	SpliceΔexon3-5, Δexon3, 5[60]	ni	ni	DS-AMKL	------
SH2	P434R[60]	ni	ni	DS-TMD	------
SH2-Pseudokinase linker	Q501H + R657Q[57]	+	+	MGS cell line (DS-AMKL)	------
Pseudokinase	M511I + V722I[61]	ni	ni	DS-ML	JAK2-M535
	A572V[11, 59]	+	+	CMK cell line (AMKL)	------
	A573V[6, 11, 60]	+	+	CMY cell line (AMKL),	------

				DS-AMKL, T-ALL	
	M576L[58]	ni	ni	AMKL	------
	A593+ A573V[58]	ni	ni	DS-AMKL	JAK3 A593: JAK2-C618
	R657Q + Q501H[57]	+	+	MGS cell line (DS-AMKL)	JAK3 R657Q: JAK1 R724, JAK2 R683
	V674A[61]	+	+	ALL	
	V722I[11, 59]	+	+	DS-AMKL	------
Pseudokinase-kinase linker	S789P[4]	ni	ni	ch-B-ALL	------
Kinase	2851-3442del592[60]	ni	ni	DS-AMKL	------
	L857P[61]	+	+	ALL	JAK2 L884P
TYK2					
FERM	G363S[2]	ni	ni	AML	------

ni: not investigated, (+): increased activity compared to wild-type kinase, (-): no effect compared to wild-type kinase.
Abbreviations: **ALL**: acute lymphoblastic leukaemia, **AMKL**: acute megakaryoblastic; leukaemia, **AML:** acute myeloid leukaemia, **B-ALL**: B cell precursor ALL, **ch:** childhood, CML: chronic myelogenous leukaemia, **CMML:** chronic myelomonocytic leukaemia, **CNL**: chronic neutrophilic leukaemia, **DS**: Down syndrome, **ET**: essential thrombocythemia, **HES:** hypereosinophilic syndrome, **IE:** idiopathic erythrocytosis, **JMML:** juvenile myelomonocytic leukaemia, **MDS/MPN-U:** unclassifiable myelodysplastic syndrome/myeloproliferative neoplasms, **ML:** myeloid leukaemia, **MPN-U**: unclassifiable or atypical myeloproliferative neoplasms, **PM:** primary myelofibrosis, **PV:** polycythemia vera, **RA**: refractory anaemia, **RAEB**: refractory anaemia with excess of blasts, **RARS**: refractory anaemia with ringed sideroblasts, **RARS-T:** RARS with thrombocytosis, **RCMD:** refractory cytopenia with multilineage dysplasia, **SM:** systemic mastocytosis, **T-ALL**: T cell ALL, **TMD:** transient myeloproliferative disorder.

[**Adapted from:** Haan, C., Behrmann, I. & Haan, S. Perspectives for the use of structural information and chemical genetics to develop inhibitors of Janus kinases. *J Cell Mol Med* **14**, 504-27 (2010)]

References:

1. Flex E, Petrangeli V, Stella L, et al. Somatically acquired JAK1 mutations in adult acute lymphoblastic leukemia. J Exp Med 2008;205:751-8.
2. Tomasson MH, Xiang Z, Walgren R, et al. Somatic mutations and germline sequence variants in the expressed tyrosine kinase genes of patients with de novo acute myeloid leukemia. Blood 2008;111:4797-808.
3. Xiang Z, Zhao Y, Mitaksov V, et al. Identification of somatic JAK1 mutations in patients with acute myeloid leukemia. Blood 2008;111:4809-12.
4. Marty C, Saint-Martin C, Pecquet C, Grosjean S, Saliba J, Mouton C, et al. Germ-line JAK2 mutations in the kinase domain are responsible for hereditary thrombocytosis and are resistant to JAK2 and HSP90 inhibitors. Blood. 2014;123(9):1372-83
5. Harvey RC, Mullighan CG, Chen IM, et al. Rearrangement of CRLF2 is associated with mutation of JAK kinases, alteration of IKZF1, Hispanic/Latino ethnicity, and a poor outcome in pediatric B-progenitor acute lymphoblastic leukemia. Blood 2010;115:5312-21.
6. Blink M, Buitenkamp TD, van den Heuvel-Eibrink MM, et al. Frequency and prognostic implications of JAK 1-3 aberrations in Down syndrome acute lymphoblastic and myeloid leukemia. Leukemia 2011;25:1365-8.

7. Mullighan CG, Collins-Underwood JR, Phillips LA, et al. Rearrangement of CRLF2 in B-progenitor- and Down syndrome-associated acute lymphoblastic leukemia. Nat Genet 2009;41:1243-6.
8. Staerk J, Kallin A, Demoulin JB, Vainchenker W, Constantinescu SN. JAK1 and Tyk2 activation by the homologous polycythemia vera JAK2 V617F mutation: cross-talk with IGF1 receptor. J Biol Chem 2005;280:41893-9.
9. Jeong EG, Kim MS, Nam HK, et al. Somatic mutations of JAK1 and JAK3 in acute leukemias and solid cancers. Clin Cancer Res 2008;14:3716-21.
10. Ma W, Kantarjian H, Zhang X, et al. Mutation profile of JAK2 transcripts in patients with chronic myeloproliferative neoplasias. J Mol Diagn 2009;11:49-53.
11. Malinge S, Ragu C, Della-Valle V, et al. Activating mutations in human acute megakaryoblastic leukemia. Blood 2008;112:4220-6.
12. Zhao L, Dong H, Zhang CC, et al. A JAK2 interdomain linker relays Epo receptor engagement signals to kinase activation. J Biol Chem 2009;284:26988-98.
13. Sayyah J, Magis A, Ostrov DA, Allan RW, Braylan RC, Sayeski PP. Z3, a novel Jak2 tyrosine kinase small-molecule inhibitor that suppresses Jak2-mediated pathologic cell growth. Mol Cancer Ther 2008;7:2308-18.
14. Percy MJ, Scott LM, Erber WN, et al. The frequency of JAK2 exon 12 mutations in idiopathic erythrocytosis patients with low serum erythropoietin levels. Haematologica 2007;92:1607-14.
15. Scott LM, Tong W, Levine RL, et al. JAK2 exon 12 mutations in polycythemia vera and idiopathic erythrocytosis. N Engl J Med 2007;356:459-68.
16. Schnittger S, Bacher U, Haferlach C, et al. Detection of JAK2 exon 12 mutations in 15 patients with JAK2V617F negative polycythemia vera. Haematologica 2009;94:414-8.
17. Ohyashiki JH, Hisatomi H, Shimizu S, Sugaya M, Ohyashiki K. Detection of low allele burden of JAK2 exon 12 mutations using TA-cloning in patients with erythrocytosis. Jpn J Clin Oncol 2009;39:509-13.
18. Pardanani A, Lasho TL, Finke C, Hanson CA, Tefferi A. Prevalence and clinicopathologic correlates of JAK2 exon 12 mutations in JAK2V617F-negative polycythemia vera. Leukemia 2007;21:1960-3.
19. Pietra D, Li S, Brisci A, et al. Somatic mutations of JAK2 exon 12 in patients with JAK2 (V617F)-negative myeloproliferative disorders. Blood 2008;111:1686-9.
20. Williams DM, Kim AH, Rogers O, Spivak JL, Moliterno AR. Phenotypic variations and new mutations in JAK2 V617F-negative polycythemia vera, erythrocytosis, and idiopathic myelofibrosis. Exp Hematol 2007;35:1641-6.
21. Scott LM. The JAK2 exon 12 mutations: a comprehensive review. Am J Hematol 2011;86:668-76.
22. Siemiatkowska A, Bieniaszewska M, Hellmann A, Limon J. JAK2 and MPL gene mutations in V617F-negative myeloproliferative neoplasms. Leuk Res 2010;34:387-9.
23. Butcher CM, Hahn U, To LB, et al. Two novel JAK2 exon 12 mutations in JAK2V617F-negative polycythaemia vera patients. Leukemia 2008;22:870-3.
24. Yeh YM, Chen YL, Cheng HY, et al. High percentage of JAK2 exon 12 mutation in Asian patients with polycythemia vera. Am J Clin Pathol 2010;134:266-70.
25. Ugo V, Tondeur S, Menot ML, et al. Interlaboratory development and validation of a HRM method applied to the detection of JAK2 exon 12 mutations in polycythemia vera patients. PLoS One 2010;5:e8893.
26. Ormazabal C, Hurtado C, Aranaz P, et al. Low frequency of JAK2 exon 12 mutations in classic and atypical CMPDs. Leuk Res 2008;32:1485-7.
27. Lee JW, Kim YG, Soung YH, et al. The JAK2 V617F mutation in de novo acute myelogenous leukemias. Oncogene 2006;25:1434-6.
28. Kratz CP, Boll S, Kontny U, Schrappe M, Niemeyer CM, Stanulla M. Mutational screen reveals a novel JAK2 mutation, L611S, in a child with acute lymphoblastic leukemia. Leukemia 2006;20:381-3.
29. Funakoshi-Tago M, Tago K, Sumi K, et al. The acute lymphoblastic leukemia-associated JAK2 L611S mutant induces tumorigenesis in nude mice. J Biol Chem 2009;284:12680-90.

30. Zhang SJ, Li JY, Li WD, Song JH, Xu W, Qiu HX. The investigation of JAK2 mutation in Chinese myeloproliferative diseases-identification of a novel C616Y point mutation in a PV patient. Int J Lab Hematol 2007;29:71-2.
31. James C, Ugo V, Le Couedic JP, et al. A unique clonal JAK2 mutation leading to constitutive signalling causes polycythaemia vera. Nature 2005;434:1144-8.
32. Kralovics R, Passamonti F, Buser AS, et al. A gain-of-function mutation of JAK2 in myeloproliferative disorders. N Engl J Med 2005;352:1779-90.
33. Levine RL, Wadleigh M, Cools J, et al. Activating mutation in the tyrosine kinase JAK2 in polycythemia vera, essential thrombocythemia, and myeloid metaplasia with myelofibrosis. Cancer Cell 2005;7:387-97.
34. Baxter EJ, Scott LM, Campbell PJ, et al. Acquired mutation of the tyrosine kinase JAK2 in human myeloproliferative disorders. Lancet 2005;365:1054-61.
35. Zhao R, Xing S, Li Z, et al. Identification of an acquired JAK2 mutation in polycythemia vera. J Biol Chem 2005;280:22788-92.
36. Jones AV, Kreil S, Zoi K, et al. Widespread occurrence of the JAK2 V617F mutation in chronic myeloproliferative disorders. Blood 2005;106:2162-8.
37. Steensma DP. JAK2 V617F in myeloid disorders: molecular diagnostic techniques and their clinical utility: a paper from the 2005 William Beaumont Hospital Symposium on Molecular Pathology. J Mol Diagn 2006;8:397-411; quiz 526.
38. Steensma DP, Tefferi A. JAK2 V617F and ringed sideroblasts: not necessarily RARS-T. Blood 2008;111:1748.
39. Tono C, Xu G, Toki T, et al. JAK2 Val617Phe activating tyrosine kinase mutation in juvenile myelomonocytic leukemia. Leukemia 2005;19:1843-4.
40. Remacha AF, Nomdedeu JF, Puget G, et al. Occurrence of the JAK2 V617F mutation in the WHO provisional entity: myelodysplastic/myeloproliferative disease, unclassifiable-refractory anemia with ringed sideroblasts associated with marked thrombocytosis. Haematologica 2006;91:719-20.
41. Szpurka H, Tiu R, Murugesan G, et al. Refractory anemia with ringed sideroblasts associated with marked thrombocytosis (RARS-T), another myeloproliferative condition characterized by JAK2 V617F mutation. Blood 2006;108:2173-81.
42. Renneville A, Quesnel B, Charpentier A, et al. High occurrence of JAK2 V617 mutation in refractory anemia with ringed sideroblasts associated with marked thrombocytosis. Leukemia 2006;20:2067-70.
43. Karow A, Waller C, Reimann C, Niemeyer CM, Kratz CP. JAK2 mutations other than V617F: a novel mutation and mini review. Leuk Res 2008;32:365-6.
44. Yoo JH, Park TS, Maeng HY, et al. JAK2 V617F/C618R mutation in a patient with polycythemia vera: a case study and review of the literature. Cancer Genet Cytogenet 2009;189:43-7.
45. Grunebach F, Bross-Bach U, Kanz L, Brossart P. Detection of a new JAK2 D620E mutation in addition to V617F in a patient with polycythemia vera. Leukemia 2006;20:2210-1.
46. Schnittger S, Bacher U, Kern W, Schroder M, Haferlach T, Schoch C. Report on two novel nucleotide exchanges in the JAK2 pseudokinase domain: D620E and E627E. Leukemia 2006;20:2195-7.
47. Ohnishi H, Hosoi K, Yoshino H, et al. A novel JAK2 splicing mutation in neonatal myeloproliferative disorder accompanying congenital anomalies. Br J Haematol 2009;145:676-8.
48. Bercovich D, Ganmore I, Scott LM, et al. Mutations of JAK2 in acute lymphoblastic leukaemias associated with Down's syndrome. Lancet 2008;372:1484-92.
49. Cario G, Zimmermann M, Romey R, et al. Presence of the P2RY8-CRLF2 rearrangement is associated with a poor prognosis in non-high-risk precursor B-cell acute lymphoblastic leukemia in children treated according to the ALL-BFM 2000 protocol. Blood 2010;115:5393-7.
50. Russell LJ, Capasso M, Vater I, et al. Deregulated expression of cytokine receptor gene, CRLF2, is involved in lymphoid transformation in B-cell precursor acute lymphoblastic leukemia. Blood 2009;114:2688-98.
51. Malinge S, Ben-Abdelali R, Settegrana C, et al. Novel activating JAK2 mutation in a patient with Down syndrome and B-cell precursor acute lymphoblastic leukemia. Blood 2007;109:2202-4.

52. Gaikwad A, Rye CL, Devidas M, et al. Prevalence and clinical correlates of JAK2 mutations in Down syndrome acute lymphoblastic leukaemia. Br J Haematol 2009;144:930-2.
53. Kearney L, Gonzalez De Castro D, Yeung J, et al. Specific JAK2 mutation (JAK2R683) and multiple gene deletions in Down syndrome acute lymphoblastic leukemia. Blood 2009;113:646-8.
54. Yoda A, Yoda Y, Chiaretti S, et al. Functional screening identifies CRLF2 in precursor B-cell acute lymphoblastic leukemia. Proc Natl Acad Sci U S A 2010;107:252-7.
55. Ensor HM, Schwab C, Russell LJ, et al. Demographic, clinical, and outcome features of children with acute lymphoblastic leukemia and CRLF2 deregulation: results from the MRC ALL97 clinical trial. Blood 2011;117:2129-36.
56. Mercher T, Wernig G, Moore SA, et al. JAK2T875N is a novel activating mutation that results in myeloproliferative disease with features of megakaryoblastic leukemia in a murine bone marrow transplantation model. Blood 2006;108:2770-9.
57. Sato T, Toki T, Kanezaki R, et al. Functional analysis of JAK3 mutations in transient myeloproliferative disorder and acute megakaryoblastic leukaemia accompanying Down syndrome. Br J Haematol 2008;141:681-8.
58. Kiyoi H, Yamaji S, Kojima S, Naoe T. JAK3 mutations occur in acute megakaryoblastic leukemia both in Down syndrome children and non-Down syndrome adults. Leukemia 2007;21:574-6.
59. Walters DK, Mercher T, Gu TL, et al. Activating alleles of JAK3 in acute megakaryoblastic leukemia. Cancer Cell 2006;10:65-75.
60. De Vita S, Mulligan C, McElwaine S, et al. Loss-of-function JAK3 mutations in TMD and AMKL of Down syndrome. Br J Haematol 2007;137:337-41.
61. Klusmann JH, Reinhardt D, Hasle H, et al. Janus kinase mutations in the development of acute megakaryoblastic leukemia in children with and without Down's syndrome. Leukemia 2007;21:1584-7.
62. Losdyck E, Hornakova T, Springuel L, Degryse S, Gielen O, Cools J, et al. Distinct Acute Lymphoblastic Leukemia (ALL)-associated Janus Kinase 3 (JAK3) Mutants Exhibit Different Cytokine-Receptor Requirements and JAK Inhibitor Specificities. J Biol Chem. 2015;290(48):29022-34
63. Milosevic Feenstra JD, Nivarthi H, Gisslinger H, Leroy E, Rumi E, Chachoua I, et al. Whole-exome sequencing identifies novel MPL and JAK2 mutations in triple-negative myeloproliferative neoplasms. Blood. 2016;127(3):325-32

Inhibitor	Other names	Company	Compound Structure	Scaffolds	Type	Disease	JAK2 IC50 (nM)*	Other Targets	Status	Side effects	Ref.
INCB018424	Ruxolitinib Jakavi®	*Incyte/ Novartis*	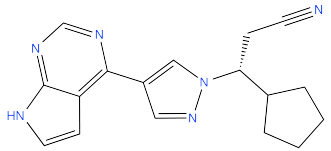	Pyrrolo-pyrimidine	Type-I	MF, PV	2.8	JAK1	FDA approved MF (2011) PV (2015)	Thrombo-cytopenia, Anemia, Neutropenia, Myelosuppression	(1-3)
LY2784544	Gandotinib	*Eli Lilly*	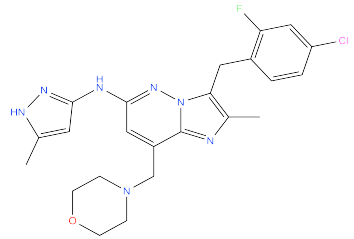	Substituted imidazo-pyridazine	Type-I	ET, PV, MF Solid tumor	3	JAK1, JAK3	Phase I/II, ongoing Preclinic	Renal impairment, tumor lysis syndrome, gastro intestinal toxicity, anemia	(4, 5)
CYT387	Momelotinib GS-0387	*Cytopia, acquired Gilead*	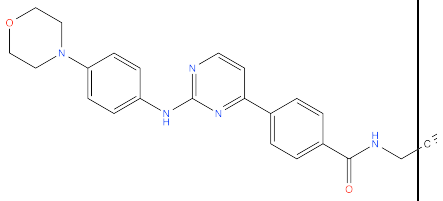	Amino-pyrimidine	Type-I	PMF, post PV MF, post ET MF	11	JAK1, TYK2 TBK1/IKK -ε	Phase III, ongoing	Withdrawal symptoms, neurological side effects	(6-9)
NS-018		*Nippon Shinyaku Co*	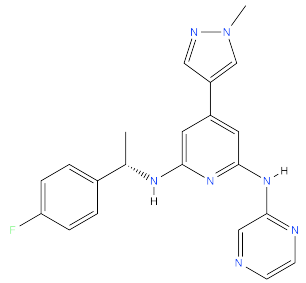	Pyridine based	Type-I	MF, post PV MF, post ET MF	< 1	Src	Phase I/II, ongoing		(10-12)

INCB028050	Baricitinib LY3009104	*Incyte/Eli Lilly*	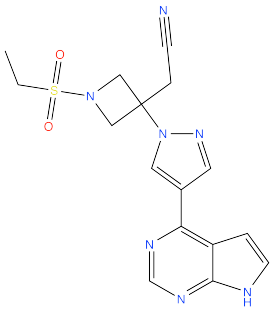	Pyrrolo-pyrimidine	Type-I	RA, Psoriasis	5.7	JAK1	Phase III (RA), Phase II (psoriasis)		(13, 14)
BMS-911543		*Bristol Myers Squibb*	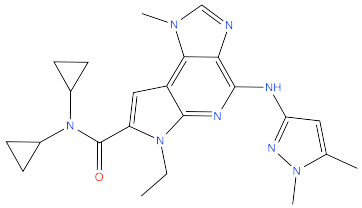	Imidazo-pyrrolo-pyridine	Type-I	MF	1	JAK1 JAK3 TYK2	Phase I/II, completed	Leukopenia, thrombocytopenia, neutropenia	(15-17)
TG101348	Fedratinib SAR302503	*TargeGene* *Sanofi Aventi*	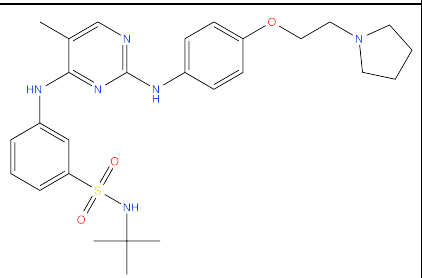	Amino-pyrimidine (thiamine analogue)	Type-I	MF	3	FLT3 RET	Phase III, development terminated in, *Nov 2013*	Wericke's encephalopathy (due to ressemblance of fedratinib with thiamine, VitB1, whose absoption was reduced by hTHTR2)	(18, 19)
CEP-701	Lestaurtinib	*Cephalon*	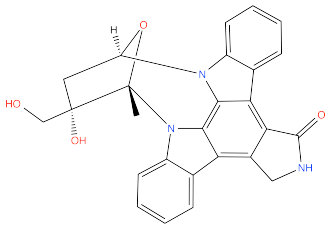	Indolo-carbazole (staurosporine analogue)	Type-I	MF,ET,PV	0.9	FLT3	Phase I/II, development terminated	Gastrointestinal toxicity, high variability in patients (due to high protein bound form)	(20)

AZD-1480		*AstraZeneca*	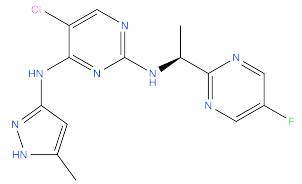	Pyrazol-pyrimidine	Type-I	Primary MF, post PV MF, post ET MF,	3	JAK1 Aurora-A FGFR1 FLT4	Phase I, development terminated	Neurological toxicities	(21)
SB1518	Pacritinib	*S*BIO, CTI biopharma*	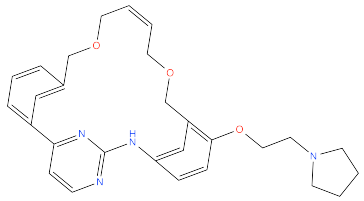	Macrocyclic pyrimidine-based	Type-I	MPN, AML, MDS	23	FLT3	Phase III, development terminated in *Feb 2016*	Intra-cerebral haemorrhage, cardiac failure and arrest, gastrointestinal toxicity	(22, 23)
XL019		*Exelixis*	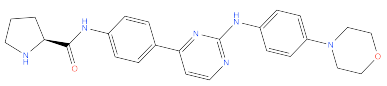	Pyrimidine based	Type-I	PV, MF	2	JAK1 JAK3 TYK2	Phase I, development terminated	Neurotoxicty (peripheral neurophathy)	(24)
NVP-CHZ868		*Novartis*	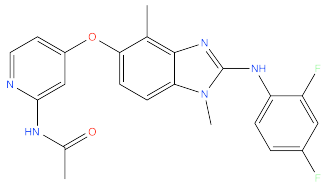	Benzimidazole	Type-II	MPN	110	KIT, as well as PDGFR and VEGFR family kinases	Preclinic		(25, 26)
NVP-BSK805		*Novartis*	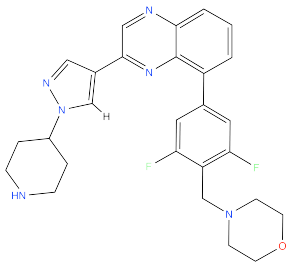	Subsituted quinoxaline	Type-I	MPN	0.48	JAK1 JAK3 TYK2	Preclinic		(27, 28)

CEP-33779		*Cephalon*	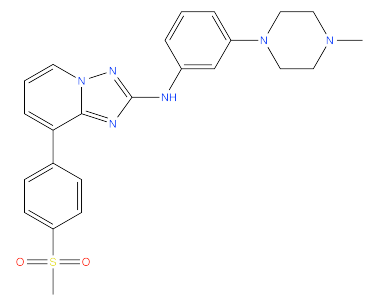	Pyridine derivative	Type-I	Colorectal Tumor	1,3	NA	Preclinic		(29)
NVP-BVB808		*Novartis*	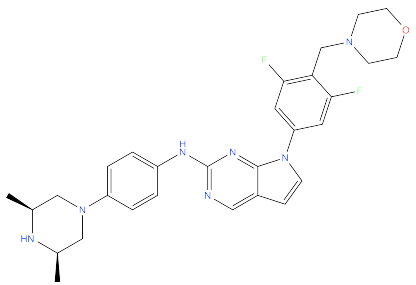	Pyrrolo-pyrimidine	Type-I		0,35	FLT3	Preclinic		(27)
TG101209		*TargeGene*	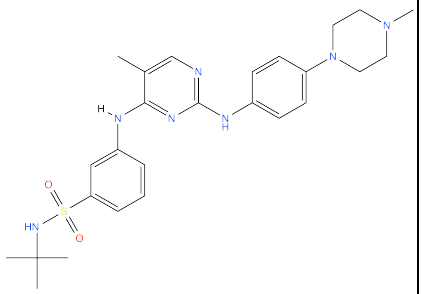	Pyrimidine based	Type-I		6	JAK3, FLT3, RET	Preclinic		(30, 31)
NVP-BBT594		*Novartis*	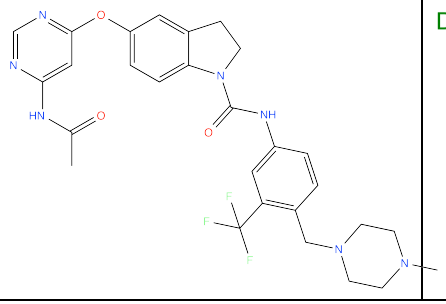	Dihydroindole	Type-II		990	Brc-Abl, KDR, FLT3, RET	Research only	Limits in specificity for JAK2, pharamacokinetics unproper for *in vivo* use	(25, 32)

AG490		*Tocris Bioscience*	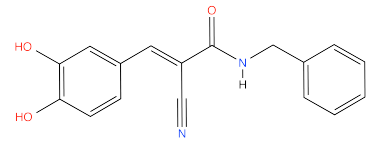	Tyrphostin (first generation)	Type-I		100	EGFR	Research only (*First JAK2 inhibitor*)	Pharamacokinetics unproper for *in vivo* use	(33, 34)
LS104			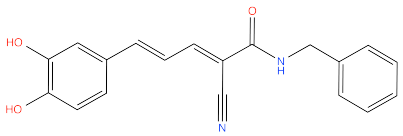	Dienamide	Allosteric			Bcr-Abl RET	Research only		(35, 36)
ON-044580		*Onconova Therapeutics*	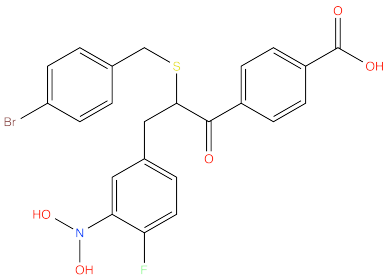	α-benzoyl styryl benzyl sulfide	Allosteric			Bcr-Abl	Research only		(37, 38)

* IC50 values from cell-free assays
** NA: not available

References:

1. Harrison C, Kiladjian JJ, Al-Ali HK, Gisslinger H, Waltzman R, Stalbovskaya V, et al. JAK inhibition with ruxolitinib versus best available therapy for myelofibrosis. N Engl J Med. 2012;366(9):787-98.
2. Verstovsek S, Mesa RA, Gotlib J, Levy RS, Gupta V, DiPersio JF, et al. A double-blind, placebo-controlled trial of ruxolitinib for myelofibrosis. N Engl J Med. 2012;366(9):799-807.
3. Vannucchi AM. Ruxolitinib versus standard therapy for the treatment of polycythemia vera. N Engl J Med. 2015;372(17):1670-1.
4. Ma L, Clayton JR, Walgren RA, Zhao B, Evans RJ, Smith MC, et al. Discovery and characterization of LY2784544, a small-molecule tyrosine kinase inhibitor of JAK2V617F. Blood Cancer J. 2013;3:e109.

5. Verstovsek S, Mesa RA, Salama ME, Giles JLK, Pitou C, Zimmermann AH, et al. Phase I Study Of LY2784544, a JAK2 Selective Inhibitor, In Patients With Myelofibrosis (MF), Polycythemia Vera (PV), and Essential Thrombocythemia (ET) Blood. 2013;122(21):665.

6. Abdelrahman RA, Begna KH, Al-Kali A, Hogan WJ, Litzow MR, Pardanani A, et al. Momelotinib treatment-emergent neuropathy: prevalence, risk factors and outcome in 100 patients with myelofibrosis. Br J Haematol. 2015;169(1):77-80.

7. Abdelrahman RA, Begna KH, Al-Kali A, Hogan WJ, Litzow MR, Tefferi A. Revised assessment of response and long-term discontinuation rates among 111 patients with myelofibrosis treated with momelotinib or ruxolitinib. Leukemia. 2015;29(2):498-500.

8. Pardanani A, Abdelrahman RA, Finke C, Lasho TT, Begna KH, Al-Kali A, et al. Genetic determinants of response and survival in momelotinib-treated patients with myelofibrosis. Leukemia. 2015;29(3):741-4.

9. Pardanani A, Gotlib JR, Gupta V, Roberts AW, Wadleigh M, Sirhan S, et al. Update On The Long-Term Efficacy and Safety Of Momelotinib, a JAK1 and JAK2 Inhibitor, For The Treatment Of Myelofibrosis. Blood. 2013;122(21):108.

10. Nakaya Y, Shide K, Naito H, Niwa T, Horio T, Miyake J, et al. Effect of NS-018, a selective JAK2V617F inhibitor, in a murine model of myelofibrosis. Blood Cancer J. 2014;4:e174.

11. Nakaya Y, Shide K, Niwa T, Homan J, Sugahara S, Horio T, et al. Efficacy of NS-018, a potent and selective JAK2/Src inhibitor, in primary cells and mouse models of myeloproliferative neoplasms. Blood Cancer J. 2011;1(7):e29.

12. Verstovsek S, Talpaz M, Ritchie EK, Wadleigh M, Odenike O, Jamieson C, et al. A Phase 1/2, Open-Label, Dose-Escalation, Multi-Center Study to Assess the Safety, Tolerability, Pharmacokinetics, and Pharmacodynamics of Orally Administered NS-018 in Patients with Primary Myelofibrosis (PMF), Post-Polycythemia Vera Myelofibrosis (postPV MF), or Post-Essential Thrombocythemia Myelofibrosis (postET MF) Blood. 2014;124(21):1839.

13. Genovese MC, Kremer J, Zamani O, Ludivico C, Krogulec M, Xie L, et al. Baricitinib in Patients with Refractory Rheumatoid Arthritis. N Engl J Med. 2016;374(13):1243-52.

14. Genovese MC, Kremer J, Zamani O, Ludivico C, Krogulec M, Xie L, et al. Baricitinib, An Oral Janus Kinase (JAK)1/JAK2 Inhibitor, in Patients with Active Rheumatoid Arthritis (RA) and an Inadequate Response to TNF Inhibitors: Results of the Phase 3 RA-Beacon Study Ann Rheum Dis. 2015;74(Suppl 2):75-6.

15. Purandare AV, McDevitt TM, Wan H, You D, Penhallow B, Han X, et al. Characterization of BMS-911543, a functionally selective small-molecule inhibitor of JAK2. Leukemia. 2012;26(2):280-8.

16. Roberts AW, Seymour JF, Burbury K, Verstovsek S, Tefferi A, Pardanani A. BMS-911543, A Selective JAK2 Inhibitor: A Multicenter Phase 1/2a Study In Myelofibrosis. Blood. 2013;122(21):664.

17. Wan H, Schroeder GM, Hart AC, Inghrim J, Grebinski J, Tokarski JS, et al. Discovery of a Highly Selective JAK2 Inhibitor, BMS-911543, for the Treatment of Myeloproliferative Neoplasms. ACS Med Chem Lett. 2015;6(8):850-5.

18. Zhang Q, Zhang Y, Diamond S, Boer J, Harris JJ, Li Y, et al. The Janus kinase 2 inhibitor fedratinib inhibits thiamine uptake: a putative mechanism for the onset of Wernicke's encephalopathy. Drug Metab Dispos. 2014;42(10):1656-62.

19. Pardanani A, Harrison C, Cortes JE, Cervantes F, Mesa RA, Milligan D, et al. Safety and Efficacy of Fedratinib in Patients With Primary or Secondary Myelofibrosis: A Randomized Clinical Trial. JAMA Oncol. 2015;1(5):643-51.

20. Hexner EO, Mascarenhas J, Prchal J, Roboz GJ, Baer MR, Ritchie EK, et al. Phase I dose escalation study of lestaurtinib in patients with myelofibrosis. Leuk Lymphoma. 2015;56(9):2543-51.

21. Verstovsek S, Hoffman R, Mascarenhas J, Soria JC, Bahleda R, McCoon P, et al. A phase I, open-label, multi-center study of the JAK2 inhibitor AZD1480 in patients with myelofibrosis. Leuk Res. 2015;39(2):157-63.

22. Komrokji RS, Seymour JF, Roberts AW, Wadleigh M, To LB, Scherber R, et al. Results of a phase 2 study of pacritinib (SB1518), a JAK2/JAK2(V617F) inhibitor, in patients with myelofibrosis. Blood. 2015;125(17):2649-55.

23. Mesa RA, Egyed M, Szoke A, Suvorov A, Perkins A, Mayer J, et al. Results of the PERSIST-1 phase III study of pacritinib (PAC) versus best available therapy (BAT) in primary myelofibrosis (PMF), post-polycythemia vera myelofibrosis (PPV-MF), or post-essential thrombocythemia-myelofibrosis (PET-MF). ASCO Annual Meeting: J Clin Oncol 33, 2015 (suppl; abstr LBA7006); 2015.

24. Verstovsek S, Tam CS, Wadleigh M, Sokol L, Smith CC, Bui LA, et al. Phase I evaluation of XL019, an oral, potent, and selective JAK2 inhibitor. Leuk Res. 2014;38(3):316-22.

25. Meyer SC, Keller MD, Chiu S, Koppikar P, Guryanova OA, Rapaport F, et al. CHZ868, a Type II JAK2 Inhibitor, Reverses Type I JAK Inhibitor Persistence and Demonstrates Efficacy in Myeloproliferative Neoplasms. Cancer Cell. 2015;28(1):15-28.

26. Wu SC, Li LS, Kopp N, Montero J, Chapuy B, Yoda A, et al. Activity of the Type II JAK2 Inhibitor CHZ868 in B Cell Acute Lymphoblastic Leukemia. Cancer Cell. 2015;28(1):29-41.

27. Ringel F, Kaeda J, Schwarz M, Oberender C, Grille P, Dorken B, et al. Effects of Jak2 type 1 inhibitors NVP-BSK805 and NVP-BVB808 on Jak2 mutation-positive and Bcr-Abl-positive cell lines. Acta Haematol. 2014;132(1):75-86.

28. Baffert F, Regnier CH, De Pover A, Pissot-Soldermann C, Tavares GA, Blasco F, et al. Potent and selective inhibition of polycythemia by the quinoxaline JAK2 inhibitor NVP-BSK805. Mol Cancer Ther. 2010;9(7):1945-55.

29. Seavey MM, Lu LD, Stump KL, Wallace NH, Hockeimer W, O'Kane TM, et al. Therapeutic efficacy of CEP-33779, a novel selective JAK2 inhibitor, in a mouse model of colitis-induced colorectal cancer. Mol Cancer Ther. 2012;11(4):984-93.

30. Pardanani A, Hood J, Lasho T, Levine RL, Martin MB, Noronha G, et al. TG101209, a small molecule JAK2-selective kinase inhibitor potently inhibits myeloproliferative disorder-associated JAK2V617F and MPLW515L/K mutations. Leukemia. 2007;21(8):1658-68.

31. Geissler K, Jager E, Barna A, Sliwa T, Knobl P, Schwarzinger I, et al. In vitro and in vivo effects of JAK2 inhibition in chronic myelomonocytic leukemia. Eur J Haematol. 2016.

32. Andraos R, Qian Z, Bonenfant D, Rubert J, Vangrevelinghe E, Scheufler C, et al. Modulation of activation-loop phosphorylation by JAK inhibitors is binding mode dependent. Cancer Discov. 2012;2(6):512-23.

33. Meydan N, Grunberger T, Dadi H, Shahar M, Arpaia E, Lapidot Z, et al. Inhibition of acute lymphoblastic leukaemia by a Jak-2 inhibitor. Nature. 1996;379(6566):645-8.

34. Miyamoto N, Sugita K, Goi K, Inukai T, Lijima K, Tezuka T, et al. The JAK2 inhibitor AG490 predominantly abrogates the growth of human B-precursor leukemic cells with 11q23 translocation or Philadelphia chromosome. Leukemia. 2001;15(11):1758-68.

35. Lipka DB, Hoffmann LS, Heidel F, Markova B, Blum MC, Breitenbuecher F, et al. LS104, a non-ATP-competitive small-molecule inhibitor of JAK2, is potently inducing apoptosis in JAK2V617F-positive cells. Mol Cancer Ther. 2008;7(5):1176-84.

36. Kasper S, Breitenbuecher F, Hoehn Y, Heidel F, Lipka DB, Markova B, et al. The kinase inhibitor LS104 induces apoptosis, enhances cytotoxic effects of chemotherapeutic drugs and is targeting the receptor tyrosine kinase FLT3 in acute myeloid leukemia. Leuk Res. 2008;32(11):1698-708.

37. Jatiani SS, Cosenza SC, Reddy MV, Ha JH, Baker SJ, Samanta AK, et al. A Non-ATP-Competitive Dual Inhibitor of JAK2 and BCR-ABL Kinases: Elucidation of a Novel Therapeutic Spectrum Based on Substrate Competitive Inhibition. Genes Cancer. 2010;1(4):331-45.

38. Samanta AK, Chakraborty SN, Wang Y, Schlette E, Reddy EP, Arlinghaus RB. Destabilization of Bcr-Abl/Jak2 Network by a Jak2/Abl Kinase Inhibitor ON044580 Overcomes Drug Resistance in Blast Crisis Chronic Myelogenous Leukemia (CML). Genes Cancer. 2010;1(4):346-59.

Acknowledgments

I have had the chance to work with a number of brilliant people who have helped me through my PhD.

I would like, first, to express my sincere gratitude to advisor Stefan, who welcome me in his lab during my master thesis work. I would like to thank him for the continuous support of my PhD, for his patience, his guidance, encouragements and his immense knowledge.

Besides my advisor, I would like to thank the members of my jury, Profs. Jean-Christophe Renauld (and special thanks for letting me use your coffee machine), Thomas Michiels, Frederic Lemaigre, Mikka Vikkula for their insightful comments and encouragements but also for the questions which incented me to widen my research from various perspectives.

My sincere thanks also go to the external members of my jury. I would like to thank Prof. Radek Skoda for the stimulating questions and discussion about the work presented in this thesis. I also would like to thank Dr. Andrew Shaw for his expertise in structural biology and for the greatly appreciated collaboration on the project. Thank you for helping me getting more insight into the world of crystallography.

I would like to thank my fellow labmates** and all the people in the institute that help me daily during the thesis. Thank you to Didier Colau for the great help with the work related to protein production and for the general help on my project! Thank you for being such a great colleague! Thank you also to Madeleine for the technical help related to this project.

Thank you to Nicolas Dauget for FACS sorting. Thank you to the administrative members of the Ludwig and de Duve Institutes (Geneviève Sapin, Nathalie Krack, Carine Lemoine and Pierre-Olivier Seroen and Julie Klein) for the help with sending and receiving all the necessary materials, items and samples necessary to properly undertake our researches. Thank you for the help on the administrative part in general. Thank you to the IT team (Jo and Jacques/Pascal). Massive thank you Jacques for the help related to "Mac issues".

Thank you to the 74+4 and 75+4 teams (JBD and JCR's groups), thank you for sharing animated lunch times and cheerful discussion but also for sharing protocols, cytokines or pipettes!

I would like to thank my friends from Brussels and elsewhere for always being there for me and for the continuous support and the encouragement, thank you for taking (a huge and important) part of the world that is outside of the PhD thesis.

Huge thank to my family (Ebly and Brussels represent), thank you to my parents, my brothers, to my aunt and cousins.

**

Labmates_part 2_ Ladies first,

Tout d'abord un énorme merci à Céline qui a toujours été là pour moi et ce, depuis le tout début. Merci pour l'aide générale dans le labo et tout ce que tu m'as appris quand je n'étais encore qu'une petite mémorante. Merci pour tout et surtout ton amitié!

Thank you to Leila, who has saved me from my solitude in the JAK2's land. Thank you for the critical reading of this work and for your endless help about "English language stuff". (and thank you for sharing some excellent belgians beers some times).

Merci à Christian, le rock de ce labo! Merci pour avoir toujours répondu aux (trop nombreuses) questions en ce qui concerne les manips, les résultats obtenus, ou encore où trouver les choses dans ce labo (trop) ordonné..... brefs les questions de la vie quoi!

Merci à Jean-Philippe pour le travail de collaboration et les discussions (souvent) très constructives au sujet des résultats. Merci pour m'avoir appris à toujours ranger mes affaires...

Merci à Ilyas (Bienvenue) pour être toujours là quand on en a besoin, merci pour ton énergie positive et ton sourire. Toujours prêt à aider tout le monde, Ilyas you're the man! Inch Allah!

Merci aux derniers arrivants de ce labo qui ont apporté une autre dyamique (bien appréciée) dans le labo. Merci à Xavier pour sa grande expertise en FACS, son (toujours très apprécié) support et son humour de doc (non sérieusement j'adore tes blagues!) Merci à Gaëlle, avec qui je partage un bureau, une orchidée et mes fluos, merci pour les discussions toujours intéressantes et pour être une collègue hors pair! Merci à Mr. (F***) Balligand pour être lui-même tout simplement! Merci pour les (nombreuses) courses chez le Chinois (merci Tam, ce dit en passant pour remplir mon estomac (presque) tous les midis). Merci de toujours répondre présent (même pour aller chercher une collègue boitante qui vient de perdre une cheville). Merci à Florian pour ses avalanches de magnésium et de sérotonine liées à un apport régulier de chocobons. Merci à Lidvine pour son (work, work, work, work, work) aide (amplement) appréciée pour les manips!

Merci aux membres passés et (tout juste) présent (Roxanna, Vitalina, Alexandra, Shwe et Anita)